

https://dspace.org/

The effect of consolidation and loading stress paths on the static liquefaction of mine tailings

Tshabalala, Lourence

2003
http://hdl.handle.net/10539/23712

Downloaded from a DSpace repository. https://dspace.org/

THE EFFECT OF CONSOLIDATION AND LOADING STRESS PATHS ON THE STATIC LIQUEFACTION OF MINE TAILINGS

Lourence Tshabalala

A dissertation submitted to the Faculty of Engineering and the Built Environment, University of the Witwatersrand, Johannesburg, in fulfilment of the requirements for the degree of Master of Science in Engineering.

Johannesburg, 2003

DECLARATION

I declare that this dissertation is my own, unaided work. It is being submitted for the Degree of Master of Science in the University of the Witwatersrand, Johannesburg. It has not been submitted before for any degree or examination in any other University.

T.Shabalala.....

17TH day of DECEMBER 2003

ABSTRACT

The reliability of using isotropically consolidated specimens in the laboratory determination of liquefaction characteristics of cohesionless sands, as is common practice today, is evaluated.

Two series of triaxial tests involved the conventional undrained loading of isotropically and anisotropically consolidated specimens. The third series of tests utilized anisotropically consolidated specimens loaded by following special undrained stress paths.

Test results revealed that liquefaction characteristics obtained from isotropically and anisotropically consolidated specimens are different. The effective angles of friction mobilized at peak shear stress and at steady state were greater for anisotropically consolidated specimens.

Loading stress path is seen to have no effect on the liquefaction characteristics derived from conventional loading of anisotropically consolidated specimens.

The critical stress ratio line is observed to be the line determining the initiation of liquefaction so that any stress path attempting to cross this line, regardless of direction of approach, immediately shows strain-softening behavior leading to liquefaction.

ACKNOWLEDGEMENTS

The author wishes to express his gratitude for the financial support provided by the Mellon Postgraduate Fund. The author also wishes to thank the University of the Witwatersrand for permission to use equipment in the soils laboratory. Supervision and mentorship of Professor A. B. Fourie of the School of Civil and Environmental Engineering of the University of the Witwatersrand is greatly acknowledged.

TABLE OF CONTENTS

Contents **Page**

DECLARATION ii

ABSTRACT iii

ACKNOWLEDGEMENTS iv

TABLE OF CONTENTS v

LIST OF FIGURES xi

LIST OF TABLES xvi

1 INTRODUCTION 1

1.1 Overview of the Chapter 2

1.2 The Merriespruit Gold Tailings Dam Flow Failure 3

1.2.1 Life of the dam 3

1.2.2 Investigations to ascertain the cause of failure 4

1.2.3 Postulated cause of failure 8

1.3 Objectives of the Present Study 10

1.4 Research Methodology 10

1.5 Organization of the Document 13

2 STATIC LIQUEFACTION OF COHESIONLESS SOILS 15

2.1 Overview 15

2.2 Definition of Liquefaction 15

2.3 Requirements for Liquefaction 16

2.4 Static Liquefaction Testing in the Triaxial Equipment 18

2.5 Postulated Observations 19

2.5.1 Contractive (strain-softening) behavior 19

2.5.2 Dilative (strain-hardening) behavior 21

Contents Page

2.5.3 Limited liquefaction behavior 22
2.6 Characterization of Liquefaction Behavior 23
2.6.1 Steady-state line "F line" 23
2.6.2 Steady-state "large strain" failure envelope 24
2.6.3 Critical void ratio line "CVR line or S line" 26
2.6.4 Critical stress ratio line "CSR line" 27
2.6.5 Phase transformation line (PT line) 28
2.7 Prediction of Undrained Behavior 29
2.7.1 The steady-state approach 29
2.7.2 State parameter 30
2.8 Liquefaction Potential of Sand 32
2.9 Liquefaction Resistance of Sand 32
2.10 Initiation of Liquefaction 33
2.11 Factors Affecting Liquefaction Behavior of Sands 34
2.11.1 Soil property 35
2.11.2 Test procedures 40
2.11.3 Stress conditions 48
2.12 Potential Errors in the Triaxial Test 49
2.12.1 Void ratio 49
2.12.2 Measured volume changes 50
2.12.3 Measured pore pressures 51
2.13 Corrections to Triaxial Test Data 53
2.13.1 Area correction 53
2.13.2 Membrane volume change corrections 53
2.13.3 Correction of pore pressure for membrane effect 56
2.13.4 Correction for strength of rubber membrane 57

Contents Page

3 LIQUEFACTION TESTING 59

3.1 Introduction 59

3.2 Monotonic Undrained Compression of Isotropically Consolidated Specimens (case 1 tests) 60

3.2.1 Test equipment 60

3.2.2 Preparation of test equipment and pre-test checks 65

3.2.3 Calibration of equipment 70

3.2.4 Preparation of test specimens 70

3.2.5 Setting up of specimens in the triaxial equipment 74

3.2.6 Saturation of specimens 76

3.2.7 Consolidation to the required isotropic stress state 84

3.2.8 Monotonic undrained loading of specimens 85

3.3 Monotonic Undrained Compression of One-Dimensionally Consolidated Specimens (case 2 tests) 87

3.3.1 Test equipment 87

3.3.2 Preparation of test equipment and pre-test checks 88

3.3.3 Calibration of equipment 88

3.3.4 Preparation of test specimens 89

3.3.5 Setting up of specimens in the triaxial equipment 89

3.3.6 Saturation of specimens 92

3.3.7 Consolidation to the required K0-condition stress state 95

3.3.8 Monotonic undrained loading of specimens 96

3.4 Variation of Stress Path Followed During Undrained Loading of One-Dimensionally Consolidated Specimens (case 3 tests) 97

3.4.1 Test equipment 97

3.4.2 Preparation of test equipment and pre-test checks 103

3.4.3 Calibration of equipment 107

Contents **Page**

3.4.4 Preparation of test specimens 108

3.4.5 Setting up of specimens in the Bishop-Wesley stress path cell 108

3.4.6 Saturation of specimens 109

3.4.7 Consolidation to the required K0-condition stress state 118

3.4.8 Undrained loading stress paths 119

4 TEST RESULTS 129

4.1 Overview 129

4.2 Monotonic Undrained Compression of Isotropically Consolidated Specimens (case 1 tests) 129

4.2.1 Description of the format of the datasheet and the calculation of various test parameters 130

4.3 Monotonic Undrained Compression of One-Dimensionally Consolidated Specimens (case 2 tests) 136

4.3.1 Description of the format of the datasheet and the calculation of various test parameters 137

4.4 Variation of Stress Path Followed During Undrained Loading of One-Dimensionally Consolidated Specimens (case 3 tests) 143

4.4.1 Description of the format of the datasheet and the calculation of various test parameters 143

5 PRESENTATION AND DISCUSSION OF RESULTS 151

5.1 Monotonic Undrained Compression of Isotropically Consolidated Specimens (case 1 tests) 151

5.1.1 CSR line and steady-state failure envelope 154

5.1.2 Variation of effective angles of friction mobilized at peak shear stress and at steady state with fines content and gradation 156

5.1.3 Steady-state line 157

5.1.4 Variation of steady-state line with fines content and gradation 160

Contents Page

5.2 Monotonic Undrained Compression of One-Dimensionally Consolidated Specimens (case 2 tests) 161

5.2.1 CSR line and steady-state failure envelope 165

5.2.2 Variation of effective angles of friction mobilized at peak shear stress and at steady state with fines content and gradation 167

5.2.3 Steady-state line 169

5.2.4 Liquefaction resistance 172

5.3 Variation of Stress Path Followed During Undrained Loading of One-Dimensional Consolidated Specimens (Case 3 tests) 173

5.3.1 CSR line and steady-state failure envelope 174

5.3.2 Steady-state line 176

5.4 Summary of Findings 177

5.4.1 Tests on isotropically consolidated specimens 177

5.4.2 Effect of anisotropic consolidation 179

5.4.3 Effect of fines content and gradation 180

5.4.4 Effect of loading stress path 181

5.5 Discussion 182

5.5.1 Effect of anisotropic consolidation 182

5.5.2 Effect of fines content and gradation 183

5.5.3 Implication of the variable loading stress path tests 184

6 CONCLUSIONS AND RECOMMENDATIONS 186

6.1 Summary and Conclusions 186

6.2 Recommendations for Future Research 188

REFERENCES 190

BIBLIOGRAPHY 200

Contents Page

APPENDIX A Calibration of Equipment for Case 1 Tests 201

APPENDIX B Calibration of Equipment for Case 3 Tests 208

APPENDIX C Test Results for Specimens Under Case 1 Tests 239

APPENDIX D Test Results for Specimens Under Case 2 Tests 307

APPENDIX E Test Results for Specimens Under Case 3 Tests 382

LIST OF FIGURES

Figure	Title	Page
Figure 1.1	Particle size distribution curves for Merriespruit gold tailings	11
Figure 1.2	Maximum and minimum void ratios for Merriespruit gold tailings	12
Figure 2.1	Undrained behavior of sands	20
Figure 2.2	Relationship between initial state of sand and undrained behavior	30
Figure 2.3	Definition of state parameter	31
Figure 3.1	The conventional triaxial apparatus	61
Figure 3.2	Details of a typical triaxial cell	62
Figure 3.3	Arrangement for displacing air in the voids of a specimen by water at the lowest pressures (Air-flushing)	79
Figure 3.4	Lateral strain indicator (K0-ring)	87
Figure 3.5	Ensuring the correct amount of mercury in the mercury chamber of the K0-ring	89
Figure 3.6	Fitting the K0-ring around the specimen	91
Figure 3.7	The Bishop-Wesley stress path cell and necessary pressure systems	98
Figure 3.8	Details of the Bishop-Wesley stress path cell	99
Figure 3.9	Schematic representation of the electronic measurement and recording of test data	103
Figure 3.10	Arrangement for displacing air in the voids of a specimen by water at the lowest pressures (Air-flushing)	111
Figure 5.1	Stress paths for isotropically consolidated Merriespruit gold tailings containing 0% fines	152

Figure **Title** **Page**

Figure 5.2 Stress paths for isotropically consolidated Merriespruit gold tailings containing 20% fines 152

Figure 5.3 Stress paths for isotropically consolidated Merriespruit gold tailings containing 30% fines 153

Figure 5.4 Stress paths for isotropically consolidated Merriespruit gold tailings containing 60% fines 153

Figure 5.5 CSR line and steady-state failure envelope for isotropically consolidated Merriespruit gold tailings containing 0% fines 154

Figure 5.6 CSR line and steady-state failure envelope for isotropically consolidated Merriespruit gold tailings containing 20% fines 155

Figure 5.7 CSR line and steady-state failure envelope for isotropically consolidated Merriespruit gold tailings containing 30% fines 155

Figure 5.8 CSR line and steady-state failure envelope for isotropically consolidated Merriespruit gold tailings containing 60% fines 156

Figure 5.9 Variation with fines content (and gradation) of effective angles of friction mobilized at peak shear stress and at steady-state for isotropically consolidated Merriespruit gold tailings 157

Figure 5.10 Steady-state line for isotropically consolidated Merriespruit gold tailings containing 0% fines 158

Figure 5.11 Steady-state line for isotropically consolidated Merriespruit gold tailings containing 20% fines 159

Figure 5.12 Steady-state line for isotropically consolidated Merriespruit gold tailings containing 30% fines 159

Figure 5.13 Steady-state line for isotropically consolidated Merriespruit gold tailings containing 60% fines 160

Figure **Title** **Page**

Figure 5.14 Variation of steady-state line of isotropically consolidated Merriespruit gold tailings with fines content (and gradation) 161

Figure 5.15 Stress paths for anisotropically consolidated Merriespruit gold tailings containing 0% fines..... 163

Figure 5.16 Stress paths for anisotropically consolidated Merriespruit gold tailings containing 20% fines..... 163

Figure 5.17 Stress paths for anisotropically consolidated Merriespruit gold tailings containing 30% fines..... 164

Figure 5.18 Stress paths for anisotropically consolidated Merriespruit gold tailings containing 60% fines..... 164

Figure 5.19 CSR lines and steady-state failure envelopes for isotropically consolidated and anisotropically consolidated Merriespruit gold tailings containing 0% fines..... 165

Figure 5.20 CSR lines and steady-state failure envelopes for isotropically consolidated and anisotropically consolidated Merriespruit gold tailings containing 20% fines..... 166

Figure 5.21 CSR lines and steady-state failure envelopes for isotropically consolidated and anisotropically consolidated Merriespruit gold tailings containing 30% fines..... 166

Figure 5.22 CSR lines and steady-state failure envelopes for isotropically consolidated and anisotropically consolidated Merriespruit gold tailings containing 60% fines..... 167

Figure 5.23 Variation with fines content (and gradation) of the effectiveangle of friction mobilized at peak shear stress for isotropically consolidated and anisotropically consolidated Merriespruit gold tailings 168

Figure **Title** **Page**

Figure 5.24 Variation with fines content (and gradation) of the effective angle of friction mobilized at steady-state for isotropically consolidated and anisotropically consolidated Merriespruit gold tailings 169

Figure 5.25 Steady-state lines for isotropically consolidated and anisotropically consolidated Merriespruit gold tailings containing 0% fines 170

Figure 5.26 Steady-state lines for isotropically consolidated and anisotropically consolidated Merriespruitgold tailings containing 20% fines 170

Figure 5.27 Steady-state lines for isotropically consolidated and anisotropically consolidated Merriespruit gold tailings containing 30% fines 171

Figure 5.28 Steady-state lines for isotropically consolidated and anisotropically consolidated Merriespruit gold tailings containing 60% fines 171

Figure 5.29 Variation of liquefaction resistance of isotropically consolidated and anisotropically consolidated specimens with effective mean normal stress after consolidation 172

Figure 5.30 Stress paths for anisotropically consolidated Merriespruit gold tailings containing 20% fines, loaded undrained by reducing the cell pressure while keeping either the deviator stress or the effectivemean normal stress constant 174

Figure 5.31 CSR lines and steady-state failure envelopes obtained during conventional and special undrained loading of anisotropically consolidated Merriespruit gold tailings containing 20% fines 175

Figure 5.32 Steady-state lines for anisotropically consolidated Merriespruit gold tailings containing 20% fines loaded undrained by following various stress paths 176

Figure A1 Calibration for cell expansion with pressure and time 206

Figure B1 Calibration of cell pressure transducer 211

Figure	Title	Page

Figure B2 Calibration of back/ pore pressure transducer 214

Figure B3 Arrangement for the calibration of load transducer against axial force 216

Figure B4 Calibration of load transducer against axial force 218

Figure B5 Calibration of load transducer against cell pressure 221

Figure B6 Arrangement for the calibration of volume change transducer 223

Figure B7 Calibration of volume change transducer 226

Figure B8 Calibration of volume change due to piston movement 229

Figure B9 Calibration for cell expansion with pressure and time 232

Figure B10 The instrument used for calibrating the axial displacement transducers.. 234

Figure B11 Calibration of axial displacement transducers 237

LIST OF TABLES

Table	Title	Page
Table 1.1	Maximum and minimum void ratios for Merriespruit gold tailings	11
Table A1	Calibration for cell expansion with pressure and time	205
Table B1	Calibration of cell pressure transducer	210
Table B2	Calibration of back/ pore pressure transducer	213
Table B3	Calibration of load transducer against axial force	217
Table B4	Calibration of load transducer against cell pressure	220
Table B5	Calibration of volume change transducer	224
Table B6	Calibration of volume change due to piston movement	228
Table B7	Calibration for cell expansion with pressure and time	231
Table B8	Calibration of axial displacement transducers	235
Table C1	Summary of results of monotonic undrained compression triaxial tests performed on isotropically consolidated Merriespruit gold tailings (present study)	240
Table C2	Summary of results of monotonic undrained compression triaxial tests performed on isotropically consolidated Merriespruit gold tailings (Fourie and Papageorgiou (2001))	241
Table D1	Summary of results of monotonic undrained compression triaxial tests performed on anisotropically consolidated Merriespruit gold tailings	308
Table E1	Summary of results of undrained compression triaxial tests performed on anisotropically consolidated Merriespruit gold tailings	383

1 INTRODUCTION

Many failures of earth structures (hydraulic fills, slopes, embankments, and foundations) have been attributed in the literature to the liquefaction of saturated sands. These failures are primarily caused by a rapid pore pressure build-up and a substantial loss of shear strength resulting from some external undrained loading (cyclic or static). The loss of shear resistance and the associated large strains that occur in a soil mass leads to the development of instabilities within the mass and places the mass of soil in a "fluid state" which result in the mass flowing until the stresses acting on it are as low as its reduced shear strength. The flow of large masses of soil structures has in many cases caused catastrophic consequences involving damage to property and loss of lives.

The majority of liquefaction failures documented in the literature were due to cyclic or dynamic loading resulting from earthquakes, classical examples being the failures that occurred in Niigata, Japan (Japan National Committee (1965); Ohsaki (1966)) and Alaska (Grantz et al. (1964); Seed and Wilson (1967)) during earthquakes in 1964. It is not surprising, therefore, that most of the research surrounding liquefaction was directed to cyclic loading conditions and lesser attention was paid to liquefaction behavior under monotonic (static) loading conditions. However, although relatively rare, liquefaction failures under monotonic (static) loading conditions have been observed in the past (Hazen (1920); Middlebrooks (1942); Senour and Turnbull (1948); Koppejan et al. (1948) Terzaghi (1956); Andresen and Bjerrum (1968); Kleiner (1976); Jennings (1979); Lucia (1981)). These failures are potentially catastrophic and equally undesirable.

The procedures used for analyzing the safety of slopes and embankments against static liquefaction failure focus on the potential for a flow failure to occur through the determination of the undrained steady-state strength corresponding to the in situ void ratio of the sand by means of laboratory tests, for example, (Poulos et al. (1985)).
The determination of undrained steady-state strength parameters in the laboratory usually utilizes isotropically consolidated specimens of the sand. However, the sand fabric developed insitu is anisotropic. Uncertainties exist in the procedure as to the ability to correlate the undrained steady-state strength measured in the laboratory to

insitu strength. The basis of the procedures is the presumption that the undrained steady-state strength is solely a function of the void ratio of the sand. However, a considerable amount of research has indicated that there are many factors that influence the undrained steady-state strength measured in the laboratory (e.g. specimen preparation method; method of loading; etc.). While some of the factors affecting the measured steady state strength have been identified and studied, the influences of many other factors are less well understood and in some cases contradictory conclusions have been drawn as to the effects of such factors on the measured undrained steady-state strength.

With reference to the Merriespruit gold tailings dam flow failure of February 1994, several of these factors are considered in the present investigation.

1.1 Overview of the Chapter

This chapter commences with a brief description of the Merriespruit gold tailings dam flow failure, section 1.2. This covers the life of the dam, from design up to failure, (section 1.2.1); the investigations done, during the inquest/ inquiry following the failure, to ascertain the cause of failure (section 1.2.2); and the postulated cause of failure thereof (section 1.2.3). Test results obtained by Fourie and Papageorgiou (2001), suggesting that the reason that the Merriespruit tailings flowed with such disastrous consequences was because of static liquefaction, are included elsewhere (Appendix C, Table C2).

Section 1.3 outlines the objectives of the present study.

The methodology for achieving the objectives of the present study is described in section 1.4.

Section 1.5 gives a brief overview of the contents of the rest of the chapters of this document.

1.2 The Merriespruit Gold Tailings Dam Flow Failure

1.2.1 Life of the dam

In the following paragraphs, a very brief description of the life, from design through to failure in February 1994, of the Merriespruit No. 4 dam is given, which eventually breached and released about 600 000 m^3 of semi-liquid tailings, killing 17 people, injuring more than 200 and causing damage estimated at R75 million. Full details are covered elsewhere (Wagener (1997); Wagener et al. (1998) and Strydom and Williams (1999)). Note that the following descriptions are actually a summary of these references.

The dam was designed in 1976 using rule of thumb, although the details did not differ much from those being used today. A geotechnical investigation was not conducted at the time.

The 'upstream semi-dry paddock' method of dam construction, widely used for gold tailings dams in South Africa, was used for construction of the dam. The initial earthworks were constructed in 1978. Instead of providing a single ringmain around the dam, as is customary today, three delivery pipes were used.

One of these pipes regularly experienced high friction head, choking and pipe bursts, resulting in difficulty with pool control and the pool frequently being located away from the penstock intakes.

On the northern side of the wall, at the point where the breach occurred, was a shallow drainage valley. The two delivery pipes, on either side of this low spot, resulted in the finer fraction of the slimes being deposited in this low section.
According to the contractor's head office supervisor, slurry received from the reduction works often had a low relative density resulting in difficult dam-building conditions with seepage and sloughing on the northern wall.

Seepage and sloughing was a continual problem and in 1991 a small dump rock buttress was placed against the face of the slope to prevent sloughing, however, this

was not successful. In 1992, an hydraulically placed buttress was formed to repair the seepage erosion area by depositing tailings into the failed area. The placing of this buttress was problematic and the buttress was therefore inspected regularly.

A stability analysis performed by the contractor in April 1993, using assumed strength parameters and a circular slip failure mode, yielded a factor of safety of 1.34 for the northern wall where the breach later occurred.

Due to continued seepage and sloughing, a decision was made by the contractor to discontinue sliming on the dam about 15 months prior to the disaster. According to the contractor, the vertical freeboard was at an acceptable 1.0m plus at the time the decision was made to decommission the dam.

Sloughing at the toe continued even after deposition supposedly stopped on the dam. The contractor continued with construction of the slime buttress. Shortly before the disaster, slips occurred on the lower slope of the dam immediately above the buttress and these were repaired by dozing in dry slime from the lower berm.

The freeboard was slowly used up as excess plant water, which must often have contained slime, was still being delivered to the dam even after the instruction to stop operating the dam. At the time of failure the vertical freeboard was only 300mm and this included the height of the daywall paddock wall, which should be disregarded as it was narrow and loosely packed.

The unauthorized deposition of water and slime reduced the freeboard to an unacceptable level and pushed the pool away from the penstock intakes towards the northern daywall prior to the failure. The Merriespruit No. 4 dam was clearly in an unacceptable condition prior to failure.

1.2.2 Investigations to ascertain the cause of failure

Following the Merriespruit gold tailings dam failure, investigations were done to ascertain the cause of the failure. The following sections briefly describe these investigations. The postulated cause of failure is given in the last

section (section 1.2.3). Detailed descriptions of the investigations are provided elsewhere (Wagener (1997); Wagener et al. (1998) and Strydom and Williams (1999)). Note, again, that the following sections are summaries of the descriptions given by these references.

Eye-witness accounts

Some useful information regarding the events on the evening of the 22 February 1994 was gathered from eye-witnesses by the police (Wagener (1997); Wagener et al. (1998) and Strydom and Williams (1999)).

Weather pattern

Measurements of rainfall: Relevant facts about the weather pattern leading up to the breaching of the slimes dam wall were established from rain-gauge records obtained from the Official Weather Bureau.

Additional information about rainfall was obtained from unofficial reports gathered by the local police in Virginia.

Rainfall calculations from radar: The Weather Bureau's Bethlehem weather radar station provided further interesting data on the storm. Estimates, from a detailed study, were made of both the intensity of downpour and the total rainfall on 22 February 1994.

The total rainfall values were in agreement with those obtained from other sources and were nowhere near the 24-hour 100-year precipitation level referred to in Regulation R287 of the Water Act (Act 54 of 1956).

Hydrological aspects

According to Midgley (1994), the 24-hour 100-year maximum precipitation in the general locality of Merriespruit was calculated as 140mm. This meant that, to comply with the regulation for the control of water on a tailings dam (Government Notice

R287 of 30 February 1976), a freeboard of at least 562mm had to be maintained on all the tailings dams in this area during the month of February 1994. This was clearly not the case for the dam under consideration.

Runoff and ponding

Photosurvey and digital terrain-mapping: A digital terrain model (DTM) of the dam was prepared from 16 600 data points, from both photogrammetrical analysis and spot heights from land survey, and contours were drawn. The data was used for the hydrological study and to provide cross-sections as required in further investigations.

From a contour survey, it was established that the top of the tailings dam tilted downward from south to north at a slope of 1 in 250. It followed that practically all the water on top of the dam that did not infiltrate or evaporate drained towards the northern wall.

It was estimated that the state of wetness prior to the storm was such that about 80 percent of a storm's precipitation would have become runoff (Midgley (1994)).

A uniform precipitation of 32mm of rain, which according to Visser (1994) fell over the full three-hour period, was estimated to have produced about 30 000m^3 of runoff. Taking the time of concentration from the main storm to be one hour, it was concluded that there would have been a lapse of nearly an hour before the bulk of the runoff reached the depression near the northern wall and this is in agreement with the eye-witness descriptions.

Freeboard requirements: A profile of the rim of the northern wall of the tailings dam was plotted from the contour survey and a stage-area-storage relationship was generated. Assuming a 24-hour 100-year storm and 80% runoff, the accumulation of water at the lower part of the tailings dam was established. Using the stage storage curve, the approximate elevation to which such an event would raise the water level on top of the dam, from a dry state, was established. The minimum freeboard requirement, according to regulation, was established.

Knowledge as to whether the dam contained water prior to the storm, was crucial in order to reveal whether the freeboard of the dam was acceptable or not. This information was obtained from satellite imagery as described below.

Satellite imagery

In order to gain relevant information about the state of the tailings dam prior to the failure, inquiries were made about the data obtained from the Satellite Applications Centre of the CSIR at Hartbeeshoek. Details of this satellite imagery provided evidence of there having being free water on top of the dam for a considerable period and that it was abutting the outer rim shortly before the breach. This was subsequently confessed to by individuals who had been aware of the situation at the time and it was then learnt that water was being pumped from the plant to the top of the dam, even on the night of the disaster.

Field tests

In order to explain the cause of failure, an understanding of the internal conditions in the dam governing the behavior of the tailings material in the sequence of events giving rise to the mechanism of failure was crucial. For this reason the available data from insitu field tests from a number of sources were studied. These comprised of piezocone tests commissioned by all the parties and conducted by Dr E Rust of the University of Pretoria, vane shear tests carried out by the CSIR, and analysis of standpipe piezometer records by the consultants. Further light was shed on some of the apparent anomalies by the findings of a small-scale seepage and over-topping experiment conducted specifically on the Merriespruit tailings dam itself.

Piezocone tests: Piezocone tests revealed low values of penetration resistance at three locations in the area between the penstock intakes and the breach. However at some locations, considerable resistance was recorded. The results of instantaneous pore pressure observations revealed the presence of shallow perched water tables. At several places, pore pressure dissipation tests were conducted, where the movement of the probe was suspended and the excess pressure allowed to

dissipate. It was noted that the slope of the pore pressure curve was less than hydrostatic.

Swedish vane tests: The vane shear test results indicated considerable variability, with insitu peak strengths from 15.7 kPa to 61.9 kPa and residual strengths from 3.2 kPa to 13.1 kPa, but this was in accordance with the observed considerable variability in moisture contents from 26.6 to 40.4 percent.

Piezometer probes: It was established that the phreatic surface was generally higher than the levels indicated by standpipes which had been installed one year before the failure. Also, the presence of shallow perched water tables was confirmed. These water tables made it impossible to determine the true phreatic surface.

It was also confirmed that pore pressure distribution was less than hydrostatic, as was earlier shown during the piezocone tests.

Overtopping and erosion experiment: In order to study the kind of erosion that might occur in tailings if the outer crest wall was overtopped and to obtain some qualitative idea of the amount of tailings that could be eroded away, a small-scale trial was conduct in the field. A ponding experiment was laid out and constructed on top of the dam wall near the south west corner of the Merriespruit tailings dam. The model was filled and overtopped twice. The experiment showed that erosion due to overtopping had an undercutting effect that was progressing headward towards the breach. It was clear that the tailings is a highly erodible material and that once the wall had breached, there was no possibility that the process could have been stopped.

1.2.3 Postulated cause of failure

Seismic action

As no seismic action was recorded during the period in which the failure occurred, seismicity was ruled out as a possible mode of failure.

Piping

Although there were eyewitness accounts of a water jet emerging from the slope during the early stages of the failure, there was consensus amongst the investigators that even if piping had been a contributory cause of the failure in its early stages, it was unlikely to have been a major cause.

Slope instability

Extensive analyses of the slope in the vicinity of the breach showed that although the slope was not as stable as it should have been, it was marginally stable. However, it was evident from the sloughing failures that occurred on the lower slope, just above the tailings buttress, prior to the disaster, that local stability was not acceptable. It was concluded that overall slope instability was not a primary reason for the failure, although localized instability could have been a triggering mechanism.

Overtopping

It was established that the dam overtopped at the breach location and that water flowed over the crest of the dam for between 1 and 2 hours. During this time considerable erosion of the tailings must have occurred. Also, eye-witnesses testified to the high silt load in the water running through the streets of Merriespruit prior to the failure and the erosion tests confirmed that the tailings is particularly susceptible to erosion. It was therefore accepted that the prime cause of failure of the dam was overtopping and that this overtopping resulted in large-scale removal of tailings on the slope face and resulted in back erosion of the crest into the dam. The net effect of this erosion was removal of support to the poorly consolidated tailings within the body of the dam.

1.3 Objectives of the Present Study

In the present study, use is made of the Merriespruit gold tailings recovered from the vicinity of the failure scar after the 1994 flow failure of the Merriespruit gold tailings dam to investigate the effect of anisotropic consolidation on the liquefaction characteristics of the tailings.

The advantage of using the Merriespruit tailings for the present study is the availability of previous test results in which this tailings was tested under isotropic conditions to determine its liquefaction characteristics (Fourie and Papageorgiou (2001)) and this would aid in the comparison of the liquefaction characteristics of isotropically consolidated and anisotropically consolidated tailings specimens.

The study by Fourie and Papageorgiou (2001) made use of various gradations of Merriespruit gold tailings, each of which had a different fines content (< 75μm). This was important because the tailings involved in the failure most probably had different gradations and fines contents due to sorting of particles along the beach of the tailings dam during deposition.

To yield comparable results, the present study also varied the gradation and fines content so as to match those used by Fourie and Papageorgiou (2001). To some degree, therefore, the present study also investigated the effect of gradation and fines content on the liquefaction characteristics of Merriespruit tailings.

Another factor that was investigated in the present study is the effect of stress path followed during undrained loading.

1.4 Research Methodology

Three series of triaxial tests were performed, viz: Monotonic undrained compression of isotropically consolidated specimens; Monotonic undrained compression of one-dimensionally consolidated specimens and Variation of stress path followed during undrained loading of one-dimensionally consolidated specimens. From hereon these tests will be referred to as case 1, case 2, and case 3 tests, respectively. All three

series involved the use of four bulk samples of Merriespruit gold tailing with different gradation and fines content. The fines contents of these bulk samples were 0%, 20%, 30% and 60% and their gradations are shown in Figure 1.1. These gradations were created by selectively sieving this tailings so as to reproduce the gradations and fines contents used by Fourie and Papageorgiou (2001).

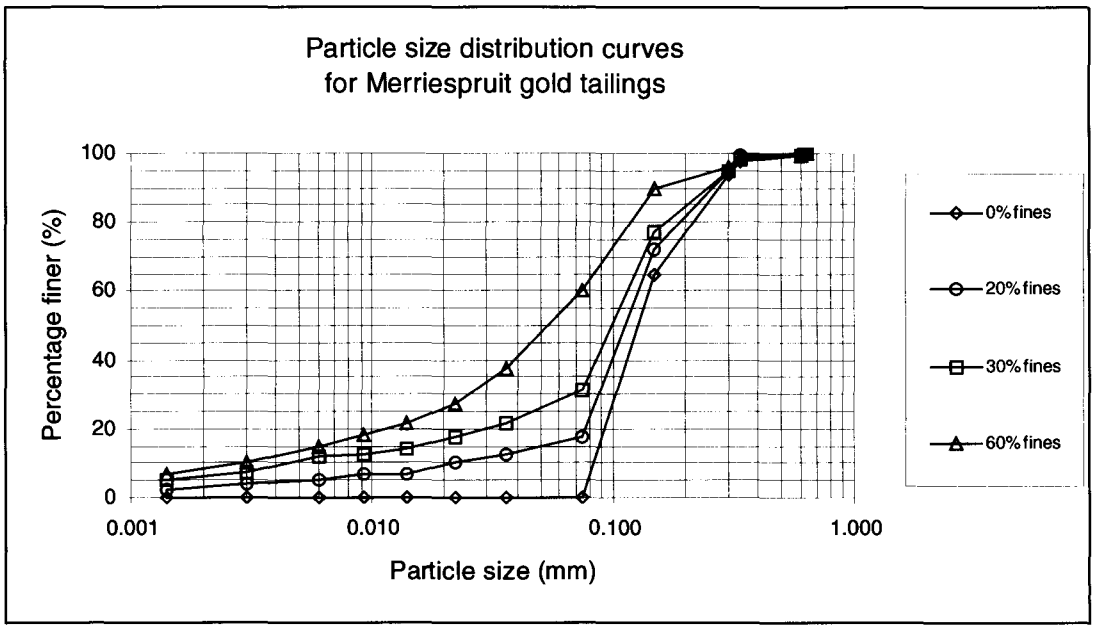


Figure 1.1 Particle size distribution curves for Merriespruit gold tailings

The maximum and minimum void ratios of these bulk samples, determined according to ASTM D4253-91 and D4254-91 (1993) are shown in Table 1.1 and Figure 1.2.

Table 1.1 Maximum and minimum void ratios for Merriespruit gold tailings

Fines content by mass (%)	Maximum void ratio (e_{max})	Minimum void ratio (e_{min})
0	1.221	0.738
20	1.326	0.696
30	1.331	0.577
60	1.827	0.655

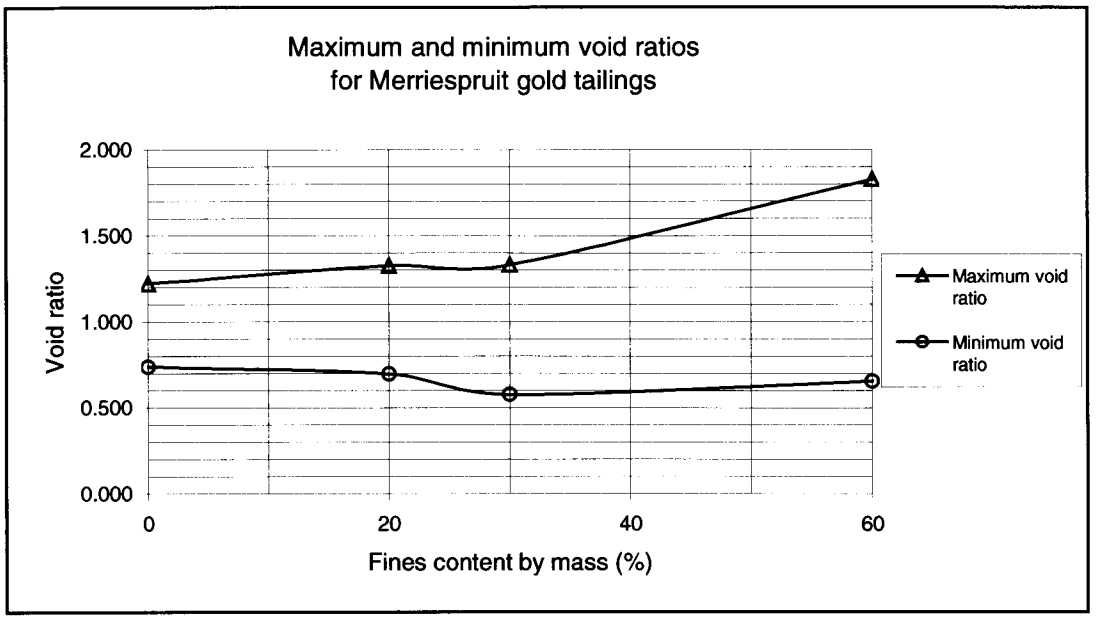


Figure 1.2 Maximum and minimum void ratios for Merriespruit gold tailings

For case 1 tests, triaxial specimens 38 mm x 76 mm and 76 mm x 152 mm were used. Specimens for case 2 tests were 76 mm x 152 mm due to the limitation that only 76 mm diameter K0-rings were available. For case 3 tests, specimens were 38 mm x 76 mm due to the limitation that the equipment for this series of tests (the Bishop-Wesley stress path cell) is designed for this size of specimens.

All triaxial specimens were reconstituted in the laboratory using the same moist tamping technique to aid in the comparison. The moist tamping technique is preferred because of its ability to produce the loosest specimens.

Saturation of specimens was carried out in two stages. First, deaired water was flushed through the specimen using the lowest possible confining pressures to keep the specimen intact and then saturation by back pressure technique, in which an effective confining pressure of 10kPa was maintained, was carried out. This saturation process minimized the loss of void ratio of the specimens because the voids are first filled with water (which is more incompressible compared to air) before application of high pressures to the specimens.

Specimens for case 1 tests were isotropically consolidated whereas specimens for cases 2 and 3 tests were anisotropically consolidated in such a way as to keep their initial lateral dimensions unchanged (K0-condition or one-dimensional consolidation). In all series of tests, specimens were consolidated to cover a wide range of void ratio and effective confining stress states.

All specimens were loaded undrained. Specimens for cases 1 and 2 tests were loaded by increasing the vertical load acting on the specimen, at a constant rate of strain, while keeping the cell confining pressure constant. Specimens for case 3 tests were loaded by reducing the cell confining pressure while keeping either the deviator stress or the effective mean normal stress constant. For the constant deviator stress tests, the rate of strain was constant and for the constant effective mean normal stress tests, the strain rate varied.

1.5 Organization of the Document

Chapter 2 describes the static liquefaction of cohesionless soils based on an extensive literature review that was carried out for the present study.

Chapter 3 gives detailed procedures that were followed for performing the liquefaction tests in this study.

Chapter 4 describes the calculation of various parameters necessary for the interpretation of test results obtained during liquefaction tests in this investigation.

In Chapter 5, the reduced liquefaction test results are presented and discussed with regard to liquefaction phenomena described in chapter 2.

In Chapter 6, the conclusions drawn in the present study and the recommendations for further research are given.

Appendix A contains the calibration procedures, calibration data and calibration curves for the test equipment used for cases 1 and 2 tests.

Appendix B contains the calibration procedures, calibration data and calibration curves for the test equipment used for case 3 tests.

Appendices C, D, and E give the liquefaction test results for each of the triaxial specimens tested in cases 1, 2, and 3 tests, respectively. Also included in Appendix C are the results of monotonic undrained compression triaxial tests performed by Fourie and Papageorgiou (2001) on isotropically consolidated specimens of Merriespruit gold tailings.

2 STATIC LIQUEFACTION OF COHESIONLESS SOILS

2.1 Overview

This chapter is concerned with the behavior of sands, silty-sands, and sandy-silts (i.e. cohesionless soils) under monotonic (static) loading. It reviews the current state of understanding of this behavior based on an extensive literature survey that was carried out in the present study. However, wherever applicable to monotonic loading condition, knowledge gained from studies on cyclic loading conditions will be referred to.

The knowledge gained over the past decades regarding liquefaction phenomena was mainly through laboratory testing of sands in the triaxial apparatus. Due to the complexities attached to laboratory testing (discussed later in this chapter), it is not surprising that throughout the years of research, although agreement was reached on the primary aspects of liquefaction, many conclusions were drawn that are not consistent and in many cases contradictory (as proven by subsequent investigations). Wherever this has been the case on any aspect, this chapter will, in an attempt at sketching the development of knowledge on liquefaction, highlight such observations and outline the current state of knowledge.

2.2 Definition of Liquefaction

Liquefaction has been defined by Castro and Poulos (1977) as follows:

"Liquefaction is a phenomenon wherein a *saturated sand* loses a large percentage of its shear resistance (due to monotonic or to cyclic loading) and *flows* in a manner resembling a liquid until the shear stresses acting on the mass are as low as its *reduced shear resistance*"

In the definition given above, the key words are written in italics and are explained further below:

Saturated: This refers to the state in which a sand has all its voids completely filled with water.

Sand: This refers to all particulate media which have zero cohesion or with a cohesion so small that it does not affect the behavior during loading. These include sands; sandy-silts; silty-sands and silts.

Flow: This refers to the large unilateral shear strains observed during a liquefaction failure. Since one can observe 'flow' features in liquefied masses, these failures have been described as 'flow slides' (Poulos et al. (1985)).

Liquid: The phenomenon of liquefaction derived its name from the fact that a soil mass appears to flow as if it was a liquid.

Reduced shear resistance: This is sometimes referred to as residual shear strength or steady-state shear strength and will be discussed in detail later.

2.3 Requirements for Liquefaction

The following requirements are fundamental to the phenomenon of liquefaction and have throughout the decades of research been accepted and confirmed through extensive laboratory testing of sands.

For liquefaction to occur:

1. The sand must be "loose" (Casagrande (1938); Casagrande (1940); Geuze (1948); Koppejan et al. (1948); Castro (1969); Poulos (1971); Castro (1975); Casagrande (1975); Castro and Poulos (1977); Poulos (1981)).

   This refers to the state of packing of sand particles as expressed by the relative density (Dr) or void ratio (e). Note that void ratio and relative density are interdependent. This condition is necessary but not sufficient for liquefaction. For example, two 'identical' sand specimens at the same void ratio but different

states of stress may behave differently during undrained loading (this is discussed in detail in section 2.7.1).

2. The condition of loading must be undrained.

   This is so that sufficient pore pressure buildup necessary for the reduction of effective stresses within the sand to the residual shear strength can occur. A sand that liquefies in an undrained loading condition may possibly not liquefy under a drained loading condition. However, if the rate of loading is rapid enough, sufficient pore pressures may develop in a drained loading condition to trigger a liquefaction failure (Lindenberg and Koning (1981)). Sladen et al. (1985) showed that up to the point of failure loading may be fully drained.

3. The sand must be fully saturated.

   A saturated soil has all its voids completely filled with water. This is necessary in order for the development of pore pressures required for liquefaction to occur during loading. In a soil that is not fully saturated, the development of pore pressure may be inhibited by the movement of water into the air-filled voids. However, according to Poulos et al. (1985), liquefaction can also occur in very large masses of sands or silts that are dry and loose and loaded so rapidly that the escape of air from the voids is restricted. In this chapter the assumption is that sands are fully saturated with water.

4. The stresses acting on the sand (the driving force) must be sufficiently large.

   According to Kramer and Seed (1988), the shear stress required to initiate liquefaction is equal to the magnitude of the shear stress increment required to mobilize the peak deviator stress during undrained loading. According to Poulos et al. (1985), if the steady-state strength is greater than the driving shear stress, then liquefaction cannot occur because the associated large unidirectional deformations are not possible.

2.4 Static Liquefaction Testing in the Triaxial Equipment

The study of the behavior of saturated sands under monotonic undrained loading is of great importance in understanding the static liquefaction of sands. A considerable amount of research has been done to characterize this behavior. These studies include, amongst many others, (Castro (1969); Castro and Poulos (1977); Begemann et al. (1977); Highter and Tobin (1980); Highter and Vallee (1980); Lindenberg and Koning (1981); Torrey (1981); Dierichs and Forster (1985); Poulos et al. (1985)).

Almost invariably, the studies were conducted in the laboratory as described below:

1. A series of monotonic undrained triaxial compression tests are performed on fully saturated specimens of a sand which are consolidated (usually isotropically) to cover a wide range of initial void ratios (ranging between e_{max} and e_{min}) and confining pressures (covering the normal geotechnical engineering confining pressures).

2. For each specimen:

   - Stress-strain curves are plotted as the observed deviator stress ($q = \sigma_1 - \sigma_3$) and induced pore pressure (Δu) against axial strain (ε).

   - Stress path is plotted as deviator stress ($q = \sigma_1 - \sigma_3$) against effective mean normal stress ($p' = (\sigma'_1 + 2\sigma'_3) / 3$).

3. The steady-state line is drawn as the best-fit line through the points representing void ratio and any effective stress parameter at steady state of deformation (see section 2.5.1 for the definition of steady state of deformation).

2.5 Postulated Observations

Three distinct behaviors of fully saturated sands during monotonic undrained compression loading in the triaxial test were observed since the work of the early pioneers (for example Castro (1969); Castro and Poulos (1977)) as described below:

2.5.1 Contractive (strain-softening) behavior

This behavior is sometimes called liquefaction behavior and is associated with flow slides due to the substantial loss of shear strength resulting from the high build-up of pore pressure within a sand as described below:

In Figures 2.1(a), 2.1(b), and 2.1(c), 'curve a' shows the deviator stress-axial strain, induced pore pressure-axial strain and stress path of a sand specimen undergoing contractive (strain-softening) behavior during monotonic undrained compression triaxial testing.

The specimen's initial state before loading corresponds to zero deviator stress condition due to isotropic consolidation to a confining pressure, $\sigma_{3c} = \sigma_{1c} = p_c'$.

As axial compressive load is increased, the specimen undergoes a rapid linear increase in deviator stress with axial strain and reaches a well-defined peak at relatively small axial strains (about 1 to 2%). During this time, there is a rapid increase in induced pore pressure but it does not reach its peak value. In the stress path, a well-defined peak is evident.

After the peak deviator stress, the specimen undergoes a marked reduction in strength with axial strain (strain-softening) until the stress stabilizes at an ultimate or residual strength at relatively large strain (about 10 to 15%), regardless of strain. The point at which the residual strength is reached corresponds to the point at which the induced pore pressure reaches its peak value. The condition of constant residual strength with additional axial strain is referred to as the steady state of deformation. Poulos (1981) defined the steady state of deformation as follows:

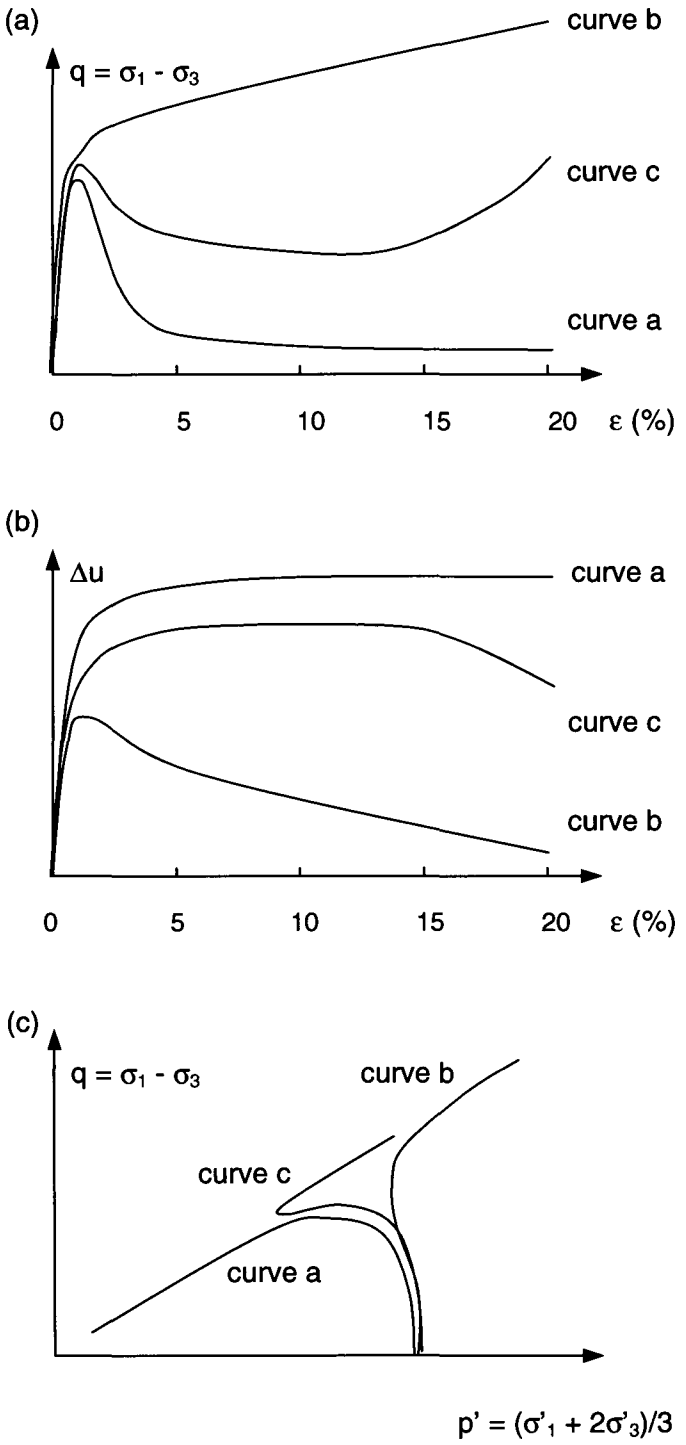


Figure 2.1 Undrained behavior of sands (adopted from Castro (1969)): (a) Deviator stress-axial strain; (b) Induced pore pressure-axial strain; (c) Stress path

"The steady state of deformation for any mass of particles is that state in which the mass is continuously deforming at constant volume, constant normal effective stress, constant shear stress, and constant velocity. The steady state of deformation is achieved only after all particle orientation has reached a statistically steady state condition and after all particle breakage, if any, is complete, so that the shear stress needed to continue deformation and the velocity of deformation remain constant."

According to Poulos (1981), due to the process of deformation, the initial structure of the sand skeleton is completely destroyed and reworked into a new "flow structure" that enables the sand to continue deforming at constant stress, constant volume and constant velocity during steady state of deformation.

Alarcon-Guzman et al. (1988) state that the strain-softening behavior (sudden loss of shear strength) of contractive sands is attributed to the "structural collapse" that occurs at small strains during undrained loading. They state that during straining, there is a sudden rearrangement of grains and loss of contact between neighboring grains resulting in the load being suddenly transferred from the sand skeleton to the water. According to Alarcon-Guzman et al. (1988), this "structural collapse" occurs close to the mobilization of the peak shear strength. The consequence of this is the substantial reduction in shear strength that leads to liquefaction. Contractive sands are said to be strain-sensitive under undrained loading in that very small strains are required to mobilize the peak shear resistance (Poulos et al. (1985)).

The residual strength during the steady state of deformation is called the steady-state strength.

2.5.2 Dilative (strain-hardening) behavior

In Figures 2.1(a), 2.1(b), and 2.1(c), 'curve b' shows the deviator stress-axial strain, induced pore pressure-axial strain and stress path of a sand specimen undergoing dilative (strain-hardening) behavior during monotonic undrained compression triaxial testing.

The specimen's initial state before loading corresponds to a zero deviator stress condition due to isotropic consolidation to a confining pressure, $\sigma_{3c} = \sigma_{1c} = p_c'$.

As axial compressive load is increased, the deviator stress increases and no peak is observed.

In the stress path, there is initially a slight tendency for contraction due to the rapid increase in induced pore pressure at small strains until the pore pressure reaches its peak value at strains of about 1 to 2%. However, dilation soon prevails as a result of the decrease in induced pore pressure and the stress path exhibits a turn around point and approaches the steady-state failure envelope.

2.5.3 Limited liquefaction behavior

This behavior is sometimes called quasi-steady state behavior. In Figures 2.1(a), 2.1(b), and 2.1(c), 'curve c' shows the deviator stress-axial strain, induced pore pressure-axial strain and stress path of a sand specimen undergoing limited liquefaction behavior during monotonic undrained compression triaxial testing.

The specimen exhibits contractive behavior, similar to the one described in section 2.5.1, but the residual strength remains constant over a limited range of axial strain (typically 7 to 15%) after which the specimen gains strength (strain-hardens) as further straining causes a reduction in pore pressure. Accordingly, the stress path shows a peak after which it moves downwards until it reaches the temporary residual strength. The stress path then shows an "elbow" as it moves back along the failure envelope to its ultimate condition.

This type of behavior was initially observed by Castro (1969) and he suggested that sand exhibiting this behavior during undrained loading should be considered to have liquefied because of the potential damage that could result from the large strains associated with this behavior. However, the state of transient minimum strength associated with this behavior cannot be regarded as a steady state of deformation (Vaid et al. (1990)). According to Vaid and Chern (1985), the contractive response of liquefaction and limited liquefaction can be treated within the same framework since

the steady-state line in the void ratio-effective stress space associated with liquefaction-type contractive response also encompasses response of the limited liquefaction-type. In other words, as noted by Castro (1969) and Mohamad and Dobry (1986), the state conditions associated with the residual strength occurring during limited liquefaction behavior lie on or near the steady-state line for a given sand.

2.6 Characterization of Liquefaction Behavior

Previous work has identified a number of lines as being useful in the characterization of static liquefaction of sands. These lines are shown in Figure 2.2 of section 2.7 and described in the following sections.

2.6.1 Steady-state line "F line"

Castro (1969) performed a considerable amount of load-controlled tests on various sands at different void ratios and consolidation stresses. He found that the residual or steady-state strength of a contractive sand was a function of grain characteristics and the void ratio of the sand. This has been supported by many subsequent studies including Castro (1975); Casagrande (1976); Castro and Poulos (1977); and Poulos (1981). Castro (1969) suggested that, for a given sand, the locus of steady-state strengths in a state diagram (a plot of void ratio against any effective stress parameter) defines a unique line referred to as the steady-state line. The line is sometimes called the F line and is defined as the best-fit line of the experimental data showing steady-state conditions (Poulos et al. (1985)). The 'F' is used because the conditions associated with the steady-state strength resemble the flow conditions occurring during the steady state of deformation of a contractive sand as described above. This F line is approximately linear when void ratio is plotted against logarithm of stress.

Several studies (Bishop (1966,1971); Ishihara et al. (1975); Vaid and Chern (1983,1985); Kuerbis et al. (1988); Vaid et al. (1990); Been et al. (1991)) have confirmed that the F line is unique for a sand and is independent of void ratio,

consolidated state of stress before loading as well as mode of loading (compression or extension).

Steady-state lines reported in the literature for moist tamped sand often suffer from considerable scatter (Castro et al. (1982)). This scatter, according to Vaid et al. (1990), could be attributed to sample nonuniformity together with fabric variation at each moist tamped density. Been et al. (1991) emphasized that in order to obtain a unique steady-state line, within the limits of testing procedures, it is important that careful control be maintained on the intrinsic material properties and to ensure that the phase transformation points are not assumed to be the same as the ultimate state. Using this rule, Been et al. (1991) reported that, for the sand they tested, the scatter about the mean steady-state line was about ±0.01 in void ratio at the typical civil engineering stress levels (0-1000kPa).

According to Castro and Poulos (1977) and Poulos et al. (1985), the slope of the F line on a semilog plot is affected mainly by the shape of the grains in a given soil, and its vertical position is affected by even small differences in grain-size distribution.

Poulos et al. (1985) state that the method of specimen preparation has no effect on the position or slope of the steady-state line of a given sand because the initial structure of a sand (which depends on the specimen preparation method) is completely remolded at the steady state of deformation.

2.6.2 Steady-state "large strain" failure envelope

The conditions associated with the steady-state line define a straight line in p'-q space called the "steady-state (large strain) failure envelope" or simply the steady-state failure envelope whose inclination, α_{ss}, is, according to Mohamad and Dobry (1986), given by:

$$\alpha_{ss} = \arctan \{(\sigma_1'_{ss} - \sigma_3'_{ss})/2] / [(\sigma_1'_{ss} + \sigma_3'_{ss})/2]\} \quad (2.1)$$

Where:

$\sigma_1'_{ss}$ and $\sigma_3'_{ss}$ are the effective major and minor principal stresses at steady state of deformation, respectively.

Like the steady-state line, the steady-state failure envelope is defined as the line of best-fit through the points representing steady state of deformation. According to Mohamad and Dobry (1886), the slope of the steady-state failure envelope is independent of void ratio.

Typical values of α_{ss} are 26.5^0 and 29.7^0 for several rounded to subrounded sands and angular tailings, respectively (Mohamad and Dobry (1986).

Effective angle of friction at steady state of deformation

Corresponding to the steady-state failure envelope, the effective angle of friction at steady state of deformation, ϕ'_{ss}, is given, according to Mohamad and Dobry (1986), by:

$$\text{Tan } \alpha_{ss} = \sin \phi'_{ss} \tag{2.2}$$

For each specimen that reaches the steady state of deformation, the effective angle of friction at steady state of deformation, ϕ'_{ss}, is given, according to Poulos et al. (1985), in terms of effective major and minor principal stresses at steady state of deformation, σ'_{1ss} and σ'_{3ss}, respectively, by:

$$\sin \phi'_{ss} = (\sigma'_{1ss}/\sigma'_{3ss} - 1) / (\sigma'_{1ss}/\sigma'_{3ss} + 1) \tag{2.3}$$

Riemer et al. (1990) indicated that during the steady state of deformation, the residual or steady-state effective friction angle (ϕ'_{ss}) is essentially the same for a given sand regardless of the density and effective confining stress level. However, Been et al. (1991), on comparing the values ϕ'_{ss} resulting from each of the tests that reached the steady state of deformation, found that there is a trend of rapidly decreasing ϕ'_{ss} with increasing void ratio, especially at very low stress levels.

Although, they admit that errors in the calculation of ϕ'_{ss} are relatively larger at low stress levels and that these errors could be the reason for the observed rapid decrease in ϕ'_{ss}, they indicate that the best fit line drawn through the steady-state points tends to be heavily weighted towards the higher stress levels due to the fact that the data points near the origin appear to be close to the steady-state line. In other words, this means that the best fit line under consideration is relatively less affected by the data points near the origin (i.e. those corresponding to high void ratios and very low steady-state stress levels) than it is affected by the data points occurring at high stress levels.

Typical values of ϕ'_{ss} are 30^0 and 35^0 for several rounded to subrounded sands and angular tailings, respectively (Mohamad and Dobry (1986).

2.6.3 Critical void ratio line "CVR line or S line"

The critical void ratio line (CVR line or S line) is the residual strength envelope obtained from constant volume drained tests on sands (Roscoe et al. (1958); Casagrande (1975)). According to Lambe and Whitman (1969), the S line is also independent of void ratio of the sand. The inclination of the S line in stress space is the same as that of the steady-state failure envelope obtained from undrained tests for a given sand (Castro (1969); Casagrande (1976)).

The S line is closely analogous to the F line in that they are both associated with continuous deformation at constant stress and constant volume. There seems to have been some uncertainty as to the difference between the steady-state line and the critical void ratio line in the past. For example, Sladen et al. (1985) assumed that the two lines are the same and Been et al. (1991) showed that, for the sands they tested, these lines were the same and independent of stress path, sample preparation method, and initial density. However, many researchers (Poulos (1971); Poulos (1981); Alarcon- Guzman and Leonards (1988); Alarcon-Guzman et al. (1988)) suggested that the lines are not necessarily the same. Alarcon-Guzman and Leonards (1988) showed that the lines are different and concluded that the difference depends upon the brittleness or "collapsiveness" of the sand skeleton which determines whether the load will be transferred from the sand skeleton to the

water by a mechanism of structural collapse or by sand compressibility. The former mechanism tends to move the lines further apart whereas the latter tends to merge them (Alarcon-Guzman et al. (1988)).

2.6.4 Critical stress ratio line "CSR line"

The critical stress ratio line (CSR line) is a line in stress space connecting the peak points of the liquefaction stress paths. According to Alarcon-Guzman et al. (1988) and Kramer and Seed (1988), the CSR line determines the initiation of strain softening behavior in monotonic undrained loading. Sladen et al. (1985) found the CSR line to be an essentially straight line whereas Vaid and Chern (1985b) and Alarcon-Guzman et al. (1988) reported curved CSR lines. Alarcon-Guzman et al. (1988) found that the location of the CSR line depends on void ratio and confining stress. Yamamuro (1993); and Yamamuro and Lade (1997) have shown that the CSR line is unique for a series of undrained compression triaxial tests performed on a sand at varying confining pressures with the same void ratio and it passes through the origin of the stress space. On the other hand, Bishop (1971); Vaid and Chern (1985); Mohamad and Dobry (1986); and Vaid et al. (1990) reported that the CSR line is unique for a sand and independent of void ratio and initial state of stress and that it is a straight line passing through the origin of the stress space. Sladen et al. (1985) reported that the location of the CSR line is also affected by the consolidation stress ratio and the subsequent stress path to failure.

According to Vaid et al. (1990), liquefaction studies using moist tamped specimens have, in general, not revealed a unique CSR line. Vaid et al. (1990) speculated that the sample inhomogeneity and possible fabric differences at each tamped density could be cited as possible reasons for this non-uniqueness.

Been and Jefferies (1985) reported that there is a linear relationship between state parameter and stress ratio at peak shear strength. This means that for a given state parameter, the CSR line is a straight line passing through the origin. This statement has been supported by Alarcon-Guzman (1986).

Effective angle of friction at peak shear resistance

Using equation (2.3), the effective angle of friction corresponding to the peak point of the stress path of a specimen (or the effective angle of friction at peak shear stress (ϕ'_{ps})), is given in terms of effective major and minor principal stresses at peak shear stress, σ'_{1ps} and σ'_{3ps}, respectively, by:

$$\sin \phi'_{ps} = (\sigma'_{1ps}/\sigma'_{3ps} - 1) / (\sigma'_{1ps}/\sigma'_{3ps} + 1) \tag{2.4}$$

Slope of the CSR line

If the CSR line is a straight line passing through the origin of the stress space, then, using equation (2.2), its slope, α_{ps}, is given in terms of the effective angle of friction mobilized at peak shear stress, ϕ_{ps}, by:

$$\text{Tan } \alpha_{ps} = \sin \phi'_{ps} \tag{2.5}$$

2.6.5 Phase transformation line (PT line)

The locus of points defining the "elbows" of the stress paths of a sand undergoing limited liquefaction behavior in monotonic undrained loading triaxial testing defines the Phase Transformation line or PT line (Alarcon-Guzman et al. (1988)). Zhang and Garga (1997) found that the post-PT effective stress paths were essentially located along the same straight line passing through the origin of the stress space. As pointed out above, Vaid and Chern (1985) suggested that the contractive response of liquefaction and limited liquefaction be treated under the same framework. This implies that the PT line and the F line are the same. Vaid et al. (1990) also treated the two lines as being the same. It is important, however, to note that the steady state of deformation which requires a constant stress condition with continued deformation, is only associated with the F line.

2.7 Prediction of Undrained Behavior

2.7.1 The steady-state approach

The steady-state approach provides a convenient framework for predicting the undrained behavior of a sand based on its initial state, in the state diagram, relative to the F line and the S line.

Several studies (Castro (1969); Selig and Chang (1981); Lindenberg and Koning (1981); Been and Jefferies (1985); Ishihara (1985); Sladen et al. (1985); Vaid and Chern (1985b); Mohamad and Dobry (1986); Alarcon-Guzman (1986); Alarcon-Guzman et al. (1988)) suggested that there are three regions in the state diagram that govern the undrained behavior of saturated sands. The three regions are separated by the steady-state line (F line) obtained from undrained tests and the critical void ratio line (CVR line or S line) obtained from drained tests into Strain Softening Region, Transition Region, and Strain Hardening Region. As shown in Figure 2.2(a), Strain Softening Region is above and to the right of the CVR line; Transition Region is the shaded region between the F line and the CVR line; and Strain Hardening Region is below and to the left of the shaded region.

The relationship between the initial state of a sand and the resulting behavior during monotonic undrained loading is illustrated, in Figure 2.2, by considering the behavior of three sand specimens (designated a, b, and c) with the same void ratio but at different levels of effective mean normal stress ($p' = (\sigma'_1 + 2\sigma'_3)/3$) placing them within Strain Softening, Transition, and Strain Hardening Regions, respectively in the state diagram (Figure 2.2(a)). In Figure 2.2(a), the initial states of the specimens are shown by open circles and their ultimate states are shown by solid circles. Accordingly, the undrained behavior of the specimen whose initial state is within the Strain Softening Region will be contractive; the specimen located in the Transition Region exhibits limited liquefaction behavior; and the specimen whose initial state places it within Strain Hardening Region dilates (strain-hardens) during undrained loading (see Figure 2.2(b)).

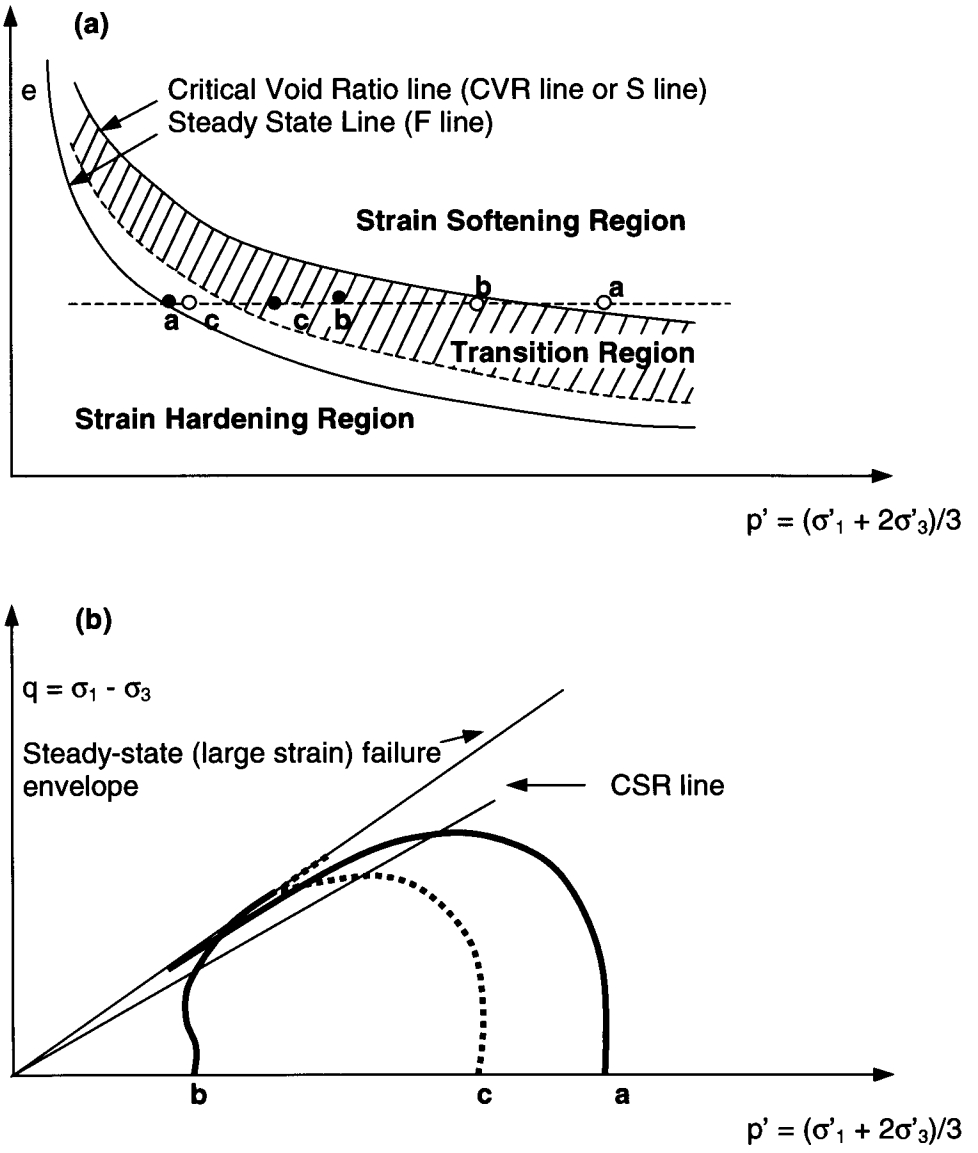


Figure 2.2 Relationship between initial state of sand and undrained behavior:
(a) State diagram; (b) Stress path plot

2.7.2 State parameter

It can be seen from the state diagram, Figure 2.2(a), that the requirement that a sand must be "loose" in order for it to liquefy during undrained loading refers to a state which is defined by both its void ratio and its effective stress level and not by its void ratio alone. For example, sand A with a void ratio lower than that of sand B is considered to be "looser" than sand B if the stress levels of these sands are such

that the initial state of sand A is above and to the right of the CVR line while that of sand B is below and to the left of the steady-state line so that the behavior of sands A and B during undrained loading will be contractive and dilative, respectively. Similarly, sand A is considered to be "looser" than sand B while both sands have the same void ratio, if their stress levels are such that the initial state of sand A in the state diagram is above and to the right of the CVR line while that of sand B is below and to the left of the steady-state line. Been and Jefferies (1985) proposed the use of a single parameter, the state parameter, to combine the effects of void ratio and effective stress level with reference to the steady state to describe sand behavior. The state parameter is defined, as shown in Figure 2.3, as the void ratio difference between the initial state and the steady state conditions at the same effective stress. Accordingly, positive state parameters correspond to states above the steady-state line whereas negative state parameters represent states below the steady-state line.

Been and Jefferies showed that sand behavior bears a strong relationship to the state parameter. For example, Been and Jefferies (1985) reported a linear relationship between state parameter and the mobilized angle of shear resistance at peak strength, ϕ'_{ps}, so that for a given state parameter, the CSR line is a straight line passing through the origin.

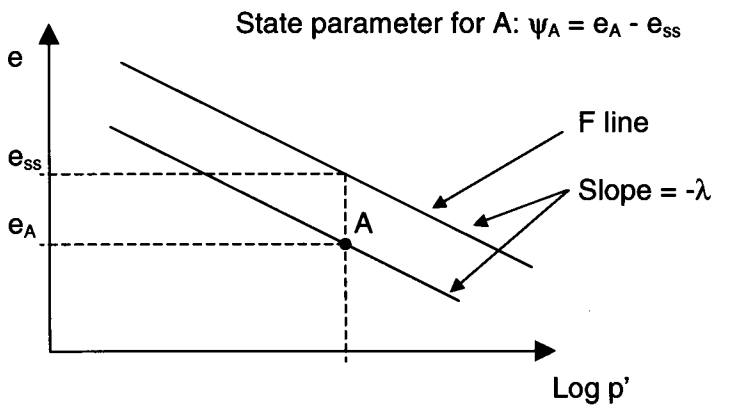


Figure 2.3 Definition of state parameter (simplified version of Been and Jefferies (1985)).

In their definition of state parameter, however, Been and Jefferies (1985) did not consider the influence of anisotropic fabric but assumed that the effect of anisotropic fabric at large strains is small.

2.8 Liquefaction Potential of Sand

Casagrande (1976) suggested the use of liquefaction potential, L_p, as a measure of the contractiveness of a sand as follows:

$$L_p = (\sigma'_{3c} - \sigma'_{3ss}) / \sigma'_{3ss} \qquad (2.6)$$

Where:

σ'_{3c} = Effective minor principal stress after consolidation;

σ'_{3ss} = Effective minor principal stress at steady state of deformation.

This definition implies that liquefaction susceptibility increases with increase in effective minor principal stress after consolidation, σ'_{3c}, for a given void ratio after consolidation.

This definition relates the stress condition after consolidation to the condition at steady state of deformation without consideration of the maximum shear resistance that has to be overcome first before the steady state of deformation can be reached. Considering that the maximum shear strength during undrained loading of sands with the same void ratio increases with increase in effective minor principal stress (Kramer and Seed (1988)) and that they achieve the same steady-state strength (Castro (1969)), it appears that the liquefaction potential defined above refers to the magnitude of the reduction in shear strength associated with a liquefaction failure and not the ease with which such a failure could be brought about.

2.9 Liquefaction Resistance of Sand

Kramer and Seed (1988) defined liquefaction resistance as the magnitude of the shear stress difference required to initiate liquefaction. This definition is consistent

with the fact that the maximum resistance of a sand has to be overcome first before the reduction in shear strength leading to liquefaction failure can occur.

According to Kramer and Seed (1988) and Konrad (1990), the peak deviator stress required to trigger strain-softening behavior increases with decreasing void ratio.

2.10 Initiation of Liquefaction

Liquefaction has been described as the process of a reduction of shear strength due to a substantial increase in pore pressure due to undrained loading. A sand is said to have liquefied only when such a process has reached its ultimate stage, i.e. when no further reduction in shear strength occurs with increase in axial strain. At this stage the sand is said to have reached the steady state of deformation and the constant shear strength is called the steady-state shear strength (Castro (1969); Castro and Poulos (1977); Poulos (1981)). The steady-state concept is only concerned with the state of a sand during the steady state of deformation and the factors affecting conditions during the steady state of deformation, mainly the void ratio of the sand, and as much as the steady-state concept initially postulated that the steady-state strength is solely a function of void ratio of a sand without considering the effect that other factors (such as those described in section 2.11) have on the steady-state strength, it also does not specify the initiation of liquefaction.

More recently, research has been done on stress conditions prevailing prior to the initiation of liquefaction. Kramer and Seed (1988); Alarcon-Guzman et al. (1988); and Vaid et al. (1990) considered the initiation of liquefaction to correspond to the point during undrained loading at which the peak deviator stress is reached. Alarcon-Guzman et al. (1988) indicated that the mobilized angle of shear resistance at the initiation of strain softening, ϕ'_{ps}, depends on the void ratio and the level of confining stress. Alarcon-Guzman (1986) and Alarcon-Guzman et al. (1988) found that shortly before the peak strength is mobilized, there was an increase in the rate of pore pressure buildup indicated by the change in curvature of the pore pressure versus time plot.

According to Kramer and Seed (1988), initiation of liquefaction is typically observed at very small strains and is characterized by a rapid increase in strain rate and increase in pore pressure to a constant value.

Alarcon-Guzman et al. (1988), using undrained monotonic torsional shear tests, suggested that during undrained shearing, collapse of the structure results in the load being suddenly transmitted from the sand skeleton to the water, thereby producing a sharp increase in pore water pressure. Accordingly, a "kink" was observed in pore pressure response. Konrad (1990) also observed the "kink" on his very loose well-rounded sands (tested by stress controlled CIU). He suggested that this kink may not always be clearly identifiable in CIU tests.

2.11 Factors Affecting Liquefaction Behavior of Sands

It may be noted from the previous sections that the steady-state approach postulates that the steady-state strength is a function solely of the void ratio of a sand (for example, Castro (1969); Poulos et al. (1985)). However, a huge amount of laboratory tests have suggested that the steady-state strength is affected by many other factors. Other factors known to affect cyclic liquefaction resistance include grain angularity, overconsolidation ratio, previous strain history, length of time under sustained pressure, and grain structure or fabric. The influence of these parameters on cyclic liquefaction resistance was summarized by Seed (1976). It seems reasonable to believe that these parameters will also affect the static liquefaction resistance of a sand to some degree.

In the following sections, the influences of some of the factors postulated to affect the steady-state strength measured in the laboratory are reviewed based on the evidence published in the literature. It may be noted, however, that inconsistency regarding the effects of these factors prevails and special attention is particularly drawn to anisotropic consolidation since this is the factor that the test program in the present study investigated. The factors are grouped under the following categories: Soil property; Test procedures and Stress conditions.

2.11.1 Soil property

Void ratio

Void ratio is a soil parameter that represents the state of packing of the particles of a soil. The state of packing of the soil particles is sometimes expressed in terms of relative density.

The void ratio of sand has since the beginning of research on liquefaction of sands been identified and shown to be the fundamental factor affecting the behavior of sands under undrained loading (for example, Castro (1969); Castro and Poulos (1977); Poulos et al. (1985)). All else being equal, small changes in void ratio can lead to rather large variations in the steady state strength as indicated by the slope of the steady-state line in the state diagram. Moreover, such changes in void ratio can sometimes alter the undrained behavior of sand, for example, from contractive to dilative.

With regard to liquefaction resistance of a sand, Kramer and Seed (1988) indicated that, within the range of void ratios constituting liquefaction and limited liquefaction behavior under a given isotropic consolidation stress level, the higher the consolidated void ratio, the lower the peak deviator stress achieved during undrained loading. This means that the liquefaction resistance of a sand specimen decreases with an increase in void ratio or a decrease in relative density.

Konrad (1990) indicated that the stress-strain and pore pressure behavior are dependent upon the void ratio after consolidation for specimens with the same consolidation pressure. However, Konrad (1990) observed that steady-state strength was not uniquely defined by void ratio.

Particle gradation

Physical characteristics of sands, such as grain size, shape, mineralogy, and gradation, have all been suggested to influence the cyclic liquefaction resistance of sands. However, the effect of gradation alone had not been dealt with in isolation

until the work of Vaid et al. (1990). In order to isolate the effect of gradation (or coefficient of uniformity) alone, Vaid et al. (1990) tested three sands with identical mean grain size, D_{50}, linear grain size distribution curves and identical mineralogy. Vaid et al. (1990) found that at high void ratios, poorly graded sand had a lower *cyclic* strength than the well-graded sands at the same void ratio. The opposite trend was observed at lower void ratios. Although these observations were made from cyclic tests, it seems reasonable to suspect that gradation will have some effect on the monotonic loading case.

According to Castro and Poulos (1977); Poulos et al. (1985); and Castro et al. (1982), the vertical position of the steady-state line is affected by even small differences in grain-size distribution. However, Pitman et al. (1994) observed that the collapse behavior of the sand they tested did not differ with variation in gradation.

Fines content

The fines content of a soil sample usually refers to the percentage of dry mass of the total sample that passes the 75 μm sieve.

Although the percent fines alone is not an adequate criterion to distinguish deposits susceptible to liquefaction from those that are not (Koester and Tsuchida (1998)), it appears that the addition of fines to a sand effectively changes the sand into a completely different sand (Lade and Yamamuro (1997)) with potentially different liquefaction characteristics. The following paragraphs outline some of the observations made by researchers regarding the effect of fines on liquefaction characteristics of sands.

Dobry et al. (1985) indicated that the steady-state lines obtained from cyclic and monotonic tests were different for specimens of the same sand having different fines content, whereas the steady-state strength envelope was the same for these sands. Been and Jefferies (1985) conducted load-controlled and strain-controlled tests on sand specimens containing 0%, 2%, 5%, and 10% fines and found that the slope of the steady-state line increases with increasing fines content.

Kuerbis et al. (1988) found that the addition of fines decreases the liquefaction potential of a sand.

Kuerbis and Vaid (1989) found that the addition of fines up to 20% did not affect the skeletal void ratio (the void ratio of the base gradation without the fines included) as the fines would occupy the void spaces and not contribute to the undrained behavior. According to Kuerbis and Vaid (1989) the skeletal void ratio is given by:

$$e_S = (V_T G_S \rho_w) / (M_t - M_f) - 1 \qquad (2.7)$$

Where:
e_S is the skeletal void ratio, V_T is total volume of specimen (cm^3), G_S is specific gravity of sand, ρ_w is density of water (g/cm^3), M_t is total mass of solids (g), and M_f is mass of fines in sample (g).

Pitman et al. (1994) found that the strain-softening behavior of the sand they tested decreased with increase in fines content up to 20% fines and as the fines content was increased beyond 20%, the undrained behavior was only dilative. They concluded that the 20% fines content marks the transition between a sand dominated by sand grain to sand grain contact and one dominated more by the fines matrix. A similar conclusion was drawn by Hird and Hassona (1986), who found that the strain-softening behavior of the sand they tested progressively decreased with fines content up to 30% fines and beyond this mark, the sand behavior was governed by fines.

Pitman et al. (1994) found that the location of the steady-state line changes with changes in fines content. Also observed by Pitman et al. (1994) was that the effective angles of friction at peak shear stress and at steady-state were essentially the same regardless of fines content

Lade and Yamamuro (1997) concluded that increasing fines content increases the liquefaction potential of a sand.

Anisotropic consolidation and sand fabric

Fabric is the term used to describe the arrangement of sand grains on a particulate scale (Been et al. (1991)). It describes particle contacts, their orientations and distribution, and cementation at contacts, if any. Anisotropy is a condition in a sand in which there will be unequal particle contacts and forces between particles in different directions (Oda (1981); Been et al. (1991)).

There are two types of anisotropy, namely, inherent and induced anisotropy. The first type is due to the process of deposition whereas the latter is due to strain associated with an applied stress (Wong and Arthur (1985)). It is the latter type that is of interest in the present investigation.

Although void ratio is often used to describe the state of packing of soils, it is incapable of characterizing the directional nature of fabric. Masad and Muhunthan (2000) studied the three dimensional anisotropic fabric of soils using computer modelling and concluded that the specimens had more voids in the horizontal direction than in the vertical one and the voids in the horizontal direction are larger than those in the vertical direction.

It has been shown by, amongst many others, Oda (1972b), that the directional distribution of particle contact tangents alters radically during strain (induced anisotropy) resulting in a gain in particle contacts with normals parallel to the major principal stress direction and a loss in particle contacts with normals parallel to the direction of the minor principal stress. According to Wong and Arthur (1985) this distribution of contacts determines the stress-strain behavior leading to failure during undrained loading. Wong and Arthur (1985) showed that small permanent shear strain of the order of 0.5% leads to significant induced anisotropy which can cause large directional variations in stiffness of sand and associated capability for pore water pressure generation.

Middlebrooks (1942) and Seed et al. (1977) noted with respect to monotonic and cyclic loading conditions, respectively, that the liquefaction characteristics of a sand are influenced by the strain history to which it has been subjected and concluded

that the liquefaction characteristics of a sand cannot be reliably determined in the laboratory tests on specimens prepared to the same void ratio as those in the field if the structure is not the same as that in the field. Mulilis et al. (1975) showed that the same sand could have the same relative density but different structures, resulting in different liquefaction characteristics. Seed et al. (1977) suggested that in order to closely approximate the liquefaction characteristics of a sand in the laboratory, it is important to conduct tests on specimens having the same void ratio, structure and K0 consolidation value existing insitu. Although the use of undisturbed samples for laboratory tests would very closely approximate the insitu fabric, reconstituted specimens are often preferred, due to the extreme difficulty of extracting undisturbed samples of cohesionless soils.

Anisotropy has been postulated to cause large differences in steady-state lines obtained in extension and compression tests (Kuirbis et al. (1988) and Vaid et al. (1990)). This is a direct consequence of anisotropic deformation properties due to anisotropic sand fabric (Vaid et al. (1990)). According to Symes et al. (1984), this fabric causes changes in the undrained deformation-strength characteristics with the direction of loading. Vaid et al. (1990) has shown that during virgin isotropic consolidation of these specimens, radial strains are larger than the axial strains and that the difference increases as the void ratio increases.

Seed and Lee tested anisotropically consolidated sands to simulate insitu conditions (Seed and Lee (1966,1969); Lee and Seed (1967); Seed et al. (1975); Lee et al. (1975); and Seed (1983)) and concluded that the cyclic liquefaction resistance increases due to anisotropic consolidation. Vaid and Chern (1983a, 1983b) showed that cyclic strength can either increase or decrease with anisotropic consolidation. On the other hand, Castro and his co-workers concluded that anisotropic consolidation reduces the seismic liquefaction resistance of sands, which is completely the opposite of the findings by Seed and Lee (1966,1969).

With regard to monotonic undrained loading, it is commonly assumed (Castro (1969); Casagrande (1976); Poulos (1981); Castro et al. (1985); Poulos et al. (1985)) that the strength at steady state of deformation, and hence the steady-state line, is unique and that the characteristics of the flow structure developed at steady state of

deformation are dependent on void ratio only and independent of initial sand fabric since, according to the definition of steady state of deformation (Poulos (1981)), the initial fabric is completely destroyed and remolded into a new 'flow structure'. Moreover, according to Castro (1975), the steady-state strength is the same for isotropically- and anisotropically consolidated sand specimens if their void ratios after consolidation are the same.

Alarcon-Guzman et al. (1988) speculated that the initial anisotropy could possibly affect the static liquefaction characteristics of a sand because the pore pressure response during undrained loading depends on the initial fabric, as shown by different liquefaction characteristics observed for different specimen preparation methods (see section 2.11.2, below).

Konrad (1990) performed undrained tests on sand specimens with different overconsolidation ratios and found that the ratio of peak deviator stress to effective confining pressure of normally consolidated specimens were lower than those of overconsolidated specimens and that amongst the overconsolidated specimens, the higher the overconsolidation ratio, the higher the ratio of peak deviator stress to effective confining pressure.

The uncertainty as to the effect of anisotropic consolidation on static liquefaction behavior of sands seems to prevail to date.

2.11.2 Test procedures

Specimen preparation method

Although the steady-state line for a sand is normally determined in the laboratory by compression tests on samples reconstituted by the moist tamping technique (Vaid et al. (1990)), several other methods of reconstitution of sand specimens for triaxial testing have been used. The effectiveness of any method of reconstitution is based on its ability to produce homogeneous (uniform) specimens and to replicate precisely several homogeneous specimens at a desired void ratio (relative density) to facilitate comparable results. Although direct quantification of fabric is not

practical, there is evidence (e.g. Oda (1972)) that fabric resulting from different preparation methods is different. The following sub-sections summarize the published observations with regard to initial density, homogeneity and repeatability of initial density, and influence on liquefaction characteristics of some of the commonly used specimen preparation methods. The details of each specimen preparation method are not given.

Initial density: According to Konrad (1990), the moist tamping technique is the only method that produces relatively high void ratios in the laboratory. Consequently, moist tamped sand samples are contractive in compression over a wide range of void ratios (Castro et al. (1982)).

Been et al. (1991) found that, for the sand they tested, it was difficult to prepare pluviated specimens at void ratios above the steady-state line (i.e. very loose specimens), consequently all the pluviated specimens in their study could only reach the steady-state line by dilation.

Mulilis et al. (1977) showed that the electrical conductivity (measured in the direction of loading) of a sand sample decreases with increase in density of the sand. By comparing the conductivities of samples prepared to the same density by dry pluviation; moist tamping; horizontal high frequency vibrations on dry sample; and horizontal high frequency vibrations on moist sample, Mulilis et al. (1977) found that the moist vibrated samples were the least conductive (or densest) followed by the moist tamped, while the dry pluviated were the most conductive (or loosest).

Homogeneity and repeatability of initial density: Although it is difficult to ensure a uniform density distribution in reconstituted laboratory specimens of sand (Gilbert and Marcuson (1988)), studies in which the uniformity of void ratio over the height of the specimens was assessed (Castro (1969); Mulilis et al. (1977); Castro et al (1982)) indicated that water-pluviated specimens tend to be relatively more uniform than specimens prepared using compaction techniques, such as moist tamping. However, Vaid and Negussey (1988) emphasized that if the fines content of the specimen is significant, pluviation methods may produce nonhomogeneous specimens due to segregation.

Studies in which the microstructure of sands was assessed using digital image processing and analysis based techniques (for example, Jang and Frost (1998)) indicate that whereas pluviation through air or water causes segregation of the graded sands, the slurry deposition method results not only in homogeneous and uniform specimens (Kuerbis and Vaid (1988)), but also simulates closely fluvial and hydraulic fill-deposition processes. According to Vaid et al (1990), the slurry deposition method yields homogeneous and uniform specimens that closely simulate fluvial and hydraulic fill-deposition processes.

X-ray radiographs were used to assess the uniformity of moist tamped specimens (Geotechnical Engineers Inc. (1982)) and revealed that thin horizontal looser zones occur between layers and that denser specimens are generally more uniform. However, measurements of average void ratio in five layers of two specimens led to the conclusion that the uniformity was about ± 0.011 in void ratio.

By quantifying the structure resulting from air-pluviation and moist tamping specimen preparation methods, Jang and Frost (1998) found that the standard deviations of the void ratio distribution of specimens prepared by air-pluviation are relatively stable and consistently lower than those of specimens prepared by moist tamping implying that moist-tamped specimens are less uniform than air-pluviated specimens.

Mulilis et al. (1977) investigated the density distribution within sand specimens prepared by pluviation of dry sand through air; high frequency vibrations applied horizontally to dry samples formed in layers; and moist tamping in layers and concluded that the pluviated sample contains continuously alternating thin layers of loose and dense material; the vibrated sample is composed of relatively uniform layers, each separated by a thin denser layer; and the moist tamped sample is the most nonuniform, each layer grading from loose to denser condition and it contains the largest amount of looser material.

Moist tamping technique has been used by many researchers studying the behavior of soils containing fines and found to produce fairly uniform specimens (Dobry et al. (1985); Baziar (1987, 1991); Koester (1992)). Ladd (1978) suggested that a modification of moist tamping using undercompaction would result in fairly uniform

samples. This technique was used by Vucetic and Dobry (1988) on silty-sands and they concluded that it yielded uniform reconstituted specimens.

Castro (1969) showed that the degree of nonuniformity tends to increase with average density of the reconstituted specimen.

Vaid and Negussey (1988) reported excellent repeatability of initial density (void ratio) using water pluviation technique.

Influence on liquefaction characteristics: Ladd (1974) suggested that different methods of reconstitution to the same density produce specimens with different structures and different liquefaction characteristics. Ladd (1977) studied the cyclic liquefaction characteristics of sand specimens prepared by different methods and concluded that the method of preparation affected the fabric, strain-development characteristics and consequently the liquefaction characteristics of the sands.

Mulilis et al. (1977) assessed the orientation of interparticle contact planes for samples prepared by pluviation of dry sand through air; high frequency vibrations applied horizontally to dry samples formed in layers; and moist tamping in layers and found that of these three sample preparation methods under consideration, the moist tamped samples had the highest distribution of normals to interparticle contact planes in the vertical direction (i.e., parallel to the loading axis) and samples prepared by dry pluvial compaction had the lowest distribution of normals to interparticle contact planes in the vertical direction. Comparing the cyclic strength results of samples prepared by the methods mentioned above and consolidated to the same void ratio and stress level, Mulilis et al. (1977) found that the cyclic strength increases as the distribution of normals to interparticle contact planes in the loading direction increases.

A similar correlation between the distribution of normals to interparticle contact planes in the loading direction and sample strength was obtained by Oda (1972) in performing static drained triaxial tests on samples of sand compacted to the same density by different methods of preparation. It seems reasonable to expect that a similar correlation exists for the static undrained loading conditions.

A comparison between cyclic strengths of undisturbed samples with those of remolded samples for various sands prepared using different methods of sample preparation (Mulilis et al. (1977)) revealed that samples prepared in this order: moist vibrated; moist tamped; dry vibrated; and dry rodded exhibited progressively lower cyclic strengths compared to their undisturbed companions. More importantly, Mulilis et al. (1977) concluded that the liquefaction characteristics of samples prepared by moist vibration and by moist tamping would be most similar to the liquefaction characteristics of undisturbed samples.

Been et al. (1991) found that for the sand used in their study, there was no difference in steady-state lines resulting from moist tamping and water pluviation methods of specimen preparation. Poulos et al. (1985) also drew the same conclusion.

Dennis (1988) concluded that, under stress-controlled loading, the slope of the steady-state line is not affected by the specimen preparation method whereas under strain controlled loading, specimens prepared by equal-volume moist tamping method exhibit higher steady-state strengths than those prepared using the equal-energy moist tamping method, all else being equal. Consequently the slopes of the steady-state lines are different. Another indication of differences in strength is the potential volume change of the specimens. According to Dennis (1988), the equal-volume moist tamping method produces specimens that are more resistant to volume change than the specimens prepared using the equal-energy moist tamping method.

DeGregorio (1990) concluded that the position of the steady-state line varied with sample preparation method (he used dry pluviation, moist tamping and moist vibration methods). He observed that samples prepared by dry pluviation, moist tamping, and moist vibration, in this order, exhibited progressively higher peak and steady-state strengths when sheared with a load-control device and that dry pluviated specimens exhibited greater peak pore-water pressure response than specimens prepared by either moist methods.

Although water pluviation method would produce specimens which would closely approximate the sand fabric similar to that produced by hydraulic fills (Oda et al

(1978)), pluviation methods of sample preparation were not used in the present study because of the postulated difficulty in achieving a "target void ratio" when using these techniques (Amini and Qi (2000)). Instead, the moist tamping specimen preparation method was used because of its ability to construct much looser specimens than the water pluviation technique (Kuerbis (1989)) and the greater control over the target void ratio. Another important reason that moist tamping was chosen for the present study is to yield comparable results with those obtained by Fourie and Papageorgiou (2001) who also used the moist tamping method of specimen preparation in their study on the same tailings.

End restraint

Friction at the ends of a triaxial specimen retards the development of lateral strains, especially, near the ends (Taylor (1941); Bishop and Henkel (1957, 1962). This results in the barreling type of deformation commonly observed in undrained triaxial tests (Lee (1978)).

Rowe (1962) was apparently the first to use a combination of rubber sheeting and silicone grease to develop "frictionless" ends for triaxial specimens. This frictionless system provides the basis for evaluating the effect of end friction on the undrained strength of sands.

Several investigators, for example (Barden and McDermott (1965); Bishop and Green (1965); Duncan and Dunlop (1968); Lee (1978)), have shown that the use of grease-rubber system eliminates the end restraint effects by producing uniform lateral strains throughout the entire height of the specimens. Roy and Lo (1971) observed that particle crushing was uniformly distributed in tests with lubricated ends whereas in the case of regular ends, particle crushing occurred largely in the central portion of the specimen and concluded that this indicates that the shear distortion is uniformly distributed in specimens with lubricated ends whereas it is larger in the center of the specimen than at the ends for specimens with regular ends. Zhang and Garga (1997) concluded that the use of lubricated ends can significantly reduce the end restraint in dense specimens, while the lubrication effect becomes small in loose specimens.

Lee (1978) showed that in undrained tests, the use of frictionless ends leads to less volume decrease, lower pore pressure build-up and higher undrained strength. Lee (1978) indicated that the effect of using lubricated ends could lead to an increase in undrained strength of about 20% of that obtained when using regular ends. A totally opposite observation was made by Zhang and Garga (1997) who found that tests that used lubricated end platens showed lower deviator stress and higher pore pressure than tests that used regular end platens.

The disadvantage of using "frictionless" ends is the difficulty of setting up specimens under such conditions and the tendency of specimens to slide laterally off one side of the platen during testing (Lee (1978)). Duncan and Dunlop (1968) concluded that the benefits in the use of lubricated ends as opposed to regular ends are outweighed by the difficulty of setting up such tests.

Lee (1978) maintained that reliable results can be obtained with soil specimens having regular ends provided the ratio of the length to the diameter is in the range 1.5 and 3.0. A ratio of the length to the diameter of 2.0 has generally been accepted as a standard for triaxial compression tests (Bishop and Henkel (1957, 1962); Lee (1978)).

For the present study, regular ends were used because it was envisioned that these would not affect the results since all specimens were very loose and the ratio of the length to the diameter was about 2.0. The use of regular ends was also to avoid the difficulty of using lubricated ends.

Method of loading

Two methods have been used for loading specimens in the triaxal test, namely, strain-controlled and load-controlled methods. The strain-controlled method of loading uses a gear-driven press operating at a constant velocity or constant rate of strain and specimens are usually loaded until a strain in excess of 25% is attained, or until the specimen evidences strong dilation and the applied force approaches the safe limit of the load cell. For the stress-controlled loading, specimens are step loaded at time intervals by initially increasing the applied force at a given increment

of the expected failure load and as specimens approach failure, the loading increment is reduced. Specimens loaded in this manner typically reach peak strength in 14-16 minutes with subsequent failure occurring in less than two tenths of a second (Dennis (1988)).

Several studies, for example, Castro et al. (1982); Sladen et al. (1985); Dennis (1988); Konrad (1990); DeGregorio (1990); Been et al. (1991), investigated the effect of method of loading (strain- versus stress- controlled) on undrained behavior of sands.

Castro et al. (1982); Sladen et al. (1985); and Dennis (1988) found that the stress-strain responses are similar for both types of loading, although due to the rapidity of failure, it is not easy to collect the post-peak data for the stress-controlled tests. Konrad (1990) concluded that stress-controlled loading does not always yield an accurate value of peak deviator stress and that constant rate of loading yields sharp peaks. Consequently, Poulos et al. (1985) recommended the use of strain-controlled triaxial tests for the determination of steady-state line.

According to Dennis (1988), strain-controlled loading yields similar steady-state strengths amongst specimens tested at the same void ratio due to the length of time period of loading allowing redistribution of void ratio within the test specimens whereas stress-controlled loading may result in significantly different steady-state strengths for specimens tested at the same void ratio. Due to the rapidity of failure (in load-controlled tests) not allowing the redistribution of void ratio to occur, the zone of failure may be at a void ratio significantly different than that at which the specimen was prepared, therefore the strength measured using stress-controlled loading tend to reflect the strength of the localized zones of loose material within the specimen (Dennis (1988)).

Dennis (1988) concluded that, at a given void ratio, specimens tested using strain-controlled loading have significantly higher strengths than those tested using stress-controlled loading and that under the same confining pressure, liquefaction could be achieved at much lower void ratios for stress-controlled loading than for strain-controlled loading.

Been et al. (1991) found that there was no significant difference in the steady-state lines obtained from stress-controlled and strain-controlled tests, however, they emphasized that this may not be the case for finer, silty-sand. A similar conclusion was drawn by Poulos et al. (1988).

According to Konrad (1990), the deviator stress at steady state of deformation is not affected by the mode of loading. Poulos et al. (1988) showed that the method of loading had no effect on the undrained behavior of Syncrude tailings. However, Hird and Hassona (1990) reported a consistent difference between load-controlled and strain-controlled tests for Leighton Buzzard sand.

DeGregorio (1990) concluded that the relative position of the steady-state line was not affected by the type of loading and that the effective angle of friction at steady state for load-controlled tests were not identical. He noted that the same peak pore-water pressure was achieved by both modes of loading.

2.11.3 Stress conditions

Effect of confining pressure

The effect of confining pressure on the undrained behavior of sands has been studied by performing monotonic undrained compression triaxial tests on specimens consolidated isotropically to various confining pressures but at the same void ratio or relative density (Sladen et al. (1985); Kramer and Seed (1988); Alarcon-Guzman et al. (1988); Konrad (1990)). A consistent finding of these studies was that the peak deviator stress achieved during undrained loading increases as the confining pressure is increased. This means, according to Kramer and Seed (1988), that the liquefaction resistance of a sand specimen increases with an increase in confining pressure. Kramer and Seed (1988) found that the peak deviator stress achieved during undrained loading increases nearly proportionally with the increase in confining pressure.

Kramer and Seed (1988) found that, for a constant void ratio, the residual deviator stress was the same regardless of confining pressure in the range (100–500kPa)

whereas Konrad (1990) observed that different confining stresses resulted in different residual deviator stresses.

Effect of initial shear stress

The effect of initial shear stress on the deviator stress required to mobilize the peak shear resistance during undrained loading was assessed by many researchers (Bjerrum et al. (1961); Castro (1969); Castro and Poulos (1977); Castro et al. (1985); Poulos et al. (1985); Alarcon-Guzman et al. (1988); Kramer and Seed (1988)) and all of them noted that the increase in deviator stress from the initial state to the peak deviator stress state decreases with an increase in the initial shear stress. This means, according to the definition of liquefaction resistance given by Kramer and Seed (1988), that the higher the initial shear stress the lower the liquefaction resistance of a sand.

Castro and Poulos (1977); Castro et al. (1982); Castro et al. (1985); and Alarcon-Guzman et al. (1988) indicate that if the insitu static shear stress is larger than the steady-state strength, relatively small increments in undrained shear will be sufficient to trigger the initiation of a flow failure, which under stress-controlled conditions (such as close to the face of a sloping ground) will have catastrophic consequences.

2.12 Potential Errors in the Triaxial Test

2.12.1 Void ratio

In the evaluation of the susceptibility of sand to liquefaction failure, the steady-state line is drawn using void ratio and corresponding steady-state effective stress parameter measured in the laboratory . The void ratio used is a global void ratio obtained from the initial dimensions of the soil and the volume changes undergone by the specimen from its preparation until the end of consolidation.

However, Shi and Winslow (1991); Desrues et al. (1996); Kuo and Frost (1996); and Frost and Jang (2000) have shown, using digital image processing and analysis based techniques, that from a microstructural point of view, the void ratio of a sand

varies widely within the specimen. Such variations in void ratios within a sand specimen could possibly lead to misleading interpretation of sand behavior, for example, the loosest portion within a sand specimen could account for the observed soil behavior while such a loose state is not taken into account in the global void ratio determination. Therefore, the microscopic nonuniformities in void ratio within the specimen could account for differences observed in steady-state conditions for specimens of the same sand loaded from the same initial global void ratio.

Gilbert and Marcuson (1988) froze completely saturated sand specimens at various void ratios and loaded to various strain levels, dissected them into numerous small elements, and determined the density of each element and hence the density distribution of each specimen. Additionally, control specimens were used to determine initial uniformity. In their study, Gilbert and Marcuson (1988) used both water pluviated and moist tamped specimens. After monotonic undrained loading, Gilbert and Marcuson (1988) found that although the density distribution within a specimen was random in the vertical direction, there was a marked variation in density distribution in the horizontal direction, with the density lower close to the center than at the peripherals. Gilbert and Marcuson (1988) also found that the uniformity of density within the specimen reduced during loading and appeared to increase with axial strain. They observed that the initially uniform specimens became less uniform with axial strain, whereas the initially non-uniform specimens became more uniform with axial strain.

2.12.2 Measured volume changes

Accuracy in the measurement of specimen volume changes during triaxial testing is essential for a reliable evaluation of changes in diameter, height and void ratio during and at the end of test.

In drained triaxial tests involving changes in confining pressure, the volume change measured is not the actual volume change of the specimen but includes the volume change corresponding to membrane penetration into or withdrawal out of the voids at the boundaries of the specimen (assuming that a correction has been made for cell expansion). In 'undrained' tests there is a possibility for a decrease in void ratio due

to volume change and drainage occurring when the membrane pushes out as the effective confining pressure is decreased in response to increasing pore pressure. A correction for volume change due to membrane penetration/ withdrawal is therefore essential.

Several studies (Newland and Alley (1959); Roscoe et al. (1963); Frydman et al. (1973); Raju and Sadasivan (1974); Kiekbusch and Schuppener (1977); Lade and Hernandez (1977); Vaid and Negussey (1984); Baldi and Nova (1984)) in which the effect of rubber membrane were investigated concluded that membrane penetration volume depends on average particle size, void ratio of specimen, magnitude and change in confining pressure, surface area covered by the membrane, thickness and rigidity of the rubber membrane.

Of the factors postulated to affect the membrane penetration volume, the mean grain size has been shown to be by far the most important (for example, Frydman et al. (1973); Baldi and Nova (1984)). According to Frydman et al. (1973), membrane penetration is negligible for soils with average particle sizes below 0.1mm-0.2mm.

Lade and Hernandez (1977) indicated that the effective strength envelope is not affected by membrane penetration.

In the present study, no correction was made for membrane penetration volume change because, as indicated by Frydman et al. (1973), membrane penetration is negligible for soils with average particle sizes below 0.1mm-0.2mm.

2.12.3 Measured pore pressures

Pore pressures measured during undrained triaxial tests on saturated sand specimens are affected by the pressure measurement system (i.e. flexibility of the tubings, fittings, connecting valves, and the compressibility of the water filling the measuring system), the penetration of the rubber membrane into the voids of the granular soil and the degree of saturation of the sand specimen. These factors are described in the following sub-sections, based on published literature.

System compliance

The measurement of pore pressures in undrained triaxial tests can be affected by the flexibility of the pore pressure measurement system and the compressibility of the fluid filling the measuring system. These effects on the measured pore pressure depend mainly on the compressibility of the soil skeleton (Martin et al. (1978)).

Due to the flexibility of the pressure measuring system, water may flow into or out of the pore space of the saturated specimen so that the test is not truly undrained and therefore the measured pore pressures are different from those that would be measured for a truly undrained test. According to Martin et al. (1978), the effects of the pressure measurement system can be minimized by using a system of low overall flexibility.

Membrane penetration

During undrained loading wherein pore pressures increase, there is a corresponding decrease in effective confining stress and a consequent reduction in membrane penetration. The volume of the specimen, therefore, increases and, as a result, the pore pressure reduces relative to the magnitude that it would have reached if there was no membrane penetration (Kiekbusch and Schuppener (1977); Lade and Hernandez (1977); Baldi and Nova (1984)). The reduced pore pressures result in higher effective stresses within the specimen. In tests wherein pore pressures decrease, the effect of membrane penetration is the opposite to the one described above.

The effects of membrane penetration on pore pressures measured during undrained loading have been shown to be potentially more important than all the other effects for specimens of granular soils (Lade and Hernandez (1977); Martin et al. (1978)).

Baldi and Nova (1984) indicated that the use of specimens with larger diameters reduces the effect of membrane penetration on measured pore pressures.

Degree of saturation

Incomplete saturation has a similar influence on the pore pressures measured during 'undrained' tests as the system compliance and membrane penetration, i.e. reducing the pore pressure to a lower value than that which would be measured in a truly undrained test on fully saturated sand (Martin et al. (1978)).

2.13 Corrections to Triaxial Test Data

2.13.1 Area correction

For a triaxial compression test, Bishop and Henkel (1957, 1962) give the following cross-sectional area correction:

$$A_c = A_o (1 + \Delta V/V_o) / (1 - \varepsilon) \qquad (2.8)$$

Where:
A_o is initial cross-sectional area of the specimen, V_o is initial volume of the specimen, ΔV is change in volume of the specimen, and ε is axial strain.

2.13.2 Membrane volume change corrections

Although membrane penetration volume correction was not done in the present study, as indicated earlier, it is considered necessary to describe the correction procedures for the sake of completeness.

Three methods for evaluating the membrane penetration volume change during triaxial tests are summarized below. One was suggested by Baldi and Nova (1984) and the other two were suggested by Vaid and Negussey (1984). For convenience the following sections are labeled with reference to the researchers who proposed the methods:

Baldi and Nova (1984)'s Method

Baldi and Nova (1984) derived the following semiempirical expression for the evaluation of membrane penetration volume:

$$V_m = [d_g V_o / (2D)] [\sigma'_3 d_g / (E_m t_m)]^{1/3} \quad (2.9)$$

Where:
V_m is membrane penetration volume, d_g is mean grain size, V_o is initial volume of specimen, D is diameter of specimen, σ'_3 is effective confining pressure, and E_m and t_m are young modulus and thickness of membrane, respectively.

The expression has been evaluated against experimental data in which the membrane penetration volume was obtained as the difference between the total volume change measured by a volume change device and the volume change calculated from measured axial and radial strains and found to be satisfactory (Baldi and Nova (1984)).

Vaid and Negussey (1984)'s Methods

Vaid and Negussey (1984) suggested two simple methods for evaluating the membrane penetration volume based on an expression for total volume change during a drained triaxial test. These methods are called multiple- and single-specimens methods and are summarized below:

According to Vaid and Negussey (1984), the total volume change during a drained triaxial test, excluding the volume change due to cell expansion, is given by:

$$\Delta V_T = \varepsilon_m A_s + \varepsilon_v \Delta V_o \quad (2.10)$$

Where:
ΔV_T is total volume change, ε_m is membrane penetration per unit membrane surface

area, ε_v is soil volumetric strain, V_o is volume of soil specimen, A_s is soil surface area covered by membrane.

Multiple specimen method: The assumption used in this method is that the volumetric strain is identical in triaxial specimens of different diameters but same density, when subjected to a given increment in effective confining pressure.

Since the ratio V_o/A_s equals D/4, where D is the diameter of the triaxial specimen, equation (2.10) is rewritten as:

$$\Delta V_T / A_s = \varepsilon_m + (\varepsilon_v / 4)D \qquad (2.11)$$

The linear relationship between D and $\Delta V_T/A_s$ in equation (2.11) is obtained by measuring the total volume change data for a given increment in effective confining pressure from triaxial tests on two or more specimens that have the same density and stress history but different diameters. The unit membrane penetration, ε_m, is obtained as the intercept and the volumetric strain as four times the slope of the straight line.

Single specimen method: The method assumes that the behavior of sand in unloading is isotropic elastic. Hence:

$$\varepsilon_{vu} = 3\varepsilon_{au} \qquad (2.12)$$

Where:

ε_{vu} and ε_{au} are volumetric and axial strains during unloading, respectively.

Therefore, equation (2.11) becomes:

$$\Delta V_{Tu} / A_s = \varepsilon_{mu} + (3\varepsilon_{au} / 4)D \qquad (2.13)$$

Where the subscript u refers to unloading.

Assessment of membrane correction is done by conducting one conventional triaxial unloading test from a suitable initial confining pressure with measurements of volume change and axial deformation corresponding to each decrement in effective confining pressure.

Experimentation using these corrections revealed that membrane penetration is the same for the same increment or decrement in effective confining pressure (Vaid and Negussey (1984)). Also, according to Vaid and Negussey (1984), the two methods yield the same membrane penetration volume, with negligible error.

2.13.3 Correction of pore pressure for membrane effect

Since the effects of membrane penetration depend on the membrane penetration volume, which for the present study was assumed to be negligible because of the average particle size of the tailings used being less than 0.2mm, the correction of measured pore pressures was not necessary. However, for the sake of completeness, the procedure for correcting pore pressures for membrane penetration effects is outlined below.

Baldi and Nova (1984) derived the following semiempirical expression for the correction to be applied to measured pore pressures to account for the effect of membrane penetration:

$$\text{Amplification factor} = 1 + f_m / (C_{11} + V_o) \qquad (2.14)$$

And

$$f_m / V_o = 4v_m / (3\sigma'_3 D) \qquad (2.15)$$

Where:

f_m is membrane flexibility, V_o is volume of the specimen, v_m is unit membrane penetration, σ'_3 is effective confining pressure, D is diameter of the specimen and C_{11} is a factor obtained by an experimental procedure as follows:

1. Consolidate isotropically a virgin sample of sand to a convenient consolidation pressure;
2. Perform a drained test at constant cell pressure until a chosen value of stress ratio is reached;
3. Increase the cell pressure to another given value maintaining σ_d constant;
4. Keep the new cell pressure constant and increase the axial load to a new value of stress ratio;
5. Repeat the procedure until failure is reached.

2.13.4 Correction for strength of rubber membrane

Rubber membrane imposes lateral restraints on the specimen it encloses and a correction to the measured stresses has to be made.

Bishop and Henkel (1957, 1962) suggested the following correction to be applied on the major principal stress for a test involving a bulging type of deformation:

$$\sigma_{1m} = (\pi d_o M \varepsilon) \ / \ A_c \qquad (2.16)$$

Where:
σ_{1m} is the correction to be added to the major principal stress, d_o is initial diameter of the specimen, M is extension Modulus of the membrane, ε is axial strain, A_c is corrected cross-sectional area of specimen at axial strain ε.

The extension modulus of the membrane is measured by the method proposed by Henkel and Gilbert (1952) or Bishop and Henkel (1957, 1962).

As noted by Bishop and Henkel (1957,1962), the rubber correction is usually fairly small. For the present study, a correction on measured axial stress for rubber restraint was taken as:

$$\sigma_{1m} = 0.5 \times \varepsilon \quad \text{, for axial strains less than 2\%} \qquad (2.17)$$
$$= 1 \quad \text{, for axial strains greater than 2\%}$$

This chapter has described the static liquefaction of cohesionless soils based on a literature review that was carried out in the present study. It has also indicated the lack of evidence on the influence of, amongst other factors, anisotropic consolidation on the static liquefaction characteristics of cohesionless sands. The next chapter, chapter 3, describes the procedures followed in performing the liquefaction tests done in the present study.

3 LIQUEFACTION TESTING

3.1 Introduction

As discussed in Chapter 1, section 1.4, the liquefaction potential of Merriespruit gold tailings was assessed by performing three series of liquefaction tests in the triaxial equipment, namely: Monotonic undrained compression of isotropically consolidated specimens; Monotonic undrained compression of one-dimensionally consolidated specimens and Variation of stress path followed during undrained loading of one-dimensionally consolidated specimens. From here on, the above tests will be referred to as case 1, case 2, and case 3 tests, respectively.

The main differences between these tests were the states of stress of specimens prior to loading and the stress path followed during loading, i.e. the way in which failure was brought about. The basic features of the tests are outlined below.

Case 1 tests (Monotonic undrained compression of isotropically consolidated specimens): Specimens were isotropically consolidated and loaded undrained by increasing the vertical stress, at a constant rate of strain, while the confining pressure was kept constant.

Case 2 tests (Monotonic undrained compression of one-dimensionally consolidated specimens): Specimens were one-dimensionally consolidated and loaded undrained by increasing the vertical stress, at a constant rate of strain, while the confining pressure was kept constant.

Case 3 tests (Variation of stress path followed during undrained loading of one-dimensionally consolidated specimens): Specimens were one-dimensionally consolidated and failure was brought about by reducing the confining pressure while keeping either the deviator stress or the effective mean normal stress constant. A constant rate of strain was used for the constant deviator stress path whereas for the constant effective mean normal stress path, the rate of strain was not constant.

In this chapter, detailed procedures used for performing the above tests are given. Section 3.2 describes case 1 tests, section 3.3 deals with case 2 tests and finally in section 3.4 the details of case 3 tests are given.

3.2 Monotonic Undrained Compression of Isotropically Consolidated Specimens (case 1 tests)

3.2.1 Test equipment

The equipment used for case 1 tests, the conventional triaxial apparatus, is shown in Figure 3.1. The features of the equipment are discussed in the following sections.

Triaxial cell

Standard triaxial cells for 38mm x 76mm specimens and 76mm x 152mm specimens were used for carrying out liquefaction tests. The details of a typical cell are shown in Figure 3.2.

The cell body and top consist of a single unit. The top has a hole (bushing) into which a loading piston is fitted. The piston is machined to a close tolerance with the bushing. When the cell is not pressurized, the piston should fall slowly under its own weight. The retaining collar of the piston prevents it being forced out if the cell is pressurized when not in position in a load frame.

The load from the loading piston is transmitted to the specimen through the top cap. The top cap is perforated and fitted with a gland for connecting a length of nylon tubing to the gland in the cell base.

A bracket fitted to the cell top forms a seating for the stem of the strain dial gauge. The air bleed valve enables filling and emptying of the cell from the base. An additional plugged hole is provided for inserting oil into cell to minimize piston friction and to limit water leakage between piston and cell bushing, if any.

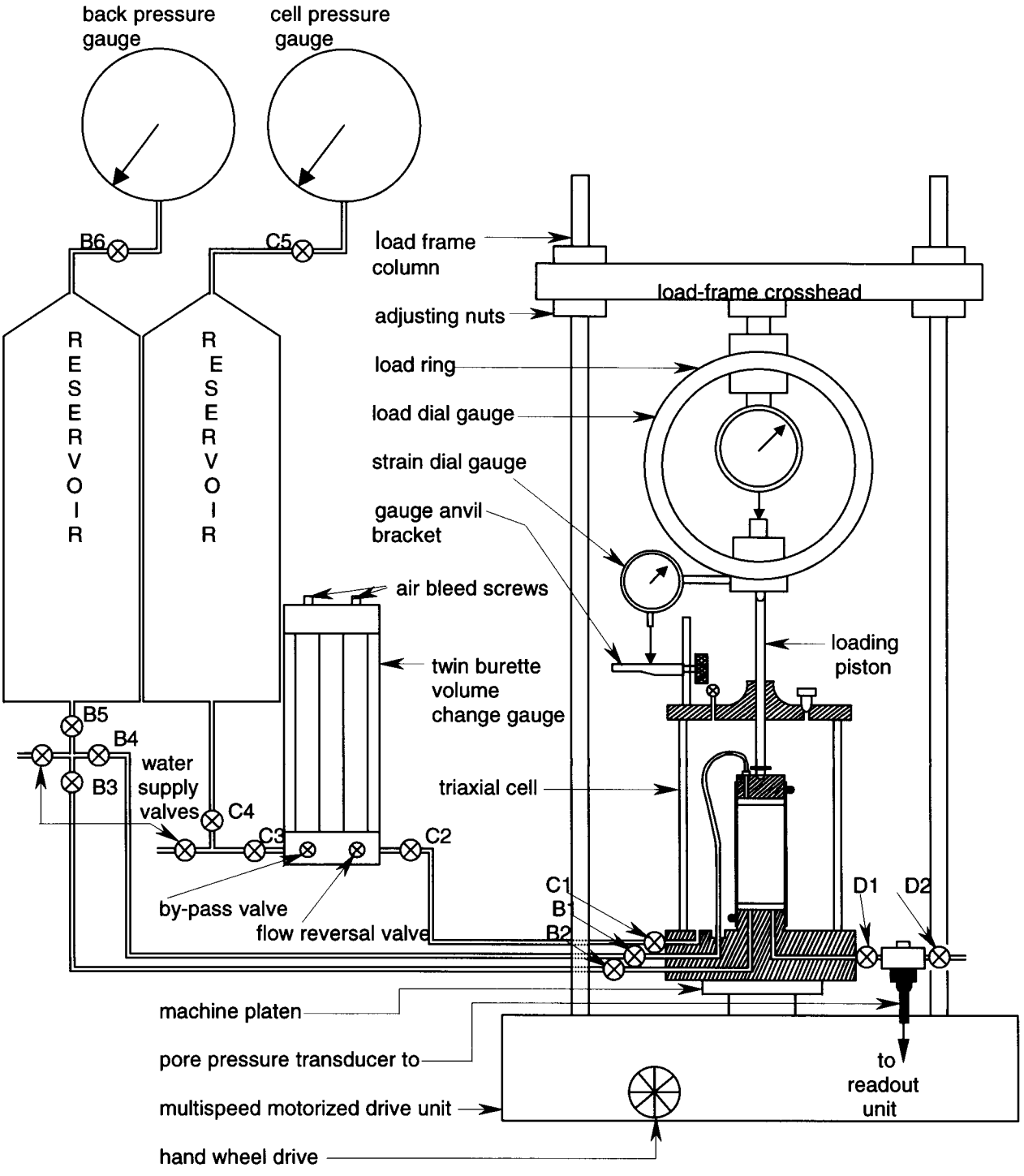


Figure 3.1 The conventional triaxial apparatus: triaxial cell in a load frame and necessary pressure systems

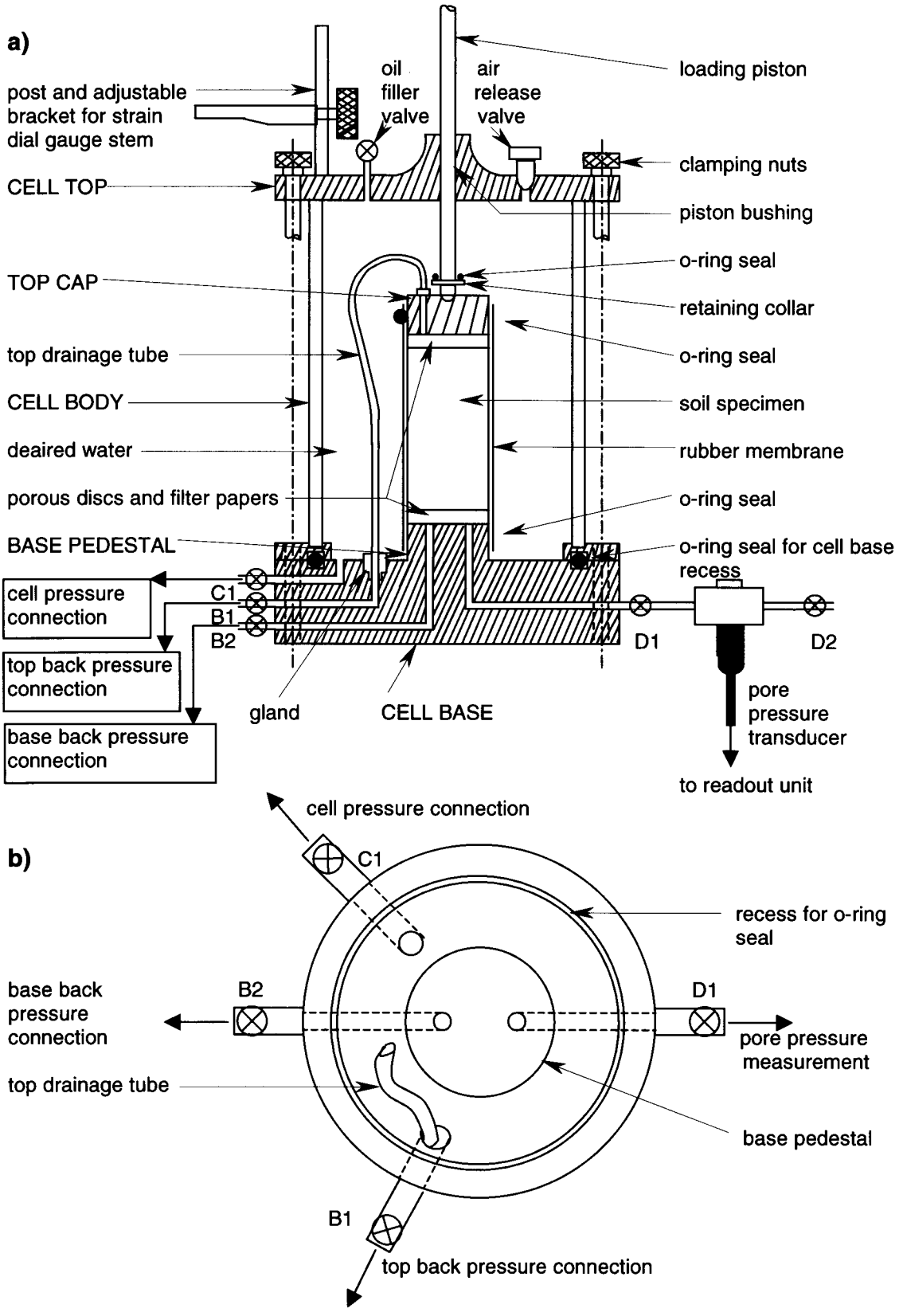


Figure 3.2 Details of a typical triaxial cell: (a) triaxial cell (b) triaxial cell base

The cell body expands when subjected to pressure, and this volume change is allowed for by calibration against cell pressure and time, see Appendix A.

The base, onto which the cell body is assembled, has four outlet ports, as shown in Figure 3.2(b), to enable application of pressures and measurement of pore pressure. Each of the outlet ports terminates at a screwed socket on the edge of the base.

Valves are fitted onto the screwed sockets to enable connection to appropriate pressure lines as follows:

Valve C1: cell chamber valve for filling, pressurizing and emptying the cell.
Valve B2: connection to base pedestal for drainage and application of back pressure to the specimen.
Valve B1: connection to top cap for drainage and application of back pressure to the specimen.
Valve D1: connection to base pedestal for pore pressure measurement.

Pressure systems

The cell pressure and back pressure lines are included in Figure 3.1. A motorized compressed air system, with a maximum working pressure of 1000kPa, was used to apply and maintain pressures in these lines. Each pressure line had a valve connecting to the overhead deaired water source. The back pressure line was connected to valves B1 and B2 to enable back pressure to be applied to the specimen through its top and base. The reservoir in the cell pressure line served as a source of deaired water for filling the cell. A twin-burette volume change gauge was included in the cell pressure line as shown in Figure 3.1. The adjustment and measurement of pressures in the lines was by means of pressure gauges, 250mm diameter, reading 0 – 1000kPa. To improve the accuracy of testing, the gauges were calibrated to relate the gauge readings to actual pressures in the lines, see Appendix A.

Axial loading system

To apply axial load to the specimen, a multispeed motorized load frame was used to lift the machine platen on which the cell base rested at a constant rate of displacement so that the specimen top cap pushed against the loading piston, the top of which was in contact with a stationary proving ring. The proving ring measured the load. A predetermined constant rate of displacement or strain was selected by setting the motor drive to an appropriate gear position.

Measurement of pore pressure within the specimen

A pressure transducer of 1000kPa capacity was connected to valve D1 of the base pedestal port, as shown in Figure 3.1, to enable measurement of pore pressure at the base of the specimen. The transducer was connected to a readout unit that displayed the pressure in digital pressure units.

Measurement of change in length of specimen

Micrometer dial gauges, reading to the accuracy of 0.01mm were used for the measurement of change in length of specimens. Gauges with a travel of 25mm were used for 38mm x 76mm specimens and for 76mm x 152mm specimens, gauges with a travel of 50mm were used.

The dial gauge was clamped to a bracket on the lower end of the proving ring, as shown in Figure 3.1. The stem of the gauge rested on an adjustable bracket supported by the triaxial cell. Movement of the cell relative to the piston was, therefore, equal to the movement of the base pedestal relative to the top cap, i.e. the change in length of the specimen.

Measurement of volume change of specimen

A 100ml twin-burette volume change gauge reading to the nearest 0.1ml was connected in the cell pressure line, as shown in Figure 3.1, to enable the measurement of volume into and out of the cell. The component for cell expansion

was deducted from the total volume change read from the volume change gauge to obtain the specimen volume change. A flow reversal valve was operated to reverse the flow in the burette should the burette capacity be reached for flow in a given direction. A separate valve was provided for by-passing the volume change gauge.

Ancillary items

The following items were also used for the test:

A supply of deaired water;
Two porous discs;
Two filter papers;
Rubber membrane;
Two rubber o-ring seals;
Membrane stretcher;
Split cylindrical o-ring stretcher.

3.2.2 Preparation of test equipment and pre-test checks

General

Prior to setting up a specimen on the triaxial equipment and starting a test, it was important to ensure that the cell pressure, back pressure and pore pressure measurement lines were air-free and contained no leaks and that all elements of the equipment were fully functional. This increased the accuracy of testing.

Back pressure line

Deairing: Initially, all valves were closed and the cell was disassembled from its base. The gauge pressure was set to zero and all valves along the back pressure line, including the water supply valve, were opened to allow entrapped air to be pushed out at the port in the base pedestal and the hole in the top cap. When all the air had been released, valves D1 and D2 were closed.

Checking for leaks: Initially, all valves were closed and the gauge pressure was set to zero. A tapered plug was fitted tightly in the hole in the top cap and all valves along the back pressure line, except the valve connecting to the base pedestal (valve B2) and the water supply valve, were opened. The gauge pressure was set to maximum working pressure and left for a period of time. Any leak(s) in the line could be identified by first drying the connecting tubings and valves in the line and observing any water that came out or wiping the tubings and valves with a dry paper. Any leakage was eliminated and the check repeated.

Cell pressure line

Deairing: All valves were initially closed and the gauge pressure was set to zero. The volume change gauge was first isolated from the cell pressure line by opening the burette by-pass valve, see Figure 3.1. All valves along the cell pressure line, including the water supply valve, were opened to allow deaired water from the water supply line to run through the line thereby removing any entrapped air at the cell pressure port. When all air had been removed, all valves were closed and the volume change gauge was introduced to the cell pressure line by closing the burette by-pass valve. The air bleed screws of the volume change gauge were opened and all valves in the cell pressure line including the water supply valve were reopened to allow deaired water to run through the line. Air in the burettes, if any, was released at the air bleed screws and air trapped in the valves, manifold or connecting pipework, if any, was pushed out through the line at the cell pressure port. When all the air had been removed, the air bleed screws of the volume change gauge and all valves in the cell pressure line were closed.

Checking for leaks: In order to check for leaks in the cell pressure line, all valves along this line, except the valve connecting to the cell base, valve C1, and the water supply valve, were opened and the cell pressure gauge was set to maximum working pressure. The pressure was left for some time. Immediately after application of pressure, there would be some volume change due to expansion of connecting tubings but this would stop if there were no leak(s) in the system. Continuous volume change implied the presence of a leak(s), which could be traced by first drying the connecting tubings and valves along the line and allowing some time. Wiping the

connecting tubings and valves, later, would reveal the location of the leaks. The leak(s), if present, were eliminated and the check repeated.

Checking the cell body for leaks

The cell body, if it had not been used before, was checked to ensure that it was leak-free as follows: The bottom surface of the cell and the top surface of the cell base were cleaned to ensure that they were free of particles and dirt. The cell body was assembled to the cell base and tightened by turning the clamping nuts or screws with controlled torque. The top air release valve was opened. The loading piston was pulled up to its fullest extent and held there. The cell was filled with deaired water from the water supply while the valve connecting to the cell pressure gauge, valve C5, was closed and the volume change gauge was by-passed. When water emerged through the top air release valve, the cell chamber valve, valve C1, and the water supply valve were closed. The valve connecting to the cell pressure gauge, valve C5, was opened and the volume change gauge introduced to the system. The gauge pressure was set to maximum working pressure and the cell chamber valve was opened. Immediately after opening the cell chamber valve, there would be an initial volume change, indicated by the volume change gauge, due to expansion of the cell and connecting tubings but this would soon stop or slow down considerably if there was no leakage(s) in the cell body, assuming that the cell pressure line had already been confirmed to be leak-free. Presence of a leak(s) in the cell would be indicated by a continuous volume change in the volume change gauge and could be easily located by drying the cell and observing any water that came out (either between the cell and the base or between the loading piston and the cell bushing). If water came out between the cell and the base, the leak would then have been due to either the presence of a particle(s) between the two surfaces, which could be removed, or a cut in the o-ring seal in the cell base, in which case the o-ring seal would be replaced. If water came out between the loading piston and the cell bushing, the o-ring seal in the cell bushing was replaced or a new recess made in the cell bushing for use with a bigger o-ring seal. This technique was used for a number of cells used in the present study. If the leakage(s) could not be eliminated, the cell was discarded.

Pore pressure measurement line

Deairing: The cell pressure line was temporarily connected to valve D2, Figure 3.1, of the pore pressure measurement line. Valves D1 and D2 and the water supply valve were opened to allow deaired water from the water supply to run through the pore pressure measurement line. Air was pushed out of the line at the cell base port. When all the air had been removed, valve D1 and the water supply valve were closed and a check for leakage(s) was performed.

Checking for leaks: While the cell pressure line was still connected to the pore pressure measurement line, valve D2 was opened and valve D1 was closed. The gauge pressure was set to maximum working pressure. Continuous volume change implied the presence of a leak(s), which could be traced and eliminated and the check redone. After this check, valve D1 was opened and valve D2 was closed. The cell pressure line was reconnected to the cell chamber valve. When reconnecting the cell pressure line back on to the cell chamber valve there was a possibility of trapping air at that connection. Trapped air, if any, was removed by allowing water from the water supply to run through the cell pressure line while the cell chamber connection was loose. The connection was tightened while water was flowing out at the connection so that trapped air could be displaced by water.

Ancillary items

Deaired water: To avoid compressing the specimen by filling the cell with water of unknown pressure from the overhead water supply source, when the specimen was being set up in the triaxial equipment, deaired water in the cell pressure line's reservoir was used to fill up the cell. This required that this reservoir be filled with deaired water from the overhead deaired water source prior to setting up the specimen. The back pressure line's reservoir was also filled with deaired water.

Porous discs: Two porous discs of the same diameter as the diameter of the specimen to be tested were boiled for 10 minutes in distilled water, to remove air, and kept under deaired water ready for use.

Filter papers: Filter papers prevent soil particles from migrating through the porous discs. Two filter papers of the same diameter as the diameter of the specimen to be tested were prepared prior to setting up the specimen.

Proving ring: A proving ring of capacity appropriate to the likely strength of the specimen to be tested was checked to ensure that there was free movement of its stem throughout its full range of travel in both directions and was set ready for use.

Dial gauge: A dial gauge of range of travel appropriate to the height of the specimen to be tested (25mm for 38mm x 76mm specimens or 50mm for 76mm x 152mm specimens) was checked for free movement of its stem throughout its range of travel. The necessary fixings and support brackets were prepared and set ready for assembly.

Rubber membrane: A rubber membrane of appropriate size to the size of the specimen to be tested was inspected for flaws or pinholes by stretching in two directions while holding against bright light. To check for leaks, the membrane was sealed onto a solid and a drainage end cap with rubber o-ring seals and inflated with air through the drainage lead while holding it under water. The presence of leak(s) would be indicated by the appearance of air bubbles, in which case the membrane would be discarded.

Rubber o-ring seals: Two rubber o-ring seals of size appropriate for the specimen to be tested were inspected by stretching them a little to ensure that they were free from nicks or weak points.

Membrane stretcher: A membrane stretcher of appropriate size to the size of specimen to be tested was set ready for use. The membrane stretcher was cylindrical and of a slightly larger diameter than the nominal diameter of specimens for which it was used. It was fitted with a thin length of tube for applying suction to the membrane inside it.

Split cylindrical o-ring stretcher: A split cylindrical o-ring stretcher of appropriate size to the size of the specimen to be tested was set ready for use. The stretcher

had a longitudinal cut so that an o-ring seal with a smaller diameter could be fitted over it by pressing on the stretcher to reduce its diameter.

3.2.3 Calibration of equipment

In order to improve the accuracy with which the output data from a triaxial test represent the physical quantity being measured, it was important that the data collection devices be calibrated against known standards. Calibrations of pressure gauges, pore pressure transducers, cell expansion volume change against pressure and time, and piston friction were necessary prior to carrying out the triaxial test. Detailed procedures used for performing these calibrations, calibration data and calibration curves are given in Appendix A.

3.2.4 Preparation of test specimens

General

Specimens for liquefaction testing in the triaxial equipment were formed by compacting moist soil in a mould. This method is called the moist tamping technique of specimen preparation.

The void ratio of a specimen formed depends on the dry mass of the soil that goes into the mould and the volume of the specimen.

To produce specimens with uniform void ratio, moist soil was compacted in the mould in five layers each with the same void ratio.

Procedure

The method that was used for preparing specimens for liquefaction testing (moist tamping technique) is outlined below:

1. A target set-up void ratio was chosen based on the maximum and minimum void ratios (determined using ASTM D4253-91 and D4254-91 (1993)) of the sample

under consideration at the moisture content to be used to prepare the specimen, in this case, 10% by dry mass. This moisture content was chosen because it yielded the 'loosest' bulk sample within the range of moisture contents that could be used to prepare the specimen. As liquefaction behavior requires high void ratios ('very loose' specimens), very high set-up void ratios were often chosen but not as high as to hamper specimen handling. Usually, a void ratio of about 90% of the maximum void ratio of the sample was chosen.

2. Using the target set-up void ratio and the estimated volume of specimen to be formed (86.193 cm^3 for 38mm x 76mm specimens or 689,542 cm^3 for 76mm x 152mm specimens), the required dry mass of the specimen was calculated as follows:

$$M_{d(required)} = V_{estimated} / [(1+ e_{target}) / G_s] \quad (3.1)$$

Where:

$M_{d(required)}$ = Required dry mass of specimen, g;

$V_{estimated}$ = Estimated volume of specimen, cm^3;

e_{target} = Target set-up void ratio of specimen;

G_s = Specific gravity of sample under consideration.

3. Since the specimen was formed in five layers, the required dry mass and height of compaction of each layer were calculated as follows:

$$M_{d(layer)} = 1/5 (M_{d(required)}) \quad (3.2)$$

$$M_{w(layer)} = 1/5 (M_{w(required)})$$

$$= 1/5[(M_{d(required)} + 1/10 \times M_{d(required)}] \quad (3.3)$$

$$L_{o(layer)} = 1/5 (L_{o(estimated)}) \quad (3.4)$$

Where:

$M_{d(layer)}$ = Required dry mass of layer, g;

$M_{w(layer)}$ = Required moist mass of layer (assuming 10% moisture content), g;

$M_{d(required)}$ = Required dry mass of specimen, g;

$M_{w(required)}$ = Required moist mass of specimen (assuming 10% moisture content), g;

$L_{o(layer)}$ = Estimated height of layer, mm;

$L_{o(estimated)}$ = Estimated height of specimen, mm.

4. An oven-dried representative sample of mass 50g in excess of the required dry mass of specimen was thoroughly mixed with deaired water of mass 10% of the total dry mass of sample in a sufficiently big container to obtain a moist sample with uniform moisture content. The additional 50g of soil was to enable the measurement of true moisture content of specimen, as this would often be slightly different to the 10% moisture content used due to evaporation.
5. Immediately after mixing the soil sample with water, three moisture samples were taken and weighed (m_{w1}, m_{w2} and m_{w3}) and placed in the oven to obtain their dry masses the next day (m_{d1}, m_{d2} and m_{d3}).
6. The moist soil sample was compacted in the mould in five layers each of mass given by equation 3.3 and height given by equation 3.4.
7. The mould was removed and the resulting specimen was immediately weighed to obtain its moist mass, Mw.
8. Immediately after recording the moist mass of the specimen, three moisture samples were taken from the remaining moist soil sample and weighed (m_{w4}, m_{w5} and m_{w6}) and placed in the oven to obtain their dry masses the next day (m_{d4}, m_{d5} and m_{d6}).
9. The initial diameter and initial height of the specimen were then measured and recorded as D_o and L_o, respectively. The diameter of the specimen was taken to be the average of three diameter measurements made at the top and bottom ends and at mid-height of the specimen. The height of the specimen was taken to be the average of four height measurements made at four diametrically opposite points at the top of the specimen.
10. The specimen was immediately set up in the triaxial equipment, as described in section 3.2.5, to avoid loss of moisture, which might result in the specimen breaking on handling.

Calculation of set-up moisture content of specimen

The moisture content of the specimen, when its moist mass was being recorded, was taken to be the average of the moisture contents obtained from the moisture

samples in steps 5 and 8 above, where the moisture content of each moisture sample was calculated as:

$$mc_i = (mw_i - md_i) / md_i \times 100\% \quad (3.5)$$

Therefore,

$$mc = (mc_1 + mc_2 + mc_3 + mc_4 + mc_5 + mc_6) / 6 \quad (3.6)$$

Where:

mc_i = Moisture content of the i'th moisture sample, %;

mw_i = Moist mass of the i'th moisture sample, g;

md_i = Dry mass of the i'th moisture sample, g;

mc = moisture content of the specimen when its wet mass was being measured, %.

Calculation of dry mass of specimen

The true dry mass of specimen was obtained from the moist mass of specimen (step 7) and true moisture content of specimen (equation 3.6) as follows:

$$M_d = M_w / (1 + mc / 100) \quad (3.7)$$

Where:

M_d = Dry mass of specimen, g;

M_w = Moist mass of specimen (step 7 above), g;

mc = True moisture content of specimen (equation 3.6), %.

Calculation of set-up void ratio of specimen

The specimen formed usually had a void ratio close to the target set-up void ratio, but not necessarily the same because the actual dimensions and dry mass of the specimen were usually slightly different from those initially targeted.

The specimen's true set-up void ratio was calculated from the dry mass and dimensions of the specimen obtained in equation 3.7 and step 9, respectively, as follows:

$$e_o = [\pi(D_o/10)^2(L_o/10) / 4 - M_d/G_s] / (M_d/G_s) \quad (3.8)$$

Where:

e_o = True initial (set-up) void ratio of the specimen;

D_o = Initial (set-up) diameter of the specimen (step 9), mm;

L_o = Initial (set-up) height of the specimen (step 9), mm;

M_d = Dry mass of the specimen (equation (3.7)), g;

G_s = Specific gravity of soil sample under consideration, g/cm^3.

3.2.5 Setting up of specimens in the triaxial equipment

Assumptions

1. The equipment had been prepared and checked according to section 3.2.2, all valves were closed and the cell was disassembled from its base.
2. The specimen had been prepared according to the method described in section 3.2.4.

Procedure

1. The base pedestal was covered with a film of deaired water from a wash bottle.
2. A deaired, saturated porous disc was slid onto the base pedestal without trapping air and a filter paper was placed on top of the disc.
3. The specimen was placed symmetrically on top of the filter paper taking care not to break it or distort its shape on handling. The specimen was held with fingers on its sides as close to its base as possible.
4. A second filter paper was placed on top of the specimen followed by the second deaired, saturated porous disc.
5. A rubber membrane was positioned inside a membrane stretcher of appropriate size so that its ends were equally distanced from the ends of the stretcher. The

ends of the membrane were rolled over the stretcher and suction was applied by sucking the tube of the stretcher to enable the membrane to stick tightly onto the stretcher.

6. A finger was placed on the end of the tube so as to maintain the suction pressure. The stretcher and membrane were positioned over the specimen, taking care not to disturb the specimen, so that the top and bottom ends of the stretcher were equally distanced from the top and bottom porous discs, respectively.
7. The finger was released from the tube, thereby releasing the suction and enabling the membrane to cling to the specimen. Air was blown through the tube to unroll the ends of the membrane and the stretcher was carefully lifted away from the specimen.
8. Two rubber o-rings were used to seal the membrane onto the base pedestal and top cap. First, one o-ring was fitted over a split cylindrical o-ring stretcher and positioned over the specimen. The o-ring was unrolled so that it sealed the bottom end of the membrane onto the base pedestal. The top end of the membrane was rolled down over the specimen so that the top surface of the porous disc was fully exposed. The second o-ring was fitted over and past the top cap so that it encircled the top cap's drainage tube. The top cap was placed on the top porous disk and rotated to such a position that the top drainage tube would not interfere with the cell body on assembling. The membrane was rolled up over the top cap. The o-ring encircling the top cap's drainage tube was fitted over the split cylindrical o-ring stretcher taking care not to disturb the specimen. The o-ring stretcher was positioned over the top cap and the o-ring unrolled so that it sealed the membrane onto the top cap. The o-ring stretcher was carefully lifted away and the upper end of the membrane rolled down over the o-ring to expose the top surface of the top cap.
9. With the loading piston pulled up to its fullest extent, the cell body was carefully lowered into position over the specimen so that it did not interfere with the specimen and the top drainage tube. The cell body was assembled to the cell base by tightening the clamping nuts or screws with controlled torque.
10. The piston was allowed to fall slowly into contact with the top cap to confirm proper alignment. The piston was then pulled up to its fullest extent and held there.

11. The top air release valve of the cell was opened and the cell was filled with deaired water from the cell pressure line's reservoir until the cell was nearly full. Oil was then introduced at the oil filler valve, Figure 3.2(a). After oil had been put in, the oil filler valve was closed and more deaired water was allowed to enter the cell until the oil started coming out through the air release valve.
12. As soon as oil emerged from the top air release valve, the cell chamber valve was closed. The top air release valve was left open until the beginning of the test.

3.2.6 Saturation of specimens

General

Saturation is the process by which the voids of the soil specimen are filled with water. The method used for saturating the specimens in this investigation was one in which the back pressure (pore pressure) was increased in stages. During this process, air in the voids was compressed as water from the back pressure line infiltrated the specimen and eventually, at high enough pore pressure, the air was absorbed into solution by the water. In all stages of saturation, a cell/confining pressure, which was higher than the back pressure, was applied to the specimen to maintain a positive effective stress within the specimen. This condition was necessary to keep the specimen intact.

When a confining pressure was applied to the specimen, the air in the voids of the specimen was compressed resulting in a reduction in void ratio. It was desirable that the specimen be saturated and consolidated to the required stress state with minimal loss in void ratio so that at the beginning of undrained loading, the void ratio of the specimen would still be high enough to cause the specimen to behave in a contractive manner (i.e. liquefy).

To minimize the loss in void ratio during saturation, which would be due to the compression of air in the void space, air in the void space of the specimen was first displaced by water at the lowest confining pressures (air-flushing) and then the specimen was saturated by applying increments of back pressure.

Air-flushing

Assumptions:

The specimen had been set up according to section 3.2.5. The cell body had been assembled to its base. Clamping nuts had been tightened. The cell had been filled with deaired water and all valves, except the top air release valve and the pore pressure measurement line, valve D1, had been closed.

Procedure:

1. The cell pressure, base back pressure and top back pressure connections to the cell base (valves C1, B1 and B2 respectively, in Figure 3.1) were disconnected while the valves were still closed. The pore pressure measurement line was left in place with valve D1 opened and valve D2 closed.
2. Three burettes of 100ml capacity and reading to the accuracy of 0.1ml were tightly fitted with flexible tubings at their bottom ends. The other ends of the flexible tubings were fitted with appropriate fittings and loosely connected to cell base valves (valves C1, B1 and B2) while these valves were still closed. The burettes were clamped to burette stands as shown in Figure 3.3.
3. The burettes were filled with deaired water, to release air at the loose connections at valves C1, B1 and B2 of the cell base. Deaired water was continuously added to the burettes until all the air had been removed at the loose connections. The connections were tightened while water was running through them, to avoid trapping air. For convenience, the levels of water in the burettes were set at 100ml, 100ml and 0ml marks for the cell pressure, base back pressure and top drainage burettes, respectively, as shown in Figure 3.3.
4. The top air release valve was closed.
5. The cell pressure burette was clamped to its stand so that the height of water in the burette was just above the highest point on the cell. The back pressure burette was clamped so that the height of water in it was a few centimeters below the height of water in the cell pressure burette. The top drainage burette was clamped so that the height of water in it was at about the same level as the specimen's top cap.

6. The cell chamber valve, valve C1, was opened and the volume in the cell pressure burette was recorded, when stable.
7. Ensuring that the level of water in the back pressure burette was lower than the level of water in the cell pressure burette after step 6, the base back pressure valve (valve B2) was opened to allow deaired water to infiltrate the specimen from its base. When the level of water in the back pressure and the cell pressure burettes had stabilized, the volumes in the burettes were recorded.
8. Ensuring that the level of water in the top drainage burette was lower than the level of water in the back pressure burette after step 7, the top drainage valve was opened.

With all three burette connections to the cell base opened, the air-flushing system had the following tendency:

- The back pressure burette's water level dropped as water was admitted into the base of the specimen;
- The top drainage burette's water level rose as air was pushed out of the top of the specimen due to a high back pressure at the base and a lower pressure at the top of the specimen;
- The cell pressure burette's water level rose with a rise in level of water in any of the other two burettes and dropped with a drop in the level of water in any of these burettes.

9. Ensuring that the height of water in the cell pressure burette was the highest followed by the height of water in the back pressure burette, the back pressure burette was raised as its water level dropped and the top drainage burette was lowered as its water level rose. When the flow of water through the specimen ceased, the cell pressure and back pressure burettes were gradually raised keeping the distance between their water levels constant until a big enough pressure gradient between the top and base of the specimen had developed for flow through the specimen to continue.
10. When the level of water in either of the back pressure or top drainage burette had come close to the extreme mark of the burette, the top drainage, back pressure and cell pressure valves, in this order, were closed and the volumes in the burettes recorded.

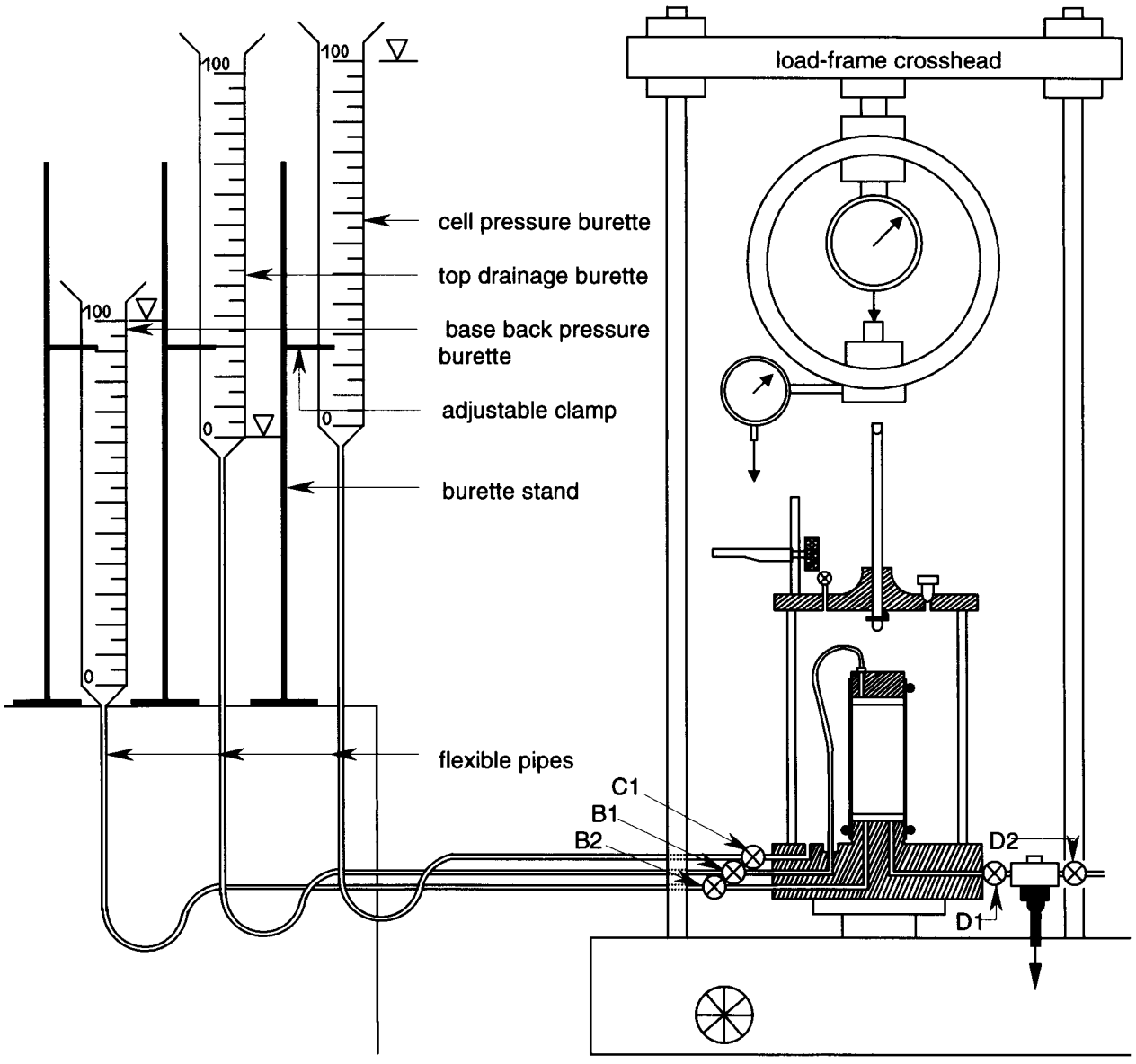


Figure 3.3 Arrangement for displacing air in the voids of a specimen by water at the lowest pressures (Air-flushing)

11. While all valves were closed, the base back pressure burette was refilled to the 100ml extreme top mark and the top drainage burette connection at valve B1, loosened to release the air that had been displaced from the specimen (collected in the tubing connecting the top drainage burette to the cell base and partially in the top drainage burette). More deaired water was added into the top drainage burette to ensure that all air was removed, and the connection was tightened while water was running out through it to avoid trapping air at the connection. The level of water in the top drainage burette was filled to the 0ml extreme bottom mark.
12. Ensuring that the height of water in the cell pressure burette remained the highest followed by the height of water in the base back pressure burrette, the cell pressure, back pressure and top drainage valves were opened in this order.
13. Steps 9 to 12 were repeated until water had flowed through the specimen and emerged across the top drainage valve, valve B1. At this point the top drainage, base back pressure and cell pressure valves were closed in this order and the volumes in the burettes recorded. However, to ensure that maximum amount of air was displaced from the specimen, steps 9 to 12 were repeated until no air bubble was detected in the top drainage tubing. This, however, did not mean that all the air in the specimen had been displaced.
14. When the maximum amount of air had been displaced by flushing, the top drainage and base back pressure valves were closed and time was allowed for the pore pressure reading to stabilize under the effect of the cell pressure (height of water in the cell pressure burette above the midheight of the specimen). The pore pressure reading was recorded, when stable, and the height of water in the cell pressure burette above the mid-height of the specimen was measured and converted to cell pressure by the following equation:

$$P = pgh \tag{3.9}$$

Where:

P = Cell pressure, kPa;

p = Density of water, 1000 kg/m^3;

g = Gravitational acceleration, 10 m/s^2;

h = Height of water in the cell pressure burette above mid-height of the specimen, m.

Notes:

- The volume change in the cell pressure burette was recorded as the volume change of the specimen (cell expansion was taken to be insignificant at these low pressures).
- The total volume change in the top drainage burette from the point when air started showing up across the top drainage valve to the point when water emerged through this valve, was equal to the volume of air displaced from the specimen. The corresponding volume change in the base back pressure burette represented the volume of water admitted into the specimen. These volumes were often almost equal.

Caution:

- There was a possibility that air released from the specimen's top into the top drainage burette's tubing could percolate through the water in the top drainage burette into the atmosphere thereby not only giving misleading measurement of volume of air displaced from the specimen, but potentially causing the top drainage burette water level to drop by such an amount as to cause an undesirable specimen compression indicated by the cell pressure burette volume change.
- The difference in heights between levels of water in the cell pressure and back pressure burettes had to be sufficiently high so as to maintain the initial structure of the specimen. However, the difference was not to be too high as to cause an undesirable compression of the specimen.

Saturation by increments of back pressure

Assumptions:

The specimen had been air-flushed as described above. All valves, except the pore pressure measurement valve, valve D1, had been closed.

Procedure:

1. All three burette connections to the cell base at valves C1, B1 and B2 were disconnected while these valves were still closed.
2. Pressure lines were loosely connected to their appropriate valves, i.e. cell pressure line at valve C1, top and base back pressure connections at valves B1 and B2 respectively. At this stage, all these valves were still closed.
3. Deaired water from the water supply was allowed to run through the pressure lines (with the volume change gauge in the cell pressure line by-passed) in order to remove any air that could have been trapped at the loose connections. While deaired water was running through the pressure lines, the connections were tightened to avoid trapping any air. The water supply valves were then closed.
4. Pressure gauges were adjusted to 0kPa and introduced to the pressure lines while the cell base valves were still closed. The volume change gauge was introduced to the cell pressure line.
5. The initial volume gauge reading corresponding to 0kPa cell pressure and a closed cell chamber valve was recorded.
6. The cell pressure and back pressure were set to 50kPa and 40 kPa, respectively.
7. The cell chamber valve was opened and time allowed for the resulting pore pressure reading to stabilize. The pore pressure reading was recorded when stable.
8. A check for the degree of saturation, B value, was performed as follows:

$$\text{B value} = (PWP_2 - PWP_1) / (CP_2 - CP_1) \qquad (3.10)$$

Where:

PWP_2 = Pore pressure reading at step 7 above, kPa;

PWP_1 = Pore pressure reading at step 14 of air-flushing, kPa;

CP_2 = Cell pressure at step 6 above, i.e. 50kPa;

CP_1 = Cell pressure at step 14 of air-flushing, i.e. equation (3.9), kPa.

9. The back pressure valves, B1 and B2, were opened and the system was left for 24 hours.

10. After 24 hours, the pore pressure and the volume gauge readings were recorded. The pressure gauges were checked to see whether they were still indicating the correct pressures they had been set to. If they indicated different pressures, these new pressures were recorded.
11. The back pressure valves were closed and time allowed for the resulting pore pressure reading to stabilize. At the same time, the back pressure was increased by 50kPa. The pore pressure reading was recorded when stable.
12. The cell chamber valve was closed and the cell pressure increased by 50kPa.
13. The cell chamber valve was opened and time was allowed for the resulting pore pressure reading to stabilize. The pore pressure reading was recorded when stable.
14. A check for the degree of saturation was performed as follows:

$$\text{B value} = (PWP_2 - PWP_1) / (CP_2 - CP_1) \qquad (3.11)$$

Where:
PWP_2 = Pore pressure reading at step 13 above, kPa;
PWP_1 = Pore pressure reading at step 11 above, kPa;
CP_2 = Cell pressure at step 12 above, kPa;
CP_1 = Cell pressure at step 10 above, kPa.

15. The back pressure valves were opened and the system was left for 24 hours.
16. Steps 10 to 15 were repeated until the B value in step 14 was equal to or greater than 0.97, at which point the specimen was considered to be fully saturated. After confirming that the specimen was fully saturated, step 15 was carried out and without having to wait for 24 hours, the specimen was immediately consolidated to the required stress state as described in section 3.2.7, below.

Notes:

- During saturation, there would sometimes be a need for reversing the flow direction in the volume change gauge due to the gauge approaching the extreme of its travel in the current flow direction. In such a case, the back pressure and cell pressure valves were closed and the volume gauge

reading recorded. The flow direction was reversed by operating the flow reversal valve. The pressure valves were then reopened.

- At the end of saturation stage, the following data had been collected:

1. Cell and back pressures at each stage of saturation.
2. B values corresponding to the 24-hour application of each cell pressure increment.
3. Total volume change corresponding to each cell pressure increment over a period of 24 hours.

3.2.7 Consolidation to the required isotropic stress state

General

Consolidation as a stage of the test was the means by which the specimen, saturated as described above, was brought to the required equilibrium effective stress state. In this series of tests the specimens were isotropically consolidated, i.e. stresses within the specimen were the same in all directions.

Procedure

1. While the cell pressure and back pressure valves were still open, the cell pressure was raised by tiny increments (typically 5-10kPa), with some time allowed between increments, to a pressure which was just less than the required consolidation cell pressure.
2. The back pressure and cell pressure valves were closed and the cell pressure was raised to the required value. This step ensured that mistakes, such as raising the cell pressure above the required amount while the cell pressure valve was open, were avoided.
3. The cell pressure and back pressure valves were opened and the system was left for a period of 24 hours after which the volume, pore pressure, cell pressure and back pressure readings were recorded. Loading of specimen was then performed as described below.

3.2.8 Monotonic undrained loading of specimens

General

Isotropically consolidated specimens were loaded undrained by increasing the vertical stress acting on the specimen at a constant rate of strain.

The method used for loading specimens was one in which the machine platen on which the cell base rested was raised by a motor drive unit at a constant rate of displacement therefore causing the cell, along with the specimen sitting on the cell base pedestal, to rise at the same speed (rate of strain) against a stationary loading piston whose bottom end was in contact with the specimen's top cap and its upper end was in contact with a proving ring mounted to a fixed load frame cross-head (see Figure 3.1). The proving ring measured the vertical force applied to the specimen.

Procedure

1. A rate of strain was calculated based on the consolidated height of the specimen and the required time to failure using the criterion that the test should not end earlier than 20% axial strain. Bishop and Henkel (1957, 1962) state that as sands are highly permeable, no pore pressure lag will occur, and the time to failure is based on the convenience of taking readings. According to Bishop and Henkel (1957, 1962), a time to failure of about one hour is commonly adopted. For the present study, six hours were usually used as the time to failure.

   The shearing rate was then calculated as follows:

   $$ROS = (\text{ultimate strain} \times \text{consolidated height}) / \text{time to failure} \quad (3.12)$$
   $$= 0.2 \times L_{cons} / \text{time to failure}$$
   $$L_{cons} = L_o (1-(\text{Chg V}) / 3V_o) \quad (3.13)$$

   Where:
   ROS = Rate of shearing or loading, mm/min;

L_{cons} = Height of the specimen, after consolidation, mm;

L_o = Initial (set-up) height of the specimen, mm;

V_o = Initial (set-up) volume of the specimen, cm^3;

Chg V = Volume change of the specimen after saturation and consolidation, cm^3.

2. The machine was set to the required speed, while off.
3. The machine platen was lowered to its lowest extreme using the hand drive.
4. The load frame cross-head was raised (by untightening the fixing nuts) to a height that allowed the proving ring to hang just above the top of the piston (which was still up at its fullest extent). The load frame cross-head was fixed at this position by tightening the fixing nuts, ensuring that it was horizontal using a leveling tool.
5. A proving ring was fitted loosely at its position on the load frame cross-head.
6. The machine platen was raised slowly by hand drive to bring the piston into contact with the proving ring ensuring that proper alignment of the piston and load ring was achieved.
7. Slowly, the machine platen was raised further to bring the top cap just below the bottom end of the loading piston. During this step, the proving ring reading was checked as the piston advanced into the cell, to see whether it was stable. Stops were made when necessary. The proving ring reading was recorded.
8. The anvil bracket of the dial gauge was fitted so that the dial gauge reading was zero.
9. The back pressure valves were closed.
10. The machine was started.
11. When the proving ring's reading pointer started to move, i.e. when full contact between the piston and top cap was achieved, the dial gauge, pore pressure and proving ring readings were recorded. The start time was also recorded. The dial gauge reading when the proving ring reading pointer started to move was taken to be the zero mark on the axial strain axis.
12. At suitable intervals, data was recorded for time, dial gauge, proving ring and pore pressure readings.
13. The machine was stopped after 20% axial strain. However, in some cases, due to the proving ring reading and/or pore pressure reading still changing, it was necessary to leave the machine running beyond the time dedicated for the test.

3.3 Monotonic Undrained Compression of One-Dimensionally Consolidated Specimens (case 2 tests)

3.3.1 Test equipment

The equipment used for this series of tests was the same as the equipment described for case 1 tests, section 3.2.1, except for one additional item: the K0-ring.

K0- ring

As discussed in Chapter 1, section 1.4, specimens for case 2 tests were saturated and consolidated in such a way that their lateral dimensions were kept constant, i.e. with zero lateral strain (K0-condition). The device used for the detection of lateral deformation of specimens, the K0-ring, is shown in Figure 3.4 and its principles are discussed below.

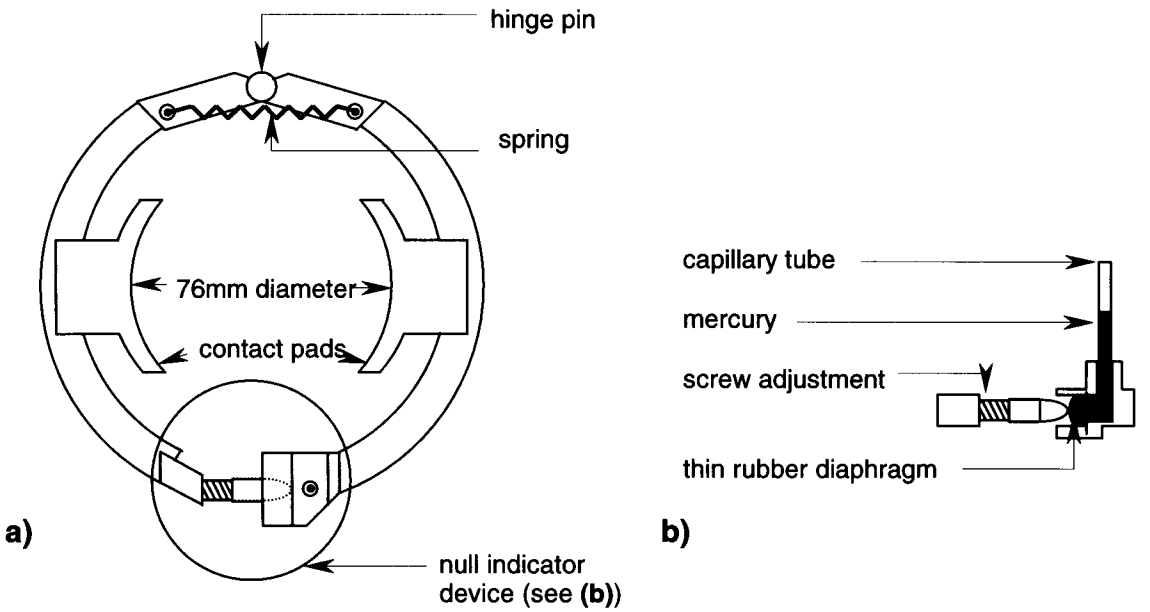


Figure 3.4 Lateral strain indicator (K0-ring): **a)** General arrangement, **b)** Details of the null indicator

Principles: The K0-ring consisted of a hinged ring which was spring loaded to maintain contact between two curved pads and the surface of the specimen it encircled. The ring was attached to the mid-height of the specimen. A small chamber of mercury was situated diametrically opposite to the hinge. The mercury in the chamber was enclosed by a thin diaphragm. Movement due to change in diameter of specimen during saturation and consolidation was doubled by the hinge and imparted to the diaphragm which caused the mercury in the chamber to rise or fall in a small graduated capillary tube. Constant diameter (K0-condition) was maintained by adjusting the cell pressure and/or the vertical load so that the mercury level remained constant.

Note:

- Only 76mm diameter K0-rings were available, therefore, only 76mm x 152mm specimens were used for this series of tests.

3.3.2 Preparation of test equipment and pre-test checks

The equipment was prepared and checked as for case 1 tests, section 3.2.2. Additionally, the K0-ring was checked as described in section 3.3.3, below.

3.3.3 Calibration of equipment

The calibration procedure for the equipment was the same as for case 1 tests, section 3.2.3. In addition, proper functioning of the K0-ring was checked as follows:

K0- ring

The K0-ring was checked to ensure that:

- There was enough mercury in the mercury chamber: it was ensured that the amount of mercury in the chamber was such that when the diaphragm was pressed fully inwards, the mercury level in the capillary tube rose to just below the top end of the tube and when the diaphragm was released, the level of mercury dropped far enough to leave a sufficient length of empty tube above its

level, see Figure 3.5. Mercury could be added into or sucked out of the capillary tube using an injection of appropriate size.

- No air was trapped in the mercury chamber and capillary tube: air was released by pressing and releasing the diaphragm a few times.
- The diaphragm was leak-free: a visual check was done when the diaphragm was stretched by the high amount of mercury in the capillary tube.
- The diaphragm was sufficiently elastic to be able to maintain a constant level of mercury in the tube: this was checked by observing the levels of mercury when the diaphragm was pressed fully inwards and when it was completely released, with time. The cycle was repeated a few times. Constant levels indicated that the diaphragm was properly functional. If the levels changed, the diaphragm was replaced or the ring discarded.



(a) Fully pressed diaphragm **(b)** Released diaphragm

Figure 3.5 Ensuring the correct amount of mercury in the mercury chamber of the K0-ring: **a)** Fully pressed diaphragm, **b)** Released diaphragm

3.3.4 Preparation of test specimens

The procedure for the preparation of specimens for case 2 tests was the same as that given for case 1 tests, section 3.2.4. However, because of the unavailability of other sizes of K0-rings, only 76mm x 152mm specimens were used.

3.3.5 Setting up of specimens in the triaxial equipment

The specimens were set up in exactly the same way as the specimens in case 1 tests, section 3.2.5. However, before assembling the cell body to the cell base, a K0-

ring was fitted to the specimen as described below. The other difference was that, unlike in the case 1 tests where the loading piston was held up at its fullest extent until the beginning of loading, here the piston was always in contact with the top cap (at its bottom end) and a proving ring (at its top end), onto which a dial gauge was mounted.

Fitting the K0-ring

Assumptions:

The K0-ring had been prepared and checked as described in section 3.3.3.

Procedure:

1. The K0-ring was opened wide and positioned around the mid-height of the specimen without closing it or disturbing the specimen.
2. The ring was closed slowly and carefully so that the curved pads just came to contact with the specimen. While holding the ring at this position, a check was done to ensure that the adjusting screw had contacted the diaphragm by observing if there was any change in level of mercury in the capillary tube from its level when the diaphragm was completely released (Figure 3.5(b)). If there was no rise in the level of mercury, the ring was reopened and carefully removed from the specimen. The adjusting screw was turned to extend the exposed length of the screw a little. If the level of mercury in the capillary tube rose substantially, the ring was removed and the adjusting screw was turned so as to reduce the exposed length of the screw. The screw was adjusted to a position that would cause a slight rise in mercury level (from its level when there was no contact between the adjusting screw and the diaphragm, Figure 3.5(b)) when the pads came into contact with the specimen.
3. When the adjusting screw had been properly adjusted, the ring was slowly released, ensuring that it was perfectly horizontal and symmetrical about the midheight of the specimen. The action of the spring ensured that the ring was firmly attached to the specimen. However, in this investigation, additional measures were taken to ensure that the ring was firmly attached to the

specimen. Little pieces of masking tape were used to 'glue' the pads to the membrane as shown in Figure 3.6. When using tape to glue the pad onto the membrane, consideration was taken to ensure that tapes did not provide additional stiffness to the membrane or prohibit free expansion and contraction of the membrane. The arrangement in Figure 3.6 in which two pieces of tape were used to glue each pad to the membrane seemed suitable. First, two pieces of tapes, tapes 1 in Figure 3.6, were glued onto the inside of each pad at its top edge leaving short lengths of tapes sticking out. Two additional short pieces of tapes, tapes 2 in Figure 3.6, were used to glue the first two tapes to the membrane.

4. When the K0-ring had been properly fitted, the level of mercury in the capillary tube was marked with a thin waterproof marker.
5. The cell body was carefully lowered into position over the specimen with the piston pulled out to its fullest extent (this step deserved great care to ensure that the cell body did not touch the K0-ring on being lowered into position).

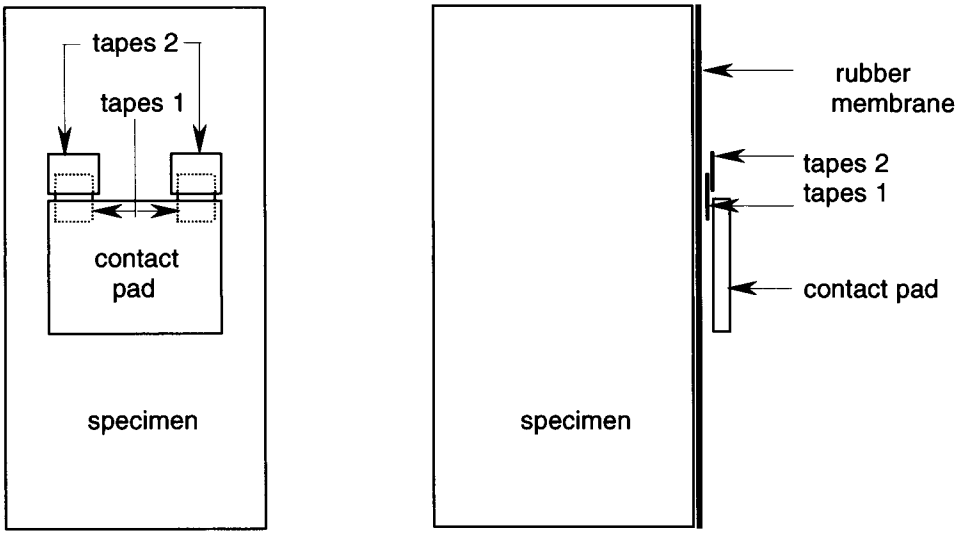


Fig 3.6 Fitting the K0-ring around the specimen

6. The cell was assembled to the base by tightening the clamping nuts or screws with controlled torque.
7. The piston was allowed to fall slowly into contact with the top cap. Proper alignment was achieved by gently rotating the piston into its position on the top cap. Unlike in case 1 tests, here the piston was left in contact with the top cap.
8. The machine platen was lowered to its lowest extent using the hand drive. The position of the machine cross-head was adjusted by turning the fixing nuts so that a proving ring fitted to the cross-head (along with a dial gauge of range 50mm, reading to the accuracy of 0.01mm) hung just above the top of the piston. The machine cross-head was fixed at this position using the fixing nuts, ensuring that it was horizontal.
9. Slowly and carefully, the machine platen was raised by hand drive to bring the top of the piston to contact with the proving ring. The anvil bracket of the dial gauge was fixed in position so that the dial gauge read zero. The 'zero-load' proving ring reading was recorded.
10. The top air release valve of the cell was opened, and the cell was filled with deaired water from the cell pressure line's reservoir until the cell was nearly full. Oil was then introduced at the oil filler valve, Figure 3.2(a). After oil had been put in, the oil filler valve was closed and more deaired water was allowed to enter the cell until the oil started coming out through the air release valve.
11. When oil emerged from the top air release valve, the cell chamber valve was closed and the top air release valve left open until the beginning of test.

3.3.6 Saturation of specimens

Air-flushing

The importance of air-flushing was discussed under case 1 tests in section 3.2.6. As the confining pressures were small during this stage, there was very little change, if any, in specimen dimensions (diameter, height). Consequently, there was insignificant, if any, movement of the mercury level in the K0-ring due to air-flushing. Therefore this stage of test was performed exactly the same as for case 1 tests, except that the loading piston was, in this case, in contact with the top cap.

Saturation by increments of back pressure

Unlike in case 1 tests, for case 2 tests, this stage involved the application of a vertical load along with each cell pressure increment to keep the diameter of the specimen constant and equal to the initial diameter, as indicated by the level of mercury in the K0-ring. In all other respects, the procedure was the same as for case 1 tests.

Assumptions:

The specimen had been air-flushed according to the procedure given in section 3.2.6 but with the loading piston being in contact with the top cap. All valves were closed except the pore pressure measurement valve, valve D1.

Procedure:

1. The burette connections at valves C1, B1 and B2, Figure 3.3, were replaced by appropriate pressure connections, i.e. the cell pressure connection at valve C1, top and bottom back pressure connections at valves B1 and B2, respectively. Air was removed at the connections as before and the connections were tightened.
2. Pressure gauges were set to 0kPa and introduced to the pressure lines with the volume change gauge of the cell pressure line included in the system. While all base valves were still closed, the initial volume change gauge reading corresponding to 0kPa cell pressure and a closed cell chamber valve was recorded.
3. The cell and back pressures were set to 50kPa and 40kPa, respectively.
4. The cell chamber valve was opened and time was allowed for the resulting pore pressure reading to stabilize. When stable, the pore pressure reading was recorded. There would be a rise in the mercury level in the capillary tube of the K0-ring due to compression of the specimen.
5. A check for B value was performed as in section 3.2.6, for isotropically consolidated specimens.
6. The top and base back pressure valves (valves B1 and B2) were opened. A vertical load was applied to the specimen by slowly turning the hand drive of the

loading machine in order to lower the level of the mercury back to its original level in (step 4, section 3.3.5). As the diameter of the specimen continued to decrease with time under the action of the cell pressure, the vertical load was increased appropriately to balance out this continuous decrease in diameter.

7. After 24 hours, the readings of the dial gauge, pore pressure, volume change, proving ring and gauge pressures were recorded.
8. The back pressure valves were closed, and time was allowed for the resulting pore pressure reading to stabilize. At the same time, the back pressure was increased by 50kPa. When stable, the pore pressure reading was recorded.
9. The cell chamber valve was closed and the cell pressure increased by 50kPa.
10. The cell chamber valve was opened and time was allowed for the resulting pore pressure reading to stabilize. The stable pore pressure reading was recorded.
11. A check for B value was performed as in section 3.2.6, for isotropically consolidated specimens.
12. The back pressure valves were opened and the vertical load was increased by slowly turning the hand drive of the loading machine so that the level of the mercury was lowered to its original level. The mercury level was lowered as it rose under the action of the cell pressure with time.
13. Steps 7 to 12 were repeated with increments of cell pressure and back pressure of 50kPa, until the B value at step 11 was equal to or more than 0.97. At this point the specimen was considered to be fully saturated and step 12 was performed but this time without having to wait for 24 hours as consolidation was immediately carried out, as described in section 3.3.7, below.

Notes:

- As in case 1 tests, during saturation there would sometimes be a need for reversal of flow in the volume change gauge due to the gauge approaching the extreme of its travel in a given direction. The procedure was as described for case 1 tests.
- At the end of saturation, the following data had been gathered.

    1. Total dial gauge deflection from its 'zero mark' (step 9, section 3.3.5)
    2. Total volume change corresponding to each cell pressure increment, over a period of 24 hours.

3. Proving ring readings, pore pressure readings and corresponding B values after 24 hours of application of each pressure increment.

3.3.7 Consolidation to the required K0-condition stress state

Consolidation in this series of tests was performed so that the diameter of the specimen was unchanged and was equal to the original diameter measured after specimen preparation. This was ensured by the level of mercury in the capillary tube (during and after consolidation) being at its original level marked in step 4, section 3.3.5.

Assumptions

The specimen had been saturated according to section 3.3.6 above.

Procedure

1. The cell pressure was increased slowly by tiny increments (typically 5-10 kPa) and at the same time the vertical load was increased in such a way as to balance out any resulting rise in the level of mercury above its original level at specimen set-up.
2. In this manner, the cell pressure was increased to an amount which was just less than the required consolidation cell pressure. At this point, all valves were closed and the cell pressure was increased to its required value. The cell pressure and back pressure valves were opened and the vertical load increased as appropriate to balance out any rise in mercury above its K0-condition level. The vertical load was continuously increased to maintain the level of the mercury at its original mark as the level continued to rise with time under the effect of cell pressure. Consolidation was allowed to occur for 24 hours after the application of the final consolidation cell pressure increment.
3. After 24 hours, the readings of the dial gauge, proving ring, volume change and pore pressure were recorded. The readings of the gauge pressures were also recorded if they had changed. Loading was then carried out as described below.

3.3.8 Monotonic undrained loading of specimens

Undrained loading of specimens was performed in the same way as in case 1 tests. The difference was that here, the loading piston was already in contact with the top cap (at its bottom) and a proving ring (at its top) and the dial gauge was in place and already had a 'zero shear strain' fixed point. Loading was therefore carried out as follows:

1. The initial readings of dial gauge, proving ring and pore pressure were recorded.
2. The shearing rate was calculated as follows:

$$ROS = \text{ultimate strain} \times \text{consolidated height} / \text{time to failure} \quad (3.14)$$
$$= 0.2 \times L_{cons} / \text{time to failure}$$
$$L_{cons} = L_o - Chg\ L \quad (3.15)$$

Where:

ROS = Rate of shearing or loading, mm/min;

L_{cons} = Height of the specimen, after consolidation, mm;

L_o = Initial (set-up) height of specimen, mm;

Chg H = Change in height of specimen from specimen preparation to the end of consolidation, mm;

= Total dial gauge deflection x 0.01mm

3. The back pressure valves were closed.
4. The machine was set to the required rate of shearing and started.
5. At suitable intervals, the readings of time from start of loading, dial gauge, proving ring and pore pressure were recorded.
6. The machine was stopped after 20% axial strain of the specimen's consolidated height if the readings had ceased to change, otherwise, the test was allowed to run beyond 20% strain.

3.4 Variation of Stress Path Followed During Undrained Loading of One-Dimensionally Consolidated Specimens (case 3 tests)

3.4.1 Test equipment

The equipment for case 3 tests, is shown diagrammatically in Figure 3.7. The various components are described in the following paragraphs.

The Bishop-Wesley stress path cell

The details of the Bishop-Wesley stress path cell are shown in Figure 3.8. The upper part of the Bishop-Wesley stress path cell is similar to a conventional triaxial cell.

A load cell, consisting of a load transducer, is screwed into the top of the cell. Four holes are present in the base: the cell chamber port, to enable filling of cell with water and application of cell pressure; two base pedestal ports, for specimen base drainage and pore pressure measurement; and a separate hole for fitting the radial strain transducer cable into the cell.

The base pedestal is mounted at the top of a loading ram, the bottom of which is inside the lower pressure chamber. The top part of the loading ram and the pedestal are inside the cell chamber. Two bellofram rolling seals are used. The upper one to contain the cell fluid and the lower one to seal the pressurizing fluid in the lower pressure chamber. The ram moves vertically in a 'rotolin' linear bearing located in the region between the rolling seals. This region is open to atmosphere.

Axial load is applied to the specimen by increasing the pressure in the lower pressure chamber to cause the ram together with the specimen sitting on the pedestal to move upwards to push the top cap against a stationary load cell.

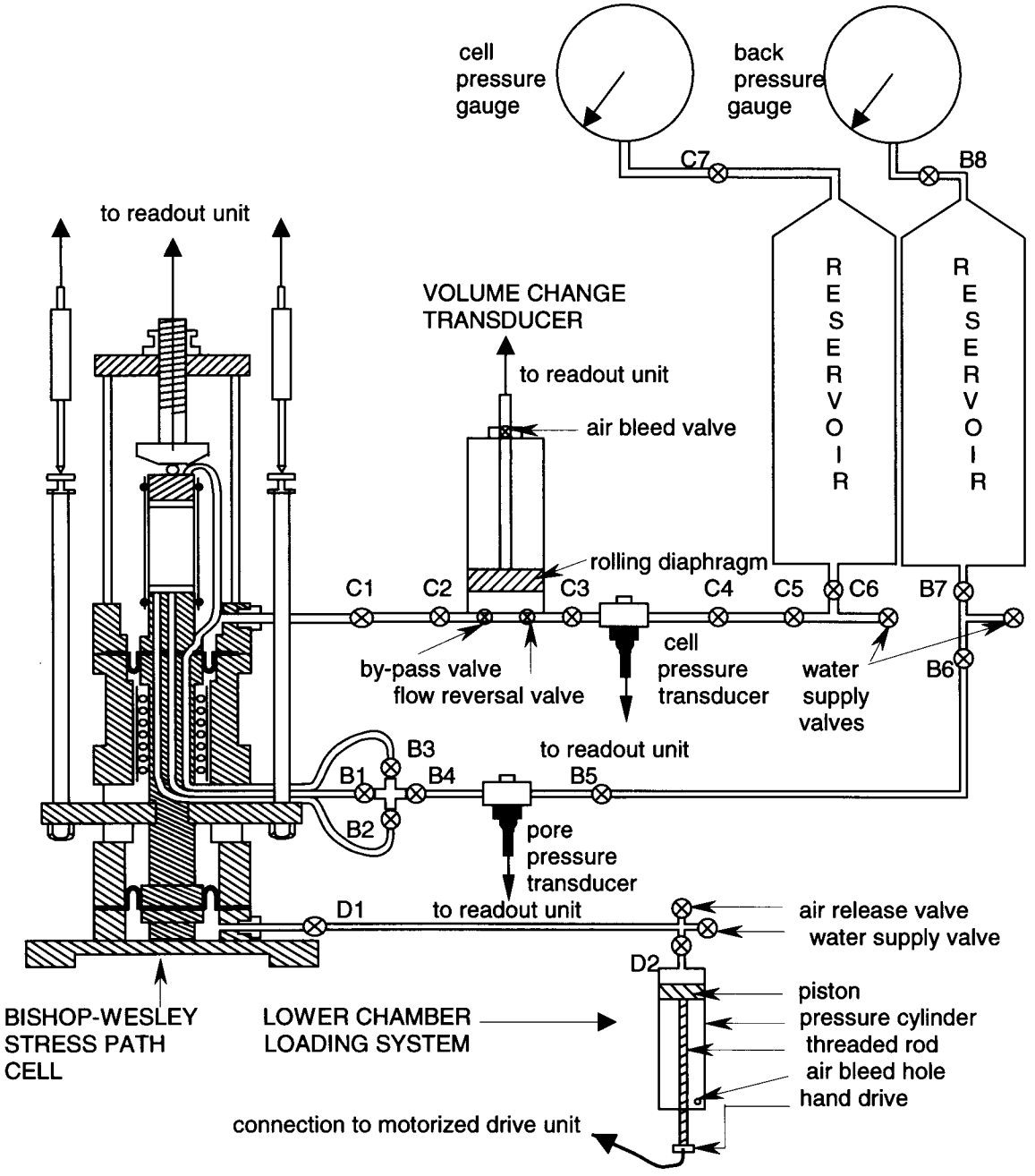


Figure 3.7 The Bishop-Wesley stress path cell and necessary pressure systems

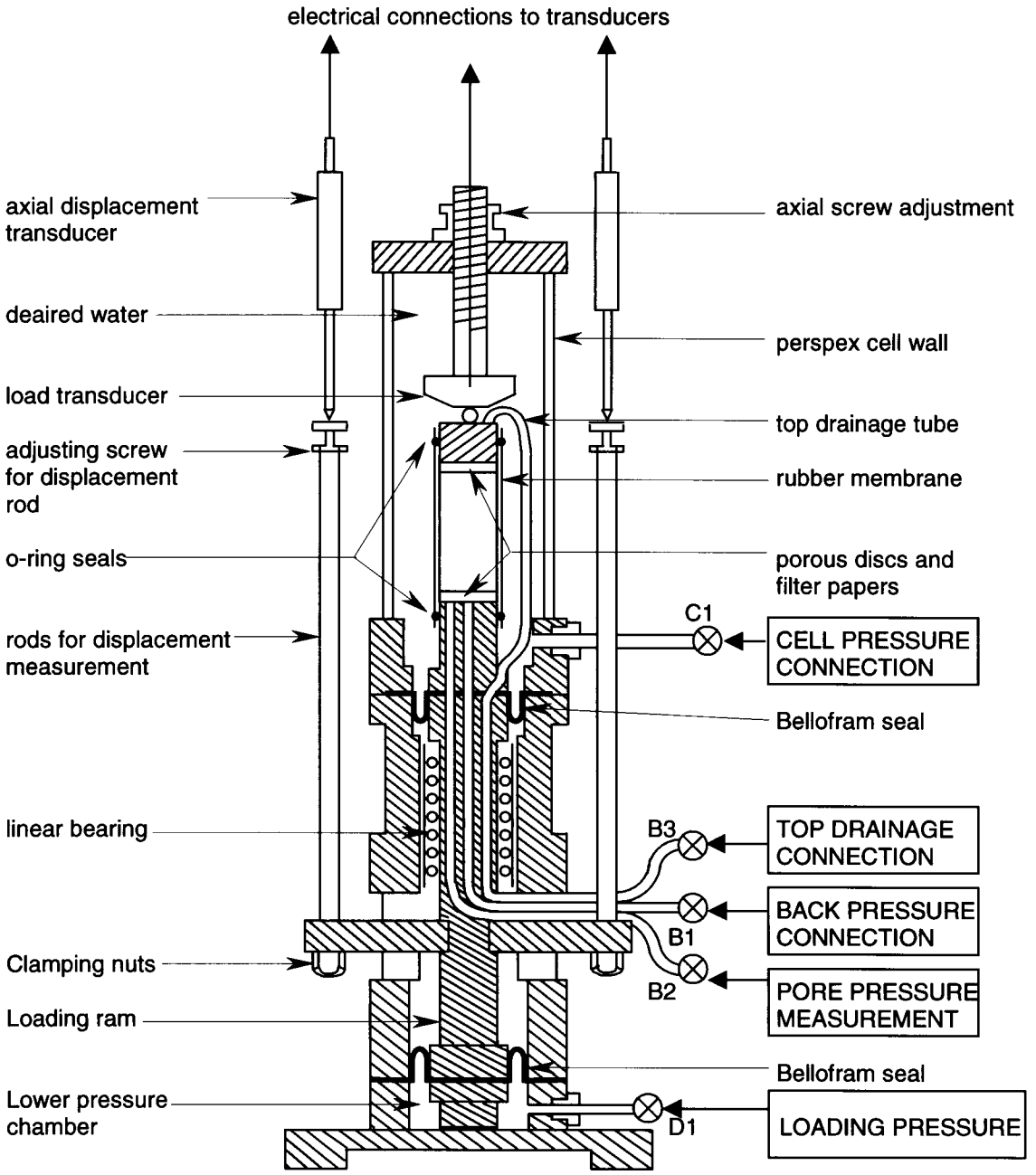


Figure 3.8 Details of the Bishop-Wesley stress path cell

The two base pedestal ports and the top cap drainage tube pass, separately, through the loading ram and exit the ram through the space between the rolling seals to their appropriate pressure connections.

The cross-arm attached to the loading ram supports two vertical rods which pass through clearance holes in the cell base and deflect the two axial displacement transducers mounted on the top of the cell. The axial transducers, therefore, measure the movement of the ram. If the top cap is in contact with the load transducer, the axial displacement transducers measure the change in length of the specimen.

Pressure systems

The cell pressure and back pressure lines are shown in Figure 3.7. Each line had a valve connecting to the overhead deaired water source. A reservoir was included in each pressure line to supply deaired water required for the test once the valves connecting to the deaired water source had been closed.

Pressures in both lines were applied and maintained by a motorized compressed air system with a maximum working pressure of 1000kPa.

Pressure transducers, one in each pressure line, were used for the measurement of pressures in the lines. The locations of the pressure transducers in each line can be seen in Figure 3.7.

A device for the measurement of volume change, the rolling diaphragm volume change transducer, was included in the cell pressure line as shown in Figure 3.7.

Back pressure was applied to the specimen through its top and base by the use of the top caps drainage connection and the two base pedestal ports.

Vertical loading system

The axial load was applied to the specimen by increasing the pressure in the lower pressure chamber. The lower chamber loading system, shown in Figure 3.7, was used for this purpose. A threaded shaft, the end of which consisted of a piston, was turned to cause the piston to progress into a pressure cylinder, whose diameter was the same as that of the piston, so as to compress water inside the cylinder. The shaft was turned automatically, at a desired speed, by using the motor drive unit or manually using the hand wheel. Axial load was measured by the load transducer.

Deaired water was supplied from the overhead deaired water source. The air bleed valve was used to remove air in the system as described in section 3.4.2.

Measurement of pore pressure

Pore pressure within the specimen was measured by the same transducer that was used to measure the back pressure. If the measurement was to be made without the effect of back pressure, valve B5 was closed to isolate the back pressure system.

Measurement of change in length of specimen

The vertical displacement of the loading ram was measured by the use of two axial displacement transducers mounted on the top of the cell. This displacement was equal to the change in length of the specimen if the specimen top cap was in contact with the stationary load transducer.

Measurement of radial deformation of specimen

Ideally, a radial strain belt similar to the K0-ring but fitted with a miniature submersible displacement transducer in place of the mercury indicator would be used for the measurement of radial deformations of the specimen. Due to the stiffness of the transducer cable, it was difficult to fit the belt to the specimen without disturbing it, especially because the specimens in this investigation were prepared 'very loose'. Instead of using the radial strain belt for the detection of lateral

deformation of specimens in order to maintain the K0-condition, the average K0 value derived from case 2 tests was used to back-calculate the axial load required to achieve the K0-condition.

Measurement of volume change

The rolling diaphragm volume change transducer in the cell pressure line was used for the measurement of volume into or out of the cell. The direction of flow in the volume change device was reversed, by operating the flow reversal valve, to allow more water to flow through the device when the rolling diaphragm had reached the end of its travel in a given flow direction. The volume change device could be isolated from the cell pressure line by operating the by-pass valve. The air bleed valve was used to deair the volume change device as described in section 3.4.2.

The actual volume change of the specimen during testing was obtained by deducting the effects of cell expansion and piston movement from the volume change measured by the volume change transducer.

Measurement and recording of test variables

Measurement of test variables, i.e. cell pressure, back pressure, pore pressure, axial load, vertical displacement of loading ram (change in length of specimen, if top cap is in contact with load cell) and volume change during testing were made electronically by the use of appropriate transducers. The locations of the individual transducers are highlighted in Figure 3.7. In Figure 3.9, a schematic layout of the electronic measurement and recording of test data is shown.

During saturation and consolidation stages of the test, there was no need to record the data by the computer as only one set of readings was recorded per day. Recording of the data was, therefore, done manually by selecting each channel on the data logger. During loading to failure, any desired time interval could be selected for scanning and recording of the data. This was useful because the computer selected each output channel in a rapid sequence without the need for manual switching.

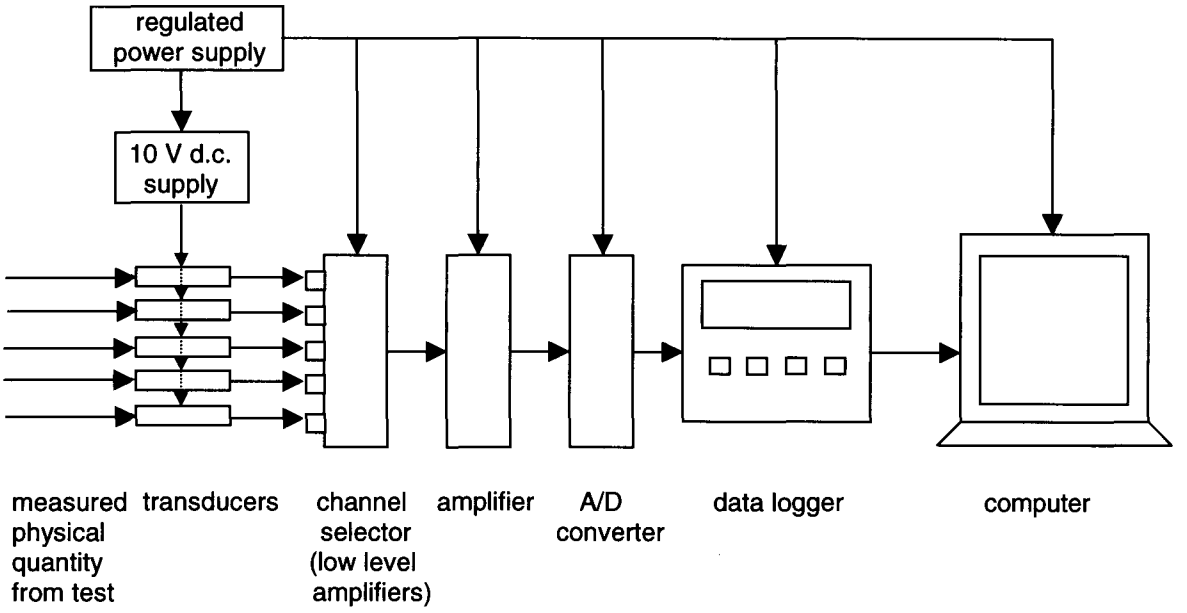


Figure 3.9 Schematic representation of the electronic measurement and recording of test data

Calibration of each transducer was necessary to obtain the relationship between the transducer electrical output (voltage or millivoltage) and the actual physical quantity being measured. Details are given in section 3.4.3.

3.4.2 Preparation of test equipment and pre-test checks

Cell and back pressure systems

Deairing: The pressure systems were deaired by allowing deaired water from the water supply to run through the lines while all valves were open (for the cell pressure system, the volume change device was first by-passed). This allowed any air in the system to be released at the cell base ports and the hole in the top cap.

When all air had been removed, the water supply valves were closed and no further deairing was required for the back pressure system.

The volume change device in the cell pressure line was deaired by allowing water from the deaired water supply to run through the line while the volume change

device was not by-passed and its air bleed valve was open. Air, if any, in the volume change device would be released through its air bleed valve while air trapped in the valves, manifold and connecting tubings would be pushed out through the line at the cell pressure port. When all the air had been removed, the air bleed valve was closed. All other valves were then closed.

Filling the reservoirs in the systems with deaired water: It was important to ensure that enough deaired water was present in the reservoirs. The reservoirs were filled with deaired water from the overhead water supply. The cell pressure reservoir was filled to capacity to enable filling of the cell before testing. The back pressure reservoir was filled to about half its capacity.

Checking for leaks in the cell pressure line: All valves leading from the cell pressure gauge to the cell base, except the water supply valve and the cell chamber valve, were opened. The volume change device was included in the system. The cell pressure gauge was set to maximum working pressure and the volume change indicated by the volume change device was observed. There would be change in volume, initially, due to the expansion of the connecting tubing but this would stop, or slow down substantially after some time if there was no leak(s) in the line. A continual change in volume indicated the presence of a leak(s), which could be traced (by first drying the connecting tubing and valves along the system and wiping with a dry paper later). The leak(s), if present, was eliminated. Having ensured that the cell pressure line was leak-free, the gauge pressure was reduced to zero and all valves were closed.

Checking for leaks in the back pressure line: Tapered plugs were tightly fitted in the two base pedestal ports and in the hole in the top cap and all valves leading from the back pressure gauge to the cell base, except the water supply valve, were opened. The back pressure gauge was set to maximum working pressure and held there for a period of time. Leak(s), if present, could be located by first drying the connecting tubing and valves along the system and wiping with a dry paper, later.

Deairing the lower pressure chamber and setting the loading ram at its extreme bottom position

Assumptions:

Initially, the cell body was not assembled to the base, the motor drive unit was off and all valves were closed.

Procedure:

1. The connections at valves D1 and D2, Figure 3.7, were loosened while these valves were closed. The water supply valve and the air bleed valve were opened to let deaired water from the water supply to flow out through the loose connections at valves D1 and D2 and the air bleed valve thereby displacing any air that could be trapped in the tubing connecting these valves. When all air had been removed, the loose connections at valves D1 and D2 were tightened and the air bleed valve was closed.
2. The valve connecting to the lower pressure chamber, valve D1, was opened to apply the overhead deaired water pressure to the lower pressure chamber to cause the loading ram to be pushed up to its extreme top position.
3. The water supply valve was closed and the air bleed valve was opened. This caused the pressure in the lower pressure chamber to drop to atmospheric pressure and allowed the loading ram to fall under its own weight thereby pushing air, if any, in the lower pressure chamber out through the air bleed valve. Additional pressure was applied by pushing the base pedestal down by hand to ensure that the loading ram reached its extreme bottom position.
4. The air bleed valve and the lower pressure chamber valve, valve D1, were closed.
5. To ensure that no air remained in the lower pressure chamber, steps 1 to 4 were repeated as many times as necessary.

Deairing the pressure cylinder and setting the loading piston of the pressure cylinder at the beginning of its travel

Assumptions:

The lower pressure chamber had been deaired as above and all valves of the lower chamber loading system were closed.

Procedure:

1. Step 1, above, was performed to deair the tubing connecting valves D1, D2, the air bleed valve and the water supply valve. All valves were closed.
2. The water supply valve and the valve connecting to the pressure cylinder, valve D2, were opened and the piston in the pressure cylinder was moved to the beginning of its travel by turning the hand wheel. When the piston was at this position, deaired water from the water supply flowed into the pressure cylinder and out through the air bleed hole located close to the end of the pressure cylinder, see Figure 3.7, thereby forcing any air in the cylinder out through this air bleed hole.
3. When all air had been removed from the pressure cylinder, the piston was driven into the pressure cylinder, by turning the hand wheel, just so that the air bleed hole was closed.
4. The pressure cylinder valve, valve D2, and the water supply valve were then closed.
5. Step 1 was repeated to ensure that no air remained in the tubing connecting valves D1, D2 the air bleed valve and the water supply valve.

Ancillary items

The following items were checked and prepared as described in section 3.2.2, for case 1 tests.

- Two porous discs;
- Two filter papers;

- Rubber membrane;
- 2 rubber o-ring seals;
- Cell body and cell base.

Electronic instruments

Power supply: With all the necessary transducers connected, the power supply was switched on a few hours before the start of a test to allow the transducers to warm up to their stable operating temperatures.

Checking the transducers: A small pressure, load or displacement was applied momentarily to the pressure transducer, load transducer or displacement transducer, respectively, to check whether the instruments and readouts were responding. For the volume change transducer, the cell pressure line was opened from the water supply through the volume change device to the cell chamber valve and the readout checked to determine whether it was responding.

Mounting the axial displacement transducers at convenient position on the cell top: Prior to starting the test, when the equipment was being used for the first time, it was convenient to ensure that the axial displacement transducers were clamped in position on to the cell top in such a way that only the straight line portion of the axial displacement transducer calibration curve would be used to interpret the axial displacement transducer readings during testing. It can be seen, from the axial displacement transducer calibration curve, Appendix B, Figure B11, that towards both extremes of the transducer stems, the calibration curve deviated from the straight line portion occurring at the middle portions of the stems. The procedure for ensuring that all the data from the axial displacement transducers fell within the straight-line portion of the calibration curve is given in Appendix B.

3.4.3 Calibration of equipment

The importance of calibration of equipment has been emphasized in section 3.2.3, for case 1 tests. For case 3 tests, each transducer was calibrated to obtain the relationship between the physical quantity being measured and the transducer

electrical readout. Detailed procedures used for the calibration of each of the transducers used for case 3 tests, calibration data and calibration curves are given in Appendix B. Also included in Appendix B are the calibration procedure, calibration data and calibration curve for cell and connecting tubing expansion volume change against pressure and time.

3.4.4 Preparation of test specimens

Specimens for liquefaction testing in the Bishop-Wesley stress path cell were prepared using the method described in section 3.2.4, for case 1 tests. However, due to the size limitation imposed by the equipment, only 38mm x 76mm specimens were used.

3.4.5 Setting up of specimens in the Bishop-Wesley stress path cell

The method used for setting up specimens in the Bishop-Wesley stress path cell was similar to that given in section 3.2.5, for case 1 tests, except that in this case the top cap was brought to contact with the load transducer before testing.

Assumptions

The equipment had been prepared and checked according to section 3.4.2.

Procedure

1. The procedure given in section 3.2.5, for setting up of specimens for case 1 tests, was followed up to the point when the specimen had been covered with a rubber membrane and the membrane was sealed onto the top cap and base pedestal by o-ring seals.
2. The axial screw adjustment of the load transducer was turned to bring the load transducer up at its fullest extent.
3. The cell body was lowered into position over the specimen, taking care not to pull the load and axial displacement transducer cables off from their connections to the power supply.

4. The cell was tightened by turning the clamping nuts with controlled torque and the initial axial displacement transducer reading was recorded. This corresponded to the loading ram being at its extreme bottom position, and would only change when the lower chamber pressure was applied to lift the loading ram.
5. The load transducer was brought into contact with the top cap by turning the axial screw adjustment, slowly and carefully, so as to avoid pressing on the specimen. The initial load transducer reading was then recorded.
6. The cell was filled with deaired water from the cell pressure line's reservoir while the volume change device was by-passed. When water emerged from the top air release valve, the cell chamber valve and the water supply valve were closed. The top air release valve was left open until the beginning of test.

3.4.6 Saturation of specimens

Air-flushing of specimens

As in case 1 and case 2 tests, specimens for liquefaction testing in the Bishop-Wesley stress path cell were air-flushed in order to minimize the loss in void ratio during the subsequent back pressure saturation stage. The arrangement for air-flushing of specimens for case 3 tests is shown in Figure 3.10.

Procedure:

1. Air-flushing of specimens for case 3 tests was carried out in the same way as described in section 3.2.6, for case 1 tests, except that here the back pressure burette was connected to both the two base pedestal ports at the same time, as shown in Figure 3.10.
2. When air-flushing was completed, valves B3 and B5 of the top drainage and back pressure burettes were closed. The cell pressure valve, valve C1, and the pore pressure measurement line (from the base of the specimen through valves B1, B2 and B4 to the pore pressure transducer) were not closed yet. Time was allowed for the pore pressure transducer reading to stabilize under the action of

the cell pressure, i.e. the height of water in the cell pressure burette above the midheight of the specimen.

3. The pore pressure transducer reading was recorded when stable. The cell chamber valve, valve C1, and the pore pressure measurement line's valves B1, B2 and B3 were closed.
4. The pore pressure transducer reading was converted to pore pressure by the relationship obtained from the calibration curve of the pore pressure transducer, Appendix B, Figure B2, as follows:

$$pwp = (pwp\ (volt) + 0.1828) / 0.1003 \quad (3.16)$$

Where:

pwp = Pore pressure in kPa;

pwp (volt) = Pore pressure transducer reading, millivolts.

5. The height of water in the cell pressure burette above the midheight of the specimen was measured and converted to cell pressure by the following equation:

$$P = pgh \quad (3.17)$$

Where:

P = Cell pressure, kPa;

p = Density of water, 1000 kg/m^3

g = Gravitational acceleration, 10 m/s^2;

h = Height of water in the cell pressure burette above the mid-height of the specimen, m.

Saturation by increments of back pressure

Saturation of specimens for case 3 tests was carried out in such a way that the ratio of the effective horizontal and effective vertical stresses acting on the specimen was constant and equal to K0 (derived from case 2 tests) throughout all stages of saturation.

Before any increments of cell and back pressure could be applied to the specimen, it was necessary to calculate the vertical load to be applied along with these pressure increments in order to maintain the K0-condition. The required load was expressed in terms of load transducer voltage reading. The correction for load transducer response to cell pressure was added to the required load transducer reading to obtain the load transducer reading to be displayed by the load transducer readout.

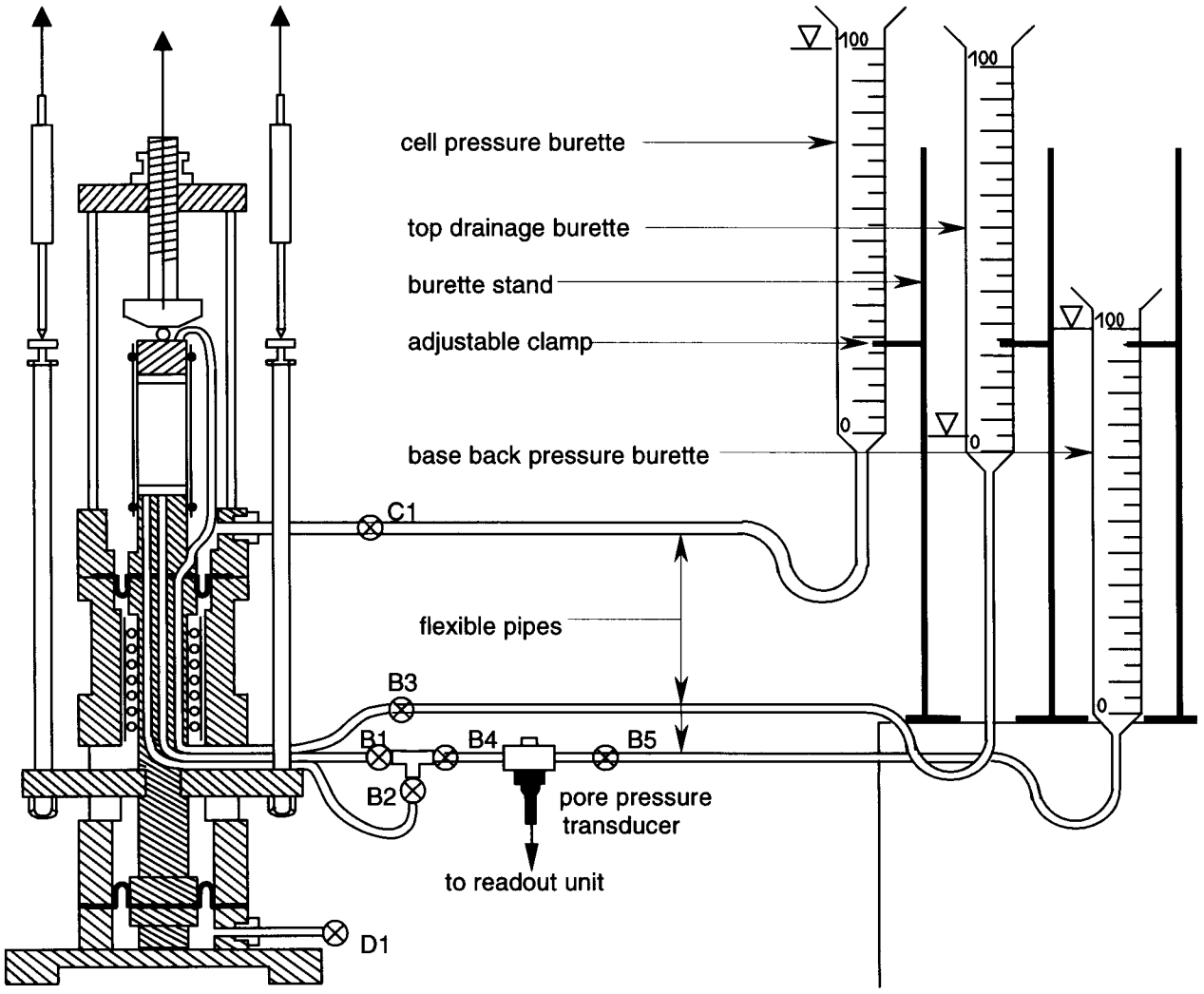


Figure 3.10 Arrangement for displacing air in the voids of a specimen by water at the lowest pressures (Air-flushing)

Determination of axial load required to maintain K0-condition during saturation

Stresses acting on specimen:

$$\sigma_H = cp \quad (3.18)$$

$$\sigma'_H = cp - bp \quad (3.19)$$

$$\sigma_V = Load_{spec} / A_o + cp \quad (3.20)$$

$$\sigma'_V = Load_{spec} / A_o + cp - bp \quad (3.21)$$

Where:

σ_H = Total horizontal stress, kPa;

σ'_H = Effective horizontal stress, kPa;

σ_V = Total vertical stress, kPa;

σ'_V = Effective vertical stress, kPa;

cp = Cell pressure, kPa;

bp = Back pressure, kPa;

$Load_{spec}$ = Axial force to be applied to the specimen by the lower chamber pressure system, for K0-condition, dN;

A_o = Initial (set-up) cross-sectional area of the specimen, cm^2.

For K0-condition:

$$\sigma'_H / \sigma'_V = K0 \quad (3.22)$$

i.e.

$$K0 = [(cp - bp)] / [(Load_{spec} / A_o) + cp - bp] \quad (3.23)$$

Therefore,

$$Load_{spec} = A_o[(cp - bp) / K0 + bp - cp] \quad (3.24)$$

Equation (3.24) was then converted to proving ring divisions using the calibration factor of the proving ring that was used to calibrate the load transducer, i.e. 25.77dN/div:

$$R = Load_{spec} / 25.77 \quad (3.25)$$

Where:

R = Proving ring divisions corresponding to the axial force to be applied to the specimen by the lower chamber pressure system, divisions.

Expressing saturation stresses in terms of transducers voltage readings

The cell pressure, back pressure and proving ring divisions required for K0-condition during saturation were expressed in terms of transducer voltage readings using the equations of the appropriate calibration curves (Appendix B: Figures B1, B2, and B4, respectively). The equations were as follows:

$$cp(volt) = 0.1004 \times cp + 0.5553 \quad (3.26)$$

$$bp(volt) = 0.1003 \times bp - 0.1828 \quad (3.27)$$

$$Load_{spec}(volt) = 0.0173 \times R - 0.0469 \quad (3.28)$$

Where:

cp(volt) = Cell pressure transducer reading, millivolts;

cp = Cell pressure, kPa;

bp(volt) = Back/ Pore pressure transducer reading, millivolts;

bp = Back pressure, kPa;

$Load_{spec}(volt)$ = Load transducer reading, Volts;

R = Proving ring divisions corresponding to the axial force to be applied to the specimen by the lower chamber pressure system, divisions.

Correction to load transducer reading for effect of cell pressure

The load transducer voltage reading displayed by the readout unit at any stage of testing represented the combined effects of the cell pressure and the axial force applied to the specimen by the lower chamber pressure system.

It was therefore necessary to add the two effects in order to obtain the correct load transducer reading that had to be displayed by the readout unit for K0-condition during back pressure saturation.

The effect of cell pressure on the load transducer reading was determined from the equation of the load transducer versus cell pressure calibration curve in Appendix B, Figure B5 as follows:

$$Load_{cp}(volt) = -6x10^{-7}(cp)^2 + 0.0008(cp) + 0.0348 \quad (3.29)$$

Where:
$Load_{cp}(volt)$ = Load transducer reading resulting from the action of cell pressure, V;
cp = Cell pressure, kPa.

The correct load transducer voltage reading required for K0-condition was obtained by adding equations (3.28) and (3.29):

$$Load_{corr}(volt) = Load_{spec}(volt) + Load_{cp}(volt) \quad (3.30)$$

Where:
$Load_{corr}(volt)$ = Corrected load transducer reading, V.

Application of cell pressure, back pressure and vertical load to the specimen

Assumptions:

The specimen had been air-flushed as described above and all valves were closed.

Procedure:

1. The burette connections at valves C1, B3 and B5, Figure 3.10, were disconnected while these valves were still closed.
2. The cell pressure and back pressure lines were loosely connected at valves C1 and B5, respectively.

3. Valves B1, B2, B3 and B4 were joined, as shown in Figure 3.7, while these valves were still closed. To remove air that could be trapped at the loose connections when the burettes were replaced by pressure connections, deaired water from the water supply was allowed to run through the pressure lines and the connections were tightened while water was dripping out of them.
4. The rolling diaphragm of the volume change device was positioned at roughly midway of its full range of travel in order to accommodate volume into the cell (due to cell pressure) and volume out of the cell (due to progression of loading ram into the cell). This was done by loosening the cell pressure line's connection to the cell chamber valve and allowing deaired water from the water supply to run through the cell pressure line via the volume change device while observing the volume change transducer reading. The connection was tightened when the volume change transducer reading approached the middle of its full range, observed during calibration.
5. All valves along the cell pressure line, except the water supply valve and the cell chamber valve, valve C1, were opened. The volume change device was included in the cell pressure line.
6. The cell pressure gauge was adjusted so that the cell pressure transducer reading corresponded to 0kPa (equation (3.26)) and the volume change transducer reading was recorded when stable (this represented the initial volume change transducer reading with the cell pressure being 0kPa and the cell chamber valve closed).
7. The cell pressure gauge was adjusted so that the cell pressure transducer reading corresponded to 50kPa (equation (3.26))
8. The cell chamber valve, valve C1, was opened to apply the cell pressure increment to the specimen and then valves B1, B2, B3 and B4 were opened to enable measurement of pore pressure. The pore pressure transducer reading was recorded when stable and was converted to pore pressure by equation (3.16).
9. The degree of saturation was calculated as follows:

$$\text{B value} = (PWP_2 - PWP_1) / (CP_2 - CP_1) \qquad (3.31)$$

Where:

PWP_2 = Pore pressure in step 8 above, kPa;

PWP_1 = Pore pressure in step 4 of air-flushing, kPa;

CP_2 = Cell pressure in step 7 above, kPa;

CP_1 = Cell pressure in step 5 of air-flushing, kPa.

10. Valve B4 was closed and all valves along the back pressure line except the water supply valve were opened. This isolated the back pressure line and the pore pressure transducer from the specimen. The back pressure gauge was adjusted so that the pore pressure transducer reading corresponded to 40kPa (equation (3.27)).
11. Valve B4 was opened to apply the back pressure increment to the specimen through its top and base.
12. All valves along the lower chamber loading system, except the water supply valve and the air bleed valve, were opened.
13. The motor drive unit of the lower chamber loading system was switched on at its lowest speed and the rate at which the load transducer reading approached the target value given by equation (3.30) was observed. If the rate was too slow, the speed was carefully increased. As soon as the load transducer reading hit the target value, the motor unit was switched off. When the motor unit was off, the load transducer reading tended to drop due to the reduction in contact between the load cell and the specimen top cap as the specimen height continued to decreased under the effect of cell pressure. It was therefore necessary to continuously adjust the lower chamber pressure to maintain the K0-condition load transducer reading.
14. After 24 hours of application of the cell pressure increment, the cell pressure, back pressure, load, axial displacement and volume change transducer readings were recorded and valve B5 was closed to isolate the back pressure system from the specimen while leaving the pore pressure transducer connected to the specimen.
15. The cell pressure transducer reading was converted to cell pressure by equation (3.26).
16. The pore pressure transducer reading was recorded when stable and converted to pore pressure by equation (3.16).

17. The cell chamber valve, valve C1, was closed and the cell pressure gauge was adjusted so that the cell pressure transducer reading corresponded to 100kPa, i.e. an increment of 50kPa, using equation (3.26).
18. The cell chamber valve was opened and time was allowed for the resulting pore pressure transducer reading to stabilize. The pore pressure transducer reading was recorded when stable and converted to pore pressure by equation (3.16).
19. The degree of saturation, B value, was calculated as follows:

$$\text{B value} = (PWP_2 - PWP_1) / (CP_2 - CP_1) \qquad (3.32)$$

Where:

PWP_2 = Pore pressure in step 18 above, kPa;

PWP_1 = Pore pressure in step 16 above, kPa;

CP_2 = Cell pressure in step 17 above, kPa;

CP_1 = Cell pressure in step 15 above, kPa.

20. Valve B4 was closed and valve B5 was opened to isolate the pore pressure transducer from the specimen and include it to the back pressure line. The back pressure gauge was adjusted so that the pore pressure transducer reading corresponded to 90kPa, i.e. an increment of 50kPa, using equation (3.27).
21. Valve B4 was opened to apply the back pressure increment to the specimen.
22. The lower chamber loading system was switched on at the previous speed and the load transducer reading observed.
23. When the load transducer reading reached the target K0-condition value calculated by equation (3.30) using the cell pressure and back pressure in steps 17 and 20, respectively, the lower chamber loading system was switched off. The lower chamber loading system was regularly operated to maintain the K0-condition load transducer reading.
24. After 24 hours of application of the cell pressure increment, the cell pressure, back pressure, load, axial displacement and volume change transducer readings were recorded and valve B5 was closed to isolate the back pressure system from the specimen while leaving the pore pressure transducer connected to the specimen.

25. Steps 15 to 24 were repeated with increments of cell pressure and back pressure of 50kPa, until the B value at step 19 was equal to or greater than 0.97, at which point the specimen was considered to be fully saturated.
26. After confirming the B value to be equal to or greater than 0.97 (step 19, above), steps 20 to 23 were carried out and consolidation was immediately performed as described below.

3.4.7 Consolidation to the required K0-condition stress state

The specimen was consolidated to the required K0-condition stress state by leaving the back pressure at its final saturation value and increasing the cell pressure and vertical load appropriately to maintain the K0-condition.

Procedure

1. Having chosen a final consolidation effective confining pressure, σ'_{Hf}, the required final consolidation cell pressure, σ_{Hf}, was calculated from the final saturation back pressure, bp_f, as follows:

$$\sigma_{Hf} = \sigma'_{Hf} + bp_f \tag{3.33}$$

2. The required final consolidation cell pressure was converted to cell pressure transducer reading by equation (3.26).
3. The corresponding load transducer reading required for K0-condition was obtained from equation (3.30), using the final cell and back pressures.
4. In order to reduce the deviation of the actual consolidation stress path from the K0-consolidation line, the cell pressure increment required to get to the final consolidation cell pressure was subdivided into smaller increments (typically 5-10kPa) and the corresponding cell pressure transducer and load transducer readings were calculated for each sub-increment by equations (3.26) and (3.30), respectively. The cell pressure and lower chamber pressure were increased simultaneously by these subdivisions until the final required cell pressure and load transducer readings were reached.

5. The lower chamber loading system was continuously operated to maintain the K0-condition load transducer reading. The specimen was allowed to consolidate for 24hours, after which undrained loading was carried out.

3.4.8 Undrained loading stress paths

Specimens for case 3 tests were loaded by following either a constant deviator stress, decreasing confining pressure undrained loading path or a constant effective mean normal stress, decreasing confining pressure undrained loading path. The procedures for each of these loading stress paths are given below.

Constant deviator stress, decreasing confining pressure- undrained loading path

This loading stress path was followed by maintaining the deviator stress acting on the specimen, before loading, constant while the loading piston progressed into the cell chamber at a constant rate of strain by appropriately reducing the cell confining pressure.

The deviator stress acting on the specimen at any point in time during loading was given by the quotient of the axial load applied to the specimen (by the bottom chamber pressure system) and the cross-sectional area of the specimen. Since the cross-sectional area of the specimen changed as the specimen was strained, the axial load applied to the specimen had to be adjusted accordingly in order to keep the deviator stress constant.

Prior to loading, it was therefore necessary to calculate the cross-sectional area of the specimen at convenient intervals of axial strains and determine the corresponding load transducer readings required to maintain the constant deviator stress condition.

During loading, the loading piston would progress into the cell chamber, at a constant rate of strain, and compress the specimen and therefore cause a rise in the load transducer reading displayed by the readout unit. To maintain a constant

deviator stress condition, the cell pressure was reduced in such a manner that the predetermined load transducer reading corresponding to the given axial strain be displayed by the readout unit. However as soon as the load transducer reading ceased to increase, it was assumed that the collapse surface had been reached and no further reduction of cell pressure was done.

The effect of cell pressure on the load transducer reading displayed by the readout unit at any time during loading was not possible to account for in the predetermination of load transducer reading required for constant deviator stress condition since this would require that the cell pressure be reduced in some controlled predetermined rate, however this was not the case since at any point during loading, the cell pressure was reduced by an amount and a rate necessary to keep the deviator stress constant and this was unknown until loading was done.

Pre-loading calculations:

Change in height of specimen after saturation and consolidation

The average slope of the straight-line portions of the axial displacement transducer calibration curves, Appendix B, Figure B11, was used.

$$\Delta L = \Delta L(volt) \times 0.2141 \qquad (3.34)$$

Where:

ΔL = Change in height of the specimen after saturation and consolidation, mm;

$\Delta L(volt)$ = Total change in axial displacement transducer reading after saturation and consolidation, V.

Consolidated height of specimen

$$L_{cons} = L_o - \Delta L \qquad (3.35)$$

Where:

L_{cons} = Height of the specimen, after consolidation, mm;

L_o = Initial (set-up) height of the specimen, mm.

Consolidated cross-sectional area of specimen

$$A_{cons} = A_o = \pi \times (D_o/10)^2 / 4 \quad (3.36)$$

Where:

A_{cons} = Cross-sectional area of the specimen, after consolidation, cm^2;

A_o = Initial (set-up) cross-sectional area of the specimen, cm^2;

D_o = Initial (set-up) diameter of specimen, mm.

Time to failure

The time to failure was chosen as for case 1 and 2 tests. Usually six hours were used. The time to failure was used to calculate the rate of loading and it was split into smaller time intervals of 30 seconds each so that the axial strain and corresponding load transducer reading required for constant deviator condition could be determined for the end of each of these time intervals.

Rate of loading [ROL(mm/s)]

ROL(mm/s) = ultimate strain x consolidated height of specimen / time to failure (3.37)

Where:

Ultimate strain was taken to be 20% of the consolidated height of the specimen.

Rate of change of axial displacement transducer reading [ROL(volt/s)]

The average slope of the straight-line portions of the axial displacement transducer calibration curves, Appendix B, Figure B11, was used.

ROL(volt/s) = ROL(mm/s) x 0.2141 (3.38)

Axial strain at any time during loading, ε_t

$$\varepsilon_t = ROS(mm/s) / L_{cons} \times t \quad (3.39)$$

Where:
t is the time, in seconds, from start of loading.

Cross-sectional area of specimen at any time during loading, A_t

$$A_t = A_{cons} / (1 - \varepsilon_t) \quad (3.40)$$

Initial deviator stress acting on the specimen, before loading

First, the load transducer reading corresponding to the force applied to the specimen by the lower chamber pressure, before loading, was calculated as follows:

$$Load_{spec(0)}(volt) = Load_0(volt) - Load_{CP(0)}(volt) \quad (3.41)$$

Where:
$Load_{spec(0)}(volt)$ = Load transducer reading corresponding to the force applied to the specimen by the lower chamber pressure before loading, V;
$Load_0(volt)$ = Load transducer reading displayed by the readout unit before loading, V;
$Load_{CP(0)}(volt)$ = Load transducer reading obtained by substituting the consolidation cell pressure into the equation of the load transducer versus cell pressure calibration curve, equation (3.29), V.

The load transducer reading in equation (3.41) was converted to force using the load transducer versus axial force calibration curve's equation, equation (3.28), and the calibration factor of the proving ring that was used to calibrate the load transducer, i.e. 25.77dN/div:

$$Load_{spec(0)} = 25.77 / 0.0173 \times [\, Load_{spec(0)}(volt) + 0.0469 \,] \quad (3.42)$$

Where:

$Load_{spec(0)}$ = Force applied to the specimen by the lower chamber pressure, before loading, dN.

The initial deviator stress was then calculated as follows:

$$q_0 = Load_{spec(0)} / A_{cons} \quad (3.43)$$

Where:

q_0 is the deviator stress before loading, kPa.

Axial force required to maintain deviator stress constant [$Load_{spec(t)}$]

$$Load_{spec(t)} = q_0 \times A_t \quad (3.44)$$

Load transducer reading corresponding to the required axial force

The load transducer versus axial force calibration equation, equation (3.28), and the proving ring calibration factor, 25.77dN/div, were used:

$$Load_{spec(t)}(volt) = (0.0173 / 25.77) \times Load_{spec(t)} - 0.0469 \quad (3.45)$$

Where:

$Load_{spec(t)}(volt)$ = Load transducer reading corresponding to the force required to maintain constant deviator stress condition (effect of cell pressure not accounted for).

Loading procedure:

1. The time to failure was split into convenient time intervals of 30 seconds each and the axial strain and corresponding load transducer reading required for constant deviator stress condition were calculated for the end of each of these time intervals using equations (3.39) and (3.45), respectively.

2. The back pressure line was isolated from the cell, while leaving the pore pressure transducer connected to the specimen, by closing valve B5.
3. The motor drive unit of the lower chamber loading system was switched on at the required rate of loading, equation (3.37), and a timer was started.
4. The cell pressure gauge was appropriately adjusted to achieve the load transducer reading required at the end of each time interval.
5. As soon as the load transducer reading ceased to change, no further reduction of cell pressure was done.
6. Loading was stopped when the time to failure had been reached. However, if the load and/or pore pressure transducer had not stabilized, the test was allowed to run beyond the required time to failure.

Constant effective mean normal stress, decreasing confining pressure-undrained loading path

This loading stress path was achieved by maintaining the effective mean normal stress acting on the specimen, before loading, constant during undrained loading.

This stress path involved the monitoring of an extra variable, the pore pressure. To reduce the number of test variables and therefore simplify the loading procedure, the cell pressure was reduced at a constant predetermined rate.

Constant effective mean normal stress was then achieved by adjusting the axial force applied to the specimen by the lower chamber pressure system (rate of loading) so that the relationship between cell pressure, pore pressure and axial force applied to the specimen by the lower chamber pressure system required for this stress path was satisfied during loading.

The rate of strain was consequently not constant during loading and the predetermination of cross sectional area of the specimen during loading was therefore not possible. In the relationship between cell pressure, pore pressure and axial force required for constant effective mean normal stress, the cross- sectional area of the specimen during loading was taken as constant and equal to the cross-sectional area after consolidation. This introduced the error in the loading path,

however, since axial strains at the initiation of liquefaction are very small, the change in cross-sectional area of the specimen at the initiation of liquefaction is also small and this error was therefore not very significant.

As in the case of constant deviator stress loading, the time to failure was split into 30 seconds time intervals. The cell pressure at the end of each 30 seconds time interval was determined. The effect of cell pressure on the load transducer readings during loading could therefore be accounted for prior to loading.

Pre-loading calculations:

In addition to equations (3.34) to (3.36), the following calculations were done prior to loading:

Time to failure

The time to failure was chosen as for case 1 and 2 tests. Six hours were usually used. The time to failure was split into 30 seconds time intervals so that cell pressures at the end of each of these time intervals and the corresponding load transducer readings could be determined prior to loading.

Effective mean normal stress acting on the specimen

$$p' = (\sigma'_1 + 2\,\sigma'_3) / 3 \qquad (3.46)$$

But

$$\sigma'_1 = Load_{spec} / A + \sigma'_3 \qquad (3.47)$$

$$\sigma'_3 = cp - pwp \qquad (3.48)$$

Where:

p' = Effective mean normal stress, kPa;

σ'_1 = Effective vertical stress, kPa;

σ'_3 = Effective horizontal stress, kPa;

$Load_{spec}$ = Axial force applied to the specimen by the lower chamber pressure system, dN;

A = Cross-sectional area of the specimen, cm^2;

cp = Cell pressure, kPa;

pwp = Pore pressure, kPa.

For constant effective mean normal stress,

$$\Delta\sigma'_1 = -2\Delta\sigma'_3 \tag{3.49}$$

Therefore,

$$-2\,\Delta[cp - pwp] = \Delta[Load_{spec} / A + cp - pwp] \tag{3.50}$$

or

$$\Delta[Load_{spec} / A] = -3\Delta cp + 3\Delta pwp \tag{3.51}$$

Equation (3.51) was expressed in terms of transducer readings using equations (3.26), (3.27) and (3.28):

$$25.77\,[\Delta Load_{spec}(volt)] / 0.0173\,A = -3\Delta cp(volt) / 0.1004 + 3\Delta pwp(volt) / 0.1003 \tag{3.52}$$

Where:

$Load_{spec}(volt)$ = Load transducer reading corresponding to the axial force applied to the specimen by the lower pressure system, V;

cp(volt) = Cell pressure transducer reading, mV;

pwp(volt) = Pore pressure transducer reading, mV.

Applying the correction for cell pressure effect on the load transducer reading, substituting A by A_{cons} and rearranging gives:

$$-3\Delta cp(volt) / 0.1004 + 3\Delta pwp(volt) / 0.1003 = 25.77\,[\Delta Load_{corr}(volt) - \Delta Load_{cp}(volt)] / 0.0173 A_{cons} \tag{3.53}$$

Where:

$Load_{corr}$(volt) = Corrected load transducer reading to be displayed by the readout unit, V;

$Load_{cp}$(volt) = Correction to load transducer reading for effect of cell pressure, equation (3.29), V.

Note that in equation (3.53), the unknowns were Δpwp(volt) and $\Delta Load_{corr}$(volt).

Loading procedure:

1. The time to failure was split into convenient time intervals of 30 seconds each. Using cell pressure decrements of 10kPa, the cell pressures at the end of each of these 30 seconds time intervals were calculated and the corresponding load transducer readings were determined by equation (3.29). The required cell pressure transducer reading at the end of each 30-second time interval was determined using equation (3.26).
2. The back pressure line was isolated from the cell, while leaving the pore pressure transducer connected to the specimen, by closing valve B5.
3. The motor drive unit of the lower chamber loading system was switched on at the previous speed and a timer was started.
4. At the beginning of each 30 seconds time interval, the cell pressure decrement was applied to the specimen.
5. The motor drive unit of the lower chamber pressure loading system was operated to adjust the speed of loading so that the relationship between pore pressure and load transducer readings given by equation (3.53) was satisfied at the end of each of the 30 seconds time intervals.
6. As soon as the load transducer reading ceased to increase, the cell pressure was left unchanged and loading was allowed to continue without adjustments of the rate of loading.
7. Loading was stopped after reaching the time to failure. However, if the transducer readings had not ceased to change, the test was allowed to continue beyond the time to failure.

This chapter has described the procedures followed to carry out the liquefaction tests in this investigation. The next chapter is concerned with the test data obtained in these test. It describes the calculation of relevant test parameters that are necessary to interprete the behavior of the Merriespruit gold tailings under the various cases of tests performed in this investigation.

4 TEST RESULTS

4.1 Overview

Data recorded during the tests described in Chapter 3 was used to calculate the relevant test parameters that are necessary to interpret the behavior of Merriespruit gold tailings under various triaxial test loading conditions.

For each test specimen, the observed and calculated data is presented in the form of a datasheet accompanied by plots of deviator stress- axial strain, pore pressure- axial strain, and stress path.

The formats of the datasheets for the various categories of undrained triaxial tests performed in this study are slightly different owing to the different test conditions and different means of measurement of test variables. Accordingly, special formats were designed for datasheets of the various test categories.

Due to the large number of tests performed in this investigation and the space taken by the results of each of the test specimens (2 A4 pages), the results for all the tests are extensive and are conveniently included in Appendices C, D, and E for case 1, case 2 and case 3 tests, respectively.

This chapter describes the calculation of relevant test parameters from the data recorded under the various categories of tests and the organization of the datasheets for each category of tests.

4.2 Monotonic Undrained Compression of Isotropically Consolidated Specimens (case 1 tests)

A typical datasheet containing the results of a triaxial test specimen under case 1 test is shown on pages 131 and 132. The plots of deviator stress- axial strain, pore pressure- axial strain and stress path are also included at the end of the datasheet, as per the format designed for this series of tests.

4.2.1 Description of the format of the datasheet and the calculation of various test parameters

The **top block of data** provides information about the type of test, the fines content and the specific gravity of the specimen under consideration, the particular triaxial cell used for the test, and the designation of the specimen.

The contents of the rest of the datasheet are considered below:

Sample physical properties

Wet mass before test, moisture content before test, and dry mass of specimen: The wet mass and moisture content of the specimen after specimen preparation were used to calculate the dry mass of the specimen using equation (3.7).

Initial height and initial diameter of the specimen: The initial height and diameter of the specimen were measured using a caliper by the method described in Chapter 3, section 3.2.4, step 9.

Cross-sectional area, volume, void ratio and dry density of the specimen: The following equations were used for the determination of the initial cross-sectional area, initial volume, initial void ratio and dry density of the specimen:

$$\text{Area} = \pi \times (\text{Diameter}/10)^2 / 4 \quad (4.1)$$

$$\text{Volume} = \text{Area} \times (\text{Height} / 10) \quad (4.2)$$

$$\text{Void ratio} = (\text{Volume} - \text{Dry mass} / \text{Specific gravity}) / (\text{Dry mass} / \text{Specific gravity}) \quad (4.3)$$

$$\text{Dry density} = \text{Dry mass} / \text{Volume} \quad (4.4)$$

Where:
Height, Diameter, Area, and Volume are expressed in mm, mm, cm^2, and cm^3, respectively.

Test	**Case 1: Monotonic Undrained Compression of Isotropically Consolidated Specimens**		
Cell No.	6 (Big)	Fines content (%)	0
Specimen	6c	Specific gravity (g/cm^3)	2.72

1.) Sample physical properties

Wet mass before test (g)	865.889	m.c before test (%)	8.30	Height (mm)	151.35	Volume (cm^3)	687.497
Wet mass after test (g)	971.427	m.c. after test (%)	21.50	Diameter (mm)	76.05		
Dry mass (g)	799.528	Dry density (kg/m^3)	1163	Area (cm^2)	45.424	Void ratio (e_0)	1.339

2.) Saturation/Consolidation

Date	C.P (kPa)	P.W.P bp closed (kPa)	B.P (kPa)	P.W.P bp open (kPa)	Change C.P (kPa)	Change P.W.P (kPa)	B value	Volume Gauge (cm^3)	Cell Expansn (cm^3)	Specimen Volume (cm^3)	Void Ratio	Comments
3/10	0		0	-1.5				0.00	0.00	687.497	1.339	
3/10	10.6		8.0	5.5				6.55	0.00	680.947	1.317	**AIR-FLUSHING**
3/10	50	15.5	40	39.5	39.4	10.0	0.25	14.93	3.82	676.387	1.301	**S**
4/10	100	60.5	90	90.0	50	21.0	0.42	20.52	7.94	674.917	1.296	**A**
5/10	150	119.0	140	140.0	50	29.0	0.58	25.89	10.71	672.317	1.287	**T**
6/10	200	176.0	190	190.0	50	36.0	0.72	30.02	12.51	669.987	1.279	**U**
7/10	250	230.5	240	240.0	50	40.5	0.81	32.68	13.93	668.747	1.275	**R**
8/10	300	283.0	290	290.0	50	43.0	0.86	35.20	15.40	667.697	1.272	**A**
9/10	350	335.5	340	340.0	50	45.5	0.91	37.52	16.91	666.887	1.269	**T**
10/10	400	387.0	390	390.0	50	47.0	0.94	39.68	18.26	666.077	1.266	**I**
11/10	450	438.0	440	440.0	50	48.0	0.96	42.37	20.38	665.507	1.264	**O**
12/10	500	489.0	490	450.0	50	49.0	0.98					**N**
12/10	700		500	500.0				57.05	27.57	658.017	1.239	**CONSOLIDATION**

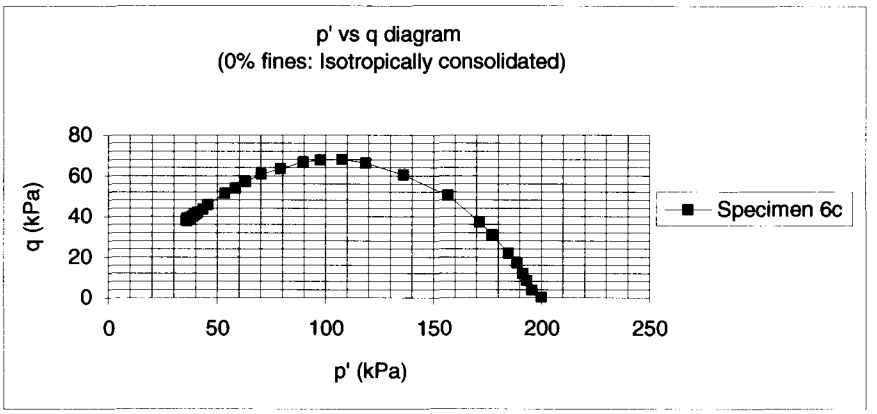
3.) Shear data

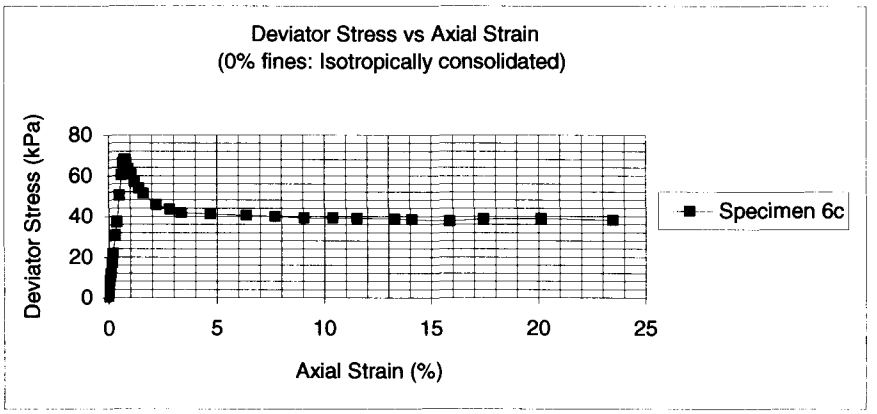
Volume change 1:		Volume change 2:		Sample Vol. change (cm^3)	29.48	B value	0.98
Air Flushing (cm^3)	6.55	Sat/Cons. (cm^3)	50.50	L_{cons} (mm)	149.19	p'consolidation (kPa)	200
Cell Expansion (cm^3)	0.00	Cell Expsn.(cm^3)	27.57	A_{cons} (cm^2)	44.126	Void ratio (e_1)	1.239

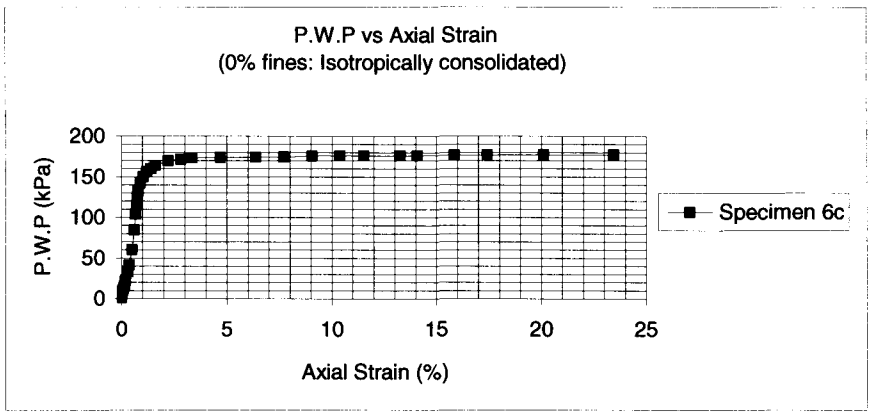
Proof ring properties		Strain gauge properties	
Proof ring No.	5153	1 strain division (mm)	0.01
Proof ring factor (dN/div)	7.512		

Strain Gauge (divs)	Axial Strain	Axial Strain (%)	Change Prf. ring (divs)	Change P.W.P (kPa)	q (Uncortd) (kPa)	Membrn. Corrctn. (kPa)	q (kPa)	t (kPa)	p' (kPa)	s' (kPa)
0	0.0000	0.0000	0.0	0.0	0.0	0.0	0.0	0.0	200.0	200.0
5	0.0003	0.0335	21.5	5.5	3.7	0.0	3.6	1.8	195.7	196.3
10	0.0007	0.0670	49.8	9.5	8.5	0.0	8.4	4.2	193.3	194.7
15	0.0010	0.1005	70.3	12.5	12.0	0.1	11.9	6.0	191.5	193.5
25	0.0017	0.1676	101.2	17.0	17.2	0.1	17.1	8.6	188.7	191.6
30	0.0020	0.2011	128.9	22.5	21.9	0.1	21.8	10.9	184.8	188.4
45	0.0030	0.3016	182.3	33.0	30.9	0.2	30.8	15.4	177.3	182.4
55	0.0037	0.3687	219.8	41.0	37.3	0.2	37.1	18.5	171.4	177.5
75	0.0050	0.5027	298.5	60.0	50.6	0.3	50.3	25.2	156.8	165.2
90	0.0060	0.6033	358.9	84.0	60.7	0.3	60.4	30.2	136.1	146.2
100	0.0067	0.6703	393.5	103.5	66.5	0.3	66.2	33.1	118.6	129.6
110	0.0074	0.7373	404.5	115.0	68.4	0.4	68.0	34.0	107.7	119.0
115	0.0077	0.7708	403.3	125.0	68.1	0.4	67.7	33.9	97.6	108.9
120	0.0080	0.8044	397.2	132.5	67.1	0.4	66.7	33.3	89.7	100.8
135	0.0090	0.9049	378.5	142.0	63.9	0.5	63.4	31.7	79.1	89.7
155	0.0104	1.0390	363.4	150.0	61.2	0.5	60.7	30.4	70.2	80.4
180	0.0121	1.2065	342.1	156.0	57.5	0.6	56.9	28.5	63.0	72.5
210	0.0141	1.4076	324.7	159.5	54.5	0.7	53.8	26.9	58.4	67.4
240	0.0161	1.6087	310.4	163.5	52.0	0.8	51.2	25.6	53.6	62.1
330	0.0221	2.2120	280.5	169.5	46.7	1.0	45.7	22.8	45.7	53.3
420	0.0282	2.8153	268.9	171.0	44.5	1.0	43.5	21.7	43.5	50.7
500	0.0335	3.3515	259.5	173.0	42.7	1.0	41.7	20.8	40.9	47.8
700	0.0469	4.6921	259.6	173.5	42.1	1.0	41.1	20.6	40.2	47.1
950	0.0637	6.3679	259.7	174.0	41.4	1.0	40.4	20.2	39.5	46.2

Strain Gauge (divs)	Axial Strain	Axial Strain (%)	Change Prf. ring (divs)	Change P.W.P (kPa)	q (Uncortd) (kPa)	Membrn. Corrctn. (kPa)	q (kPa)	t (kPa)	p' (kPa)	s' (kPa)
1150	0.0771	7.7085	259.8	174.5	40.8	1.0	39.8	19.9	38.8	45.4
1350	0.0905	9.0491	259.9	175.5	40.2	1.0	39.2	19.6	37.6	44.1
1550	0.1039	10.3897	263.6	176.0	40.2	1.0	39.2	19.6	37.1	43.6
1720	0.1153	11.5292	265.5	176.0	40.0	1.0	39.0	19.5	37.0	43.5
1980	0.1327	13.2720	269.1	176.0	39.7	1.0	38.7	19.4	36.9	43.4
2100	0.1408	14.0763	269.3	176.0	39.4	1.0	38.4	19.2	36.8	43.2
2365	0.1585	15.8526	269.8	176.5	38.6	1.0	37.6	18.8	36.0	42.3
2600	0.1743	17.4278	282.3	176.5	39.7	1.0	38.7	19.3	36.4	42.8
3000	0.2011	20.1090	293.7	177.0	39.9	1.0	38.9	19.5	36.0	42.5
3500	0.2346	23.4605	300.2	177.0	39.1	1.0	38.1	19.1	35.7	42.1







Wet mass after test and moisture content after test: The moisture content of the specimen after testing was measured and the wet mass of the specimen after test ing was determined by substituting this moisture content and the dry mass of the specimen into equation (3.7).

Saturation / consolidation

This section of the datasheet contains the following data pertaining to the air-flushing, saturation and consolidation stages of the test:

Cell pressure and back pressure: The cell pressure and back pressure applied to the specimen and the resulting pore pressure within the specimen at the end of the period during which the stresses were acting (written as P.W.P bp open).

Volume gauge reading: The volume gauge reading at the end of the period of action of the given set of stresses.

Cumulative cell expansion volume change: The cumulative cell expansion volume change resulting from the action of a given increment in cell pressure over a period of 24 hours. (This information was obtained from the cell expansion calibration data pertaining to the particular cell used, Appendix A, Table A1 and Figure A1).

Specimen volume change: The specimen volume change at the end of action of the given set of stresses. (This was obtained by subtracting the difference between the change in volume gauge reading and the change in cell expansion volume brought about by the action of the given increment of cell pressure).

Void ratio: The void ratio of the specimen at the end of action of a given increment of cell pressure was calculated by equation (4.3) using the volume of the specimen at the end of action of the given increment of cell pressure.

Change in cell pressure, change in pore pressure, and B value: For the saturation part of the test, additional data about the change in pore pressure

resulting from the change in cell pressure applied to the specimen (while the back pressure line was closed) and the corresponding B value are given. The B value was calculated as:

B value = (Change in pore pressure) / (Change in cell pressure) (4.5)

Shear data

This section of the datasheet contains data about the shearing/ loading stage of the test.

The **first block of data** contains a summary of data from the air-flushing, saturation, and consolidation stages of the test as follows:

Volume change after air-flushing: Measured during air-flushing of the specimen.

Cell expansion due to air-flushing: This was taken as zero since the cell pressures during air-flushing were small (< 15kPa).

Volume change due to saturation and consolidation: Measured by the volume change gauge.

Cumulative cell expansion volume change: At the end of saturation and consolidation.

Sample volume change: Calculated as the difference between the total volume change during air-flushing, saturation and consolidation and the total cumulative cell expansion volume change.

Final height and cross-sectional area: The final height and cross-sectional area of the specimen at the end of consolidation, L_{cons} and A_{cons}, were calculated as:

$$L_{cons} = L_0 (1 - (\Delta V / 3V_0)) \quad (4.6)$$

$$A_{cons} = A_0 (1 - (2\Delta V / 3V_0)) \quad (4.7)$$

Where:

L_0 = Initial (set-up) height of the specimen, mm;

ΔV = Specimen volume change at the end of consolidation, cm^3;

V_0 = Initial (set-up) volume of the specimen, cm^3;

A_0 = Initial (set-up) cross-sectional area of the specimen, cm^2.

B value: The B value at the end of saturation was calculated by equation (3.11).

Effective confining pressure: At the end of consolidation, $p'_{consolidation}$.

Final void ratio: The final void ratio at the end of consolidation, e_1, was calculated by equation (4.3).

The **second block of data** contains relevant information about the proving ring and the strain dial gauge used for the test.

The **last block of data** contains data recorded during the shearing/loading stage of the test and the calculated data thereof.

Recorded data include:

- Strain dial gauge reading, divisions;
- Change in proving ring reading, divisions;
- Change in pore water pressure, kPa.

Calculated data include:

$$\text{Axial strain} = \text{strain gauge reading} \times 0.01 / (L_{cons}) \quad (4.8)$$

$$\text{Axial strain (\%)} = \text{axial strain} \times 100\% \quad (4.9)$$

$$q(\text{uncorrected}) = (\Delta R \times F) / (A_{cons} / (1 - \text{axial strain})) \quad (4.10)$$

Membrane correction = 1/2 x (axial strain (%)) , for axial strain < 2% (4.11)

= 1 , for axial strain > 2% (4.12)

$$q = q(\text{uncorrected}) - \text{membrane correction} \quad (4.13)$$

$$t = q / 2 \quad (4.14)$$

$$p' = (q / 3) + p'_{consolidation} - \Delta P.W.P \quad (4.15)$$

$$s' = (q / 2) + p'_{consolidation} - \Delta P.W.P \quad (4.16)$$

Where:

ΔR = Change in proving ring reading, divisions;

F = Proving ring factor, dN/div;

q = Deviator stress, kPa;

t = Stress invariant, kPa;

p' = Effective mean normal stress, kPa;

$p'_{consolidation}$ = Effective mean normal stress after consolidation, kPa;

$\Delta P.W.P$ = Change in pore water pressure reading, kPa;

s' = Stress invariant, kPa.

4.3 Monotonic Undrained Compression of One-Dimensionally Consolidated Specimens (case 2 tests)

A typical datasheet containing the results of a triaxial test specimen under case 2 test is shown on pages 138 and 139. The plots of deviator stress- axial strain, pore pressure- axial strain and stress path are also included at the end of the datasheet, as per the format designed for this series of tests.

4.3.1 Description of the format of the datasheet and the calculation of various test parameters

The **top block of data** provides information about the type of test, the fines content and the specific gravity of the specimen under consideration, the particular triaxial cell used for the test, and the designation of the specimen.

The contents of the rest of the datasheet are considered below:

Sample physical properties

Same as for case 1 datasheet.

Saturation / consolidation

The format of this section of the datasheet is different from that for case 1 tests because of the additional measurement of axial force applied to the specimen during saturation and consolidation. Furthermore, due to space constraints, data about the changes in cell pressure and the corresponding changes in pore pressure during the determination of the degree of saturation (B value), specimen volume and void ratio at the end of action of a given increment of cell pressure were not included. The data was presented as follows:

The **first block of data** contains information about the proving ring, strain dial gauge, and loading ram of the particular triaxial cell used.

Area $[ram]_1$ and Area $[ram]_2$ under loading ram properties refer to the cross-sectional area of the front portion of the loading ram and the cross-sectional area of the loading piston. (note that the front portion of the loading ram had a fitting to enable proper seating on the top cap, resulting in a larger cross-sectional area than that of the piston).

The **second block of data** provides data about the air-flushing, saturation, and consolidation stages of the test.

Test	**Case 2: Monotonic Undrained Compression of One-Dimensionally Consolidated Specimens**		
Cell No.	3 (Big)	Fines content (%)	0
Specimen	K0-1	Specific gravity (g/cm^3)	2.72

1.) Sample physical properties

Wet mass before test (g)	841.609	m.c before test (%)	9.65	Height (mm)	151.25	Volume (cm^3)	697.926
Wet mass after test (g)	974.854	m.c. after test (%)	27.01	Diameter (mm)	76.65		
Dry mass (g)	767.541	Dry density (kg/m^3)	1100	Area (cm^2)	46.144	Void ratio (e_0)	1.473

2.) Saturation / Consolidation

Proof ring properties		Strain gauge properties		Loading ram properties	
Proof ring No.	5153	1 strain division (mm)	0.01	Area [ram]$_1$ (cm^2)	7.905
Proof ring factor (dN/div)	7.512			Area [ram]$_2$ (cm^2)	5.004

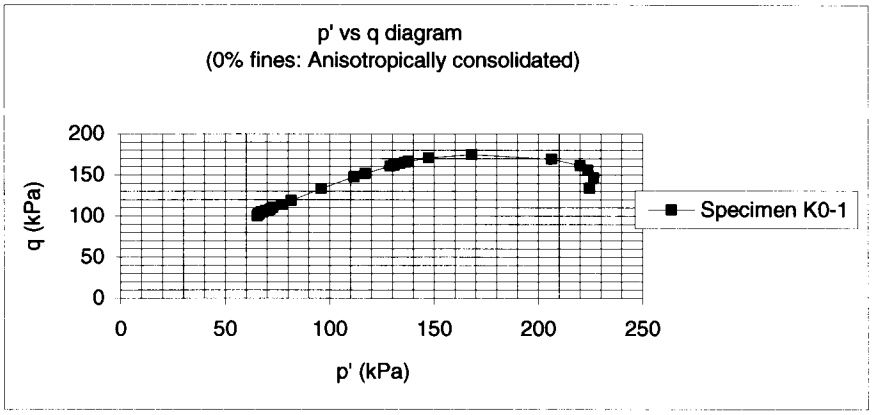
Date	Strain Gauge (divs)	Change Length (mm)	Cell Pressure (kPa)	Proof Ring (div)	Pore Pressure (kPa)	P_1 (kPa)	P'_3 (kPa)	P'_1 (kPa)	q (kPa)	p' (kPa)	K0	Volume Gauge (cm^3)	Cell Expansn (cm^3)
3/3	0	0.000	0	0.0	0.0						\	0.00	0.00
3/3	0	0.000	12.5		8.0	A I R - F L U S H I N G					\	8.00	0.00
3/3	195	1.950	50	125.0	40.0	61.8	10	21.8	11.8	13.9	0.46	33.41	6.08
4/3	324	3.240	100	168.2	90.0	110.3	10	20.3	10.3	13.4	0.49	52.13	8.77
5/3	512	5.120	150	202.1	140.0	157.2	10	17.2	7.2	12.4	0.58	62.00	10.65
6/3	694	6.940	200	250.5	190.0	206.5	10	16.5	6.5	12.2	0.61	69.57	12.00
7/3	826	8.260	250	305.2	240.0	256.9	10	16.9	6.9	12.3	0.59	74.49	13.63
8/3	933	9.330	300	362.7	290.0	307.7	10	17.7	7.7	12.6	0.57	78.03	15.06
9/3	1103	11.030	350	412.3	340.0	357.2	10	17.2	7.2	12.4	0.58	81.95	16.08
10/3	1255	12.550	400	650.0	350.0	437.3	50	87.3	37.3	62.4	0.57	86.49	18.12
11/3	1404	14.040	450	853.3	350.0	511.8	100	161.8	61.8	120.6	0.62	90.07	19.91
12/3	1700	17.000	550	1400.0	370.0	683.7	180	313.7	133.7	224.6	0.57	117.55	22.28

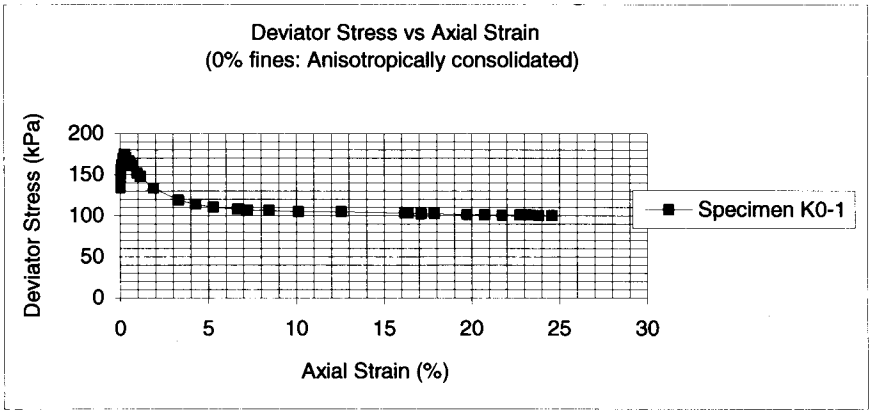
3.) Shear data

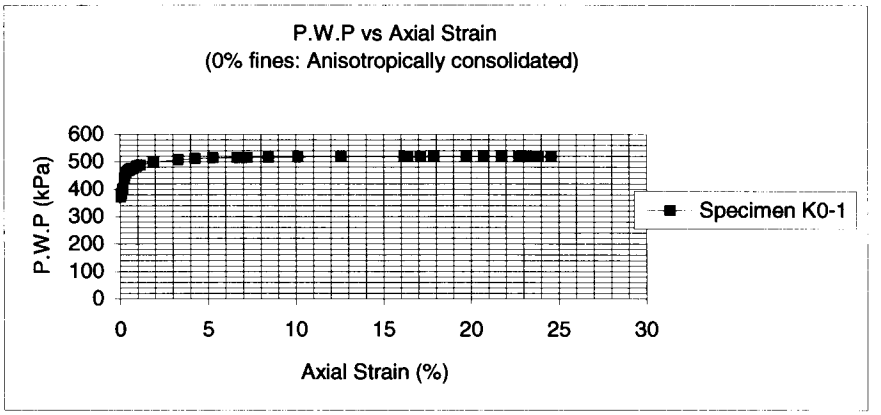
Volume change 1:		Volume change 2:		Sample Vol. change (cm^3)	103.78	B value	0.99
Air Flushing (cm^3)	8.00	Sat/Cons. (cm^3)	109.55	L_{cons} (mm)	134.25	K0	0.57
Cell Expsn. (cm^3)	0.00	Cell Expsn. (cm^3)	22.28	A_{cons} (cm^2)	46.144	Void ratio (e_1)	1.106
		Ram into cell (cm^3)	8.51				

Strain Gauge (divs)	Axial Strain (%)	Cell Press. (kPa)	Proof Ring (divs)	Pore Pressure (kPa)	Membrane Correction (kPa)	P_1 (kPa)	q (kPa)	t (kPa)	p' (kPa)	s' (kPa)
0	0.0000	550	1400.2	370.0	0.0	683.7	133.7	66.9	224.6	246.9
2	0.0149	550	1475.7	372.0	0.0	696.0	146.0	73.0	226.7	251.0
6	0.0447	550	1535.0	378.0	0.0	705.6	155.6	77.8	223.9	249.8
13	0.0968	550	1570.5	383.5	0.0	711.2	161.2	80.6	220.2	247.1
22	0.1639	550	1620.7	400.0	0.1	719.3	169.3	84.6	206.4	234.6
35	0.2607	550	1655.9	440.0	0.1	724.8	174.8	87.4	168.3	197.4
45	0.3352	550	1632.4	459.5	0.2	720.8	170.8	85.4	147.4	175.9
65	0.4842	550	1607.5	467.5	0.2	716.4	166.4	83.2	138.0	165.7
70	0.5214	550	1600.0	469.0	0.3	715.1	165.1	82.6	136.0	163.6
75	0.5587	550	1591.3	471.0	0.3	713.6	163.6	81.8	133.5	160.8
80	0.5959	550	1580.2	473.0	0.3	711.8	161.8	80.9	130.9	157.9
95	0.7076	550	1575.1	474.5	0.4	710.7	160.7	80.3	129.1	155.8
130	0.9683	550	1521.7	483.5	0.5	701.5	151.5	75.8	117.0	142.3
155	1.1546	550	1500.0	487.5	0.6	697.7	147.7	73.8	111.7	136.3
255	1.8994	550	1418.6	498.5	0.9	683.2	133.2	66.6	95.9	118.1
445	3.3147	550	1340.5	508.0	1.0	668.9	118.9	59.4	81.6	101.4
575	4.2831	550	1315.9	511.0	1.0	663.9	113.9	56.9	77.0	95.9
710	5.2886	550	1300.1	514.0	1.0	660.2	110.2	55.1	72.7	91.1
895	6.6667	550	1295.5	514.5	1.0	657.9	107.9	54.0	71.5	89.5
970	7.2253	550	1292.4	515.0	1.0	656.8	106.8	53.4	70.6	88.4
1135	8.4544	550	1298.0	516.0	1.0	656.2	106.2	53.1	69.4	87.1
1360	10.1304	550	1302.3	517.0	1.0	654.9	104.9	52.4	68.0	85.4
1690	12.5885	550	1320.4	517.5	1.0	654.5	104.5	52.3	67.3	84.8
2175	16.2011	550	1340.7	518.0	1.0	652.9	102.9	51.5	66.3	83.5

Strain Gauge (divs)	Axial Strain (%)	Cell Press. (kPa)	Proof Ring (divs)	Pore Pressure (kPa)	Membrane Correction (kPa)	P_1 (kPa)	q (kPa)	t (kPa)	p' (kPa)	s' (kPa)
2200	16.3873	550	1342.3	518.0	1.0	652.9	102.9	51.5	66.3	83.5
2300	17.1322	550	1343.2	518.0	1.0	652.1	102.1	51.1	66.0	83.1
2400	17.8771	550	1350.4	518.0	1.0	652.2	102.2	51.1	66.1	83.1
2650	19.7393	550	1360.0	518.0	1.0	651.1	101.1	50.5	65.7	82.5
2785	20.7449	550	1367.2	518.0	1.0	650.7	100.7	50.4	65.6	82.4
2920	21.7505	550	1373.8	518.0	1.0	650.3	100.3	50.1	65.4	82.1
3055	22.7561	550	1386.9	518.0	1.0	650.6	100.6	50.3	65.5	82.3
3125	23.2775	550	1393.0	518.0	1.0	650.7	100.7	50.3	65.6	82.3
3200	23.8361	550	1393.7	518.0	1.0	650.0	100.0	50.0	65.3	82.0
3300	24.5810	550	1400.0	518.0	1.0	649.8	99.8	49.9	65.3	81.9







Recorded data include:

- Strain dial gauge reading;
- Cell pressure;
- Proving ring reading;
- Pore pressure;
- Volume gauge reading.

Calculated data include:

$$\Delta L = \text{strain dial gauge} \times 0.01 \quad (4.17)$$

$$P_1 = (R \times F) / A_0 + cp \left(1 - \text{Area[ram]}_1 / A_0 \right) \quad (4.18)$$

$$P'_3 = cp - pwp \quad (4.19)$$

$$P'_1 = P_1 - pwp \quad (4.20)$$

$$q = P_1 - cp \quad (4.21)$$

$$p' = (P'_1 - 2\,P'_3) / 3 \quad (4.22)$$

$$K0 = P'_3 / P'_1 \quad (4.23)$$

Where:

ΔL = Change in height of the specimen, mm;
P_1 = Total axial stress acting on the specimen, kPa;
R = Proving ring reading, divisions;
F = Proving ring factor, dN/div;
A_0 = Initial (set-up) cross-sectional area of the specimen, cm^2;
cp = Cell pressure, kPa;
P'_3 = Effective confining pressure, kPa;
pwp = Pore pressure, kPa;
P'_1 = Effective axial stress, kPa;

q = Deviator stress, kPa;

p' = Effective mean normal stress, kPa;

K0 = Ratio of effective confining pressure to effective vertical stress.

Shear data

Except for the following data, the **first block of data** contains a summary of data pertaining to the air-flushing, saturation, and consolidation stages of the test obtained similarly as for case 1 tests:

$$\Delta V_{R/PEN} = (\Delta L_T / 10) \times \text{Area[ram]}_2 \quad (4.24)$$

$$\Delta V_S = \Delta V_{A/F} + \Delta V_{S/C} - \Delta V_{C/EXP} + \Delta V_{R/PEN} \quad (4.25)$$

$$L_{cons} = L_0 - \Delta L_T \quad (4.26)$$

$$A_{cons} = A_0 \quad (4.27)$$

Where:

$\Delta V_{R/PEN}$ = Volume change due to ram penetration into the cell chamber, cm^3;

ΔL_T = Total change in height of the specimen at the end of consolidation, mm;

ΔV_S = Total specimen volume change, cm^3;

$\Delta V_{A/F}$ = Volume change due to air-flushing, cm^3;

$\Delta V_{S/C}$ = Volume change due to saturation and consolidation, cm^3;

$\Delta V_{C/EXP}$ = Volume change due to cell expansion, cm^3;

L_{cons} = Final height of the specimen at the end of consolidation, mm;

L_0 = Initial (set-up) height of the specimen, mm;

ΔL_T = Total change in height of the specimen after consolidation, mm;

A_{cons} = Final cross-sectional area of the specimen, cm^2;

A_0 = Initial (set-up) cross-sectional area of the specimen, cm^2.

K0, the ratio of effective confining pressure to effective vertical stress after consolidation was calculated by equation (4.23).

The **second block of data** contains data recorded during the shearing/ loading stage of the test and the calculated data thereof.

Recorded data include:

- Strain dial gauge reading, divisions;
- Cell pressure, kPa;
- Proving ring reading, divisions;
- Pore water pressure, kPa.

Calculated data include:

Axial strain (%) , (calculated as before);

Membrane correction, (calculated as before);

$P_1 = R \times F / A -$ membrane correction $+ cp\ (1 - Area[ram]_1 / A)$ (4.28)

$A = A_0 / (1 -$ axial strain (%) $/ 100)$ (4.29)

q = (refer to equation (4.21));

$t = q / 2$ (4.30)

p' = (refer to equation (4.22));

$s' = (P_1 - pwp + (cp - pwp)) / 2$ (4.31)

4.4 Variation of Stress Path Followed During Undrained Loading of One-Dimensionally Consolidated Specimens (case 3 tests)

A typical datasheet containing the results of a triaxial test specimen under case 3 test is shown on pages 144 and 145. The plots of deviator stress- axial strain, pore pressure- axial strain and stress path are also included at the end of the datasheet, as per the format designed for this series of tests.

4.4.1 Description of the format of the datasheet and the calculation of various test parameters

The top block of data provides information about the type of test, the fines content and the specific gravity of the specimen under consideration, the particular triaxial cell used for the test, and the designation of the specimen.

The contents of the rest of the datasheet are discussed below:

Sample physical properties

Same as for case 1 datasheet.

Saturation / consolidation

The format of this section of the datasheet is different from those of case 1 and case 2 tests because of the different means of measurement of test variables. Furthermore, as for case 2 tests, data about the changes in cell pressure and the corresponding changes in pore pressure during the determination of the degree of saturation (B value), calculated specimen volume and void ratio at the end of the action of the given increment of cell pressure were not included. The data was split into observed data and processed data.

Test	**Case 3: Constant Deviator Stress Undrained Loading, One-Dimensionally Consolidated**		
Cell No.	Bishop-Wesley stress path cell	Fines content (%)	20
Sample	Specimen BW-1	Specific gravity (g/cm^3)	2.72

1.) Sample physical properties

Wet mass before test (g)	102.753	m.c before test (%)	9.66	Height (mm)	75.95	Volume (cm^3)	86.363
Wet mass after test (g)	124.229	m.c. after test (%)	32.58	Diameter (mm)	38.05		
Dry mass (g)	93.701	Dry density (kg/m^3)	1085	Area (cm^2)	11.371	Void ratio (e_0)	1.507

2.) Saturation / Consolidation

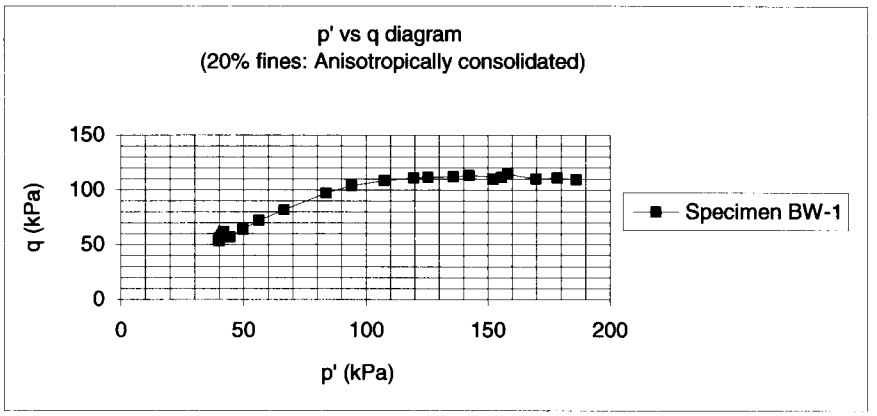
Observed Data								Processed Data							
Date	Cell Press Trd (mV)	Pore Press Trd (mV)	Axial LVDT (V)	Volume change transducer measrd. (V)	Volume change transducer cell expans. (V)	Volume change transducer piston movmnt. (V)	Load Trd (V)	Cell Press. (kPa)	Proof Ring (div)	Pore Press. (kPa)	P_1 (kPa)	P'_3 (kPa)	P'_1 (kPa)	q (kPa)	p' (kPa)	K0
8/3			-2.788	-2.976	0.000	0.000		0.0	0.0	0.0						\
8/3	A I R - F L U S H I N G							9.8		4.1						\
8/3	5.58	3.88	-2.592	-2.896	0.296	0.415	0.241	50.0	12.4	40.5	78.2	9.5	37.6	28.1	18.9	0.25
9/3	10.59	8.85	-2.463	-2.710	0.583	0.688	0.152	99.9	5.2	90.1	111.8	9.9	21.7	11.8	13.8	0.46
10/3	15.64	13.90	-2.394	-2.477	0.856	0.834	0.189	150.2	5.5	140.4	162.6	9.8	22.2	12.4	14.0	0.44
11/3	20.66	18.89	-2.322	-2.321	1.111	0.987	0.181	200.2	3.3	190.2	207.7	10.1	17.6	7.5	12.6	0.57
12/3	25.63	23.88	-2.265	-2.120	1.404	1.108	0.197	249.7	2.7	239.9	255.9	9.8	16.0	6.1	11.9	0.62
13/3	30.69	28.93	-2.193	-1.971	1.677	1.260	0.230	300.1	3.2	290.3	307.5	9.9	17.2	7.3	12.3	0.57
14/3	35.70	33.93	-2.156	-1.765	1.928	1.339	0.251	350.0	3.3	340.1	357.5	9.9	17.4	7.4	12.4	0.57
15/3	40.70	38.98	-2.112	-1.600	2.163	1.432	0.268	399.8	3.2	390.5	407.2	9.4	16.7	7.4	11.8	0.56
16/3	45.76	44.00	-2.071	-1.437	2.391	1.519	0.280	450.2	3.1	440.5	457.3	9.7	16.8	7.0	12.1	0.58
17/3	70.86	55.02	-1.732	-0.998	3.421	2.237	1.087	700.2	48.2	550.4	809.4	149.9	259.0	109.1	186.2	0.58

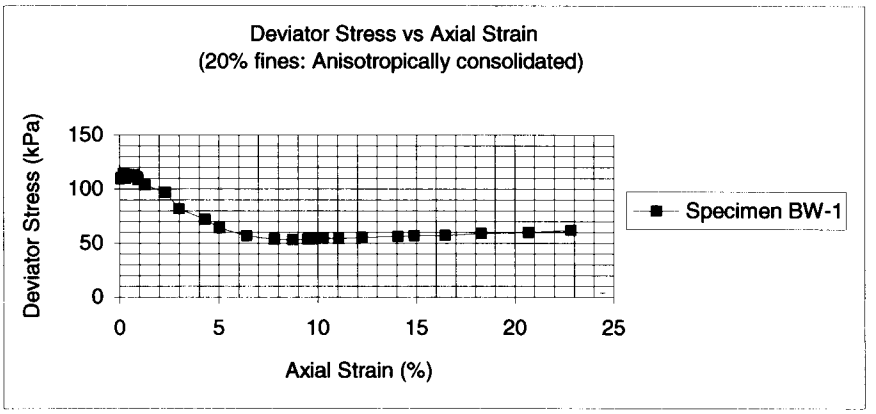
3.) Shear data

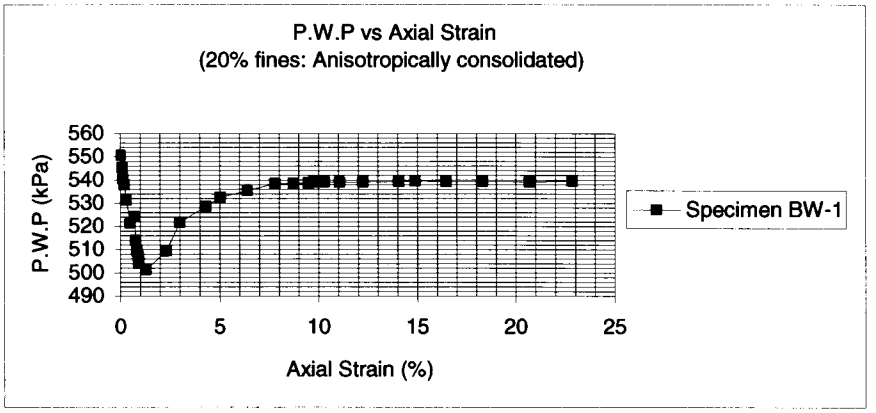
Volume change 1:		Volume change 2:		Sample Vol. change (cm^3)	12.357	K0	0.58		
Air Flushing (cm^3)	2.050	Sat/Cons. (cm^3)	25.688	L_{cons} (mm)	71.02			Void ratio (e_1)	1.148
Cell Expsn. (cm^3)	0.000	Cell Expsn.(cm^3)	44.429	A_{cons} (cm^2)	11.371	B value	0.99		
		Piston pen.(cm^3)	29.047						

Raw Data				Processed Data									
Cell Press Trd (mV)	Pore Press Trd (mV)	Axial LVDT (V)	Load Trd (V)	Change in Length (mm)	Axial Strain (%)	Cell Press (kPa)	Proof Ring (div)	Pore Press (kPa)	P_1 (kPa)	q (kPa)	t (kPa)	p' (kPa)	s' (kPa)
70.88	55.04	-1.732	1.088	0.000	0.000	700.4	48.2	550.6	809.7	109.3	54.6	186.3	204.5
69.52	54.51	-1.718	1.100	0.065	0.092	686.9	48.9	545.3	797.5	110.6	55.3	178.5	196.9
68.17	54.01	-1.710	1.096	0.103	0.145	673.5	48.6	540.3	783.5	110.0	55.0	169.8	188.1
66.60	53.76	-1.701	1.130	0.145	0.204	657.8	50.6	537.8	772.2	114.4	57.2	158.1	177.2
65.52	53.10	-1.685	1.094	0.220	0.309	647.1	48.5	531.2	756.6	109.5	54.8	152.3	170.6
64.80	52.11	-1.655	1.111	0.360	0.506	639.9	49.5	521.4	751.3	111.4	55.7	155.7	174.2
63.69	52.39	-1.622	1.127	0.514	0.723	628.8	50.5	524.2	742.0	113.2	56.6	142.4	161.3
62.06	51.37	-1.613	1.117	0.556	0.783	612.6	50.0	514.0	724.5	111.9	56.0	135.9	154.6
60.57	50.90	-1.604	1.112	0.598	0.842	597.8	49.7	509.3	709.1	111.3	55.7	125.6	144.1
59.77	50.67	-1.595	1.107	0.640	0.901	589.8	49.5	507.0	700.5	110.7	55.3	119.7	138.1
58.38	50.42	-1.588	1.089	0.673	0.947	575.9	48.5	504.5	684.4	108.4	54.2	107.6	125.6
56.87	50.10	-1.534	1.055	0.925	1.302	560.9	46.7	501.3	664.6	103.7	51.9	94.1	111.4
56.85	50.90	-1.380	1.013	1.644	2.315	560.7	44.2	509.3	657.6	96.9	48.5	83.7	99.9
56.88	52.14	-1.276	0.898	2.130	2.999	561.0	37.6	521.7	642.6	81.6	40.8	66.5	80.1
56.87	52.84	-1.077	0.830	3.059	4.308	560.9	33.6	528.6	632.9	72.0	36.0	56.3	68.2
56.88	53.23	-0.965	0.769	3.582	5.044	561.0	30.1	532.5	624.8	63.8	31.9	49.7	60.4
56.88	53.52	-0.758	0.719	4.549	6.406	561.0	27.2	535.4	617.8	56.8	28.4	44.5	54.0
56.85	53.82	-0.546	0.698	5.539	7.800	560.7	26.0	538.4	614.1	53.4	26.7	40.1	49.0
56.86	53.83	-0.405	0.701	6.198	8.727	560.8	26.2	538.5	614.0	53.2	26.6	40.0	48.9
56.87	53.85	-0.289	0.708	6.740	9.490	560.9	26.6	538.7	614.5	53.6	26.8	40.0	49.0
56.86	53.87	-0.252	0.711	6.913	9.734	560.8	26.8	538.9	614.6	53.8	26.9	39.8	48.8
56.89	53.89	-0.168	0.718	7.305	10.286	561.1	27.2	539.1	615.4	54.3	27.1	40.1	49.1
56.89	53.88	-0.050	0.721	7.856	11.062	561.1	27.3	539.0	615.2	54.1	27.1	40.1	49.2

Raw Data				Processed Data									
Cell Press Trd (mV)	Pore Press Trd (mV)	Axial LVDT (V)	Load Trd (V)	Change in Length (mm)	Axial Strain (%)	Cell Press (kPa)	Proof Ring (div)	Pore Press (kPa)	P_1 (kPa)	q (kPa)	t (kPa)	p' (kPa)	s' (kPa)
56.87	53.89	0.131	0.736	8.702	12.253	560.9	28.2	539.1	616.0	55.1	27.6	40.2	49.3
56.88	53.91	0.407	0.756	9.991	14.068	561.0	29.4	539.3	617.2	56.2	28.1	40.4	49.8
56.91	53.93	0.533	0.765	10.579	14.897	561.3	29.9	539.5	618.0	56.6	28.3	40.7	50.1
56.90	53.90	0.771	0.778	11.691	16.462	561.2	30.6	539.2	618.2	57.0	28.5	41.0	50.5
56.87	53.91	1.053	0.806	13.008	18.316	560.9	32.3	539.3	619.6	58.7	29.4	41.2	51.0
56.85	53.89	1.414	0.833	14.694	20.691	560.7	33.8	539.1	620.5	59.8	29.9	41.5	51.5
56.86	53.93	1.742	0.870	16.226	22.848	560.8	36.0	539.5	622.7	61.9	30.9	41.9	52.2







Observed data include:

- Cell pressure transducer reading, mV;
- Pore pressure transducer reading, mV;
- Axial displacement transducer reading, V;
- Volume change transducer reading (measured), V;
- Cell expansion volume change, V;
  (obtained from the cell expansion volume change calibration data in Appendix B, Table B7 and Figure B9)
- Volume change due to piston movement, V;
  determined using the average slope of the calibration curves for volume change due to piston movement, Appendix B, Table B6 and Figure B8, as follows:

$$\Delta V_{P/M} = 2.118 \times \Delta L(volt) \quad (4.32)$$

Where:

$\Delta V_{P/M}$ = Change in volume change transducer reading due to piston movement, V;

$\Delta L(volt)$ = Change in axial displacement transducer reading, V;

2.118 = Average slope of the calibration curves.

- Load transducer reading, V.

Processed data include:

$$cp = [cp(volt) - 0.5553] / 0.1004 \quad (4.33)$$

$$R = [Load(volt) - Load_{CP}(volt) + 0.0469] / 0.0173 \quad (4.34)$$

$$Load_{CP}(volt) = -6x10^{-7}(cp)^2 + 0.0008\,(cp) + 0.0348 \quad (4.35)$$

$$pwp = [pwp(volt) + 0.1828] / 0.1003 \quad (4.36)$$

$P_1 = (R \times 25.77) / A_0 + cp$ (4.37)

$P'_3 = cp - pwp$ (4.38)

$P'_1 = P_1 - pwp$ (4.39)

$q = P_1 - cp$ (4.40)

$p' = (P'_1 - 2\,P'_3) / 3$ (4.41)

$K0 = P'_3 / P'_1$ (4.42)

Where:

cp = Cell pressure, kPa;

cp(volt) = Cell pressure transducer reading, mV;

R = Proving ring reading, divisions;

Load(volt) = Load transducer reading, V;

$Load_{CP}$(volt) = Load transducer reading due to action of cell pressure, V;

pwp = Pore pressure, kPa;

pwp(volt) = Pore pressure transducer reading, mV.

Shear data

The **first block of data** contains the following data:

Volume change after air-flushing: Measured during air-flushing of the specimen.

Cell expansion due to air-flushing: Which was taken as zero since the cell pressures during air-flushing were small (< 15kPa).

Volume change during saturation and consolidation: The average slope of the volume change transducer calibration curves, Appendix B, Table B5 and Figure B7, was used for the following volume change conversions:

$$\Delta V_{S/C}\,(cm^3) = \Delta V_{S/C}(V) / 0.077 \quad (4.43)$$

$$\Delta V_{C/EXP}\,(cm^3) = \Delta V_{C/EXP}\,(V) / 0.077 \quad (4.44)$$

$$\Delta V_{P/M}\,(cm^3) = \Delta V_{P/M}\,(V) / 0.077 \quad (4.45)$$

Where:

$\Delta V_{S/C}(cm^3)$ = Change in volume due to saturation and consolidation, cm^3;

$\Delta V_{C/EXP}(cm^3)$= Change in volume due to cell expansion, cm^3;

$\Delta V_{P/M}(cm^3)$ = Change in volume due to piston movement, cm^3;

$\Delta V_{S/C}(V)$ = Change in volume due to saturation and consolidation, V;

$\Delta V_{C/EXP}(V)$ = Change in volume due to cell expansion, V;

$\Delta V_{P/M}(V)$ = Change in volume due to piston movement, V;

0.077 = Average slope of the volume change transducer calibration curves.

Sample volume change: Sample volume change at the end of consolidation was calculated as:

$$\Delta V_S(cm^3) = \Delta V_{A/F}(cm^3) + \Delta V_{S/C}(cm^3) - \Delta V_{C/EXP}(cm^3) + \Delta V_{P/M}(cm^3) \quad (4.46)$$

Where:

$\Delta V_S(cm^3)$ = Sample volume change, at the end of consolidation, cm^3;

$\Delta V_{A/F}(cm^3)$ = Volume change due to air-flushing, cm^3.

Final height of specimen: The average slope of the axial displacement transducer calibration curves, Appendix B, Table B8 and Figure B11, was used to obtain the final height of the specimen after consolidation as:

$$L_{cons} = L_0 - \Delta L_{S/C}(volt) / 0.2141 \quad (4.47)$$

Where:

L_{cons} = Final height of the specimen after consolidation, mm;

L_0 = Initial (set-up) height of the specimen, mm;

$\Delta L_{S/C}$(volt) = Change in axial displacement transducer reading, after saturation and consolidation, V;

0.2141 = Average slope of the axial displacement calibration curves;

A_{cons}, K0, B value, and e_1 were calculated as for case 2 tests.

The **second block of data** was split into observed and processed data as follows:

Observed data include:

- Cell pressure transducer reading, mV;
- Pore pressure transducer reading, mV;
- Axial displacement transducer reading, V;
- Load transducer reading, V.

Processed data include:

$$\Delta L = \Delta L_S(volt) \ / \ 0.2141 \qquad (4.48)$$

Axial strain (calculated as before)

cp (equation (4.33))

R (equation (4.34))

pwp (equation (4.36))

$$P_1 = (R \times 25.77) / A - 1/2 \times (\text{axial strain}(\%)) + cp, \quad \text{for axial strain} < 2\% \qquad (4.49)$$

$$P_1 = (R \times 25.77) / A - 1 + cp \quad , \quad \text{for axial strain} > 2\% \qquad (4.50)$$

$$A = A_0 / (1 - \text{axial strain}(\%) / 100) \qquad (4.51)$$

$$q = P_1 - cp \qquad (4.52)$$

$$t = q / 2 \tag{4.53}$$

$$p' = [P_1 - pwp + 2(cp - pwp)] / 3 \tag{4.54}$$

$$s' = [P_1 - pwp + cp - pwp] / 2 \tag{4.55}$$

This chapter has described the equations used to interpret the data recorded under the different series of tests performed in this investigation and it has also explained the formats of the datasheets containing the recorded and the calculated data for each series of tests.

As pointed out earlier, the datasheets for the individual test specimens are included in Appendices C, D, and E for specimens of case 1, case 2 and case 3 tests, respectively.

In the next chapter, Chapter 5, the undrained behavior of Merriespruit gold tailings under the various series of tests performed in this study is analyzed and discussed by first comparing behavior of specimens within each series of tests and then by comparing the behavior observed under different series of tests.

5 PRESENTATION AND DISCUSSION OF RESULTS

5.1 Monotonic Undrained Compression of Isotropically Consolidated Specimens (case 1 tests)

The results of monotonic undrained compression triaxial tests on isotropically consolidated Merriespruit gold tailings specimens are given in Appendix C and summarized in Table C1. In Table C2 the results obtained by Fourie and Papageorgiou (2001) from similar tests on the same tailings are shown. The stress paths for the tests performed in this study on Merriespruit gold tailings containing 0%, 20%, 30% and 60% fines (defined as percentage finer than 75μm) are shown in Figures 5.1, 5.2, 5.3 and 5.4, respectively.

All specimens showed liquefaction behavior with the deviator stress increasing sharply with axial strain and reaching a peak at small axial strains of about 1% (for all tests, the minimum and maximum axial strains at peak deviator stress were 0.73 and 1.17%, respectively). After its peak, the deviator stress showed a marked decrease until it stabilized at a residual/steady-state value at relatively large strains of about 10-15%. The pore pressure increased rapidly at small strains and after about the peak deviator stress point, the pore pressure continued to increase at a lower rate until it reached a maximum value at roughly the point when the deviator stress reached its residual/steady-state value. The stress paths showed well defined peaks followed by declines leading to well defined residual/steady state points.

This behavior was observed for all isotropically consolidated Merriespruit gold tailings specimens. However, some of the specimens containing 60% fines (specimens 6e, 3g, 6f, 2h and 2i) showed a limited liquefaction behavior with the deviator stress showing an increase after reaching the above-mentioned residual/ steady-state value. For these specimens, the quasi steady-state strength was reached at axial strains of about 7% and remained constant up to axial strains of about 15% after which the strength increased for the rest of the test.

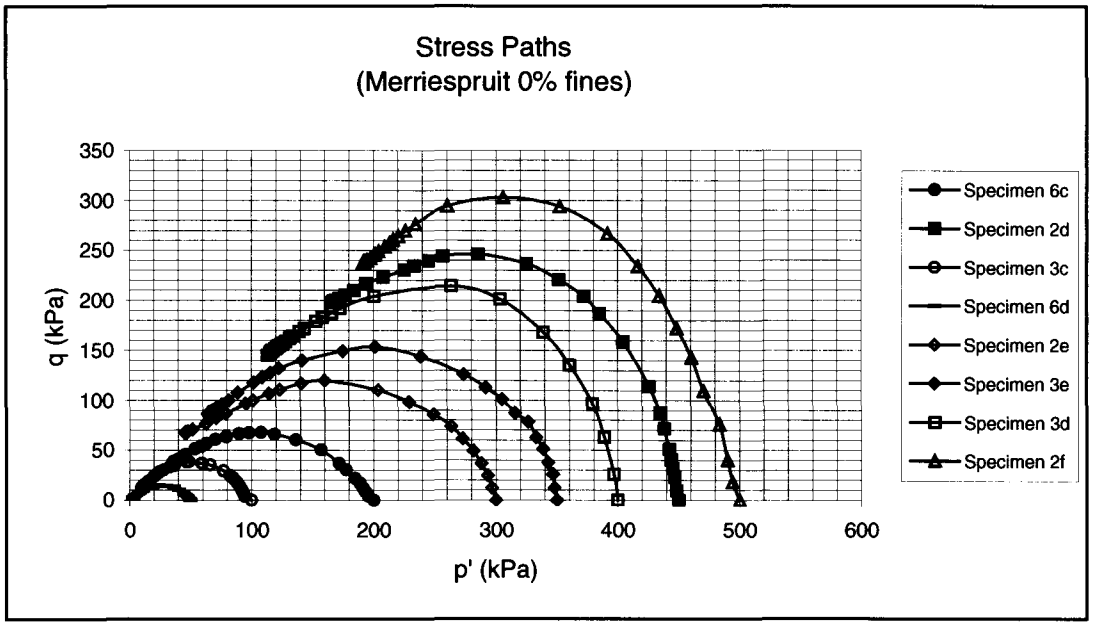


Figure 5.1 Stress paths for isotropically consolidated Merriespruit gold tailings containing 0% fines

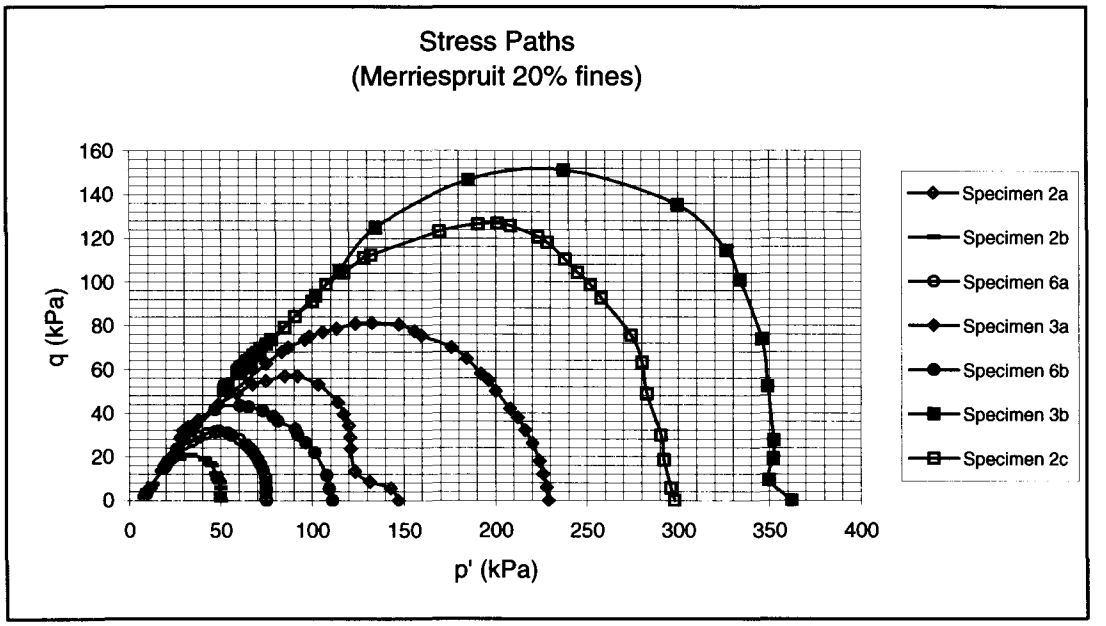


Figure 5.2 Stress paths for isotropically consolidated Merriespruit gold tailings containing 20% fines

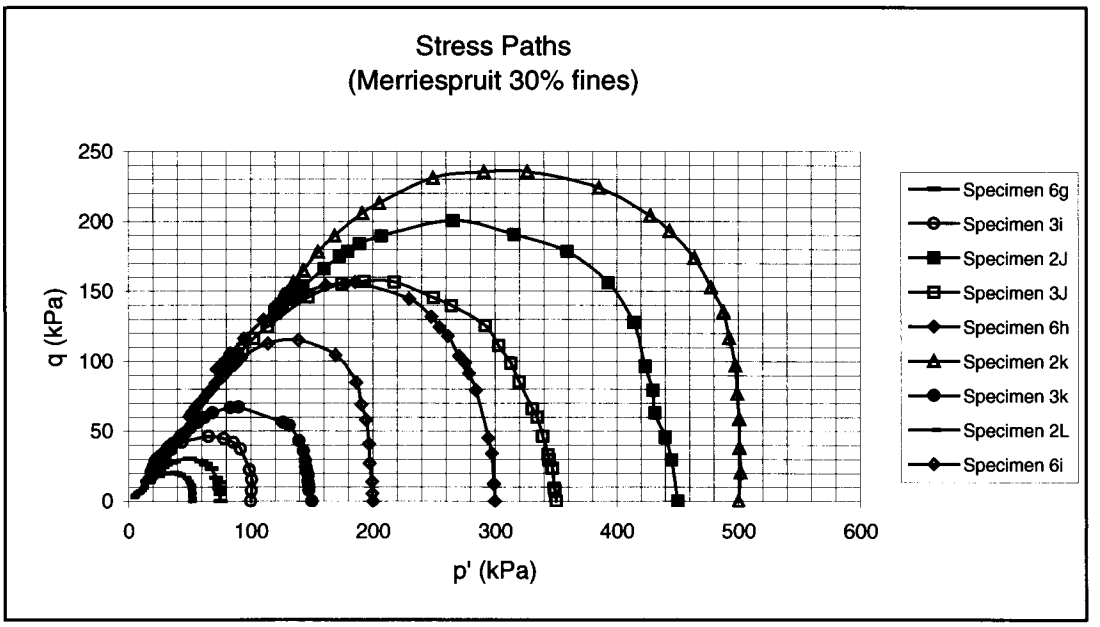


Figure 5.3 Stress paths for isotropically consolidated Merriespruit gold tailings containing 30% fines

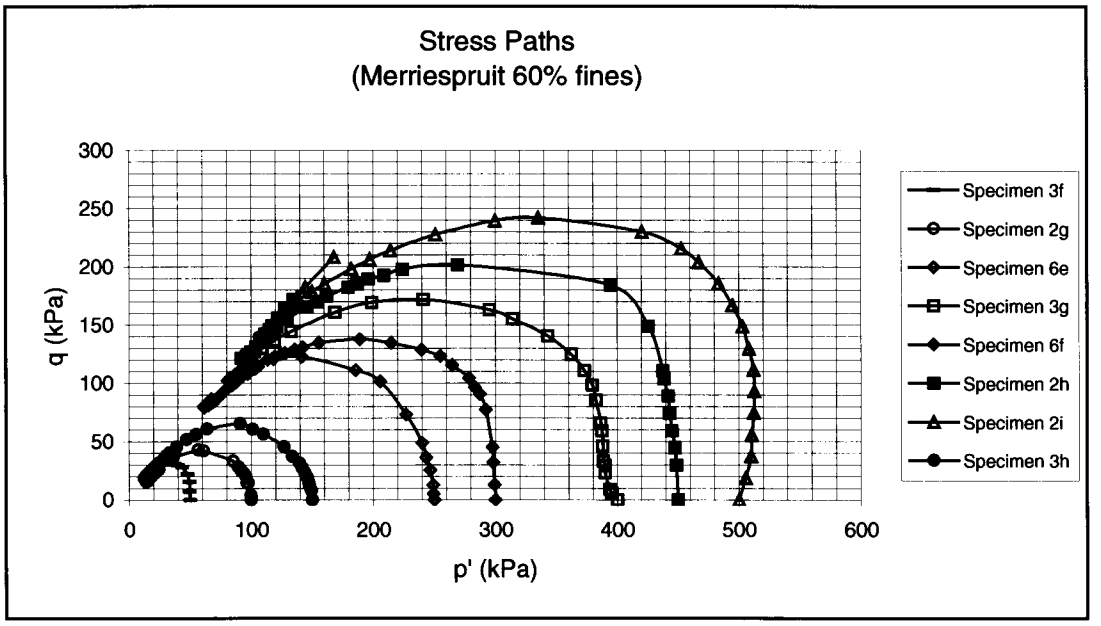


Figure 5.4 Stress paths for isotropically consolidated Merriespruit gold tailings containing 60% fines

During the time when the deviator stress was constant, the pore pressure was also constant at its maximum value, however, as the specimens continued to be strained, the pore pressure dropped, precipitating the observed increase in deviator stress.

5.1.1 CSR line and steady-state failure envelope

For all the specimens containing the same percentage of fines, the deviator stress and the effective mean normal stress corresponding to the peak and residual/ steady-state strengths were carefully selected and used to construct the Critical Stress Ratio line (CSR line) and the steady-state failure envelope, respectively. In Figures 5.5, 5.6, 5.7 and 5.8 the CSR line and the steady-state failure envelope for isotropically consolidated Merriespruit gold tailings containing 0%, 20%, 30% and 60% fines are shown, respectively. Also included in these figures are the CRS lines and steady-state failure envelopes obtained in a similar study on the same tailings by Fourie and Papageorgiou (2001). In Figures 5.5, 5.6, 5.7, and 5.8, solid and open symbols correspond to CSR line and steady-state failure envelope, respectively.

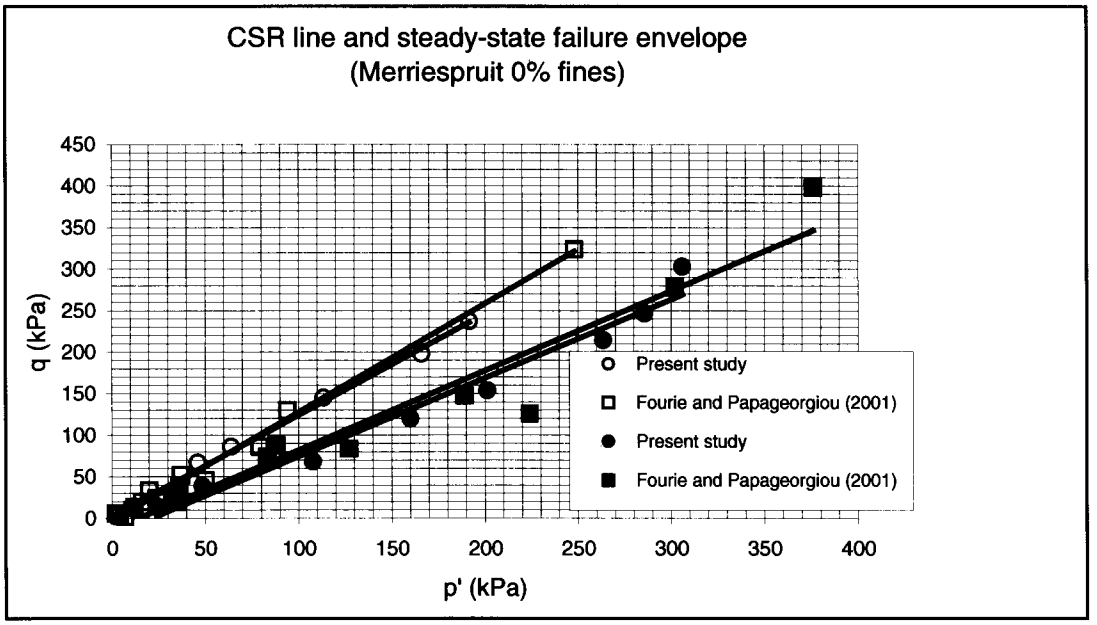


Figure 5.5 CSR line and steady-state failure envelope for isotropically consolidated Merriespruit gold tailings containing 0% fines

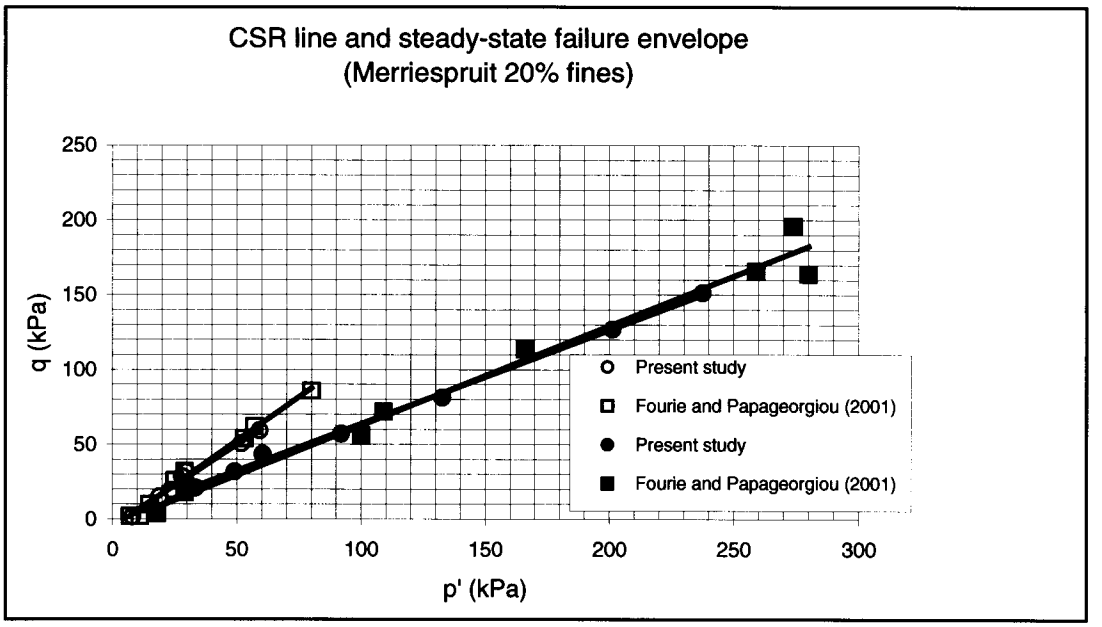


Figure 5.6 CSR line and steady-state failure envelope for isotropically consolidated Merriespruit gold tailings containing 20% fines

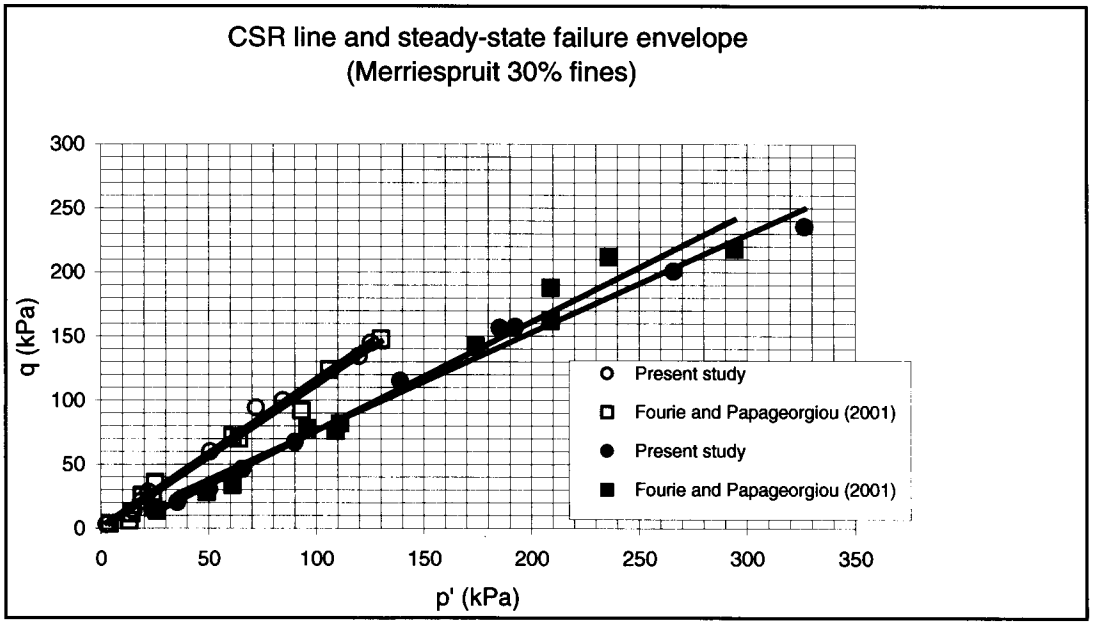


Figure 5.7 CSR line and steady-state failure envelope for isotropically consolidated Merriespruit gold tailings containing 30% fines

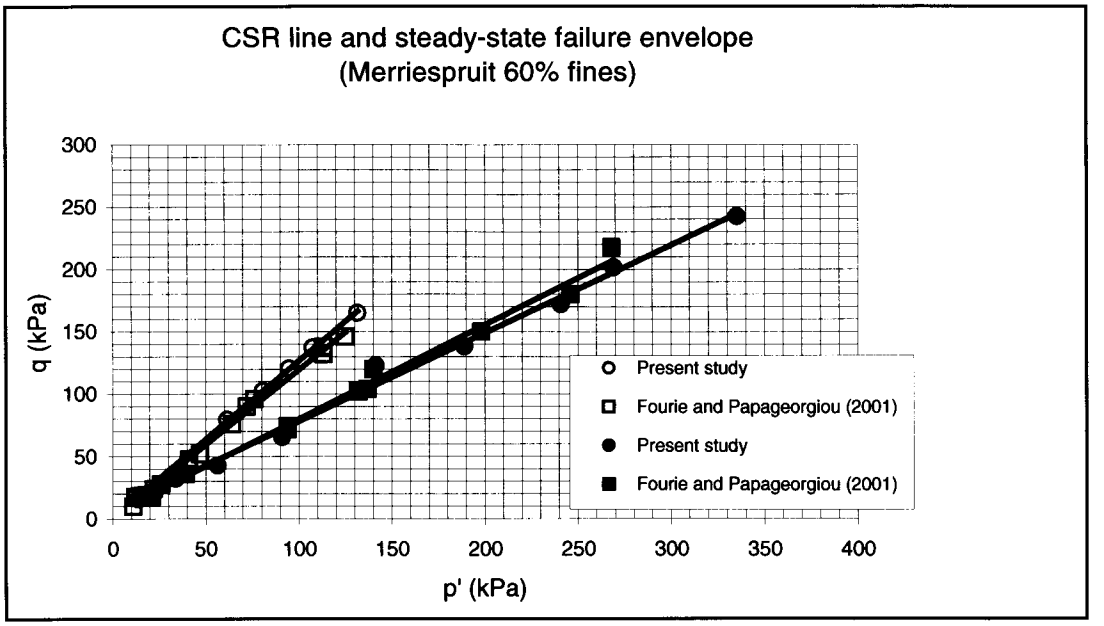


Figure 5.8 CSR line and steady-state failure envelope for isotropically consolidated Merriespruit gold tailings containing 60% fines

It can be seen in Figures 5.5, 5.6, 5.7 and 5.8 that although in both this study and the study by Fourie and Papageorgiou (2001) there was some scatter in the points representing the CSR line and the steady-state failure envelope, the best-fit lines drawn though such points are relatively unique, since for both studies these best-fit lines are essentially the same. These lines are straight and essentially pass through the origin of the stress space.

5.1.2 Variation of effective angles of friction mobilized at peak shear stress and at steady state with fines content and gradation

The effective angles of friction mobilized at peak shear stress and at steady state are plotted against fines content in Figure 5.9. For each fines content, the averages of the effective angles of friction at peak shear stress and at steady-state were calculated and plotted in Figure 5.9 and lines through these average values were drawn as shown in Figure 5.9. In Figure 5.9, the variation with fines content of the effective angles of friction mobilized at peak shear stress and at steady-state is evident (it must be borne in mind, however, that the gradations of the tailings at different fines contents were also different so that the observed variation of effective

angles of friction is not necessarily due to the variation in fines content alone). It is clear in Figure 5.9 that increasing fines content from 0% to 20% resulted a decrease in both effective angles of friction whereas increasing fines content beyond 20% caused these friction angles to increase. The larger drop of average effective angle of friction at steady-state seen at 20% fines is due to the very low effective angle of friction at steady-state exhibited by one of the test specimens. This specimen's effective angle of friction at steady-state was about 5 degrees.

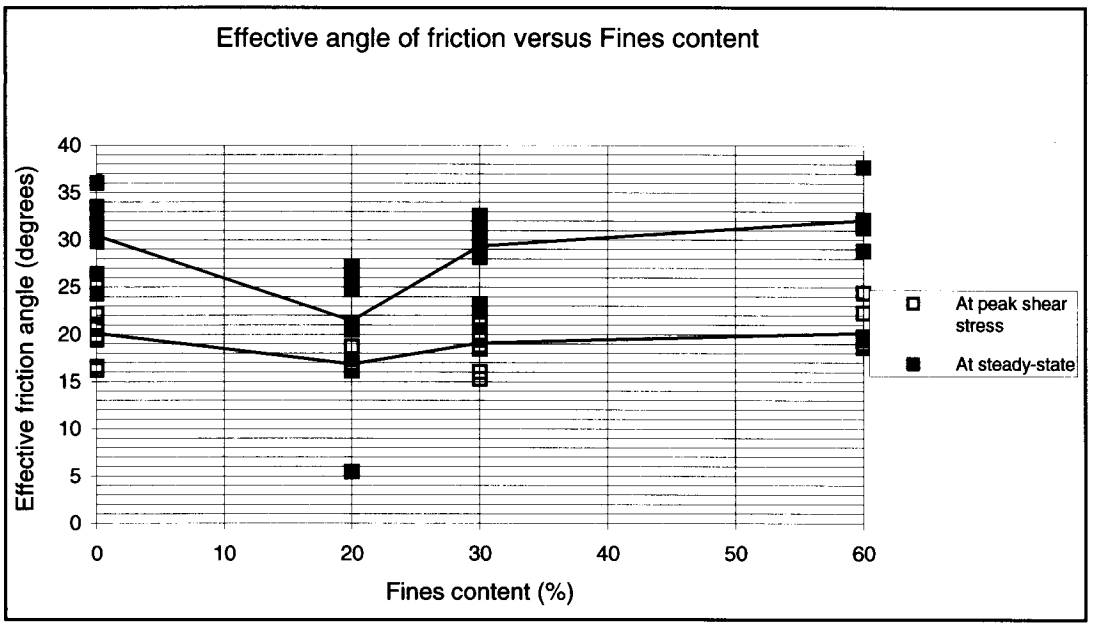


Figure 5.9 Variation with fines content (and gradation) of effective angles of friction mobilized at peak shear stress and at steady-state for isotropically consolidated Merriespruit gold tailings

5.1.3 Steady-state line

For all the specimens containing the same percentage of fines, the void ratio after consolidation was plotted against the logarithm of the effective mean normal stress at steady state and the best-fit straight line was drawn through the data points to obtain the steady-state line.

In Figures 5.10, 5.11, 5.12 and 5.13 the steady-state lines for isotropically consolidated Merriespruit gold tailings containing 0%, 20%, 30% and 60% are shown, respectively. Also included in these Figures are the steady-state lines obtained by Fourie and Papageorgiou (2001).

Again, the steady-state points show some scatter but the steady-state lines, the best-fit straight lines through these data points, are essentially the same for this study and the study performed by Fourie and Papageorgiou (2001).

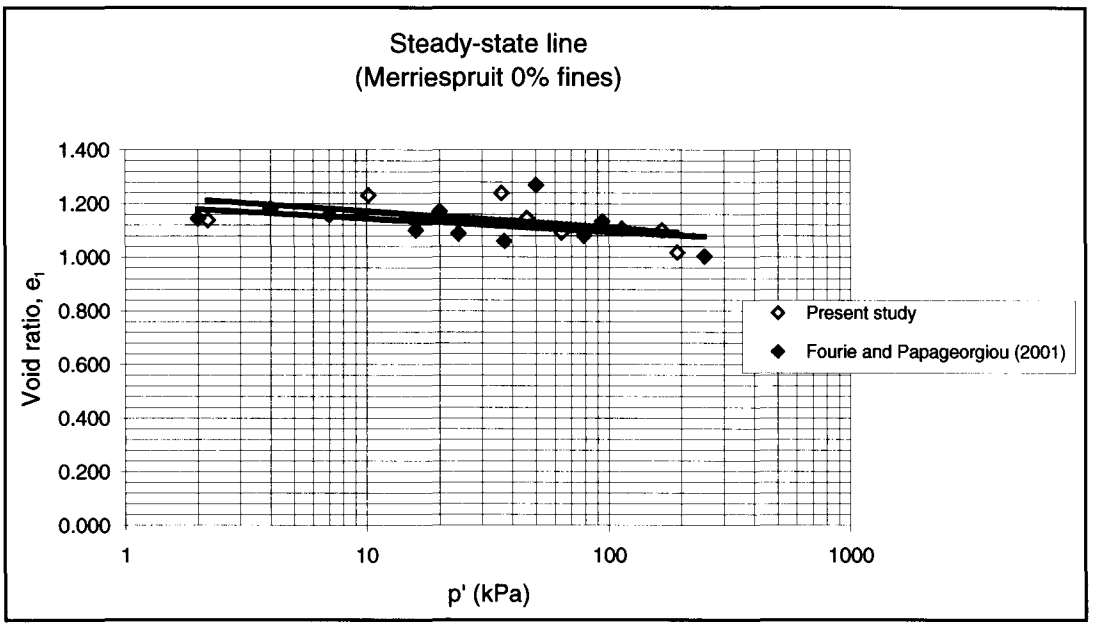


Figure 5.10 Steady-state line for isotropically consolidated Merriespruit gold tailings containing 0% fines

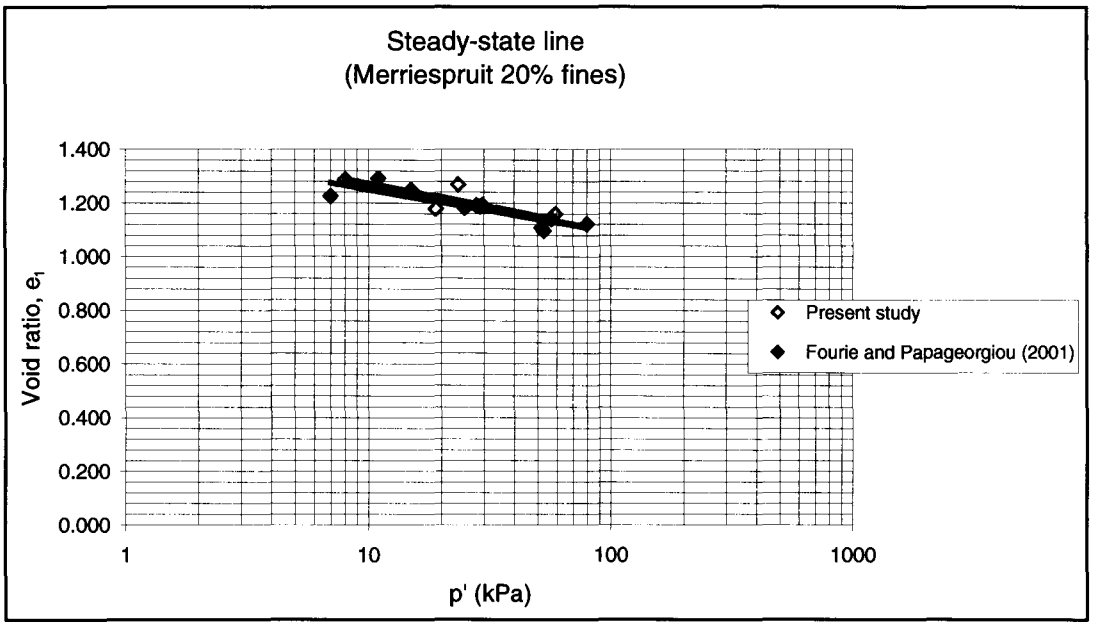


Figure 5.11 Steady-state line for isotropically consolidated Merriespruit gold tailings containing 20% fines

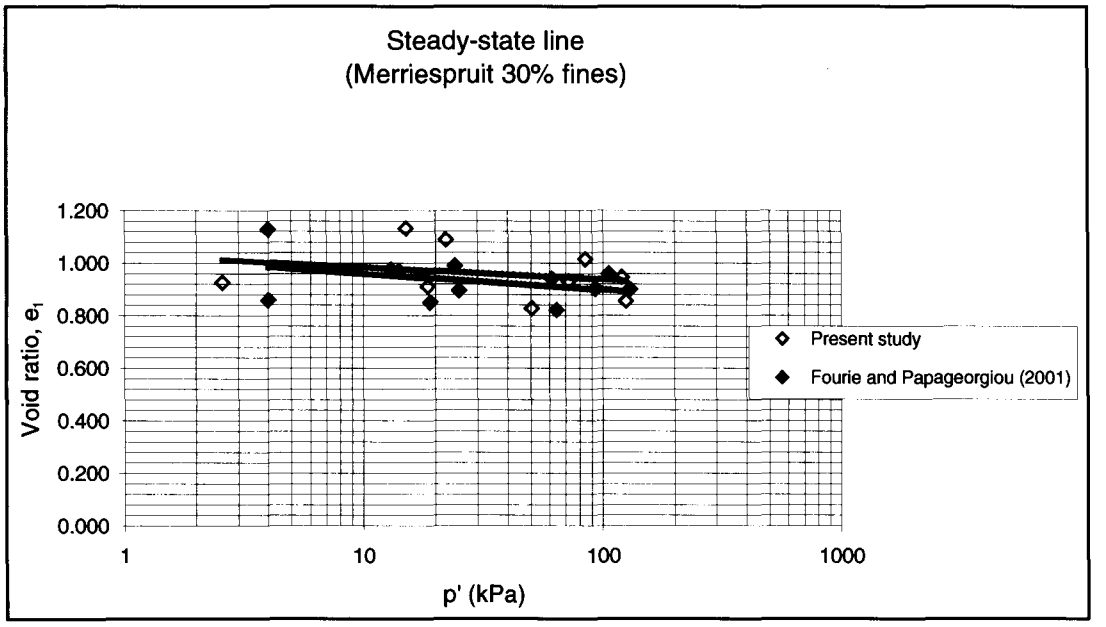


Figure 5.12 Steady-state line for isotropically consolidated Merriespruit gold tailings containing 30% fines

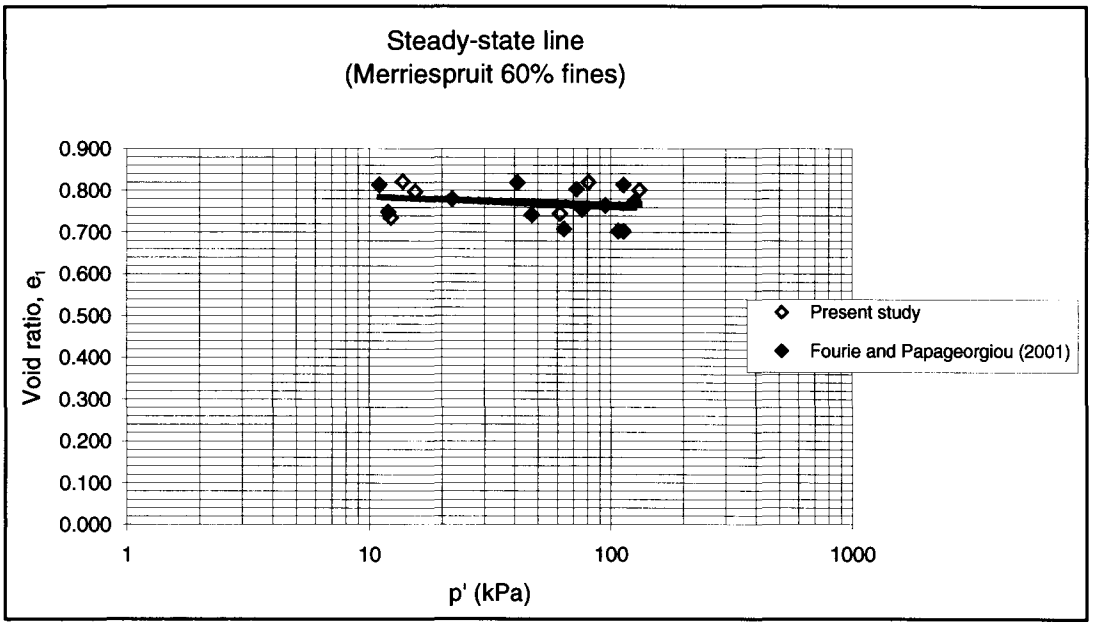


Figure 5.13 Steady-state line for isotropically consolidated Merriespruit gold tailings containing 60% fines

5.1.4 Variation of steady-state line with fines content and gradation

In the state diagram, Figure 5.14, the steady-state lines for the various fines contents (and gradations) of Merriespruit gold tailings were drawn together for the sake of comparison.

It can be seen in Figure 5.14 that the position of the steady-state line changed with fines content (and gradation) and that except for the 20% fines content steady-state line, all the steady-state lines were essentially parallel. The increase in fines content from 0% to 20% resulted in the steady-state line shifting upwards and getting somewhat steeper. As fines content was increased beyond 20%, the steady-state line moved progressively downwards while essentially maintaining the slope of the 0% fines steady-state line.

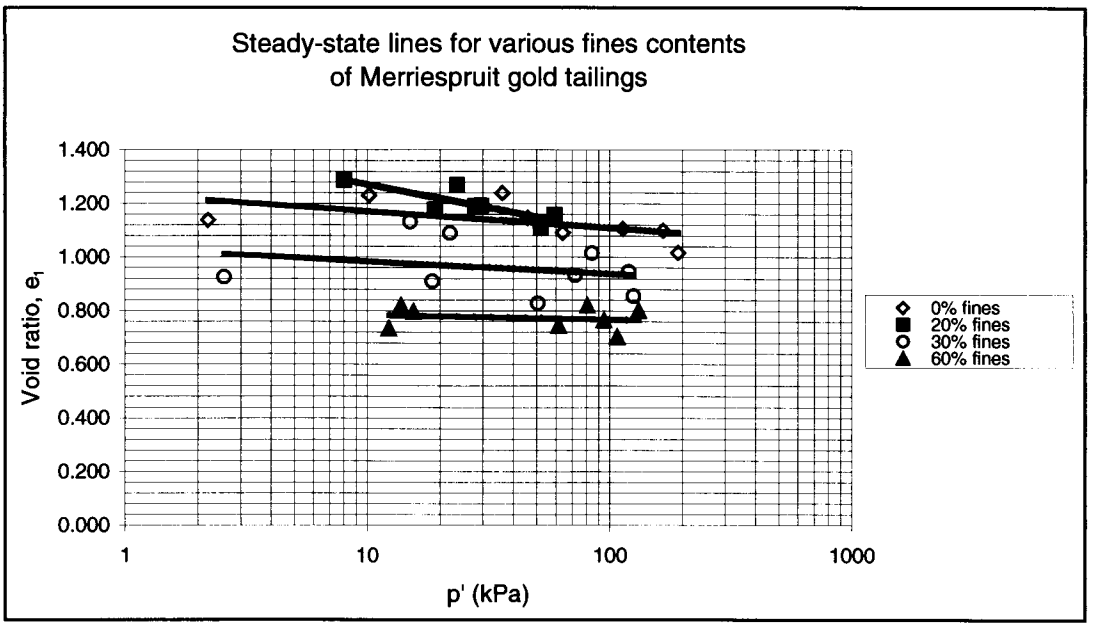


Figure 5.14 Variation of steady-state line of isotropically consolidated Merriespruit gold tailings with fines content (and gradation)

5.2 Monotonic Undrained Compression of One-Dimensionally Consolidated Specimens (case 2 tests)

The results of monotonic undrained compression triaxial tests on anisotropically consolidated Merriespruit gold tailings specimens are given in Appendix D and summarized in Table D1. In Figures 5.15, 5.16, 5.17 and 5.18, the stress paths for Merriespruit gold tailings containing 0%, 20%, 30% and 60% fines are shown, respectively.

The specimens were initially at stress states representing more or less the laboratory derived K0 value of about 0.60.

During undrained loading, in which the vertical force was increased at a constant rate of strain, the specimens exhibited a rapid increase in deviator stress at small strains and reached a peak deviator stress at axial strains generally smaller than those at which the peak deviator stress of isotropically consolidated specimens was mobilized (the minimum and maximum axial strains at peak deviator stress for all anisotropically consolidated specimens were 0.058 and 0.636%, respectively). After

reaching the peak deviator stress, the specimens showed a marked reduction in deviator stress as the deviator stress decreased with further straining until it stabilized at a residual/ steady-state strength at relatively large axial strains of about 7-15%. The pore pressure showed a steep increase initially and continued to increase at a lower rate roughly after the strains at which the deviator stress reached its peak. The pore pressure reached its maximum value at about the same axial strains at which the residual/ steady state shear strength was reached.

The pore pressure then remained essentially constant for the rest of the test except for specimens K0-17, K0-23, K0-29, K0-30 and K0-31, which contained 60% fines. For these specimens, the pore pressure remained constant up to axial strains of about 15%. Further straining of these specimens resulted in a decrease in pore pressure, which in turn precipitated an increase in deviator stress for the rest of the tests. These specimens therefore exhibited quasi steady-state behavior, which was also evident in some of the isotropically consolidated specimens with 60% fines content.

The stress paths in Figures 5.15, 5.16, 5.17, and 5.18 accordingly showed peak points followed by declines to the residual/ steady-state points. For all the tests, except for specimens K0-17, K0-23, K0-29, K0-30 and K0-31, the stress paths remained at the steady-state point for the rest of the test duration. For specimens K0-17, K0-23, K0-29, K0-30 and K0-31 the stress paths continued to rise after reaching their quasi steady-state points and remaining there for a while (from axial strains of about 7-15%). This is typical of quasi steady-state behavior.

As in the case of the quasi steady-state behavior observed in isotropically consolidated Merriespruit gold tailings containing 60% fines, the paths followed by the quasi steady-state stress paths (after the residual strength point) for anisotropically consolidated specimens of Merriespruit gold tailings containing 60% fines, appeared to project back to the origin of the stress space.

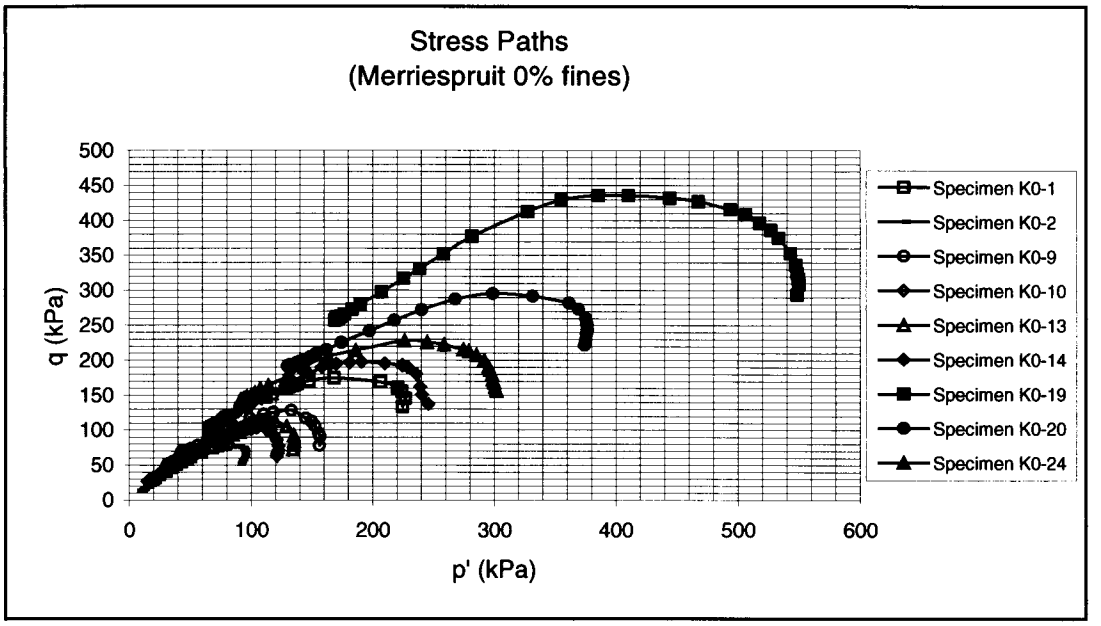


Figure 5.15 Stress paths for anisotropically consolidated Merriespruit gold tailings containing 0% fines

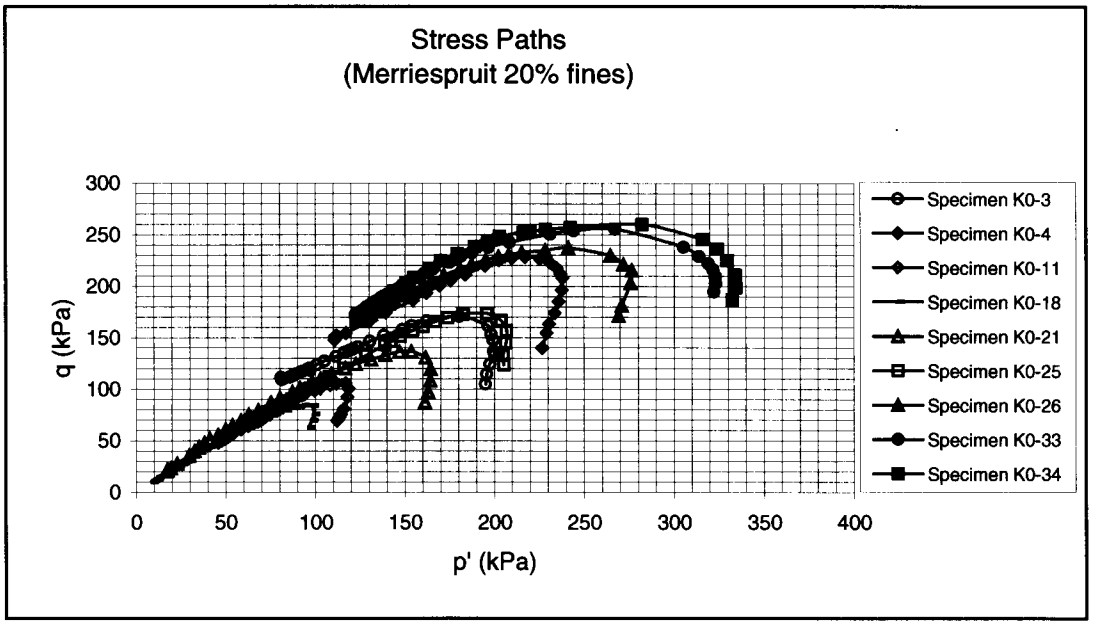


Figure 5.16 Stress paths for anisotropically consolidated Merriespruit gold tailings containing 20% fines

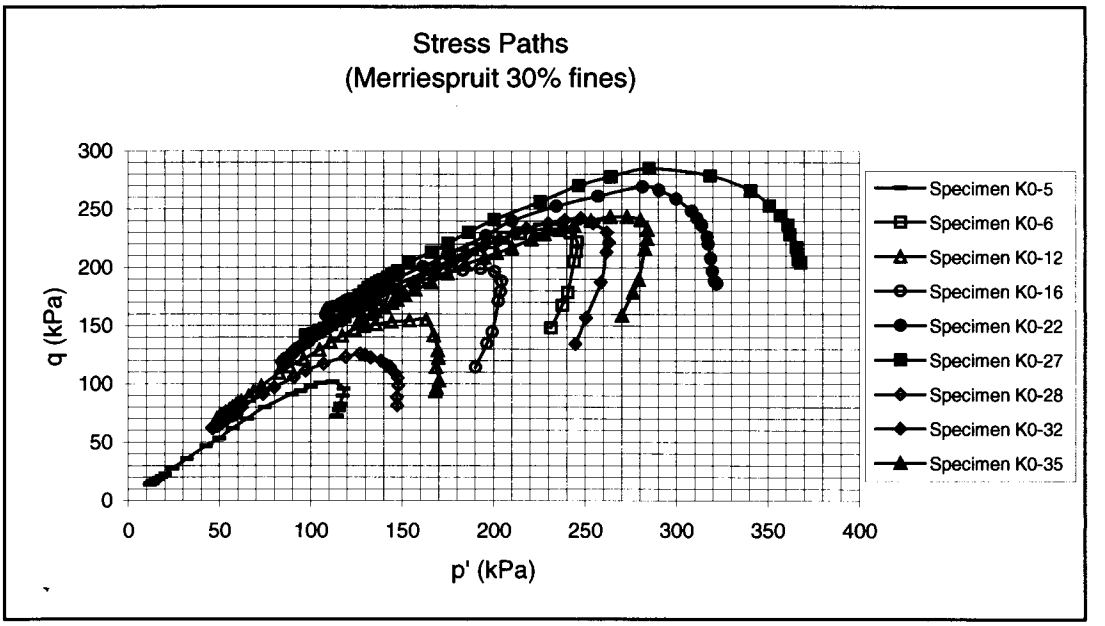


Figure 5.17 Stress paths for anisotropically consolidated Merriespruit gold tailings containing 30% fines

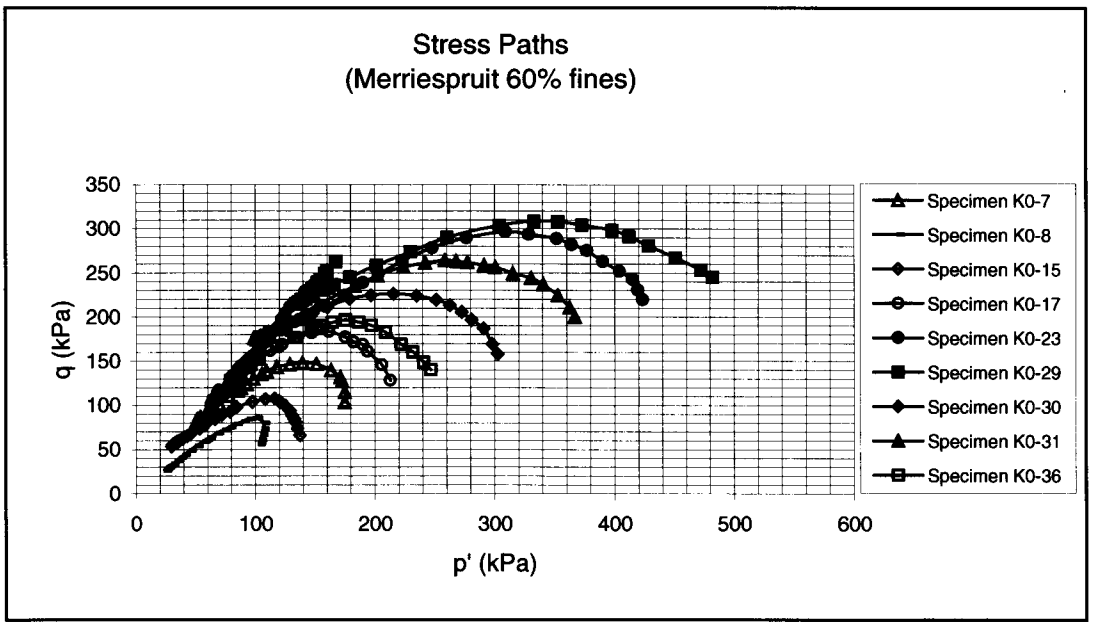


Figure 5.18 Stress paths for anisotropically consolidated Merriespruit gold tailings containing 60% fines

5.2.1 CSR line and steady-state failure envelope

The critical stress ratio lines (CSR lines) and steady-state failure envelopes obtained from monotonic undrained loading of anisotropically consolidated specimens of Merriespruit gold tailings containing 0%, 20%, 30% and 60% fines are shown in Figures 5.19, 5.20, 5.21, and 5.22, respectively. For comparison, the CRS lines and steady-state failure envelopes of isotropically consolidated Merriespruit gold tailings specimens containing 0%, 20%, 30% and 60% are appropriately included in these figures. In Figures 5.19, 5.20, 5.21, and 5.22, solid and open symbols correspond to CSR line and steady-state failure envelope, respectively. As before, some scatter in the data points is evident.

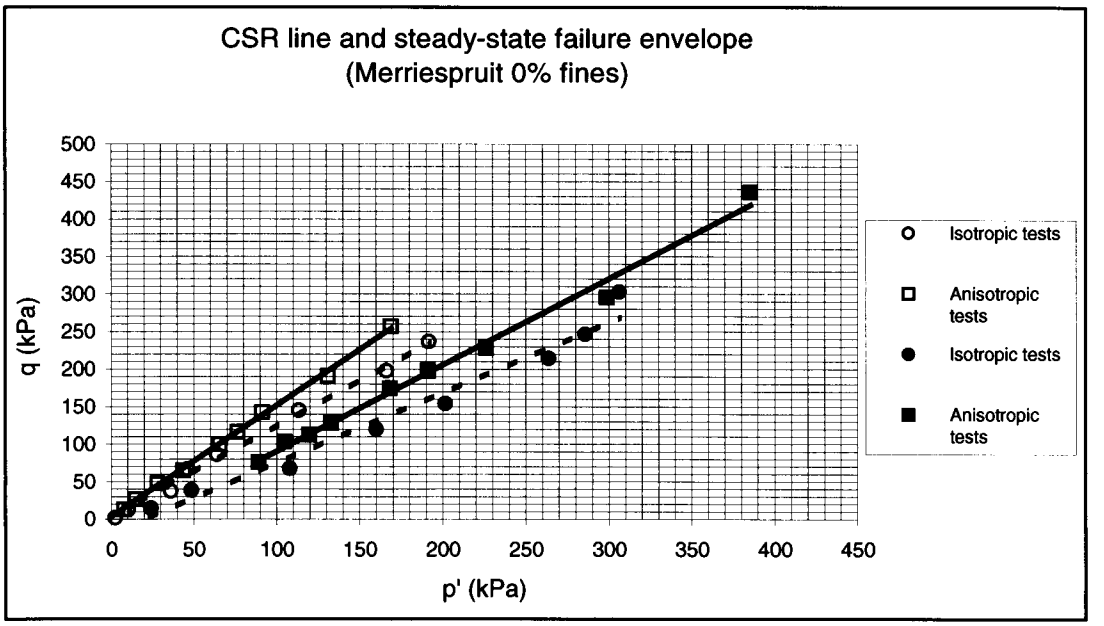


Figure 5.19 CSR lines and steady-state failure envelopes for isotropically consolidated and anisotropically consolidated Merriespruit gold tailings containing 0% fines

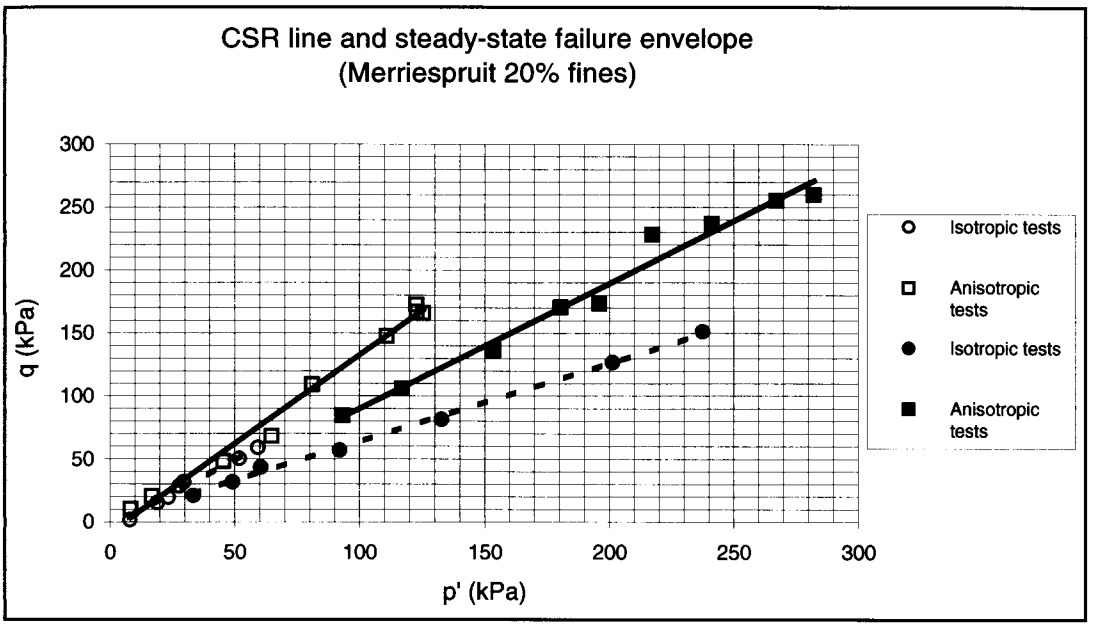


Figure 5.20 CSR lines and steady-state failure envelopes for isotropically consolidated and anisotropically consolidated Merriespruit gold tailings containing 20% fines

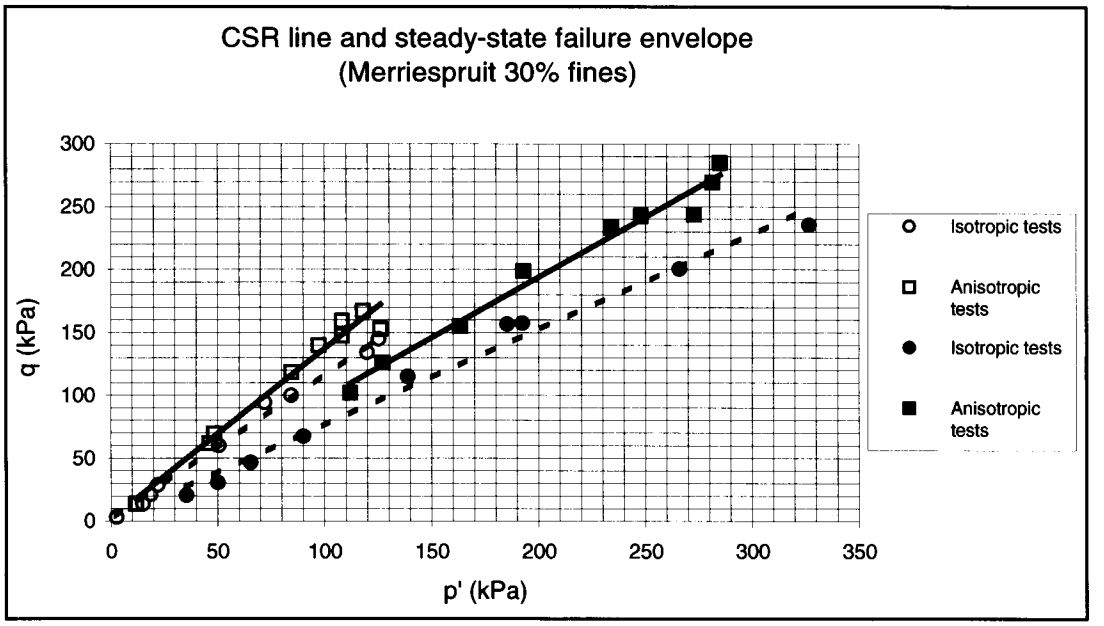


Figure 5.21 CSR lines and steady-state failure envelopes for isotropically consolidated and anisotropically consolidated Merriespruit gold tailings containing 30% fines

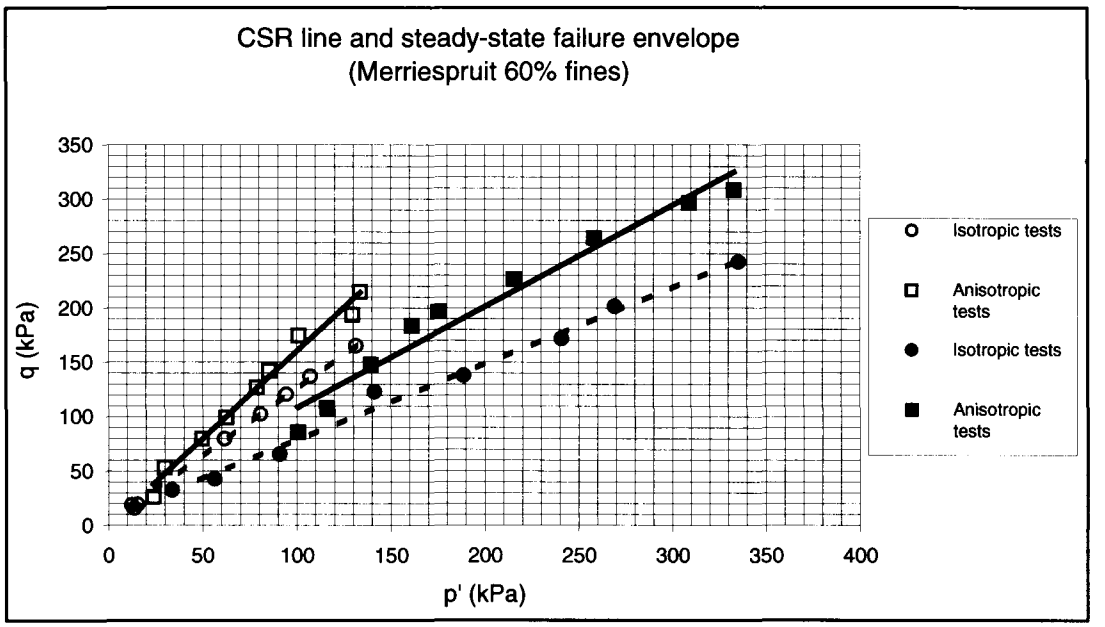


Figure 5.22 CSR lines and steady-state failure envelopes for isotropically consolidated and anisotropically consolidated Merriespruit gold tailings containing 60% fines

It can be seen in Figures 5.19, 5.20, 5.21, and 5.22 that the CSR line and steady-state failure envelope for various fines contents of Merriespruit gold tailings are different for isotropically- and anisotropically consolidated specimens. Although for both consolidation stress states the lines essentially pass through the origin of the stress space, the lines for anisotropically consolidated specimens were consistently higher (or steeper) in the stress space.

5.2.2 Variation of effective angles of friction mobilized at peak shear stress and at steady state with fines content and gradation

In Figure 5.23, the effective angle of friction mobilized at peak shear stress for isotropically consolidated and anisotropically consolidated Merriespruit gold tailings specimens are plotted against fines content. For each consolidation stress state and fines content, the averages of the friction angles were calculated and included in Figure 5.23 and lines through these average friction angles were drawn.

Figure 5.24 shows the effective angle of friction at steady-state for isotropically consolidated and anisotropically consolidated Merriespruit gold tailings against fines content. Also included in Figure 5.24, are the lines joining the averages of the data points.

It is clear in Figures 5.23 and 5.24, that for each consolidation stress state, both effective angles of friction changed with changes in fines content (and, ofcourse, gradation). The increase in fines content from 0% to 20% resulted in some decrease in the effective angles of friction mobilized at peak shear stress and at steady state. As mentioned before, the larger reduction in the average effective angle of friction at steady-state observed at 20% fines content was due to the extremely low effective angle of friction, about 5°, exhibited by one of the isotropically consolidated specimens. As fines content was increased beyond 20%, both effective friction angles increased.

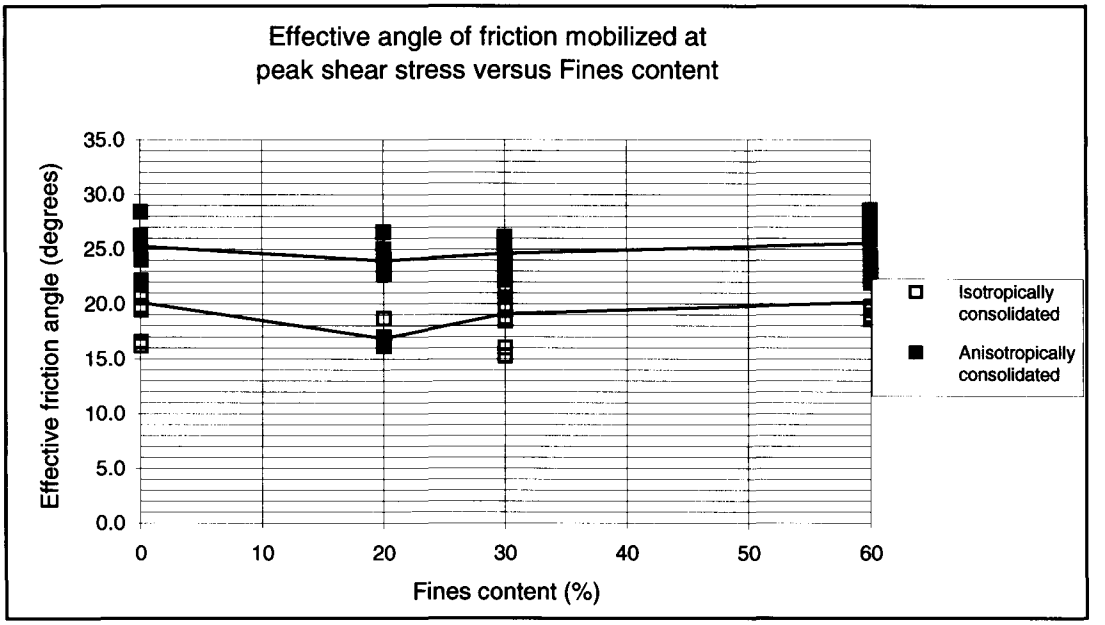


Figure 5.23 Variation with fines content (and gradation) of the effective angle of friction mobilized at peak shear stress for isotropically consolidated and anisotropically consolidated Merriespruit gold tailings

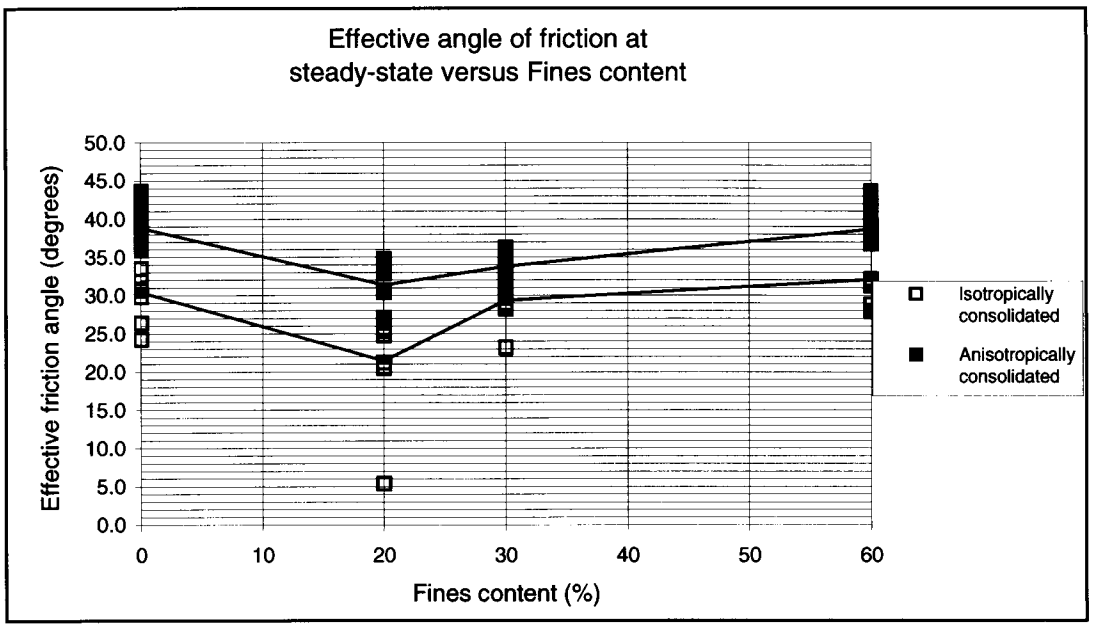


Figure 5.24 Variation with fines content (and gradation) of the effective angle of friction mobilized at steady-state for isotropically consolidated and anisotropically consolidated Merriespruit gold tailings

It can be seen in Figures 5.23 and 5.24 that, for all fines contents, the effective angles of friction mobilized at peak shear stress and at steady-state for anisotropically consolidated Merriespruit gold tailings were higher than those for the isotropically consolidated specimens. This follows directly from the fact that the CRS lines and steady-state failure envelopes were also different.

5.2.3 Steady-state line

The steady-state lines for anisotropically consolidated Merriespruit gold tailings containing 0%, 20%, 30% and 60% fines are shown in Figures 5.25, 5.26, 5.27, and 5.28, respectively. For comparison the steady-state lines for isotropically consolidated Merriespruit gold tailings containing 0%, 20%, 30% and 60% are appropriately included in these Figures.

As shown in Figures 5.25, 5.26, 5.27, and 5.28, the steady-state lines for isotropically consolidated and anisotropically consolidated Merriespruit gold tailings are parallel but the steady-state lines for the anisotropically consolidated specimens

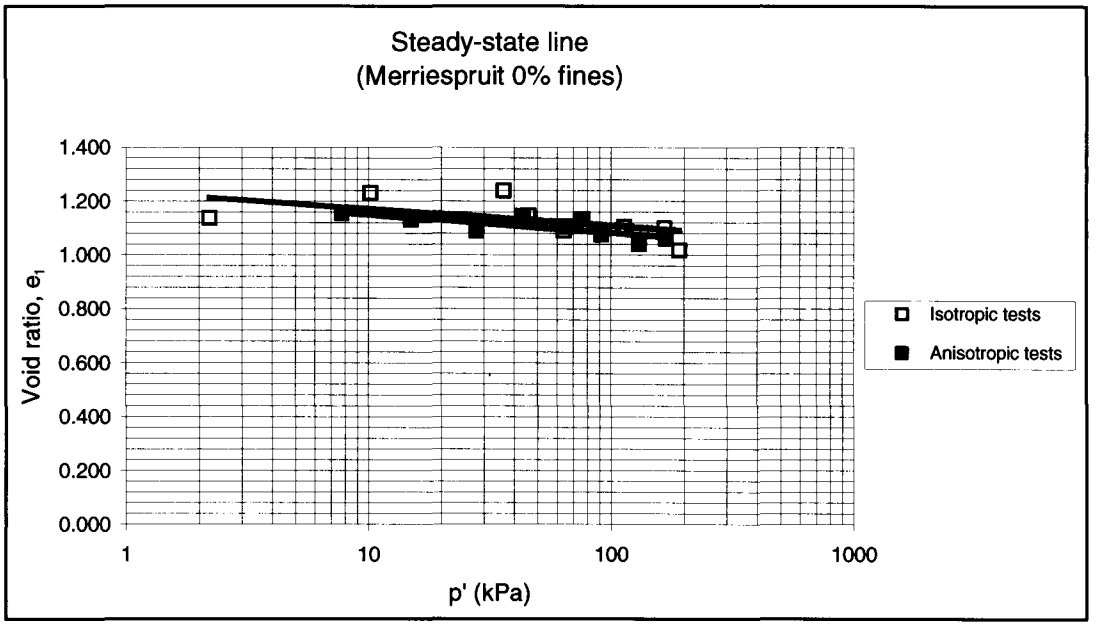


Figure 5.25 Steady-state lines for isotropically consolidated and anisotropically consolidated Merriespruit gold tailings containing 0% fines

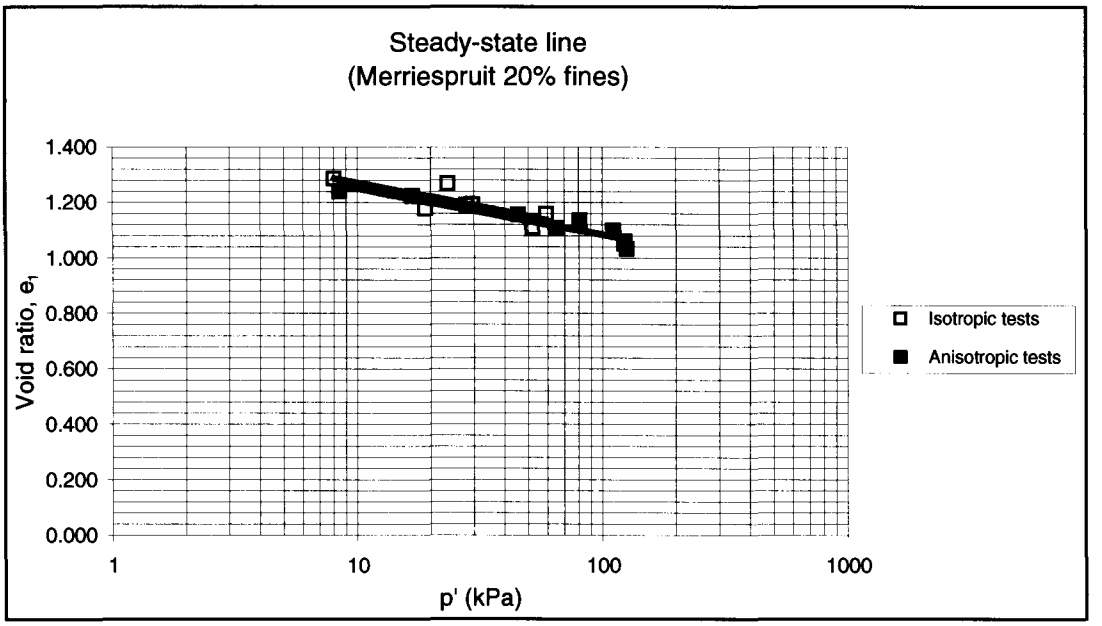


Figure 5.26 Steady-state lines for isotropically consolidated and anisotropically consolidated Merriespruit gold tailings containing 20% fines

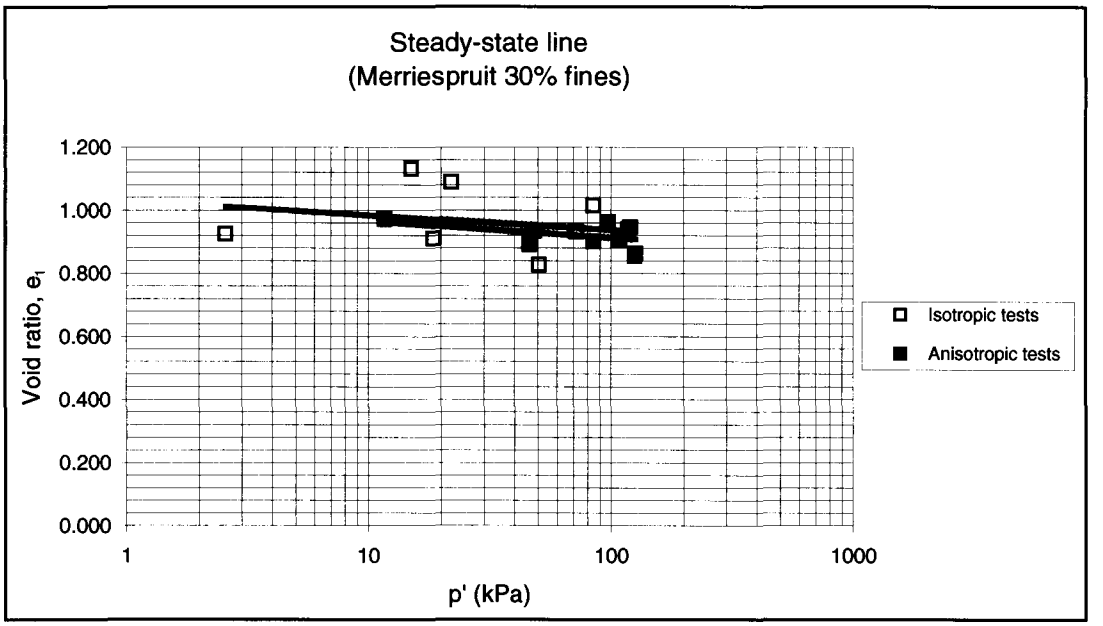


Figure 5.27 Steady-state lines for isotropically consolidated and anisotropically consolidated Merriespruit gold tailings containing 30% fines

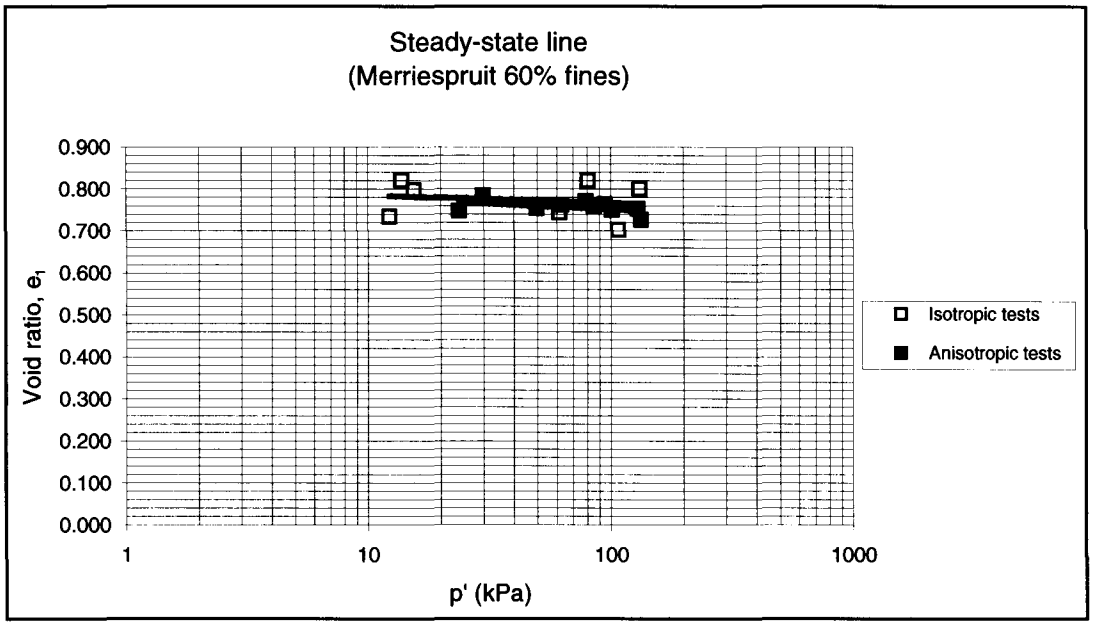


Figure 5.28 Steady-state lines for isotropically consolidated and anisotropically consolidated Merriespruit gold tailings containing 60% fines

are slightly lower that those of the isotropically consolidated specimens for all the fines contents. For a given fines content, the difference in the vertical positions of these steady-state lines is small.

5.2.4 Liquefaction resistance

Liquefaction, the loss of shear resistance due to rapid build up of pore pressure, initiates when the peak shear resistance is mobilized (Vaid et al. (1990)). The liquefaction resistance of a sand specimen was defined as the magnitude of the increase in deviator stress needed to initiate liquefaction (Kramer and Seed (1988)). As noted by, amongst many others, Castro et al. (1985), the liquefaction resistance of anisotropically consolidated sand is significantly lower than that of an isotropically consolidated sand. This statement is supported by test results observed in this study as shown in Figure 5.29, in which the liquefaction resistances of isotropically consolidated and anisotropically consolidated specimens of Merriespruit gold tailings containing various percentages of fines were plotted against effective mean normal stress after consolidation.

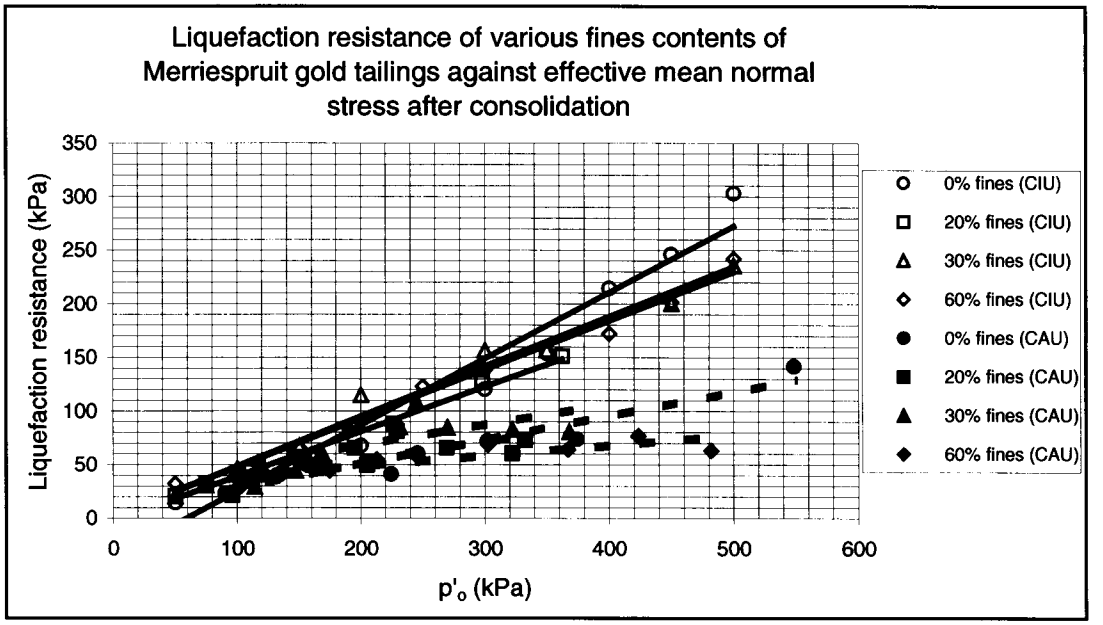


Figure 5.29 Variation of liquefaction resistance of isotropically consolidated and anisotropically consolidated specimens with effective mean normal stress after consolidation

Figure 5.29 also shows that the increase in liquefaction resistance of anisotropically consolidated Merriespruit gold tailings specimens with effective mean normal stress after consolidation is lower than that of isotropically consolidated specimens.

5.3 Variation of Stress Path Followed During Undrained Loading of One-Dimensional Consolidated Specimens (Case 3 tests)

The results of undrained tests in which anisotropically consolidated Merriespruit gold tailings containing 20% fines were loaded by reducing the confining pressure while keeping either the deviator stress or the effective mean normal stress constant are given in Appendix E and summarized in Table E1. The stress paths for these tests are shown in Figure 5.30.

For the tests in which an attempt was made to keep the effective mean normal stress constant, specimens BW-2 and BW-5, the deviator stress increased rapidly until it reached its peak at axial strains of 0.89 and 0.87%, respectively. After reaching the peak, the deviator stress decreased considerably and reached its steady-state value at axial strains of about 9% and 7%, respectively. The pore pressure in specimen BW-2 increased until it reached its maximum value at axial strain of about 9%. In specimen BW-5, the pore pressure decreased substantially up to an axial strain of about 1% and then increased until it reached its maximum at an axial strain of about 7%. The stress paths for these specimens showed well defined peaks followed by declines to steady-state points.

For tests in which an attempt was made to keep the deviator stress constant, specimens BW-1, BW-3, and BW 4, the effective mean normal stress decreased continuously until it reached its steady-state value. In all these specimens, the pore pressure decreased with axial strain up to axial strains of about 1.6, 0.7, and 0.8% respectively. The pore pressures in these specimens then started to increase reaching their maximum values at axial strains of about 9, 9, and 7% respectively.

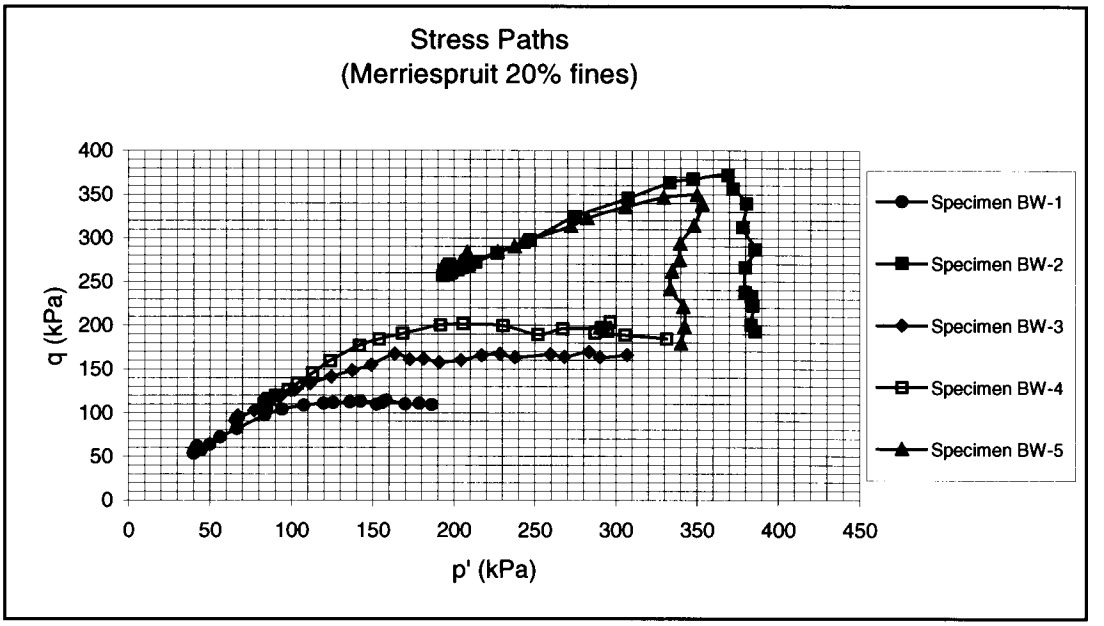


Figure 5.30 Stress paths for anisotropically consolidated Merriespruit gold tailings containing 20% fines, loaded undrained by reducing the cell pressure while keeping either the deviator stress or the effective mean normal stress constant

As mentioned in chapter 3, section 3.4.8, the attempt to keep the deviator stress in these specimens constant was by reducing the cell pressure in such a way as to balance the increase in deviator stress indicated by the load transducer reading and as soon as the deviator stress ceased to increase with further straining, the cell pressure was left unchanged. This condition was taken as the initiation of liquefaction and it corresponds to the points on the stress paths of specimens BW-1, BW-3, and BW-4, Figure 5.30, at which the deviator stress started to decrease continuously until it reached the steady-state value.

5.3.1 CSR line and steady-state failure envelope

In Figure 5.31, the stress conditions corresponding to the peak deviator stress in specimens BW-2, and BW-5 and the stress condition corresponding to the points at which the deviator stress in specimens BW-1, BW-3, and BW-4 started to decrease continuously to the steady state value were used to construct the CSR line. The steady-state failure envelope was constructed as before. In Figure 5.31, Solid and

open symbols correspond to CSR line and steady-state failure envelope, respectively.

Also included in Figure 5.31, is the CSR line and the steady-state failure envelope for anisotropically consolidated Merriespruit gold tailings containing 20% fines loaded in the conventional manner, i.e. by increasing the vertical stress while keeping the confining pressure constant.

It is clear in Figure 5.31 that the CSR line and the steady-state failure envelope for Merriespruit gold tailings loaded by reducing the cell pressure while keeping either the deviator stress or the effective mean normal stress constant are essentially the same as those obtained under conventional loading of Merriespruit gold tailings containing the same fines content (20%).

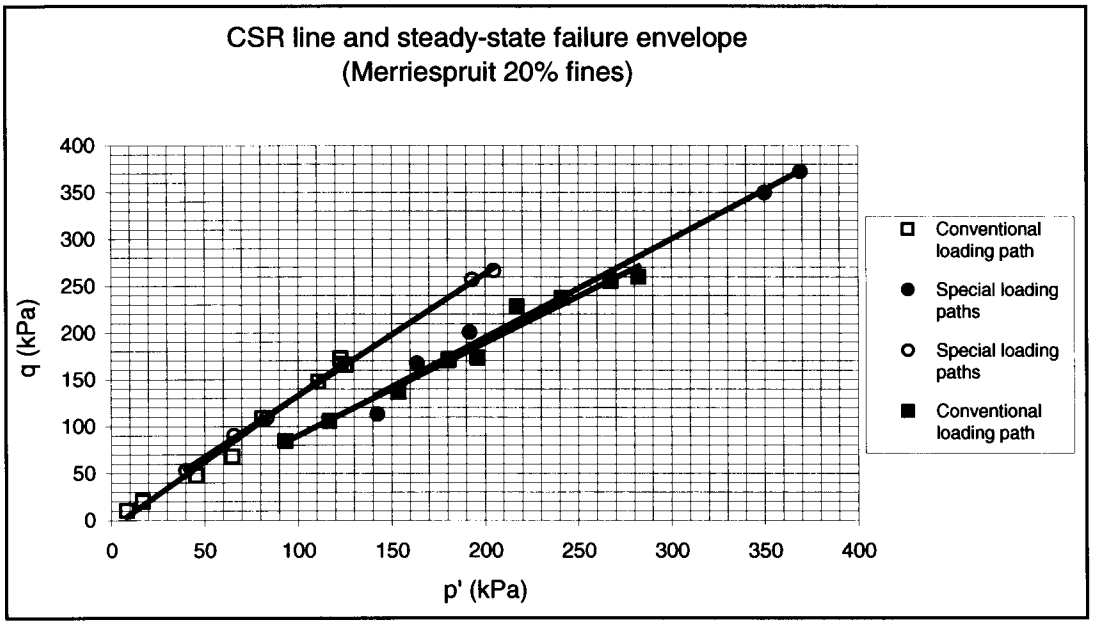


Figure 5.31 CSR lines and steady-state failure envelopes obtained during conventional and special undrained loading of anisotropically consolidated Merriespruit gold tailings containing 20% fines

5.3.2 Steady-state line

The steady-state line for Merriespruit gold tailings containing 20% fines, loaded by reducing the cell pressure while keeping either the deviator stress or the effective mean normal stress constant is plotted together with the steady-state line for anisotropically consolidated Merriespruit gold tailings containing 20% fines loaded in the conventional manner in Figure 5.32. It can be seen in Figure 5.32 that the steady-state line defined by the tests in which failure was brought about by reducing the cell pressure while keeping either the deviator stress or the effective mean normal stress constant is not different from that obtained using conventional loading.

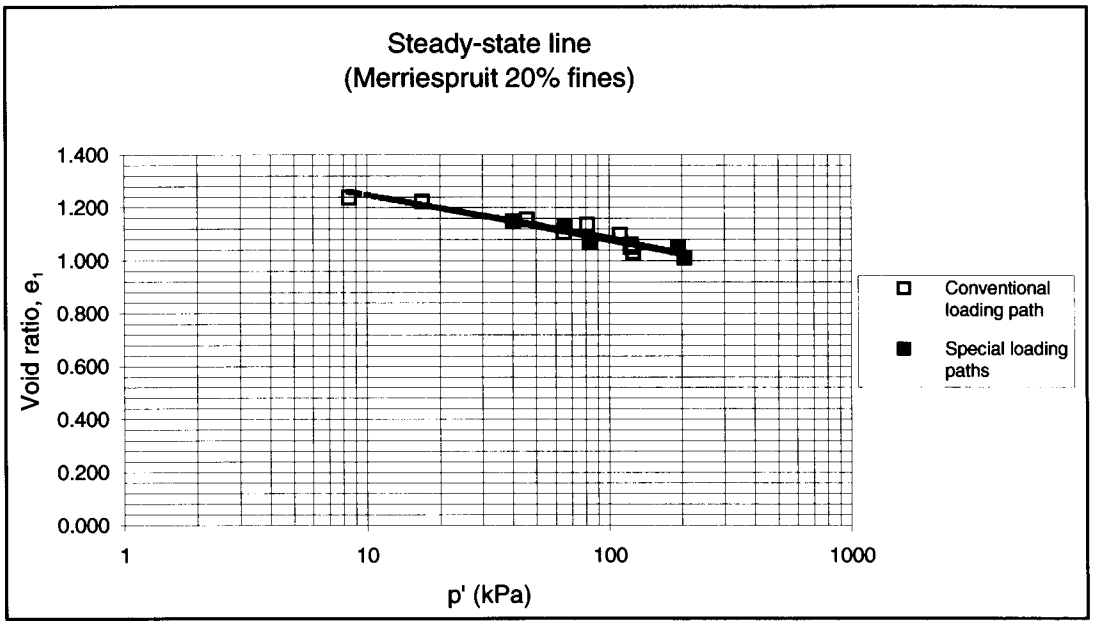


Figure 5.32 Steady-state lines for anisotropically consolidated Merriespruit gold tailings containing 20% fines loaded undrained by following various stress paths

5.4 Summary of Findings

5.4.1 Tests on isotropically consolidated specimens

Strain-softening behavior

The strain-softening behavior observed for isotropically consolidated specimens containing various fractions of fines (percentage finer than 75μm) was in accordance with the typical liquefaction behavior postulated in the literature (for example, Castro (1969); Castro and Poulos (1977)) in which the peak deviator stress is reached at small strains of about 1 to 2% and the steady-state strength is achieved at axial strains of about 10 to 15%.

Limited liquefaction behavior

For isotropically consolidated specimens that exhibited limited liquefaction behavior (all of which contained 60% fines), this behavior was in accordance with that postulated in the literature (for example, Castro (1969); Castro and Poulos (1977); Alarcon-Guzman et al. (1988)) with axial strains at peak deviator stress of about 1-2% and axial strains at residual strength of about 7-15%.

CSR line

Despite some scatter, results of monotonic undrained tests on isotropically consolidated specimens showed that, for a given fines content, the CSR line is unique and independent of void ratio and initial confining pressure and that it is a straight line passing through the origin of the stress space. This is in accordance with the observations made by Bishop (1971); Vaid and Chern (1985); Vaid et al. (1990); and Mohamad and Dobry (1986). For a given void ratio, the uniqueness of the CSR line for isotropically consolidated specimens, was also supported by reasonable agreement when comparison was made between the CSR line obtained in this study with the CSR line obtained by Fourie and Papageorgiou (2001) in a similar study on the same tailings.

Steady-state failure envelope

For a given fines content, the results of monotonic undrained compression tests on isotropically consolidated specimens indicated that the steady-state failure envelope is unique and independent of void ratio and effective confining pressure and it passes through the origin of the stress space. Mohamad and Dobry (1986) also observed that the steady-state failure envelope is independent of void ratio. A comparison of the steady-state lines observed for isotropically consolidated specimens with the steady-state lines reported by Fourie and Papageorgiou (2001) in a similar study on the same tailings further supported the uniqueness of the steady-state failure envelope.

Steady-state strength

For a given sand, the steady-state strength is postulated in the literature to be a unique function of void ratio (for example, Castro (1969); Casagrande (1976); Castro (1975); Castro and Poulos (1977); and Poulos (1981)). The uniqueness of the steady-state strength with void ratio could not be assessed in the present study since, under each series of tests, specimens were consolidated to different void ratios in order to facilitate the construction of the CSR line; steady-state failure envelope; and the steady-state line. It could have been possible to prepare specimens for each series of tests at various void ratios but such that the void ratios of some of the specimens under these three series of tests are the same. This would have enabled an even better evaluation of the effect of consolidation stress state, fines content, and loading stress path.

Test results of the present study, however, imply that the steady-state strength for Merriespruit gold tailings was different for different fines contents and different consolidation stress states because the steady-state failure envelopes (which are lines joining the steady-state strengths in the stress space) for these different test conditions were different.

Steady-state line

Although the steady-state lines observed in this study suffered from some scatter, which according to Vaid et al. (1990) could be due to specimen nonuniformity and fabric variation at each moist tamped density, the uniqueness of these lines for isotropically consolidated specimens was evident since, for a given fines content, the steady-state line obtained in this study was in good agreement with that obtained in a similar study on the same tailings (Fourie and Papageorgiou (2001)).

5.4.2 Effect of anisotropic consolidation

Strain-softening behavior

Anisotropically consolidated specimens exhibited a strain-softening behavior under the conventional monotonic undrained loading condition (case 2 tests) similar to that shown by isotropically consolidated specimens (case 1 tests). However, it was noted that both the shear stress and axial strain required to mobilize the peak shear resistance decreased substantially with anisotropic consolidation. This is in accord with the reports made in the literature (for example, Bjerrum et al. (1961); Castro (1969); Bishop (1973); Alarcon-Guzman et al. (1988); Kramer and Seed (1988)).

Limited liquefaction behavior

The limited liquefaction behavior shown by Merriespruit gold tailings specimens that were anisotropically consolidated (all of which contained 60% fines) was similar to that shown by their isotropically consolidated companions, although, the shear stress increments and axial strains required to mobilize their peak shear resistance were considerably lower than those required for their isotropically consolidated companions.

CSR line

For a given fines content, the CSR line obtained from anisotropically consolidated specimens was different from that obtained from isotropically

consolidated specimens. The CRS lines for anisotropically consolidated Merriespruit gold tailings specimens were consistently steeper than those of isotropically consolidated specimens.

The CSR lines for anisotropically consolidated specimens were also independent of void ratio and initial confining pressure and passed through the origin of the stress apace.

Steady-state failure envelope

The steady-state failure envelope obtained from anisotropically consolidated specimens was different from that obtained using isotropically consolidated specimens containing the same fines content. Steady-state lines obtained from anisotropic tests were steeper than those obtained from isotropically consolidated tests.

Like the CSR line, for a given fines content, the steady-state failure envelope for anisotropically consolidated specimens was unique and independent of void ratio and effective confining pressure and passed through the origin of the stress space.

Steady-state line

For a given fines content, the steady-state lines obtained from anisotropic tests were parallel to and somewhat lower than those obtained from isotropic tests. However, the difference in these steady-state lines was small.

5.4.3 Effect of fines content and gradation

CSR line

The variation of the CSR line with fines content (and gradation) was evident when the effective angle of friction mobilized at peak shear stress was plotted against fines content for specimens under either case 1 or case 2 tests. For both series of tests (case 1 and case 2 tests), the increase of fines from 0% to 20% resulted in a

reduction in the effective angle of friction mobilized at peak shear stress whereas the increase of fines beyond 20% resulted in an increase in the effective angle of friction mobilized at peak shear stress.

Steady-state failure envelope

The results of the case 1 and case 2 tests showed that the steady-state failure envelope changes with changes in fines content (and gradation).

The variation of the steady-state failure envelope with fines content (and gradation) was assessed by plotting the effective angle of friction at steady state against fines content. The effective angle of friction at steady state was seen to decrease as fines content was increased from 0% to 20%. The increase of fines content beyond 20% resulted in an increase in the effective angle of friction. This variation of effective angle of friction at steady state with fines content is similar to the variation of the effective angle of friction at peak shear stress with fines content.

Steady-state line

The present study indicates that the steady-state line of Merriespruit gold tailings changed as fines content (and gradation) was changed. With increase of fines content from 0 to 20%, the steady-state line plotted higher and somewhat steeper whereas increasing fines content beyond 20% resulted in the steady state line plotting lower but with no essential change in slope from that of the 0% fines steady-state line.

5.4.4 Effect of loading stress path

CRS line, steady-state failure envelope, and steady-state line

The special undrained loading stress path tests (case 3 tests) performed in the present study indicated that for a given fines content (in this case 20%), the CSR line, the steady-state failure envelope and the steady-state line obtained from

anisotropically consolidated specimens are independent of the stress path leading to failure.

5.5 Discussion

5.5.1 Effect of anisotropic consolidation

It is clear that the application of vertical stress, along with a confining pressure, under drained conditions during saturation and consolidation of a triaxial specimens induces an anisotropic fabric in which there will be unequal particle contacts and forces between particles in different directions (Oda (1981); Been et al. (1991)).

The distribution of particle contacts and forces at the start of undrained loading determines the stress-strain and pore pressure generation characteristics leading to failure of the sand (Wong and Arthur (1985)).

In the present study, the effect that anisotropic consolidation had on Merriespruit gold tailings with different gradations and different fines contents was clear. For all gradations and fines contents, both the CSR line and the steady-state failure envelope were steeper for anisotropically consolidated specimens when compared with those obtained for isotropically consolidated specimens whereas not much difference to the steady-state line was brought about as a result of anisotropic consolidation.

The fact that the present study tested Merriespruit gold tailings with different gradations and fines contents (and essentially, therefore, different sands) probably justifies the generalization of the postulation that for any sand, the effect of anisotropic consolidation is to bring about a sand fabric with higher particle contacts and forces in the vertical direction than the particle contacts and forces that would be achieved if the same sand had been consolidated isotropically and that this results in steeper CRS line, steeper steady-state failure envelope, but essentially the same steady-state line due to different stress-strain and pore pressure generation characteristics both at small strains (< 0.5%) and large strains (> 0.5%) associated with these different fabrics.

5.5.2 Effect of fines content and gradation

All other physical characteristics of a sand (grain size, grain shape, mineralogy, and gradation) being constant, it is clear that the addition of fines to a sand changes the sand into a completely different sand with potentially different liquefaction characteristics (Been and Jefferies (1985); Kuerbis et al. (1988); Pitman et al. (1994); Lade and Yamamuro (1997)).

Observations reported in the literature regarding the effect of fines content on the liquefaction characteristics of sand have not generally indicated the same findings. For example, Kuerbis et al. (1988) and Pitman et al. (1994) concluded that the increase in fines decreases the liquefaction potential whereas Sladen et al. (1985) and Lade and Yamamuro (1997) showed that the liquefaction potential increases with increase in fines content.

The key to the manner in which the increase in fines will alter the liquefaction characteristics of a sand seems, therefore, to lie on the physical characteristics (grain size, grain shape, mineralogy, and gradation) of the parent sand onto which the fines are added because these determine the interaction that occurs between the fines and the parent sand. Also, for a given sand the amount of fines added determines the type of interaction between the sand grains and the fines. For example, Kuerbis and Vaid (1989) observed that the addition of fines up to 20% did not change the skeletal void ratio as the fines occupied the void spaces and did not have any contribution to undrained behavior and Pitman et al. (1994) found that the increase of fines content beyond 20% changed the sand from a sand whose undrained behavior is dominated by a sand grain to sand grain contact to one whose undrained behavior is dominated by the fine matrix.

The change in gradation of a sand certainly changes the fabric of a sand. Some researchers (for example Castro and Poulos (1977) and Poulos et al. (1985)) have indicated that the steady-state line is sensitive to even small differences in gradation while some researchers (for example Pitman et al. (1994)) concluded that gradation did not have an effect in the collapse behavior of a sand.

In the present study, both gradation and fines content were varied simultaneously. It was therefore not possible to isolate the effect of fines content or gradation alone. It was observed, however, that the simultaneous variation of fines content and gradation had a significant effect on the liquefaction characteristics of Merriespruit gold tailings.

It seems reasonable to suspect that, although the gradation was also changed, the addition of fines up to 60% led to the tailings being more dominated by the fines matrix and that this must have caused the observed shift from contractive behavior to limited liquefaction behavior. However, since gradation was not kept constant, this postulation is questionable.

5.5.3 Implication of the variable loading stress path tests

Uniqueness of CRS line, steady-state failure envelope and steady-state line

The fact that the CSR line, the steady-state failure envelope, and the steady-state line for anisotropically consolidated Merriespruit gold tailings containing 20% fines were the same regardless of the stress path followed during undrained loading supports the postulation that for a given sand fabric (with the same gradation and fines content) these lines are unique and independent of void ratio, initial effective confining pressure, and loading stress path.

CRS line marks initiation of strain-softening behavior

Tests in which the loading stress path was varied showed that the CSR line determines the initiation of liquefaction behavior under undrained loading because any stress path that attempted to cross this line, regardless of the direction of approach, immediately developed strain-softening behavior leading to liquefaction failure. The CSR line therefore defines a state boundary above which no stress state is possible. Sladen et al. (1985) suggested that for a given void ratio, there exists a straight line above which no stress state can exist. This implied that a series of these straight lines associated with various void ratios define a surface in the effective

mean normal stress-deviator stress-void ratio space defining initiation of collapse. Sladen et al. (1985) called this surface the collapse surface. A somewhat similar surface was proposed by Sasitharan et al. (1993) who suggested that the postpeak portion (from peak to steady-state) of a constant void ratio stress path defines a state boundary surface determining initiation of strain-softening behavior so that for various void ratios, this state boundary defined a surface in the effective mean normal stress-deviator stress-void ratio space. Contrary to the above-mentioned surfaces, the present study observed that the CSR line, which is independent of void ratio, defined the initiation of strain-softening behavior.

In this chapter, the results of the liquefaction tests performed in the present study were presented and discussed under the framework of the steady-state approach. Results from each of the series of tests carried out in the present investigation were compared by plotting them on the same graph and findings were discussed. Results of isotropic tests performed in this study (case 1 tests) were compared with those obtained by Fourie and Papageorgiou (2001) and the findings were discussed. Results of case 1 and case 2 tests were plotted on common graphs to evaluate the effect of anisotropic consolidation and results of case 2 and case 3 tests were plotted together to evaluate the effect of loading stress path on liquefaction characteristics.

In the next chapter, chapter 6, the findings of the present investigation are summarized and the conclusions are given. Also included in chapter 6 are the recommendations for future research.

6 CONCLUSIONS AND RECOMMENDATIONS

6.1 Summary and Conclusions

The primary objective of the present study was to investigate the effect of anisotropic consolidation on the static liquefaction characteristics of tailings. This is important because the current procedures for assessing the static liquefaction characteristics of sands make use of isotropically consolidated specimens of a sand in laboratory tests whereas it is clear that the sand fabric existing insitu is anisotropic.

Another factor that was investigated by the present study is the effect of stress path followed during undrained loading. This was important because it would reveal whether the liquefaction characteristics determined using the conventional monotonic undrained loading, wherein the triaxial specimen is loaded by increasing the axial force at a constant rate of strain, are different from those resulting from a different loading stress path.

Use was made of the Merriespruit gold tailings recovered from the vicinity of the failure scar after the 1994 flow failure of the Merriespruit gold tailings dam to reconstitute triaxial specimens for use in the present study. The availability of previous test results in which this tailings was tested under isotropic conditions to determine its liquefaction characteristics (Fourie and Papageorgiou (2001)) offered the benefit of being able to compare results from the present study with those obtained by Fourie and Papageorgiou (2001).

Since Fourie and Papageorgiou (2001) made use of various gradations of Merriespruit gold tailings, each of which had a different fines content, the present study also had to vary these parameters simultaneously so as to match those used by Fourie and Papageorgiou (2001) to aid in the comparison. To some extent, therefore, the present study also studied the effect of gradation and fines content on the liquefaction characteristics of tailing.

Three series of laboratory tests were performed (case 1, case 2, and case 3 tests). Each series of tests involved the use of four bulk samples of Merriespruit gold

tailings with different gradations and fines contents. The fines contents of these bulk samples were 0%, 20%, 30%, and 60%. All specimens were prepared using the same moist tamping technique to aid in the comparison. Specimens for case 1 tests were consolidated isotropically whereas specimens for cases 2 and 3 tests were consolidated anisotropically. Specimens for cases 1 and 2 tests were loaded undrained in the conventional manner, i.e. by increasing the axial stress at a constant rate of strain. Specimens for case 3 tests were loaded undrained by reducing the cell confining pressure while keeping either the deviator stress or the effective mean normal stress constant.

The results of the present study revealed that, all else being constant, the simultaneous variation of gradation and fines content results in different liquefaction characteristics of Merriespruit gold tailings. Fourie and Papageorgiou (2001) reached the same conclusion.

A comparison of results obtained in the present study for specimens that were consolidated isotropically (case 1 tests) with those obtained by Fourie and Papageorgiou (2001) showed that the liquefaction characteristics obtained from these two studies were in agreement. For a given fines content (and gradation) the CSR lines and the steady-state failure envelopes determined from this study were essentially the same as those reported by Fourie and Papageorgiou (2001). Both the CSR line and the steady-state failure envelope were straight lines, independent of void ratio and initial confining pressure, and passed through the origin of the stress space. The steady-state lines obtained in this study and in the study by Fourie and Papageorgiou (2001) were essentially the same.

Comparing results obtained from tests in which specimens were isotropically consolidated and loaded in the conventional manner (case 1 tests) with the results obtained from tests in which the specimens were consolidated anisotropically and loaded in the conventional manner (case 2 tests), for a given fines content (and gradation), it was clear that the liquefaction characteristics derived from anisotropically consolidated specimens were different from those obtained from isotropically consolidated specimens. For a given fines content (and gradation) the CSR line and steady-state failure envelope obtained for anisotropically consolidated

specimens were steeper than those derived from isotropically consolidated specimens. Accordingly, the effective angles of friction mobilized at peak shear stress and at steady-state for anisotropically consolidated specimens were greater than those obtained from isotropically consolidated specimens. For a given fines content (and gradation) the steady-state lines obtained for anisotropically consolidated specimens were somewhat lower than those obtained from isotropically consolidated specimens whereas their slopes were essentially the same. However, the differences in these steady-state lines were small.

Comparing results of tests in which anisotropically consolidated Merriespruit gold tailings specimens containing 20% fines were loaded in the conventional manner (case 2 tests) with results of tests in which anisotropically consolidated Merriespruit gold tailings specimens containing 20% fines were loaded by reducing the cell pressure while keeping either the deviator stress or the effective mean normal stress constant (case 3 tests), it was clear that the undrained stress path by which the specimen is brought to failure did not affect the liquefaction characteristics of the specimens. It was concluded that the CSR line, steady-state failure envelope, and steady-state line of Merriespruit gold tailings are unique for a given fines content (and gradation) and consolidation stress state (isotropic or anisotropic). Moreover, the CSR line was seen to be an important line determining the initiation of strain-softening behavior under undrained loading so that any stress path attempting to cross this line, regardless of the direction of approach, immediately declines to the residual/ steady-state strength conditions.

6.2 Recommendations for Future Research

The present study clearly showed that the variation of gradation and fines content of Merriespruit gold tailings significantly alters the liquefaction characteristics of this tailings. However, since gradation and fines content were varied simultaneously, it was not possible to isolate the effect of the one from that of the other. It is therefore recommended that, in order to study the effect of gradation alone, the fines content of specimens be kept constant while the gradation is changed. Similarly, in order to study the effect of fines, gradation must be kept constant.

The present study utilized Merriespruit gold tailings specimens consolidated to various void ratios and effective confining pressures without an effort to achieve the same void ratio for specimens under the different series of tests. Although this was sufficient to achieve the objective of the present study, it is recommended that for future study, the variation of void ratio after consolidation be controlled so that some of the specimens under different series of tests have identical void ratios.

Although tests in which undrained loading was done by reducing the cell pressure (case 3 tests) revealed the independence of liquefaction characteristics on the stress path through which failure is brought about, it is recommended that more tests be done using different gradations and fines contents since only five specimens were tested in this study and all of these specimens had the same gradation and fines content (20%).

REFERENCES

Alarcon-Guzman, A. (1986). "Cyclic stress-strain and liquefaction characteristics of sands." thesis presented to Purdue University, at West Lafayette, Ind., in partial fulfillment of the requirements for the degree of Doctor of Philosophy.

Alarcon, A., and Leonards, G. A. (1988). Discussion of "Liquefaction evaluation procedure." by S. J. Poulos, G. Castro, and J. W. France. *J. Geotech. Engrg.*, ASCE, 114(2), 232-236.

Alarcon-Guzman, A., Leonards, G. A., and Chameau, J. L. (1988). " Undrained monotonic and cyclic strength of sands." *J. Geotech. Engrg.*, ASCE, 114(10), 1089-1110.

Amini, F., and Qi, G. Z. (2000). "Liquefaction testing of stratified silty sands." *J. Geotech. and Geoenvir. Engrg.*, ASCE, 126(3), 208-217.

Andresen, A., and Bjerrum, L. (1968). "Slides in subaqueous slopes in loose sand and silt." *Norwegian Geotech. Inst. Pub. No. 81*, Norwegian Geotechnical Institute, Oslo, Norway, 1-9.

ASTM (1993). Standard test method for minimum and maximum index density and unit weight of soils (D4253-91 and D4254-91). In *annual book of ASTM standards*, Sect. 4, Vol. 04-08. ASTM. Philadelphia.

Baldi, G., and Nova, R. (1984). "Membrane penetration effects in triaxial testing." *J. Geotech. Engrg.*, ASCE, 110(3), 403-420.

Barden, L., and McDermott, J. W. (1965). "The use of free ends in triaxial testing of clays." *Journal of the Soil Mechanics and Foundation Div.*, ASCE, Vol. 91. No. SM6, proc. paper 4535, 1-24.

Baziar, M. H. (1987). "Influence of the testing technique on the steady state lines of a sand." thesis presented to Rensselaer Polytechnic Institute, Troy, N.Y., in partial fulfillment of the requirements for the degree of Master of Science.

Baziar, M. H. (1991). "Permanent deformations due to seismically induced liquefaction." PhD dissertation, Rensselaer Polytechnic Institute, Troy, N.Y.

Been, K., and Jefferies, M. G. (1985). " A state parameter for sands." *Geotechnique*, 35(2), 99-112.

Been, K., Jefferies, M. G., and Hachey, J. (1991). "The critical state of sands." *Geotechnique*, London, 41(3), 365-381.

Begemann, H. K. S. P., Koning, H. L., and Lindenberg, J. (1977). "Critical density of sand." *Proceedings of the Ninth International Conference on Soil Mechanics and Foundation*, Tokyo, Japan, Vol. 1, 43-46.

Bishop, A. W., and Henkel, D. J. (1957). "The measurement of soil properties in the triaxial test." Edward Arnold, London.

Bishop, A. W., and Henkel, D. J. (1962). "The measurement of soil properties in the triaxial test." Edward Arnold, London.

Bishop, A. W., and Green, G. E. (1965). "The influence of end restraint on the compression strength of a cohesionless soil." *Geotechnique*, Vol. 15, No.3, 143-265.

Bishop, A. W. (1966). "Strength of soils as engineering materials." 6th Rankine Lecture. *Geotechnique*, Vol.16, 89-130.

Bishop, A. W. (1971). "Shear strength parameters for undisturbed and remolded soil specimens." Roscoe Memorial Symposium, Cambridge University, 3-58.

Bishop, A. W. (1973). "The stability of tips and spoil heaps." *J. Engrg. Geology*, Vol. 6, 335-376.

Bjerrum, L., Kringsted, S., and Kummeneje, O. (1961). "The shear strength of a fine sand." Proceedings of the fifth International Conference on Soil Mechanics and Foundation Engineering, Paris, France, 29-37.

Casagrande, A. (1938). "The shearing resistance of soils and its relation to the stability of earth dams." *Proceedings of the soils and foundations conference of the U.S. Engineer Department*, 1-20.

Casagrande, A. (1940). "Characteristics of cohesionless soil affecting the stability of slopes and earth fills," Contributions to soil mechanics, 1925-1940, *Boston Society of Civil Engineers*, Oct., 1940, 257-276. (originally published in the *Journal of the Boston Society of Civil Engineers*, Jan., 1936).

Casagrande, A. (1975). "Liquefaction and cyclic deformation of sands, A critical review." *Proceedings of the 5th Pan-American Conference on Soil Mechanics and Foundation Engineering*, Vol. 5, Buenos Aires, Argentina, 79-133.

Casagrande, A. (1976). "Liquefaction and cyclic deformation of sands-a critical review." *Harvard Soil Mechanics Series No. 88*, Harvard Univ., Cambridge, Mass.

Castro, G. (1969). "Liquefaction of sands." *Harvard soil mechanics series*, 81, Harvard Univ., Cambridge, Mass, 1-112.

Castro, G. (1975). "Liquefaction and cyclic mobility of saturated sands." *J. of Geotech. Engrg. Div.*, ASCE, 101(GT6), 551-569.

Castro, G., and Poulos, S. J. (1977). "Factors affecting liquefaction and cyclic mobility." *J. Geotech. Engrg. Div.*, ASCE, 103(6), 501-515.

Castro, G., Poulos, S. J., France, J. W., and Enos, J. L. (1982). "Liquefaction induced by cyclic loading." Report to National Science Foundation, Washington, D.C.

Castro, G., Poulos, S. J., and Leathers, F. D. (1985). "Re-examination of slide of lower San Fernando dam." *J. Geotech. Engrg.*, ASCE, 111(9), 1093-1107.

DeGregorio, V. B. (1990). "Loading systems, sample preparation, and liquefaction." *J. Geotech. Engrg.*, ASCE, 116(5), 805-820.

Dennis, N. D. (1988). "Influence of specimen preparation techniques and testing procedures on undrained steady state shear strength." *Advanced triaxial testing of soil and rock*, ASTM, STP 977, 642-654.

Desrues, J., Chambon, R., Mokni, M., and Mazerolle, F. (1996). "Void ratio evolution inside shear bands in triaxial sand specimens studied by computed tomography." *Geotechnique*, London, 46(2), 529-546.

Dierichs, D., and Forster, W. (1985). "Results of liquefaction tests under static conditions." *Proceedings, XI International Conference on Soil Mechanics and Foundation Engineering*, San Fransisco, Calif., Vol. 2, 437-441.

Dobry, R., Vasquez-Herrera, A., Ramli, M., and Vucetic, M. (1985). "Liquefaction flow failure of silty sand by torsional cyclic tests." *Advances in the art of testing soils under cyclic conditions*, ASCE Annual Convention, Detroit, Mich., 29-50.

Duncan, J. M., and Dunlop, P. (1968). "The significance of cap and base restraint." *Journal of the Soil Mechanics and Foundations Division*, ASCE, Vol. 94, No. SM1, proc. paper 5768, 271-290.

Fourie, A. B., and Papageorgiou, G. (2001). "Defining an appropriate steady state line for Merriespruit gold tailings." *Canadian Geotechnical Journal*. Vol. 38, No.4, 695-706.

Frost, J. D., and Jang, D. –J. (2000). "Evolution of sand microstructure during shear." *J. Geotech. and Goenvir. Engrg.*, ASCE, 126(2), 116-130.

Frydman, S., Zeitlen, J. G., and Alpan, I. (1973). "The membrane effects in triaxial-testing of granular soils." *Journal of Testing and Evaluation*, ASTM, Vol. 1, 37-41.

Geotechnical Engineers Inc. (1982). "Liquefaction induced by cyclic loading." *Report to National Science Foundation*, Mar., Winchester, Mass.

Geuze, E. (1948). "Critical density of some Dutch sans." *Proceedings, Second International Conference on Soil Mechanics and Foundation Engineering*, Vol. 3, Rotterdam, Holand, 125-130.

Gilbert, P. A., and Marcuson III, W. F. (1988). "Density variation in specimens subjected to cyclic and monotonic loads." *J. Geotech. Engrg.*, ASCE, 114(1), 1-20.

Grantz, A., Plafker, G., and Kachedoorian, R. (1964). "Alaska's Good Friday earthquake, March 27, 1964." *Circular 491*, Geological Survey, U.S. Dept. of the Interior, Washington, D.C.

Hazen, A. (1920). "Hydraulic fill dams." *Trans.*, ASCE, Vol. LXXXIII, 1713-1745.

Henkel, D. J., and Gilbert, C. D. (1952). "The effect of the rubber membrane on the measured triaxial compression strength of clay samples." *Geotechnique*, Vol.3, 20-29.

Highter, W. H., and Tobin, R. F. (1980). "Flow slides and the undrained brittleness index of some mine tailings." *Eng. Geol.*, 16(1/2), 71-82.

Highter, W. H., and Vallee, R. P. (1980). "The Liquefaction of different mine tailings under stress-controlled loading." *Eng. Geol.*, 16(1/2), 147-150.

Hird, C. C., and Hassona, F. A. K. (1986). "Discussion on: A state parameter for sand." *Geotechnique*, Vol 36, 124-127.

Ishihara, K., Tatsuoka, F., and Yasuda, S. (1975). "Undrained deformation and liquefaction of sand under cyclic stresses." *Soils and Foundations*, 15(1), 29-44.

Ishihara, K. (1985). "Stability of natural deposits during earthquakes." *Poc., 11th Int. Conf. Soil Mechanics and Foundation Engineering*, San Francisco, Calif. Vol. 1, 321-376.

Jang, D. –J., and Frost, J. D. (1998). "Sand structure differences resulting from specimen preparation procedures." Proc., *Geotech. Earthquake Engrg. and Soil Dyn.*, III, ASCE, Reston, Va, 234-245.

Japan National Committee on Earthquake Engineering. (1965). "Niigata earthquake of 1964." *Proc., Third World Conference on Earthquake Engineering*, New Zealand, Feb.

Jennings, J. E. (1979). "The failure of a slimes dam at Bafokeng." *Civ. Eng. S. Afr.*, 6, June., 135-140.

Jennings, J. E., Williams, A. A. B., Wilson, L. C., Wates, J. A., Wagener, F., Rudd, R. T., Schwartz, H. I., Midgley, D. D., and Olivier, H. (1979). "The failure of a slimes dam at Bafokeng." *The Civil Engineer in South Africa*, No. 6, June 1979.

Kiekbusch, M., and Schuppener, B. (1977). "Membrane penetration and its effects on pore pressures." *J. Geotech. Engrg. Div.*, ASCE, 103(GT11), 1267-1280.

Kleiner, D. E. (1976). "Design and construction of an embankment dam to impound gypsum wastes." *Proceedings, 12th International Congress on Large Dams,* International Commission on Large Dams, Mexico City, Mexico, 235-249.

Koester, J. P. (1992). "Cyclic strength and pore pressure generation characteristics of fine-grained soils, PhD dissertation, University of Colorado, Denver.

Koester, J. P., and Tsuchida, T. (1998). "Earthquake-induced liquefaction of fine-grained soils – considerations from Japanese research." Rep. Prepared for the U.S. Army Corps of Engineers, U.S. Army Corps of Engineers, Washington, D. C.

Konrad, J.-M. (1990). "The minimum undrained strength of two sands." *J. Geotech. Engrg.*, ASCE, 116(6), 932-947.

Koppejan, A. W., Wamelan, B. M., and Weinberg, L. J. (1948). "Coastal flowslides in the Dutch province of Zeeland." *Proceedings, Second International Conference on Soil Mechanics and Foundation Engineering*, Rotterdam, the Netherlands, Vol. 5, 89-96.

Kramer, S. L., and Seed, H. B. (1988). "Initiation of soil liquefaction under static loading conditions." *J. Geotech. Engrg.*, ASCE, 114(4), 412-430.

Kuerbis, R. H., and Vaid, Y. P. (1988). "Sand sample preparation- the slurry deposition method." *Sols Found.*, 28(4), 107-118.

Kuerbis, R. H., Negussey, D., and Vaid, Y P. (1988). "Effect of gradation and fines content on the undrained response of sand." In: *Hydraulic fill structures.* Geotechnical Special Publication 21, ASCE, New York, 330-345.

Kuerbis, R. H. (1989). "The effect of gradation and fines content on the undrained loading response of sand." MS thesis, University of British Columbia, Vancouver, Canada.

Kuerbis, R. H., and Vaid, Y. P. (1989). "Undrained behavior of clean and silty sands." In *Proc. of Discussion session on influence of local conditions on seismic response.* 12th International Conference on Soil Mechanics and Foundation Engineering, 91-100.

Kuo, C. –Y., and Frost, J. D. (1996). "Uniformity evaluation of cohesionless specimens using image analysis." *J. Geotech. Engrg.*, ASCE, 122(5), 390-396.

Ladd, R. S. (1974). "Specimen preparation and liquefaction of sand." *J. Geotech. Engrg. Div.*, ASCE, 100(10), 1180-1184.

Ladd, R. S. (1977). "Specimen preparation and cyclic stability of sands." *J. Geotech. Engrg. Div.*, ASCE, 103(GT6), 535-547.

Ladd, R. S. (1978). "Preparing test specimens using undercompaction." *Geotech. Testing J.*, STM, 1(1), 16-23.

Lade, P. V., and Hernandez, S. B. (1977). "Membrane penetration effects in undrained tests." *J. Geotech. Engrg. Div.* ASCE, 103(GT2), 109-125.

Lade, P. V., and Yamamuro, J. A. (1997). " Effect of nonplastic fines on static liquefaction of sands." *Canadian Geotechnical Journal*, Vol 34, 918-928.

Lambe, T. W., and Whitman, R. V. (1969) "Soil mechanics." John Wiley and Sons, New York, N.Y.

Lee, K. L., and Seed, H. B. (1967). "Cyclic stress conditions causing liquefaction of sand." *J. Soil Mech. Found. Div.*, ASCE, 93 (SM1), 47-70.

Lee, K. L., Seed, H. B., Idriss, I. M., and Makdisi, F. I. (1975). "Properties of soil in the San Fernando hydraulic fill dams." *J. Geotech. Engrg. Div.*, ASCE, Vol. 101, No. GT8, 801-821.

Lee, K. L. (1978). "End restraint effects on undrained static triaxial strength of sand." *J. Geotech. Engrg. Div.*, ASCE, 104(GT6), 687-704.

Lindenberg, J., and Koning, H. L. (1981). "Critical density of sand." *Geotechnique*, 31(2), June, 231-245.

Lucia, P. C. (1981). "Flow failures of tailings dam, waste impoundments, and embankments." thesis presented to the University of California at Berkeley, Calif., in partial fulfillment of the requirements for the degree of Doctor of Philosophy.

Martin, G. R., Finn, W. D. L., and Seed, H. B. (1978). "Effect of system compliance on liquefaction tests." *J. Geotech. Engrg. Div.*, ASCE, 104(GT4), 463-479.

Masad, E., and Muhunthan, B. (2000). "Three-dimensional characterization and simulation of anisotropic soil fabric." *J. Geotech. and Geoenvir. Engrg.*, ASCE, 126(3), 199-207.

Middlebrooks, T. A. (1942). " Fort Peck slide." *Trans.*, ASCE, Vol. 107, 723-764.

Midgley, D. C. (1994). "Merriespruit tailings dam failure." A report to the CSIR.

Mohamad, R., and Dobry R. (1986). "Undrained monotonic and cyclic triaxial strength of sand." *J. Geotech. Engrg.*, 112(10), 941-958.

Mulilis, J. P., Chan, C, K., and Seed, H. B. (1975). "The effects of method of preparation on the cyclic stress-strain behavior of sands." *Report No. EERC 75-18*, Univ. of California, Berkeley, Calif.

Mulilis, J. P., Seed, H. B., Chan C. K., Mitchell, J. K., and Arulanandan, K. (1977). "Effects of sample preparation on sand liquefaction." *J. Geotech. Engrg. Div.*, ASCE, 103(GT2), 91-109.

Newland, P. L., and Alley, B. H. (1959). "Volume changes in drained triaxial tests on granular materials." *Geotechnique*, Vol. 9, 174-182.

Oda, M. (1972a). "Initial fabrics and their relations to mechanical properties of granular material." *Soils and Foundations*, Japanese Society of Soil Mechanics and Foundation Engineering, Tokyo, Japan, Vol.12, No.1, Mar., 17-36.

Oda, M. (1972b). "The mechanism of fabric changes during compressional deformation of sand." *Soils and Foundations*, Japanese Society of Soil Mechanics and Foundation Engineering, Tokyo, Japan, Vol.12, No.2, July, 1-18.

Oda, M. (1972c). "Deformation mechanism of sand in triaxial compression tests." *Soils and Foundations*, Japanese Society of Soil Mechanics and Foundation Engineering, Tokyo, Japan, Vol.12, No.4, Dec., 45-63.

Oda, M., Koishikawa, I., and Higuchi, T. (1978)."Experimental study of anisotropic shear strength of sand by plane strain test." *Soils and Foundations*, Vol. 18(1), 25-38.

Oda, M. (1981). "Anisotropic strength of cohesionless sands." *J. Geotech. Engrg. Div.*, ASCE, 107, 1219-1231.

Ohsaki, Y. (1966). "Niigata earthquakes, 1964 building damage and soil condition." *Soils Found.*, 6(2), 14-37.

Pitman, T. D., Robertson, P. K., and Sego, D. C. (1994). "Influence of fines on the collapse of loose sands." *Canadian Geotechnical Journal*, Vol 31, 728-739.

Poulos, S. J. (1971). "The stress-strain curves of soils." Geotechnical Engineers, Inc., Winchester, Mass, 1-82.

Poulos, S. J. (1981). "The steady state of deformation." *J. Geotech. Engrg. Div.*, ASCE, 107(GT5), 553-562.

Poulos, S. J., Castro G., and France, J. (1985). "Liquefaction evaluation procedure." *J. Geotech. Engrg.*, 111(6), 772-792.

Poulos, S. J., Castro, G., and France, J. W. (1988). "Closure to discussion: Liquefaction evaluation procedure." *J. Geotech. Engrg.*, ASCE, 114(2), 251-259.

Raju, V. S., and Sadasivan, S. K. (1974). "Membrane penetration in triaxial-tests on sands." *J. Geotech. Engrg. Div.*, ASCE, 100(GT4), 482-489.

Roscoe, K. H., Schofield, M. A., and Wroth, C. P. (1958). " On the yielding of soils." *Geotechnique*, Vol. 8, London, England, 22-53.

Riemer, M. F., Seed, R. B., Nicholson, P. G., and Jong, H. L. (1990). "Steady state testing of loose sands: Limiting minimum density." *J. Geotech. Engrg.*, Vol. 116, No. 2, 332-337.

Roscoe, K. H., Schofield, A. N., and Thurairajah, A. (1963). "An evaluation of test data for selecting a yield criterion for soils." *Laboratory shear testing of soils*, ASTM, STP 361, 111-128.

Rowe, D. W. (1962). "The stress-dilatency relation for static equilibrium of and assembly of particles in contact." Proceedings of the Royal Society, London, England, series A, Vol. 269, 500-527.

Roy, M., and Lo, K. Y. (1971). "Effect of end restraint on high pressure tests of granular materials." *Revue Canadienne de Geotechnique*, Vol. 8, No. 4, 579-588.

Sasitharan, S., Robertson, P. K., Sego, D. C., and Morgenstern, N. R. (1993). "Collapse behavior of sand." *Canadian Geotechnical Journal*, Vol. 30, 569-577.

Seed, H. B., and Lee, K. L. (1966). "Liquefaction of saturated sands during cyclic loading." *J. Soil Mech. Found. Div.*, ASCE, 92(SM6), 105-134.

Seed, H. B., and Wilson, S. W. (1967). "The Turnagain Heights landslide, Anchorage, Alaska." *J. Soil Mech. Found. Div.*, ASCE, 93(SM4), 325-353.

Seed, H. B., and Lee, K. L. (1969). "Pore-water pressure in earth slopes under seismic loading conditions." *Proceedings, 4th World Conference on Earthquake Engineering*, Vol. 3, A-5, Santiago, Chile, 1-11.

Seed, H. B., Lee, K. L., Idriss, I. M., and Makdisi, F. I. (1975a). "The slides in the San Fernando dams during the earthquake of February 9, 1971." *J. Geotech. Engrg. Div.*, ASCE, Vol. 101(GT7), 651-689.

Seed, H. B., Lee, K. L., Idriss, I. M., and Makdisi, F. I. (1975b). "Dynamic analyses of the slide in the lower San Fernando dam during the earthquake of February 9, 1971." *J. Geotech. Engrg. Div.*, ASCE, Vol. 101(GT9), 889-911.

Seed, H. B. (1976). " Evaluation of soil liquefaction effects on level ground during earthquakes." Preprint 2752, ASCE Annual meeting, Philadelphia, Pa.

Seed, H. B., Martin, P. P., and Cysmer, J. (1976). " Pore water pressure changes during soil liquefaction." *J. Geotech. Engrg. Div.*, 102(4), ASCE, April 1976.

Seed, H. B., Mori, K., and Chan, C. K. (1977). "Influence of seismic history on liquefaction of sands." *J. Geotech. Engrg. Div.* ASCE, 103(GT4), 257-270.

Seed, H. B. (1983). "Earthquake resistance design of earth dams." Proc. Symp. on Seismic Design of Embankments and Caverns, ASCE, Vol. 1, 41-64.

Selig, E. T., and Chang, C. S. (1981). "Soil failure modes in undrained cyclic loading." *J. Geotech. Engrg. Div.*, ASCE, 107(GT5), 539-551.

Senour, C., and Turnbull, W.J. (1948). "A study of foundations failures on a river bank revetment." *Proceedings, Second International Conference on Soil Mechanics and Foundation Engineering*, Rotterdam, the Netherlands, Vol. 7, 117-121.

Shi, D., and Winslow, D. N. (1991). "Accuracy of a volume fraction measurement using areal image analysis." *ASTM J. Testing and Evaluation*, 19(3), 210-213.

Sladen, J. A., D'Hollander, R. D., and Krahn, J. (1985). " The liquefaction of sands, a collapse surface approach." *Can. Geotech. J.*, 22(4), 564-578.

Strydom, J. H., and Williams, A. A. B. (1999). "A review of important and interesting technical findings regarding the tailings dam failure at Merriespruit." *Journal of the South African Institution of Civil Engineering*, Vol.41, No.4, 1-9.

Symes, M. J. P. R., Gens, A. and Hight, D. W. (1984). "Undrained anisotropy and principal stress rotation in saturated sand." *Geotechnique*, 34(1), 11-27.

Taylor, D. W. (1941). "Seventh progress report on shear research to U.S. Engineers." M.I.T. Publication.

Terzaghi, K. (1956). "Varieties of submarine slope failures." *Proceedings. Eighth Texas Conference on Soil Mechanics and Foundation Engineering*, 1-41.

Torrey, V. H. (1981). "Some effects of rate of loading, method of loading, and applied total stress path on the critical void ratio of fine uniform sand." Thesis presented to Texas A&M University, at College Station, Tex., in partial fulfillment of the requirements of the degree of Doctor of Philosophy.

Vaid, Y. P., and Chern, J. C. (1983a). "Mechanics of deformation during cyclic undrained loading of saturated sands." *Soil Dynamics and earthquake Engineering*, 2(3), 171-177.

Vaid, Y. P., and Chern, J. C. (1983b)."Effects of static shear on resistance to liquefaction." *Soils Found.*, JSSMFE, 23(1), 47-60.

Vaid, Y. P., and Negussey, D. (1984). "A critical assessment of membrane penetration in the triaxial test." *Geotechnical Testing Journal*, 7, 70-76.

Vaid, Y. P., and Chern, J. C. (1985a). closure to "Effects of static shear on resistance to liquefaction." by Y. P. Vaid and J. C. Chern. *Soils Found.*, JSSMFE, 25(3), 154-156.

Vaid, Y. P., and Chern, J. C. (1985b). "Cyclic and monotonic undrained response of saturated sands." *Advances in the art of testing soils under cyclic conditions*, ASCE Annual Convention, Detroit, Mich., 120-147.

Vaid, Y. P., and Negussey, D. (1988). "Preparation of reconstituted sand specimens." *Advanced triaxial testing of soil and rock*, ASTM, STP 977, 405-417.

Vaid, Y., Chung, E., and Kuerbis, R. (1990). "Stress path and steady state." *Can. Geotech. J.*, Ottawa, 27(1), 1-7.

Visser, P. J. M. (1994). "Voorlopige verslag van radar data oor Virginia op 22 Februarie 1994." *Weerburo.* (Appendix 2 of Midgley's report).

Vucetic, M., and Dobry, R. (1988). "Cyclic triaxial strain-controlled testing of liquefiable sands." *Advanced triaxial testing of soil and rock*, R. T. Doaghe, R. C. Chaney, and M. L. Silver, eds., ASTM, West Conshohocken, Pa., 475-485.

Wagener, F. (1997). "The Merriespruit slimes dam failure: Overview and lessons learnt." *Journal of the South African Institution of Civil Engineering*, Vol.39, No.3, 11-15.

Wagener, F., Craig, H. J., Blight, G. E., McPhail, G., Williams, A. A. B., and Strydom, J. H. (1998). "The Merriespruit tailings dam failure- A review." *Proc Tailings and Mine Waste '98*, Colorado State University, January 1998, 925-952.

Wong, R. K. S and Arthur, J. R. F. (1985). "Induced and inherent anisotropy in sand." *Geotechnique*, Vol. 35, No. 4, 471-481.

Yamamuro, J. A. (1993). "Instability and behavior of granular materials at high pressures. Ph.D. thesis, University of California, Los Angeles, Calif.

Yamamuro, J. A., and Lade, P. V. (1997). "Static liquefaction of very loose sands." *Canadian Geotechnical Journal*, Vol. 34, 905-917.

Zhang, H., and Garga, V. K. (1997). "Quasi-steady state: a real behavior?" *Can. Geotech. J.*, Ottawa, Vol. 34, 749-761.

BIBLIOGRAPHY

Bjerrum, L. (1971). "Subaqueous slope failures in norwegian fjords." *Norwegian Geotech. Inst. Pub. No. 88*, Norwegian Geotechnical Institute, Oslo, Norway.

Blight, G. E., and Steffen, O. K. H. (1978). "Geotechnics of gold mining waste disposal." In: *Current geotechnical Practice in mine waste disposal*, ASCE, 1979, 1-52.

Blight, G. E. (1998a). "Some less familiar aspects of hydraulic fill structures." *Proceedings*, ASCE Conference on Hydraulic Fill Structures, Geotechnical Special Publication 21, ASCE, New York, 1000-1027.

Blight, G. E. (1998b). "Destructive mudflows as a consequence of tailings dyke failures." *Proceedings Institution of Civil Engineers*, Vol.125, 9-18.

Fourie, A. B., Papageorgiou, G., and Blight, G. E. (2000). "Static liquefaction as an explanation for two catastrophic tailings dam failures in South Africa." Proc Tailings and Mine Waste '00, Colorado State University, January 2000, 149-158.

Garga, V. K., and Zhang, H. (1997). "Volume changes in undrained triaxial tests on sands." *Canadian Geotechnical Journal*, Vol. 34, 762-772.

Ishihara, K., and Takatsu, H. (1979). "Effects of overconsolidation and K_0 conditions on the liquefaction characteristics of sands." *Soils and foundations*, Vol. 19(4), 59-68.

Ishihara, K. (1993). " Liquefaction and flow failure during earthquakes." The 33rd Rankine Lecture, *Geotechnique*, 43(3), 351-415.

Konrad, J.-M. (1990). "Minimum undrained strength versus steady-state strength of sands." *J. Geotech. Engrg.*, ASCE, 116(6), 948-963.

La Rochelle, P., Leroueil, S., Trak, B., Blais-Leroux, L., and Tavenas, F. (1988). "Observational approach to membrane and area corrections in triaxial tests." *Advanced triaxial testing of soil and rock*, ASTM, STP 977, 715-731.

Lee, K. L., and Farhoomand, I. (1967). "Compressibility and crushing of granular soil in anisotropic triaxial compression." *Can. Geotech. J.*, 4(1), 68-86.

Mulilis, J P., Townsend, F C., and Horz, R C. (1978). "Triaxial testing techniques and sand liquefaction". in *Dynamic geotechnical testing*, ASTM, SPT 654, 265-279.

Sasitharan, S., Robertson, P. K., Sego, D. C., and Morgenstern, N. R. (1994). "State-Boundary surface for very loose sand and its practical implications." *Canadian Geotechnical Journal*, Vol.31, 321-334.

SABS 0286 (1998). Code of practice for mine residue deposits. Pretoria, South Africa. SABS.

Wagener, F., Strydom, K., Craig, H., and Blight, G. (1997). "The tailings dam flow failure at Merriespruit, South Africa, Causes and Consequences." *Conference on Tailings and Mine Waste '97*, Colorado State University, January 1997. 657-666.

APPENDIX A

CALIBRATION OF EQUIPMENT FOR CASE 1 TESTS

A CALIBRATION OF EQUIPMENT FOR CASE 1 TESTS

This section gives the details of the procedures used to calibrate the equipment for case 1 tests. Also included are the calibration data and calibration curves.

A.1 Calibration of Pressure Gauges

To measure the cell pressure and back pressure applied to a specimen, ideally, a pressure transducer calibrated against proven standards is incorporated in each of these pressure lines. Alternatively, pressure gauges are calibrated against a proven pressuremeter to relate the gauge pressure readings to the actual pressures. The latter method was used in this investigation. The procedure is outlined below:

1. The valve connecting the pressure gauge to the appropriate pressure line (valve B6 and valve C5 for back pressure and cell pressure, respectively in Figure 3.1) was disconnected and a calibrated pressuremeter was connected to the pressure gauge at that point.
2. The pressure gauge was adjusted so that the pressuremeter read 0kPa. The corresponding gauge reading was recorded after tapping the gauge to ensure that the indicator was stable.
3. The pressure gauge was adjusted so that the pressuremeter read 10kPa and the corresponding gauge reading was recorded, after tapping the gauge.
4. Step 3 was repeated with pressure increments of 10kPa up to the maximum working pressure of the pressuremeter, i.e. 700kPa.
5. Three cycles of calibrations were performed for each gauge and the averages of the calibration data were calculated.
6. From the plot of the average of the calibrations, an extrapolation was done to provide the gauge pressure readings corresponding to pressures beyond 700kPa, i.e. from 700kPa to 1000kPa.
7. The resulting average of the calibration data and its plot were placed next to the appropriate gauge to enable correct settings of the gauge pressures during testing.

A.2 Calibration of Pore Pressure Transducer

The procedure for the calibration of pore pressure transducer is outlined below:

1. The cell pressure line was connected to the pore pressure measurement line at valve D2 and the line was deaired and checked for leaks as described in section 3.2.2. The level of water in the cell pressure line was set to the same level as the transducer.
2. At valve C5 of the cell pressure line, a proven pressuremeter was connected to the cell pressure line.
3. The pressure gauge was adjusted so that the pressuremeter read 0kPa and the corresponding pore pressure transducer reading was recorded.
4. Step 3 was repeated with pressure increments of 10kPa up to the maximum working pressure of the pressuremeter, i.e. 700kPa.
5. Three cycles of calibrations were performed and the averages of the data were calculated.
6. From the plot of the average of the calibration data, an extrapolation was done to enable interpretation of pore pressure measurements beyond 700kPa i.e. from 700kPa to 1000kPa.
7. The resulting average of the calibration data and its plot were used to relate pore pressure transducer readings to actual pore pressures during testing.

A.3 Calibration for Cell Expansion with Pressure and Time

When the pressure in a triaxial cell is increased, the cell and connecting tubings immediately expand and if this pressure increment is left for a period of time, the cell and connecting tubings will continue to expand due to creep effects. When using the cell pressure line's volume change gauge to measure the specimen volume change during testing, as was the case in this investigation, it was necessary that the volume change due to expansion of cell and connecting tubings be deducted from the total volume change measured by the volume change gauge.

The procedure for measuring the expansion of a cell and connecting tubings is outlined below:

A.3.1 Procedure

1. At valve C5, a proven pressuremeter was connected to the cell pressure line.
2. The cell pressure system was deaired as described in section 3.2.2.
3. The cell was assembled to its base and the cell clamping nuts or screws were tightened with controlled torque.
4. The cell was filled with deaired water from the water supply while its top air release valve was opened, its loading piston was held up at its fullest extent and the volume gauge was by-passed. When water emerged from the top air release valve, the cell chamber valve and the water supply valve were closed and then the top air release valve was closed.
5. The volume change gauge was introduced to the system.
6. The cell pressure gauge was set to 0kPa, the cell chamber valve was opened and the initial volume change gauge reading was recorded.
7. The cell chamber valve was closed and the cell pressure was increased by 50kPa.
8. The cell chamber valve was opened and the immediate volume change was recorded. The system was left for 24 hours.
9. After 24 hours, the volume change reading was recorded.
10. Steps 7 to 9 were repeated with pressure increments of 50kPa up to 1000kPa.

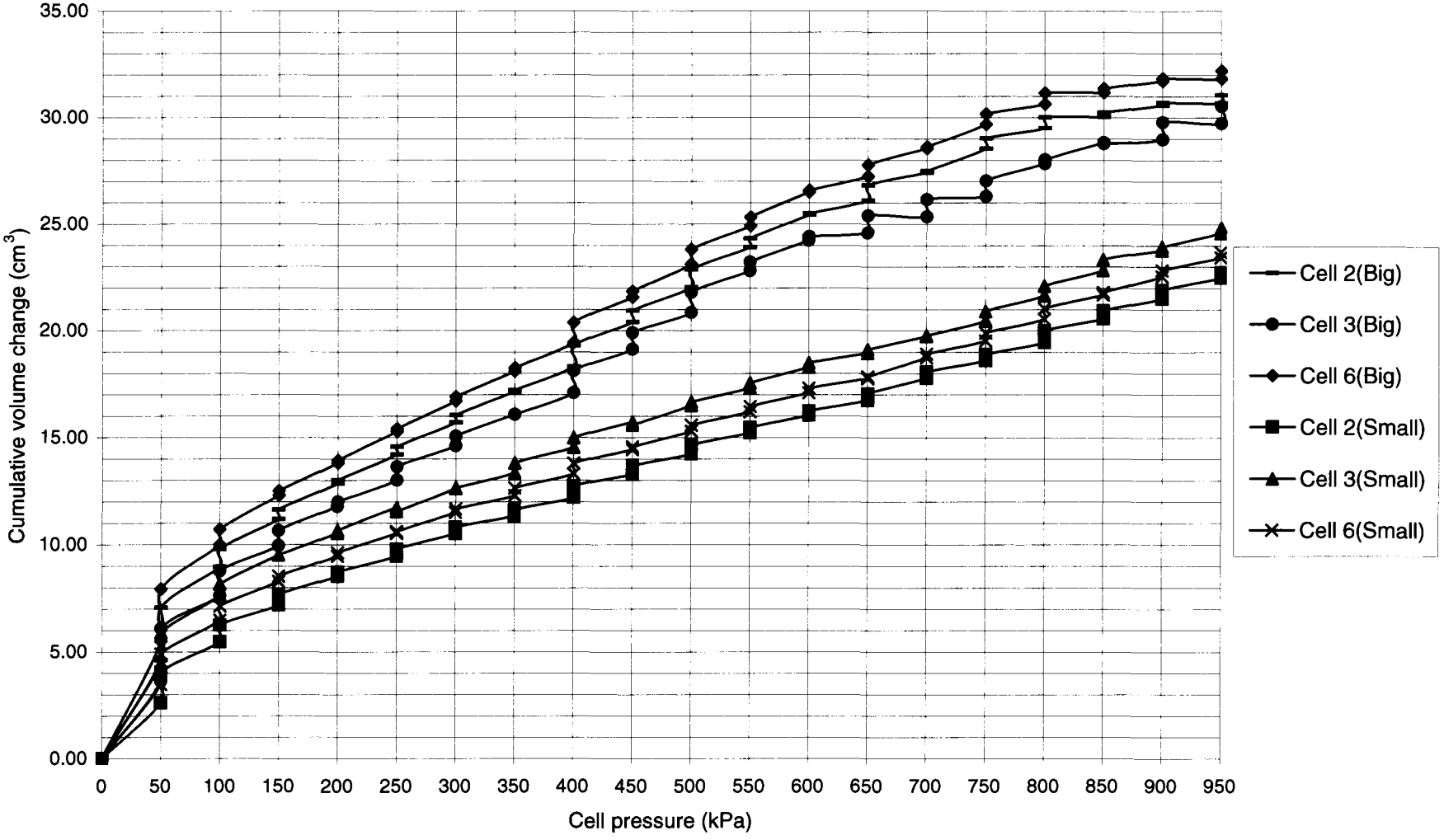
The average calibration data and corresponding plots for three cycles of calibrations for cell and connecting tubing expansion of 6 cells used in this investigation are given in Table A1 and Figure A1, respectively.

Table A1 Calibration for cell expansion with pressure and time

Cell Pressure (kPa)		Cumulative volume change (cm^3)					
		Cell 2 (Big)	Cell 3 (Big)	Cell 6 (Big)	Cell 2 (Small)	Cell 3 (Small)	Cell 6 (Small)
0		0.00	0.00	0.00	0.00	0.00	0.00
50	Instantaneous	4.61	3.63	5.49	2.61	4.46	3.47
50	After 24hours	7.06	6.08	7.94	4.04	5.89	4.89
100	Instantaneous	8.98	7.63	10.01	5.47	7.62	6.48
100	After 24hours	9.79	8.77	10.71	6.24	8.17	7.14
150	Instantaneous	11.18	9.96	12.30	7.18	9.52	8.28
150	After 24hours	11.63	10.65	12.50	7.67	9.52	8.53
200	Instantaneous	12.85	11.79	13.81	8.53	10.54	9.46
200	After 24hours	13.02	12.00	13.93	8.73	10.66	9.63
250	Instantaneous	14.20	13.02	15.28	9.47	11.72	10.52
250	After 24hours	14.57	13.63	15.40	9.79	11.56	10.61
300	Instantaneous	15.71	14.61	16.71	10.53	12.62	11.50
300	After 24hours	16.03	15.06	16.91	10.81	12.66	11.67
350	Instantaneous	17.14	16.08	18.09	11.34	13.35	12.28
350	After 24hours	17.22	16.08	18.26	11.63	13.80	12.65
400	Instantaneous	18.32	17.10	19.44	12.20	14.54	13.30
400	After 24hours	19.30	18.12	20.38	12.73	14.98	13.79
450	Instantaneous	20.40	19.14	21.56	13.30	15.72	14.44
450	After 24hours	20.93	19.91	21.85	13.67	15.60	14.56
500	Instantaneous	22.03	20.85	23.11	14.24	16.49	15.30
500	After 24hours	22.85	21.79	23.81	14.65	16.66	15.58
550	Instantaneous	23.91	22.81	24.91	15.22	17.31	16.20
550	After 24hours	24.32	23.22	25.32	15.46	17.55	16.44
600	Instantaneous	25.42	24.24	26.50	16.03	18.29	17.09
600	After 24hours	25.50	24.40	26.58	16.24	18.49	17.30
650	Instantaneous	26.10	24.59	27.24	16.73	18.95	17.76
650	After 24hours	26.82	25.39	27.77	17.05	19.12	17.85
700	Instantaneous	27.42	25.34	28.56	17.79	19.73	18.74
700	After 24hours	27.49	26.15	28.63	18.07	19.77	18.91
750	Instantaneous	28.54	26.30	29.68	18.60	20.46	19.52
750	After 24hours	29.02	27.03	30.16	18.89	20.91	19.89
800	Instantaneous	29.50	27.83	30.64	19.46	21.65	20.54
800	After 24hours	30.01	28.03	31.15	19.99	22.09	21.03
850	Instantaneous	30.04	28.83	31.18	20.56	22.83	21.68
850	After 24hours	30.22	28.78	31.36	20.93	23.34	21.80
900	Instantaneous	30.57	28.98	31.71	21.50	23.77	22.54
900	After 24hours	30.70	29.78	31.84	21.91	23.93	22.82
950	Instantaneous	30.69	29.73	31.83	22.48	24.58	23.44
950	After 24hours	31.06	30.54	32.20	22.73	24.83	23.68

FIGURE A1

CALIBRATION FOR CELL EXPANSION WITH PRESSURE AND TIME



A.4 Calibration for Piston Friction

During loading of triaxial specimens, the machine platen is raised at a constant rate by the drive unit causing the cell (and the specimen resting on the base pedestal) to move upwards against a stationary piston in the cell bushing. The force applied to the specimen by the piston is measured by the proving ring fixed between the machine cross-head and the upper end of the piston.

Friction between the piston and cell bushing, if any, increases the force that is measured by the proving ring and therefore causes errors in the calculation of the vertical force applied to the specimen. The friction between the piston and the cell bushing was measured by running the machine at the rate of strain used for the test with the cell filled with deaired water (with a layer of oil on top of the cell water) and under the same pressure as it was during loading but with the loading piston not in contact with the top cap.

The friction could be reduced to an insignificant amount by including a layer of oil on top of the cell water, as was the case in this investigation.

APPENDIX B

CALIBRATION OF EQUIPMENT FOR CASE 3 TESTS

B CALIBRATION OF EQUIPMENT FOR CASE 3 TESTS

This section contains the procedures used for the calibration of equipment for case 3 tests. The calibration data and calibration curves are also included.

B.1 Calibration of Pressure Transducers

Pressure transducers, one in each pressure line, were calibrated by incorporating a proven pressuremeter in the pressure line and relating the pressuremeter readings to the voltage outputs of the transducer.

B.1.1 Cell pressure transducer

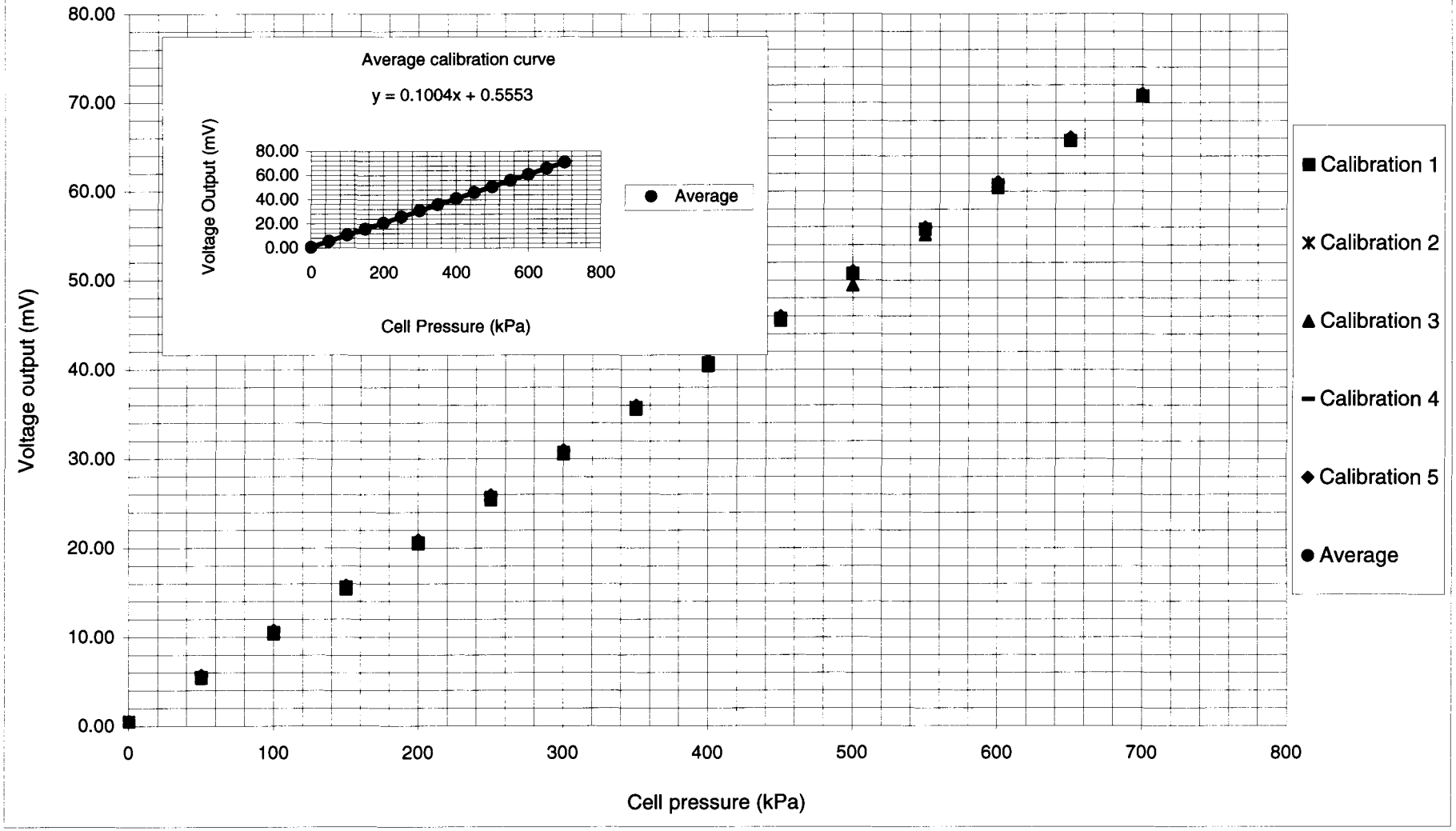
1. The cell pressure gauge was set to zero.
2. Valve C7, connecting the pressure gauge to the reservoir, see Figure 3.7, was disconnected and a proven pressuremeter was connected at that point.
3. The volume change device was by-passed and the cell pressure line was deaired as described in section 3.4.2.
4. After deairing, the water supply valve and the valve immediately after the cell pressure transducer, valve C3, were closed.
5. The gauge was adjusted so that the pressuremeter read 0kPa and the corresponding cell pressure transducer voltage output was recorded when stable.
6. Step 5 was repeated with pressure increments of 50kPa up to 700 kPa (the maximum working pressure of the pressuremeter).
7. Five cycles of calibration of the cell pressure transducer were performed and the averages of the data were calculated.
8. An extrapolation was done from the curve of the average of the calibration data to obtain the cell pressure transducer readings for cell pressures beyond 700kPa. i.e. from 700kPa to 1000kPa.

Table B1 Calibration of cell pressure transducer

Cell Pressure (kPa)	Voltage output (mV) Calibration No. 1	2	3	4	5	Average Voltage (mV)	Calculated Voltage (mV)	% Error (calculated - maximum deviation) x100%
0	0.47	0.48	0.48	0.52	0.51	0.49	0.56	6.39
50	5.49	5.52	5.41	5.69	5.71	5.56	5.58	2.97
100	10.5	10.52	10.36	10.71	10.77	10.57	10.60	2.22
150	15.6	15.62	15.4	15.81	15.81	15.65	15.62	1.38
200	20.58	20.62	20.46	20.79	20.89	20.67	20.64	-1.23
250	25.64	25.65	25.4	25.89	25.95	25.71	25.66	-1.15
300	30.67	30.69	30.53	30.86	30.96	30.74	30.68	-0.93
350	35.7	35.73	35.55	35.95	35.97	35.78	35.70	-0.77
400	40.7	40.72	40.43	40.98	40.96	40.76	40.72	0.70
450	45.67	45.7	45.47	45.98	46.00	45.76	45.74	-0.58
500	50.73	50.74	49.42	50.95	51.04	50.58	50.76	2.63
550	55.72	55.74	55.12	55.96	55.99	55.71	55.78	1.18
600	60.68	60.74	60.4	60.98	61.05	60.77	60.80	0.65
650	65.67	65.72	65.98	65.99	66.08	65.89	65.82	-0.40
700	70.67	70.82	70.95	71.05	71	70.90	70.84	-0.30
750	EXTRAPOLATION FROM AVERAGE CALIBRATION CURVE'S EQUATION						75.86	
800							80.88	
850							85.90	
900							90.92	
950							95.94	
1000							100.96	

FIGURE B1

CALIBRATION OF CELL PRESSURE TRANSDUCER



B.1.2 Back pressure (pore pressure) transducer

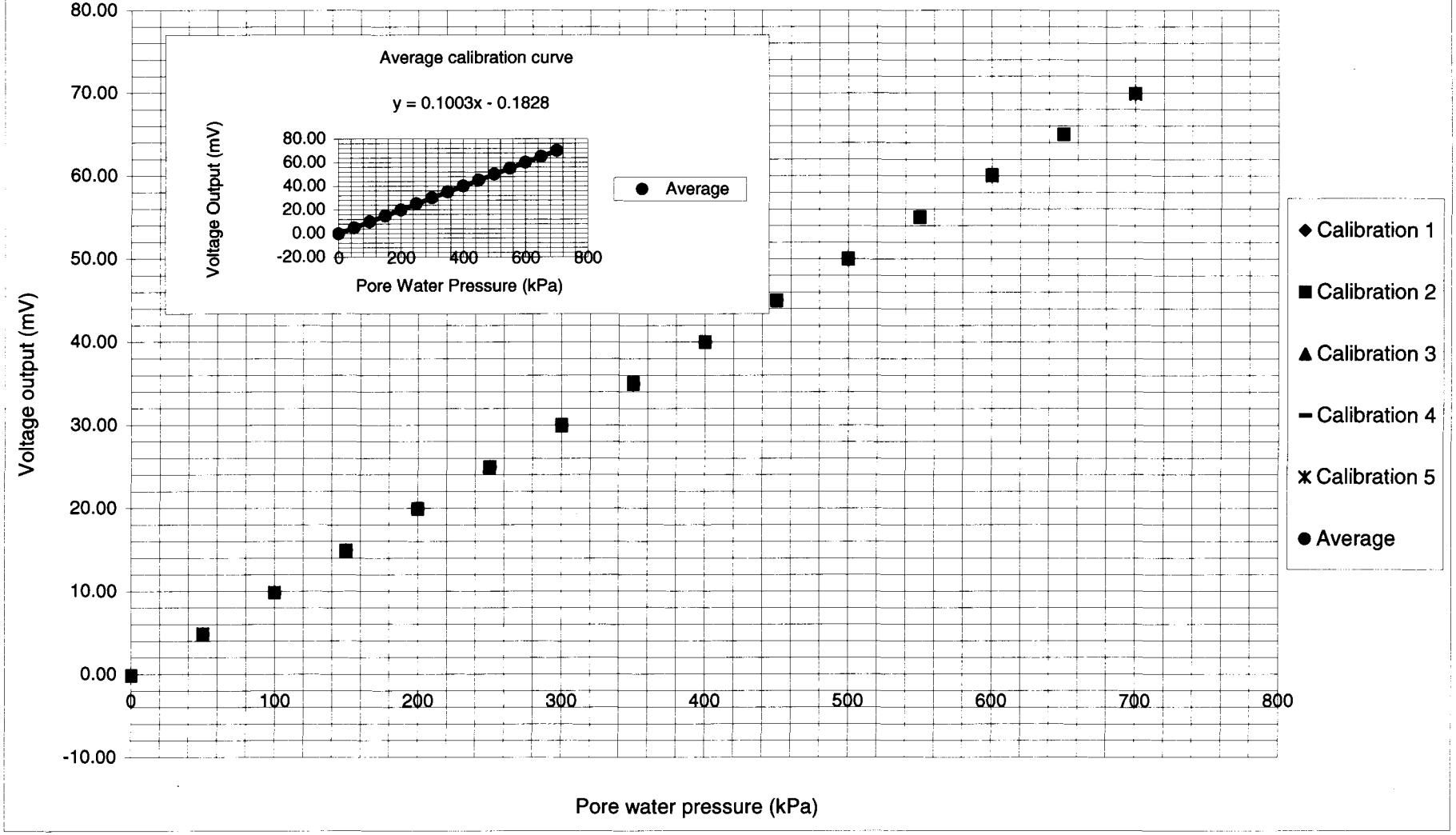
1. The back pressure gauge was set to zero.
2. The valve connecting the back pressure gauge to the reservoir, valve B8 in Figure 3.7, was disconnected and a proven pressuremeter was connected at that point.
3. The back pressure line was deaired as described in section 3.4.2.
4. When all air had been removed, the water supply valve and valve immediately after the back pressure transducer, valve B4, were closed.
5. The back pressure gauge was adjusted so that the pressuremeter read 0kPa and the resulting pore pressure transducer voltage reading was recorded when stable.
6. Step 5 was repeated with pressure increments of 50kPa up to 700kPa (the maximum working pressure of the pressuremeter).
7. Five cycles of calibration of the pore pressure transducer were preformed and the averages of the data were calculated.
8. The curve of the average of the calibration data was extrapolated to obtain the pore pressure transducer readings for pore pressures in excess of 700kPa. i.e. from 700kPa tom 1000kPa.

Table B2 Calibration of back/ pore pressure transducer

Applied Pressure (kPa)	Voltage output (mV) Calibration No. 1	2	3	4	5	Average Voltage (mV)	Calculated Voltage (mV)	% Error (calculated – maximum deviation) x100%
0	-0.19	-0.17	-0.18	-0.17	-0.18	-0.18	-0.18	7.00
50	4.77	4.79	4.70	4.78	4.89	4.79	4.83	2.74
100	9.82	9.82	9.81	9.75	9.88	9.82	9.85	0.99
150	14.78	14.88	14.79	14.85	14.96	14.85	14.86	-0.66
200	19.86	19.92	19.87	19.92	19.88	19.89	19.88	-0.22
250	24.86	24.98	24.86	24.93	24.96	24.92	24.89	-0.35
300	29.83	30.02	29.86	29.93	29.98	29.92	29.91	-0.38
350	34.88	35.06	34.91	34.94	34.98	34.95	34.92	-0.39
400	39.99	40.02	39.95	39.97	39.98	39.98	39.94	-0.21
450	44.94	45.02	44.94	45.00	44.96	44.97	44.95	-0.15
500	49.89	50.05	49.93	49.98	49.96	49.96	49.97	-0.17
550	54.96	55.06	54.96	55.04	54.95	54.99	54.98	-0.14
600	60.02	60.09	60.02	60.07	59.93	60.03	60.00	-0.15
650	65.02	65.02	64.94	65.06	64.92	64.99	65.01	0.14
700	69.96	69.96	70.03	70.05	69.85	69.97	70.03	0.25
750	EXTRAPOLATION FROM AVERAGE CALIBRATION CURVE'S EQUATION						75.04	
800							80.06	
850							85.07	
900							90.09	
950							95.10	
1000							100.12	

FIGURE B2

CALIBRATION OF BACK/ PORE PRESSURE TRANSDUCER



B.2 Calibration of Load Transducer

Two different calibrations were performed for the load transducer. The first calibration related the load transducer voltage output to the axial force applied to the transducer. The second calibration related the load transducer voltage output to cell pressure.

B.2.1 Calibration of load transducer against axial force

Procedure

1. The load transducer voltage reading when the load transducer was in position in the empty cell and the load transducer was not in contact with anything was recorded, ensuring that it was stable.
2. The load transducer was disassembled from the cell and its loading bolt was removed. The load transducer was then placed between a machine platen and a calibrated proving ring mounted to the load frame cross-head as shown in Figure B3. The load transducer was initially not in contact with the proving ring. The load transducer voltage reading was recorded when stable (this corresponded to the weight of the transducer).
3. The proving ring reading (in divisions), corresponding to the proving ring being attached to the load frame cross-head and not in contact with the load transducer was recorded.
4. The machine platen was raised slowly by turning the hand wheel of the machine to bring the load transducer to contact with the proving ring, ensuring that the load transducer was vertical and the proving ring was properly aligned with the load transducer.
5. The machine platen was raised further so that the proving ring deflected by 20 divisions. The resulting voltage reading of the load transducer was recorded when stable.
6. Step 5 was repeated with increments in the divisions of the proving ring of 20 up to the maximum working force of the load transducer.
7. Six cycles of calibration of the load transducer against axial force were performed and the averages of the calibrations were calculated.

8. The load transducer was weighed and its weight was converted to the number of divisions of the proving ring using the calibration factor of the proving ring, i.e. 25.77 dN/div.
9. The proving ring divisions obtained in step 8 were then added to the calibration data in step 7 to give the correct proving ring divisions corresponding each load transducer reading.

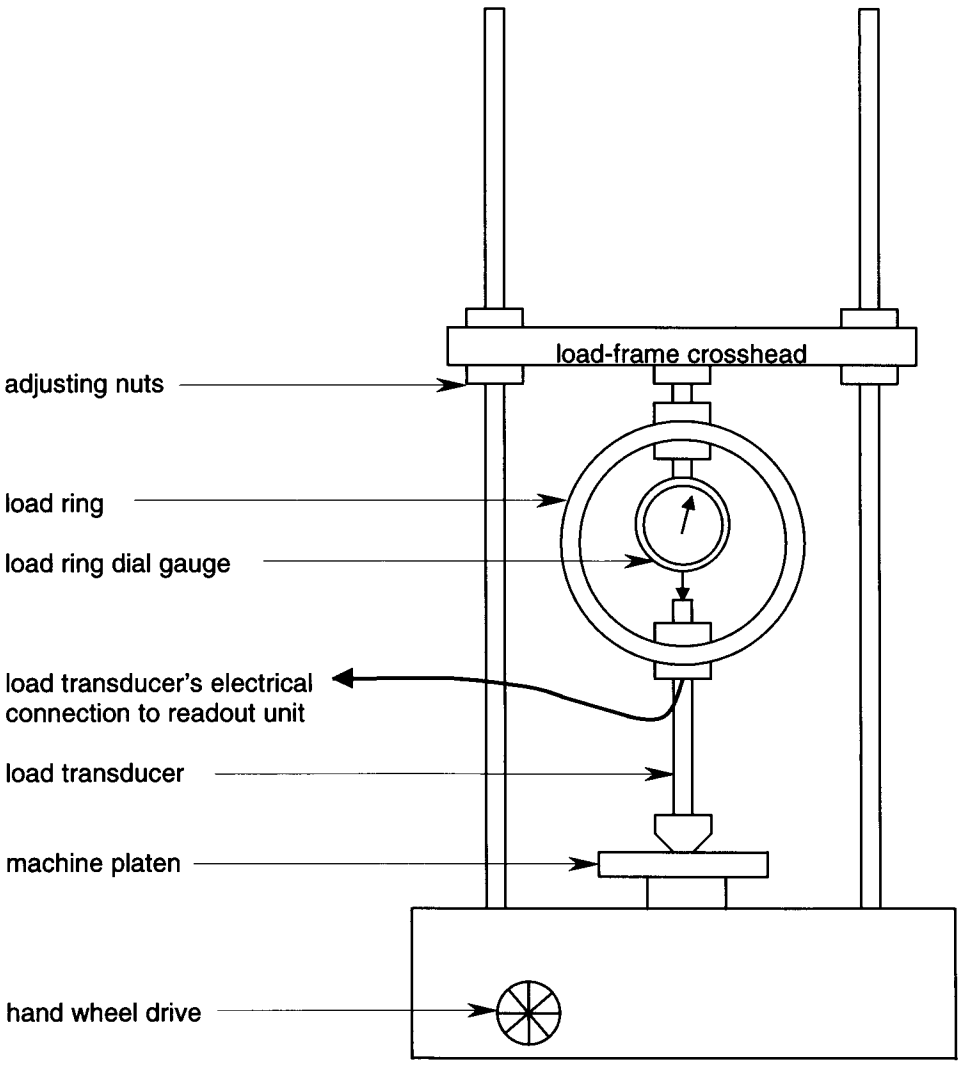


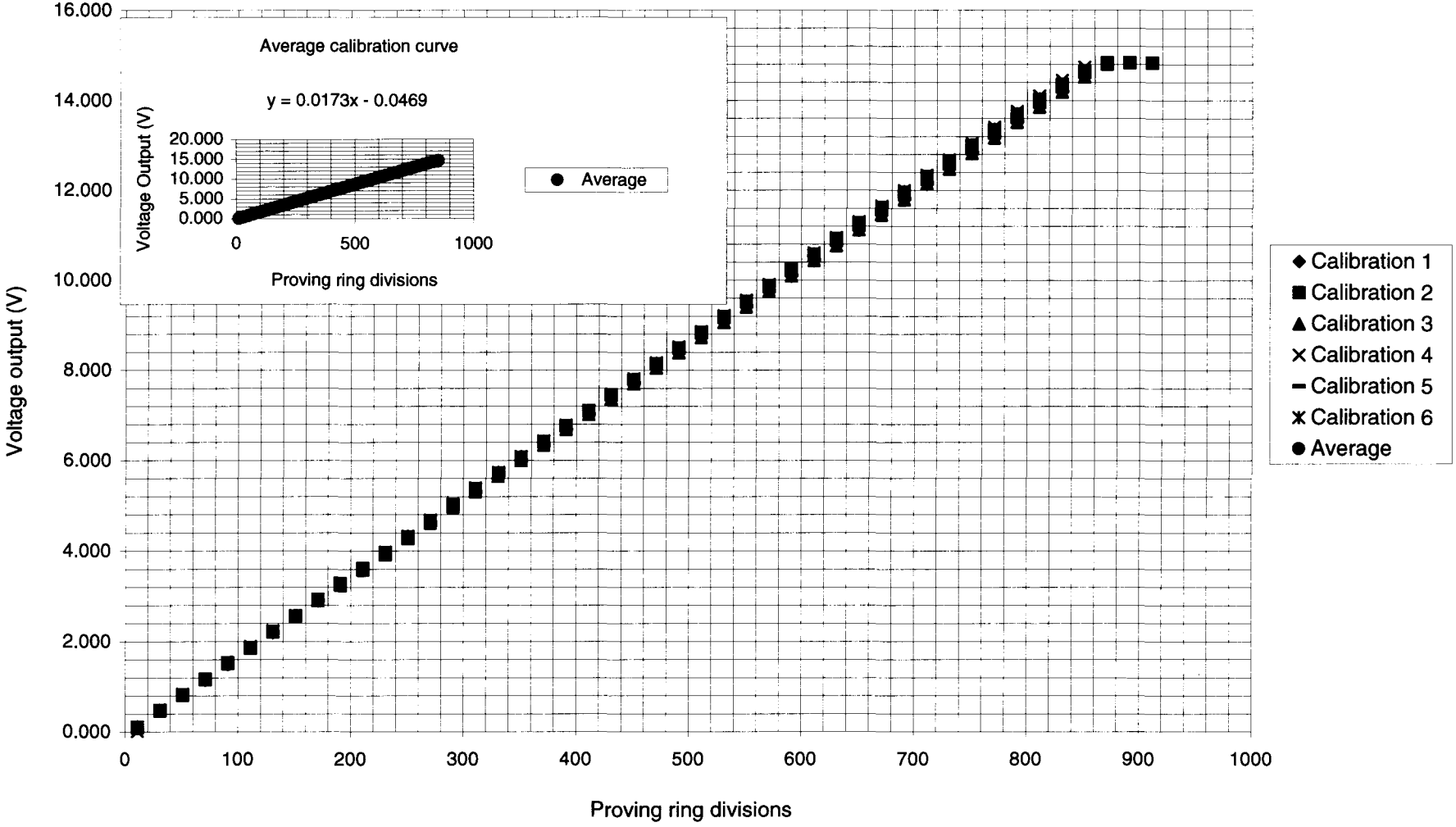
Figure B3 Arrangement for the calibration of load transducer against axial force

Table B3 Calibration of load transducer against axial force

Proof Ring (Div)	Voltage output (mV) Calibration No. 1	2	3	4	5	6	Average Voltage (V)	Calculatd Voltage (V)	% Error (calculated –maximum deviation)x100%
10.8	0.090	0.103	0.095	0.011	0.010	0.109	0.069	0.140	9.307
30.8	0.463	0.477	0.467	0.487	0.461	0.477	0.472	0.486	5.132
50.8	0.807	0.820	0.811	0.833	0.800	0.825	0.816	0.832	3.839
70.8	1.143	1.166	1.162	1.168	1.154	1.172	1.161	1.178	2.966
90.8	1.488	1.528	1.510	1.526	1.500	1.516	1.511	1.524	2.358
110.8	1.849	1.857	1.853	1.886	1.852	1.860	1.860	1.870	1.120
130.8	2.188	2.214	2.206	2.232	2.198	2.216	2.209	2.216	1.261
150.8	2.540	2.557	2.552	2.568	2.548	2.566	2.555	2.562	0.856
170.8	2.900	2.924	2.894	2.928	2.898	2.922	2.911	2.908	0.000
190.8	3.245	3.279	3.239	3.284	3.244	3.273	3.261	3.254	0.000
210.8	3.587	3.613	3.581	3.613	3.583	3.610	3.598	3.600	0.526
230.8	3.923	3.961	3.917	3.972	3.919	3.959	3.942	3.946	0.733
250.8	4.268	4.309	4.276	4.321	4.268	4.313	4.293	4.292	-0.677
270.8	4.611	4.661	4.614	4.677	4.616	4.664	4.641	4.638	-0.842
290.8	4.960	5.014	4.966	5.033	4.967	5.016	4.993	4.984	-0.984
310.8	5.303	5.367	5.303	5.389	5.304	5.369	5.339	5.330	-1.108
330.8	5.652	5.709	5.648	5.726	5.648	5.726	5.685	5.676	-0.882
350.8	5.995	6.057	5.994	6.073	5.994	6.079	6.032	6.022	-0.948
370.8	6.340	6.408	6.335	6.424	6.338	6.415	6.377	6.368	-0.880
390.8	6.683	6.757	6.678	6.771	6.679	6.764	6.722	6.714	-0.850
410.8	7.020	7.091	7.016	7.102	7.019	7.102	7.058	7.060	0.622
430.8	7.364	7.445	7.356	7.453	7.365	7.447	7.405	7.406	0.674
450.8	7.699	7.786	7.694	7.809	7.708	7.795	7.749	7.752	0.747
470.8	8.043	8.138	8.046	8.162	8.051	8.150	8.098	8.098	-0.791
490.8	8.385	8.487	8.387	8.515	8.392	8.493	8.443	8.444	-0.842
510.8	8.725	8.835	8.726	8.860	8.732	8.839	8.786	8.790	-0.797
530.8	9.062	9.184	9.057	9.206	9.066	9.180	9.126	9.136	0.864
550.8	9.399	9.525	9.401	9.552	9.412	9.531	9.470	9.482	0.875
570.8	9.743	9.875	9.751	9.899	9.751	9.877	9.816	9.828	0.864
590.8	10.085	10.225	10.089	10.252	10.100	10.230	10.164	10.174	0.874
610.8	10.425	10.569	10.433	10.598	10.438	10.575	10.506	10.520	0.902
630.8	10.763	10.915	10.761	10.941	10.777	10.919	10.846	10.866	0.966
650.8	11.103	11.262	11.110	11.293	11.123	11.266	11.193	11.212	0.972
670.8	11.449	11.612	11.449	11.645	11.461	11.614	11.538	11.558	0.943
690.8	11.787	11.961	11.791	11.993	11.801	11.970	11.884	11.904	0.982
710.8	12.133	12.307	12.139	12.340	12.147	12.312	12.230	12.250	0.955
730.8	12.472	12.647	12.472	12.680	12.484	12.654	12.568	12.596	0.984
750.8	12.810	12.996	12.816	13.038	12.822	13.003	12.914	12.942	1.019
770.8	13.160	13.343	13.160	13.404	13.173	13.352	13.265	13.288	0.963
790.8	13.506	13.686	13.510	13.750	13.520	13.701	13.612	13.634	0.938
810.8	13.848	14.015	13.850	14.098	13.862	14.031	13.951	13.980	0.944
830.8	14.184	14.346	14.183	14.440	14.198	14.358	14.285	14.326	0.998
850.8	14.515	14.640	14.515	14.735	14.520	14.645	14.595	14.672	1.070
870.8	14.806	14.834	14.804	14.834	14.815	14.834	14.821	15.018	1.425
890.8	14.834	14.834	14.834	14.834	14.834	14.834	14.834	15.364	3.449
910.8	14.834	14.834	14.834	14.834	14.834	14.834	14.834	15.710	5.576

FIGURE B4

CALIBRATION OF LOAD TRANSDUCER AGAINST AXIAL FORCE
(Proving ring factor = 25.77dN/div)



B.2.2 Calibration of load transducer against cell pressure

Procedure

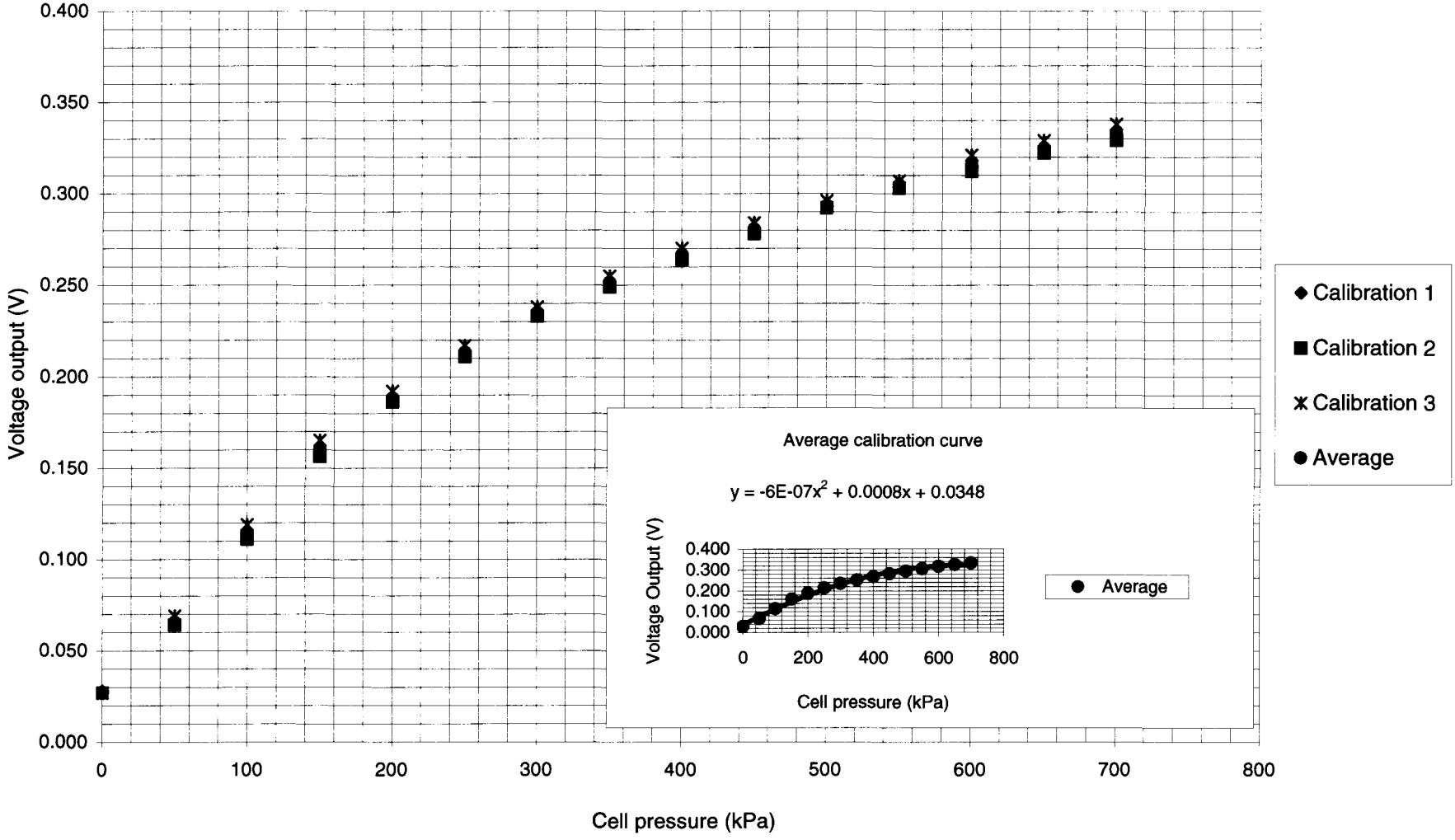
1. The valve connecting the cell pressure gauge to the reservoir, valve C7 in Figure 3.7, was disconnected and at that point a proven pressuremeter was connected to the cell pressure line.
2. The cell pressure and back pressure lines were deaired as described in section 3.4.2. When all the air had been removed from both pressure systems, all valves were closed and the volume change device was by-passed.
3. The cell was assembled and tightened to the cell base by turning the clamping nuts with controlled torque.
4. The cell was filled with deaired water from the water supply while its top air bleed valve was open. When water emerged from the top air release valve, the water supply and cell chamber valves were closed. The top air release valve was then closed.
5. The cell pressure gauge was adjusted so that the pressuremeter read 0kPa. The cell chamber valve was opened and time was allowed for the resulting load transducer voltage reading to stabilize. When stable, the voltage reading of the load transducer was recorded and then the cell chamber valve was closed.
6. Step 5 was repeated with cell pressure increments of 50 kPa up to the maximum working pressure of the pressuremeter (700kPa).
7. Three cycles of calibration of the load transducer against cell pressure were performed and the averages of the data were calculated.
8. From the plot of the average of the calibration data, an extrapolation was done to obtain the load transducer readings for cell pressures beyond 700kPa, i.e. from 700kPa to 1000kPa.

Table B4 Calibration of load transducer against cell pressure

Cell Pressure (kPa)	Voltage output (V) Calibration No. 1	2	3	Average Voltage (V)	Calculated Voltage (V)	% Error (calculated – maximum deviation) x100%
0	0.028	0.027	0.027	0.027	0.0443	39.05
50	0.064	0.064	0.069	0.066	0.0783	18.26
100	0.114	0.111	0.119	0.115	0.1103	-7.89
150	0.159	0.156	0.165	0.160	0.1403	-17.61
200	0.187	0.186	0.192	0.188	0.1683	-14.08
250	0.212	0.211	0.217	0.213	0.1943	-11.68
300	0.234	0.233	0.238	0.235	0.2183	-9.02
350	0.251	0.249	0.255	0.252	0.2403	-6.12
400	0.266	0.264	0.27	0.267	0.2603	-3.73
450	0.28	0.278	0.284	0.281	0.2783	-2.05
500	0.292	0.292	0.296	0.293	0.2943	0.78
550	0.304	0.303	0.307	0.305	0.3083	1.72
600	0.314	0.312	0.321	0.316	0.3203	2.59
650	0.323	0.322	0.329	0.325	0.3303	2.51
700	0.332	0.329	0.338	0.333	0.3383	2.75
750	EXTRAPOLATION FROM AVERAGE CALIBRATION CURVE'S EQUATION				0.3443	
800					0.3483	
850					0.3503	
900					0.3503	
950					0.3483	
1000					0.3443	

FIGURE B5

CALIBRATION OF LOAD TRANSDUCER AGAINST CELL PRESSURE



B.3 Calibration of Volume Change Transducer

The volume change transducer was calibrated by relating the change in voltage readings of the volume change transducer to the volume of water that flowed through the volume change device. Figure B6 shows the arrangement for the calibration of volume change transducer.

Procedure

1. The cell pressure line was isolated from the cell by disconnecting the cell chamber valve while all other valves were closed.
2. The cell pressure line and its volume change device were deaired as in section 3.4.2. When all the air had been removed from the system, the air bleed valve of the volume change device and the water supply valve were closed. The reservoir in the cell pressure line was by-passed by closing valve C6.
3. The rolling diaphragm of the volume change device was set to the extreme of its travel in any one direction by allowing deaired water from the water supply to run through the cell pressure line, while the volume change device was not by-passed, until no more flow occurred (meaning that the rolling diaphragm had reached the end of its travel in the current flow direction setup of the volume change device).
4. The voltage reading of the volume change transducer, corresponding to the rolling diaphragm being at the extreme of its travel, was recorded.
5. The valve immediately before the volume change device, valve C3, was closed and the flow reversal valve was set to change the direction of flow in the volume change device
6. A 100ml burette reading to the accuracy of 0.1ml was filled with water such that the bottom of the meniscus was at the extreme bottom mark of the burette (the 100ml mark) and the burette was placed below the disconnected end of the cell pressure line, as shown in Figure B6, to allow water flowing from the water supply through the volume change device to collect in it.
7. The valve immediately before the volume change device, valve C3, was opened slightly and carefully, while the water supply valve was open, and closed as soon as 1ml of water had dropped into the burette, i.e. when the bottom of the

meniscus was at 99ml mark. The resulting voltage reading of the volume change transducer was recorded when stable. It was possible to fill the burette with the exact amount of water required by opening the valve slowly and carefully.

8. Step 7 was repeated until the rolling diaphragm had reached the end of its travel in the current flow direction.
9. The burette was emptied, dried and filled with water so that the bottom of the meniscus was at the 100ml extreme bottom mark. The flow direction in the volume change device was reversed and the voltage reading of the volume change device was recorded.

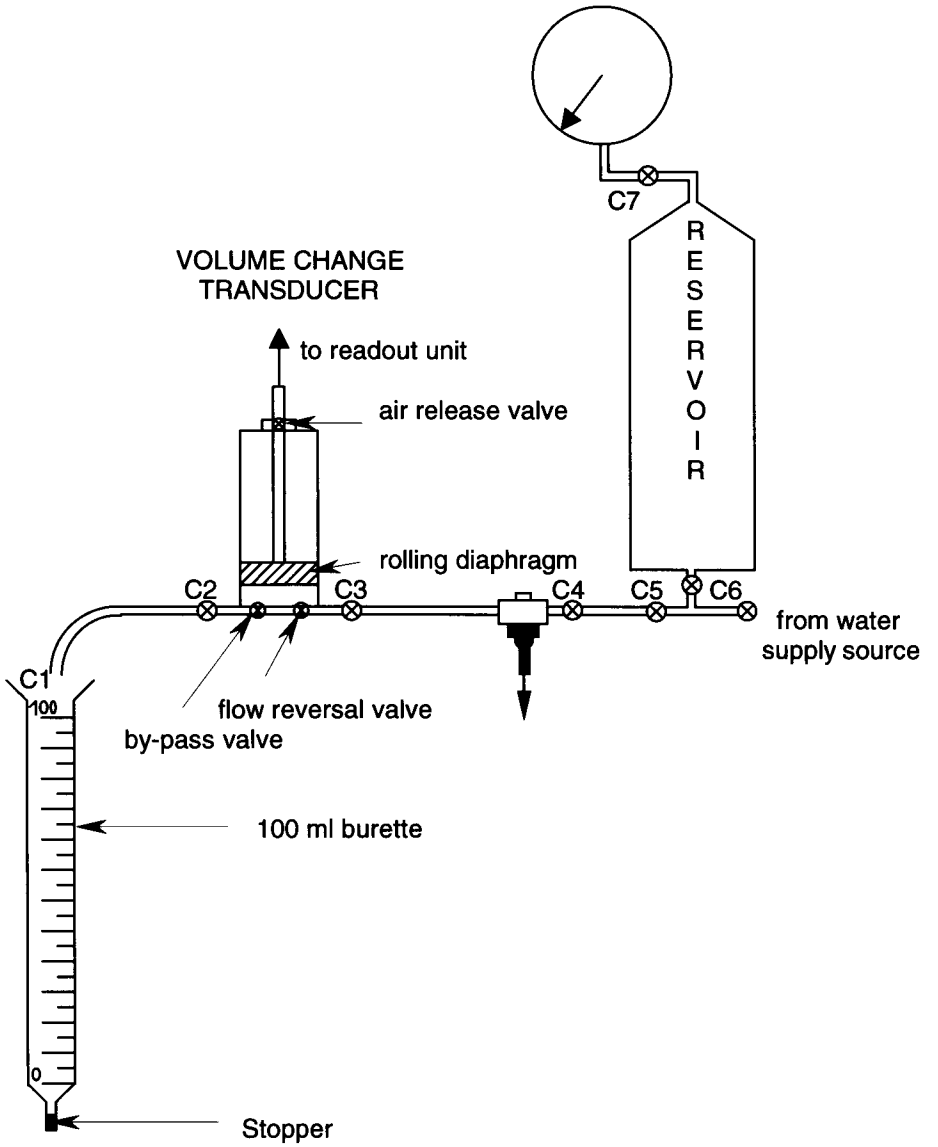


Figure B6 Arrangement for the calibration of volume change transducer

10. Steps 7 to 9 were repeated to give one full cycle of calibration consisting of flow in both directions through the volume change device.
11. Two cycles of calibrations of the volume change transducer were performed and the average slope of the calibration curves was calculated.

Table B5 Calibration of volume change transducer

Volume into Cell			**Volume out of Cell**		
Burette Volume (cm^3)	Calibration 1 (V)	Calibration 3 (V)	Burette Volume (cm^3)	Calibration 2 (V)	Calibration 4 (V)
0	-3.690	-3.680	88	3.185	3.188
1	-3.589	-3.616	87	3.099	3.102
2	-3.520	-3.544	86	3.005	3.020
3	-3.434	-3.472	85	2.942	2.942
4	-3.370	-3.395	84	2.858	2.859
5	-3.291	-3.315	83	2.780	2.790
6	-3.218	-3.235	82	2.698	2.712
7	-3.138	-3.160	81	2.622	2.626
8	-3.060	-3.081	80	2.546	2.543
9	-2.982	-3.004	79	2.469	2.471
10	-2.905	-2.898	78	2.390	2.396
11	-2.827	-2.854	77	2.307	2.318
12	-2.752	-2.772	76	2.231	2.232
13	-2.673	-2.699	75	2.152	2.159
14	-2.595	-2.625	74	2.076	2.075
15	-2.520	-2.545	73	1.996	1.994
16	-2.445	-2.470	72	1.923	1.898
17	-2.365	-2.392	71	1.843	1.843
18	-2.289	-2.315	70	1.767	1.767
19	-2.214	-2.239	69	1.690	1.689
20	-2.134	-2.164	68	1.609	1.618
21	-2.055	-2.088	67	1.527	1.532
22	-1.981	-2.008	66	1.458	1.453
23	-1.906	-1.928	65	1.374	1.377
24	-1.830	-1.856	64	1.304	1.301
25	-1.753	-1.768	63	1.227	1.222
26	-1.673	-1.704	62	1.145	1.142
27	-1.601	-1.625	61	1.069	1.062
28	-1.524	-1.552	60	0.990	0.992
29	-1.448	-1.469	59	0.910	0.914
30	-1.372	-1.401	58	0.832	0.831
31	-1.299	-1.324	57	0.758	0.762
32	-1.219	-1.250	56	0.678	0.677
33	-1.147	-1.172	55	0.600	0.605
34	-1.073	-1.097	54	0.520	0.526
35	-0.994	-1.023	53	0.444	0.449
36	-0.918	-0.944	52	0.364	0.376
37	-0.843	-0.870	51	0.289	0.292
38	-0.766	-0.802	50	0.215	0.212
39	-0.694	-0.722	49	0.140	0.139
40	-0.616	-0.652	48	0.058	0.058
41	-0.540	-0.571	47	-0.015	-0.023

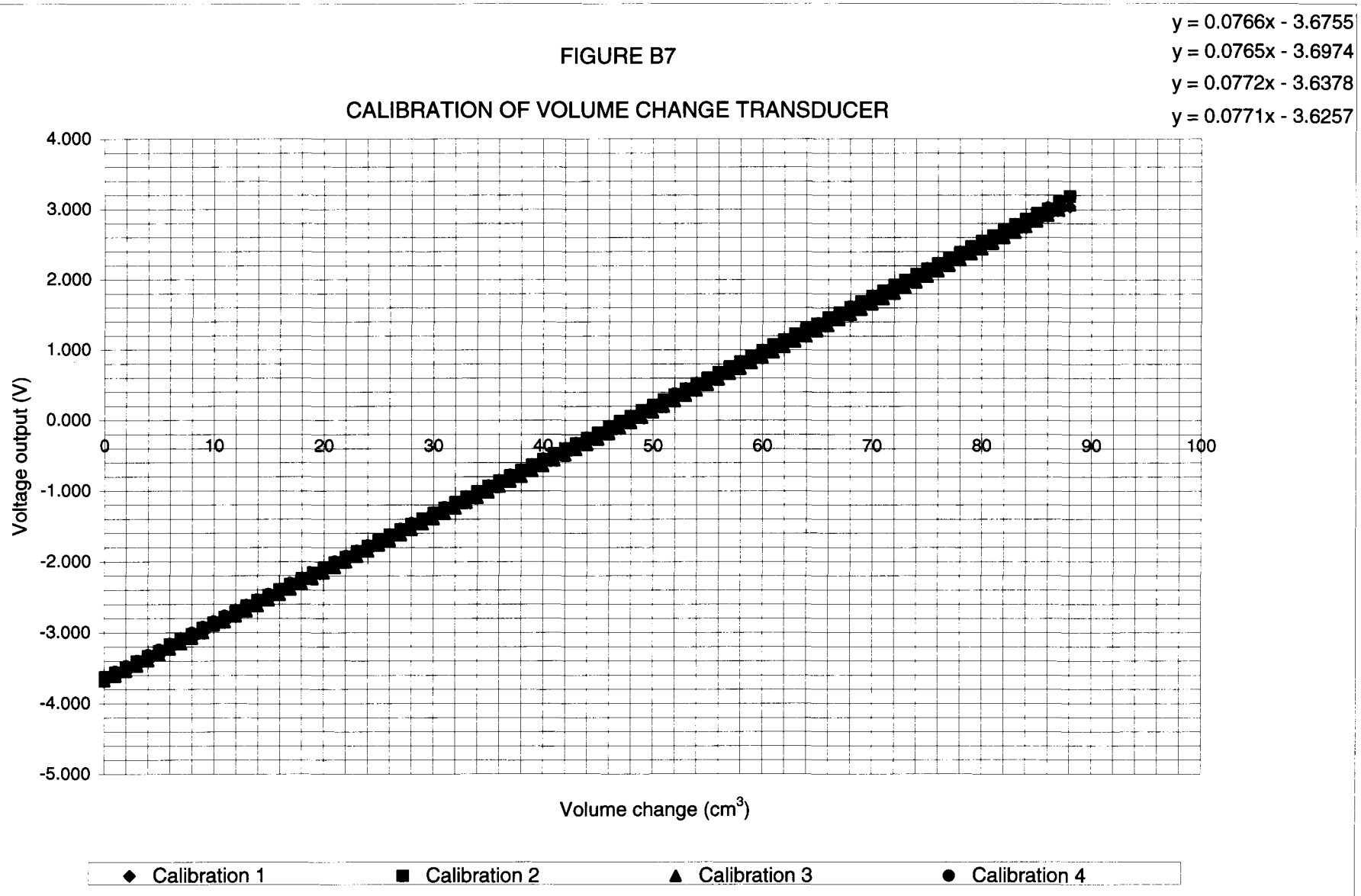
Volume into Cell			Volume out of Cell		
Burette Volume (cm^3)	Calibration 1 (V)	Calibration 3 (V)	Burette Volume (cm^3)	Calibration 2 (V)	Calibration 4 (V)
42	-0.466	-0.496	46	-0.095	-0.093
43	-0.389	-0.419	45	-0.174	-0.178
44	-0.314	-0.344	44	-0.252	-0.246
45	-0.239	-0.269	43	-0.327	-0.322
46	-0.162	-0.192	42	-0.402	-0.397
47	-0.083	-0.116	41	-0.473	-0.476
48	-0.011	-0.038	40	-0.558	-0.546
49	0.067	0.036	39	-0.634	-0.627
50	0.144	0.116	38	-0.709	-0.703
51	0.222	0.191	37	-0.786	-0.775
52	0.298	0.269	36	-0.859	-0.853
53	0.372	0.345	35	-0.934	-0.930
54	0.451	0.423	34	-1.012	-1.010
55	0.529	0.500	33	-1.089	-1.082
56	0.601	0.576	32	-1.166	-1.164
57	0.681	0.656	31	-1.245	-1.235
58	0.758	0.729	30	-1.318	-1.313
59	0.833	0.811	29	-1.395	-1.400
60	0.914	0.890	28	-1.475	-1.460
61	0.991	0.962	27	-1.551	-1.540
62	1.067	1.041	26	-1.624	-1.619
63	1.146	1.115	25	-1.704	-1.696
64	1.221	1.192	24	-1.782	-1.771
65	1.298	1.269	23	-1.857	-1.847
66	1.376	1.343	22	-1.936	-1.920
67	1.456	1.424	21	-2.011	-1.998
68	1.530	1.502	20	-2.085	-2.081
69	1.609	1.573	19	-2.162	-2.153
70	1.693	1.651	18	-2.240	-2.233
71	1.763	1.728	17	-2.320	-2.305
72	1.841	1.804	16	-2.393	-2.393
73	1.920	1.884	15	-2.475	-2.459
74	1.996	1.962	14	-2.547	-2.538
75	2.081	2.044	13	-2.627	-2.617
76	2.156	2.123	12	-2.706	-2.693
77	2.238	2.198	11	-2.786	-2.766
78	2.319	2.277	10	-2.861	-2.845
79	2.390	2.361	9	-2.936	-2.922
80	2.470	2.431	8	-3.024	-3.003
81	2.547	2.512	7	-3.089	-3.079
82	2.626	2.596	6	-3.166	-3.162
83	2.707	2.668	5	-3.260	-3.240
84	2.785	2.747	4	-3.334	-3.316
85	2.863	2.826	3	-3.408	-3.397
86	2.942	2.905	2	-3.487	-3.474
87	3.005	2.984	1	-3.565	-3.548
88	3.040	3.063	0	-3.630	-3.624

Slope =	**0.0766**	**0.0765**	Slope =	**0.0772**	**0.0771**

AVERAGE SLOPE = **0.077**

FIGURE B7

CALIBRATION OF VOLUME CHANGE TRANSDUCER



B.4 Calibration for Volume Change due to Movement of Loading Ram into Cell Chamber

B.4.1 Assumptions

1. The lower chamber loading system had been deaired according to section 3.4.2, the loading ram was at its extreme bottom position and all valves were closed.
2. The cell pressure and back pressure lines had been deaired and checked for leaks according to section 3.4.2. All valves were closed.

B.4.2 Procedure

1. The cell was assembled and tightened to its base by turning the clamping nuts with controlled torque.
2. The volume change device was by-passed and the cell was filled with deaired water from the water supply while the top air release valve was open. When water emerged from the top air release valve, the cell chamber valve and the water supply valve were closed.
3. The cell pressure gauge was set to zero, the volume change device was introduced to the cell pressure line and all valves in the cell pressure line, except the water supply valve, were opened.
4. The readings of the axial displacement and volume change transducers were recorded when stable. These corresponded to the loading ram being at its extreme bottom position, i.e. zero displacement of loading ram.
5. Valves D1 and D2, of the lower chamber loading system were opened to connect the pressure cylinder to the lower pressure chamber.
6. The motor drive unit of the lower chamber loading system was switched on at its lowest speed and the readings of the axial displacement and volume change transducers were observed. If the rate of change of these readings was too slow, the speed was increased a little.
7. After a short displacement of the loading ram, the lower pressure chamber valve, valve D1, was closed and the readings of the axial displacement and volume change transducers were recorded when stable.

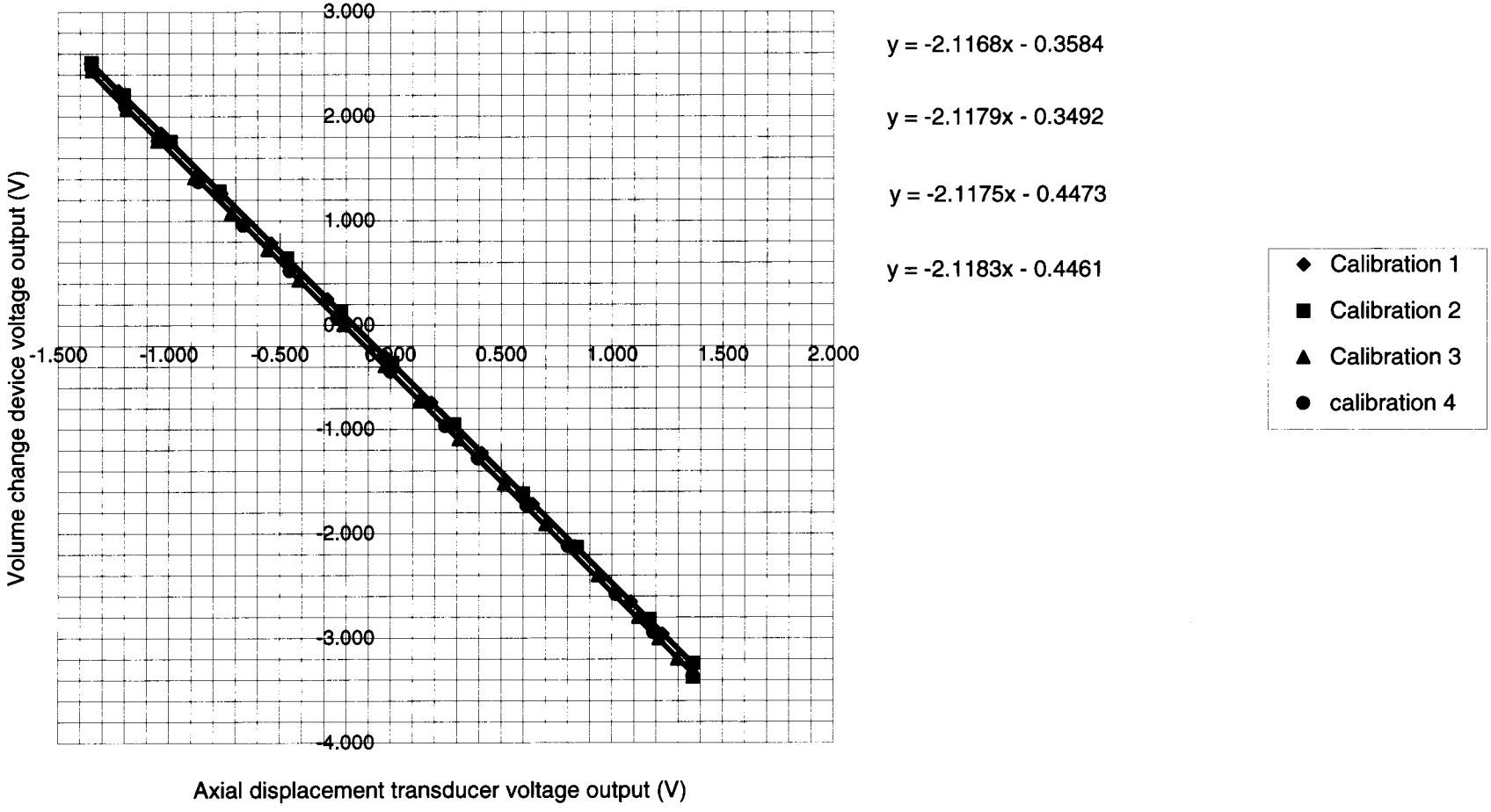
8. The lower pressure chamber valve was opened to lift the loading ram further.
9. Steps 7 and 8 were repeated until the loading ram reached its extreme top position. This gave half a cycle of calibration.
10. The motor drive unit was switched off and all valves in the lower chamber loading system, except valve D1, were closed.
11. The air bleed valve of the lower chamber loading system was opened for a short period and closed to allow the loading ram to fall for a short displacement under the action of its own weight and the height of water in the cell pressure line's reservoir. The readings of the axial displacement and volume change transducers were recorded when stable.
12. Step 11 was repeated until the loading ram reached its extreme bottom position. This gave a full cycle of calibration.
13. Two cycles of calibrations were performed and the average slope of the calibration data was calculated.

Table B6 Calibration of volume change due to piston movement

CALIBRATION 1		CALIBRATION 2		CALIBRATION 3		CALIBRATION 4	
Piston displt. (V)	Volume chng (V)	Piston displt. (V)	Volume chng (V)	Piston displt. (V)	Volume chng (V)	Piston displt. (V)	Volume chng (V)
-1.353	2.508	1.365	-3.241	-1.348	2.434	1.366	-3.369
-1.229	2.243	1.169	-2.824	-1.192	2.076	1.365	-3.362
-1.037	1.837	0.842	-2.132	-1.053	1.766	1.187	-2.946
-0.766	1.261	0.599	-1.619	-0.887	1.412	1.018	-2.580
-0.540	0.784	0.288	-0.957	-0.721	1.067	0.801	-2.119
-0.287	0.249	0.007	-0.365	-0.556	0.725	0.614	-1.731
-0.032	-0.290	-0.224	0.127	-0.416	0.432	0.395	-1.280
0.183	-0.746	-0.468	0.640	-0.212	0.004	0.247	-0.970
0.411	-1.230	-0.772	1.282	-0.026	-0.392	0.000	-0.449
0.642	-1.718	-0.993	1.756	0.131	-0.724	-0.241	0.064
0.833	-2.122	-1.205	2.204	0.308	-1.097	-0.457	0.518
1.085	-2.654	-1.351	2.512	0.513	-1.522	-0.667	0.954
1.229	-2.961			0.700	-1.911	-0.868	1.373
1.364	-3.245			0.938	-2.400	-1.050	1.761
1.365	-3.247			1.119	-2.798	-1.198	2.093
				1.212	-3.004	-1.347	2.437
				1.296	-3.199		
				1.365	-3.369		
				1.365	-3.369		
Slope =	**-2.1168**	Slope =	**-2.1179**	Slope =	**-2.1175**	Slope =	**-2.1183**
AVERAGE SLOPE =	**-2.118**						

FIGURE B8

CALIBRATION OF VOLUME CHANGE DUE TO PISTON MOVEMENT



B.5 Calibration for Cell Expansion Against Pressure and Time

B.5.1 Procedure

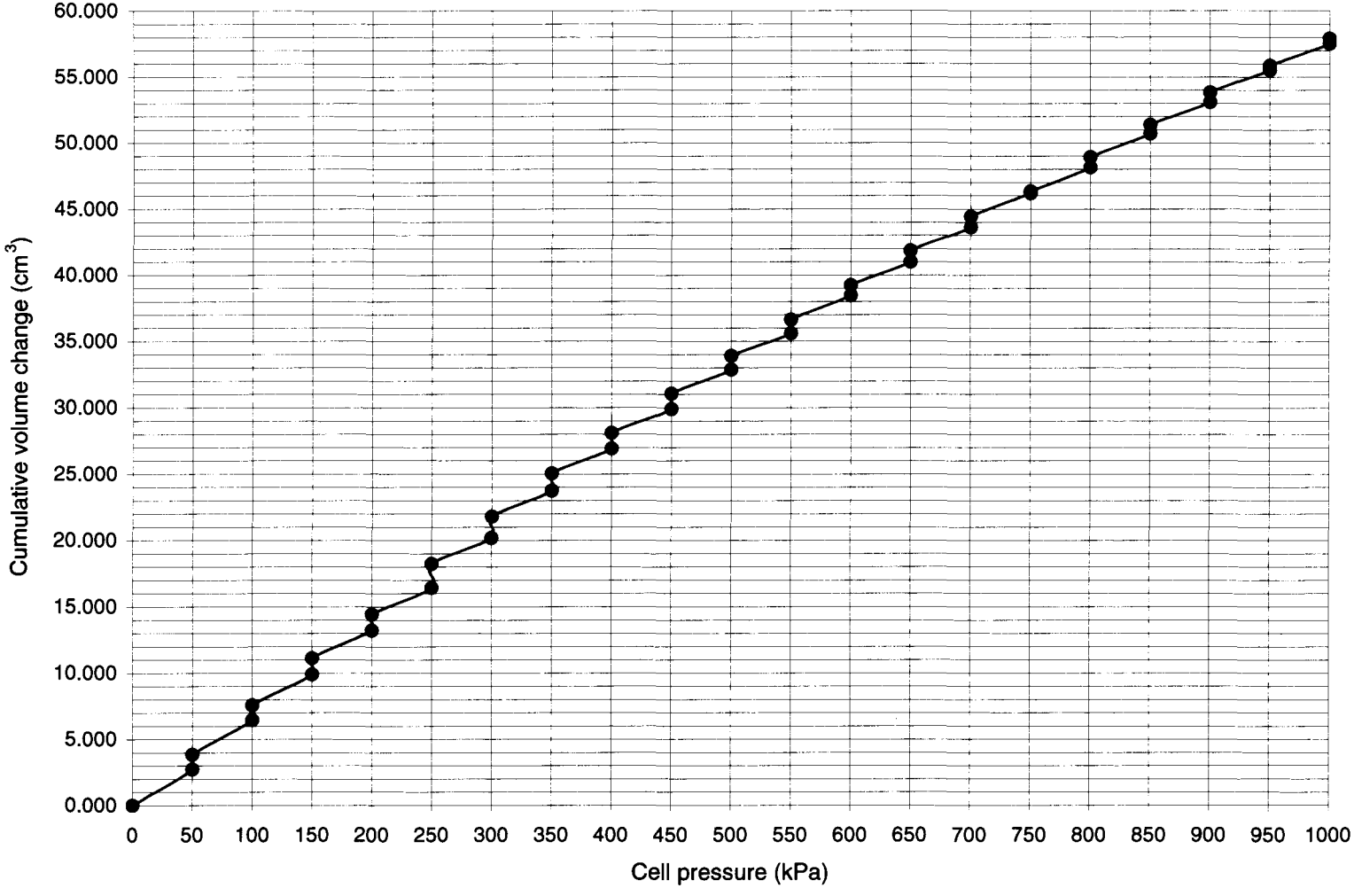
1. The cell pressure and back pressure lines were deaired as in section 3.4.2, and the back pressure line was isolated by closing valve B5.
2. The cell was assembled and tightened to the cell base by turning the clamping nuts with controlled torque.
3. The volume change device was by-passed and the cell was filled with deaired water from the water supply while the top air release valve was open. When water emerged from the top air release valve, the water supply valve was closed. The cell chamber valve and the top air release valve were not closed yet.
4. The volume change device was introduced to the cell pressure system and deaired water from the water supply was allowed to run through the system to bring the rolling diaphragm to the extreme of its travel in the current flow direction. When flow ceased to occur, the cell chamber valve, the water supply valve and the top air release valve of the cell were closed.
5. The direction of flow in the volume change device was reversed.
6. The cell pressure gauge was adjusted so that the cell pressure transducer voltage reading corresponded to 0kPa, using the cell pressure transducer calibration curve's equation, Figure B1, and the cell pressure gauge was introduced to the cell pressure line while the cell chamber valve was closed.
7. The voltage reading of the volume change device, corresponding to 0kPa cell pressure and a closed cell chamber valve, was recorded when stable.
8. The cell pressure gauge was adjusted so that the cell pressure transducer voltage reading corresponded to 50kPa, using the cell pressure transducer calibration curve's equation, Figure B1.
9. The cell chamber valve was opened to apply the cell pressure increment to the cell and the immediate volume change transducer voltage reading was recorded.
10. After 24 hours of application of the cell pressure increment, the cell chamber valve was closed and the volume change transducer voltage reading was recorded.
11. Steps 8 to10 were repeated with cell pressure increments of 50kPa up to 1000kPa.

Table B7 Calibration for cell expansion with pressure and time

Cell Pressure (kPa)		Volume transducer reading (V)	Cumulative volume change (V)	Cumulative volume change (cm^3)
0		-3.650	0.000	0.000
50	Instantaneous	-3.440	0.210	2.727
50	After 24 hours	-3.354	0.296	3.843
100	Instantaneous	-3.153	0.497	6.454
100	After 24 hours	-3.067	0.583	7.568
150	Instantaneous	-2.888	0.762	9.893
150	After 24 hours	-2.794	0.856	11.120
200	Instantaneous	-2.632	1.018	13.224
200	After 24 hours	-2.539	1.111	14.423
250	Instantaneous	-2.385	1.265	16.423
250	After 24 hours	-2.246	1.404	18.228
300	Instantaneous	-2.096	1.554	20.176
300	After 24 hours	-1.973	1.677	21.784
350	Instantaneous	-1.824	1.826	23.719
350	After 24 hours	-1.722	1.928	25.036
400	Instantaneous	-1.578	2.072	26.907
400	After 24 hours	-1.487	2.163	28.085
450	Instantaneous	-1.348	2.302	29.890
450	After 24 hours	-1.259	2.391	31.058
500	Instantaneous	-1.121	2.529	32.850
500	After 24 hours	-1.041	2.609	33.882
550	Instantaneous	-0.910	2.740	35.584
550	After 24 hours	-0.830	2.820	36.624
600	Instantaneous	-0.689	2.961	38.455
600	After 24 hours	-0.629	3.021	39.228
650	Instantaneous	-0.494	3.156	40.981
650	After 24 hours	-0.428	3.222	41.838
700	Instantaneous	-0.292	3.358	43.604
700	After 24 hours	-0.229	3.421	44.426
750	Instantaneous	-0.094	3.556	46.187
750	After 24 hours	-0.083	3.567	46.330
800	Instantaneous	0.056	3.706	48.131
800	After 24 hours	0.117	3.767	48.920
850	Instantaneous	0.254	3.904	50.698
850	After 24 hours	0.304	3.954	51.356
900	Instantaneous	0.437	4.087	53.081
900	After 24 hours	0.493	4.143	53.803
950	Instantaneous	0.624	4.274	55.505
950	After 24 hours	0.651	4.301	55.852
1000	Instantaneous	0.778	4.428	57.509
1000	After 24 hours	0.807	4.457	57.888

FIGURE B9

CALIBRATION FOR CELL EXPANSION WITH PRESSURE AND TIME



B.6 Calibration of Axial Displacement Transducers

B.6.1 Procedure

1. The two axial displacement transducers were clamped on to the calibrating instrument, shown in Figure B10, so that their stems were fully out and just in contact with the sliding plate of the instrument. The sliding plate slide on the base plate such that its surface maintained right angles to the axis of the transducers. A spring, whose one end was fixed to a stationary plate, pushed against the sliding plate so that the displacement of the plate could be accurately adjusted when the shaft of the displacement-measuring tool (on the other side of the sliding plate) pushed or moved away from the plate on turning of the adjusting nut. The displacement of the sliding plate was the same as the displacement of the stems of the transducers. The displacement-measuring tool measured to the accuracy of 0.05mm.
2. The initial displacement reading, indicated by the displacement-measuring tool, when the stems of the transducers were just in contact with the sliding plate was recorded against the voltage reading of the transducers.
3. The adjusting nut was turned to displace the transducers by 0.5mm and the resulting voltage reading of the transducers was recorded when stable.
4. Step 3 was repeated with displacement increments of 0.5mm up to 47mm. This gave half a cycle of calibration.
5. When the axial displacement transducer voltage reading corresponding to the 47mm displacement had been recorded, the adjusting nut was turned, in steps of 0.5mm, so that the sliding plate moved away from the stems of the transducers. The voltage readings of the transducers were recorded at each step. This gave one full cycle of calibration.
6. Two cycles of calibration were performed and the average slope of the linear portions of the calibration curves was calculated.

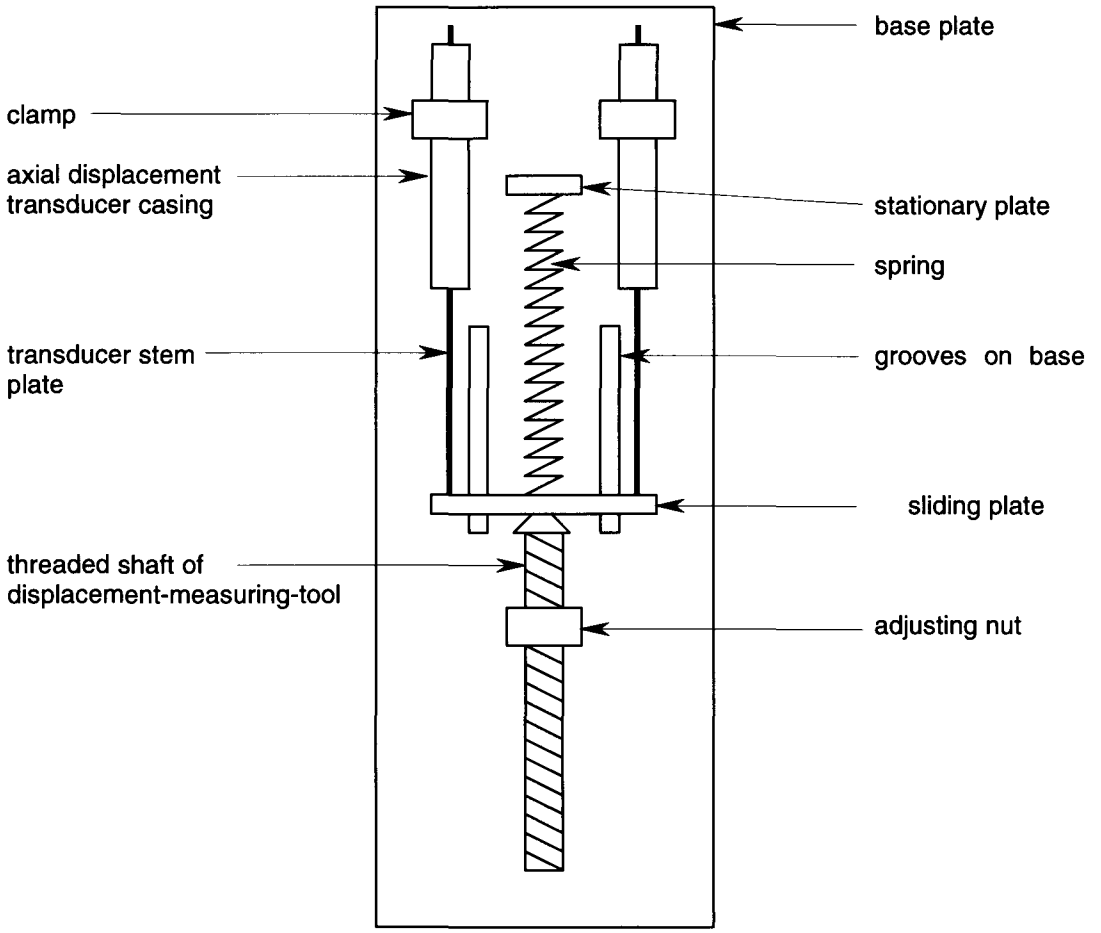


Figure B10 The instrument used for calibrating the axial displacement transducers

Table B8 Calibration of axial displacement transducers

Displacement (mm)	Calibration 1 (V)	Calibration 2 (V)	Calibration 3 (V)	Calibration 4 (V)
0.0	-3.548	-3.546	-3.558	-3.556
0.5	-3.582	-3.581	-3.590	-3.589
1.0	-3.610	-3.608	-3.619	-3.617
1.5	-3.635	-3.633	-3.641	-3.639
2.0	-3.654	-3.653	-3.659	-3.658
2.5	-3.667	-3.665	-3.671	-3.670
3.0	-3.672	-3.670	-3.674	-3.673
3.5	-3.673	-3.671	-3.670	-3.668
4.0	-3.665	-3.664	-3.660	-3.658
4.5	-3.649	-3.648	-3.643	-3.642
5.0	-3.625	-3.623	-3.619	-3.617
5.5	-3.593	-3.591	-3.584	-3.582
6.0	-3.555	-3.554	-3.543	-3.542
6.5	-3.509	-3.507	-3.496	-3.494
7.0	-3.456	-3.455	-3.443	-3.441
7.5	-3.397	-3.395	-3.383	-3.381
8.0	-3.333	-3.333	-3.316	-3.315
8.5	-3.263	-3.261	-3.242	-3.241
9.0	-3.189	-3.188	-3.168	-3.166
9.5	-3.109	-3.108	-3.087	-3.086
10.0	-3.027	-3.026	-3.005	-3.003
10.5	-2.941	-2.940	-2.918	-2.917
11.0	-2.849	-2.847	-2.830	-2.828
11.5	-2.758	-2.756	-2.737	-2.736
12.0	-2.664	-2.663	-2.642	-2.640
12.5	-2.568	-2.567	-2.546	-2.544
13.0	-2.471	-2.470	-2.451	-2.450
13.5	-2.372	-2.370	-2.352	-2.350
14.0	-2.271	-2.269	-2.241	-2.240
14.5	-2.170	-2.168	-2.147	-2.145
15.0	-2.065	-2.064	-2.042	-2.041
15.5	-1.958	-1.957	-1.937	-1.935
16.0	-1.850	-1.849	-1.830	-1.828
16.5	-1.743	-1.741	-1.721	-1.720
17.0	-1.637	-1.635	-1.613	-1.611
17.5	-1.528	-1.526	-1.504	-1.502
18.0	-1.419	-1.417	-1.394	-1.392
18.5	-1.310	-1.309	-1.285	-1.283
19.0	-1.200	-1.199	-1.175	-1.174
19.5	-1.091	-1.090	-1.066	-1.065
20.0	-0.982	-0.980	-0.958	-0.956
20.5	-0.873	-0.871	-0.848	-0.847
21.0	-0.767	-0.765	-0.740	-0.739
21.5	-0.659	-0.658	-0.633	-0.631
22.0	-0.552	-0.550	-0.526	-0.524
22.5	-0.444	-0.442	-0.418	-0.417
23.0	-0.338	-0.337	-0.312	-0.310
23.5	-0.231	-0.230	-0.206	-0.204
24.0	-0.125	-0.123	-0.099	-0.098
24.5	-0.019	-0.017	0.007	0.008
25.0	0.087	0.085	0.116	0.114
25.5	0.193	0.191	0.222	0.221
26.0	0.299	0.297	0.328	0.327
26.5	0.405	0.404	0.435	0.433
27.0	0.512	0.511	0.541	0.540
27.5	0.618	0.616	0.648	0.646
28.0	0.725	0.724	0.754	0.752
28.5	0.832	0.830	0.862	0.860

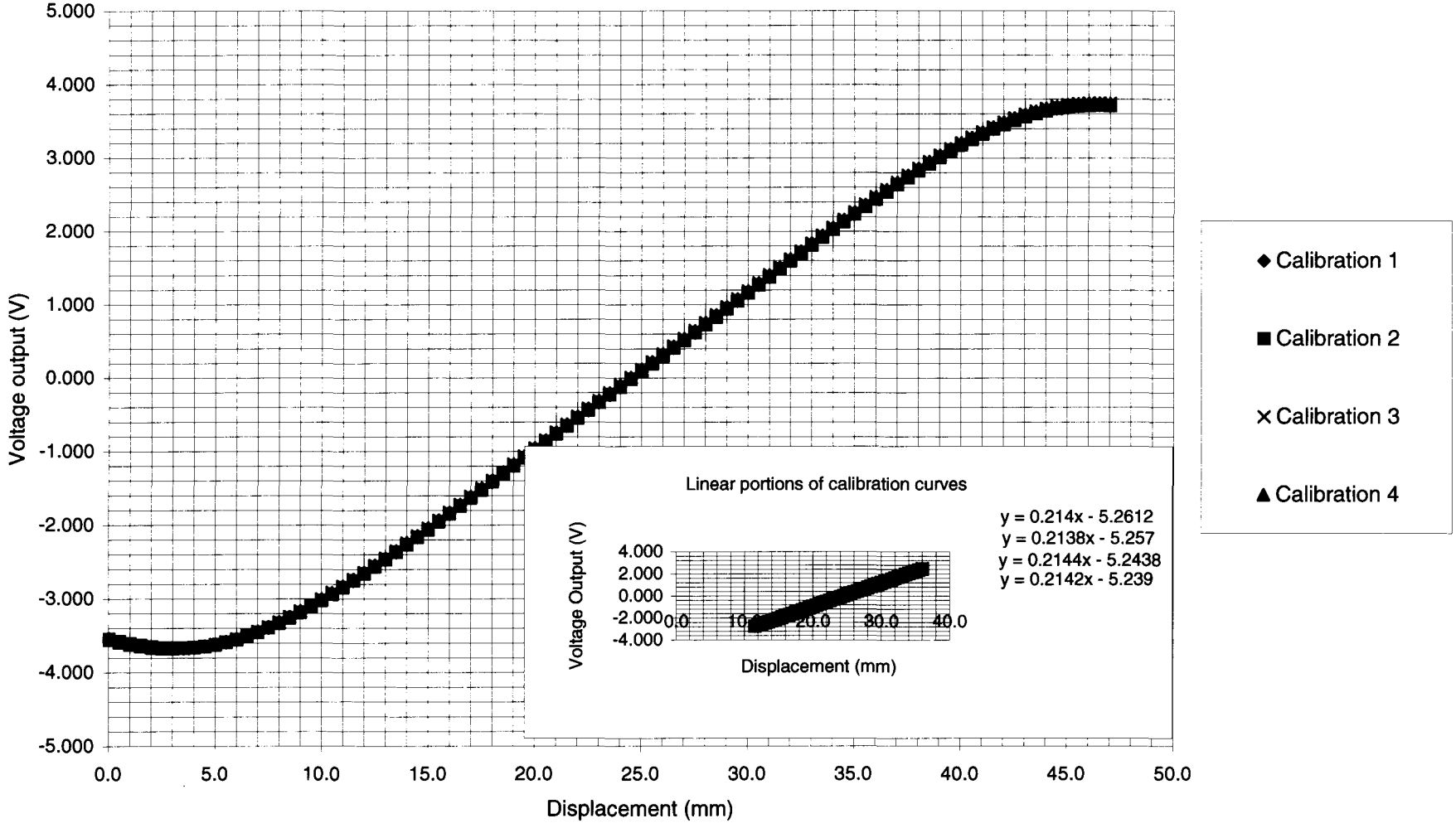
Displacement (mm)	Calibration 1 (V)	Calibration 2 (V)	Calibration 3 (V)	Calibration 4 (V)
29.0	0.940	0.938	0.968	0.967
29.5	1.048	1.047	1.078	1.076
30.0	1.157	1.156	1.185	1.184
30.5	1.266	1.264	1.295	1.293
31.0	1.375	1.373	1.404	1.402
31.5	1.484	1.482	1.513	1.511
32.0	1.593	1.592	1.621	1.620
32.5	1.701	1.700	1.729	1.728
33.0	1.809	1.807	1.838	1.836
33.5	1.916	1.915	1.944	1.943
34.0	2.022	2.020	2.052	2.050
34.5	2.128	2.126	2.158	2.156
35.0	2.233	2.231	2.262	2.261
35.5	2.336	2.335	2.366	2.364
36.0	2.438	2.437	2.468	2.467
36.5	2.539	2.537	2.570	2.568
37.0	2.638	2.637	2.668	2.666
37.5	2.735	2.733	2.765	2.764
38.0	2.829	2.827	2.859	2.858
38.5	2.921	2.919	2.951	2.949
39.0	3.009	3.007	3.039	3.037
39.5	3.094	3.092	3.124	3.122
40.0	3.175	3.174	3.205	3.203
40.5	3.251	3.250	3.281	3.280
41.0	3.324	3.322	3.355	3.353
41.5	3.392	3.390	3.422	3.421
42.0	3.453	3.451	3.485	3.484
42.5	3.511	3.509	3.545	3.543
43.0	3.563	3.561	3.593	3.592
43.5	3.604	3.603	3.637	3.635
44.0	3.640	3.639	3.673	3.671
44.5	3.670	3.669	3.702	3.701
45.0	3.690	3.688	3.725	3.723
45.5	3.704	3.702	3.738	3.737
46.0	3.711	3.710	3.745	3.744
46.5	3.714	3.713	3.747	3.745
47.0	3.710	3.708	3.741	3.740

Slope =	**0.2140**	**0.2138**	**0.2144**	**0.2142**

AVERAGE SLOPE = **0.2141**

FIGURE B11

CALIBRATION OF AXIAL DISPLACEMENT TRANSDUCERS



B.6.2 Mounting the axial displacement transducers at convenient position on the cell top

Before performing liquefaction testing in the Bishop-Wesley stress path cell, The two axial displacement transducers were clamped in position onto the brackets fixed on the cell top so that when the cell was assembled, with the loading ram at its extreme bottom position, the initial axial transducers voltage reading was within the straight line portion of the average axial displacement transducer calibration curve, Figure B11, and near the beginning of this curve for upward movement of the loading ram.

It was also important to ensure that the transducers were clamped identically i.e. in such a way that the exposed lengths of their stems, measured from the top of the vertical rod on which their stems rested to the bottom of the transducer casing, were equal. This was to ensure that the transducers were operated in the same way that they were calibrated. The adjusting screws of the vertical rods were turned, if necessary, to make finer adjustments to ensure that the exposed lengths of the transducers were equal.

APPENDIX C

TEST RESULTS FOR SPECIMENS UNDER CASE 1 TESTS

Table C1 Summary of results of monotonic undrained compression triaxial tests performed on isotropically consolidated Merriespruit gold tailings (present study)

Specimen No.	Fines Content	Initial stress state		Void ratio		Behavior	Peak shear resistance			Steady-state strength			L_P	L_R
		q_0	p'_0	Setup	Final		q_P	p'_P	ϕ'_P	q_{SS}	p'_{SS}	ϕ'_{SS}		
	(%)	(kPa)	(kPa)				(kPa)	(kPa)	(Degrees)	(kPa)	(kPa)	(Degrees)		(kPa)
6c	0	0	200	1.339	1.239	Liquefaction	68.0	107.7	16.6	37.6	36.0	26.4	7.5	68.0
2d	0	0	450	1.467	1.101	Liquefaction	246.3	285.6	22.1	197.9	166.0	29.8	3.5	246.3
3c	0	0	100	1.545	1.231	Liquefaction	38.6	48.4	20.6	12.5	10.2	30.7	15.7	38.6
6d	0	0	50	1.296	1.137	Liquefaction	14.7	23.9	16.2	2.1	2.2	24.3	32.3	14.7
2e	0	0	300	1.468	1.146	Liquefaction	120.0	160.0	19.5	67.1	45.9	36.0	11.8	120.0
3e	0	0	350	1.421	1.091	Liquefaction	153.8	201.3	19.8	86.3	63.8	33.5	9.0	153.8
3d	0	0	400	1.486	1.106	Liquefaction	214.6	263.5	21.0	145.1	113.4	31.8	5.2	214.6
2f	0	0	500	1.292	1.018	Liquefaction	303.1	306.0	25.2	237.0	191.5	30.9	3.4	303.1
2a	20	0	147	1.501	1.191	Liquefaction	57.0	92.0	16.3	28.4	28.0	25.7	6.9	57.0
2b	20	0	50	1.510	1.287	Liquefaction	20.8	33.4	16.4	1.6	8.0	5.4	5.7	20.8
6a	20	0	75	1.504	1.270	Liquefaction	31.8	49.1	17.0	19.3	23.4	21.3	3.4	31.8
3a	20	0	229	1.449	1.193	Liquefaction	81.4	132.6	16.2	31.8	29.6	27.1	11.1	81.4
6b	20	0	111	1.478	1.179	Liquefaction	43.4	60.5	18.7	15.1	19.0	20.5	6.9	43.4
3b	20	0	362	1.481	1.160	Liquefaction	151.3	237.4	16.7	59.1	59.2	25.3	8.2	151.3
2c	20	0	298	1.428	1.109	Liquefaction	126.9	201.3	16.6	50.5	51.8	24.8	7.5	126.9
6g	30	0	75	1.440	1.132	Liquefaction	30.5	50.2	16.0	13.6	15.0	23.2	6.1	30.5
3i	30	0	100	1.415	0.911	Liquefaction	46.4	65.5	18.5	21.1	18.5	28.6	7.7	46.4
2J	30	0	450	1.499	0.947	Liquefaction	200.6	265.9	19.6	134.3	119.8	28.2	5.0	200.6
3J	30	0	350	1.503	1.015	Liquefaction	157.2	192.4	21.1	99.9	84.3	29.7	5.9	157.2
6h	30	0	300	1.430	0.933	Liquefaction	156.7	185.2	21.8	94.3	71.9	32.5	6.4	156.7
2k	30	0	500	1.407	0.855	Liquefaction	235.7	326.6	18.8	144.8	125.3	29.0	5.5	235.7
3k	30	0	150	1.356	1.090	Liquefaction	67.4	90.0	19.5	28.5	22.0	32.2	11.0	67.4
2L	30	0	50	1.260	0.926	Liquefaction	20.4	35.3	15.3	3.2	2.6	31.0	32.3	20.4
6i	30	0	200	1.493	0.828	Liquefaction	115.1	138.9	21.4	60.1	50.5	29.8	5.6	115.1
3f	60	0	50	0.983	0.798	Liquefaction	32.4	33.8	24.4	19.5	15.5	31.3	4.6	32.4
2g	60	0	100	1.173	0.821	Liquefaction	43.0	56.3	19.8	15.8	13.8	28.8	10.8	43.0
6e	60	0	250	0.995	0.745	Lim liqfction	122.9	141.5	22.3	79.5	61.5	32.1	6.1	122.9

Specimen No.	Fines Content (%)	Initial stress state		Void ratio		Behavior	Peak shear resistance			Steady-state strength			L_P	L_R (kPa)
		q_0 (kPa)	p'_0 (kPa)	Setup	Final		q_P (kPa)	p'_P (kPa)	ϕ'_P (Degrees)	q_{ss} (kPa)	p'_{ss} (kPa)	ϕ'_{ss} (Degrees)		
3g	60	0	400	1.189	0.765	Lim liqfction	172.1	240.9	18.6	120.4	94.6	31.7	6.3	172.1
6f	60	0	300	1.243	0.820	Lim liqfction	138.0	189.0	19.0	102.5	80.7	31.6	5.5	138.0
2h	60	0	450	1.039	0.703	Lim liqfction	201.7	269.2	19.5	137.3	107.3	31.8	6.3	201.7
2i	60	0	500	1.212	0.801	Lim liqfction	242.3	335.3	18.8	165.1	131.5	31.3	5.5	242.3
3h	60	0	150	1.198	0.735	Liquefaction	65.6	90.9	18.8	18.9	12.3	37.7	24.0	65.6

Table C2 Summary of results of monotonic undrained compression triaxial tests performed on isotropically consolidated Merriespruit gold tailings (Fourie and Papageorgiou (2001))

Specimen No.	Fines Content (%)	Initial stress state		Void ratio		Behavior	Peak shear resistance			Steady-state strength			L_P	L_R (kPa)
		q_0 (kPa)	p'_0 (kPa)	Setup	Final		q_P (kPa)	p'_P (kPa)	ϕ'_P (Degrees)	q_{ss} (kPa)	p'_{ss} (kPa)	ϕ'_{ss} (Degrees)		
1	0	0	400	1.231	1.004	Liquefaction	398	376	26.7	324	248	32.4	1.9	398.0
5	0	0	20	1.412	1.145	Liquefaction	14	12	29.2	6	2	-	-	14.0
6	0	0	50	1.445	1.156	Liquefaction	20	35	15.1	2	7	7.8	6.9	20.0
7	0	0	455	1.241	1.081	Liquefaction	148	189	20.3	86	79	27.4	8.0	148.0
8	0	0	70	1.494	1.182	Liquefaction	22	33	17.5	4	4	25.4	25.3	22.0
9	0	0	310	1.577	1.269	Liquefaction	126	224	14.9	46	50	23.5	7.9	126.0
12	0	0	460	1.380	1.133	Liquefaction	278	302	23.5	130	94	34.2	8.1	278.0
13	0	0	230	1.405	1.088	Liquefaction	84	127	17.3	24	24	25.4	13.4	84.0
1	20	0	150	1.454	1.249	Liquefaction	56	100	14.8	10	15	17.5	11.9	56.0
2	20	0	50	1.508	1.292	Liquefaction	18	29	16.3	2	11	5.1	3.8	18.0
3	20	0	400	1.416	1.097	Liquefaction	166	259	16.8	54	53	25.8	10.4	166.0
4	20	0	470	1.491	1.141	Liquefaction	164	280	15.5	62	57	27.4	11.9	164.0
5	20	0	200	1.505	1.182	Liquefaction	72	109	17.3	26	25	26.3	11.2	72.0

Specimen No.	Fines Content	Initial stress state		Void ratio		Behavior	Peak shear resistance			Steady-state strength			L_P	L_R
		q_0	p'_0	Setup	Final		q_P	p'_P	ϕ'_P	q_{SS}	p'_{SS}	ϕ'_{SS}		
	(%)	(kPa)	(kPa)				(kPa)	(kPa)	(Degrees)	(kPa)	(kPa)	(Degrees)		(kPa)
6	20	0	300	1.464	1.187	Liquefaction	114	166	17.9	32	29	27.8	15.4	114.0
7	20	0	30	1.428	1.225	Liquefaction	4	18	6.2	2	7	7.8	3.7	4.0
8	20	0	505	1.324	1.122	Liquefaction	196	274	18.6	86	80	27.1	8.8	196.0
3	30	0	400	1.649	0.821	Liquefaction	162	209	20.1	70	64	27.6	8.8	162.0
4	30	0	50	1.597	1.129	Liquefaction	14	26	14.3	4	4	25.4	17.8	14.0
5	30	0	80	1.432	0.976	Liquefaction	28	49	15.1	6	13	12.4	6.3	28.0
6	30	0	150	1.289	0.895	Liquefaction	82	111	19.2	36	25	35.5	10.5	82.0
7	30	0	450	0.955	0.902	Liquefaction	188	209	23.0	92	93	25.1	6.2	188.0
8	30	0	280	1.043	0.941	Liquefaction	142	174	21.1	72	61	29.5	6.6	142.0
9	30	0	90	1.470	0.970	Liquefaction	34	61	14.8	12	14	22.0	8.0	34.0
10	30	0	500	1.154	0.960	Liquefaction	218	294	19.3	124	106	29.3	6.7	218.0
11	30	0	200	1.309	0.991	Liquefaction	76	109	18.2	24	24	25.4	11.5	76.0
12	30	0	400	0.924	0.900	Liquefaction	212	236	23.0	148	130	28.6	4.0	212.0
1	60	0	260	1.622	0.803	Lim liqfction	104	137	19.7	90	72	31.1	5.2	104.0
3	60	0	265	1.361	0.703	Lim liqfction	150	198	19.7	138	113	30.5	3.0	150.0
4	60	0	290	1.253	0.755	Liquefaction	120	140	22.0	96	76	31.4	5.6	120.0
5	60	0	270	1.180	0.708	Liquefaction	102	132	20.0	76	64	29.7	6.0	102.0
6	60	0	190	1.189	0.742	Liquefaction	74	94	20.4	52	47	27.8	5.4	74.0
7	60	0	160	1.020	0.819	Liquefaction	72	94	19.9	48	41	29.3	5.4	72.0
8	60	0	50	1.181	0.749	Liquefaction	28	26	27.2	18	12	36.9	7.3	28.0
9	60	0	50	0.963	0.780	Liquefaction	36	39	23.6	24	22	27.5	2.6	36.0
10	60	0	410	0.997	0.814	Liquefaction	180	246	19.0	132	113	29.3	4.9	180.0
11	60	0	20	0.966	0.814	Liquefaction	18	21	22.0	10	11	23.2	1.6	18.0
12	60	0	460	0.993	0.773	Liquefaction	218	268	21.0	146	125	29.3	5.0	218.0

Test	**Case 1: Monotonic Undrained Compression of Isotropically Consolidated Specimens**		
Cell No.	6 (Big)	Fines content (%)	0
Specimen	6c	Specific gravity (g/cm^3)	2.72

1.) Sample physical properties

Wet mass before test (g)	865.889	m.c before test (%)	8.30	Height (mm)	151.35	Volume (cm^3)	687.497
Wet mass after test (g)	971.427	m.c. after test (%)	21.50	Diameter (mm)	76.05		
Dry mass (g)	799.528	Dry density (kg/m^3)	1163	Area (cm^2)	45.424	Void ratio (e_0)	1.339

2.) Saturation/Consolidation

Date	C.P (kPa)	P.W.P bp closed (kPa)	B.P (kPa)	P.W.P bp open (kPa)	Change C.P (kPa)	Change P.W.P (kPa)	B value	Volume Gauge (cm^3)	Cell Expansn (cm^3)	Specimen Volume (cm^3)	Void Ratio	Comments
3/10	0		0	-1.5				0.00	0.00	687.497	1.339	
3/10	10.6		8.0	5.5				6.55	0.00	680.947	1.317	**AIR-FLUSHING**
3/10	50	15.5	40	39.5	39.4	10.0	0.25	14.93	3.82	676.387	1.301	**S**
4/10	100	60.5	90	90.0	50	21.0	0.42	20.52	7.94	674.917	1.296	**A**
5/10	150	119.0	140	140.0	50	29.0	0.58	25.89	10.71	672.317	1.287	**T**
6/10	200	176.0	190	190.0	50	36.0	0.72	30.02	12.51	669.987	1.279	**U**
7/10	250	230.5	240	240.0	50	40.5	0.81	32.68	13.93	668.747	1.275	**R**
8/10	300	283.0	290	290.0	50	43.0	0.86	35.20	15.40	667.697	1.272	**A**
9/10	350	335.5	340	340.0	50	45.5	0.91	37.52	16.91	666.887	1.269	**T**
10/10	400	387.0	390	390.0	50	47.0	0.94	39.68	18.26	666.077	1.266	**I**
11/10	450	438.0	440	440.0	50	48.0	0.96	42.37	20.38	665.507	1.264	**O**
12/10	500	489.0	490	450.0	50	49.0	0.98					**N**
12/10	700		500	500.0				57.05	27.57	658.017	1.239	**CONSOLIDATION**

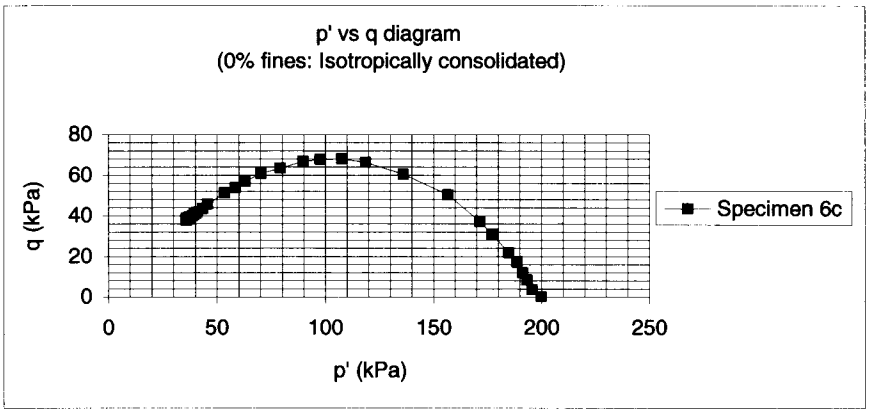
3.) Shear data

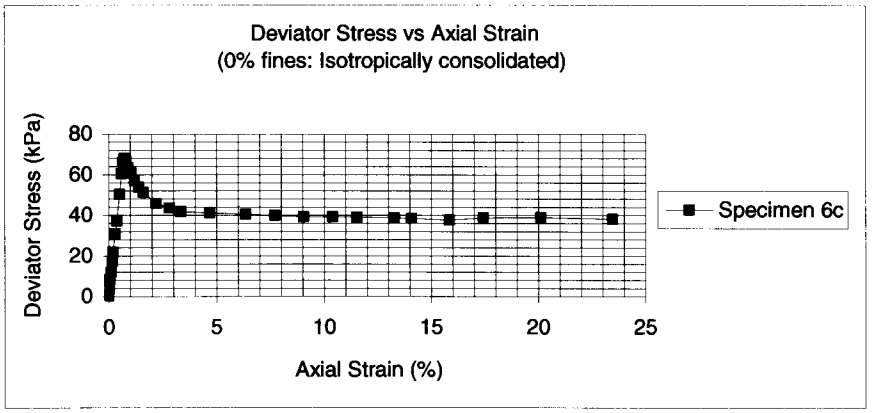
Volume change 1:		Volume change 2:		Sample Vol. change (cm^3)	29.48	B value	0.98
Air Flushing (cm^3)	6.55	Sat/Cons. (cm^3)	50.50	L_{cons} (mm)	149.19	p'consolidation (kPa)	200
Cell Expansion (cm^3)	0.00	Cell Expsn.(cm^3)	27.57	A_{cons} (cm^2)	44.126	Void ratio (e_1)	1.239

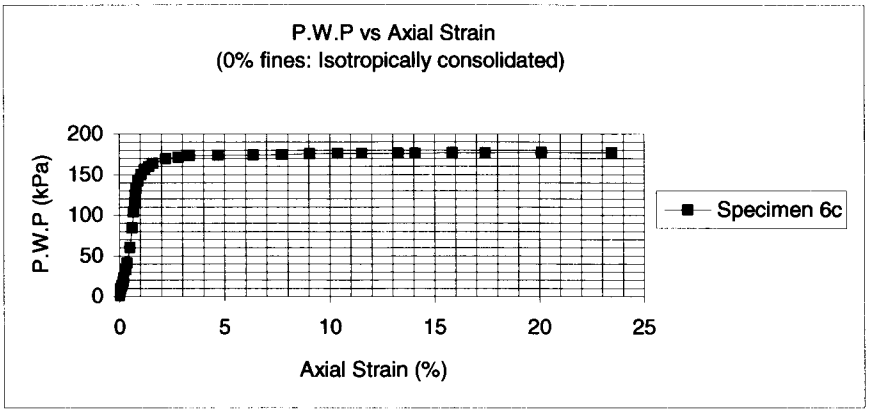
Proof ring properties		Strain gauge properties	
Proof ring No.	5153	1 strain division (mm)	0.01
Proof ring factor (dN/div)	7.512		

Strain Gauge (divs)	Axial Strain	Axial Strain (%)	Change Prf. ring (divs)	Change P.W.P (kPa)	q (Uncortd) (kPa)	Membrn. Corrctn. (kPa)	q (kPa)	t (kPa)	p' (kPa)	s' (kPa)
0	0.0000	0.0000	0.0	0.0	0.0	0.0	0.0	0.0	200.0	200.0
5	0.0003	0.0335	21.5	5.5	3.7	0.0	3.6	1.8	195.7	196.3
10	0.0007	0.0670	49.8	9.5	8.5	0.0	8.4	4.2	193.3	194.7
15	0.0010	0.1005	70.3	12.5	12.0	0.1	11.9	6.0	191.5	193.5
25	0.0017	0.1676	101.2	17.0	17.2	0.1	17.1	8.6	188.7	191.6
30	0.0020	0.2011	128.9	22.5	21.9	0.1	21.8	10.9	184.8	188.4
45	0.0030	0.3016	182.3	33.0	30.9	0.2	30.8	15.4	177.3	182.4
55	0.0037	0.3687	219.8	41.0	37.3	0.2	37.1	18.5	171.4	177.5
75	0.0050	0.5027	298.5	60.0	50.6	0.3	50.3	25.2	156.8	165.2
90	0.0060	0.6033	358.9	84.0	60.7	0.3	60.4	30.2	136.1	146.2
100	0.0067	0.6703	393.5	103.5	66.5	0.3	66.2	33.1	118.6	129.6
110	0.0074	0.7373	404.5	115.0	68.4	0.4	68.0	34.0	107.7	119.0
115	0.0077	0.7708	403.3	125.0	68.1	0.4	67.7	33.9	97.6	108.9
120	0.0080	0.8044	397.2	132.5	67.1	0.4	66.7	33.3	89.7	100.8
135	0.0090	0.9049	378.5	142.0	63.9	0.5	63.4	31.7	79.1	89.7
155	0.0104	1.0390	363.4	150.0	61.2	0.5	60.7	30.4	70.2	80.4
180	0.0121	1.2065	342.1	156.0	57.5	0.6	56.9	28.5	63.0	72.5
210	0.0141	1.4076	324.7	159.5	54.5	0.7	53.8	26.9	58.4	67.4
240	0.0161	1.6087	310.4	163.5	52.0	0.8	51.2	25.6	53.6	62.1
330	0.0221	2.2120	280.5	169.5	46.7	1.0	45.7	22.8	45.7	53.3
420	0.0282	2.8153	268.9	171.0	44.5	1.0	43.5	21.7	43.5	50.7
500	0.0335	3.3515	259.5	173.0	42.7	1.0	41.7	20.8	40.9	47.8
700	0.0469	4.6921	259.6	173.5	42.1	1.0	41.1	20.6	40.2	47.1
950	0.0637	6.3679	259.7	174.0	41.4	1.0	40.4	20.2	39.5	46.2

Strain Gauge (divs)	Axial Strain	Axial Strain (%)	Change Prf. ring (divs)	Change P.W.P (kPa)	q (Uncortd) (kPa)	Membm. Corrctn. (kPa)	q (kPa)	t (kPa)	p' (kPa)	s' (kPa)
1150	0.0771	7.7085	259.8	174.5	40.8	1.0	39.8	19.9	38.8	45.4
1350	0.0905	9.0491	259.9	175.5	40.2	1.0	39.2	19.6	37.6	44.1
1550	0.1039	10.3897	263.6	176.0	40.2	1.0	39.2	19.6	37.1	43.6
1720	0.1153	11.5292	265.5	176.0	40.0	1.0	39.0	19.5	37.0	43.5
1980	0.1327	13.2720	269.1	176.0	39.7	1.0	38.7	19.4	36.9	43.4
2100	0.1408	14.0763	269.3	176.0	39.4	1.0	38.4	19.2	36.8	43.2
2365	0.1585	15.8526	269.8	176.5	38.6	1.0	37.6	18.8	36.0	42.3
2600	0.1743	17.4278	282.3	176.5	39.7	1.0	38.7	19.3	36.4	42.8
3000	0.2011	20.1090	293.7	177.0	39.9	1.0	38.9	19.5	36.0	42.5
3500	0.2346	23.4605	300.2	177.0	39.1	1.0	38.1	19.1	35.7	42.1







Test	**Case 1: Monotonic Undrained Compression of Isotropically Consolidated Specimens**		
Cell No.	2 (Big)	Fines content (%)	0
Specimen	2d	Specific gravity (g/cm^3)	2.72

1.) Sample physical properties

Wet mass before test (g)	835.393	m.c before test (%)	11.20	Height (mm)	150.00	Volume (cm^3)	681.365
Wet mass after test (g)	911.270	m.c. after test (%)	21.30	Diameter (mm)	76.05		
Dry mass (g)	751.253	Dry density (kg/m^3)	1103	Area (cm^2)	45.424	Void ratio (e_0)	1.467

2.) Saturation/Consolidation

Date	C.P (kPa)	P.W.P bp closed (kPa)	B.P (kPa)	P.W.P bp open (kPa)	Change C.P (kPa)	Change P.W.P (kPa)	B value	Volume Gauge (cm^3)	Cell Expansn (cm^3)	Specimen Volume (cm^3)	Void Ratio	Comments
16/10	0		0	-2.5				0.00	0.00	681.365	1.467	
16/10	11.5		8.3	5.0				7.85	0.00	673.515	1.439	**AIR-FLUSHING**
16/10	50	16.0	40	39.5	38.5	11.0	0.29	22.66	3.12	661.825	1.396	**S**
17/10	100	61.0	90	90.0	50	21.5	0.43	39.33	7.06	649.095	1.350	**A**
18/10	150	120.0	140	140.0	50	30.0	0.60	51.99	9.79	639.165	1.314	**T**
19/10	200	176.0	190	190.0	50	36.0	0.72	60.88	11.63	632.115	1.289	**U**
20/10	250	230.5	240	240.0	50	40.5	0.81	67.54	13.02	626.845	1.270	**R**
21/10	300	282.5	290	290.0	50	42.5	0.85	73.47	14.57	622.465	1.254	**A**
22/10	350	335.0	340	340.0	50	45.0	0.90	77.47	16.03	619.925	1.245	**T**
23/10	400	387.0	390	390.0	50	47.0	0.94	80.06	17.22	618.525	1.239	**I**
24/10	450	438.0	440	440.0	50	48.0	0.96	83.21	19.30	617.455	1.236	**O**
25/10	500	488.5	450	450.0	50	48.5	0.97					**N**
25/10	900		450	450.0				128.57	27.43	580.225	1.101	**CONSOLIDATION**

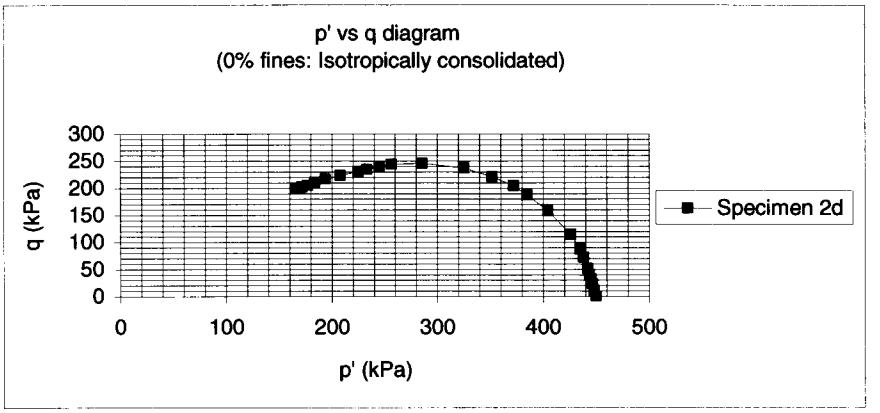
3.) Shear data

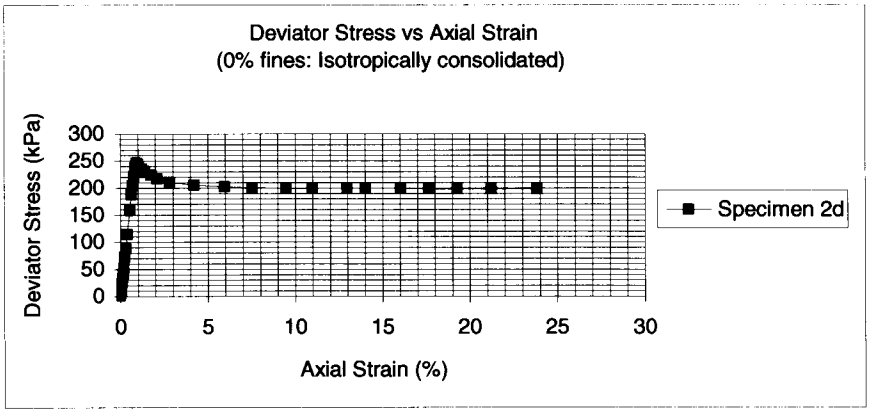
Volume change 1:		Volume change 2:		Sample Vol. change (cm^3)	101.14	B value	0.97
Air Flushing (cm^3)	7.85	Sat/Cons. (cm^3)	120.72	L_{cons} (mm)	142.58	p'consolidation (kPa)	450
Cell Expansion (cm^3)	0.00	Cell Expsn.(cm^3)	27.43	A_{cons} (cm^2)	40.929	Void ratio (e_1)	1.101

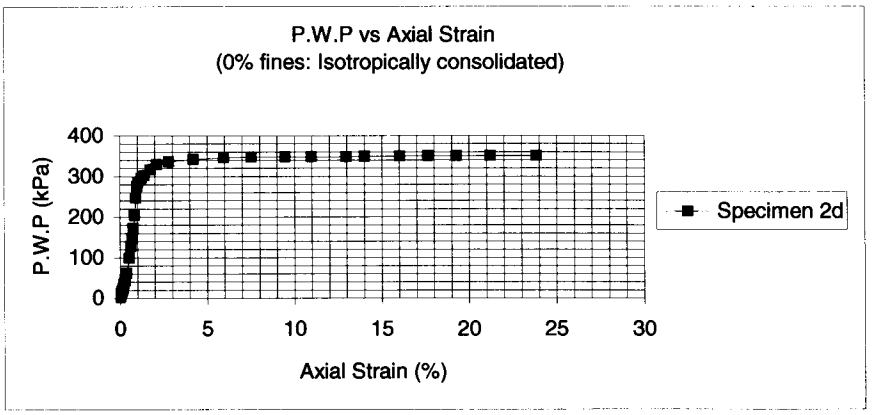
Proof ring properties		Strain gauge properties	
Proof ring No.	4541	1 strain division (mm)	0.01
Proof ring factor (dN/div)	25.77		

Strain Gauge (divs)	Axial Strain	Axial Strain (%)	Change Prf. ring (divs)	Change P.W.P (kPa)	q (Uncortd) (kPa)	Membrn. Corrctn. (kPa)	q (kPa)	t (kPa)	p' (kPa)	s' (kPa)
0	0.0000	0.0000	0.0	0.0	0.0	0.0	0.0	0.0	450.0	450.0
5	0.0004	0.0351	15.2	5.0	9.6	0.0	9.5	4.8	448.2	449.8
10	0.0007	0.0701	36.7	11.0	23.1	0.0	23.1	11.5	446.7	450.5
15	0.0011	0.1052	51.3	15.5	32.3	0.1	32.2	16.1	445.2	450.6
20	0.0014	0.1403	64.7	20.0	40.7	0.1	40.6	20.3	443.5	450.3
25	0.0018	0.1753	82.0	25.0	51.5	0.1	51.5	25.7	442.2	450.7
35	0.0025	0.2455	114.9	36.0	72.2	0.1	72.0	36.0	438.0	450.0
45	0.0032	0.3156	139.8	44.5	87.7	0.2	87.6	43.8	434.7	449.3
55	0.0039	0.3858	182.5	62.0	114.5	0.2	114.3	57.1	426.1	445.1
75	0.0053	0.5260	253.6	98.5	158.8	0.3	158.6	79.3	404.4	430.8
90	0.0063	0.6312	299.7	127.5	187.5	0.3	187.2	93.6	384.9	416.1
100	0.0070	0.7014	327.6	146.0	204.8	0.4	204.5	102.2	372.2	406.2
110	0.0077	0.7715	354.4	172.0	221.4	0.4	221.0	110.5	351.7	388.5
120	0.0084	0.8416	380.1	204.0	237.3	0.4	236.9	118.4	325.0	364.4
130	0.0091	0.9118	395.5	246.5	246.7	0.5	246.3	123.1	285.6	326.6
140	0.0098	0.9819	392.8	275.0	244.9	0.5	244.4	122.2	256.5	297.2
150	0.0105	1.0521	385.6	285.0	240.2	0.5	239.7	119.9	244.9	284.9
175	0.0123	1.2274	378.3	295.0	235.3	0.6	234.6	117.3	233.2	272.3
200	0.0140	1.4027	372.8	302.0	231.4	0.7	230.7	115.4	224.9	263.4
250	0.0175	1.7534	362.4	316.5	224.2	0.9	223.3	111.6	207.9	245.1
300	0.0210	2.1041	353.6	328.5	218.0	1.0	217.0	108.5	193.8	230.0
400	0.0281	2.8055	345.1	336.0	211.2	1.0	210.2	105.1	184.1	219.1
600	0.0421	4.2082	342.2	341.5	206.4	1.0	205.4	102.7	177.0	211.2
850	0.0596	5.9616	342.8	345.5	203.0	1.0	202.0	101.0	171.8	205.5

Strain Gauge (divs)	Axial Strain	Axial Strain (%)	Change Prf. ring (divs)	Change P.W.P (kPa)	q (Uncortd) (kPa)	Membrn. Corrctn. (kPa)	q (kPa)	t (kPa)	p' (kPa)	s' (kPa)
1075	0.0754	7.5397	345.6	347.0	201.2	1.0	200.2	100.1	169.7	203.1
1350	0.0947	9.4685	351.0	348.0	200.1	1.0	199.1	99.5	168.4	201.5
1565	0.1098	10.9764	357.4	348.0	200.3	1.0	199.3	99.7	168.4	201.7
1850	0.1298	12.9753	366.8	348.0	201.0	1.0	200.0	100.0	168.7	202.0
2000	0.1403	14.0274	370.9	349.0	200.8	1.0	199.8	99.9	167.6	200.9
2285	0.1603	16.0263	378.7	349.5	200.2	1.0	199.2	99.6	166.9	200.1
2515	0.1764	17.6395	384.3	350.0	199.3	1.0	198.3	99.1	166.1	199.1
2750	0.1929	19.2877	392.2	350.0	199.3	1.0	198.3	99.2	166.1	199.2
3025	0.2122	21.2164	401.0	350.0	198.9	1.0	197.9	99.0	166.0	199.0
3400	0.2385	23.8466	415.6	350.0	199.3	1.0	198.3	99.1	166.1	199.1







Test	**Case 1: Monotonic Undrained Compression of Isotropically Consolidated Specimens**		
Cell No.	3 (Big)	Fines content (%)	0
Specimen	3c	Specific gravity (g/cm^3)	2.72

1.) Sample physical properties

Wet mass before test (g)	801.306	m.c before test (%)	8.50	Height (mm)	152.55	Volume (cm^3)	691.127
Wet mass after test (g)	890.668	m.c. after test (%)	20.60	Diameter (mm)	75.95		
Dry mass (g)	738.531	Dry density (kg/m^3)	1069	Area (cm^2)	45.305	Void ratio (e_0)	1.545

2.) Saturation/Consolidation

Date	C.P (kPa)	P.W.P bp closed (kPa)	B.P (kPa)	P.W.P bp open (kPa)	Change C.P (kPa)	Change P.W.P (kPa)	B value	Volume Gauge (cm^3)	Cell Expansn (cm^3)	Specimen Volume (cm^3)	Void Ratio	Comments
3/10	0		0	-1.0				0.00	0.00	691.127	1.545	
3/10	8.4		5.6	2.5				8.00	0.00	683.127	1.516	**AIR-FLUSHING**
3/10	50	13.5	40	39.5	41.6	11.0	0.26	24.83	2.51	668.807	1.463	**S**
4/10	100	59.5	90	90.0	50	20.0	0.40	44.46	6.08	652.747	1.404	**A**
5/10	150	119.0	140	140.0	50	29.0	0.58	56.96	8.77	642.937	1.368	**T**
6/10	200	175.0	190	190.0	50	35.0	0.70	65.78	10.65	635.997	1.342	**U**
7/10	250	229.5	240	240.0	50	39.5	0.79	72.35	12.00	630.777	1.323	**R**
8/10	300	282.0	290	290.0	50	42.0	0.84	77.16	13.63	627.597	1.311	**A**
9/10	350	335.0	340	340.0	50	45.0	0.90	81.88	15.06	624.307	1.299	**T**
10/10	400	386.5	390	390.0	50	46.5	0.93	85.26	16.08	621.947	1.291	**I**
11/10	450	437.5	440	440.0	50	47.5	0.95	88.13	18.12	621.117	1.288	**O**
12/10	500	488.5	450	450.0	50	48.5	0.97					**N**
12/10	550		450	450.0				107.65	22.28	605.757	1.231	**CONSOLIDATION**

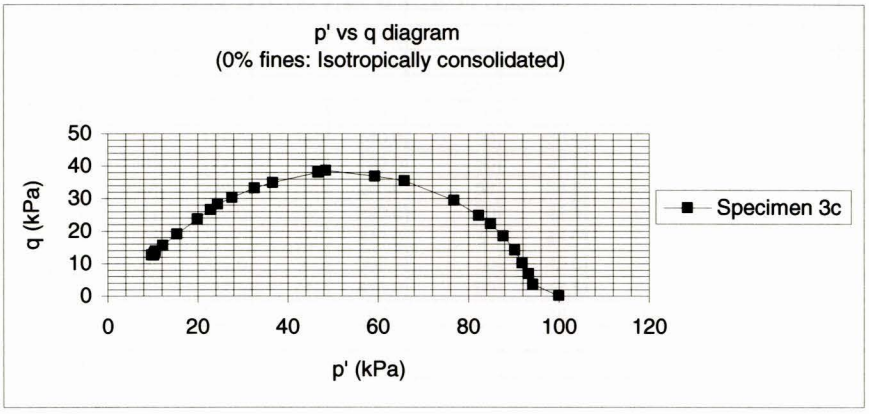
3.) Shear data

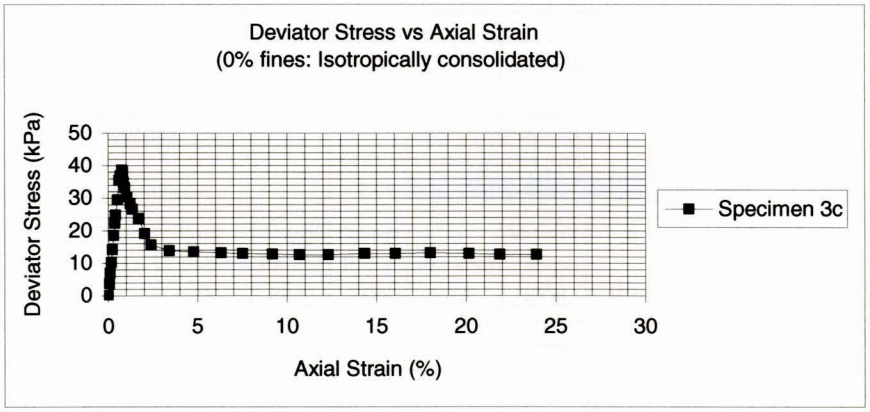
Volume change 1:		Volume change 2:		Sample Vol. change (cm^3)	85.37	B value	0.97
Air Flushing (cm^3)	8.00	Sat/Cons. (cm^3)	99.65	L_{cons} (mm)	146.27	p'consolidation (kPa)	100
Cell Expansion (cm^3)	0.00	Cell Expsn.(cm^3)	22.28	A_{cons} (cm^2)	41.574	Void ratio (e_1)	1.231

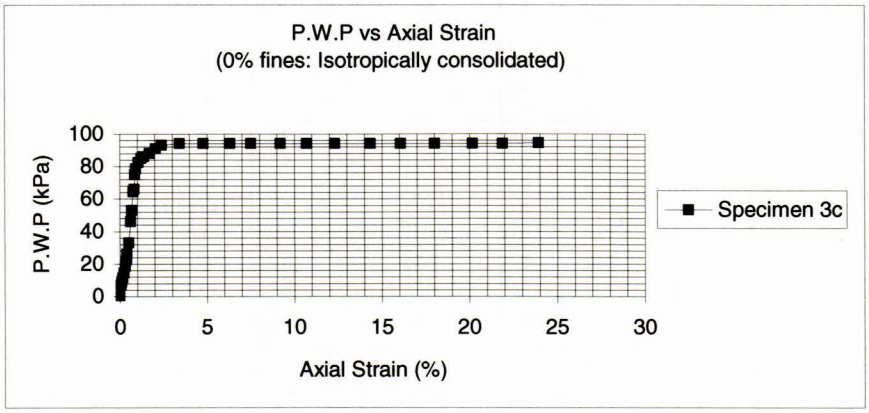
Proof ring properties		Strain gauge properties	
Proof ring No.	1800	1 strain division (mm)	0.01
Proof ring factor (dN/div)	14.846		

Strain Gauge (divs)	Axial Strain	Axial Strain (%)	Change Prf. ring (divs)	Change P.W.P (kPa)	q (Uncortd) (kPa)	Membrn. Corrctn. (kPa)	q (kPa)	t (kPa)	p' (kPa)	s' (kPa)
0	0.0000	0.0000	0.0	0.0	0.0	0.0	0.0	0.0	100.0	100.0
10	0.0007	0.0684	10.3	7.0	3.7	0.0	3.6	1.8	94.2	94.8
15	0.0010	0.1026	19.4	9.0	6.9	0.1	6.9	3.4	93.3	94.4
25	0.0017	0.1709	28.8	11.5	10.3	0.1	10.2	5.1	91.9	93.6
35	0.0024	0.2393	40.1	14.5	14.3	0.1	14.2	7.1	90.2	92.6
45	0.0031	0.3077	52.3	18.5	18.6	0.2	18.5	9.2	87.7	90.7
55	0.0038	0.3760	63.0	22.5	22.4	0.2	22.2	11.1	84.9	88.6
60	0.0041	0.4102	70.4	26.0	25.0	0.2	24.8	12.4	82.3	86.4
75	0.0051	0.5128	83.7	33.0	29.7	0.3	29.5	14.7	76.8	81.7
90	0.0062	0.6153	100.9	46.0	35.8	0.3	35.5	17.8	65.8	71.8
100	0.0068	0.6837	104.8	53.0	37.2	0.3	36.8	18.4	59.3	65.4
112	0.0077	0.7657	110.0	64.5	39.0	0.4	38.6	19.3	48.4	54.8
120	0.0082	0.8204	108.7	66.0	38.5	0.4	38.1	19.0	46.7	53.0
125	0.0085	0.8546	99.7	75.0	35.3	0.4	34.9	17.4	36.6	42.4
135	0.0092	0.9230	95.2	78.5	33.7	0.5	33.2	16.6	32.6	38.1
155	0.0106	1.0597	87.3	82.5	30.8	0.5	30.3	15.2	27.6	32.7
180	0.0123	1.2306	81.8	85.0	28.9	0.6	28.2	14.1	24.4	29.1
200	0.0137	1.3673	77.4	86.0	27.3	0.7	26.6	13.3	22.9	27.3
250	0.0171	1.7092	69.9	88.0	24.5	0.9	23.7	11.8	19.9	23.8
300	0.0205	2.0510	57.5	91.0	20.1	1.0	19.1	9.6	15.4	18.6
350	0.0239	2.3929	47.8	93.0	16.7	1.0	15.7	7.8	12.2	14.8
500	0.0342	3.4184	43.0	94.0	14.8	1.0	13.8	6.9	10.6	12.9
700	0.0479	4.7857	42.6	94.0	14.5	1.0	13.5	6.7	10.5	12.7
925	0.0632	6.3240	42.4	94.0	14.2	1.0	13.2	6.6	10.4	12.6

Strain Gauge (divs)	Axial Strain	Axial Strain (%)	Change Prf. ring (divs)	Change P.W.P (kPa)	q (Uncortd) (kPa)	Membrn. Corrctn. (kPa)	q (kPa)	t (kPa)	p' (kPa)	s' (kPa)
1100	0.0752	7.5204	42.1	94.0	13.9	1.0	12.9	6.5	10.3	12.5
1345	0.0920	9.1954	42.5	94.0	13.8	1.0	12.8	6.4	10.3	12.4
1565	0.1070	10.6995	42.6	94.0	13.6	1.0	12.6	6.3	10.2	12.3
1800	0.1231	12.3061	43.2	94.0	13.5	1.0	12.5	6.3	10.2	12.3
2100	0.1436	14.3571	45.7	94.0	14.0	1.0	13.0	6.5	10.3	12.5
2350	0.1607	16.0663	46.6	94.0	14.0	1.0	13.0	6.5	10.3	12.5
2635	0.1801	18.0148	48.4	94.0	14.2	1.0	13.2	6.6	10.4	12.6
2950	0.2017	20.1683	48.9	94.0	13.9	1.0	12.9	6.5	10.3	12.5
3200	0.2188	21.8775	49.0	94.0	13.7	1.0	12.7	6.3	10.2	12.3
3500	0.2393	23.9285	50.4	94.5	13.7	1.0	12.7	6.3	9.7	11.8







Test	**Case 1: Monotonic Undrained Compression of Isotropically Consolidated Specimens**		
Cell No.	6 (Small)	Fines content (%)	0
Specimen	6d	Specific gravity (g/cm^3)	2.72

1.) Sample physical properties

Wet mass before test (g)	114.123	m.c before test (%)	10.80	Height (mm)	76.45	Volume (cm^3)	86.931
Wet mass after test (g)	128.337	m.c. after test (%)	24.60	Diameter (mm)	38.05		
Dry mass (g)	102.999	Dry density (kg/m^3)	1185	Area (cm^2)	11.371	Void ratio (e_0)	1.296

2.) Saturation/Consolidation

Date	C.P (kPa)	P.W.P bp closed (kPa)	B.P (kPa)	P.W.P bp open (kPa)	Change C.P (kPa)	Change P.W.P (kPa)	B value	Volume Gauge (cm^3)	Cell Expansn (cm^3)	Specimen Volume (cm^3)	Void Ratio	Comments
15/11	0		0	-1.0				0.00	0.00	86.931	1.296	
15/11	7.5		5.1	3.0				2.05	0.00	84.881	1.242	**AIR-FLUSHING**
15/11	50	18.5	40	39.5	42.5	15.5	0.36	6.35	3.12	83.701	1.210	**S**
16/11	100	65.0	90	89.5	50	25.5	0.51	9.11	4.89	82.711	1.184	**A**
17/11	150	119.5	140	140.0	50	30.0	0.60	11.89	7.14	82.181	1.170	**T**
18/11	200	177.0	190	190.0	50	37.0	0.74	13.68	8.53	81.781	1.160	**U**
19/11	250	229.5	240	240.0	50	39.5	0.79	14.99	9.63	81.571	1.154	**R**
20/11	300	282.0	290	290.0	50	42.0	0.84	16.14	10.61	81.401	1.150	**A**
21/11	350	334.0	340	340.0	50	44.0	0.88	17.39	11.67	81.211	1.145	**T**
22/11	400	385.5	390	390.0	50	45.5	0.91	18.50	12.65	81.081	1.141	**I**
23/11	450	437.5	440	440.0	50	47.5	0.95	19.71	13.79	81.011	1.139	**O**
24/11	500	488.5	450	450.0	50	48.5	0.97					**N**
24/11	500		450	450.0				21.58	15.58	80.931	1.137	**CONSOLIDATION**

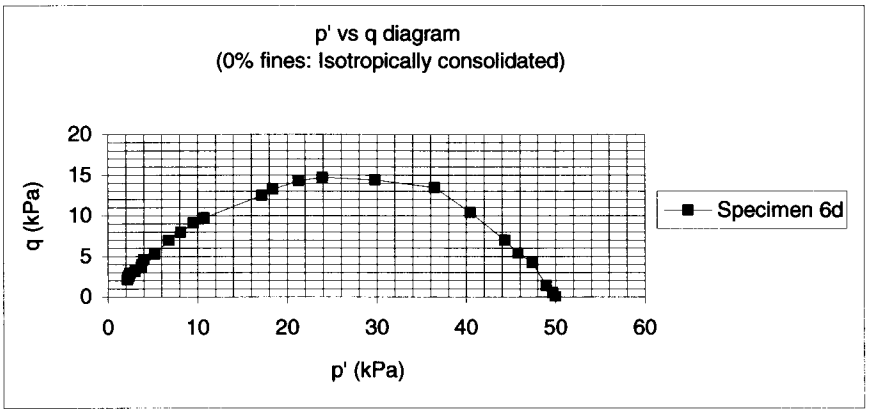
3.) Shear data

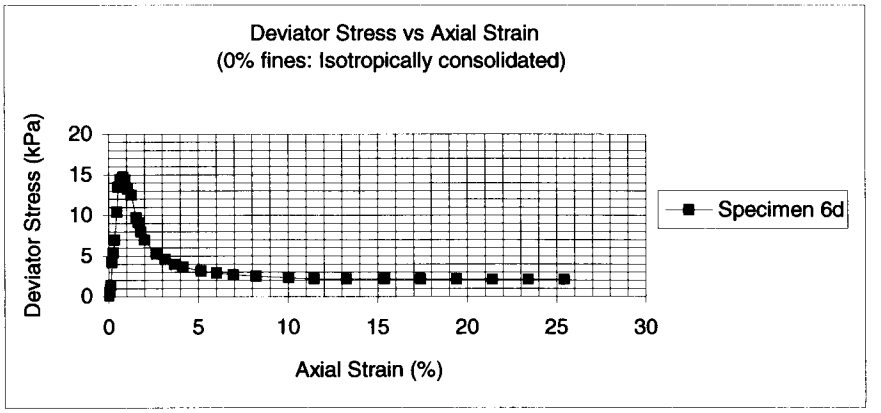
Volume change 1:		Volume change 2:		Sample Vol. change (cm^3)	6.00	B value	0.97
Air Flushing (cm^3)	2.05	Sat/Cons. (cm^3)	19.53	L_{cons} (mm)	74.69	p'consolidation (kPa)	50
Cell Expansion (cm^3)	0.00	Cell Expsn.(cm^3)	15.58	A_{cons} (cm^2)	10.848	Void ratio (e_1)	1.137

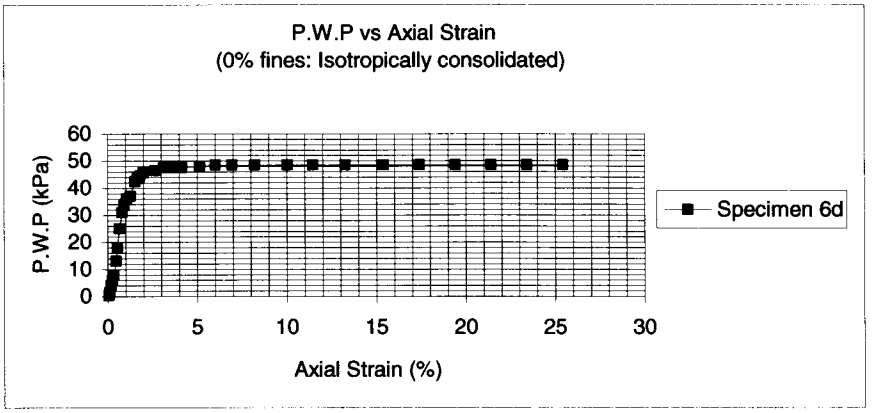
Proof ring properties		Strain gauge properties	
Proof ring No.	5153	1 strain division (mm)	0.01
Proof ring factor (dN/div)	7.512		

Strain Gauge (divs)	Axial Strain	Axial Strain (%)	Change Prf. ring (divs)	Change P.W.P (kPa)	q (Uncortd) (kPa)	Membrn. Corrctn. (kPa)	q (kPa)	t (kPa)	p' (kPa)	s' (kPa)
0	0.0000	0.0000	0.0	0.0	0.0	0.0	0.0	0.0	50.0	50.0
5	0.0007	0.0669	0.8	0.5	0.6	0.0	0.5	0.3	49.7	49.8
10	0.0013	0.1339	2.1	1.5	1.5	0.1	1.4	0.7	49.0	49.2
15	0.0020	0.2008	6.2	4.0	4.3	0.1	4.2	2.1	47.4	48.1
20	0.0027	0.2678	8.0	6.0	5.5	0.1	5.4	2.7	45.8	46.7
25	0.0033	0.3347	10.3	8.0	7.1	0.2	6.9	3.5	44.3	45.5
35	0.0047	0.4686	15.4	13.0	10.6	0.2	10.4	5.2	40.5	42.2
40	0.0054	0.5355	19.9	18.0	13.7	0.3	13.4	6.7	36.5	38.7
50	0.0067	0.6694	21.4	25.0	14.7	0.3	14.4	7.2	29.8	32.2
60	0.0080	0.8033	22.0	31.0	15.1	0.4	14.7	7.4	23.9	26.4
70	0.0094	0.9372	21.5	33.5	14.7	0.5	14.3	7.1	21.3	23.6
80	0.0107	1.0711	20.1	36.0	13.8	0.5	13.2	6.6	18.4	20.6
95	0.0127	1.2719	19.2	37.0	13.1	0.6	12.5	6.2	17.2	19.2
115	0.0154	1.5397	15.4	42.5	10.5	0.8	9.7	4.9	10.7	12.4
125	0.0167	1.6736	14.6	43.5	9.9	0.8	9.1	4.6	9.5	11.1
135	0.0181	1.8074	13.0	44.5	8.8	0.9	7.9	4.0	8.1	9.5
150	0.0201	2.0083	11.7	45.5	7.9	1.0	6.9	3.5	6.8	8.0
200	0.0268	2.6777	9.2	46.5	6.2	1.0	5.2	2.6	5.2	6.1
235	0.0315	3.1463	8.3	47.5	5.6	1.0	4.6	2.3	4.0	4.8
275	0.0368	3.6818	7.4	47.5	4.9	1.0	3.9	2.0	3.8	4.5
310	0.0415	4.1504	7.0	47.5	4.6	1.0	3.6	1.8	3.7	4.3
385	0.0515	5.1546	6.3	48.0	4.1	1.0	3.1	1.6	3.0	3.6
450	0.0602	6.0248	6.0	48.5	3.9	1.0	2.9	1.5	2.5	3.0
520	0.0696	6.9620	5.7	48.5	3.7	1.0	2.7	1.3	2.4	2.8

Strain Gauge (divs)	Axial Strain	Axial Strain (%)	Change Prf. ring (divs)	Change P.W.P (kPa)	q (Uncortd) (kPa)	Membrn. Corrctn. (kPa)	q (kPa)	t (kPa)	p' (kPa)	s' (kPa)
615	0.0823	8.2339	5.5	48.5	3.5	1.0	2.5	1.2	2.3	2.7
750	0.1004	10.0414	5.3	48.5	3.3	1.0	2.3	1.2	2.3	2.7
855	0.1145	11.4471	5.2	48.5	3.2	1.0	2.2	1.1	2.2	2.6
990	0.1325	13.2546	5.2	48.5	3.1	1.0	2.1	1.1	2.2	2.6
1150	0.1540	15.3967	5.4	48.5	3.2	1.0	2.2	1.1	2.2	2.6
1300	0.1741	17.4050	5.5	48.5	3.1	1.0	2.1	1.1	2.2	2.6
1450	0.1941	19.4133	5.6	48.5	3.1	1.0	2.1	1.1	2.2	2.6
1600	0.2142	21.4215	5.7	48.5	3.1	1.0	2.1	1.1	2.2	2.6
1750	0.2343	23.4298	5.8	48.5	3.1	1.0	2.1	1.0	2.2	2.5
1900	0.2544	25.4381	6.0	48.5	3.1	1.0	2.1	1.0	2.2	2.5







Test	Case 1: Monotonic Undrained Compression of Isotropically Consolidated Specimens		
Cell No.	2 (Small)	Fines content (%)	0
Specimen	2e	Specific gravity (g/cm^3)	2.72

1.) Sample physical properties

Wet mass before test (g)	104.367	m.c before test (%)	9.65	Height (mm)	76.55	Volume (cm^3)	86.360
Wet mass after test (g)	118.644	m.c. after test (%)	24.65	Diameter (mm)	37.90		
Dry mass (g)	95.182	Dry density (kg/m^3)	1102	Area (cm^2)	11.282	Void ratio (e_0)	1.468

2.) Saturation/Consolidation

Date	C.P (kPa)	P.W.P bp closed (kPa)	B.P (kPa)	P.W.P bp open (kPa)	Change C.P (kPa)	Change P.W.P (kPa)	B value	Volume Gauge (cm^3)	Cell Expansn (cm^3)	Specimen Volume (cm^3)	Void Ratio	Comments
16/10	0		0	-2.0				0.00	0.00	86.360	1.468	
16/10	7.3		5.1	3.0				1.85	0.00	84.510	1.415	**AIR-FLUSHING**
16/10	50	13.0	40	39.5	42.7	10.0	0.23	5.57	2.02	82.810	1.366	**S**
17/10	100	60.0	90	90.0	50	20.5	0.41	9.12	4.04	81.280	1.323	**A**
18/10	150	119.0	140	140.0	50	29.0	0.58	12.51	6.24	80.090	1.289	**T**
19/10	200	175.5	190	190.0	50	35.5	0.71	15.25	7.67	78.780	1.251	**U**
20/10	250	230.0	240	240.0	50	40.0	0.80	17.35	8.73	77.740	1.222	**R**
21/10	300	282.5	290	290.0	50	42.5	0.85	19.27	9.79	76.880	1.197	**A**
22/10	350	335.0	340	340.0	50	45.0	0.90	20.54	10.81	76.630	1.190	**T**
23/10	400	387.0	390	390.0	50	47.0	0.94	21.55	11.63	76.440	1.184	**I**
24/10	450	438.0	440	440.0	50	48.0	0.96	22.78	12.73	76.310	1.181	**O**
25/10	500	488.5	450	450.0	50	48.5	0.97					**N**
25/10	750		450	450.0				28.67	17.42	75.110	1.146	**CONSOLIDATION**

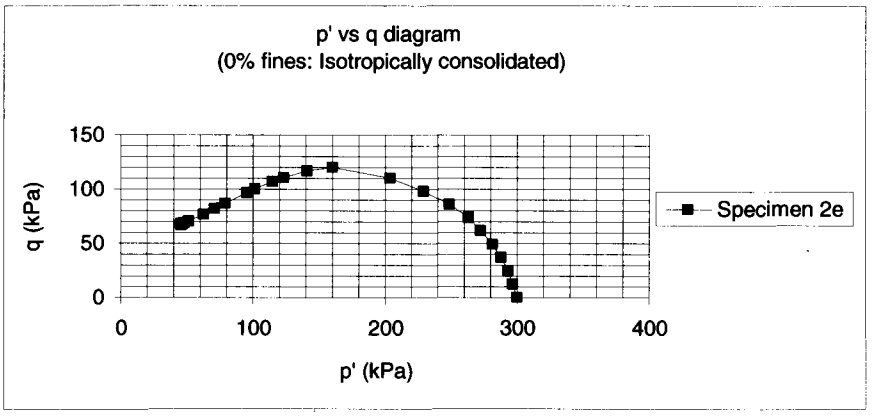
3.) Shear data

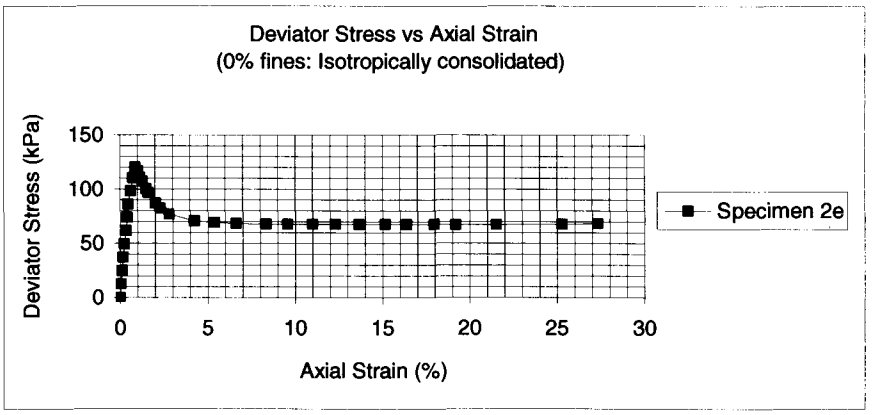
Volume change 1:		Volume change 2:		Sample Vol. change (cm^3)	11.25	B value	0.97
Air Flushing (cm^3)	1.85	Sat/Cons. (cm^3)	26.82	L_{cons} (mm)	73.23	p'consolidation (kPa)	300
Cell Expansion (cm^3)	0.00	Cell Expsn.(cm^3)	17.42	A_{cons} (cm^2)	10.302	Void ratio (e_1)	1.146

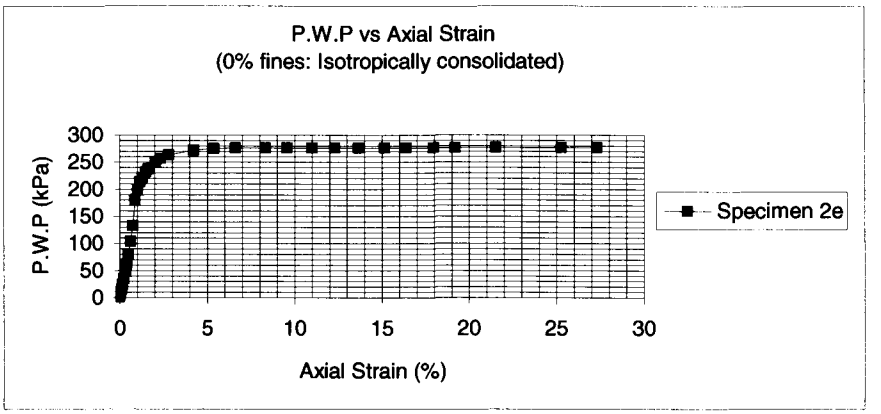
Proof ring properties		Strain gauge properties	
Proof ring No.	1800	1 strain division (mm)	0.01
Proof ring factor (dN/div)	14.846		

Strain Gauge (divs)	Axial Strain	Axial Strain (%)	Change Prf. ring (divs)	Change P.W.P (kPa)	q (Uncortd) (kPa)	Membrn. Corrctn. (kPa)	q (kPa)	t (kPa)	p' (kPa)	s' (kPa)
0	0.0000	0.0000	0.0	0.0	0.0	0.0	0.0	0.0	300.0	300.0
3	0.0004	0.0410	8.6	7.5	12.4	0.0	12.4	6.2	296.6	298.7
8	0.0011	0.1093	17.2	15.0	24.8	0.1	24.7	12.4	293.2	297.4
12	0.0016	0.1639	25.8	24.5	37.1	0.1	37.0	18.5	287.8	294.0
18	0.0025	0.2458	34.4	35.0	49.5	0.1	49.3	24.7	281.4	289.7
25	0.0034	0.3414	43.0	48.0	61.8	0.2	61.6	30.8	272.5	282.8
30	0.0041	0.4097	51.6	61.5	74.1	0.2	73.9	36.9	263.1	275.4
35	0.0048	0.4780	60.2	80.0	86.3	0.2	86.1	43.1	248.7	263.1
45	0.0061	0.6145	68.8	103.5	98.5	0.3	98.2	49.1	229.2	245.6
55	0.0075	0.7511	77.4	133.0	110.7	0.4	110.3	55.2	203.8	222.2
65	0.0089	0.8877	84.3	180.0	120.4	0.4	120.0	60.0	160.0	180.0
75	0.0102	1.0242	82.2	198.0	117.2	0.5	116.7	58.4	140.9	160.4
85	0.0116	1.1608	78.0	213.5	111.1	0.6	110.5	55.3	123.3	141.8
95	0.0130	1.2974	75.6	221.0	107.5	0.6	106.9	53.4	114.6	132.4
110	0.0150	1.5022	71.1	232.0	100.9	0.8	100.2	50.1	101.4	118.1
120	0.0164	1.6388	68.8	237.0	97.5	0.8	96.7	48.4	95.2	111.4
150	0.0205	2.0485	62.2	250.0	87.8	1.0	86.8	43.4	78.9	93.4
170	0.0232	2.3216	59.0	256.5	83.1	1.0	82.1	41.0	70.9	84.5
205	0.0280	2.7996	55.5	263.0	77.7	1.0	76.7	38.4	62.6	75.4
310	0.0423	4.2335	51.9	272.0	71.6	1.0	70.6	35.3	51.5	63.3
395	0.0539	5.3943	51.3	275.0	69.9	1.0	68.9	34.5	48.0	59.5
485	0.0662	6.6233	51.5	276.0	69.3	1.0	68.3	34.2	46.8	58.2
610	0.0833	8.3304	52.0	276.0	68.7	1.0	67.7	33.8	46.6	57.8
700	0.0956	9.5594	52.7	276.5	68.7	1.0	67.7	33.8	46.1	57.3

Strain Gauge (divs)	Axial Strain	Axial Strain (%)	Change Prf. ring (divs)	Change P.W.P (kPa)	q (Uncortd) (kPa)	Membrn. Corrctn. (kPa)	q (kPa)	t (kPa)	p' (kPa)	s' (kPa)
805	0.1099	10.9934	53.4	276.5	68.5	1.0	67.5	33.7	46.0	57.2
900	0.1229	12.2907	54.2	276.5	68.5	1.0	67.5	33.8	46.0	57.3
1000	0.1366	13.6564	55.0	276.5	68.4	1.0	67.4	33.7	46.0	57.2
1110	0.1516	15.1586	56.0	276.5	68.5	1.0	67.5	33.7	46.0	57.2
1200	0.1639	16.3876	56.7	276.5	68.3	1.0	67.3	33.7	45.9	57.2
1315	0.1796	17.9581	57.8	276.5	68.3	1.0	67.3	33.7	45.9	57.2
1405	0.1919	19.1872	58.5	276.5	68.1	1.0	67.1	33.6	45.9	57.1
1575	0.2151	21.5088	60.5	277.0	68.4	1.0	67.4	33.7	45.5	56.7
1850	0.2526	25.2643	63.7	277.0	68.6	1.0	67.6	33.8	45.5	56.8
2000	0.2731	27.3127	66.0	277.0	69.1	1.0	68.1	34.1	45.7	57.1







Test	Case 1: Monotonic Undrained Compression of Isotropically Consolidated Specimens		
Cell No.	3 (Big)	Fines content (%)	0
Specimen	3e	Specific gravity (g/cm^3)	2.72

1.) Sample physical properties

Wet mass before test (g)	853.877	m.c before test (%)	10.05	Height (mm)	152.85	Volume (cm^3)	690.663
Wet mass after test (g)	931.467	m.c. after test (%)	20.05	Diameter (mm)	75.85		
Dry mass (g)	775.899	Dry density (kg/m^3)	1123	Area (cm^2)	45.186	Void ratio (e_0)	1.421

2.) Saturation/Consolidation

Date	C.P (kPa)	P.W.P bp closed (kPa)	B.P (kPa)	P.W.P bp open (kPa)	Change C.P (kPa)	Change P.W.P (kPa)	B value	Volume Gauge (cm^3)	Cell Expansn (cm^3)	Specimen Volume (cm^3)	Void Ratio	Comments
1/11	0		0	-0.5				0.00	0.00	690.663	1.421	
1/11	10.2		8.5	6.5				7.65	0.00	683.013	1.394	**AIR-FLUSHING**
1/11	50	16.5	40	39.5	39.8	10.0	0.25	24.37	2.51	668.803	1.345	**S**
2/11	100	61.5	90	90.0	50	22.0	0.44	45.31	6.08	651.433	1.284	**A**
3/11	150	119.5	140	140.0	50	29.5	0.59	58.21	8.77	641.223	1.248	**T**
4/11	200	176.0	190	190.0	50	36.0	0.72	66.17	10.65	635.143	1.227	**U**
5/11	250	230.5	240	240.0	50	40.5	0.81	72.62	12.00	630.043	1.209	**R**
6/11	300	283.0	290	290.0	50	43.0	0.86	77.40	13.63	626.893	1.198	**A**
7/11	350	335.5	340	340.0	50	45.5	0.91	81.78	15.06	623.943	1.187	**T**
8/11	400	387.0	390	390.0	50	47.0	0.94	84.35	16.08	622.393	1.182	**I**
9/11	450	438.0	440	440.0	50	48.0	0.96	87.27	18.12	621.513	1.179	**O**
10/11	500	489.0	450	450.0	50	49.0	0.98					**N**
10/11	800		450	450.0				118.27	24.18	596.573	1.091	**CONSOLIDATION**

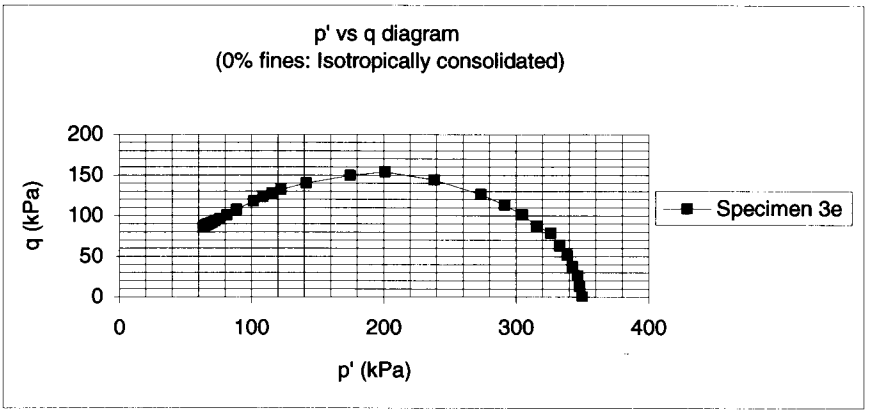
3.) Shear data

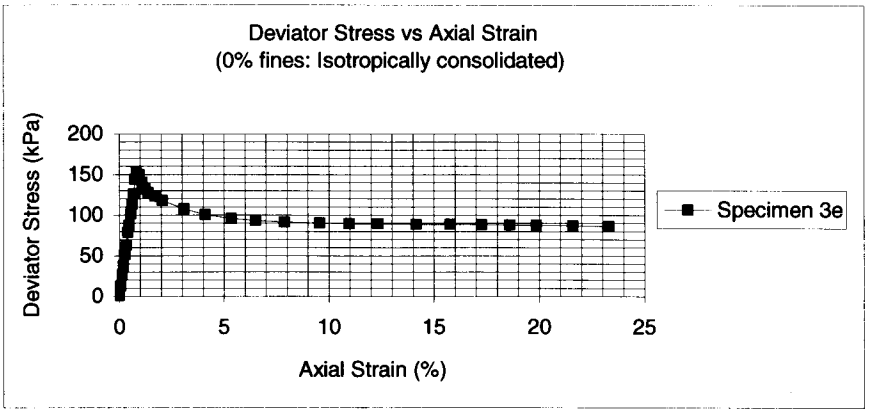
Volume change 1:		Volume change 2:		Sample Vol. change (cm^3)	94.09	B value	0.98
Air Flushing (cm^3)	7.65	Sat/Cons. (cm^3)	110.62	L_{cons} (mm)	145.91	p'consolidation (kPa)	350
Cell Expansion (cm^3)	0.00	Cell Expsn.(cm^3)	24.18	A_{cons} (cm^2)	41.082	Void ratio (e_1)	1.091

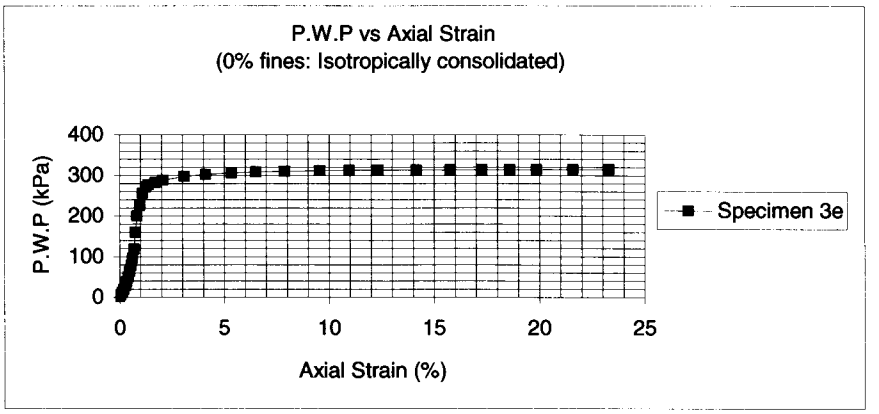
Proof ring properties		Strain gauge properties	
Proof ring No.	1800	1 strain division (mm)	0.01
Proof ring factor (dN/div)	14.846		

Strain Gauge (divs)	Axial Strain	Axial Strain (%)	Change Prf. ring (divs)	Change P.W.P (kPa)	q (Uncortd) (kPa)	Membrn. Corrctn. (kPa)	q (kPa)	t (kPa)	p' (kPa)	s' (kPa)
0	0.0000	0.0000	0.0	0.0	0.0	0.0	0.0	0.0	350.0	350.0
10	0.0007	0.0685	34.7	6.0	12.5	0.0	12.5	6.2	348.2	350.2
20	0.0014	0.1371	72.3	12.0	26.1	0.1	26.0	13.0	346.7	351.0
30	0.0021	0.2056	104.9	20.0	37.8	0.1	37.7	18.9	342.6	348.9
40	0.0027	0.2741	143.2	28.5	51.6	0.1	51.5	25.7	338.7	347.2
50	0.0034	0.3427	174.9	38.0	63.0	0.2	62.8	31.4	332.9	343.4
60	0.0041	0.4112	218.7	50.0	78.7	0.2	78.5	39.3	326.2	339.3
70	0.0048	0.4798	243.3	63.5	87.5	0.2	87.3	43.6	315.6	330.1
80	0.0055	0.5483	281.8	78.5	101.3	0.3	101.0	50.5	305.2	322.0
90	0.0062	0.6168	315.6	96.0	113.3	0.3	113.0	56.5	291.7	310.5
100	0.0069	0.6854	352.4	118.5	126.5	0.3	126.1	63.1	273.5	294.6
110	0.0075	0.7539	402.6	159.5	144.4	0.4	144.0	72.0	238.5	262.5
120	0.0082	0.8224	430.4	200.0	154.3	0.4	153.8	76.9	201.3	226.9
140	0.0096	0.9595	418.9	225.0	149.9	0.5	149.4	74.7	174.8	199.7
160	0.0110	1.0966	393.5	255.0	140.6	0.5	140.1	70.0	141.7	165.0
180	0.0123	1.2336	372.1	271.5	132.8	0.6	132.2	66.1	122.6	144.6
200	0.0137	1.3707	360.6	277.0	128.5	0.7	127.8	63.9	115.6	136.9
250	0.0171	1.7134	348.8	282.0	123.9	0.9	123.0	61.5	109.0	129.5
300	0.0206	2.0561	335.5	287.5	118.7	1.0	117.7	58.9	101.7	121.4
450	0.0308	3.0841	309.9	297.0	108.5	1.0	107.5	53.8	88.8	106.8
600	0.0411	4.1122	292.2	302.0	101.3	1.0	100.3	50.1	81.4	98.1
780	0.0535	5.3458	283.0	306.0	96.8	1.0	95.8	47.9	75.9	91.9
950	0.0651	6.5109	279.1	308.5	94.3	1.0	93.3	46.6	72.6	88.1
1150	0.0788	7.8816	277.2	310.0	92.3	1.0	91.3	45.6	70.4	85.6

Strain Gauge (divs)	Axial Strain	Axial Strain (%)	Change Prf. ring (divs)	Change P.W.P (kPa)	q (Uncortd) (kPa)	Membrn. Corrctn. (kPa)	q (kPa)	t (kPa)	p' (kPa)	s' (kPa)
1395	0.0956	9.5608	279.4	311.5	91.3	1.0	90.3	45.2	68.6	83.7
1600	0.1097	10.9657	280.6	312.0	90.3	1.0	89.3	44.6	67.8	82.6
1800	0.1234	12.3365	285.2	313.0	90.3	1.0	89.3	44.7	66.8	81.7
2065	0.1415	14.1527	288.9	313.0	89.6	1.0	88.6	44.3	66.5	81.3
2300	0.1576	15.7632	294.6	313.0	89.7	1.0	88.7	44.3	66.6	81.3
2520	0.1727	17.2710	298.5	314.0	89.2	1.0	88.2	44.1	65.4	80.1
2715	0.1861	18.6075	302.0	314.0	88.8	1.0	87.8	43.9	65.3	79.9
2900	0.1988	19.8754	304.6	314.0	88.2	1.0	87.2	43.6	65.1	79.6
3150	0.2159	21.5888	309.9	314.5	87.8	1.0	86.8	43.4	64.4	78.9
3400	0.2330	23.3022	315.0	315.0	87.3	1.0	86.3	43.2	63.8	78.2







Test	**Case 1: Monotonic Undrained Compression of Isotropically Consolidated Specimens**		
Cell No.	3 (Small)	Fines content (%)	0
Specimen	3d	Specific gravity (g/cm^3)	2.72

1.) Sample physical properties

Wet mass before test (g)	104.067	m.c before test (%)	9.85	Height (mm)	76.15	Volume (cm^3)	86.590
Wet mass after test (g)	114.204	m.c. after test (%)	20.55	Diameter (mm)	38.05		
Dry mass (g)	94.736	Dry density (kg/m^3)	1094	Area (cm^2)	11.371	Void ratio (e_0)	1.486

2.) Saturation/Consolidation

Date	C.P (kPa)	P.W.P bp closed (kPa)	B.P (kPa)	P.W.P bp open (kPa)	Change C.P (kPa)	Change P.W.P (kPa)	B value	Volume Gauge (cm^3)	Cell Expansn (cm^3)	Specimen Volume (cm^3)	Void Ratio	Comments
16/10	0		0	-0.5				0.00	0.00	86.590	1.486	
16/10	7.3		5.5	3.5				2.15	0.00	84.440	1.424	**AIR-FLUSHING**
16/10	50	17.5	40	38.5	42.7	14.0	0.33	7.63	3.81	82.770	1.376	**S**
17/10	100	65.5	90	89.5	50	27.0	0.54	11.57	5.89	80.910	1.323	**A**
18/10	150	119.5	140	140.0	50	30.0	0.60	15.20	8.17	79.560	1.284	**T**
19/10	200	175.5	190	190.0	50	35.5	0.71	17.52	9.52	78.590	1.256	**U**
20/10	250	230.0	240	240.0	50	40.0	0.80	19.88	10.66	77.370	1.221	**R**
21/10	300	283.5	290	290.0	50	43.5	0.87	21.51	11.56	76.640	1.200	**A**
22/10	350	335.5	340	340.0	50	45.5	0.91	22.98	12.66	76.270	1.190	**T**
23/10	400	387.0	390	390.0	50	47.0	0.94	24.29	13.80	76.100	1.185	**I**
24/10	450	438.0	440	440.0	50	48.0	0.96	25.61	14.98	75.960	1.181	**O**
25/10	500	489.0	440	440.0	50	49.0	0.98					**N**
25/10	850		450	450.0				34.87	21.63	73.350	1.106	**CONSOLIDATION**

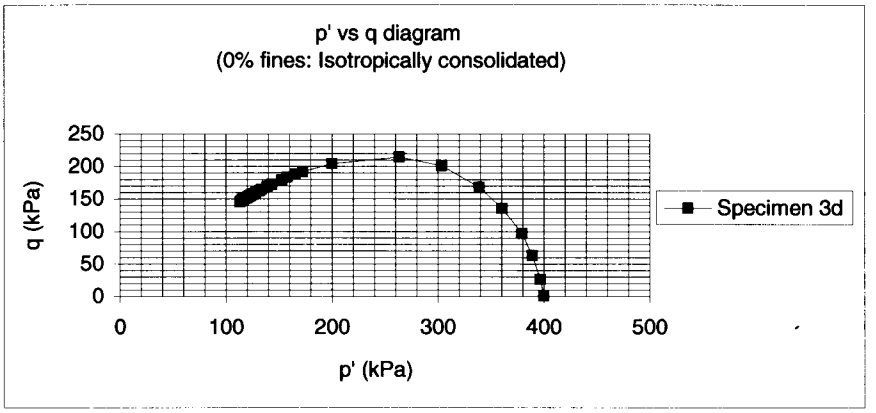
3.) Shear data

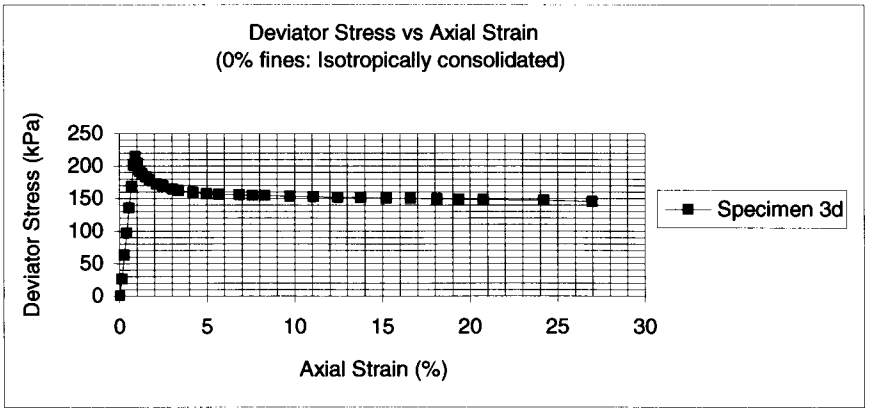
Volume change 1:		Volume change 2:		Sample Vol. change (cm^3)	13.24	B value	0.98
Air Flushing (cm^3)	2.15	Sat/Cons. (cm^3)	32.72	L_{cons} (mm)	72.27	p'consolidation (kPa)	400
Cell Expansion (cm^3)	0.00	Cell Expsn.(cm^3)	21.63	A_{cons} (cm^2)	10.212	Void ratio (e_1)	1.106

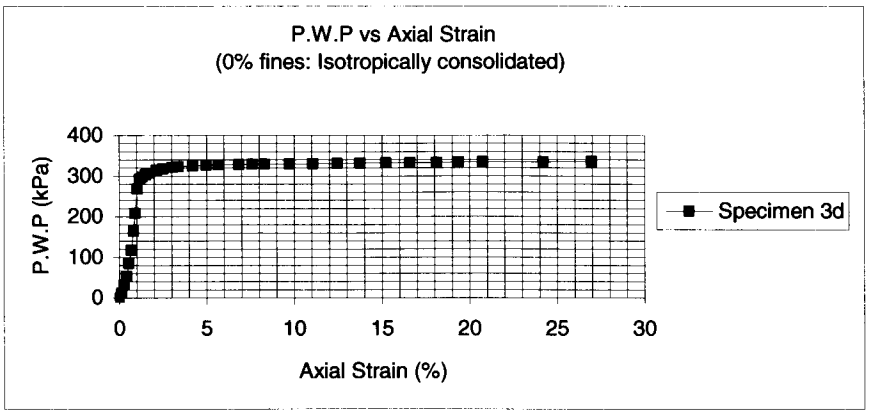
Proof ring properties		Strain gauge properties	
Proof ring No.	5153	1 strain division (mm)	0.01
Proof ring factor (dN/div)	7.512		

Strain Gauge (divs)	Axial Strain	Axial Strain (%)	Change Prf. ring (divs)	Change P.W.P (kPa)	q (Uncortd) (kPa)	Membrn. Corrctn. (kPa)	q (kPa)	t (kPa)	p' (kPa)	s' (kPa)
0	0.0000	0.0000	0.0	0.0	0.0	0.0	0.0	0.0	400.0	400.0
10	0.0014	0.1384	35.6	12.0	26.2	0.1	26.1	13.0	396.7	401.0
20	0.0028	0.2767	85.8	32.0	62.9	0.1	62.8	31.4	388.9	399.4
30	0.0042	0.4151	132.4	53.0	97.0	0.2	96.8	48.4	379.3	395.4
40	0.0055	0.5535	185.5	84.5	135.7	0.3	135.4	67.7	360.6	383.2
50	0.0069	0.6919	230.5	117.0	168.4	0.3	168.0	84.0	339.0	367.0
60	0.0083	0.8302	276.4	163.5	201.6	0.4	201.2	100.6	303.6	337.1
66	0.0091	0.9133	295.0	208.0	215.0	0.5	214.6	107.3	263.5	299.3
75	0.0104	1.0378	281.2	268.0	204.7	0.5	204.2	102.1	200.1	234.1
85	0.0118	1.1762	264.6	291.5	192.4	0.6	191.8	95.9	172.4	204.4
95	0.0131	1.3145	259.2	297.0	188.2	0.7	187.5	93.8	165.5	196.8
110	0.0152	1.5221	253.8	303.0	183.9	0.8	183.1	91.5	158.0	188.5
125	0.0173	1.7297	248.9	307.0	179.9	0.9	179.1	89.5	152.7	182.5
155	0.0214	2.1448	240.1	314.0	172.8	1.0	171.8	85.9	143.3	171.9
180	0.0249	2.4907	236.8	317.0	169.9	1.0	168.9	84.4	139.3	167.4
220	0.0304	3.0442	231.9	321.0	165.4	1.0	164.4	82.2	133.8	161.2
245	0.0339	3.3901	229.6	322.5	163.2	1.0	162.2	81.1	131.6	158.6
305	0.0422	4.2204	227.3	325.0	160.1	1.0	159.1	79.6	128.0	154.6
360	0.0498	4.9814	226.2	326.5	158.1	1.0	157.1	78.6	125.9	152.1
410	0.0567	5.6733	226.5	327.5	157.2	1.0	156.2	78.1	124.6	150.6
495	0.0685	6.8494	228.4	328.0	156.5	1.0	155.5	77.8	123.8	149.8
550	0.0761	7.6105	229.1	328.5	155.7	1.0	154.7	77.4	123.1	148.9
600	0.0830	8.3023	230.7	329.0	155.6	1.0	154.6	77.3	122.5	148.3
705	0.0976	9.7552	232.4	329.5	154.3	1.0	153.3	76.6	121.6	147.1

Strain Gauge (divs)	Axial Strain	Axial Strain (%)	Change Prf. ring (divs)	Change P.W.P (kPa)	q (Uncortd) (kPa)	Membrn. Corrctn. (kPa)	q (kPa)	t (kPa)	p' (kPa)	s' (kPa)
800	0.1107	11.0698	234.6	330.0	153.5	1.0	152.5	76.2	120.8	146.2
900	0.1245	12.4535	237.0	330.5	152.6	1.0	151.6	75.8	120.0	145.3
995	0.1377	13.7680	240.2	331.0	152.4	1.0	151.4	75.7	119.5	144.7
1100	0.1522	15.2210	242.1	332.0	151.0	1.0	150.0	75.0	118.0	143.0
1200	0.1660	16.6047	246.6	333.0	151.3	1.0	150.3	75.1	117.1	142.1
1310	0.1813	18.1268	249.2	333.0	150.1	1.0	149.1	74.5	116.7	141.5
1400	0.1937	19.3721	252.3	333.5	149.6	1.0	148.6	74.3	116.0	140.8
1500	0.2076	20.7558	255.7	334.0	149.1	1.0	148.1	74.0	115.4	140.0
1750	0.2422	24.2152	265.8	334.0	148.2	1.0	147.2	73.6	115.1	139.6
1950	0.2698	26.9826	272.0	335.0	146.1	1.0	145.1	72.5	113.4	137.5







Test	**Case 1: Monotonic Undrained Compression of Isotropically Consolidated Specimens**		
Cell No.	2 (Big)	Fines content (%)	0
Specimen	2f	Specific gravity (g/cm^3)	2.72

1.) Sample physical properties

Wet mass before test (g)	893.513	m.c before test (%)	9.05	Height (mm)	152.40	Volume (cm^3)	690.447
Wet mass after test (g)	975.367	m.c. after test (%)	19.04	Diameter (mm)	75.95		
Dry mass (g)	819.361	Dry density (kg/m^3)	1187	Area (cm^2)	45.305	Void ratio (e_0)	1.292

2.) Saturation/Consolidation

Date	C.P (kPa)	P.W.P bp closed (kPa)	B.P (kPa)	P.W.P bp open (kPa)	Change C.P (kPa)	Change P.W.P (kPa)	B value	Volume Gauge (cm^3)	Cell Expansn (cm^3)	Specimen Volume (cm^3)	Void Ratio	Comments
1/11	0		0	0.0				0.00	0.00	690.447	1.292	
1/11	9.8		7.3	5.0				9.35	0.00	681.097	1.261	**AIR-FLUSHING**
1/11	50	15.5	40	39.5	40.2	10.5	0.26	20.79	3.12	672.777	1.233	**S**
2/11	100	62.0	90	89.5	50	22.5	0.45	34.37	7.06	663.137	1.201	**A**
3/11	150	121.0	140	139.5	50	31.5	0.63	43.90	9.79	656.337	1.179	**T**
4/11	200	177.0	190	190.0	50	37.5	0.75	51.76	11.63	650.317	1.159	**U**
5/11	250	232.0	240	240.0	50	42.0	0.84	57.54	13.02	645.927	1.144	**R**
6/11	300	285.5	290	290.0	50	45.5	0.91	61.99	14.57	643.027	1.135	**A**
7/11	350	337.0	340	340.0	50	47.0	0.94	65.22	16.03	641.257	1.129	**T**
8/11	400	388.0	390	390.0	50	48.0	0.96	67.13	17.22	640.537	1.126	**I**
9/11	450	439.0	400	400.0	50	49.0	0.98					**O**
												N
9/11	900		400	400.0				109.60	26.90	607.747	1.018	**CONSOLIDATION**

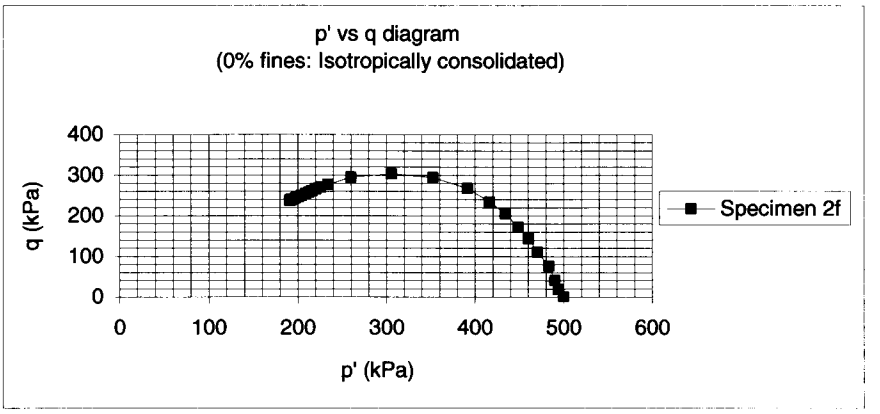
3.) Shear data

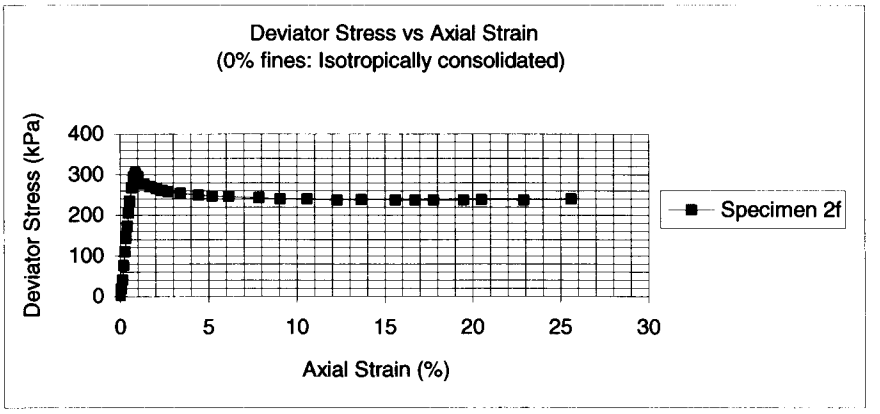
Volume change 1:		Volume change 2:		Sample Vol. change (cm^3)	82.70	B value	0.98
Air Flushing (cm^3)	9.35	Sat/Cons. (cm^3)	100.25	L_{cons} (mm)	146.32	p'consolidation (kPa)	500
Cell Expansion (cm^3)	0.00	Cell Expsn.(cm^3)	26.90	A_{cons} (cm^2)	41.687	Void ratio (e_1)	1.018

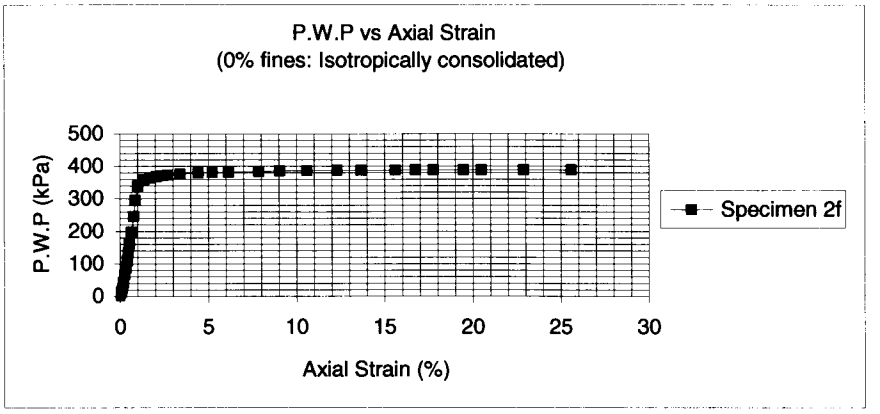
Proof ring properties		Strain gauge properties	
Proof ring No.	4541	1 strain division (mm)	0.01
Proof ring factor (dN/div)	25.77		

Strain Gauge (divs)	Axial Strain	Axial Strain (%)	Change Prf. ring (divs)	Change P.W.P (kPa)	q (Uncortd) (kPa)	Membrn. Corrctn. (kPa)	q (kPa)	t (kPa)	p' (kPa)	s' (kPa)
0	0.0000	0.0000	0.0	0.0	0.0	0.0	0.0	0.0	500.0	500.0
10	0.0007	0.0683	30.0	12.0	18.5	0.0	18.5	9.2	494.2	497.2
20	0.0014	0.1367	65.8	23.5	40.6	0.1	40.6	20.3	490.0	496.8
30	0.0021	0.2050	123.5	42.0	76.2	0.1	76.1	38.0	483.4	496.0
40	0.0027	0.2734	178.1	66.0	109.8	0.1	109.7	54.8	470.6	488.8
50	0.0034	0.3417	232.4	87.0	143.2	0.2	143.0	71.5	460.7	484.5
60	0.0041	0.4101	280.6	109.0	172.7	0.2	172.5	86.3	448.5	477.3
70	0.0048	0.4784	333.3	134.0	205.1	0.2	204.8	102.4	434.3	468.4
80	0.0055	0.5468	381.2	161.5	234.4	0.3	234.1	117.0	416.5	455.5
95	0.0065	0.6493	435.4	197.5	267.4	0.3	267.1	133.5	391.5	436.0
115	0.0079	0.7860	479.9	245.5	294.3	0.4	293.9	147.0	352.5	401.5
128	0.0087	0.8748	495.3	295.0	303.5	0.4	303.1	151.5	306.0	356.5
150	0.0103	1.0252	482.2	338.0	295.0	0.5	294.5	147.3	260.2	309.3
200	0.0137	1.3669	454.5	358.0	277.1	0.7	276.4	138.2	234.1	280.2
250	0.0171	1.7086	445.3	364.0	270.6	0.9	269.7	134.9	225.9	270.9
300	0.0205	2.0504	438.7	368.0	265.6	1.0	264.6	132.3	220.2	264.3
350	0.0239	2.3921	433.8	371.0	261.7	1.0	260.7	130.4	215.9	259.4
400	0.0273	2.7338	430.3	373.0	258.7	1.0	257.7	128.9	212.9	255.9
500	0.0342	3.4173	426.7	375.5	254.8	1.0	253.8	126.9	209.1	251.4
650	0.0444	4.4425	423.5	379.0	250.2	1.0	249.2	124.6	204.1	245.6
765	0.0523	5.2284	422.3	381.0	247.4	1.0	246.4	123.2	201.1	242.2
900	0.0615	6.1511	425.4	381.5	246.8	1.0	245.8	122.9	200.4	241.4
1150	0.0786	7.8597	427.8	383.5	243.7	1.0	242.7	121.3	197.4	237.8
1325	0.0906	9.0558	428.2	385.0	240.7	1.0	239.7	119.9	194.9	234.9

Strain Gauge (divs)	Axial Strain	Axial Strain (%)	Change Prf. ring (divs)	Change P.W.P (kPa)	q (Uncortd) (kPa)	Membrn. Corrctn. (kPa)	q (kPa)	t (kPa)	p' (kPa)	s' (kPa)
1550	0.1059	10.5936	435.5	386.0	240.7	1.0	239.7	119.8	193.9	233.8
1800	0.1230	12.3022	440.0	387.0	238.5	1.0	237.5	118.8	192.2	231.8
2000	0.1367	13.6691	447.6	387.5	238.9	1.0	237.9	118.9	191.8	231.4
2285	0.1562	15.6170	456.3	387.5	238.0	1.0	237.0	118.5	191.5	231.0
2450	0.1674	16.7447	462.8	388.0	238.2	1.0	237.2	118.6	191.1	230.6
2600	0.1777	17.7698	468.6	388.0	238.2	1.0	237.2	118.6	191.1	230.6
2850	0.1948	19.4785	478.4	388.0	238.1	1.0	237.1	118.6	191.0	230.6
3000	0.2050	20.5037	486.1	388.0	238.9	1.0	237.9	118.9	191.3	230.9
3350	0.2290	22.8958	500.0	388.0	238.3	1.0	237.3	118.7	191.1	230.7
3745	0.2560	25.5954	523.0	388.0	240.6	1.0	239.6	119.8	191.9	231.8







Test	**Case 1: Monotonic Undrained Compression of Isotropically Consolidated Specimens**		
Cell No.	2 (Big)	Fines content (%)	20
Specimen	2a	Specific gravity (g/cm^3)	2.72

1.) Sample physical properties

Wet mass before test (g)	817.398	m.c before test (%)	9.60	Height (mm)	150.95	Volume (cm^3)	685.680
Wet mass after test (g)	935.980	m.c. after test (%)	25.50	Diameter (mm)	76.05		
Dry mass (g)	745.801	Dry density (kg/m^3)	1088	Area (cm^2)	45.424	Void ratio (e_0)	1.501

2.) Saturation/Consolidation

Date	C.P (kPa)	P.W.P bp closed (kPa)	B.P (kPa)	P.W.P bp open (kPa)	Change C.P (kPa)	Change P.W.P (kPa)	B value	Volume Gauge (cm^3)	Cell Expansn (cm^3)	Specimen Volume (cm^3)	Void Ratio	Comments
3/9	0		0	0.0				0.00	0.00	685.680	1.501	
3/9	8.9		6.0	4.5				7.50	0.00	678.180	1.473	**AIR-FLUSHING**
3/9	50	15.0	40	37.5	41.1	10.5	0.26	47.64	7.06	645.100	1.353	**S**
4/9	100	60.0	90	88.5	50	22.5	0.45	60.41	9.79	635.060	1.316	**A**
5/9	150	120.0	140	139.5	50	31.5	0.63	69.19	11.63	628.120	1.291	**T**
6/9	200	176.5	190	190.0	50	37.0	0.74	74.78	13.02	623.920	1.275	**U**
7/9	250	231.5	240	240.5	50	41.5	0.83	79.01	14.57	621.240	1.266	**R**
8/9	300	285.5	290	290.0	50	45.0	0.90	82.20	16.03	619.510	1.259	**A**
9/9	350	337.0	340	340.0	50	47.0	0.94	88.67	17.22	614.230	1.240	**T**
10/9	400	388.0	390	390.0	50	48.0	0.96	92.34	19.30	612.640	1.234	**I**
11/9	450	439.0	400	400.0	50	49.0	0.98					**O**
												N
11/9	547		400	400.0				109.00	24.12	600.800	1.191	**CONSOLIDATION**

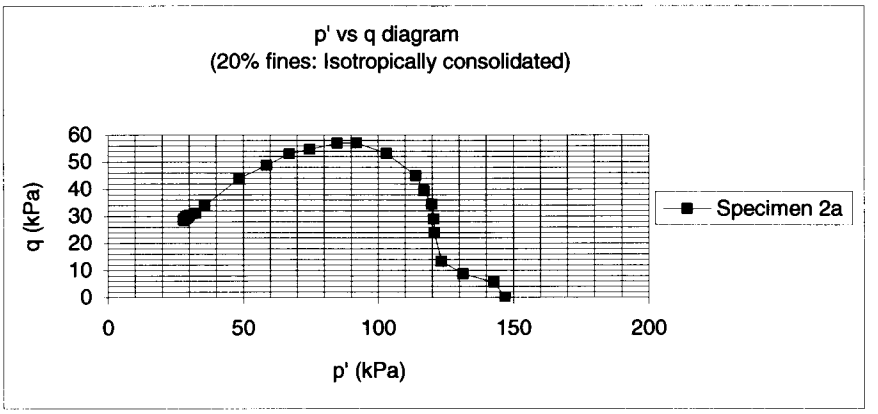
3.) Shear data

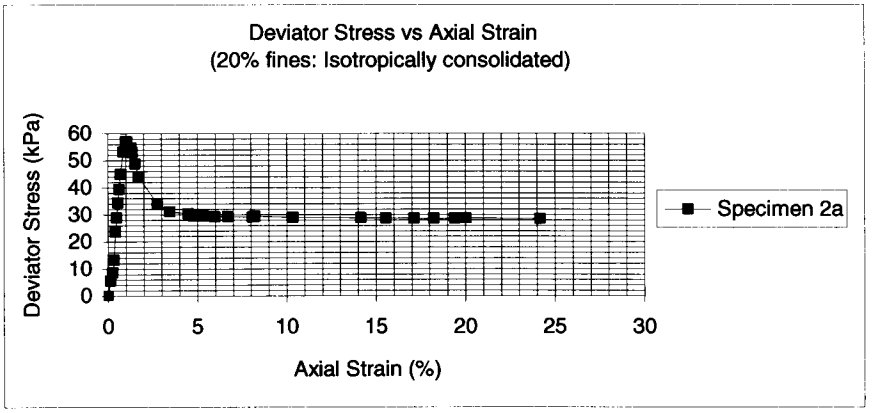
Volume change 1:		Volume change 2:		Sample Vol. change (cm^3)	84.88	B value	0.98
Air Flushing (cm^3)	7.50	Sat/Cons. (cm^3)	101.50	L_{cons} (mm)	144.72	p'consolidation (kPa)	147
Cell Expansion (cm^3)	0.00	Cell Expsn.(cm^3)	24.12	A_{cons} (cm^2)	41.676	Void ratio (e_1)	1.191

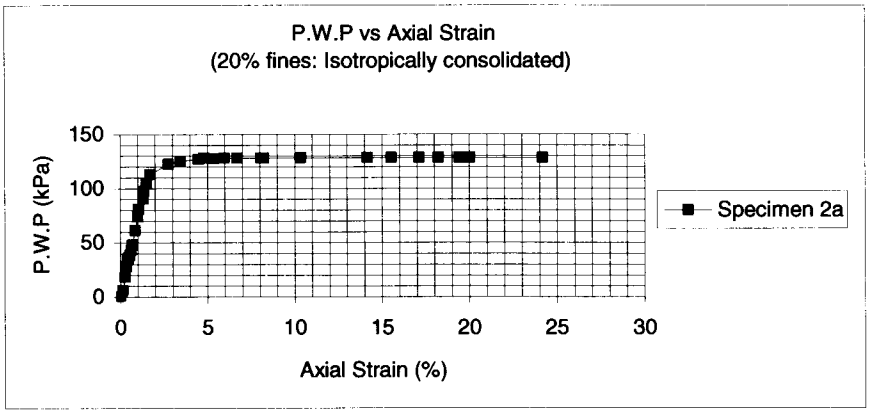
Proof ring properties		Strain gauge properties	
Proof ring No.	5153	1 strain division (mm)	0.01
Proof ring factor (dN/div)	7.512		

Strain Gauge (divs)	Axial Strain	Axial Strain (%)	Change Prf. ring (divs)	Change P.W.P (kPa)	q (Uncortd) (kPa)	Membrn. Corrctn. (kPa)	q (kPa)	t (kPa)	p' (kPa)	s' (kPa)
0	0.0000	0.0000	0.0	0.0	0.0	0.0	0.0	0.0	147.0	147.0
20	0.0014	0.1382	31.2	6.0	5.6	0.1	5.5	2.8	142.8	143.8
40	0.0028	0.2764	48.9	18.5	8.8	0.1	8.7	4.3	131.4	132.8
50	0.0035	0.3455	75.0	28.0	13.5	0.2	13.3	6.6	123.4	125.6
60	0.0041	0.4146	133.5	34.0	24.0	0.2	23.8	11.9	120.9	124.9
70	0.0048	0.4837	162.6	36.0	29.2	0.2	28.9	14.5	120.6	125.5
80	0.0055	0.5528	193.3	38.5	34.6	0.3	34.4	17.2	120.0	125.7
90	0.0062	0.6219	221.7	43.0	39.7	0.3	39.4	19.7	117.1	123.7
100	0.0069	0.6910	252.8	48.0	45.3	0.3	44.9	22.5	114.0	121.5
125	0.0086	0.8637	299.9	61.5	53.6	0.4	53.2	26.6	103.2	112.1
145	0.0100	1.0019	322.2	74.0	57.5	0.5	57.0	28.5	92.0	101.5
155	0.0107	1.0710	322.4	81.0	57.5	0.5	57.0	28.5	85.0	94.5
190	0.0131	1.3129	311.3	90.5	55.4	0.7	54.7	27.4	74.7	83.9
200	0.0138	1.3820	302.4	97.5	53.8	0.7	53.1	26.5	67.2	76.0
220	0.0152	1.5202	278.9	104.5	49.5	0.8	48.7	24.4	58.7	66.9
250	0.0173	1.7275	253.2	113.0	44.9	0.9	44.0	22.0	48.7	56.0
400	0.0276	2.7639	199.8	122.5	35.0	1.0	34.0	17.0	35.8	41.5
500	0.0345	3.4549	184.3	125.0	32.1	1.0	31.1	15.5	32.4	37.5
650	0.0449	4.4914	182.1	127.0	31.3	1.0	30.3	15.2	30.1	35.2
695	0.0480	4.8023	178.2	128.0	30.6	1.0	29.6	14.8	28.9	33.8
775	0.0536	5.3551	178.1	127.5	30.4	1.0	29.4	14.7	29.3	34.2
865	0.0598	5.9770	178.0	128.0	30.2	1.0	29.2	14.6	28.7	33.6
970	0.0670	6.7025	180.4	128.0	30.3	1.0	29.3	14.7	28.8	33.7
1170	0.0808	8.0845	181.3	128.0	30.0	1.0	29.0	14.5	28.7	33.5

Strain Gauge (divs)	Axial Strain	Axial Strain (%)	Change Prf. ring (divs)	Change P.W.P (kPa)	q (Uncortd) (kPa)	Membm. Corrctn. (kPa)	q (kPa)	t (kPa)	p' (kPa)	s' (kPa)
1180	0.0815	8.1536	182.5	128.0	30.2	1.0	29.2	14.6	28.7	33.6
1190	0.0822	8.2227	183.7	128.0	30.4	1.0	29.4	14.7	28.8	33.7
1500	0.1036	10.3647	185.6	128.5	30.0	1.0	29.0	14.5	28.2	33.0
2050	0.1417	14.1652	192.7	128.5	29.8	1.0	28.8	14.4	28.1	32.9
2250	0.1555	15.5471	195.2	128.5	29.7	1.0	28.7	14.4	28.1	32.9
2480	0.1714	17.1364	197.8	128.5	29.5	1.0	28.5	14.3	28.0	32.8
2640	0.1824	18.2420	200.3	128.5	29.5	1.0	28.5	14.3	28.0	32.8
2810	0.1942	19.4166	203.5	128.5	29.6	1.0	28.6	14.3	28.0	32.8
2900	0.2004	20.0385	205.9	128.5	29.7	1.0	28.7	14.3	28.1	32.8
3500	0.2418	24.1844	215.2	128.5	29.4	1.0	28.4	14.2	28.0	32.7







Test	**Case 1: Monotonic Undrained Compression of Isotropically Consolidated Specimens**		
Cell No.	2 (Small)	Fines content (%)	20
Specimen	2b	Specific gravity (g/cm^3)	2.72

1.) Sample physical properties

Wet mass before test (g)	101.813	m.c before test (%)	9.30	Height (mm)	76.00	Volume (cm^3)	85.966
Wet mass after test (g)	116.624	m.c. after test (%)	25.20	Diameter (mm)	37.95		
Dry mass (g)	93.150	Dry density (kg/m^3)	1084	Area (cm^2)	11.311	Void ratio (e_0)	1.510

2.) Saturation/Consolidation

Date	C.P (kPa)	P.W.P bp closed (kPa)	B.P (kPa)	P.W.P bp open (kPa)	Change C.P (kPa)	Change P.W.P (kPa)	B value	Volume Gauge (cm^3)	Cell Expansn (cm^3)	Specimen Volume (cm^3)	Void Ratio	Comments
16/9	0		0	0.5				0.00	0.00	85.966	1.510	
16/9	9.0		7.0	5.5				1.85	0.00	84.116	1.456	**AIR-FLUSHING**
16/9	50	17.0	40	39.5	41.0	11.5	0.28	7.03	4.04	82.976	1.423	**S**
17/9	100	61.0	90	90.0	50	21.5	0.43	10.14	6.24	82.066	1.396	**A**
18/9	150	120.0	140	140.0	50	30.0	0.60	12.67	7.67	80.966	1.364	**T**
19/9	200	175.5	190	190.0	50	35.5	0.71	14.18	8.73	80.516	1.351	**U**
20/9	250	231.0	240	240.0	50	41.0	0.82	15.51	9.79	80.246	1.343	**R**
21/9	300	282.5	290	290.0	50	42.5	0.85	16.79	10.81	79.986	1.336	**A**
22/9	350	335.0	340	340.0	50	45.0	0.90	17.85	11.63	79.746	1.329	**T**
23/9	400	386.5	390	390.0	50	46.5	0.93	19.30	12.73	79.396	1.318	**I**
24/9	450	437.0	440	440.0	50	47.0	0.94	20.48	13.67	79.156	1.311	**O**
25/9	500	488.5	450	450.0	50	48.5	0.97					**N**
25/9	500		450	450.0				22.29	14.65	78.326	1.287	**CONSOLIDATION**

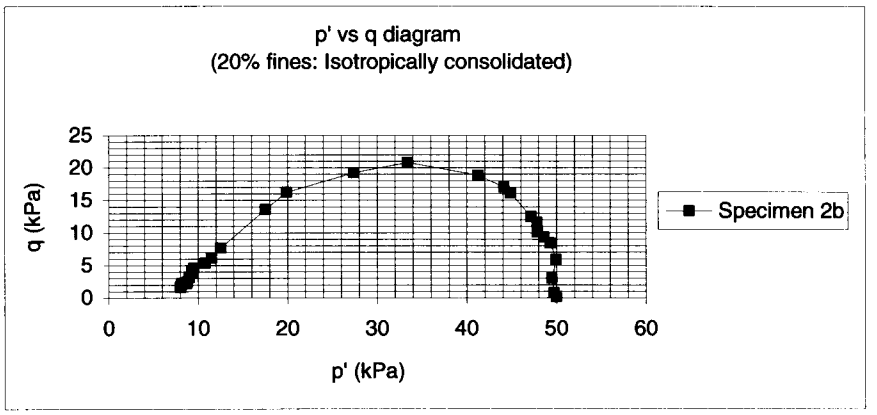
3.) Shear data

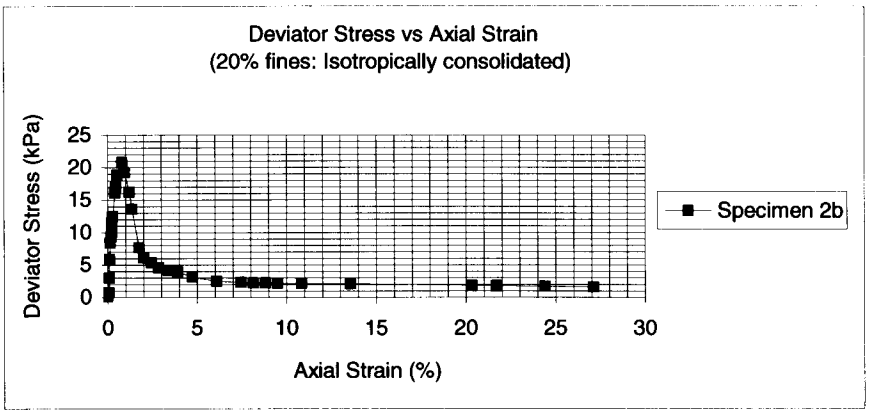
Volume change 1:		Volume change 2:		Sample Vol. change (cm^3)	7.64	B value	0.97
Air Flushing (cm^3)	1.85	Sat/Cons. (cm^3)	20.44	L_{cons} (mm)	73.75	p'consolidation (kPa)	50
Cell Expansion (cm^3)	0.00	Cell Expsn.(cm^3)	14.65	A_{cons} (cm^2)	10.641	Void ratio (e_1)	1.287

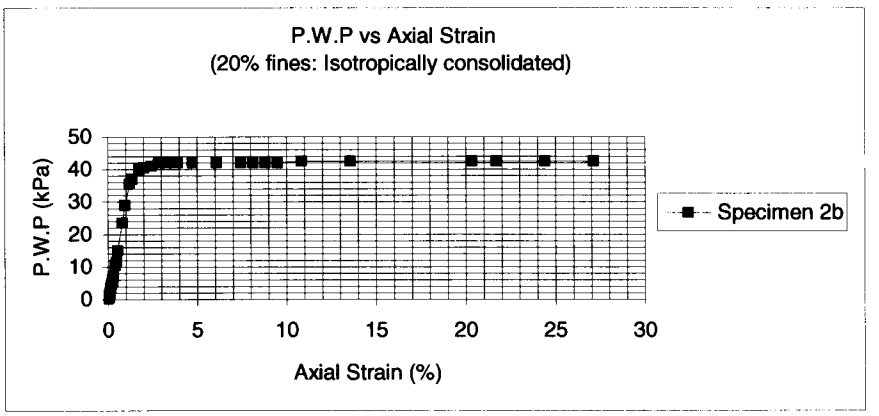
Proof ring properties		Strain gauge properties	
Proof ring No.	5153	1 strain division (mm)	0.01
Proof ring factor (dN/div)	7.512		

Strain Gauge (divs)	Axial Strain	Axial Strain (%)	Change Prf. ring (divs)	Change P.W.P (kPa)	q (Uncortd) (kPa)	Membrn. Corrctn. (kPa)	q (kPa)	t (kPa)	p' (kPa)	s' (kPa)
0	0.0000	0.0000	0.0	0.0	0.0	0.0	0.0	0.0	50.0	50.0
5	0.0007	0.0678	1.1	0.5	0.8	0.0	0.7	0.4	49.7	49.9
7	0.0009	0.0949	4.3	1.5	3.0	0.0	3.0	1.5	49.5	50.0
8	0.0011	0.1085	8.4	2.0	5.9	0.1	5.9	2.9	50.0	50.9
10	0.0014	0.1356	12.0	3.5	8.5	0.1	8.4	4.2	49.3	50.7
15	0.0020	0.2034	13.4	4.5	9.4	0.1	9.3	4.7	48.6	50.2
17	0.0023	0.2305	14.5	5.5	10.2	0.1	10.1	5.0	47.9	49.5
19	0.0026	0.2576	16.6	6.0	11.7	0.1	11.6	5.8	47.9	49.8
21	0.0028	0.2848	17.9	7.0	12.6	0.1	12.5	6.2	47.2	49.2
30	0.0041	0.4068	23.2	10.5	16.3	0.2	16.1	8.1	44.9	47.6
35	0.0047	0.4746	24.5	11.5	17.2	0.2	17.0	8.5	44.2	47.0
40	0.0054	0.5424	27.2	15.0	19.1	0.3	18.8	9.4	41.3	44.4
60	0.0081	0.8136	30.3	23.5	21.2	0.4	20.8	10.4	33.4	36.9
70	0.0095	0.9492	28.2	29.0	19.7	0.5	19.2	9.6	27.4	30.6
90	0.0122	1.2204	24.1	35.5	16.8	0.6	16.2	8.1	19.9	22.6
100	0.0136	1.3560	20.5	37.0	14.3	0.7	13.6	6.8	17.5	19.8
130	0.0176	1.7627	12.3	40.0	8.5	0.9	7.6	3.8	12.5	13.8
150	0.0203	2.0339	10.2	40.5	7.1	1.0	6.1	3.0	11.5	12.5
180	0.0244	2.4407	9.2	41.0	6.3	1.0	5.3	2.7	10.8	11.7
210	0.0285	2.8475	8.1	42.0	5.6	1.0	4.6	2.3	9.5	10.3
250	0.0339	3.3899	7.5	42.0	5.1	1.0	4.1	2.1	9.4	10.1
290	0.0393	3.9323	7.2	42.0	4.9	1.0	3.9	1.9	9.3	9.9
350	0.0475	4.7459	6.1	42.0	4.1	1.0	3.1	1.6	9.0	9.6
450	0.0610	6.1018	5.2	42.0	3.4	1.0	2.4	1.2	8.8	9.2

Strain Gauge (divs)	Axial Strain	Axial Strain (%)	Change Prf. ring (divs)	Change P.W.P (kPa)	q (Uncortd) (kPa)	Membrn. Corrctn. (kPa)	q (kPa)	t (kPa)	p' (kPa)	s' (kPa)
550	0.0746	7.4578	5.1	42.0	3.3	1.0	2.3	1.2	8.8	9.2
600	0.0814	8.1358	5.0	42.0	3.2	1.0	2.2	1.1	8.7	9.1
650	0.0881	8.8137	5.0	42.0	3.2	1.0	2.2	1.1	8.7	9.1
700	0.0949	9.4917	5.0	42.0	3.2	1.0	2.2	1.1	8.7	9.1
800	0.1085	10.8477	5.0	42.5	3.1	1.0	2.1	1.1	8.2	8.6
1000	0.1356	13.5596	5.0	42.5	3.1	1.0	2.1	1.0	8.2	8.5
1500	0.2034	20.3394	5.0	42.5	2.8	1.0	1.8	0.9	8.1	8.4
1600	0.2170	21.6953	5.0	42.5	2.8	1.0	1.8	0.9	8.1	8.4
1800	0.2441	24.4073	5.0	42.5	2.7	1.0	1.7	0.8	8.1	8.3
2000	0.2712	27.1192	5.0	42.5	2.6	1.0	1.6	0.8	8.0	8.3







Test	Case 1: Monotonic Undrained Compression of Isotropically Consolidated Specimens		
Cell No.	6 (Small)	Fines content (%)	20
Specimen	6a	Specific gravity (g/cm^3)	2.72

1.) Sample physical properties

Wet mass before test (g)	102.643	m.c before test (%)	10.00	Height (mm)	75.95	Volume (cm^3)	85.910
Wet mass after test (g)	113.654	m.c. after test (%)	21.80	Diameter (mm)	37.95		
Dry mass (g)	93.312	Dry density (kg/m^3)	1086	Area (cm^2)	11.311	Void ratio (e_0)	1.504

2.) Saturation/Consolidation

Date	C.P (kPa)	P.W.P bp closed (kPa)	B.P (kPa)	P.W.P bp open (kPa)	Change C.P (kPa)	Change P.W.P (kPa)	B value	Volume Gauge (cm^3)	Cell Expansn (cm^3)	Specimen Volume (cm^3)	Void Ratio	Comments
3/9	0		0	-2.0				0.00	0.00	85.910	1.504	
3/9	10.8		8.0	6.0				1.79	0.00	84.120	1.452	**AIR-FLUSHING**
3/9	50	17.0	40	38.5	39.2	11.0	0.28	8.13	4.89	82.670	1.410	**S**
4/9	100	60.5	90	89.5	50	22.0	0.44	11.10	7.14	81.950	1.389	**A**
5/9	150	118.0	140	139.5	50	28.5	0.57	13.24	8.53	81.200	1.367	**T**
6/9	200	176.0	190	189.5	50	36.5	0.73	15.00	9.63	80.540	1.348	**U**
7/9	250	230.0	240	240.0	50	40.5	0.81	16.85	10.61	79.670	1.322	**R**
8/9	300	282.5	290	290.0	50	42.5	0.85	18.20	11.67	79.380	1.314	**A**
9/9	350	335.0	340	340.0	50	45.0	0.90	19.60	12.65	78.960	1.302	**T**
10/9	400	386.0	390	390.0	50	46.0	0.92	21.00	13.79	78.700	1.294	**I**
11/9	450	437.0	440	440.0	50	47.0	0.94	22.00	14.56	78.470	1.287	**O**
12/9	500	489.5	450	450.0	50	49.5	0.99					**N**
12/9	525		450	450.0				24.14	16.09	77.860	1.270	**CONSOLIDATION**

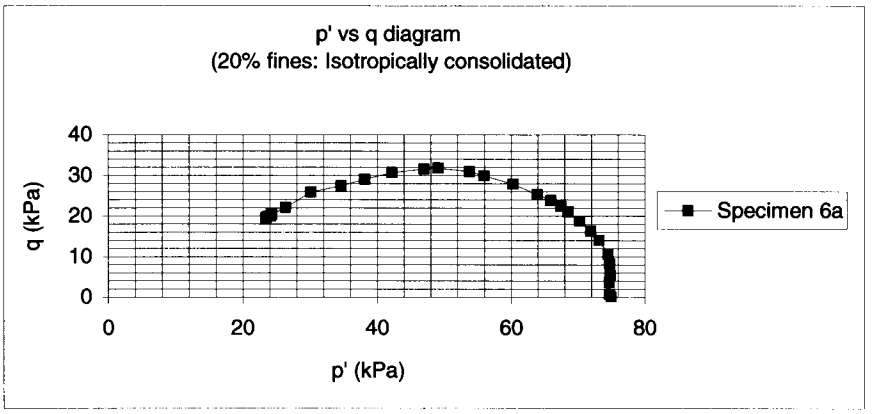
3.) Shear data

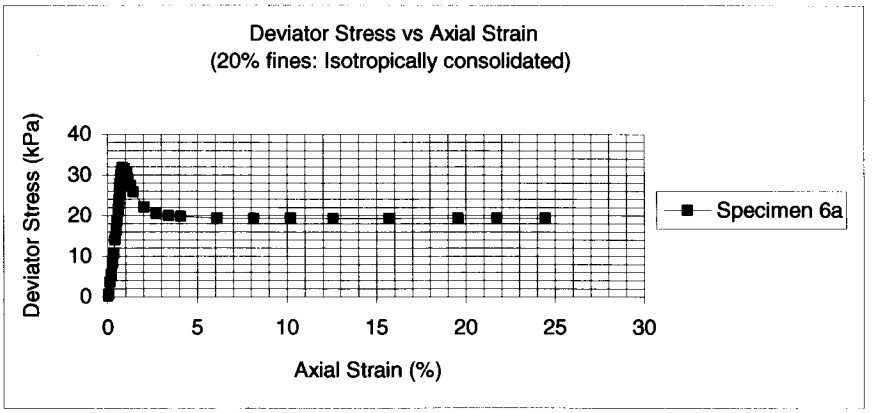
Volume change 1:		Volume change 2:		Sample Vol. change (cm^3)	8.05	B value	0.99
Air Flushing (cm^3)	1.79	Sat/Cons. (cm^3)	22.35	L_{cons} (mm)	73.58	p'consolidation (kPa)	75
Cell Expansion (cm^3)	0.00	Cell Expsn.(cm^3)	16.09	A_{cons} (cm^2)	10.605	Void ratio (e_1)	1.270

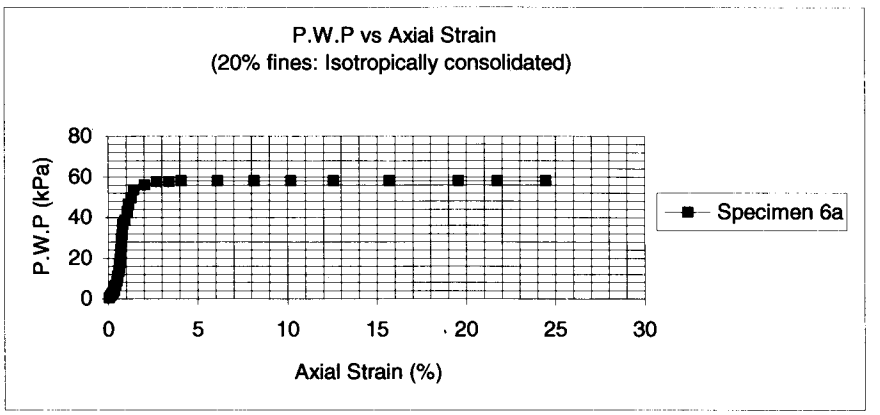
Proof ring properties		Strain gauge properties	
Proof ring No.	5153	1 strain division (mm)	0.01
Proof ring factor (dN/div)	7.512		

Strain Gauge (divs)	Axial Strain	Axial Strain (%)	Change Prf. ring (divs)	Change P.W.P (kPa)	q (Uncortd) (kPa)	Membm. Corrctn. (kPa)	q (kPa)	t (kPa)	p' (kPa)	s' (kPa)
0	0.0000	0.0000	0.0	0.0	0.0	0.0	0.0	0.0	75.0	75.0
5	0.0007	0.0680	1.1	0.5	0.8	0.0	0.7	0.4	74.7	74.9
10	0.0014	0.1359	5.2	1.5	3.7	0.1	3.6	1.8	74.7	75.3
15	0.0020	0.2039	7.9	2.0	5.6	0.1	5.5	2.7	74.8	75.7
20	0.0027	0.2718	11.8	3.0	8.3	0.1	8.2	4.1	74.7	76.1
25	0.0034	0.3398	15.2	4.0	10.7	0.2	10.6	5.3	74.5	76.3
30	0.0041	0.4077	20.1	6.5	14.2	0.2	14.0	7.0	73.2	75.5
35	0.0048	0.4757	23.4	8.5	16.5	0.2	16.3	8.1	71.9	74.6
40	0.0054	0.5436	27.0	11.0	19.0	0.3	18.8	9.4	70.3	73.4
45	0.0061	0.6116	30.3	13.5	21.3	0.3	21.0	10.5	68.5	72.0
46	0.0063	0.6252	32.2	15.0	22.7	0.3	22.4	11.2	67.5	71.2
48	0.0065	0.6524	34.3	17.0	24.1	0.3	23.8	11.9	65.9	69.9
50	0.0068	0.6796	36.4	19.5	25.6	0.3	25.3	12.6	63.9	68.1
52	0.0071	0.7067	40.1	24.0	28.2	0.4	27.9	13.9	60.3	64.9
55	0.0075	0.7475	43.0	29.0	30.2	0.4	29.9	14.9	56.0	60.9
58	0.0079	0.7883	44.5	31.5	31.3	0.4	30.9	15.4	53.8	58.9
60	0.0082	0.8155	45.8	36.5	32.2	0.4	31.8	15.9	49.1	54.4
70	0.0095	0.9514	45.6	38.5	32.0	0.5	31.5	15.8	47.0	52.3
80	0.0109	1.0873	44.5	43.0	31.2	0.5	30.6	15.3	42.2	47.3
85	0.0116	1.1552	42.3	46.5	29.6	0.6	29.0	14.5	38.2	43.0
95	0.0129	1.2912	40.1	49.5	28.0	0.6	27.4	13.7	34.6	39.2
105	0.0143	1.4271	38.0	53.5	26.5	0.7	25.8	12.9	30.1	34.4
150	0.0204	2.0387	33.2	56.0	23.0	1.0	22.0	11.0	26.3	30.0
200	0.0272	2.7182	31.0	57.5	21.4	1.0	20.4	10.2	24.3	27.7

Strain Gauge (divs)	Axial Strain	Axial Strain (%)	Change Prf. ring (divs)	Change P.W.P (kPa)	q (Uncortd) (kPa)	Membm. Corrctn. (kPa)	q (kPa)	t (kPa)	p' (kPa)	s' (kPa)
250	0.0340	3.3978	30.6	57.5	20.9	1.0	19.9	10.0	24.1	27.5
300	0.0408	4.0773	30.5	58.0	20.7	1.0	19.7	9.9	23.6	26.9
450	0.0612	6.1160	30.6	58.0	20.4	1.0	19.4	9.7	23.5	26.7
600	0.0815	8.1546	31.2	58.0	20.3	1.0	19.3	9.6	23.4	26.6
750	0.1019	10.1933	32.0	58.0	20.4	1.0	19.4	9.7	23.5	26.7
925	0.1257	12.5717	32.8	58.0	20.3	1.0	19.3	9.7	23.4	26.7
1155	0.1570	15.6977	34.0	58.0	20.3	1.0	19.3	9.7	23.4	26.7
1440	0.1957	19.5711	35.8	58.0	20.4	1.0	19.4	9.7	23.5	26.7
1600	0.2175	21.7457	36.7	58.0	20.3	1.0	19.3	9.7	23.4	26.7
1800	0.2446	24.4639	38.0	58.0	20.3	1.0	19.3	9.7	23.4	26.7







Test	**Case 1: Monotonic Undrained Compression of Isotropically Consolidated Specimens**		
Cell No.	3 (Big)	Fines content (%)	20
Specimen	3a	Specific gravity (g/cm^3)	2.72

1.) Sample physical properties

Wet mass before test (g)	832.613	m.c before test (%)	8.50	Height (mm)	151.90	Volume (cm^3)	690.903
Wet mass after test (g)	945.419	m.c. after test (%)	23.20	Diameter (mm)	76.10		
Dry mass (g)	767.385	Dry density (kg/m^3)	1111	Area (cm^2)	45.484	Void ratio (e_0)	1.449

2.) Saturation/Consolidation

Date	C.P (kPa)	P.W.P bp closed (kPa)	B.P (kPa)	P.W.P bp open (kPa)	Change C.P (kPa)	Change P.W.P (kPa)	B value	Volume Gauge (cm^3)	Cell Expansn (cm^3)	Specimen Volume (cm^3)	Void Ratio	Comments
4/9	0		0	-3.0				0.00	0.00	690.903	1.449	
4/9	10.0		7.0	5.0				7.15	0.00	683.753	1.424	**AIR-FLUSHING**
4/9	50	14.5	40	38.5	40.0	9.5	0.24	28.65	6.08	668.333	1.369	**S**
5/9	100	59.0	90	88.5	50	20.5	0.41	40.51	8.77	659.163	1.336	**A**
6/9	150	117.0	140	139.0	50	28.5	0.57	52.49	10.65	649.063	1.301	**T**
7/9	200	174.0	190	189.0	50	35.0	0.70	59.01	12.00	643.893	1.282	**U**
8/9	250	228.5	240	238.5	50	39.5	0.79	64.08	13.63	640.453	1.270	**R**
9/9	300	280.5	290	289.5	50	42.0	0.84	68.00	15.06	637.963	1.261	**A**
10/9	350	334.5	340	340.0	50	45.0	0.90	70.98	16.08	636.003	1.254	**T**
11/9	400	386.5	390	390.0	50	46.5	0.93	74.62	18.12	634.403	1.249	**I**
12/9	450	437.5	440	440.0	50	47.5	0.95	77.09	19.91	633.723	1.246	**O**
13/9	500	489.0	450	450.0	50	49.0	0.98					**N**
13/9	679		450	450.0				96.66	24.46	618.703	1.193	**CONSOLIDATION**

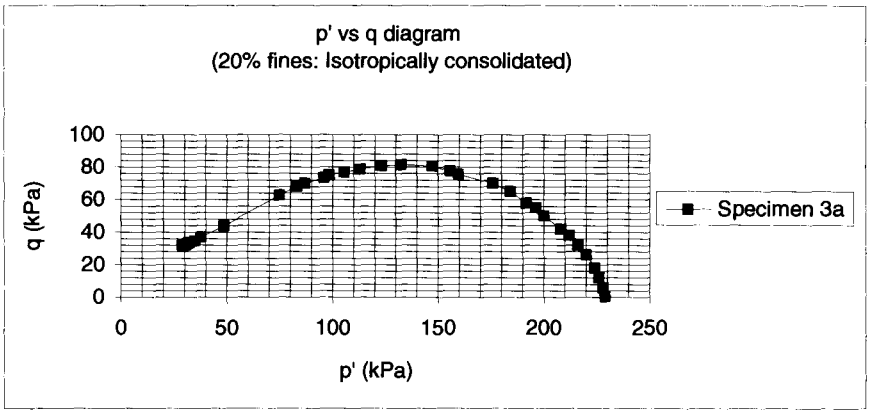
3.) Shear data

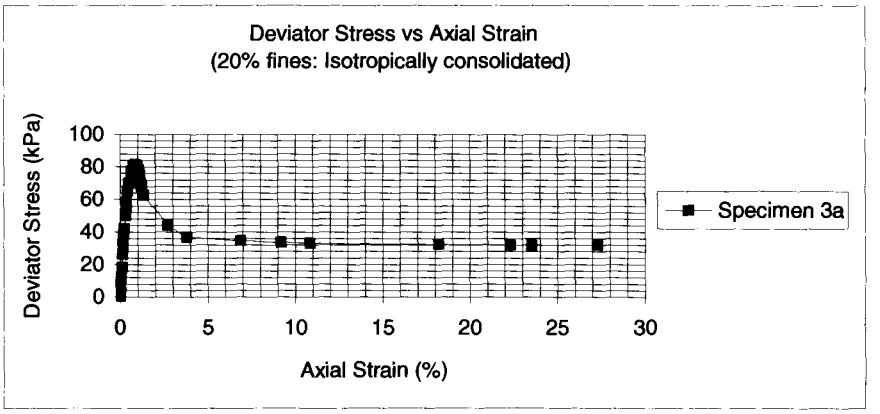
Volume change 1:		Volume change 2:		Sample Vol. change (cm^3)	72.20	B value	0.98
Air Flushing (cm^3)	7.15	Sat/Cons. (cm^3)	89.51	L_{cons} (mm)	146.61	p'consolidation (kPa)	229
Cell Expansion (cm^3)	0.00	Cell Expsn.(cm^3)	24.46	A_{cons} (cm^2)	42.315	Void ratio (e_1)	1.193

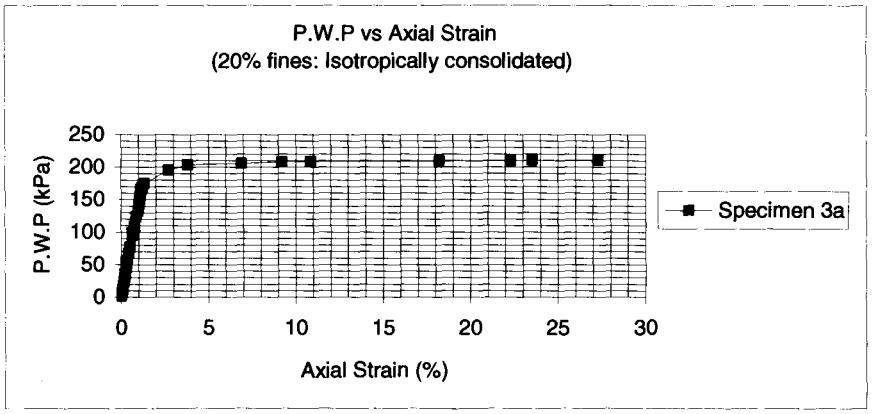
Proof ring properties		Strain gauge properties	
Proof ring No.	5153	1 strain division (mm)	0.01
Proof ring factor (dN/div)	7.512		

Strain Gauge (divs)	Axial Strain	Axial Strain (%)	Change Prf. ring (divs)	Change P.W.P (kPa)	q (Uncortd) (kPa)	Membrn. Corrctn. (kPa)	q (kPa)	t (kPa)	p' (kPa)	s' (kPa)
0	0.0000	0.0000	0.0	0.0	0.0	0.0	0.0	0.0	229.0	229.0
5	0.0003	0.0341	33.9	3.0	6.0	0.0	6.0	3.0	228.0	229.0
10	0.0007	0.0682	67.8	7.0	12.0	0.0	12.0	6.0	226.0	228.0
15	0.0010	0.1023	101.7	11.0	18.0	0.1	18.0	9.0	224.0	227.0
20	0.0014	0.1364	147.0	17.5	26.1	0.1	26.0	13.0	220.2	224.5
25	0.0017	0.1705	181.0	23.5	32.1	0.1	32.0	16.0	216.2	221.5
30	0.0020	0.2046	215.0	29.5	38.1	0.1	38.0	19.0	212.2	218.5
35	0.0024	0.2387	237.7	35.0	42.1	0.1	42.0	21.0	208.0	215.0
45	0.0031	0.3069	283.3	45.5	50.1	0.2	50.0	25.0	200.2	208.5
50	0.0034	0.3410	311.8	51.0	55.2	0.2	55.0	27.5	196.3	205.5
55	0.0038	0.3751	328.9	56.5	58.2	0.2	58.0	29.0	191.8	201.5
65	0.0044	0.4434	369.0	66.5	65.2	0.2	65.0	32.5	184.2	195.0
75	0.0051	0.5116	397.7	76.5	70.2	0.3	70.0	35.0	175.8	187.5
95	0.0065	0.6480	430.0	94.5	75.8	0.3	75.5	37.8	159.7	172.3
97	0.0066	0.6616	441.2	99.0	77.8	0.3	77.5	38.7	155.8	168.7
115	0.0078	0.7844	459.8	108.5	81.0	0.4	80.6	40.3	147.4	160.8
130	0.0089	0.8867	464.9	123.5	81.8	0.4	81.4	40.7	132.6	146.2
145	0.0099	0.9890	463.2	132.5	81.4	0.5	80.9	40.5	123.5	137.0
150	0.0102	1.0231	451.1	142.0	79.3	0.5	78.8	39.4	113.3	126.4
155	0.0106	1.0572	441.2	149.0	77.5	0.5	77.0	38.5	105.7	118.5
160	0.0109	1.0913	430.3	155.5	75.6	0.5	75.0	37.5	98.5	111.0
165	0.0113	1.1254	422.4	157.5	74.1	0.6	73.6	36.8	96.0	108.3
170	0.0116	1.1595	402.5	165.5	70.6	0.6	70.0	35.0	86.8	98.5
180	0.0123	1.2278	390.9	168.5	68.5	0.6	67.9	34.0	83.1	94.5

Strain Gauge (divs)	Axial Strain	Axial Strain (%)	Change Prf. ring (divs)	Change P.W.P (kPa)	q (Uncortd) (kPa)	Membrn. Corrctn. (kPa)	q (kPa)	t (kPa)	p' (kPa)	s' (kPa)
200	0.0136	1.3642	361.6	175.0	63.3	0.7	62.6	31.3	74.9	85.3
400	0.0273	2.7283	259.8	195.0	44.9	1.0	43.9	21.9	48.6	55.9
558	0.0381	3.8060	221.2	203.5	37.8	1.0	36.8	18.4	37.8	43.9
1010	0.0689	6.8891	215.2	205.5	35.6	1.0	34.6	17.3	35.0	40.8
1350	0.0921	9.2082	215.2	208.0	34.7	1.0	33.7	16.8	32.2	37.8
1590	0.1085	10.8452	215.4	208.5	34.1	1.0	33.1	16.5	31.5	37.0
2670	0.1821	18.2117	229.4	209.0	33.3	1.0	32.3	16.2	30.8	36.2
3270	0.2230	22.3043	238.9	209.5	33.0	1.0	32.0	16.0	30.2	35.5
3450	0.2353	23.5320	241.4	210.0	32.8	1.0	31.8	15.9	29.6	34.9
4000	0.2728	27.2835	255.3	210.5	33.0	1.0	32.0	16.0	29.2	34.5







Test	Case 1: Monotonic Undrained Compression of Isotropically Consolidated Specimens		
Cell No.	6 (Big)	Fines content (%)	20
Specimen	6b	Specific gravity (g/cm^3)	2.72

1.) Sample physical properties

Wet mass before test (g)	826.127	m.c before test (%)	9.60	Height (mm)	152.00	Volume (cm^3)	686.823
Wet mass after test (g)	945.976	m.c. after test (%)	25.50	Diameter (mm)	75.85		
Dry mass (g)	753.766	Dry density (kg/m^3)	1097	Area (cm^2)	45.186	Void ratio (e_0)	1.478

2.) Saturation/Consolidation

Date	C.P (kPa)	P.W.P bp closed (kPa)	B.P (kPa)	P.W.P bp open (kPa)	Change C.P (kPa)	Change P.W.P (kPa)	B value	Volume Gauge (cm^3)	Cell Expansn (cm^3)	Specimen Volume (cm^3)	Void Ratio	Comments
16/9	0		0	-2.0				0.00	0.00	686.823	1.478	
16/9	11.3		8.6	5.5				9.50	0.00	677.323	1.444	**AIR-FLUSHING**
16/9	50	15.5	40	40.0	38.7	10.0	0.26	29.64	7.94	665.123	1.400	**S**
17/9	100	61.5	90	90.0	50	21.5	0.43	40.05	10.71	657.483	1.373	**A**
18/9	150	119.0	140	140.0	50	29.0	0.58	49.61	12.51	649.723	1.345	**T**
19/9	200	175.0	190	190.0	50	35.0	0.70	58.43	13.93	642.323	1.318	**U**
20/9	250	230.5	240	240.0	50	40.5	0.81	66.73	15.41	635.503	1.293	**R**
21/9	300	283.0	290	290.0	50	43.0	0.86	72.31	16.91	631.423	1.279	**A**
22/9	350	335.5	340	340.0	50	45.5	0.91	76.81	18.26	628.273	1.267	**T**
23/9	400	386.5	390	390.0	50	46.5	0.93	82.00	20.38	625.203	1.256	**I**
24/9	450	437.5	440	440.0	50	47.5	0.95	88.00	21.85	620.673	1.240	**O**
25/9	500	489.5	490	490.0	50	49.5	0.99					**N**
25/9	611		500	500.0				109.41	26.43	603.843	1.179	**CONSOLIDATION**

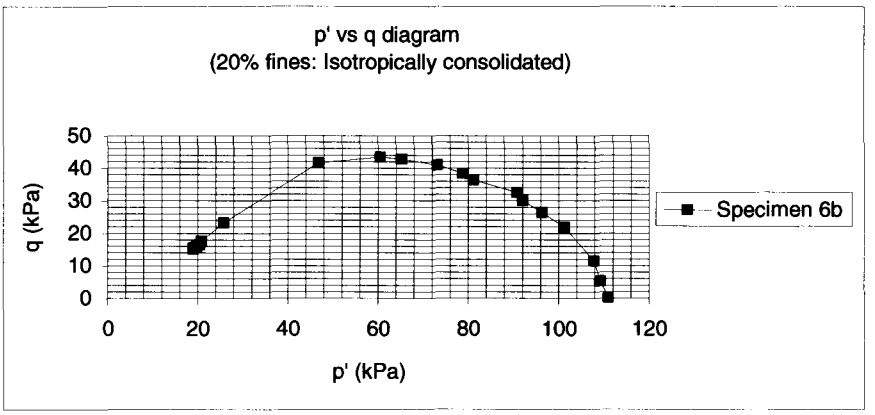
3.) Shear data

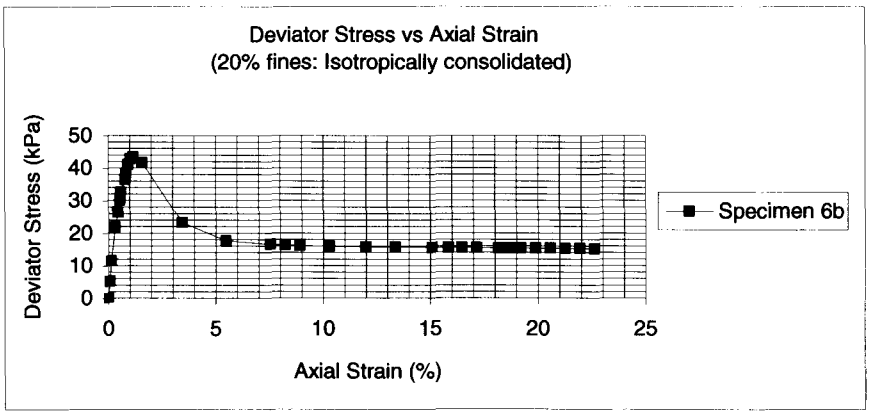
Volume change 1:		Volume change 2:		Sample Vol. change (cm^3)	82.98	B value	0.99
Air Flushing (cm^3)	9.50	Sat/Cons. (cm^3)	99.91	L_{cons} (mm)	145.88	p'consolidation (kPa)	111
Cell Expansion (cm^3)	0.00	Cell Expsn.(cm^3)	26.43	A_{cons} (cm^2)	41.546	Void ratio (e_1)	1.179

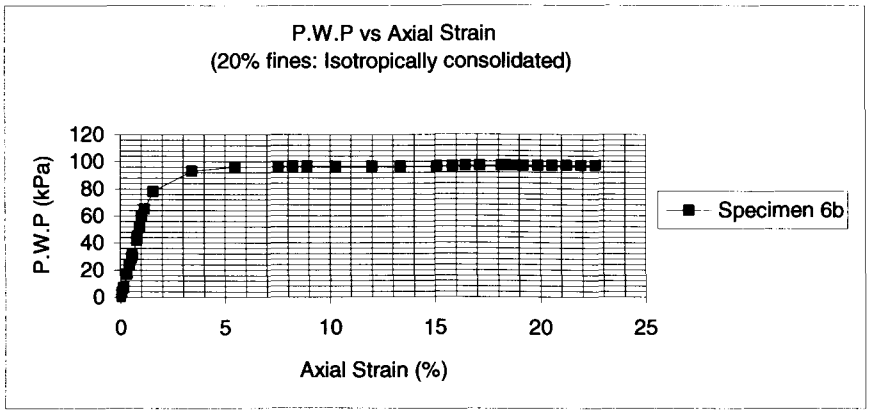
Proof ring properties		Strain gauge properties	
Proof ring No.	1800	1 strain division (mm)	0.01
Proof ring factor (dN/div)	14.846		

Strain Gauge (divs)	Axial Strain	Axial Strain (%)	Change Prf. ring (divs)	Change P.W.P (kPa)	q (Uncortd) (kPa)	Membm. Corrctn. (kPa)	q (kPa)	t (kPa)	p' (kPa)	s' (kPa)
0	0.0000	0.0000	0.0	0.0	0.0	0.0	0.0	0.0	111.0	111.0
10	0.0007	0.0686	14.9	3.5	5.3	0.0	5.3	2.6	109.3	110.1
20	0.0014	0.1371	32.3	7.0	11.5	0.1	11.5	5.7	107.8	109.7
45	0.0031	0.3085	61.7	17.0	22.0	0.2	21.8	10.9	101.3	104.9
65	0.0045	0.4456	74.9	23.5	26.6	0.2	26.4	13.2	96.3	100.7
80	0.0055	0.5484	85.3	29.0	30.3	0.3	30.0	15.0	92.0	97.0
85	0.0058	0.5827	92.3	31.0	32.8	0.3	32.5	16.2	90.8	96.2
115	0.0079	0.7883	103.6	42.0	36.7	0.4	36.3	18.2	81.1	87.2
120	0.0082	0.8226	109.3	45.0	38.7	0.4	38.3	19.2	78.8	85.2
135	0.0093	0.9254	117.2	51.5	41.5	0.5	41.0	20.5	73.2	80.0
150	0.0103	1.0283	122.4	60.0	43.3	0.5	42.8	21.4	65.3	72.4
170	0.0117	1.1654	124.6	65.0	44.0	0.6	43.4	21.7	60.5	67.7
230	0.0158	1.5767	120.4	78.0	42.3	0.8	41.6	20.8	46.9	53.8
500	0.0343	3.4275	70.3	93.0	24.3	1.0	23.3	11.6	25.8	29.6
800	0.0548	5.4840	55.1	96.0	18.6	1.0	17.6	8.8	20.9	23.8
1100	0.0754	7.5405	53.0	96.0	17.5	1.0	16.5	8.3	20.5	23.3
1200	0.0823	8.2260	52.8	96.5	17.3	1.0	16.3	8.2	19.9	22.7
1300	0.0891	8.9115	52.6	96.5	17.1	1.0	16.1	8.1	19.9	22.6
1500	0.1028	10.2825	52.7	96.5	16.9	1.0	15.9	7.9	19.8	22.4
1750	0.1200	11.9963	53.2	96.5	16.7	1.0	15.7	7.9	19.7	22.4
1950	0.1337	13.3673	54.0	96.5	16.7	1.0	15.7	7.9	19.7	22.4
2200	0.1508	15.0810	54.5	96.5	16.5	1.0	15.5	7.8	19.7	22.3
2310	0.1584	15.8351	55.0	96.5	16.5	1.0	15.5	7.8	19.7	22.3
2400	0.1645	16.4520	55.4	97.0	16.5	1.0	15.5	7.8	19.2	21.8

Strain Gauge (divs)	Axial Strain	Axial Strain (%)	Change Prf. ring (divs)	Change P.W.P (kPa)	q (Uncortd) (kPa)	Membrn. Corrctn. (kPa)	q (kPa)	t (kPa)	p' (kPa)	s' (kPa)
2500	0.1714	17.1375	55.6	97.0	16.5	1.0	15.5	7.7	19.2	21.7
2650	0.1817	18.1658	55.8	97.0	16.3	1.0	15.3	7.7	19.1	21.7
2700	0.1851	18.5085	56.0	97.0	16.3	1.0	15.3	7.7	19.1	21.7
2750	0.1885	18.8513	56.3	97.0	16.3	1.0	15.3	7.7	19.1	21.7
2800	0.1919	19.1940	56.4	97.0	16.3	1.0	15.3	7.6	19.1	21.6
2900	0.1988	19.8795	56.9	97.0	16.3	1.0	15.3	7.6	19.1	21.6
3000	0.2057	20.5650	57.4	97.0	16.3	1.0	15.3	7.6	19.1	21.6
3100	0.2125	21.2505	57.8	97.0	16.3	1.0	15.3	7.6	19.1	21.6
3200	0.2194	21.9360	58.2	97.0	16.2	1.0	15.2	7.6	19.1	21.6
3300	0.2262	22.6216	58.2	97.0	16.1	1.0	15.1	7.5	19.0	21.5







Test	**Case 1: Monotonic Undrained Compression of Isotropically Consolidated Specimens**		
Cell No.	3 (Big)	Fines content (%)	20
Specimen	3b	Specific gravity (g/cm^3)	2.72

1.) Sample physical properties

Wet mass before test (g)	817.697	m.c before test (%)	7.90	Height (mm)	151.75	Volume (cm^3)	691.128
Wet mass after test (g)	963.200	m.c. after test (%)	27.10	Diameter (mm)	76.15		
Dry mass (g)	757.829	Dry density (kg/m^3)	1097	Area (cm^2)	45.544	Void ratio (e_0)	1.481

2.) Saturation/Consolidation

Date	C.P (kPa)	P.W.P bp closed (kPa)	B.P (kPa)	P.W.P bp open (kPa)	Change C.P (kPa)	Change P.W.P (kPa)	B value	Volume Gauge (cm^3)	Cell Expansn (cm^3)	Specimen Volume (cm^3)	Void Ratio	Comments
17/9	0		0	0.0				0.00	0.00	691.128	1.481	
17/9	14.5		10.0	7.5				6.50	0.00	684.628	1.457	**AIR-FLUSHING**
17/9	50	17.0	40	39.0	35.5	9.5	0.27	35.00	6.08	662.208	1.377	**S**
18/9	100	61.0	90	90.0	50	22.0	0.44	47.25	8.77	652.648	1.342	**A**
19/9	150	120.0	140	139.5	50	30.0	0.60	54.21	10.65	647.568	1.324	**T**
20/9	200	175.5	190	190.0	50	36.0	0.72	62.13	12.00	640.998	1.301	**U**
21/9	250	229.5	240	240.0	50	39.5	0.79	66.79	13.63	637.968	1.290	**R**
22/9	300	282.5	290	290.0	50	42.5	0.85	70.21	15.06	635.978	1.283	**A**
23/9	350	335.0	340	340.0	50	45.0	0.90	72.69	16.08	634.518	1.277	**T**
24/9	400	386.0	390	390.0	50	46.0	0.92	76.25	18.12	632.998	1.272	**I**
25/9	450	437.5	440	440.0	50	47.5	0.95	79.00	19.91	632.038	1.269	**O**
26/9	500	489.0	490	490.0	50	49.0	0.98					**N**
26/9	852		490	490.0				114.10	24.77	601.798	1.160	**CONSOLIDATION**

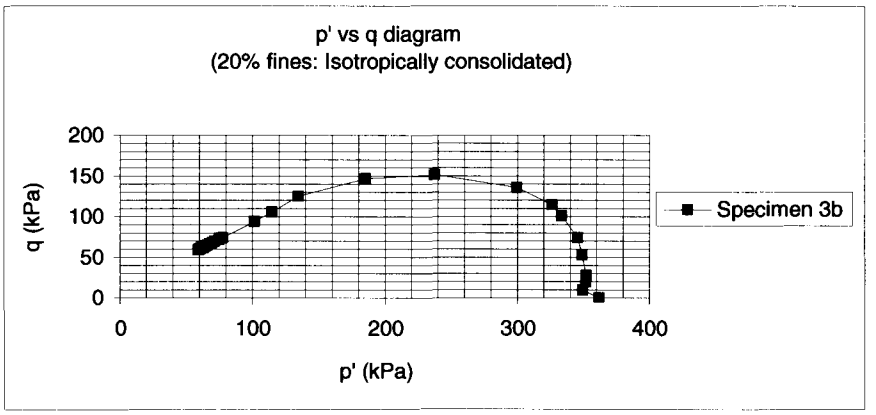
3.) Shear data

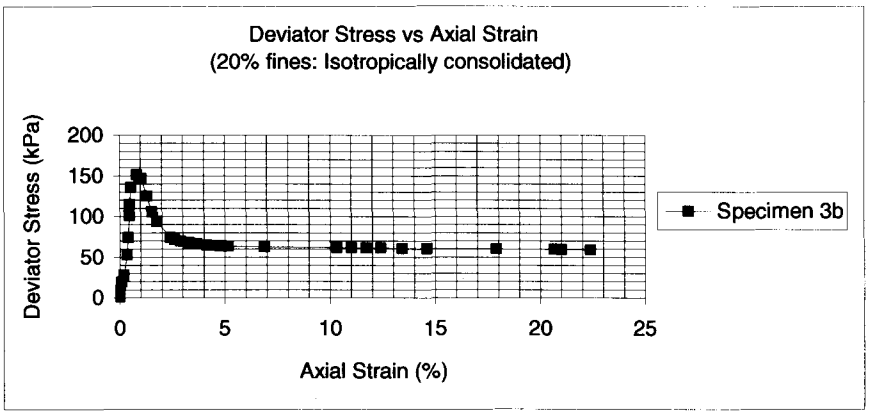
Volume change 1:		Volume change 2:		Sample Vol. change (cm^3)	89.33	B value	0.98
Air Flushing (cm^3)	6.50	Sat/Cons. (cm^3)	107.60	L_{cons} (mm)	145.21	p'consolidation (kPa)	362
Cell Expansion (cm^3)	0.00	Cell Expsn.(cm^3)	24.77	A_{cons} (cm^2)	41.619	Void ratio (e_1)	1.160

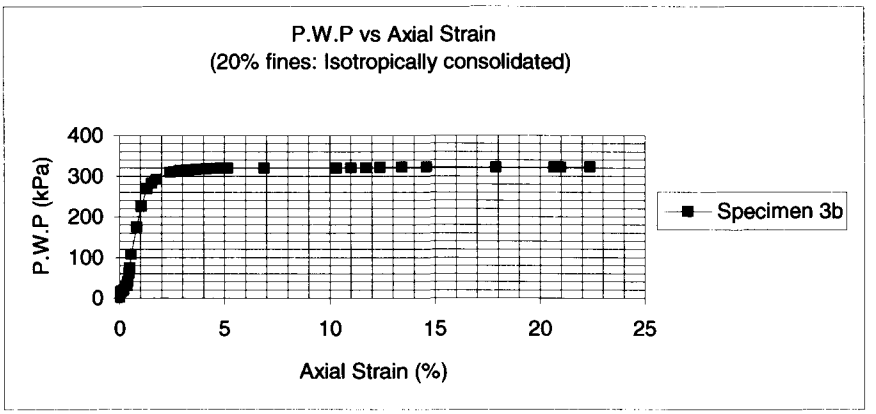
Proof ring properties		Strain gauge properties	
Proof ring No.	4541	1 strain division (mm)	0.01
Proof ring factor (dN/div)	25.77		

Strain Gauge (divs)	Axial Strain	Axial Strain (%)	Change Prf. ring (divs)	Change P.W.P (kPa)	q (Uncortd) (kPa)	Membm. Corrctn. (kPa)	q (kPa)	t (kPa)	p' (kPa)	s' (kPa)
0	0.0000	0.0000	0.0	0.0	0.0	0.0	0.0	0.0	362.0	362.0
1	0.0001	0.0083	15.2	15.5	9.4	0.0	9.4	4.7	349.6	351.2
12	0.0009	0.0854	31.5	16.5	19.5	0.0	19.4	9.7	352.0	355.2
28	0.0019	0.1928	44.9	19.0	27.7	0.1	27.7	13.8	352.2	356.8
52	0.0036	0.3581	85.3	30.5	52.6	0.2	52.4	26.2	349.0	357.7
58	0.0040	0.3994	120.2	41.0	74.1	0.2	73.9	37.0	345.6	358.0
67	0.0046	0.4614	164.1	62.0	101.1	0.2	100.9	50.5	333.6	350.5
72	0.0050	0.4958	186.2	74.0	114.7	0.2	114.5	57.2	326.2	345.2
80	0.0055	0.5509	220.3	107.5	135.7	0.3	135.4	67.7	299.6	322.2
120	0.0083	0.8264	247.0	175.0	151.7	0.4	151.3	75.6	237.4	262.6
150	0.0103	1.0330	240.3	225.5	147.3	0.5	146.7	73.4	185.4	209.9
190	0.0131	1.3084	205.2	269.0	125.4	0.7	124.7	62.4	134.6	155.4
225	0.0155	1.5495	174.4	282.5	106.3	0.8	105.5	52.8	114.7	132.3
255	0.0176	1.7561	155.6	291.5	94.7	0.9	93.8	46.9	101.8	117.4
350	0.0241	2.4103	123.7	309.0	74.7	1.0	73.7	36.9	77.6	89.9
380	0.0262	2.6169	120.4	311.0	72.6	1.0	71.6	35.8	74.9	86.8
420	0.0289	2.8923	117.3	313.5	70.5	1.0	69.5	34.8	71.7	83.3
480	0.0331	3.3055	114.8	315.0	68.7	1.0	67.7	33.9	69.6	80.9
530	0.0365	3.6498	112.9	316.5	67.4	1.0	66.4	33.2	67.6	78.7
600	0.0413	4.1319	110.2	317.5	65.4	1.0	64.4	32.2	66.0	76.7
650	0.0448	4.4762	109.9	318.5	65.0	1.0	64.0	32.0	64.8	75.5
700	0.0482	4.8205	109.5	319.0	64.5	1.0	63.5	31.8	64.2	74.8
750	0.0516	5.1649	109.4	319.0	64.2	1.0	63.2	31.6	64.1	74.6
1000	0.0689	6.8865	110.3	319.5	63.6	1.0	62.6	31.3	63.4	73.8

Strain Gauge (divs)	Axial Strain	Axial Strain (%)	Change Prf. ring (divs)	Change P.W.P (kPa)	q (Uncortd) (kPa)	Membrn. Corrctn. (kPa)	q (kPa)	t (kPa)	p' (kPa)	s' (kPa)
1500	0.1033	10.3297	113.1	319.5	62.8	1.0	61.8	30.9	63.1	73.4
1600	0.1102	11.0184	113.5	320.0	62.5	1.0	61.5	30.8	62.5	72.8
1700	0.1171	11.7070	114.0	320.5	62.3	1.0	61.3	30.7	61.9	72.2
1800	0.1240	12.3957	114.6	321.0	62.2	1.0	61.2	30.6	61.4	71.6
1950	0.1343	13.4286	115.0	321.5	61.6	1.0	60.6	30.3	60.7	70.8
2120	0.1460	14.5993	116.5	321.5	61.6	1.0	60.6	30.3	60.7	70.8
2600	0.1790	17.9049	120.0	321.5	61.0	1.0	60.0	30.0	60.5	70.5
3000	0.2066	20.6595	123.4	322.0	60.6	1.0	59.6	29.8	59.9	69.8
3050	0.2100	21.0038	123.5	322.0	60.4	1.0	59.4	29.7	59.8	69.7
3250	0.2238	22.3811	125.0	322.5	60.1	1.0	59.1	29.5	59.2	69.0







Test	**Case 1: Monotonic Undrained Compression of Isotropically Consolidated Specimens**		
Cell No.	2 (Big)	Fines content (%)	20
Specimen	2c	Specific gravity (g/cm^3)	2.72

1.) Sample physical properties

Wet mass before test (g)	824.032	m.c before test (%)	7.70	Height (mm)	150.55	Volume (cm^3)	682.964
Wet mass after test (g)	932.679	m.c. after test (%)	21.90	Diameter (mm)	76.00		
Dry mass (g)	765.118	Dry density (kg/m^3)	1120	Area (cm^2)	45.365	Void ratio (e_0)	1.428

2.) Saturation/Consolidation

Date	C.P (kPa)	P.W.P bp closed (kPa)	B.P (kPa)	P.W.P bp open (kPa)	Change C.P (kPa)	Change P.W.P (kPa)	B value	Volume Gauge (cm^3)	Cell Expansn (cm^3)	Specimen Volume (cm^3)	Void Ratio	Comments
3/10	0		0	-1.0				0.00	0.00	682.964	1.428	
3/10	16.0		12.7	9.5				11.70	0.00	671.264	1.386	**AIR-FLUSHING**
3/10	50	19.0	40	39.0	34.0	9.5	0.28	27.52	7.06	662.504	1.355	**S**
4/10	100	68.0	90	89.0	50	29.0	0.58	39.78	9.79	652.974	1.321	**A**
5/10	150	125.0	140	138.5	50	36.0	0.72	49.61	11.63	644.984	1.293	**T**
6/10	200	179.0	190	190.0	50	40.5	0.81	55.39	13.02	640.594	1.277	**U**
7/10	250	233.0	240	240.0	50	43.0	0.86	62.31	14.57	635.224	1.258	**R**
8/10	300	285.5	290	290.0	50	45.5	0.91	68.12	16.03	630.874	1.243	**A**
9/10	350	336.5	340	340.0	50	46.5	0.93	71.11	17.22	629.074	1.236	**T**
10/10	400	387.5	390	390.0	50	47.5	0.95	74.56	19.30	627.704	1.231	**I**
11/10	450	438.0	440	440.0	50	48.0	0.96	77.25	20.93	626.644	1.228	**O**
12/10	500	489.5	490	490.0	50	49.5	0.99					**N**
12/10	788		490	490.0				117.65	27.93	593.244	1.109	**CONSOLIDATION**

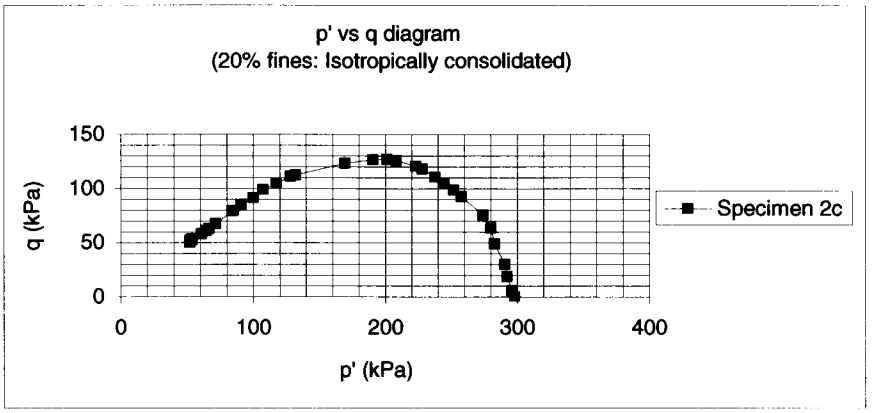
3.) Shear data

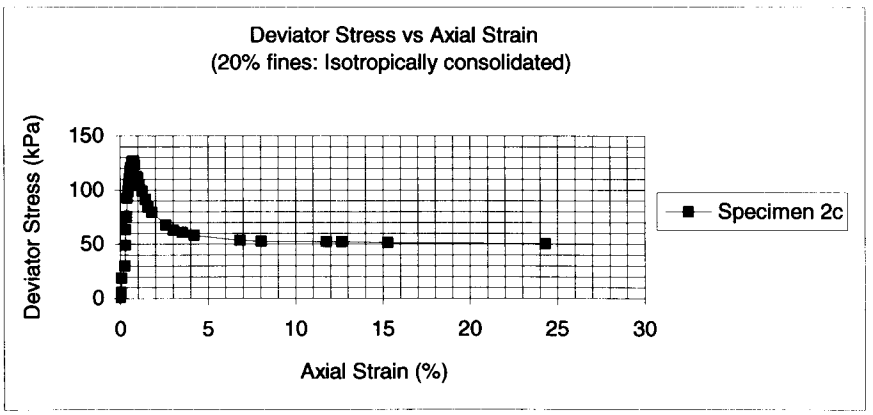
Volume change 1:		Volume change 2:		Sample Vol. change (cm^3)	89.72	B value	0.99
Air Flushing (cm^3)	11.70	Sat/Cons. (cm^3)	105.95	L_{cons} (mm)	143.96	p'consolidation (kPa)	298
Cell Expansion (cm^3)	0.00	Cell Expsn.(cm^3)	27.93	A_{cons} (cm^2)	41.392	Void ratio (e_1)	1.109

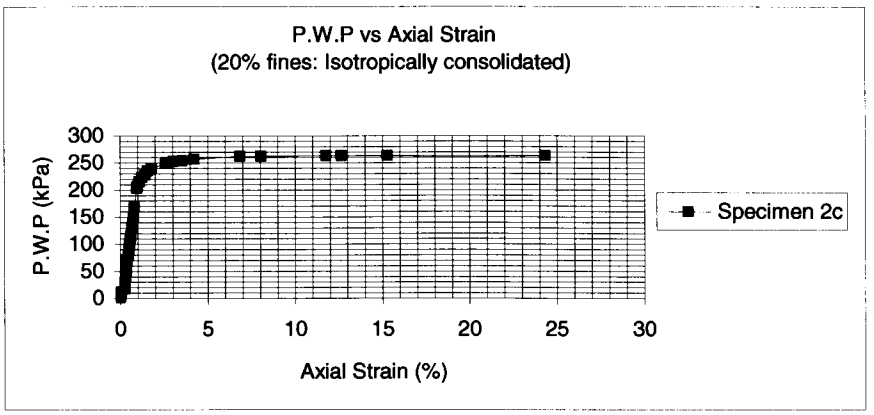
Proof ring properties		Strain gauge properties	
Proof ring No.	4541	1 strain division (mm)	0.01
Proof ring factor (dN/div)	25.77		

Strain Gauge (divs)	Axial Strain	Axial Strain (%)	Change Prf. ring (divs)	Change P.W.P (kPa)	q (Uncortd) (kPa)	Membrn. Corrctn. (kPa)	q (kPa)	t (kPa)	p' (kPa)	s' (kPa)
0	0.0000	0.0000	0.0	0.0	0.0	0.0	0.0	0.0	298.0	298.0
5	0.0003	0.0347	9.3	4.0	5.8	0.0	5.8	2.9	295.9	296.9
10	0.0007	0.0695	30.0	12.0	18.7	0.0	18.6	9.3	292.2	295.3
39	0.0027	0.2709	48.5	17.5	30.1	0.1	30.0	15.0	290.5	295.5
43	0.0030	0.2987	78.9	31.5	49.0	0.1	48.8	24.4	282.8	290.9
45	0.0031	0.3126	102.3	39.0	63.5	0.2	63.3	31.7	280.1	290.7
53	0.0037	0.3682	122.1	49.0	75.7	0.2	75.6	37.8	274.2	286.8
58	0.0040	0.4029	149.7	71.0	92.8	0.2	92.6	46.3	257.9	273.3
65	0.0045	0.4515	159.6	79.0	98.9	0.2	98.7	49.3	251.9	268.3
71	0.0049	0.4932	168.9	88.0	104.6	0.2	104.4	52.2	244.8	262.2
77	0.0053	0.5349	178.9	97.0	110.8	0.3	110.5	55.3	237.8	256.3
84	0.0058	0.5835	191.2	109.0	118.3	0.3	118.1	59.0	228.4	248.0
89	0.0062	0.6182	195.4	115.0	120.9	0.3	120.6	60.3	223.2	243.3
98	0.0068	0.6808	203.8	131.5	126.0	0.3	125.7	62.8	208.4	229.3
105	0.0073	0.7294	205.9	139.0	127.3	0.4	126.9	63.4	201.3	222.4
112	0.0078	0.7780	205.5	149.5	126.9	0.4	126.6	63.3	190.7	211.8
120	0.0083	0.8336	200.2	169.5	123.6	0.4	123.2	61.6	169.6	190.1
137	0.0095	0.9517	183.0	203.5	112.8	0.5	112.4	56.2	132.0	150.7
144	0.0100	1.0003	181.2	207.0	111.7	0.5	111.2	55.6	128.1	146.6
159	0.0110	1.1045	170.4	215.5	104.9	0.6	104.4	52.2	117.3	134.7
183	0.0127	1.2712	161.9	223.5	99.5	0.6	98.9	49.4	107.5	123.9
209	0.0145	1.4518	149.8	228.5	91.9	0.7	91.2	45.6	99.9	115.1
226	0.0157	1.5699	138.9	235.5	85.1	0.8	84.3	42.2	90.6	104.7
258	0.0179	1.7922	131.2	239.5	80.2	0.9	79.3	39.7	84.9	98.2

Strain Gauge (divs)	Axial Strain	Axial Strain (%)	Change Prf. ring (divs)	Change P.W.P (kPa)	q (Uncortd) (kPa)	Membm. Corrctn. (kPa)	q (kPa)	t (kPa)	p' (kPa)	s' (kPa)
375	0.0260	2.6049	113.2	249.0	68.6	1.0	67.6	33.8	71.5	82.8
435	0.0302	3.0217	105.5	252.5	63.7	1.0	62.7	31.3	66.4	76.8
510	0.0354	3.5427	102.7	254.0	61.7	1.0	60.7	30.3	64.2	74.3
608	0.0422	4.2235	99.0	256.5	59.0	1.0	58.0	29.0	60.8	70.5
985	0.0684	6.8423	93.5	262.0	54.2	1.0	53.2	26.6	53.7	62.6
1158	0.0804	8.0440	93.5	262.0	53.5	1.0	52.5	26.3	53.5	62.3
1695	0.1177	11.7743	96.8	263.0	53.2	1.0	52.2	26.1	52.4	61.1
1820	0.1264	12.6426	97.9	263.0	53.2	1.0	52.2	26.1	52.4	61.1
2200	0.1528	15.2823	99.4	263.0	52.4	1.0	51.4	25.7	52.1	60.7
3500	0.2431	24.3127	109.3	263.0	51.5	1.0	50.5	25.3	51.8	60.3







Test	Case 1: Monotonic Undrained Compression of Isotropically Consolidated Specimens		
Cell No.	6 (Small)	Fines content (%)	30
Specimen	6g	Specific gravity (g/cm^3)	2.72

1.) Sample physical properties

Wet mass before test (g)	103.835	m.c before test (%)	9.30	Height (mm)	75.55	Volume (cm^3)	85.232
Wet mass after test (g)	118.332	m.c. after test (%)	24.56	Diameter (mm)	37.90		
Dry mass (g)	95.000	Dry density (kg/m^3)	1115	Area (cm^2)	11.282	Void ratio (e_0)	1.440

2.) Saturation/Consolidation

Date	C.P (kPa)	P.W.P bp closed (kPa)	B.P (kPa)	P.W.P bp open (kPa)	Change C.P (kPa)	Change P.W.P (kPa)	B value	Volume Gauge (cm^3)	Cell Expansn (cm^3)	Specimen Volume (cm^3)	Void Ratio	Comments
3/12	0		0	0.0				0.00	0.00	85.232	1.440	
3/12	12.2		9.0	6.5				1.12	0.00	84.112	1.408	**AIR-FLUSHING**
3/12	50	18.5	40	39.5	37.8	12.0	0.32	8.07	4.89	82.052	1.349	**S**
4/12	100	61.5	90	90.0	50	22.0	0.44	11.67	7.14	80.702	1.311	**A**
5/12	150	119.0	140	140.0	50	29.0	0.58	14.05	8.53	79.712	1.282	**T**
6/12	200	175.0	190	190.0	50	35.0	0.70	15.97	9.63	78.892	1.259	**U**
7/12	250	230.0	240	240.0	50	40.0	0.80	18.10	10.61	77.742	1.226	**R**
8/12	300	282.0	290	290.0	50	42.0	0.84	20.03	11.67	76.872	1.201	**A**
9/12	350	335.0	340	340.0	50	45.0	0.90	21.74	12.65	76.142	1.180	**T**
10/12	400	386.5	390	390.0	50	46.5	0.93	23.15	13.79	75.872	1.172	**I**
11/12	450	437.5	440	440.0	50	47.5	0.95	24.19	14.56	75.602	1.165	**O**
12/12	500	489.0	450	450.0	50	49.0	0.98					**N**
12/12	525		450	450.0				26.87	16.09	74.452	1.132	**CONSOLIDATION**

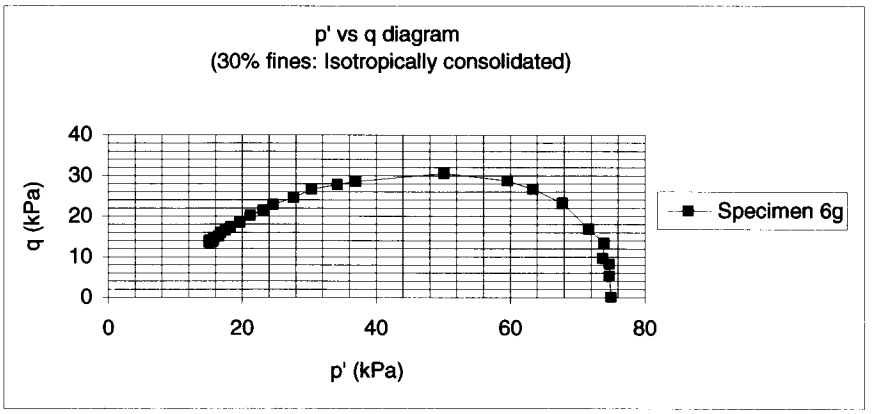
3.) Shear data

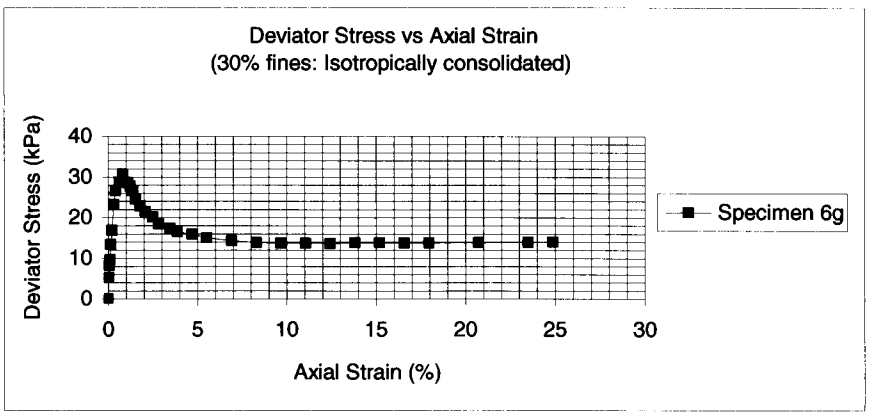
Volume change 1:		Volume change 2:		Sample Vol. change (cm^3)	10.78	B value	0.98
Air Flushing (cm^3)	1.12	Sat/Cons. (cm^3)	25.75	L_{cons} (mm)	72.36	p'consolidation (kPa)	75
Cell Expansion (cm^3)	0.00	Cell Expsn.(cm^3)	16.09	A_{cons} (cm^2)	10.330	Void ratio (e_1)	1.132

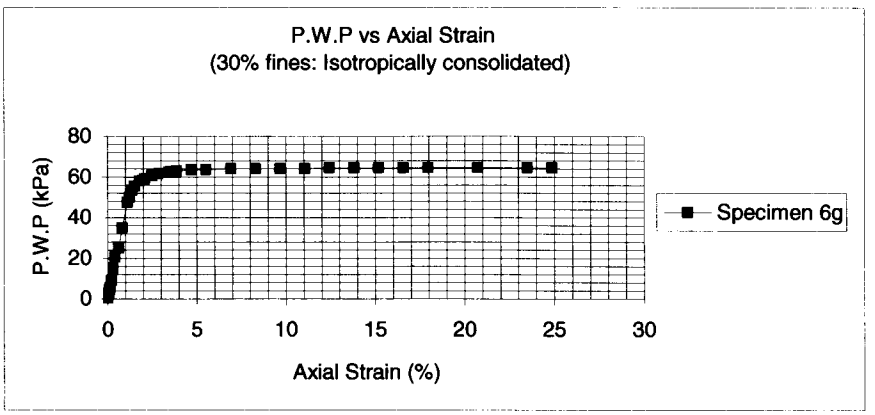
Proof ring properties		Strain gauge properties	
Proof ring No.	4541	1 strain division (mm)	0.01
Proof ring factor (dN/div)	25.77		

Strain Gauge (divs)	Axial Strain	Axial Strain (%)	Change Prf. ring (divs)	Change P.W.P (kPa)	q (Uncortd) (kPa)	Membm. Corrctn. (kPa)	q (kPa)	t (kPa)	p' (kPa)	s' (kPa)
0	0.0000	0.0000	0.0	0.0	0.0	0.0	0.0	0.0	75.0	75.0
3	0.0004	0.0415	2.1	2.0	5.2	0.0	5.2	2.6	74.7	75.6
5	0.0007	0.0691	3.3	3.0	8.2	0.0	8.2	4.1	74.7	76.1
8	0.0011	0.1106	3.9	4.5	9.7	0.1	9.7	4.8	73.7	75.3
11	0.0015	0.1520	5.4	5.5	13.5	0.1	13.4	6.7	74.0	76.2
15	0.0021	0.2073	6.8	9.0	16.9	0.1	16.8	8.4	71.6	74.4
22	0.0030	0.3040	9.4	15.0	23.4	0.2	23.2	11.6	67.7	71.6
30	0.0041	0.4146	10.8	20.5	26.8	0.2	26.6	13.3	63.4	67.8
45	0.0062	0.6218	11.7	25.0	29.0	0.3	28.7	14.3	59.6	64.3
60	0.0083	0.8291	12.5	35.0	30.9	0.4	30.5	15.3	50.2	55.3
80	0.0111	1.1055	11.8	47.5	29.1	0.6	28.6	14.3	37.0	41.8
90	0.0124	1.2437	11.5	50.0	28.3	0.6	27.7	13.9	34.2	38.9
100	0.0138	1.3819	11.1	53.5	27.3	0.7	26.6	13.3	30.4	34.8
110	0.0152	1.5201	10.3	55.5	25.3	0.8	24.5	12.3	27.7	31.8
130	0.0180	1.7965	9.7	58.0	23.8	0.9	22.9	11.4	24.6	28.4
150	0.0207	2.0728	9.2	59.0	22.5	1.0	21.5	10.7	23.2	26.7
180	0.0249	2.4874	8.7	60.5	21.2	1.0	20.2	10.1	21.2	24.6
205	0.0283	2.8329	8.0	61.5	19.4	1.0	18.4	9.2	19.6	22.7
250	0.0345	3.4547	7.6	62.5	18.3	1.0	17.3	8.7	18.3	21.2
280	0.0387	3.8693	7.3	63.0	17.5	1.0	16.5	8.3	17.5	20.3
340	0.0470	4.6984	7.1	63.5	16.9	1.0	15.9	7.9	16.8	19.4
400	0.0553	5.5275	6.8	63.5	16.0	1.0	15.0	7.5	16.5	19.0
500	0.0691	6.9094	6.6	64.0	15.3	1.0	14.3	7.2	15.8	18.2
600	0.0829	8.2913	6.5	64.0	14.9	1.0	13.9	6.9	15.6	17.9

Strain Gauge (divs)	Axial Strain	Axial Strain (%)	Change Prf. ring (divs)	Change P.W.P (kPa)	q (Uncortd) (kPa)	Membrn. Corrctn. (kPa)	q (kPa)	t (kPa)	p' (kPa)	s' (kPa)
700	0.0967	9.6732	6.5	64.0	14.6	1.0	13.6	6.8	15.5	17.8
800	0.1106	11.0551	6.6	64.0	14.6	1.0	13.6	6.8	15.5	17.8
900	0.1244	12.4370	6.7	64.5	14.6	1.0	13.6	6.8	15.0	17.3
1000	0.1382	13.8189	6.9	64.5	14.8	1.0	13.8	6.9	15.1	17.4
1100	0.1520	15.2007	7.0	64.5	14.8	1.0	13.8	6.9	15.1	17.4
1200	0.1658	16.5826	7.1	64.5	14.8	1.0	13.8	6.9	15.1	17.4
1300	0.1796	17.9645	7.2	64.5	14.7	1.0	13.7	6.9	15.1	17.4
1500	0.2073	20.7283	7.5	64.5	14.8	1.0	13.8	6.9	15.1	17.4
1700	0.2349	23.4921	7.8	64.5	14.9	1.0	13.9	6.9	15.1	17.4
1800	0.2487	24.8740	8.0	64.5	15.0	1.0	14.0	7.0	15.2	17.5







Test	**Case 1: Monotonic Undrained Compression of Isotropically Consolidated Specimens**		
Cell No.	3 (Small)	Fines content (%)	30
Specimen	3i	Specific gravity (g/cm^3)	2.72

1.) Sample physical properties

Wet mass before test (g)	106.193	m.c before test (%)	9.60	Height (mm)	76.05	Volume (cm^3)	86.023
Wet mass after test (g)	118.886	m.c. after test (%)	22.70	Diameter (mm)	37.95		
Dry mass (g)	96.891	Dry density (kg/m^3)	1126	Area (cm^2)	11.311	Void ratio (e_0)	1.415

2.) Saturation/Consolidation

Date	C.P (kPa)	P.W.P bp closed (kPa)	B.P (kPa)	P.W.P bp open (kPa)	Change C.P (kPa)	Change P.W.P (kPa)	B value	Volume Gauge (cm^3)	Cell Expansn (cm^3)	Specimen Volume (cm^3)	Void Ratio	Comments
3/1	0		0	-0.5				0.00	0.00	86.023	1.415	
3/1	9.5		7.4	4.5				1.95	0.00	84.073	1.360	**AIR-FLUSHING**
3/1	50	16.0	40	40.0	40.5	11.5	0.28	9.94	5.89	81.973	1.301	**S**
4/1	100	62.0	90	90.0	50	22.0	0.44	13.77	8.17	80.423	1.258	**A**
5/1	150	120.0	140	140.0	50	30.0	0.60	16.93	9.52	78.613	1.207	**T**
6/1	200	175.5	190	190.0	50	35.5	0.71	19.83	10.66	76.853	1.157	**U**
7/1	250	229.5	240	240.0	50	39.5	0.79	22.61	11.56	74.973	1.105	**R**
8/1	300	282.5	290	290.0	50	42.5	0.85	25.03	12.66	73.653	1.068	**A**
9/1	350	335.0	340	340.0	50	45.0	0.90	27.44	13.80	72.383	1.032	**T**
10/1	400	386.5	390	390.0	50	46.5	0.93	29.55	14.98	71.453	1.006	**I**
11/1	450	437.5	440	440.0	50	47.5	0.95	31.08	15.60	70.543	0.980	**O**
12/1	500	489.0	450	450.0	50	49.0	0.98					**N**
12/1	550		450	450.0				35.35	17.39	68.063	0.911	**CONSOLIDATION**

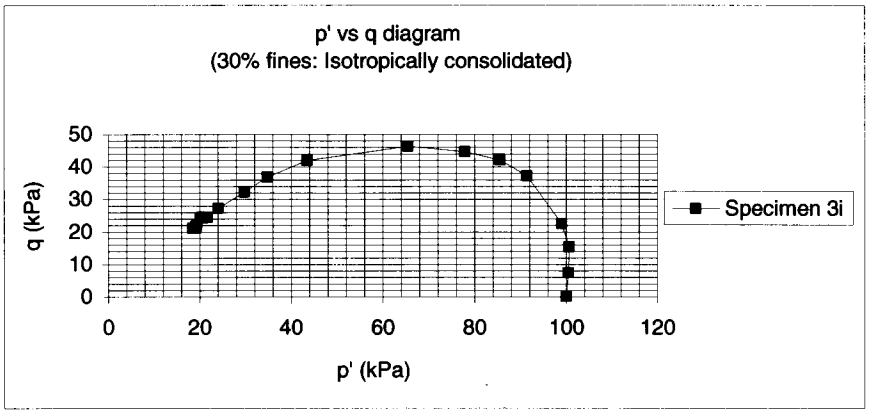
3.) Shear data

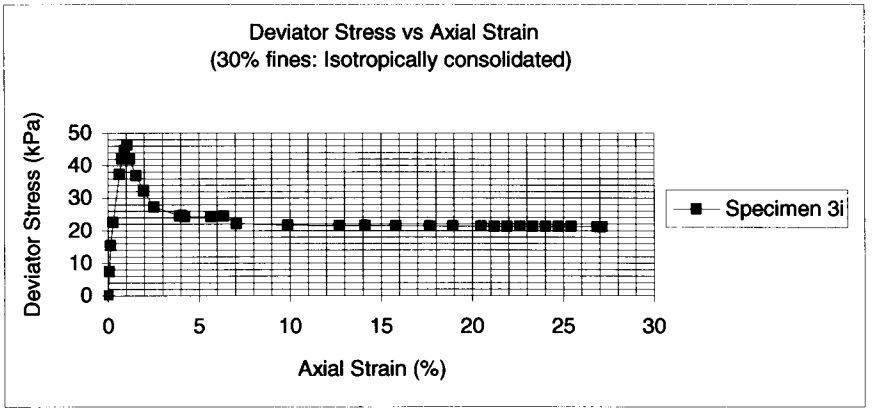
Volume change 1:		Volume change 2:		Sample Vol. change (cm^3)	17.96	B value	0.98
Air Flushing (cm^3)	1.95	Sat/Cons. (cm^3)	33.40	L_{cons} (mm)	70.76	p'consolidation (kPa)	100
Cell Expansion (cm^3)	0.00	Cell Expsn.(cm^3)	17.39	A_{cons} (cm^2)	9.737	Void ratio (e_1)	0.911

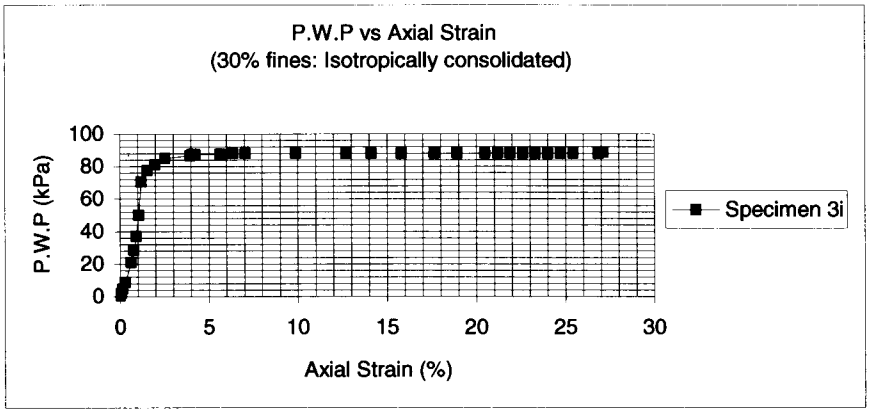
Proof ring properties		Strain gauge properties	
Proof ring No.	1800	1 strain division (mm)	0.01
Proof ring factor (dN/div)	14.846		

Strain Gauge (divs)	Axial Strain	Axial Strain (%)	Change Prf. ring (divs)	Change P.W.P (kPa)	q (Uncortd) (kPa)	Membrn. Corrctn. (kPa)	q (kPa)	t (kPa)	p' (kPa)	s' (kPa)
0	0.0000	0.0000	0.0	0.0	0.0	0.0	0.0	0.0	100.0	100.0
5	0.0007	0.0707	4.9	2.0	7.5	0.0	7.4	3.7	100.5	101.7
10	0.0014	0.1413	10.2	4.5	15.5	0.1	15.5	7.7	100.7	103.2
20	0.0028	0.2827	14.9	8.5	22.7	0.1	22.5	11.3	99.0	102.8
45	0.0064	0.6360	24.8	21.0	37.6	0.3	37.3	18.6	91.4	97.6
55	0.0078	0.7773	28.1	28.5	42.5	0.4	42.1	21.1	85.5	92.6
65	0.0092	0.9186	29.9	37.0	45.2	0.5	44.7	22.4	77.9	85.4
75	0.0106	1.0600	31.1	50.0	46.9	0.5	46.4	23.2	65.5	73.2
85	0.0120	1.2013	28.3	70.5	42.6	0.6	42.0	21.0	43.5	50.5
110	0.0155	1.5546	25.1	77.5	37.7	0.8	36.9	18.4	34.8	40.9
140	0.0198	1.9786	22.2	81.0	33.2	1.0	32.2	16.1	29.7	35.1
180	0.0254	2.5439	19.0	85.0	28.2	1.0	27.2	13.6	24.1	28.6
280	0.0396	3.9572	17.4	86.5	25.5	1.0	24.5	12.2	21.7	25.7
290	0.0410	4.0985	17.5	87.5	25.6	1.0	24.6	12.3	20.7	24.8
300	0.0424	4.2398	17.3	87.5	25.3	1.0	24.3	12.1	20.6	24.6
400	0.0565	5.6531	17.6	87.5	25.3	1.0	24.3	12.2	20.6	24.7
450	0.0636	6.3598	17.8	88.0	25.4	1.0	24.4	12.2	20.1	24.2
500	0.0707	7.0664	16.3	88.0	23.1	1.0	22.1	11.0	19.4	23.0
700	0.0989	9.8930	16.5	88.0	22.7	1.0	21.7	10.8	19.2	22.8
900	0.1272	12.7195	16.9	88.0	22.5	1.0	21.5	10.7	19.2	22.7
1000	0.1413	14.1328	17.2	88.0	22.5	1.0	21.5	10.8	19.2	22.8
1120	0.1583	15.8287	17.5	88.0	22.5	1.0	21.5	10.7	19.2	22.7
1250	0.1767	17.6660	17.8	88.0	22.3	1.0	21.3	10.7	19.1	22.7
1340	0.1894	18.9380	18.1	88.0	22.4	1.0	21.4	10.7	19.1	22.7

Strain Gauge (divs)	Axial Strain	Axial Strain (%)	Change Prf. ring (divs)	Change P.W.P (kPa)	q (Uncortd) (kPa)	Membrn. Corrctn. (kPa)	q (kPa)	t (kPa)	p' (kPa)	s' (kPa)
1450	0.2049	20.4926	18.4	88.0	22.3	1.0	21.3	10.7	19.1	22.7
1500	0.2120	21.1992	18.5	88.0	22.2	1.0	21.2	10.6	19.1	22.6
1550	0.2191	21.9058	18.7	88.0	22.3	1.0	21.3	10.6	19.1	22.6
1600	0.2261	22.6125	18.9	88.0	22.3	1.0	21.3	10.7	19.1	22.7
1650	0.2332	23.3191	19.0	88.0	22.2	1.0	21.2	10.6	19.1	22.6
1700	0.2403	24.0258	19.2	88.0	22.2	1.0	21.2	10.6	19.1	22.6
1750	0.2473	24.7324	19.4	88.0	22.3	1.0	21.3	10.6	19.1	22.6
1800	0.2544	25.4390	19.6	88.0	22.3	1.0	21.3	10.6	19.1	22.6
1900	0.2685	26.8523	19.9	88.0	22.2	1.0	21.2	10.6	19.1	22.6
1920	0.2713	27.1350	19.9	88.5	22.1	1.0	21.1	10.6	18.5	22.1







Test	**Case 1: Monotonic Undrained Compression of Isotropically Consolidated Specimens**		
Cell No.	2 (Small)	Fines content (%)	30
Specimen	2J	Specific gravity (g/cm^3)	2.72

1.) Sample physical properties

Wet mass before test (g)	103.762	m.c before test (%)	9.80	Height (mm)	76.15	Volume (cm^3)	86.818
Wet mass after test (g)	117.654	m.c. after test (%)	24.50	Diameter (mm)	38.10		
Dry mass (g)	94.501	Dry density (kg/m^3)	1088	Area (cm^2)	11.401	Void ratio (e_0)	1.499

2.) Saturation/Consolidation

Date	C.P (kPa)	P.W.P bp closed (kPa)	B.P (kPa)	P.W.P bp open (kPa)	Change C.P (kPa)	Change P.W.P (kPa)	B value	Volume Gauge (cm^3)	Cell Expansn (cm^3)	Specimen Volume (cm^3)	Void Ratio	Comments
17/1	0		0	-2.5				0.00	0.00	86.818	1.499	
17/1	10.0		7.6	4.5				1.90	0.00	84.918	1.444	**AIR-FLUSHING**
17/1	50	16.0	40	39.0	40.0	11.5	0.29	8.49	4.04	82.368	1.371	**S**
18/1	100	61.5	90	89.5	50	22.5	0.45	12.80	6.24	80.258	1.310	**A**
19/1	150	120.5	140	139.5	50	31.0	0.62	15.91	7.67	78.578	1.262	**T**
20/1	200	176.0	190	190.0	50	36.5	0.73	18.55	8.73	76.998	1.216	**U**
21/1	250	231.0	240	240.0	50	41.0	0.82	20.98	9.79	75.628	1.177	**R**
22/1	300	283.0	290	290.0	50	43.0	0.86	23.57	10.81	74.058	1.132	**A**
23/1	350	334.5	340	340.0	50	44.5	0.89	25.89	11.63	72.558	1.088	**T**
24/1	400	386.0	390	390.0	50	46.0	0.92	28.55	12.73	70.998	1.044	**I**
25/1	450	437.5	440	440.0	50	47.5	0.95	29.91	13.67	70.578	1.031	**O**
26/1	500	488.5	450	450.0	50	48.5	0.97					**N**
26/1	900		450	450.0				38.45	19.26	67.628	0.947	**CONSOLIDATION**

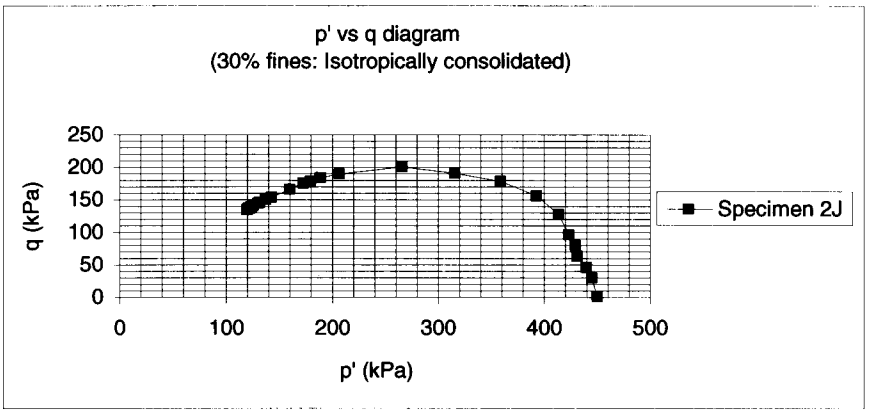
3.) Shear data

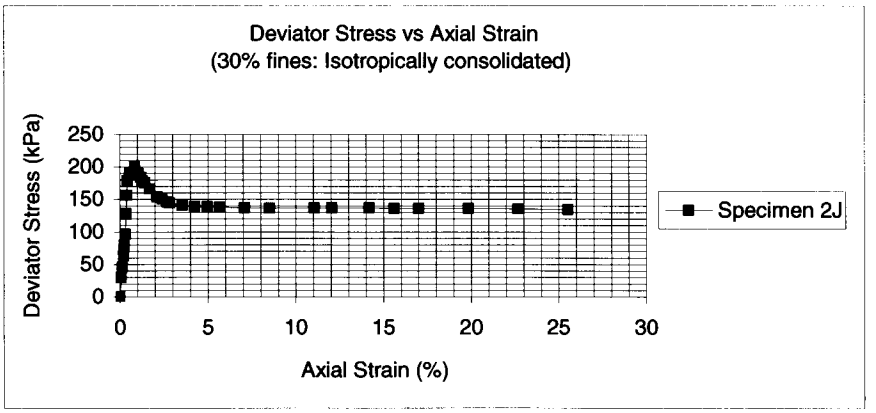
Volume change 1:		Volume change 2:		Sample Vol. change (cm^3)	19.19	B value	0.97
Air Flushing (cm^3)	1.90	Sat/Cons. (cm^3)	36.55	L_{cons} (mm)	70.54	p'consolidation (kPa)	450
Cell Expansion (cm^3)	0.00	Cell Expsn.(cm^3)	19.26	A_{cons} (cm^2)	9.721	Void ratio (e_1)	0.947

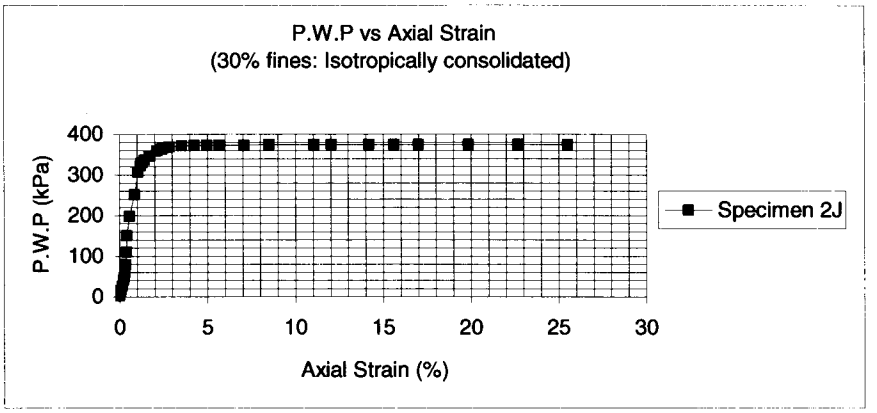
Proof ring properties		Strain gauge properties	
Proof ring No.	5153	1 strain division (mm)	0.01
Proof ring factor (dN/div)	7.512		

Strain Gauge (divs)	Axial Strain	Axial Strain (%)	Change Prf. ring (divs)	Change P.W.P (kPa)	q (Uncortd) (kPa)	Membrn. Corrctn. (kPa)	q (kPa)	t (kPa)	p' (kPa)	s' (kPa)
0	0.0000	0.0000	0.0	0.0	0.0	0.0	0.0	0.0	450.0	450.0
5	0.0007	0.0709	38.7	15.0	29.9	0.0	29.8	14.9	444.9	449.9
10	0.0014	0.1418	59.4	25.5	45.8	0.1	45.8	22.9	439.8	447.4
15	0.0021	0.2126	82.3	40.0	63.5	0.1	63.4	31.7	431.1	441.7
18	0.0026	0.2552	103.2	47.0	79.5	0.1	79.4	39.7	429.5	442.7
22	0.0031	0.3119	125.5	59.0	96.7	0.2	96.5	48.3	423.2	439.3
25	0.0035	0.3544	166.4	79.0	128.1	0.2	128.0	64.0	413.7	435.0
28	0.0040	0.3969	203.3	109.5	156.5	0.2	156.3	78.1	392.6	418.6
30	0.0043	0.4253	232.1	150.5	178.6	0.2	178.4	89.2	359.0	388.7
40	0.0057	0.5671	248.7	198.0	191.1	0.3	190.8	95.4	315.6	347.4
60	0.0085	0.8506	262.4	251.0	201.0	0.4	200.6	100.3	265.9	299.3
75	0.0106	1.0632	248.9	306.5	190.3	0.5	189.8	94.9	206.8	238.4
85	0.0121	1.2050	241.8	322.5	184.6	0.6	184.0	92.0	188.8	219.5
90	0.0128	1.2759	234.9	330.0	179.2	0.6	178.6	89.3	179.5	209.3
100	0.0142	1.4176	231.2	336.0	176.1	0.7	175.4	87.7	172.5	201.7
120	0.0170	1.7012	219.8	345.5	167.0	0.9	166.1	83.1	159.9	187.6
150	0.0213	2.1265	204.7	358.5	154.8	1.0	153.8	76.9	142.8	168.4
170	0.0241	2.4100	200.8	363.0	151.4	1.0	150.4	75.2	137.1	162.2
190	0.0269	2.6935	195.0	367.0	146.6	1.0	145.6	72.8	131.5	155.8
200	0.0284	2.8353	193.6	368.0	145.4	1.0	144.4	72.2	130.1	154.2
250	0.0354	3.5441	190.1	371.5	141.7	1.0	140.7	70.3	125.4	148.8
300	0.0425	4.2529	189.0	372.0	139.8	1.0	138.8	69.4	124.3	147.4
350	0.0496	4.9618	190.3	373.0	139.8	1.0	138.8	69.4	123.3	146.4
400	0.0567	5.6706	190.7	373.0	139.0	1.0	138.0	69.0	123.0	146.0

Strain Gauge (divs)	Axial Strain	Axial Strain (%)	Change Prf. ring (divs)	Change P.W.P (kPa)	q (Uncortd) (kPa)	Membrn. Corrctn. (kPa)	q (kPa)	t (kPa)	p' (kPa)	s' (kPa)
500	0.0709	7.0882	192.3	373.5	138.1	1.0	137.1	68.5	122.2	145.0
600	0.0851	8.5059	194.4	374.5	137.4	1.0	136.4	68.2	121.0	143.7
780	0.1106	11.0577	200.5	374.5	137.8	1.0	136.8	68.4	121.1	143.9
850	0.1205	12.0500	202.7	374.5	137.8	1.0	136.8	68.4	121.1	143.9
1000	0.1418	14.1765	207.8	374.5	137.8	1.0	136.8	68.4	121.1	143.9
1100	0.1559	15.5941	209.9	374.5	136.9	1.0	135.9	68.0	120.8	143.5
1200	0.1701	17.0118	213.2	374.5	136.7	1.0	135.7	67.9	120.7	143.4
1400	0.1985	19.8471	221.3	374.5	137.1	1.0	136.1	68.0	120.9	143.5
1600	0.2268	22.6824	228.0	374.5	136.2	1.0	135.2	67.6	120.6	143.1
1800	0.2552	25.5177	235.1	375.0	135.3	1.0	134.3	67.2	119.8	142.2







Test	**Case 1: Monotonic Undrained Compression of Isotropically Consolidated Specimens**		
Cell No.	3 (Big)	Fines content (%)	30
Specimen	3J	Specific gravity (g/cm^3)	2.72

1.) Sample physical properties

Wet mass before test (g)	817.799	m.c before test (%)	9.10	Height (mm)	152.05	Volume (cm^3)	689.769
Wet mass after test (g)	925.739	m.c. after test (%)	23.50	Diameter (mm)	76.00		
Dry mass (g)	749.587	Dry density (kg/m^3)	1087	Area (cm^2)	45.365	Void ratio (e_0)	1.503

2.) Saturation/Consolidation

Date	C.P (kPa)	P.W.P bp closed (kPa)	B.P (kPa)	P.W.P bp open (kPa)	Change C.P (kPa)	Change P.W.P (kPa)	B value	Volume Gauge (cm^3)	Cell Expansn (cm^3)	Specimen Volume (cm^3)	Void Ratio	Comments
16/1	0		0	-1.5				0.00	0.00	689.769	1.503	
16/1	15.6		12.3	7.5				8.20	0.00	681.569	1.473	**AIR-FLUSHING**
16/1	50	15.5	40	37.5	34.4	8.0	0.23	31.24	6.08	664.609	1.412	**S**
17/1	100	54.0	90	88.0	50	16.5	0.33	50.08	8.77	648.459	1.353	**A**
18/1	150	112.5	140	139.5	50	24.5	0.49	64.88	10.65	635.539	1.306	**T**
19/1	200	169.5	190	188.5	50	30.0	0.60	78.74	12.00	623.029	1.261	**U**
20/1	250	224.0	240	240.0	50	35.5	0.71	88.02	13.63	615.379	1.233	**R**
21/1	300	277.5	290	290.0	50	37.5	0.75	94.89	15.06	609.939	1.213	**A**
22/1	350	331.0	340	340.0	50	41.0	0.82	99.16	16.08	606.689	1.201	**T**
23/1	400	383.0	390	390.0	50	43.0	0.86	103.23	18.12	604.659	1.194	**I**
24/1	450	437.0	440	440.0	50	47.0	0.94	106.33	19.91	603.349	1.189	**O**
25/1	500	488.5	450	450.0	50	48.5	0.97					**N**
25/1	800		450	450.0				158.60	24.18	555.349	1.015	**CONSOLIDATION**

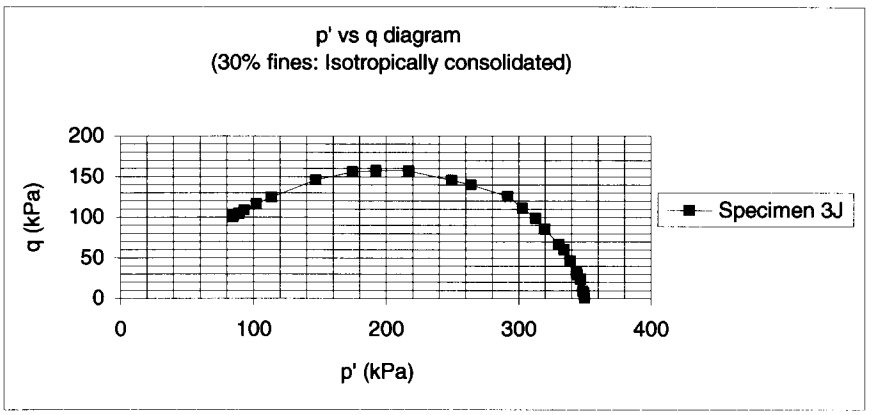
3.) Shear data

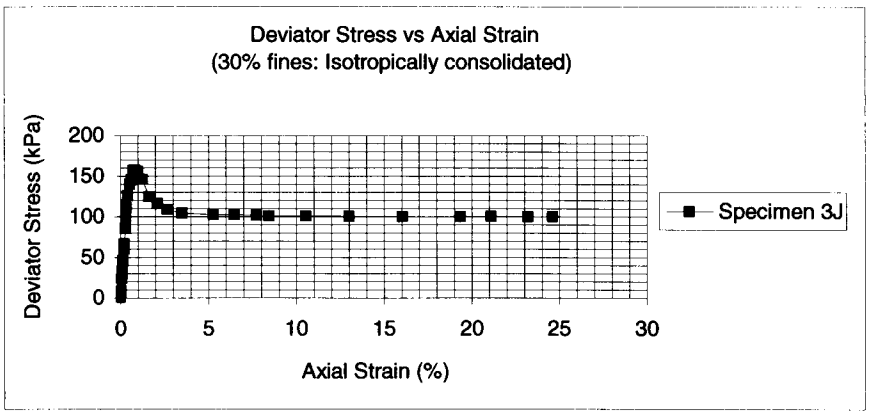
Volume change 1:		Volume change 2:		Sample Vol. change (cm^3)	134.42	B value	0.97
Air Flushing (cm^3)	8.20	Sat/Cons. (cm^3)	150.40	L_{cons} (mm)	142.17	p'consolidation (kPa)	350
Cell Expansion (cm^3)	0.00	Cell Expsn.(cm^3)	24.18	A_{cons} (cm^2)	39.471	Void ratio (e_1)	1.015

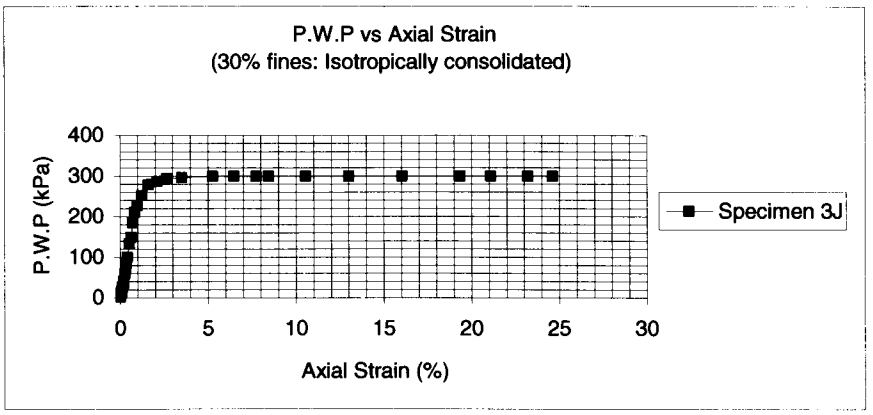
Proof ring properties		Strain gauge properties	
Proof ring No.	4541	1 strain division (mm)	0.01
Proof ring factor (dN/div)	25.77		

Strain Gauge (divs)	Axial Strain	Axial Strain (%)	Change Prf. ring (divs)	Change P.W.P (kPa)	q (Uncortd) (kPa)	Membm. Corrctn. (kPa)	q (kPa)	t (kPa)	p' (kPa)	s' (kPa)
0	0.0000	0.0000	0.0	0.0	0.0	0.0	0.0	0.0	350.0	350.0
2	0.0001	0.0141	11.2	3.0	7.3	0.0	7.3	3.7	349.4	350.7
5	0.0004	0.0352	14.2	4.5	9.3	0.0	9.3	4.6	348.6	350.1
10	0.0007	0.0703	36.4	11.0	23.7	0.0	23.7	11.9	346.9	350.9
12	0.0008	0.0844	45.2	15.5	29.5	0.0	29.4	14.7	344.3	349.2
15	0.0011	0.1055	51.0	17.5	33.3	0.1	33.2	16.6	343.6	349.1
20	0.0014	0.1407	71.3	26.5	46.5	0.1	46.4	23.2	339.0	346.7
30	0.0021	0.2110	92.4	35.5	60.2	0.1	60.1	30.0	334.5	344.5
30	0.0021	0.2110	101.9	41.5	66.4	0.1	66.3	33.1	330.6	341.6
40	0.0028	0.2813	131.3	58.5	85.5	0.1	85.3	42.7	319.9	334.2
45	0.0032	0.3165	152.2	70.0	99.1	0.2	98.9	49.4	313.0	329.4
50	0.0035	0.3517	171.1	84.0	111.3	0.2	111.1	55.6	303.0	321.6
60	0.0042	0.4220	193.7	100.0	125.9	0.2	125.7	62.9	291.9	312.9
75	0.0053	0.5275	215.9	132.5	140.2	0.3	140.0	70.0	264.2	287.5
90	0.0063	0.6330	224.8	149.0	145.8	0.3	145.5	72.8	249.5	273.8
105	0.0074	0.7385	242.4	185.0	157.1	0.4	156.7	78.4	217.2	243.4
120	0.0084	0.8440	243.5	210.0	157.6	0.4	157.2	78.6	192.4	218.6
140	0.0098	0.9847	241.6	227.0	156.2	0.5	155.7	77.8	174.9	200.8
180	0.0127	1.2661	227.3	251.5	146.5	0.6	145.9	72.9	147.1	171.4
230	0.0162	1.6177	195.4	278.0	125.5	0.8	124.7	62.4	113.6	134.4
300	0.0211	2.1101	183.5	286.5	117.3	1.0	116.3	58.1	102.3	121.6
380	0.0267	2.6728	172.4	293.0	109.5	1.0	108.5	54.3	93.2	111.3
500	0.0352	3.5168	167.3	295.5	105.4	1.0	104.4	52.2	89.3	106.7
750	0.0528	5.2753	167.0	299.0	103.3	1.0	102.3	51.1	85.1	102.1

Strain Gauge (divs)	Axial Strain	Axial Strain (%)	Change Prf. ring (divs)	Change P.W.P (kPa)	q (Uncortd) (kPa)	Membm. Corrctn. (kPa)	q (kPa)	t (kPa)	p' (kPa)	s' (kPa)
920	0.0647	6.4710	169.2	299.0	103.3	1.0	102.3	51.2	85.1	102.2
1100	0.0774	7.7371	170.1	299.0	102.5	1.0	101.5	50.7	84.8	101.7
1200	0.0844	8.4404	170.4	299.0	101.9	1.0	100.9	50.4	84.6	101.4
1500	0.1055	10.5505	174.3	299.0	101.8	1.0	100.8	50.4	84.6	101.4
1850	0.1301	13.0123	178.5	299.0	101.4	1.0	100.4	50.2	84.5	101.2
2280	0.1604	16.0368	184.6	299.0	101.2	1.0	100.2	50.1	84.4	101.1
2750	0.1934	19.3426	192.0	299.0	101.1	1.0	100.1	50.1	84.4	101.1
3000	0.2110	21.1011	196.5	299.0	101.2	1.0	100.2	50.1	84.4	101.1
3300	0.2321	23.2112	201.8	299.0	101.2	1.0	100.2	50.1	84.4	101.1
3500	0.2462	24.6179	205.0	299.0	100.9	1.0	99.9	49.9	84.3	100.9







Test	Case 1: Monotonic Undrained Compression of Isotropically Consolidated Specimens		
Cell No.	6 (Big)	Fines content (%)	30
Specimen	6h	Specific gravity (g/cm^3)	2.72

1.) Sample physical properties

Wet mass before test (g)	838.535	m.c before test (%)	8.90	Height (mm)	151.85	Volume (cm^3)	687.955
Wet mass after test (g)	955.576	m.c. after test (%)	24.10	Diameter (mm)	75.95		
Dry mass (g)	770.005	Dry density (kg/m^3)	1119	Area (cm^2)	45.305	Void ratio (e_0)	1.430

2.) Saturation/Consolidation

Date	C.P (kPa)	P.W.P bp closed (kPa)	B.P (kPa)	P.W.P bp open (kPa)	Change C.P (kPa)	Change P.W.P (kPa)	B value	Volume Gauge (cm^3)	Cell Expansn (cm^3)	Specimen Volume (cm^3)	Void Ratio	Comments
15/12	0		0	-1.0				0.00	0.00	687.955	1.430	
15/12	18.0		15.3	10.0				10.70	0.00	677.255	1.392	**AIR-FLUSHING**
15/12	50	19.0	40	37.5	32.0	9.0	0.28	43.00	7.94	652.895	1.306	**S**
16/12	100	59.5	90	88.5	50	22.0	0.44	61.00	10.71	637.665	1.253	**A**
17/12	150	116.5	140	139.0	50	28.0	0.56	74.00	12.51	626.465	1.213	**T**
18/12	200	175.5	190	189.5	50	36.5	0.73	83.00	13.93	618.885	1.186	**U**
19/12	250	229.0	240	240.0	50	39.5	0.79	91.00	15.40	612.355	1.163	**R**
20/12	300	282.5	290	290.0	50	42.5	0.85	99.10	16.91	605.765	1.140	**A**
21/12	350	336.5	340	340.0	50	46.5	0.93	103.15	18.26	603.065	1.130	**T**
22/12	400	387.0	390	390.0	50	47.0	0.94	107.00	20.38	601.335	1.124	**I**
23/12	450	437.5	440	440.0	50	47.5	0.95	109.58	21.85	600.225	1.120	**O**
24/12	500	488.5	490	490.0	50	48.5	0.97					**N**
24/12	800		500	500.0				169.70	28.88	547.135	0.933	**CONSOLIDATION**

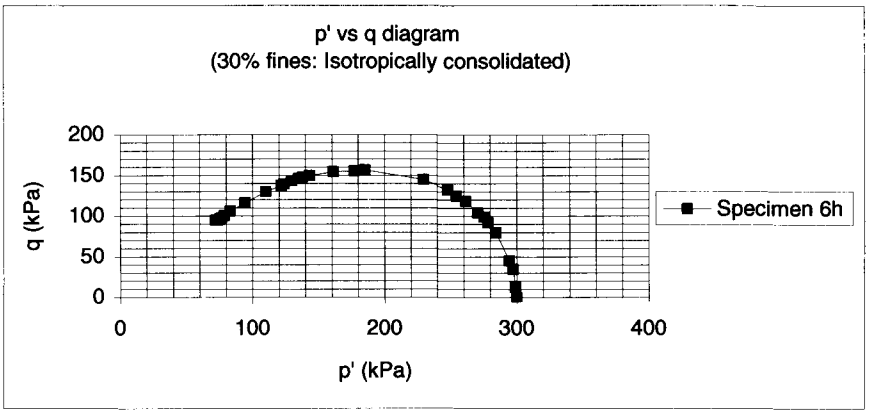
3.) Shear data

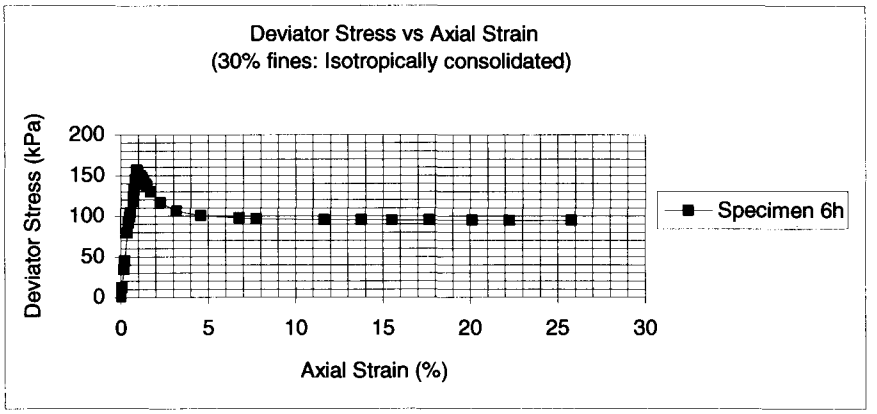
Volume change 1:		Volume change 2:		Sample Vol. change (cm^3)	140.82	B value	0.97
Air Flushing (cm^3)	10.70	Sat/Cons. (cm^3)	159.00	L_{cons} (mm)	141.49	p'consolidation (kPa)	300
Cell Expansion (cm^3)	0.00	Cell Expsn.(cm^3)	28.88	A_{cons} (cm^2)	39.123	Void ratio (e_1)	0.933

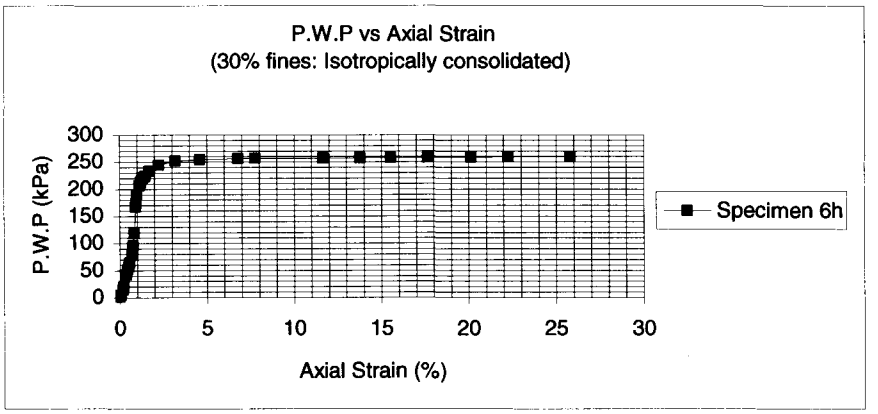
Proof ring properties		Strain gauge properties	
Proof ring No.	4541	1 strain division (mm)	0.01
Proof ring factor (dN/div)	25.77		

Strain Gauge (divs)	Axial Strain	Axial Strain (%)	Change Prf. ring (divs)	Change P.W.P (kPa)	q (Uncortd) (kPa)	Membrn. Corrctn. (kPa)	q (kPa)	t (kPa)	p' (kPa)	s' (kPa)
0	0.0000	0.0000	0.0	0.0	0.0	0.0	0.0	0.0	300.0	300.0
10	0.0007	0.0707	18.7	5.0	12.3	0.0	12.3	6.1	299.1	301.1
25	0.0018	0.1767	52.3	14.0	34.4	0.1	34.3	17.2	297.4	303.2
35	0.0025	0.2474	68.9	20.5	45.3	0.1	45.1	22.6	294.5	302.1
55	0.0039	0.3887	121.3	42.0	79.6	0.2	79.4	39.7	284.5	297.7
65	0.0046	0.4594	140.0	52.0	91.8	0.2	91.6	45.8	278.5	293.8
75	0.0053	0.5301	151.4	57.5	99.2	0.3	98.9	49.5	275.5	292.0
80	0.0057	0.5654	158.9	64.0	104.1	0.3	103.8	51.9	270.6	287.9
100	0.0071	0.7068	181.2	78.0	118.5	0.4	118.2	59.1	261.4	281.1
105	0.0074	0.7421	190.8	87.0	124.7	0.4	124.4	62.2	254.5	275.2
110	0.0078	0.7774	202.3	96.0	132.2	0.4	131.8	65.9	247.9	269.9
120	0.0085	0.8481	222.1	118.5	145.1	0.4	144.6	72.3	229.7	253.8
130	0.0092	0.9188	240.8	167.0	157.2	0.5	156.7	78.3	185.2	211.3
135	0.0095	0.9541	239.1	174.5	156.0	0.5	155.5	77.8	177.3	203.3
140	0.0099	0.9895	237.3	190.0	154.8	0.5	154.3	77.1	161.4	187.1
160	0.0113	1.1308	230.2	206.5	149.9	0.6	149.4	74.7	143.3	168.2
170	0.0120	1.2015	227.4	211.0	148.0	0.6	147.4	73.7	138.1	162.7
175	0.0124	1.2368	225.0	213.5	146.4	0.6	145.8	72.9	135.1	159.4
185	0.0131	1.3075	221.1	218.0	143.7	0.7	143.1	71.5	129.7	153.5
200	0.0141	1.4135	215.6	222.5	140.0	0.7	139.3	69.7	123.9	147.2
210	0.0148	1.4842	212.3	224.0	137.8	0.7	137.0	68.5	121.7	144.5
240	0.0170	1.6962	201.4	233.0	130.4	0.8	129.6	64.8	110.2	131.8
320	0.0226	2.2617	182.2	244.5	117.3	1.0	116.3	58.2	94.3	113.7
450	0.0318	3.1805	167.5	252.0	106.8	1.0	105.8	52.9	83.3	100.9

Strain Gauge (divs)	Axial Strain	Axial Strain (%)	Change Prf. ring (divs)	Change P.W.P (kPa)	q (Uncortd) (kPa)	Membrn. Corrctn. (kPa)	q (kPa)	t (kPa)	p' (kPa)	s' (kPa)
650	0.0459	4.5940	161.3	254.5	101.4	1.0	100.4	50.2	79.0	95.7
960	0.0678	6.7850	160.8	256.0	98.7	1.0	97.7	48.9	76.6	92.9
1100	0.0777	7.7745	160.4	256.5	97.4	1.0	96.4	48.2	75.6	91.7
1650	0.1166	11.6617	165.2	257.0	96.1	1.0	95.1	47.6	74.7	90.6
1950	0.1378	13.7820	169.3	257.5	96.1	1.0	95.1	47.6	74.2	90.1
2200	0.1555	15.5489	172.4	258.0	95.9	1.0	94.9	47.5	73.6	89.5
2500	0.1767	17.6692	176.5	258.0	95.7	1.0	94.7	47.4	73.6	89.4
2850	0.2014	20.1429	181.9	258.5	95.7	1.0	94.7	47.3	73.1	88.8
3150	0.2226	22.2632	186.1	259.5	95.3	1.0	94.3	47.1	71.9	87.6
3650	0.2580	25.7970	195.2	259.5	95.4	1.0	94.4	47.2	72.0	87.7







Test	Case 1: Monotonic Undrained Compression of Isotropically Consolidated Specimens		
Cell No.	2 (Big)	Fines content (%)	30
Specimen	2k	Specific gravity (g/cm^3)	2.72

1.) Sample physical properties

Wet mass before test (g)	852.204	m.c before test (%)	9.40	Height (mm)	152.15	Volume (cm^3)	689.314
Wet mass after test (g)	953.549	m.c. after test (%)	22.41	Diameter (mm)	75.95		
Dry mass (g)	778.980	Dry density (kg/m^3)	1130	Area (cm^2)	45.305	Void ratio (e_0)	1.407

2.) Saturation/Consolidation

Date	C.P (kPa)	P.W.P bp closed (kPa)	B.P (kPa)	P.W.P bp open (kPa)	Change C.P (kPa)	Change P.W.P (kPa)	B value	Volume Gauge (cm^3)	Cell Expansn (cm^3)	Specimen Volume (cm^3)	Void Ratio	Comments
29/1	0		0	0.0				0.00	0.00	689.314	1.407	
29/1	19.7		15.5	11.0				13.10	0.00	676.214	1.361	**AIR-FLUSHING**
29/1	50	17.0	40	37.5	30.3	6.0	0.20	38.09	7.06	658.284	1.299	**S**
30/1	100	58.5	90	89.0	50	21.0	0.42	57.86	9.79	641.244	1.239	**A**
31/1	150	120.0	140	140.0	50	31.0	0.62	74.59	11.63	626.354	1.187	**T**
1/2	200	175.0	190	190.0	50	35.0	0.70	86.10	13.02	616.234	1.152	**U**
2/2	250	230.0	240	240.0	50	40.0	0.80	96.87	14.57	607.014	1.120	**R**
3/2	300	282.0	290	290.0	50	42.0	0.84	107.15	16.03	598.194	1.089	**A**
4/2	350	334.5	340	340.0	50	44.5	0.89	114.98	17.22	591.554	1.066	**T**
5/2	400	386.0	390	390.0	50	46.0	0.92	120.57	19.30	588.044	1.053	**I**
6/2	450	437.0	440	440.0	50	47.0	0.94	125.42	20.93	584.824	1.042	**O**
7/2	500	488.5	450	450.0	50	48.5	0.97					**N**
7/2	950		450	450.0				185.60	27.66	531.374	0.855	**CONSOLIDATION**

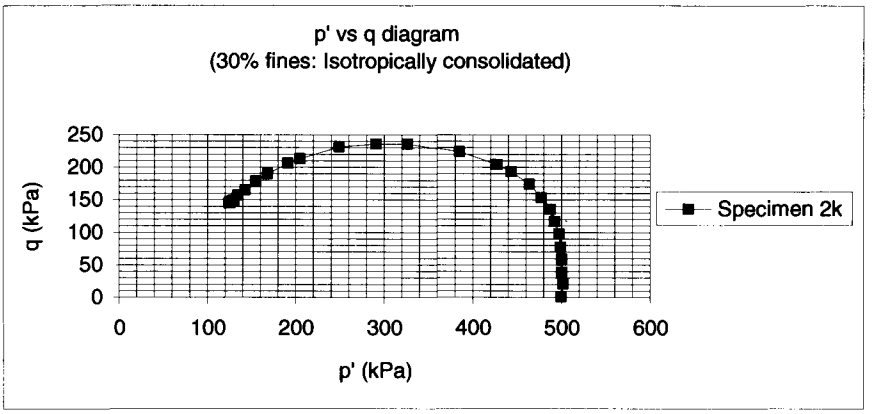
3.) Shear data

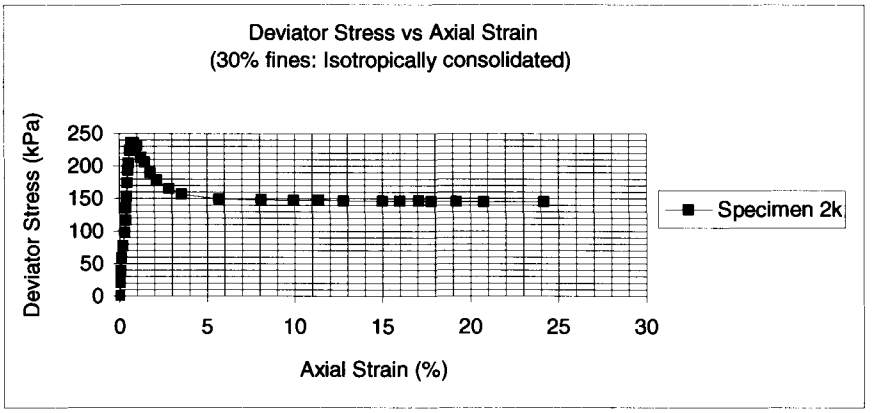
Volume change 1:		Volume change 2:		Sample Vol. change (cm^3)	157.94	B value	0.97
Air Flushing (cm^3)	13.10	Sat/Cons. (cm^3)	172.50	L_{cons} (mm)	140.53	p'consolidation (kPa)	500
Cell Expansion (cm^3)	0.00	Cell Expsn.(cm^3)	27.66	A_{cons} (cm^2)	38.385	Void ratio (e_1)	0.855

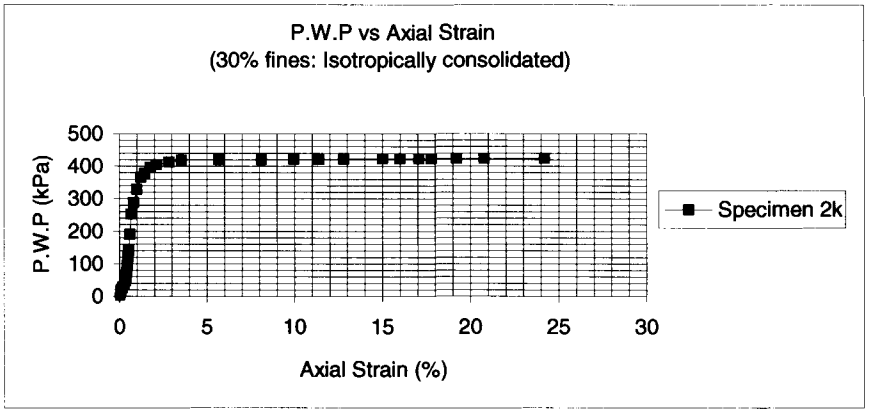
Proof ring properties		Strain gauge properties	
Proof ring No.	1800	1 strain division (mm)	0.01
Proof ring factor (dN/div)	14.846		

Strain Gauge (divs)	Axial Strain	Axial Strain (%)	Change Prf. ring (divs)	Change P.W.P (kPa)	q (Uncortd) (kPa)	Membm. Corrctn. (kPa)	q (kPa)	t (kPa)	p' (kPa)	s' (kPa)
0	0.0000	0.0000	0.0	0.0	0.0	0.0	0.0	0.0	500.0	500.0
5	0.0004	0.0356	53.4	5.0	20.6	0.0	20.6	10.3	501.9	505.3
10	0.0007	0.0712	99.2	12.0	38.3	0.0	38.3	19.2	500.8	507.2
15	0.0011	0.1067	152.5	19.0	58.9	0.1	58.9	29.4	500.6	510.4
25	0.0018	0.1779	199.5	26.5	77.0	0.1	76.9	38.5	499.1	512.0
40	0.0028	0.2846	252.3	35.0	97.3	0.1	97.2	48.6	497.4	513.6
50	0.0036	0.3558	303.1	46.5	116.8	0.2	116.6	58.3	492.4	511.8
55	0.0039	0.3914	352.2	57.5	135.7	0.2	135.5	67.7	487.7	510.2
60	0.0043	0.4270	397.9	73.5	153.2	0.2	153.0	76.5	477.5	503.0
65	0.0046	0.4625	452.3	94.0	174.1	0.2	173.9	86.9	464.0	492.9
70	0.0050	0.4981	502.5	121.0	193.4	0.2	193.1	96.6	443.4	475.6
75	0.0053	0.5337	531.6	140.5	204.5	0.3	204.2	102.1	427.6	461.6
85	0.0060	0.6049	583.4	189.5	224.3	0.3	224.0	112.0	385.2	422.5
95	0.0068	0.6760	614.5	252.0	236.1	0.3	235.7	117.9	326.6	365.9
115	0.0082	0.8183	614.9	287.5	235.9	0.4	235.5	117.7	291.0	330.2
140	0.0100	0.9962	605.0	328.0	231.7	0.5	231.2	115.6	249.1	287.6
175	0.0125	1.2453	559.6	366.0	213.7	0.6	213.1	106.6	205.0	240.6
205	0.0146	1.4588	542.1	377.5	206.6	0.7	205.9	102.9	191.1	225.4
250	0.0178	1.7790	502.3	395.0	190.8	0.9	189.9	95.0	168.3	200.0
300	0.0213	2.1348	473.5	404.5	179.2	1.0	178.2	89.1	154.9	184.6
400	0.0285	2.8464	442.1	412.0	166.1	1.0	165.1	82.6	143.0	170.6
500	0.0356	3.5580	422.4	417.5	157.6	1.0	156.6	78.3	134.7	160.8
800	0.0569	5.6928	412.3	419.5	150.4	1.0	149.4	74.7	130.3	155.2
1140	0.0811	8.1122	420.5	420.0	149.4	1.0	148.4	74.2	129.5	154.2

Strain Gauge (divs)	Axial Strain	Axial Strain (%)	Change Prf. ring (divs)	Change P.W.P (kPa)	q (Uncortd) (kPa)	Membrn. Corrctn. (kPa)	q (kPa)	t (kPa)	p' (kPa)	s' (kPa)
1400	0.0996	9.9623	425.9	420.5	148.3	1.0	147.3	73.7	128.6	153.2
1600	0.1139	11.3855	433.3	421.0	148.5	1.0	147.5	73.8	128.2	152.8
1800	0.1281	12.8087	438.7	422.0	147.9	1.0	146.9	73.5	127.0	151.5
2110	0.1501	15.0146	448.6	423.0	147.5	1.0	146.5	73.2	125.8	150.2
2250	0.1601	16.0109	453.5	423.0	147.3	1.0	146.3	73.2	125.8	150.2
2400	0.1708	17.0783	460.2	423.0	147.6	1.0	146.6	73.3	125.9	150.3
2500	0.1779	17.7899	461.5	423.0	146.7	1.0	145.7	72.9	125.6	149.9
2700	0.1921	19.2131	468.8	423.0	146.5	1.0	145.5	72.7	125.5	149.7
2920	0.2078	20.7786	476.0	423.0	145.8	1.0	144.8	72.4	125.3	149.4
3400	0.2419	24.1942	498.3	423.5	146.1	1.0	145.1	72.5	124.9	149.0







Test	**Case 1: Monotonic Undrained Compression of Isotropically Consolidated Specimens**		
Cell No.	3 (Big)	Fines content (%)	30
Specimen	3k	Specific gravity (g/cm^3)	2.72

1.) Sample physical properties

Wet mass before test (g)	862.445	m.c before test (%)	9.00	Height (mm)	151.90	Volume (cm^3)	685.466
Wet mass after test (g)	969.262	m.c. after test (%)	22.50	Diameter (mm)	75.80		
Dry mass (g)	791.234	Dry density (kg/m^3)	1154	Area (cm^2)	45.126	Void ratio (e_0)	1.356

2.) Saturation/Consolidation

Date	C.P (kPa)	P.W.P bp closed (kPa)	B.P (kPa)	P.W.P bp open (kPa)	Change C.P (kPa)	Change P.W.P (kPa)	B value	Volume Gauge (cm^3)	Cell Expansn (cm^3)	Specimen Volume (cm^3)	Void Ratio	Comments
29/1	0		0	-3.0				0.00	0.00	685.466	1.356	
29/1	13.4		10.0	7.6				7.72	0.00	677.746	1.330	**AIR-FLUSHING**
29/1	50	16.0	40	39.0	36.6	8.4	0.23	30.21	6.08	661.336	1.273	**S**
30/1	100	59.5	90	89.0	50	20.5	0.41	45.89	8.77	648.346	1.229	**A**
31/1	150	118.0	140	140.0	50	29.0	0.58	56.91	10.65	639.206	1.197	**T**
1/2	200	176.0	190	189.5	50	36.0	0.72	65.87	12.00	631.596	1.171	**U**
2/2	250	229.5	240	240.0	50	40.0	0.80	73.16	13.63	625.936	1.152	**R**
3/2	300	283.0	290	290.0	50	43.0	0.86	79.68	15.06	620.846	1.134	**A**
4/2	350	335.0	340	340.0	50	45.0	0.90	85.41	16.08	616.136	1.118	**T**
5/2	400	386.5	390	390.0	50	46.5	0.93	89.76	18.12	613.826	1.110	**I**
6/2	450	437.0	440	440.0	50	47.0	0.94	92.37	19.91	613.006	1.107	**O**
7/2	500	489.0	450	450.0	50	49.0	0.98					**N**
7/2	600		450	450.0				100.61	23.05	607.906	1.090	**CONSOLIDATION**

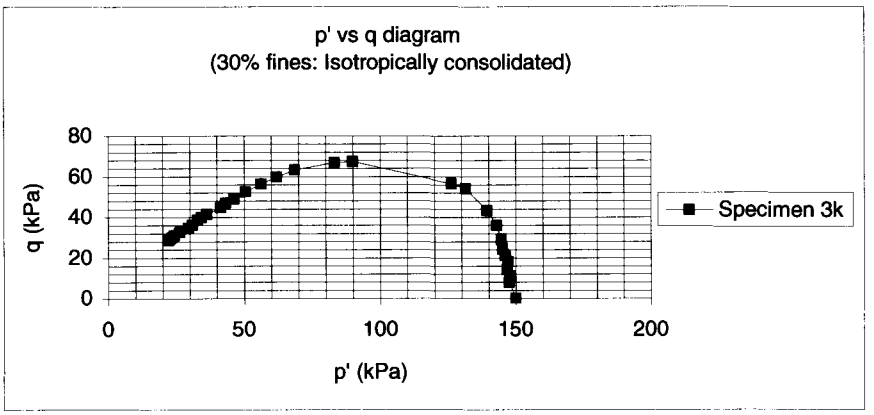
3.) Shear data

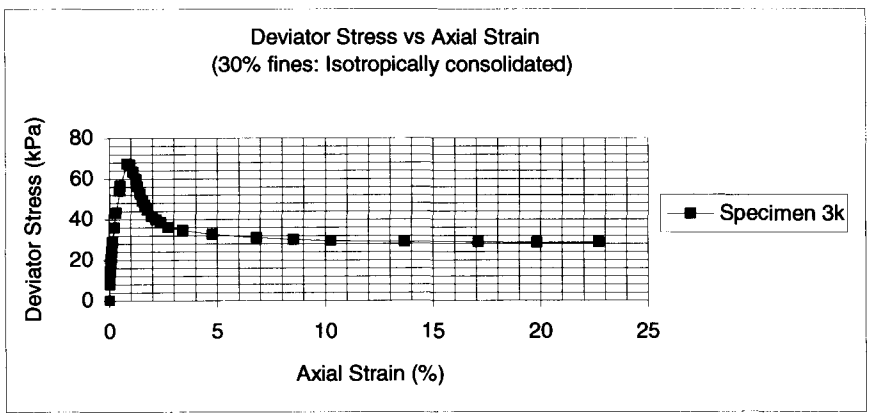
Volume change 1:		Volume change 2:		Sample Vol. change (cm^3)	77.56	B value	0.98
Air Flushing (cm^3)	7.72	Sat/Cons. (cm^3)	92.89	L_{cons} (mm)	146.17	p'consolidation (kPa)	150
Cell Expansion (cm^3)	0.00	Cell Expsn.(cm^3)	23.05	A_{cons} (cm^2)	41.722	Void ratio (e_1)	1.090

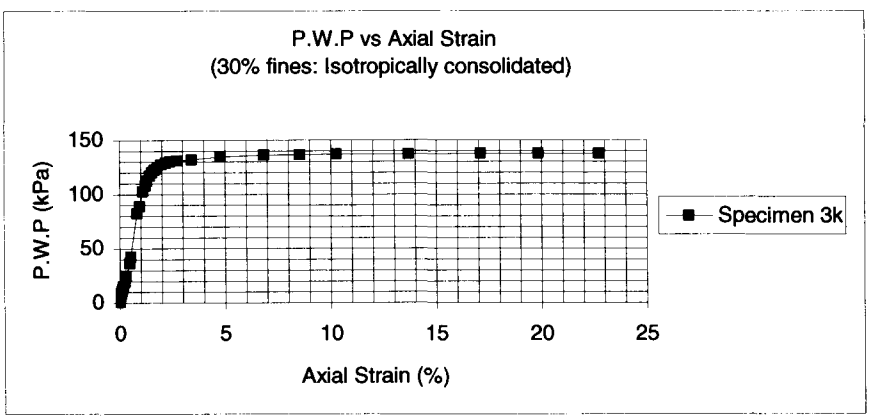
Proof ring properties		Strain gauge properties	
Proof ring No.	1800	1 strain division (mm)	0.01
Proof ring factor (dN/div)	14.846		

Strain Gauge (divs)	Axial Strain	Axial Strain (%)	Change Prf. ring (divs)	Change P.W.P (kPa)	q (Uncortd) (kPa)	Membrn. Corrctn. (kPa)	q (kPa)	t (kPa)	p' (kPa)	s' (kPa)
0	0.0000	0.0000	0.0	0.0	0.0	0.0	0.0	0.0	150.0	150.0
2	0.0001	0.0137	22.3	5.0	7.9	0.0	7.9	4.0	147.6	149.0
5	0.0003	0.0342	31.2	6.0	11.1	0.0	11.1	5.5	147.7	149.5
8	0.0005	0.0547	40.2	8.0	14.3	0.0	14.3	7.1	146.8	149.1
10	0.0007	0.0684	51.4	9.0	18.3	0.0	18.2	9.1	147.1	150.1
15	0.0010	0.1026	59.8	11.0	21.3	0.1	21.2	10.6	146.1	149.6
20	0.0014	0.1368	68.9	13.0	24.5	0.1	24.4	12.2	145.1	149.2
25	0.0017	0.1710	81.8	15.0	29.1	0.1	29.0	14.5	144.7	149.5
35	0.0024	0.2394	101.4	19.0	36.0	0.1	35.9	17.9	143.0	148.9
45	0.0031	0.3079	122.3	25.0	43.4	0.2	43.2	21.6	139.4	146.6
70	0.0048	0.4789	153.2	36.5	54.3	0.2	54.0	27.0	131.5	140.5
75	0.0051	0.5131	160.0	42.5	56.6	0.3	56.4	28.2	126.3	135.7
120	0.0082	0.8210	192.2	82.5	67.8	0.4	67.4	33.7	90.0	101.2
140	0.0096	0.9578	190.9	89.0	67.3	0.5	66.8	33.4	83.3	94.4
160	0.0109	1.0946	181.4	102.5	63.8	0.5	63.3	31.6	68.6	79.1
180	0.0123	1.2314	171.8	108.0	60.4	0.6	59.8	29.9	61.9	71.9
190	0.0130	1.2998	162.3	112.5	57.0	0.6	56.4	28.2	56.3	65.7
210	0.0144	1.4367	151.5	117.0	53.1	0.7	52.4	26.2	50.5	59.2
225	0.0154	1.5393	142.1	120.0	49.8	0.8	49.0	24.5	46.3	54.5
240	0.0164	1.6419	136.3	122.5	47.7	0.8	46.9	23.4	43.1	50.9
260	0.0178	1.7787	130.5	123.5	45.6	0.9	44.7	22.4	41.4	48.9
290	0.0198	1.9840	121.6	127.5	42.4	1.0	41.4	20.7	36.3	43.2
320	0.0219	2.1892	117.4	129.0	40.9	1.0	39.9	19.9	34.3	40.9
350	0.0239	2.3945	114.1	130.0	39.6	1.0	38.6	19.3	32.9	39.3

Strain Gauge (divs)	Axial Strain	Axial Strain (%)	Change Prf. ring (divs)	Change P.W.P (kPa)	q (Uncortd) (kPa)	Membrn. Corrctn. (kPa)	q (kPa)	t (kPa)	p' (kPa)	s' (kPa)
400	0.0274	2.7365	107.2	131.0	37.1	1.0	36.1	18.1	31.0	37.1
500	0.0342	3.4207	103.6	132.0	35.6	1.0	34.6	17.3	29.5	35.3
700	0.0479	4.7889	99.2	134.5	33.6	1.0	32.6	16.3	26.4	31.8
1000	0.0684	6.8413	96.5	136.0	32.0	1.0	31.0	15.5	24.3	29.5
1250	0.0855	8.5516	95.4	136.5	31.0	1.0	30.0	15.0	23.5	28.5
1500	0.1026	10.2620	95.3	137.0	30.4	1.0	29.4	14.7	22.8	27.7
2000	0.1368	13.6826	97.5	137.0	29.9	1.0	28.9	14.5	22.6	27.5
2500	0.1710	17.1033	101.2	137.5	29.9	1.0	28.9	14.4	22.1	26.9
2900	0.1984	19.8398	103.3	137.5	29.5	1.0	28.5	14.2	22.0	26.7
3320	0.2271	22.7131	107.5	137.5	29.6	1.0	28.6	14.3	22.0	26.8







Test	Case 1: Monotonic Undrained Compression of Isotropically Consolidated Specimens		
Cell No.	2 (Big)	Fines content (%)	30
Specimen	2L	Specific gravity (g/cm^3)	2.72

1.) Sample physical properties

Wet mass before test (g)	897.805	m.c before test (%)	9.20	Height (mm)	151.35	Volume (cm^3)	682.984
Wet mass after test (g)	980.350	m.c. after test (%)	19.24	Diameter (mm)	75.80		
Dry mass (g)	822.166	Dry density (kg/m^3)	1204	Area (cm^2)	45.126	Void ratio (e_0)	1.260

2.) Saturation/Consolidation

Date	C.P (kPa)	P.W.P bp closed (kPa)	B.P (kPa)	P.W.P bp open (kPa)	Change C.P (kPa)	Change P.W.P (kPa)	B value	Volume Gauge (cm^3)	Cell Expansn (cm^3)	Specimen Volume (cm^3)	Void Ratio	Comments
11/2	0		0	-0.5				0.00	0.00	682.984	1.260	
11/2	17.0		14.8	10.0				12.55	0.00	670.434	1.218	**AIR-FLUSHING**
11/2	50	18.0	40	37.5	33.0	8.0	0.24	44.78	7.06	645.264	1.135	**S**
12/2	100	59.0	90	88.0	50	21.5	0.43	68.88	9.79	623.894	1.064	**A**
13/2	150	117.0	140	139.5	50	29.0	0.58	82.91	11.63	611.704	1.024	**T**
14/2	200	175.0	190	190.0	50	35.5	0.71	94.87	13.02	601.134	0.989	**U**
15/2	250	230.5	240	240.0	50	40.5	0.81	102.20	14.57	595.354	0.970	**R**
16/2	300	282.0	290	290.0	50	42.0	0.84	105.86	16.03	593.154	0.962	**A**
17/2	350	335.5	340	340.0	50	45.5	0.91	109.83	17.22	590.374	0.953	**T**
18/2	400	387.0	390	390.0	50	47.0	0.94	113.54	19.30	588.744	0.948	**I**
19/2	450	437.5	440	440.0	50	47.5	0.95	116.35	20.93	587.564	0.944	**O**
20/2	500	489.0	490	490.0	50	49.0	0.98					**N**
20/2	550		500	500.0				125.15	24.32	582.154	0.926	**CONSOLIDATION**

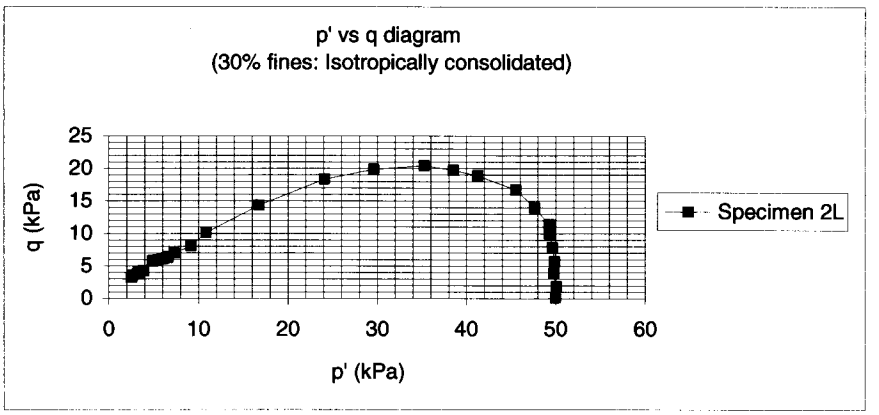
3.) Shear data

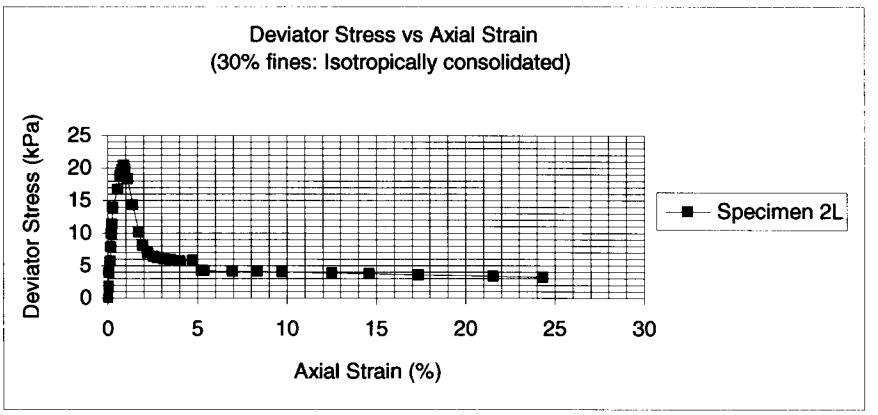
Volume change 1:		Volume change 2:		Sample Vol. change (cm^3)	100.83	B value	0.98
Air Flushing (cm^3)	12.55	Sat/Cons. (cm^3)	112.60	L_{cons} (mm)	143.90	p'consolidation (kPa)	50
Cell Expansion (cm^3)	0.00	Cell Expsn.(cm^3)	24.32	A_{cons} (cm^2)	40.685	Void ratio (e_1)	0.926

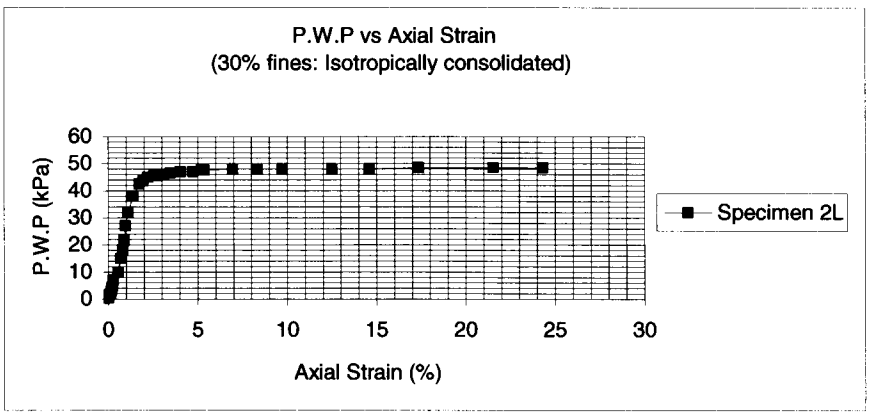
Proof ring properties		Strain gauge properties	
Proof ring No.	5153	1 strain division (mm)	0.01
Proof ring factor (dN/div)	7.512		

Strain Gauge (divs)	Axial Strain	Axial Strain (%)	Change Prf. ring (divs)	Change P.W.P (kPa)	q (Uncortd) (kPa)	Membrn. Corrctn. (kPa)	q (kPa)	t (kPa)	p' (kPa)	s' (kPa)
0	0.0000	0.0000	0.0	0.0	0.0	0.0	0.0	0.0	50.0	50.0
5	0.0003	0.0347	10.0	0.5	1.8	0.0	1.8	0.9	50.1	50.4
8	0.0006	0.0556	21.3	1.5	3.9	0.0	3.9	2.0	49.8	50.5
20	0.0014	0.1390	31.1	2.0	5.7	0.1	5.7	2.8	49.9	50.8
25	0.0017	0.1737	43.2	3.0	8.0	0.1	7.9	3.9	49.6	50.9
30	0.0021	0.2085	54.5	4.0	10.0	0.1	9.9	5.0	49.3	51.0
34	0.0024	0.2363	62.3	4.5	11.5	0.1	11.4	5.7	49.3	51.2
40	0.0028	0.2780	76.5	7.0	14.1	0.1	13.9	7.0	47.6	50.0
80	0.0056	0.5559	92.4	10.0	17.0	0.3	16.7	8.3	45.6	48.3
100	0.0069	0.6949	104.9	15.0	19.2	0.3	18.9	9.4	41.3	44.4
115	0.0080	0.7992	109.8	18.0	20.1	0.4	19.7	9.9	38.6	41.9
130	0.0090	0.9034	114.0	21.5	20.9	0.5	20.4	10.2	35.3	38.7
140	0.0097	0.9729	111.2	27.0	20.3	0.5	19.8	9.9	29.6	32.9
160	0.0111	1.1119	103.5	32.0	18.9	0.6	18.3	9.2	24.1	27.2
200	0.0139	1.3898	82.4	38.0	15.0	0.7	14.3	7.2	16.8	19.2
250	0.0174	1.7373	60.5	42.5	11.0	0.9	10.1	5.1	10.9	12.6
280	0.0195	1.9458	49.9	43.5	9.0	1.0	8.1	4.0	9.2	10.5
320	0.0222	2.2237	44.2	45.0	8.0	1.0	7.0	3.5	7.3	8.5
370	0.0257	2.5712	41.0	45.5	7.4	1.0	6.4	3.2	6.6	7.7
400	0.0278	2.7797	40.2	45.5	7.2	1.0	6.2	3.1	6.6	7.6
450	0.0313	3.1271	39.3	46.0	7.0	1.0	6.0	3.0	6.0	7.0
500	0.0347	3.4746	38.8	46.5	6.9	1.0	5.9	3.0	5.5	6.5
580	0.0403	4.0305	37.7	47.0	6.7	1.0	5.7	2.8	4.9	5.8
680	0.0473	4.7254	38.6	47.0	6.8	1.0	5.8	2.9	4.9	5.9

Strain Gauge (divs)	Axial Strain	Axial Strain (%)	Change Prf. ring (divs)	Change P.W.P (kPa)	q (Uncortd) (kPa)	Membrn. Corrctn. (kPa)	q (kPa)	t (kPa)	p' (kPa)	s' (kPa)
750	0.0521	5.2119	30.0	47.5	5.3	1.0	4.3	2.1	3.9	4.6
770	0.0535	5.3509	29.8	47.5	5.2	1.0	4.2	2.1	3.9	4.6
1000	0.0695	6.9492	29.7	48.0	5.1	1.0	4.1	2.1	3.4	4.1
1200	0.0834	8.3390	30.0	48.0	5.1	1.0	4.1	2.0	3.4	4.0
1400	0.0973	9.7288	30.0	48.0	5.0	1.0	4.0	2.0	3.3	4.0
1800	0.1251	12.5085	30.0	48.0	4.8	1.0	3.8	1.9	3.3	3.9
2100	0.1459	14.5933	30.0	48.0	4.7	1.0	3.7	1.9	3.2	3.9
2500	0.1737	17.3729	30.0	48.5	4.6	1.0	3.6	1.8	2.7	3.3
3100	0.2154	21.5424	30.0	48.5	4.3	1.0	3.3	1.7	2.6	3.2
3500	0.2432	24.3221	30.0	48.5	4.2	1.0	3.2	1.6	2.6	3.1







Test	**Case 1: Monotonic Undrained Compression of Isotropically Consolidated Specimens**		
Cell No.	6 (Small)	Fines content (%)	30
Specimen	6i	Specific gravity (g/cm^3)	2.72

1.) Sample physical properties

Wet mass before test (g)	104.048	m.c before test (%)	10.00	Height (mm)	76.25	Volume (cm^3)	86.704
Wet mass after test (g)	118.615	m.c. after test (%)	25.40	Diameter (mm)	38.05		
Dry mass (g)	94.589	Dry density (kg/m^3)	1091	Area (cm^2)	11.371	Void ratio (e_0)	1.493

2.) Saturation/Consolidation

Date	C.P (kPa)	P.W.P bp closed (kPa)	B.P (kPa)	P.W.P bp open (kPa)	Change C.P (kPa)	Change P.W.P (kPa)	B value	Volume Gauge (cm^3)	Cell Expansn (cm^3)	Specimen Volume (cm^3)	Void Ratio	Comments
27/12	0		0	-1.0				0.00	0.00	86.704	1.493	
27/12	10.0		8.1	4.5				2.20	0.00	84.504	1.430	**AIR-FLUSHING**
27/12	50	14.5	40	37.5	40.0	10.0	0.25	12.34	4.89	79.254	1.279	**S**
28/12	100	60.0	90	88.0	50	22.5	0.45	17.61	7.14	76.234	1.192	**A**
29/12	150	119.0	140	140.0	50	31.0	0.62	21.67	8.53	73.564	1.115	**T**
30/12	200	177.5	190	190.0	50	37.5	0.75	25.10	9.63	71.234	1.048	**U**
31/12	250	229.5	240	240.0	50	39.5	0.79	28.31	10.61	69.004	0.984	**R**
1/1	300	282.5	290	290.0	50	42.5	0.85	31.24	11.67	67.134	0.931	**A**
2/1	350	335.5	340	340.0	50	45.5	0.91	33.41	12.65	65.944	0.896	**T**
3/1	400	386.0	390	390.0	50	46.0	0.92	35.29	13.79	65.204	0.875	**I**
4/1	450	438.0	440	440.0	50	48.0	0.96	36.45	14.56	64.814	0.864	**O**
5/1	500	488.5	450	450.0	50	48.5	0.97					**N**
5/1	650		450	450.0				40.25	17.11	63.564	0.828	**CONSOLIDATION**

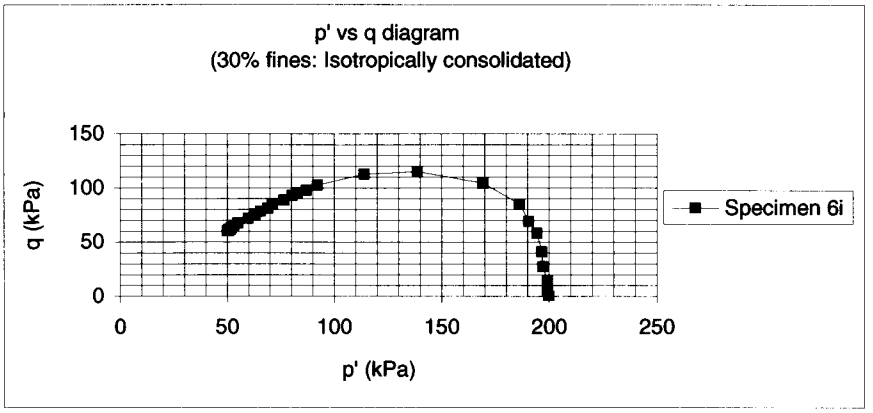
3.) Shear data

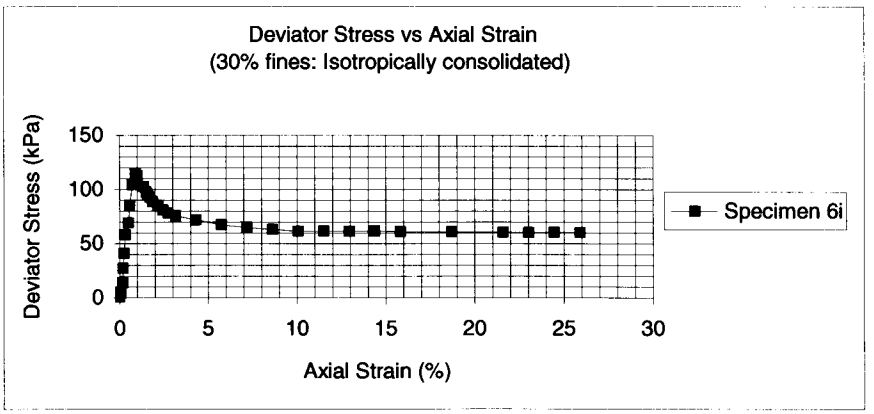
Volume change 1:		Volume change 2:		Sample Vol. change (cm^3)	23.14	B value	0.97
Air Flushing (cm^3)	2.20	Sat/Cons. (cm^3)	38.05	L_{cons} (mm)	69.47	p'consolidation (kPa)	200
Cell Expansion (cm^3)	0.00	Cell Expsn.(cm^3)	17.11	A_{cons} (cm^2)	9.348	Void ratio (e_1)	0.828

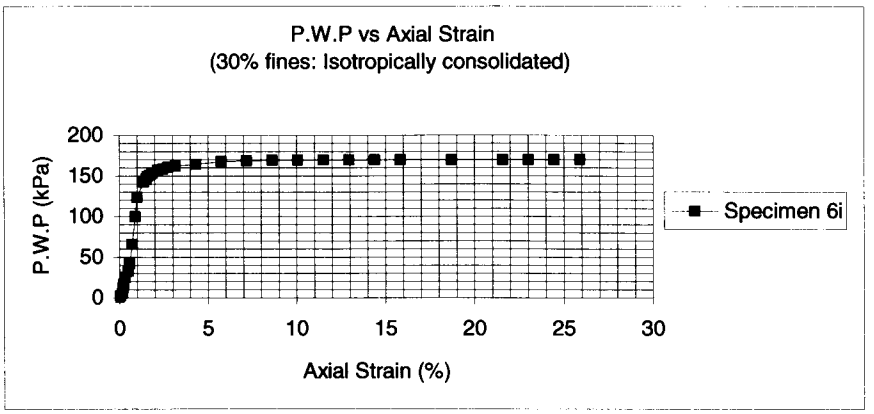
Proof ring properties		Strain gauge properties	
Proof ring No.	4541	1 strain division (mm)	0.01
Proof ring factor (dN/div)	25.77		

Strain Gauge (divs)	Axial Strain	Axial Strain (%)	Change Prf. ring (divs)	Change P.W.P (kPa)	q (Uncortd) (kPa)	Membrn. Corrctn. (kPa)	q (kPa)	t (kPa)	p' (kPa)	s' (kPa)
0	0.0000	0.0000	0.0	0.0	0.0	0.0	0.0	0.0	200.0	200.0
5	0.0007	0.0720	2.0	2.5	5.5	0.0	5.5	2.7	199.3	200.2
12	0.0017	0.1727	5.1	5.5	14.0	0.1	13.9	7.0	199.1	201.5
14	0.0020	0.2015	9.9	12.0	27.2	0.1	27.1	13.6	197.0	201.6
17	0.0024	0.2447	14.9	17.0	41.0	0.1	40.9	20.4	196.6	203.4
22	0.0032	0.3167	21.2	25.0	58.3	0.2	58.1	29.1	194.4	204.1
35	0.0050	0.5038	25.3	32.5	69.4	0.3	69.1	34.6	190.5	202.1
40	0.0058	0.5758	31.1	42.0	85.2	0.3	85.0	42.5	186.3	200.5
50	0.0072	0.7198	38.3	65.5	104.8	0.4	104.5	52.2	169.3	186.7
62	0.0089	0.8925	42.3	99.5	115.6	0.4	115.1	57.6	138.9	158.1
70	0.0101	1.0077	41.5	123.5	113.3	0.5	112.7	56.4	114.1	132.9
95	0.0137	1.3676	38.0	142.0	103.3	0.7	102.6	51.3	92.2	109.3
105	0.0151	1.5115	36.2	145.5	98.3	0.8	97.5	48.8	87.0	103.3
110	0.0158	1.5835	35.5	149.0	96.3	0.8	95.5	47.8	82.8	98.8
120	0.0173	1.7274	34.6	150.5	93.7	0.9	92.9	46.4	80.5	95.9
130	0.0187	1.8714	33.1	153.0	89.5	0.9	88.6	44.3	76.5	91.3
150	0.0216	2.1593	31.7	157.0	85.5	1.0	84.5	42.3	71.2	85.3
170	0.0245	2.4472	30.5	158.0	82.0	1.0	81.0	40.5	69.0	82.5
190	0.0274	2.7351	29.6	160.5	79.4	1.0	78.4	39.2	65.6	78.7
220	0.0317	3.1670	28.7	162.0	76.6	1.0	75.6	37.8	63.2	75.8
300	0.0432	4.3186	27.6	164.0	72.8	1.0	71.8	35.9	59.9	71.9
400	0.0576	5.7582	26.3	167.5	68.3	1.0	67.3	33.7	54.9	66.2
500	0.0720	7.1977	25.6	168.5	65.5	1.0	64.5	32.2	53.0	63.7
600	0.0864	8.6372	25.5	169.0	64.2	1.0	63.2	31.6	52.1	62.6

Strain Gauge (divs)	Axial Strain	Axial Strain (%)	Change Prf. ring (divs)	Change P.W.P (kPa)	q (Uncortd) (kPa)	Membm. Corrctn. (kPa)	q (kPa)	t (kPa)	p' (kPa)	s' (kPa)
700	0.1008	10.0768	25.2	169.0	62.5	1.0	61.5	30.7	51.5	61.7
800	0.1152	11.5163	25.7	169.5	62.7	1.0	61.7	30.8	51.1	61.3
900	0.1296	12.9559	26.0	169.5	62.4	1.0	61.4	30.7	51.0	61.2
1000	0.1440	14.3954	26.5	169.5	62.5	1.0	61.5	30.8	51.0	61.3
1100	0.1583	15.8349	26.8	169.5	62.2	1.0	61.2	30.6	50.9	61.1
1300	0.1871	18.7140	27.6	169.5	61.8	1.0	60.8	30.4	50.8	60.9
1500	0.2159	21.5931	28.4	169.5	61.4	1.0	60.4	30.2	50.6	60.7
1600	0.2303	23.0326	28.8	169.5	61.1	1.0	60.1	30.1	50.5	60.6
1700	0.2447	24.4722	29.5	169.5	61.4	1.0	60.4	30.2	50.6	60.7
1800	0.2591	25.9117	30.0	170.0	61.3	1.0	60.3	30.1	50.1	60.1







Test	**Case 1: Monotonic Undrained Compression of Isotropically Consolidated Specimens**		
Cell No.	3 (Small)	Fines content (%)	60
Specimen	3f	Specific gravity (g/cm^3)	2.72

1.) Sample physical properties

Wet mass before test (g)	129.564	m.c before test (%)	9.80	Height (mm)	75.85	Volume (cm^3)	86.023
Wet mass after test (g)	145.848	m.c. after test (%)	23.60	Diameter (mm)	38.00		
Dry mass (g)	118.000	Dry density (kg/m^3)	1372	Area (cm^2)	11.341	Void ratio (e_0)	0.983

2.) Saturation/Consolidation

Date	C.P (kPa)	P.W.P bp closed (kPa)	B.P (kPa)	P.W.P bp open (kPa)	Change C.P (kPa)	Change P.W.P (kPa)	B value	Volume Gauge (cm^3)	Cell Expansn (cm^3)	Specimen Volume (cm^3)	Void Ratio	Comments
15/11	0		0	-0.5				0.00	0.00	86.023	0.983	
15/11	7.3		5.5	3.5				2.35	0.00	83.673	0.929	**AIR-FLUSHING**
15/11	50	17.5	40	38.5	42.7	14.0	0.33	7.54	3.81	82.293	0.897	**S**
16/11	100	65.5	90	89.5	50	27.0	0.54	10.56	5.89	81.353	0.875	**A**
17/11	150	119.5	140	140.0	50	30.0	0.60	13.42	8.17	80.773	0.862	**T**
18/11	200	175.5	190	190.0	50	35.5	0.71	14.99	9.52	80.553	0.857	**U**
19/11	250	230.0	240	240.0	50	40.0	0.80	16.54	10.66	80.143	0.847	**R**
20/11	300	283.5	290	290.0	50	43.5	0.87	17.98	11.56	79.603	0.835	**A**
21/11	350	335.5	340	340.0	50	45.5	0.91	19.37	12.66	79.313	0.828	**T**
22/11	400	387.0	390	390.0	50	47.0	0.94	21.19	13.80	78.633	0.813	**I**
23/11	450	438.0	440	440.0	50	48.0	0.96	22.55	14.98	78.453	0.808	**O**
24/11	500	489.0	440	440.0	50	49.0	0.98					**N**
24/11	500		450	450.0				24.70	16.66	77.983	0.798	**CONSOLIDATION**

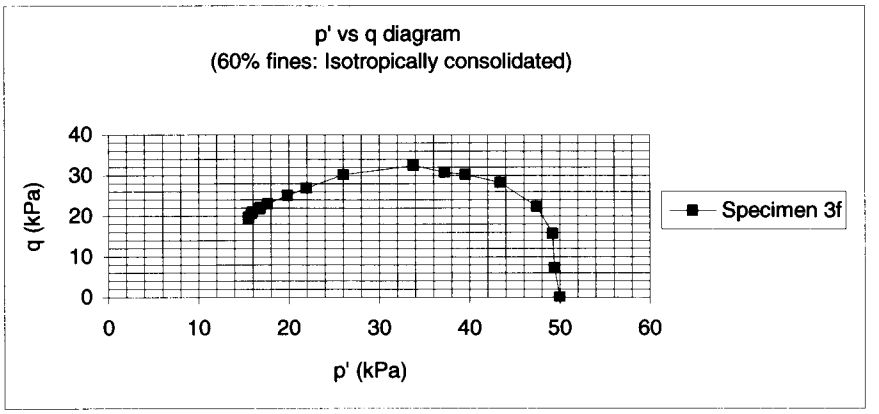
3.) Shear data

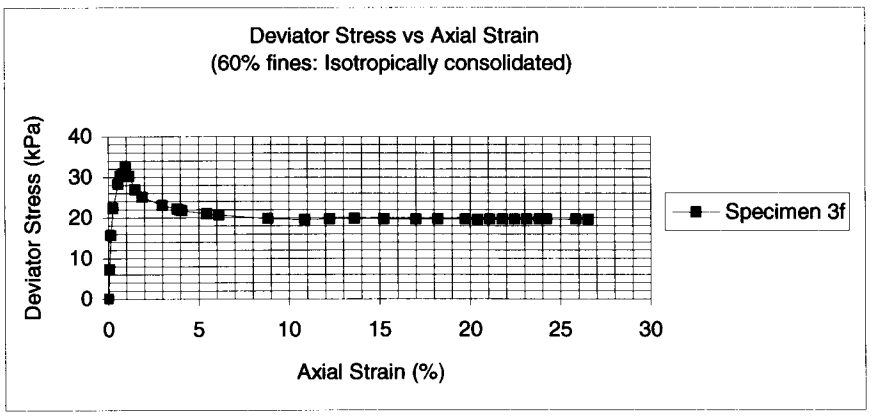
Volume change 1:		Volume change 2:		Sample Vol. change (cm^3)	8.04	B value	0.98
Air Flushing (cm^3)	2.35	Sat/Cons. (cm^3)	22.35	L_{cons} (mm)	73.49	p'consolidation (kPa)	50
Cell Expansion (cm^3)	0.00	Cell Expsn.(cm^3)	16.66	A_{cons} (cm^2)	10.634	Void ratio (e_1)	0.798

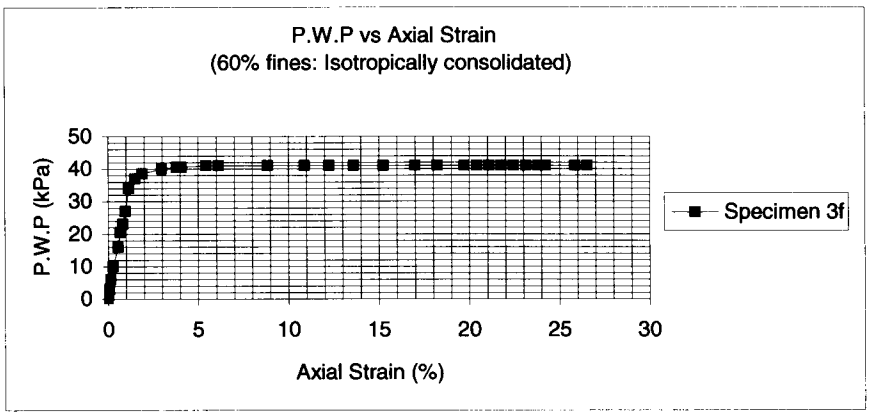
Proof ring properties		Strain gauge properties	
Proof ring No.	1800	1 strain division (mm)	0.01
Proof ring factor (dN/div)	14.846		

Strain Gauge (divs)	Axial Strain	Axial Strain (%)	Change Prf. ring (divs)	Change P.W.P (kPa)	q (Uncortd) (kPa)	Membrn. Corrctn. (kPa)	q (kPa)	t (kPa)	p' (kPa)	s' (kPa)
0	0.0000	0.0000	0.0	0.0	0.0	0.0	0.0	0.0	50.0	50.0
5	0.0007	0.0680	5.2	3.0	7.3	0.0	7.2	3.6	49.4	50.6
10	0.0014	0.1361	11.3	6.0	15.8	0.1	15.7	7.8	49.2	51.8
20	0.0027	0.2722	16.1	10.0	22.4	0.1	22.3	11.1	47.4	51.1
40	0.0054	0.5443	20.5	16.0	28.5	0.3	28.2	14.1	43.4	48.1
50	0.0068	0.6804	22.0	20.5	30.5	0.3	30.2	15.1	39.6	44.6
60	0.0082	0.8165	22.5	23.0	31.2	0.4	30.7	15.4	37.2	42.4
70	0.0095	0.9526	23.8	27.0	32.9	0.5	32.4	16.2	33.8	39.2
85	0.0116	1.1567	22.3	34.0	30.8	0.6	30.2	15.1	26.1	31.1
110	0.0150	1.4969	20.1	37.0	27.6	0.7	26.9	13.4	22.0	26.4
140	0.0191	1.9051	19.0	38.5	26.0	1.0	25.1	12.5	19.9	24.0
220	0.0299	2.9937	17.7	40.0	24.0	1.0	23.0	11.5	17.7	21.5
280	0.0381	3.8102	17.2	40.5	23.1	1.0	22.1	11.0	16.9	20.5
290	0.0395	3.9463	17.1	40.5	22.9	1.0	21.9	11.0	16.8	20.5
300	0.0408	4.0824	17.0	40.5	22.8	1.0	21.8	10.9	16.8	20.4
400	0.0544	5.4431	16.6	41.0	21.9	1.0	20.9	10.5	16.0	19.5
450	0.0612	6.1235	16.5	41.0	21.6	1.0	20.6	10.3	15.9	19.3
650	0.0885	8.8451	16.3	41.0	20.7	1.0	19.7	9.9	15.6	18.9
800	0.1089	10.8863	16.5	41.0	20.5	1.0	19.5	9.8	15.5	18.8
900	0.1225	12.2471	16.9	41.0	20.7	1.0	19.7	9.9	15.6	18.9
1000	0.1361	13.6079	17.2	41.0	20.7	1.0	19.7	9.9	15.6	18.9
1120	0.1524	15.2408	17.5	41.0	20.7	1.0	19.7	9.9	15.6	18.9
1250	0.1701	17.0098	17.8	41.0	20.6	1.0	19.6	9.8	15.5	18.8
1340	0.1823	18.2345	18.1	41.0	20.7	1.0	19.7	9.8	15.6	18.8

Strain Gauge (divs)	Axial Strain	Axial Strain (%)	Change Prf. ring (divs)	Change P.W.P (kPa)	q (Uncortd) (kPa)	Membm. Corrctn. (kPa)	q (kPa)	t (kPa)	p' (kPa)	s' (kPa)
1450	0.1973	19.7314	18.4	41.0	20.6	1.0	19.6	9.8	15.5	18.8
1500	0.2041	20.4118	18.5	41.0	20.6	1.0	19.6	9.8	15.5	18.8
1550	0.2109	21.0922	18.7	41.0	20.6	1.0	19.6	9.8	15.5	18.8
1600	0.2177	21.7726	18.9	41.0	20.6	1.0	19.6	9.8	15.5	18.8
1650	0.2245	22.4530	19.0	41.0	20.6	1.0	19.6	9.8	15.5	18.8
1700	0.2313	23.1334	19.2	41.0	20.6	1.0	19.6	9.8	15.5	18.8
1750	0.2381	23.8138	19.4	41.0	20.6	1.0	19.6	9.8	15.5	18.8
1780	0.2422	24.2220	19.5	41.0	20.6	1.0	19.6	9.8	15.5	18.8
1900	0.2585	25.8549	19.9	41.0	20.6	1.0	19.6	9.8	15.5	18.8
1950	0.2654	26.5353	20.0	41.0	20.5	1.0	19.5	9.8	15.5	18.8







Test	**Case 1: Monotonic Undrained Compression of Isotropically Consolidated Specimens**		
Cell No.	2 (Big)	Fines content (%)	60
Specimen	2g	Specific gravity (g/cm^3)	2.72

1.) Sample physical properties

Wet mass before test (g)	915.142	m.c before test (%)	9.20	Height (mm)	148.20	Volume (cm^3)	669.652
Wet mass after test (g)	999.281	m.c. after test (%)	19.24	Diameter (mm)	75.85		
Dry mass (g)	838.042	Dry density (kg/m^3)	1251	Area (cm^2)	45.186	Void ratio (e_0)	1.173

2.) Saturation/Consolidation

Date	C.P (kPa)	P.W.P bp closed (kPa)	B.P (kPa)	P.W.P bp open (kPa)	Change C.P (kPa)	Change P.W.P (kPa)	B value	Volume Gauge (cm^3)	Cell Expansn (cm^3)	Specimen Volume (cm^3)	Void Ratio	Comments
2/12	0		0	0.0				0.00	0.00	669.652	1.173	
2/12	9.8		7.3	5.0				11.25	0.00	658.402	1.137	**AIR-FLUSHING**
2/12	50	15.5	40	39.5	40.2	10.5	0.26	34.62	3.12	638.152	1.071	**S**
3/12	100	62.0	90	89.5	50	22.5	0.45	52.11	7.06	624.602	1.027	**A**
4/12	150	121.0	140	139.5	50	31.5	0.63	68.04	9.79	611.402	0.984	**T**
5/12	200	177.0	190	190.0	50	37.5	0.75	79.29	11.63	601.992	0.954	**U**
6/12	250	232.0	240	240.0	50	42.0	0.84	88.29	13.02	594.382	0.929	**R**
7/12	300	285.5	290	290.0	50	45.5	0.91	95.27	14.57	588.952	0.912	**A**
8/12	350	337.0	340	340.0	50	47.0	0.94	100.24	16.03	585.442	0.900	**T**
9/12	400	388.0	390	390.0	50	48.0	0.96	103.05	17.22	583.822	0.895	**I**
10/12	450	439.0	400	400.0	50	49.0	0.98					**O**
												N
10/12	500		400	400.0				130.85	22.32	561.122	0.821	**CONSOLIDATION**

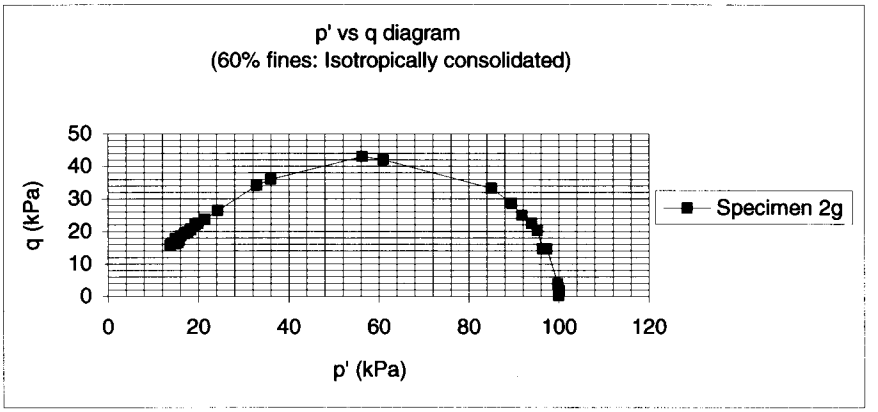
3.) Shear data

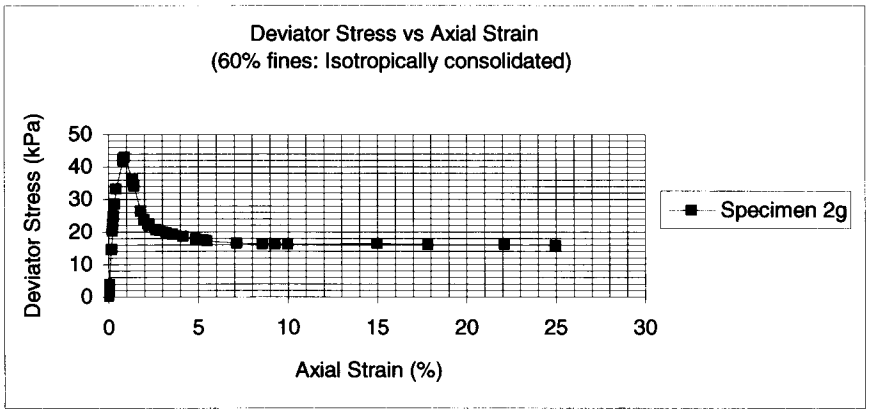
Volume change 1:		Volume change 2:		Sample Vol. change (cm^3)	108.53	B value	0.98
Air Flushing (cm^3)	11.25	Sat/Cons. (cm^3)	119.60	L_{cons} (mm)	140.19	p'consolidation (kPa)	100
Cell Expansion (cm^3)	0.00	Cell Expsn.(cm^3)	22.32	A_{cons} (cm^2)	40.304	Void ratio (e_1)	0.821

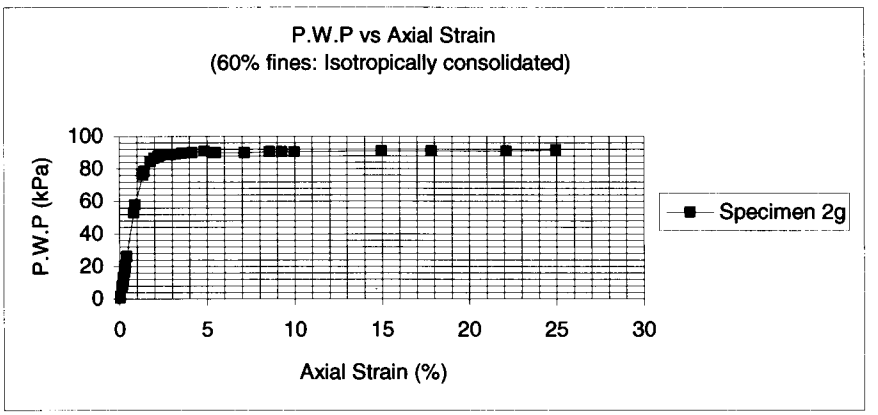
Proof ring properties		Strain gauge properties	
Proof ring No.	5153	1 strain division (mm)	0.01
Proof ring factor (dN/div)	7.512		

Strain Gauge (divs)	Axial Strain	Axial Strain (%)	Change Prf. ring (divs)	Change P.W.P (kPa)	q (Uncortd) (kPa)	Membrn. Corrctn. (kPa)	q (kPa)	t (kPa)	p' (kPa)	s' (kPa)
0	0.0000	0.0000	0.0	0.0	0.0	0.0	0.0	0.0	100.0	100.0
5	0.0004	0.0357	9.9	0.5	1.8	0.0	1.8	0.9	100.1	100.4
8	0.0006	0.0571	21.1	1.5	3.9	0.0	3.9	2.0	99.8	100.5
20	0.0014	0.1427	78.6	7.5	14.6	0.1	14.6	7.3	97.4	99.8
25	0.0018	0.1783	78.9	8.5	14.7	0.1	14.6	7.3	96.4	98.8
30	0.0021	0.2140	109.6	11.5	20.4	0.1	20.3	10.1	95.3	98.6
34	0.0024	0.2425	121.2	13.5	22.5	0.1	22.4	11.2	94.0	97.7
40	0.0029	0.2853	134.8	16.5	25.1	0.1	24.9	12.5	91.8	96.0
48	0.0034	0.3424	154.6	20.0	28.7	0.2	28.5	14.3	89.5	94.3
60	0.0043	0.4280	180.2	26.0	33.4	0.2	33.2	16.6	85.1	90.6
115	0.0082	0.8203	229.6	53.0	42.4	0.4	42.0	21.0	61.0	68.0
125	0.0089	0.8916	235.0	58.0	43.4	0.4	43.0	21.5	56.3	63.5
190	0.0136	1.3553	199.5	76.0	36.7	0.7	36.0	18.0	36.0	42.0
200	0.0143	1.4266	189.7	78.5	34.9	0.7	34.1	17.1	32.9	38.6
250	0.0178	1.7832	148.9	84.5	27.3	0.9	26.4	13.2	24.3	28.7
280	0.0200	1.9972	135.2	86.5	24.7	1.0	23.7	11.8	21.4	25.3
310	0.0221	2.2112	128.3	87.5	23.4	1.0	22.4	11.2	20.0	23.7
320	0.0228	2.2826	125.7	88.0	22.9	1.0	21.9	10.9	19.3	22.9
370	0.0264	2.6392	119.2	88.5	21.6	1.0	20.6	10.3	18.4	21.8
400	0.0285	2.8532	118.1	88.5	21.4	1.0	20.4	10.2	18.3	21.7
450	0.0321	3.2098	114.9	89.0	20.7	1.0	19.7	9.9	17.6	20.9
500	0.0357	3.5665	112.5	89.5	20.2	1.0	19.2	9.6	16.9	20.1
580	0.0414	4.1371	109.3	90.0	19.5	1.0	18.5	9.3	16.2	19.3
680	0.0485	4.8504	105.7	91.0	18.7	1.0	17.7	8.9	14.9	17.9

Strain Gauge (divs)	Axial Strain	Axial Strain (%)	Change Prf. ring (divs)	Change P.W.P (kPa)	q (Uncortd) (kPa)	Membrn. Corrctn. (kPa)	q (kPa)	t (kPa)	p' (kPa)	s' (kPa)
750	0.0535	5.3497	104.3	90.0	18.4	1.0	17.4	8.7	15.8	18.7
770	0.0549	5.4924	103.5	90.0	18.2	1.0	17.2	8.6	15.7	18.6
1000	0.0713	7.1330	101.1	90.0	17.5	1.0	16.5	8.2	15.5	18.2
1200	0.0856	8.5596	101.5	90.5	17.3	1.0	16.3	8.1	14.9	17.6
1300	0.0927	9.2729	101.8	90.5	17.2	1.0	16.2	8.1	14.9	17.6
1400	0.0999	9.9862	102.4	90.5	17.2	1.0	16.2	8.1	14.9	17.6
2100	0.1498	14.9793	109.6	91.0	17.4	1.0	16.4	8.2	14.5	17.2
2500	0.1783	17.8325	111.7	91.0	17.1	1.0	16.1	8.1	14.4	17.1
3100	0.2211	22.1123	117.9	91.0	17.1	1.0	16.1	8.1	14.4	17.1
3500	0.2497	24.9654	120.3	91.5	16.8	1.0	15.8	7.9	13.8	16.4







Test	**Case 1: Monotonic Undrained Compression of Isotropically Consolidated Specimens**		
Cell No.	6 (Small)	Fines content (%)	60
Specimen	6e	Specific gravity (g/cm^3)	2.72

1.) Sample physical properties

Wet mass before test (g)	127.002	m.c before test (%)	9.50	Height (mm)	75.20	Volume (cm^3)	85.061
Wet mass after test (g)	145.443	m.c. after test (%)	25.40	Diameter (mm)	37.95		
Dry mass (g)	115.984	Dry density (kg/m^3)	1364	Area (cm^2)	11.311	Void ratio (e_0)	0.995

2.) Saturation/Consolidation

Date	C.P (kPa)	P.W.P bp closed (kPa)	B.P (kPa)	P.W.P bp open (kPa)	Change C.P (kPa)	Change P.W.P (kPa)	B value	Volume Gauge (cm^3)	Cell Expansn (cm^3)	Specimen Volume (cm^3)	Void Ratio	Comments
2/11	0		0	-1.0				0.00	0.00	85.061	0.995	
2/11	7.5		5.1	3.0				1.24	0.00	83.821	0.966	**AIR-FLUSHING**
2/11	50	18.5	40	39.5	42.5	15.5	0.36	5.89	3.12	82.291	0.930	**S**
3/11	100	65.0	90	89.5	50	25.5	0.51	8.51	4.89	81.441	0.910	**A**
4/11	150	119.5	140	140.0	50	30.0	0.60	11.32	7.14	80.881	0.897	**T**
5/11	200	177.0	190	190.0	50	37.0	0.74	13.45	8.53	80.141	0.879	**U**
6/11	250	229.5	240	240.0	50	39.5	0.79	15.41	9.63	79.281	0.859	**R**
7/11	300	282.0	290	290.0	50	42.0	0.84	17.10	10.61	78.571	0.843	**A**
8/11	350	334.0	340	340.0	50	44.0	0.88	18.95	11.67	77.781	0.824	**T**
9/11	400	385.5	390	390.0	50	45.5	0.91	20.41	12.65	77.301	0.813	**I**
10/11	450	437.5	440	440.0	50	47.5	0.95	21.63	13.79	77.221	0.811	**O**
11/11	500	488.5	450	450.0	50	48.5	0.97					**N**
11/11	700		450	450.0				28.76	18.09	74.391	0.745	**CONSOLIDATION**

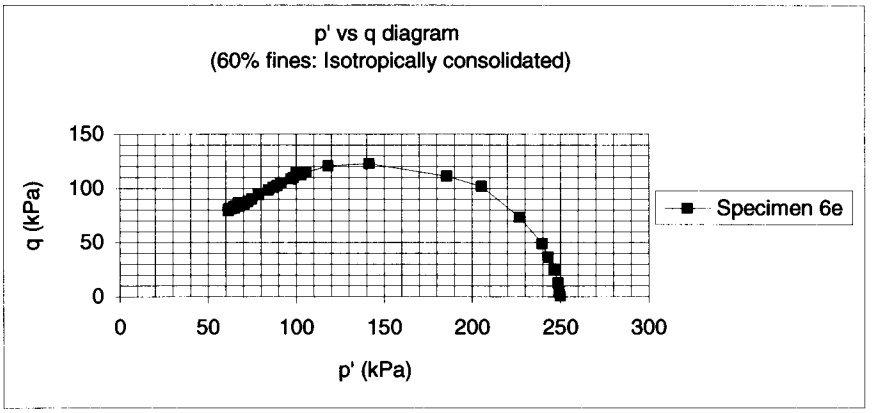
3.) Shear data

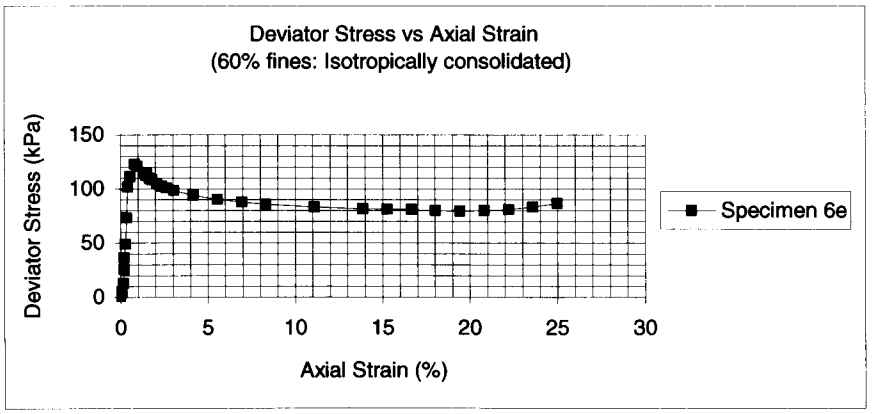
Volume change 1:		Volume change 2:		Sample Vol. change (cm^3)	10.67	B value	0.97
Air Flushing (cm^3)	1.24	Sat/Cons. (cm^3)	27.52	L_{cons} (mm)	72.06	p'consolidation (kPa)	250
Cell Expansion (cm^3)	0.00	Cell Expsn.(cm^3)	18.09	A_{cons} (cm^2)	10.365	Void ratio (e_1)	0.745

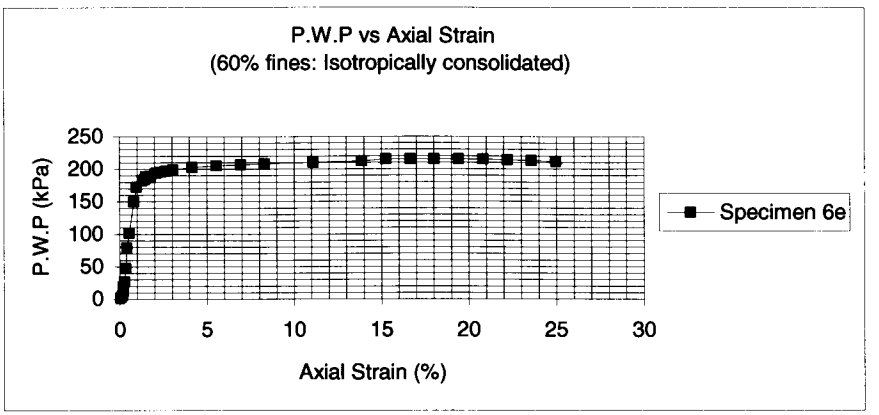
Proof ring properties		Strain gauge properties	
Proof ring No.	4541	1 strain division (mm)	0.01
Proof ring factor (dN/div)	25.77		

Strain Gauge (divs)	Axial Strain	Axial Strain (%)	Change Prf. ring (divs)	Change P.W.P (kPa)	q (Uncortd) (kPa)	Membm. Corrctn. (kPa)	q (kPa)	t (kPa)	p' (kPa)	s' (kPa)
0	0.0000	0.0000	0.0	0.0	0.0	0.0	0.0	0.0	250.0	250.0
5	0.0007	0.0694	2.1	2.5	5.2	0.0	5.2	2.6	249.2	250.1
12	0.0017	0.1665	5.2	5.5	12.9	0.1	12.8	6.4	248.8	250.9
14	0.0019	0.1943	10.3	12.0	25.6	0.1	25.5	12.7	246.5	250.7
15	0.0021	0.2082	14.7	19.0	36.5	0.1	36.4	18.2	243.1	249.2
20	0.0028	0.2776	19.8	26.5	49.1	0.1	49.0	24.5	239.8	248.0
25	0.0035	0.3470	29.6	47.5	73.3	0.2	73.2	36.6	226.9	239.1
30	0.0042	0.4163	41.2	78.5	102.0	0.2	101.8	50.9	205.4	222.4
40	0.0056	0.5551	45.1	101.5	111.5	0.3	111.2	55.6	185.6	204.1
60	0.0083	0.8327	50.0	149.5	123.3	0.4	122.9	61.4	141.5	161.9
70	0.0097	0.9715	49.2	172.0	121.1	0.5	120.6	60.3	118.2	138.3
95	0.0132	1.3184	47.0	182.5	115.3	0.7	114.6	57.3	105.7	124.8
105	0.0146	1.4572	46.2	184.5	113.2	0.7	112.5	56.2	103.0	121.7
110	0.0153	1.5266	46.9	188.0	114.8	0.8	114.1	57.0	100.0	119.0
120	0.0167	1.6654	45.2	188.0	110.5	0.8	109.7	54.8	98.6	116.8
130	0.0180	1.8042	44.8	189.0	109.4	0.9	108.5	54.2	97.2	115.2
150	0.0208	2.0817	43.5	193.5	105.9	1.0	104.9	52.4	91.5	108.9
170	0.0236	2.3593	42.6	195.0	103.4	1.0	102.4	51.2	89.1	106.2
190	0.0264	2.6369	42.1	196.5	101.9	1.0	100.9	50.5	87.1	104.0
220	0.0305	3.0532	41.3	198.5	99.5	1.0	98.5	49.3	84.3	100.8
300	0.0416	4.1634	39.9	202.5	95.1	1.0	94.1	47.0	78.9	94.5
400	0.0555	5.5513	38.8	205.0	91.1	1.0	90.1	45.1	75.0	90.1
500	0.0694	6.9391	38.3	206.5	88.6	1.0	87.6	43.8	72.7	87.3
600	0.0833	8.3269	38.0	208.0	86.6	1.0	85.6	42.8	70.5	84.8

Strain Gauge (divs)	Axial Strain	Axial Strain (%)	Change Prf. ring (divs)	Change P.W.P (kPa)	q (Uncortd) (kPa)	Membm. Corrctn. (kPa)	q (kPa)	t (kPa)	p' (kPa)	s' (kPa)
800	0.1110	11.1025	38.1	210.0	84.2	1.0	83.2	41.6	67.7	81.6
1000	0.1388	13.8782	38.5	212.0	82.4	1.0	81.4	40.7	65.1	78.7
1100	0.1527	15.2660	39.0	215.0	82.2	1.0	81.2	40.6	62.1	75.6
1200	0.1665	16.6538	39.6	215.0	82.1	1.0	81.1	40.5	62.0	75.5
1300	0.1804	18.0416	39.7	215.0	80.9	1.0	79.9	39.9	61.6	74.9
1400	0.1943	19.4294	40.2	215.0	80.5	1.0	79.5	39.8	61.5	74.8
1500	0.2082	20.8172	41.1	215.0	80.9	1.0	79.9	40.0	61.6	75.0
1600	0.2221	22.2051	42.3	214.0	81.8	1.0	80.8	40.4	62.9	76.4
1700	0.2359	23.5929	44.4	213.0	84.3	1.0	83.3	41.7	64.8	78.7
1800	0.2498	24.9807	47.0	211.5	87.7	1.0	86.7	43.3	67.4	81.8







Test	**Case 1: Monotonic Undrained Compression of Isotropically Consolidated Specimens**		
Cell No.	3 (Big)	Fines content (%)	60
Specimen	3g	Specific gravity (g/cm^3)	2.72

1.) Sample physical properties

Wet mass before test (g)	897.566	m.c before test (%)	8.50	Height (mm)	147.55	Volume (cm^3)	665.836
Wet mass after test (g)	996.108	m.c. after test (%)	20.41	Diameter (mm)	75.80		
Dry mass (g)	827.250	Dry density (kg/m^3)	1242	Area (cm^2)	45.126	Void ratio (e_0)	1.189

2.) Saturation/Consolidation

Date	C.P (kPa)	P.W.P bp closed (kPa)	B.P (kPa)	P.W.P bp open (kPa)	Change C.P (kPa)	Change P.W.P (kPa)	B value	Volume Gauge (cm^3)	Cell Expansn (cm^3)	Specimen Volume (cm^3)	Void Ratio	Comments
3/12	0		0	-1.0				0.00	0.00	665.836	1.189	
3/12	8.4		5.6	2.5				8.10	0.00	657.736	1.163	**AIR-FLUSHING**
3/12	50	13.5	40	39.5	41.6	11.0	0.26	27.98	2.51	640.366	1.106	**S**
4/12	100	59.5	90	90.0	50	20.0	0.40	48.52	6.08	623.396	1.050	**A**
5/12	150	119.0	140	140.0	50	29.0	0.58	65.32	8.77	609.286	1.003	**T**
6/12	200	175.0	190	190.0	50	35.0	0.70	81.26	10.65	595.226	0.957	**U**
7/12	250	229.5	240	240.0	50	39.5	0.79	92.39	12.00	585.446	0.925	**R**
8/12	300	282.0	290	290.0	50	42.0	0.84	102.83	13.63	576.636	0.896	**A**
9/12	350	335.0	340	340.0	50	45.0	0.90	108.68	15.06	572.216	0.881	**T**
10/12	400	386.5	390	390.0	50	46.5	0.93	113.85	16.08	568.066	0.868	**I**
11/12	450	437.5	440	440.0	50	47.5	0.95	117.79	18.12	566.166	0.862	**O**
12/12	500	488.5	450	450.0	50	48.5	0.97					**N**
12/12	850		450	450.0				153.88	24.74	536.696	0.765	**CONSOLIDATION**

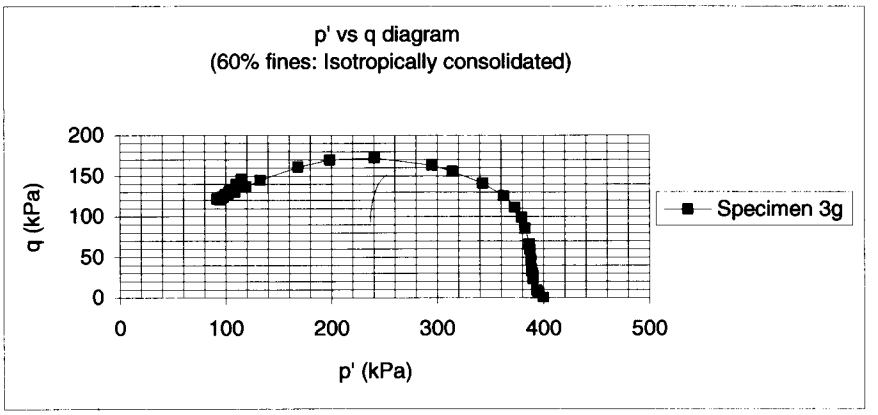
3.) Shear data

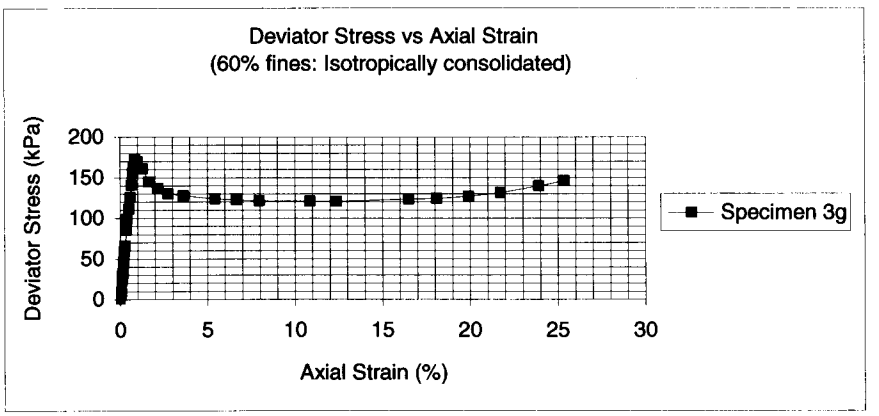
Volume change 1:		Volume change 2:		Sample Vol. change (cm^3)	129.14	B value	0.97
Air Flushing (cm^3)	8.10	Sat/Cons. (cm^3)	145.78	L_{cons} (mm)	138.01	p'consolidation (kPa)	400
Cell Expansion (cm^3)	0.00	Cell Expsn.(cm^3)	24.74	A_{cons} (cm^2)	39.291	Void ratio (e_1)	0.765

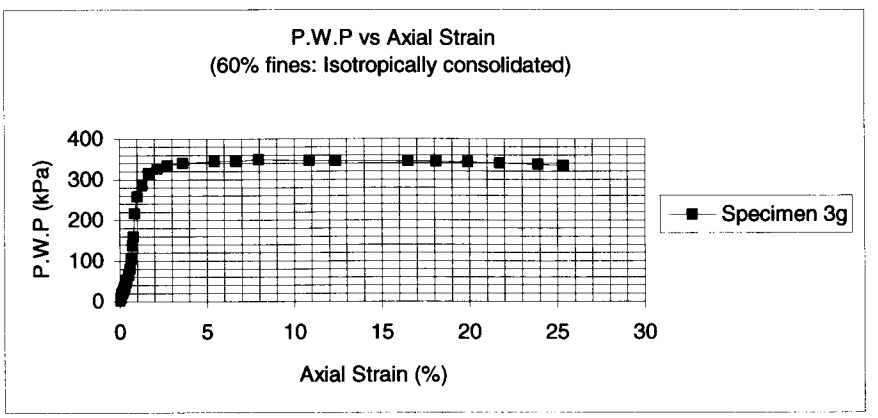
Proof ring properties		Strain gauge properties	
Proof ring No.	4541	1 strain division (mm)	0.01
Proof ring factor (dN/div)	25.77		

Strain Gauge (divs)	Axial Strain	Axial Strain (%)	Change Prf. ring (divs)	Change P.W.P (kPa)	q (Uncortd) (kPa)	Membm. Corrctn. (kPa)	q (kPa)	t (kPa)	p' (kPa)	s' (kPa)
0	0.0000	0.0000	0.0	0.0	0.0	0.0	0.0	0.0	400.0	400.0
5	0.0004	0.0362	9.6	7.0	6.3	0.0	6.3	3.1	395.1	396.1
10	0.0007	0.0725	14.1	9.5	9.2	0.0	9.2	4.6	393.6	395.1
15	0.0011	0.1087	35.8	18.0	23.5	0.1	23.4	11.7	389.8	393.7
20	0.0014	0.1449	45.2	20.0	29.6	0.1	29.5	14.8	389.8	394.8
25	0.0018	0.1811	51.0	22.5	33.4	0.1	33.3	16.6	388.6	394.1
30	0.0022	0.2174	71.2	27.5	46.6	0.1	46.5	23.2	388.0	395.7
35	0.0025	0.2536	90.8	32.5	59.4	0.1	59.3	29.6	387.3	397.1
40	0.0029	0.2898	101.2	35.5	66.2	0.1	66.0	33.0	386.5	397.5
50	0.0036	0.3623	131.2	46.0	85.7	0.2	85.6	42.8	382.5	396.8
55	0.0040	0.3985	151.4	53.5	98.9	0.2	98.7	49.4	379.4	395.9
70	0.0051	0.5072	170.6	64.0	111.3	0.3	111.1	55.5	373.0	391.5
80	0.0058	0.5797	192.3	79.5	125.4	0.3	125.1	62.6	362.2	383.1
90	0.0065	0.6521	216.5	104.0	141.1	0.3	140.7	70.4	342.9	366.4
100	0.0072	0.7246	239.1	137.5	155.7	0.4	155.3	77.7	314.3	340.2
110	0.0080	0.7970	251.2	159.0	163.4	0.4	163.0	81.5	295.3	322.5
120	0.0087	0.8695	265.4	216.5	172.6	0.4	172.1	86.1	240.9	269.6
140	0.0101	1.0144	262.2	258.0	170.2	0.5	169.7	84.9	198.6	226.9
180	0.0130	1.3042	249.8	285.0	161.7	0.7	161.0	80.5	168.7	195.5
230	0.0167	1.6665	225.5	315.5	145.4	0.8	144.6	72.3	132.7	156.8
300	0.0217	2.1737	214.7	326.5	137.8	1.0	136.8	68.4	119.1	141.9
380	0.0275	2.7534	205.5	334.5	131.1	1.0	130.1	65.0	108.9	130.5
500	0.0362	3.6229	203.3	340.0	128.5	1.0	127.5	63.8	102.5	123.8
750	0.0543	5.4344	201.1	344.0	124.7	1.0	123.7	61.9	97.2	117.9

Strain Gauge (divs)	Axial Strain	Axial Strain (%)	Change Prf. ring (divs)	Change P.W.P (kPa)	q (Uncortd) (kPa)	Membm. Corrctn. (kPa)	q (kPa)	t (kPa)	p' (kPa)	s' (kPa)
920	0.0667	6.6661	201.9	345.0	123.6	1.0	122.6	61.3	95.9	116.3
1100	0.0797	7.9704	203.0	348.5	122.5	1.0	121.5	60.8	92.0	112.3
1500	0.1087	10.8687	208.4	346.0	121.8	1.0	120.8	60.4	94.3	114.4
1710	0.1239	12.3903	211.3	345.5	121.4	1.0	120.4	60.2	94.6	114.7
2280	0.1652	16.5204	226.9	344.5	124.2	1.0	123.2	61.6	96.6	117.1
2500	0.1811	18.1145	233.1	343.5	125.2	1.0	124.2	62.1	97.9	118.6
2750	0.1993	19.9260	243.7	342.5	128.0	1.0	127.0	63.5	99.8	121.0
3000	0.2174	21.7374	257.8	340.0	132.3	1.0	131.3	65.7	103.8	125.7
3300	0.2391	23.9112	281.2	336.5	140.3	1.0	139.3	69.7	109.9	133.2
3500	0.2536	25.3603	300.0	333.5	146.9	1.0	145.9	72.9	115.1	139.4







Test	**Case 1: Monotonic Undrained Compression of Isotropically Consolidated Specimens**		
Cell No.	6 (Big)	Fines content (%)	60
Specimen	6f	Specific gravity (g/cm^3)	2.72

1.) Sample physical properties

Wet mass before test (g)	904.550	m.c before test (%)	10.00	Height (mm)	149.65	Volume (cm^3)	677.988
Wet mass after test (g)	996.650	m.c. after test (%)	21.20	Diameter (mm)	75.95		
Dry mass (g)	822.318	Dry density (kg/m^3)	1213	Area (cm^2)	45.305	Void ratio (e_0)	1.243

2.) Saturation/Consolidation

Date	C.P (kPa)	P.W.P bp closed (kPa)	B.P (kPa)	P.W.P bp open (kPa)	Change C.P (kPa)	Change P.W.P (kPa)	B value	Volume Gauge (cm^3)	Cell Expansn (cm^3)	Specimen Volume (cm^3)	Void Ratio	Comments
14/11	0		0	-1.5				0.00	0.00	677.988	1.243	
14/11	10.6		8.0	5.5				12.60	0.00	665.388	1.201	**AIR-FLUSHING**
14/11	50	15.5	40	39.5	39.4	10.0	0.25	37.88	3.82	643.928	1.130	**S**
15/11	100	60.5	90	90.0	50	21.0	0.42	65.36	7.94	620.568	1.053	**A**
16/11	150	119.0	140	140.0	50	29.0	0.58	81.96	10.71	606.738	1.007	**T**
17/11	200	176.0	190	190.0	50	36.0	0.72	93.17	12.51	597.328	0.976	**U**
18/11	250	230.5	240	240.0	50	40.5	0.81	102.62	13.93	589.298	0.949	**R**
19/11	300	283.0	290	290.0	50	43.0	0.86	109.43	15.40	583.958	0.932	**A**
20/11	350	335.5	340	340.0	50	45.5	0.91	113.94	16.91	580.958	0.922	**T**
21/11	400	387.0	390	390.0	50	47.0	0.94	117.35	18.26	578.898	0.915	**I**
22/11	450	438.0	440	440.0	50	48.0	0.96	120.09	20.38	578.278	0.913	**O**
23/11	500	489.0	490	450.0	50	49.0	0.98					**N**
23/11	800		500	500.0				156.59	28.88	550.278	0.820	**CONSOLIDATION**

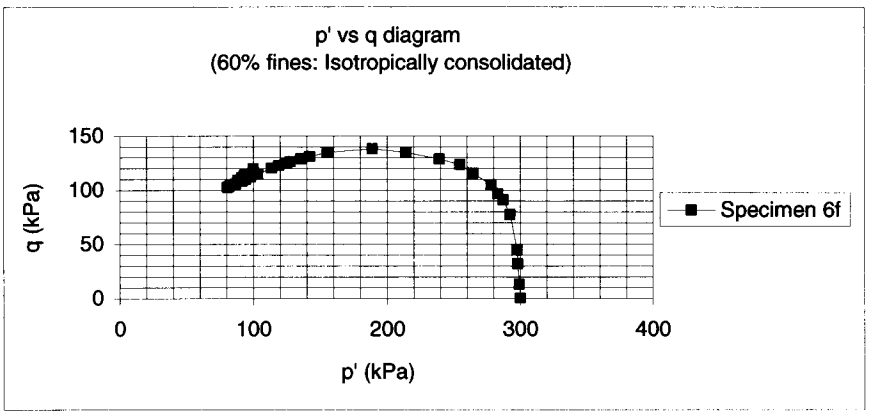
3.) Shear data

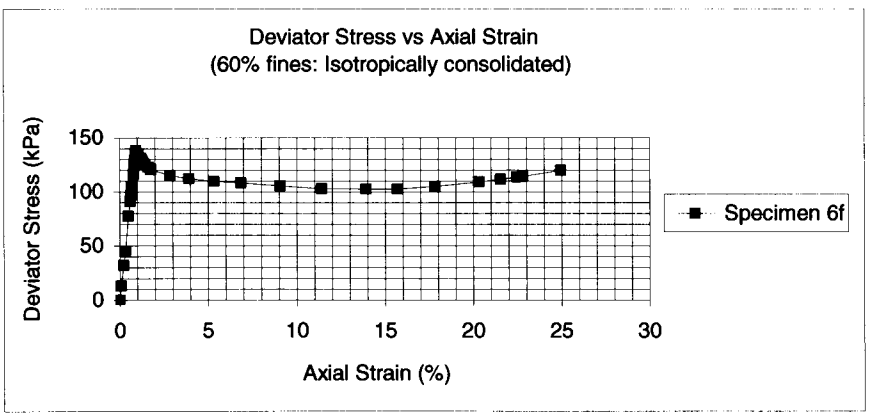
Volume change 1:		Volume change 2:		Sample Vol. change (cm^3)	127.71	B value	0.98
Air Flushing (cm^3)	12.60	Sat/Cons. (cm^3)	143.99	L_{cons} (mm)	140.25	p'consolidation (kPa)	300
Cell Expansion (cm^3)	0.00	Cell Expsn.(cm^3)	28.88	A_{cons} (cm^2)	39.616	Void ratio (e_1)	0.820

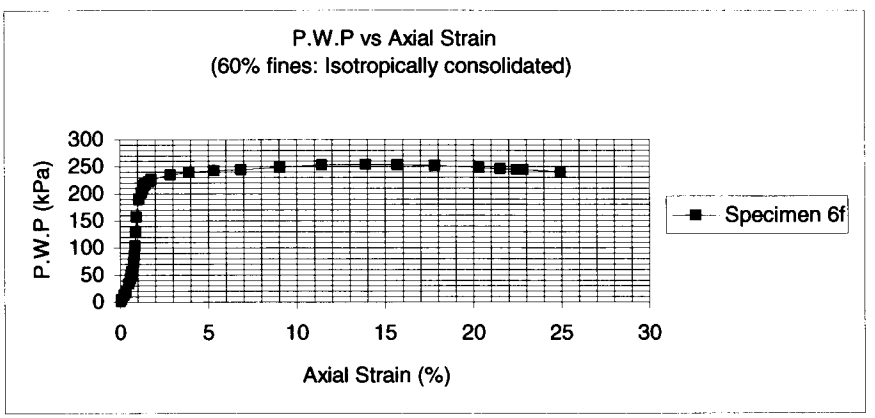
Proof ring properties		Strain gauge properties	
Proof ring No.	4541	1 strain division (mm)	0.01
Proof ring factor (dN/div)	25.77		

Strain Gauge (divs)	Axial Strain	Axial Strain (%)	Change Prf. ring (divs)	Change P.W.P (kPa)	q (Uncortd) (kPa)	Membm. Corrctn. (kPa)	q (kPa)	t (kPa)	p' (kPa)	s' (kPa)
0	0.0000	0.0000	0.0	0.0	0.0	0.0	0.0	0.0	300.0	300.0
10	0.0007	0.0713	20.0	5.0	13.0	0.0	13.0	6.5	299.3	301.5
30	0.0021	0.2139	49.6	12.5	32.2	0.1	32.1	16.0	298.2	303.5
45	0.0032	0.3208	69.8	17.5	45.3	0.2	45.1	22.5	297.5	305.0
70	0.0050	0.4991	119.9	33.5	77.6	0.2	77.4	38.7	292.3	305.2
85	0.0061	0.6060	141.1	43.0	91.2	0.3	90.9	45.5	287.3	302.5
90	0.0064	0.6417	149.9	49.0	96.9	0.3	96.6	48.3	283.2	299.3
95	0.0068	0.6773	162.3	56.5	104.9	0.3	104.5	52.3	278.3	295.8
110	0.0078	0.7843	179.8	74.0	116.0	0.4	115.7	57.8	264.6	283.8
115	0.0082	0.8199	192.1	86.5	123.9	0.4	123.5	61.8	254.7	275.3
120	0.0086	0.8556	200.2	103.5	129.1	0.4	128.7	64.3	239.4	260.8
125	0.0089	0.8912	209.7	130.5	135.2	0.4	134.7	67.4	214.4	236.9
130	0.0093	0.9269	214.9	157.0	138.5	0.5	138.0	69.0	189.0	212.0
150	0.0107	1.0695	210.2	189.5	135.3	0.5	134.7	67.4	155.4	177.9
170	0.0121	1.2121	204.9	201.5	131.7	0.6	131.1	65.5	142.2	164.0
180	0.0128	1.2834	202.0	207.5	129.7	0.6	129.1	64.5	135.5	157.0
190	0.0135	1.3547	197.8	214.5	126.9	0.7	126.2	63.1	127.6	148.6
200	0.0143	1.4260	196.1	217.0	125.7	0.7	125.0	62.5	124.7	145.5
230	0.0164	1.6399	192.9	222.0	123.4	0.8	122.6	61.3	118.9	139.3
250	0.0178	1.7825	189.8	226.5	121.3	0.9	120.4	60.2	113.6	133.7
400	0.0285	2.8520	183.7	235.0	116.1	1.0	115.1	57.5	103.4	122.5
550	0.0392	3.9215	181.1	239.5	113.2	1.0	112.2	56.1	97.9	116.6
750	0.0535	5.3475	179.9	242.5	110.8	1.0	109.8	54.9	94.1	112.4
960	0.0684	6.8447	180.2	244.5	109.2	1.0	108.2	54.1	91.6	109.6

Strain Gauge (divs)	Axial Strain	Axial Strain (%)	Change Prf. ring (divs)	Change P.W.P (kPa)	q (Uncortd) (kPa)	Membrn. Corrctn. (kPa)	q (kPa)	t (kPa)	p' (kPa)	s' (kPa)
1270	0.0906	9.0550	180.2	248.5	106.6	1.0	105.6	52.8	86.7	104.3
1600	0.1141	11.4079	180.2	253.0	103.8	1.0	102.8	51.4	81.3	98.4
1950	0.1390	13.9034	184.8	253.5	103.5	1.0	102.5	51.2	80.7	97.7
2200	0.1569	15.6859	188.9	253.0	103.6	1.0	102.6	51.3	81.2	98.3
2500	0.1782	17.8248	198.1	252.0	105.9	1.0	104.9	52.4	83.0	100.4
2850	0.2032	20.3203	212.2	248.0	110.0	1.0	109.0	54.5	88.3	106.5
3020	0.2153	21.5324	220.6	246.0	112.6	1.0	111.6	55.8	91.2	109.8
3150	0.2246	22.4593	227.0	244.5	114.5	1.0	113.5	56.7	93.3	112.2
3200	0.2282	22.8158	229.3	244.0	115.1	1.0	114.1	57.1	94.0	113.1
3500	0.2495	24.9548	247.5	240.0	120.8	1.0	119.8	59.9	99.9	119.9







Test	**Case 1: Monotonic Undrained Compression of Isotropically Consolidated Specimens**		
Cell No.	2 (Small)	Fines content (%)	60
Specimen	2h	Specific gravity (g/cm^3)	2.72

1.) Sample physical properties

Wet mass before test (g)	124.766	m.c before test (%)	8.30	Height (mm)	76.35	Volume (cm^3)	86.362
Wet mass after test (g)	143.199	m.c. after test (%)	24.30	Diameter (mm)	37.95		
Dry mass (g)	115.204	Dry density (kg/m^3)	1334	Area (cm^2)	11.311	Void ratio (e_0)	1.039

2.) Saturation/Consolidation

Date	C.P (kPa)	P.W.P bp closed (kPa)	B.P (kPa)	P.W.P bp open (kPa)	Change C.P (kPa)	Change P.W.P (kPa)	B value	Volume Gauge (cm^3)	Cell Expansn (cm^3)	Specimen Volume (cm^3)	Void Ratio	Comments
14/12	0		0	-2.0				0.00	0.00	86.362	1.039	
14/12	7.3		5.1	3.0				1.95	0.00	84.412	0.993	**AIR-FLUSHING**
14/12	50	13.0	40	39.5	42.7	10.0	0.23	6.10	2.02	82.282	0.943	**S**
15/12	100	60.0	90	90.0	50	20.5	0.41	9.21	4.04	81.192	0.917	**A**
16/12	150	119.0	140	140.0	50	29.0	0.58	12.60	6.24	80.002	0.889	**T**
17/12	200	175.5	190	190.0	50	35.5	0.71	15.67	7.67	78.362	0.850	**U**
18/12	250	230.0	240	240.0	50	40.0	0.80	17.54	8.73	77.552	0.831	**R**
19/12	300	282.5	290	290.0	50	42.5	0.85	19.48	9.79	76.672	0.810	**A**
20/12	350	335.0	340	340.0	50	45.0	0.90	21.00	10.81	76.172	0.798	**T**
21/12	400	387.0	390	390.0	50	47.0	0.94	22.41	11.63	75.582	0.785	**I**
22/12	450	438.0	440	440.0	50	48.0	0.96	23.90	12.73	75.192	0.775	**O**
23/12	500	488.5	450	450.0	50	48.5	0.97					**N**
23/12	900		450	450.0				33.48	19.26	72.142	0.703	**CONSOLIDATION**

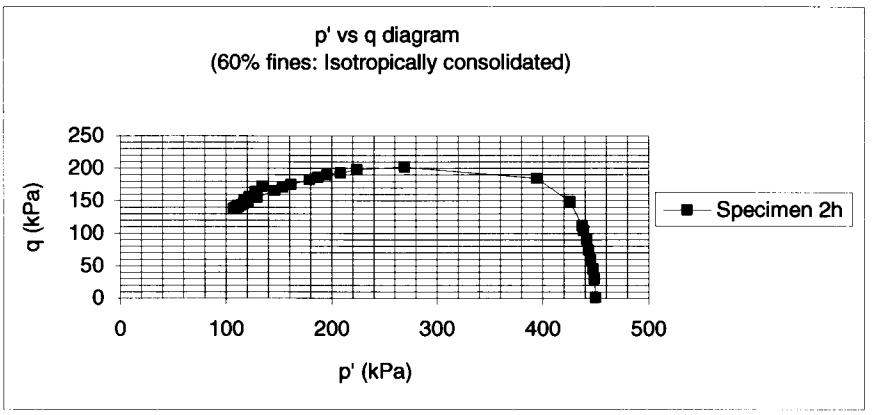
3.) Shear data

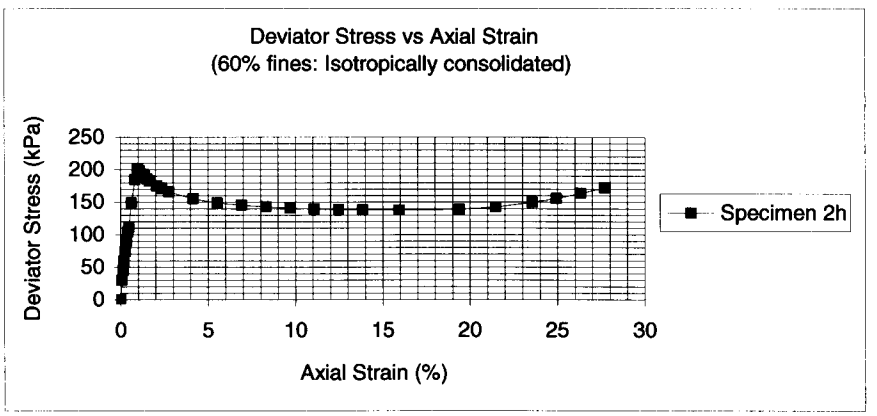
Volume change 1:		Volume change 2:		Sample Vol. change (cm^3)	14.22	B value	0.97
Air Flushing (cm^3)	1.95	Sat/Cons. (cm^3)	31.53	L_{cons} (mm)	72.16	p'consolidation (kPa)	450
Cell Expansion (cm^3)	0.00	Cell Expsn.(cm^3)	19.26	A_{cons} (cm^2)	10.070	Void ratio (e_1)	0.703

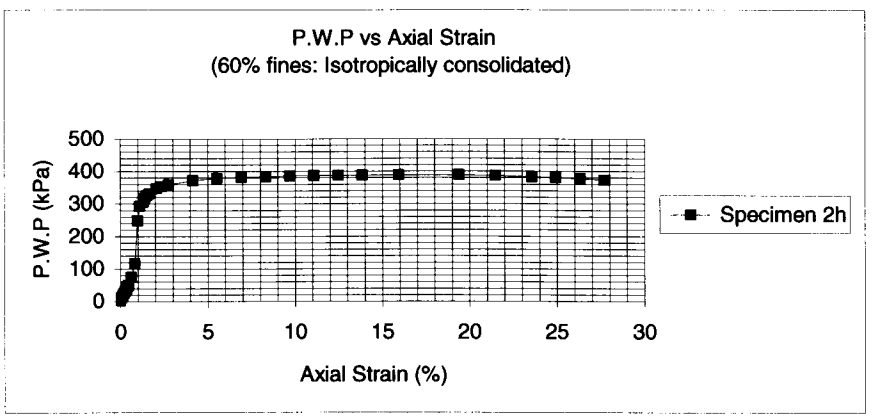
Proof ring properties		Strain gauge properties	
Proof ring No.	5153	1 strain division (mm)	0.01
Proof ring factor (dN/div)	7.512		

Strain Gauge (divs)	Axial Strain	Axial Strain (%)	Change Prf. ring (divs)	Change P.W.P (kPa)	q (Uncortd) (kPa)	Membm. Corrctn. (kPa)	q (kPa)	t (kPa)	p' (kPa)	s' (kPa)
0	0.0000	0.0000	0.0	0.0	0.0	0.0	0.0	0.0	450.0	450.0
5	0.0007	0.0693	39.9	11.0	29.7	0.0	29.7	14.9	448.9	453.9
10	0.0014	0.1386	60.2	17.5	44.8	0.1	44.8	22.4	447.4	454.9
15	0.0021	0.2079	79.8	24.5	59.4	0.1	59.3	29.7	445.3	455.2
20	0.0028	0.2772	99.8	31.5	74.2	0.1	74.1	37.1	443.2	455.6
25	0.0035	0.3465	120.3	38.0	89.4	0.2	89.3	44.6	441.8	456.6
30	0.0042	0.4157	140.2	46.0	104.2	0.2	103.9	52.0	438.6	456.0
35	0.0049	0.4850	149.7	49.5	111.1	0.2	110.9	55.4	437.5	455.9
45	0.0062	0.6236	201.2	74.0	149.2	0.3	148.8	74.4	425.6	450.4
60	0.0083	0.8315	249.9	117.0	184.9	0.4	184.5	92.2	394.5	425.2
72	0.0100	0.9978	273.8	248.0	202.2	0.5	201.7	100.9	269.2	302.9
80	0.0111	1.1087	269.2	292.0	198.6	0.6	198.0	99.0	224.0	257.0
95	0.0132	1.3165	262.5	305.5	193.2	0.7	192.6	96.3	208.7	240.8
100	0.0139	1.3858	258.9	317.5	190.5	0.7	189.8	94.9	195.8	227.4
110	0.0152	1.5244	254.0	325.0	186.6	0.8	185.8	92.9	186.9	217.9
120	0.0166	1.6630	249.7	331.5	183.2	0.8	182.3	91.2	179.3	209.7
150	0.0208	2.0787	240.5	346.5	175.7	1.0	174.7	87.3	161.7	190.8
170	0.0236	2.3559	235.1	353.0	171.3	1.0	170.3	85.1	153.8	182.1
200	0.0277	2.7716	229.7	359.0	166.6	1.0	165.6	82.8	146.2	173.8
300	0.0416	4.1575	218.6	372.0	156.3	1.0	155.3	77.6	129.8	155.6
400	0.0554	5.5433	212.2	378.5	149.5	1.0	148.5	74.3	121.0	145.8
500	0.0693	6.9291	210.3	381.5	146.0	1.0	145.0	72.5	116.8	141.0
600	0.0831	8.3149	210.3	383.5	143.8	1.0	142.8	71.4	114.1	137.9
700	0.0970	9.7007	210.8	385.0	142.0	1.0	141.0	70.5	112.0	135.5

Strain Gauge (divs)	Axial Strain	Axial Strain (%)	Change Prf. ring (divs)	Change P.W.P (kPa)	q (Uncortd) (kPa)	Membrn. Corrctn. (kPa)	q (kPa)	t (kPa)	p' (kPa)	s' (kPa)
800	0.1109	11.0865	211.9	386.0	140.6	1.0	139.6	69.8	110.5	133.8
900	0.1247	12.4724	213.7	387.0	139.5	1.0	138.5	69.3	109.2	132.3
1000	0.1386	13.8582	216.2	387.5	138.9	1.0	137.9	69.0	108.5	131.5
1150	0.1594	15.9369	220.5	388.5	138.3	1.0	137.3	68.6	107.3	130.1
1400	0.1940	19.4015	232.3	388.0	139.7	1.0	138.7	69.3	108.2	131.3
1550	0.2148	21.4802	244.8	386.0	143.4	1.0	142.4	71.2	111.5	135.2
1700	0.2356	23.5589	264.5	382.5	150.8	1.0	149.8	74.9	117.4	142.4
1800	0.2494	24.9447	280.1	380.0	156.8	1.0	155.8	77.9	121.9	147.9
1900	0.2633	26.3306	299.6	377.0	164.7	1.0	163.7	81.8	127.6	154.8
2000	0.2772	27.7164	321.0	373.0	173.1	1.0	172.1	86.0	134.4	163.0







Test	**Case 1: Monotonic Undrained Compression of Isotropically Consolidated Specimens**		
Cell No.	2 (Big)	Fines content (%)	60
Specimen	2i	Specific gravity (g/cm^3)	2.72

1.) Sample physical properties

Wet mass before test (g)	904.226	m.c before test (%)	10.00	Height (mm)	147.20	Volume (cm^3)	668.646
Wet mass after test (g)	996.621	m.c. after test (%)	21.24	Diameter (mm)	76.05		
Dry mass (g)	822.024	Dry density (kg/m^3)	1229	Area (cm^2)	45.424	Void ratio (e_0)	1.212

2.) Saturation/Consolidation

Date	C.P (kPa)	P.W.P bp closed (kPa)	B.P (kPa)	P.W.P bp open (kPa)	Change C.P (kPa)	Change P.W.P (kPa)	B value	Volume Gauge (cm^3)	Cell Expansn (cm^3)	Specimen Volume (cm^3)	Void Ratio	Comments
4/1	0		0	-2.5				0.00	0.00	668.646	1.212	
4/1	11.5		8.3	5.0				10.20	0.00	658.446	1.179	**AIR-FLUSHING**
4/1	50	16.0	40	39.5	38.5	11.0	0.29	30.78	3.12	640.986	1.121	**S**
5/1	100	61.0	90	90.0	50	21.5	0.43	56.77	7.06	618.936	1.048	**A**
6/1	150	120.0	140	140.0	50	30.0	0.60	74.21	9.79	604.226	0.999	**T**
7/1	200	176.0	190	190.0	50	36.0	0.72	85.04	11.63	595.236	0.970	**U**
8/1	250	230.5	240	240.0	50	40.5	0.81	94.79	13.02	586.876	0.942	**R**
9/1	300	282.5	290	290.0	50	42.5	0.85	102.59	14.57	580.626	0.921	**A**
10/1	350	335.0	340	340.0	50	45.0	0.90	108.44	16.03	576.236	0.907	**T**
11/1	400	387.0	390	390.0	50	47.0	0.94	112.55	17.22	573.316	0.897	**I**
12/1	450	438.0	440	440.0	50	48.0	0.96	115.91	19.30	572.036	0.893	**O**
13/1	500	488.5	450	450.0	50	48.5	0.97					**N**
13/1	950		450	450.0				152.08	27.66	544.226	0.801	**CONSOLIDATION**

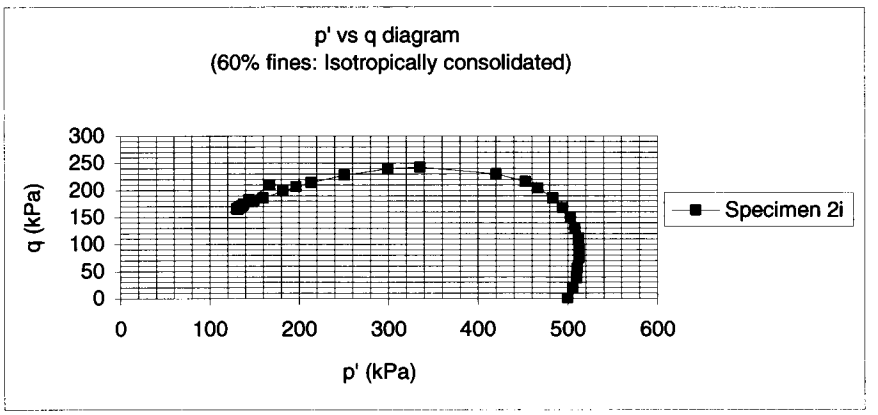
3.) Shear data

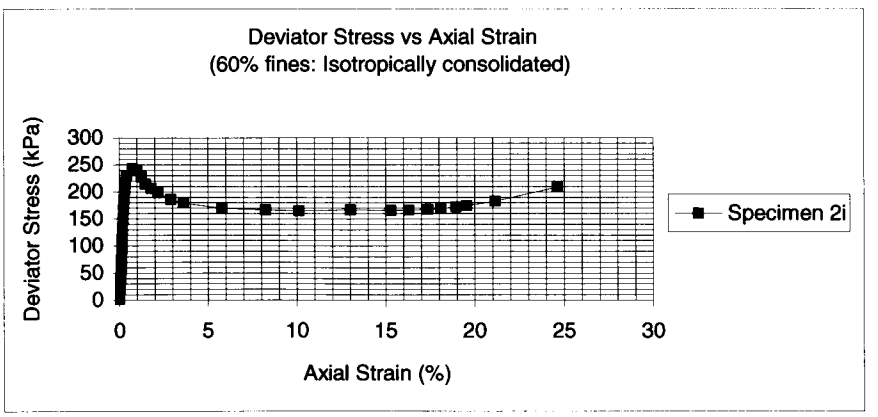
Volume change 1:		Volume change 2:		Sample Vol. change (cm^3)	124.42	B value	0.97
Air Flushing (cm^3)	10.20	Sat/Cons. (cm^3)	141.88	L_{cons} (mm)	138.07	p'consolidation (kPa)	500
Cell Expansion (cm^3)	0.00	Cell Expsn.(cm^3)	27.66	A_{cons} (cm^2)	39.789	Void ratio (e_1)	0.801

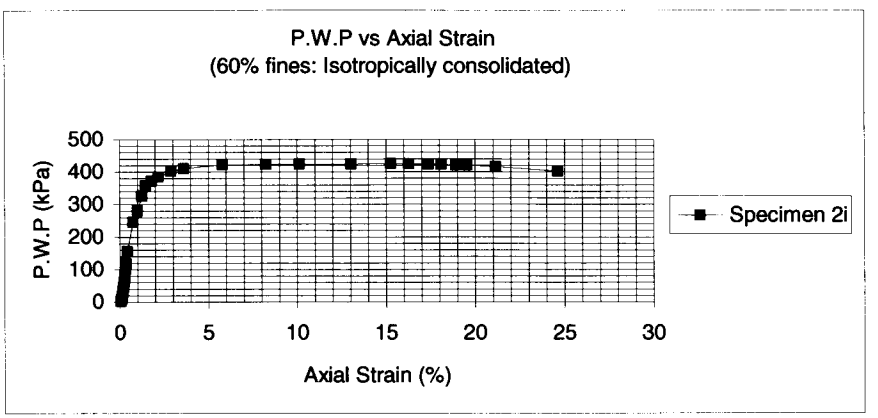
Proof ring properties		Strain gauge properties	
Proof ring No.	1800	1 strain division (mm)	0.01
Proof ring factor (dN/div)	14.846		

Strain Gauge (divs)	Axial Strain	Axial Strain (%)	Change Prf. ring (divs)	Change P.W.P (kPa)	q (Uncortd) (kPa)	Membrn. Corrctn. (kPa)	q (kPa)	t (kPa)	p' (kPa)	s' (kPa)
0	0.0000	0.0000	0.0	0.0	0.0	0.0	0.0	0.0	500.0	500.0
5	0.0004	0.0362	50.1	0.5	18.7	0.0	18.7	9.3	505.7	508.8
10	0.0007	0.0724	101.2	2.5	37.7	0.0	37.7	18.8	510.1	516.3
15	0.0011	0.1086	149.6	8.0	55.8	0.1	55.7	27.9	510.6	519.9
18	0.0013	0.1304	200.2	12.5	74.6	0.1	74.5	37.3	512.3	524.8
20	0.0014	0.1449	249.8	18.5	93.1	0.1	93.0	46.5	512.5	528.0
23	0.0017	0.1666	299.8	25.0	111.7	0.1	111.6	55.8	512.2	530.8
25	0.0018	0.1811	348.9	35.0	129.9	0.1	129.9	64.9	508.3	529.9
30	0.0022	0.2173	400.1	46.5	149.0	0.1	148.9	74.4	503.1	527.9
35	0.0025	0.2535	449.5	61.0	167.3	0.1	167.2	83.6	494.7	522.6
40	0.0029	0.2897	499.8	78.5	185.9	0.1	185.8	92.9	483.4	514.4
45	0.0033	0.3259	548.9	101.0	204.1	0.2	204.0	102.0	467.0	501.0
50	0.0036	0.3621	580.2	119.0	215.7	0.2	215.5	107.8	452.8	488.8
60	0.0043	0.4346	620.3	156.5	230.4	0.2	230.2	115.1	420.2	458.6
105	0.0076	0.7605	655.3	245.5	242.6	0.4	242.3	121.1	335.3	375.6
140	0.0101	1.0140	650.0	280.0	240.1	0.5	239.6	119.8	299.9	339.8
175	0.0127	1.2675	620.2	325.0	228.5	0.6	227.8	113.9	250.9	288.9
205	0.0148	1.4848	584.7	357.5	214.9	0.7	214.2	107.1	213.9	249.6
250	0.0181	1.8107	565.6	372.0	207.2	0.9	206.3	103.2	196.8	231.2
300	0.0217	2.1728	545.7	384.0	199.2	1.0	198.2	99.1	182.1	215.1
400	0.0290	2.8971	514.9	402.0	186.6	1.0	185.6	92.8	159.9	190.8
500	0.0362	3.6214	500.0	410.0	179.8	1.0	178.8	89.4	149.6	179.4
800	0.0579	5.7942	485.2	421.5	170.5	1.0	169.5	84.8	135.0	163.3
1140	0.0826	8.2567	489.8	423.0	167.7	1.0	166.7	83.3	132.6	160.3

Strain Gauge (divs)	Axial Strain	Axial Strain (%)	Change Prf. ring (divs)	Change P.W.P (kPa)	q (Uncortd) (kPa)	Membm. Corrctn. (kPa)	q (kPa)	t (kPa)	p' (kPa)	s' (kPa)
1400	0.1014	10.1398	495.3	423.5	166.1	1.0	165.1	82.5	131.5	159.0
1800	0.1304	13.0369	516.2	424.0	167.5	1.0	166.5	83.2	131.5	159.2
2110	0.1528	15.2821	526.1	425.0	166.3	1.0	165.3	82.6	130.1	157.6
2250	0.1630	16.2961	534.7	424.0	167.0	1.0	166.0	83.0	131.3	159.0
2400	0.1738	17.3825	545.0	423.0	168.0	1.0	167.0	83.5	132.7	160.5
2500	0.1811	18.1068	556.9	422.0	170.2	1.0	169.2	84.6	134.4	162.6
2615	0.1894	18.9397	572.2	420.0	173.1	1.0	172.1	86.0	137.4	166.0
2700	0.1956	19.5553	583.1	420.0	175.0	1.0	174.0	87.0	138.0	167.0
2920	0.2115	21.1487	623.4	416.5	183.4	1.0	182.4	91.2	144.3	174.7
3400	0.2463	24.6252	745.0	402.0	209.5	1.0	208.5	104.3	167.5	202.3







Test	**Case 1: Monotonic Undrained Compression of Isotropically Consolidated Specimens**		
Cell No.	3 (Big)	Fines content (%)	60
Specimen	3h	Specific gravity (g/cm^3)	2.72

1.) Sample physical properties

Wet mass before test (g)	902.210	m.c before test (%)	8.70	Height (mm)	149.05	Volume (cm^3)	670.832
Wet mass after test (g)	996.241	m.c. after test (%)	20.03	Diameter (mm)	75.70		
Dry mass (g)	830.000	Dry density (kg/m^3)	1237	Area (cm^2)	45.007	Void ratio (e_0)	1.198

2.) Saturation/Consolidation

Date	C.P (kPa)	P.W.P bp closed (kPa)	B.P (kPa)	P.W.P bp open (kPa)	Change C.P (kPa)	Change P.W.P (kPa)	B value	Volume Gauge (cm^3)	Cell Expansn (cm^3)	Specimen Volume (cm^3)	Void Ratio	Comments
16/12	0		0	-0.5				0.00	0.00	670.832	1.198	
16/12	10.2		8.5	6.5				7.80	0.00	663.032	1.173	**AIR-FLUSHING**
16/12	50	16.5	40	39.5	39.8	10.0	0.25	33.45	2.51	639.892	1.097	**S**
17/12	100	61.5	90	90.0	50	22.0	0.44	67.17	6.08	609.742	0.998	**A**
18/12	150	119.5	140	140.0	50	29.5	0.59	86.35	8.77	593.252	0.944	**T**
19/12	200	176.0	190	190.0	50	36.0	0.72	97.46	10.65	584.022	0.914	**U**
20/12	250	230.5	240	240.0	50	40.5	0.81	106.38	12.00	576.452	0.889	**R**
21/12	300	283.0	290	290.0	50	43.0	0.86	113.71	13.63	570.752	0.870	**A**
22/12	350	335.5	340	340.0	50	45.5	0.91	118.72	15.06	567.172	0.859	**T**
23/12	400	387.0	390	390.0	50	47.0	0.94	124.83	16.08	562.082	0.842	**I**
24/12	450	438.0	440	440.0	50	48.0	0.96	128.00	18.12	560.952	0.838	**O**
25/12	500	489.0	450	450.0	50	49.0	0.98					**N**
25/12	600		450	450.0				164.51	23.05	529.372	0.735	**CONSOLIDATION**

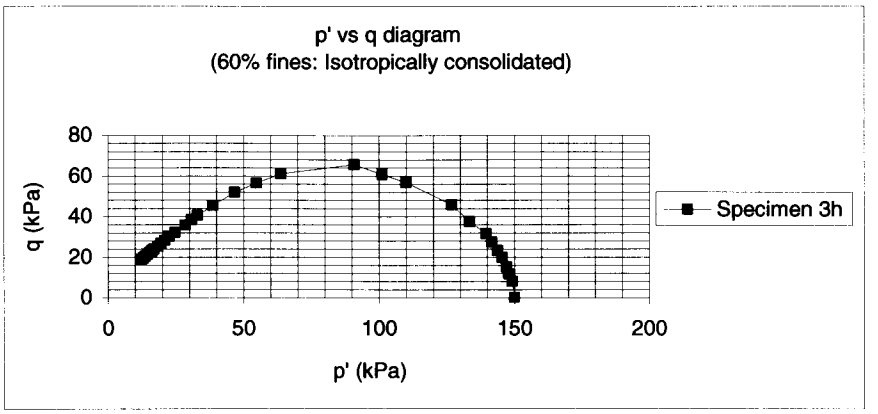
3.) Shear data

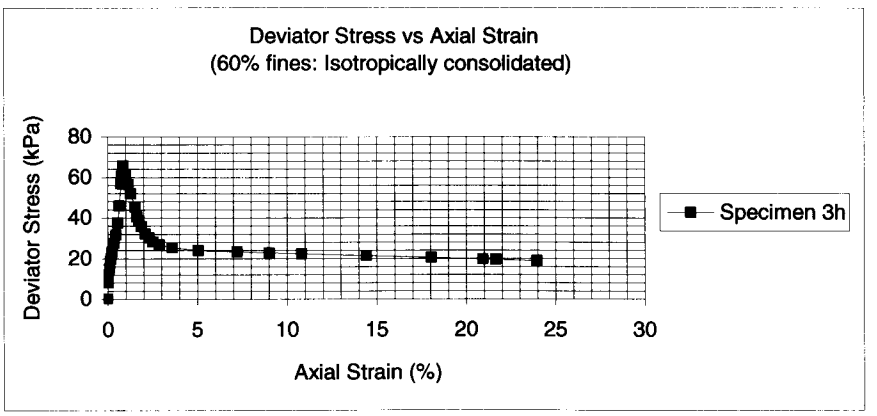
Volume change 1:		Volume change 2:		Sample Vol. change (cm^3)	141.46	B value	0.98
Air Flushing (cm^3)	7.80	Sat/Cons. (cm^3)	156.71	L_{cons} (mm)	138.57	p'consolidation (kPa)	150
Cell Expansion (cm^3)	0.00	Cell Expsn.(cm^3)	23.05	A_{cons} (cm^2)	38.680	Void ratio (e_1)	0.735

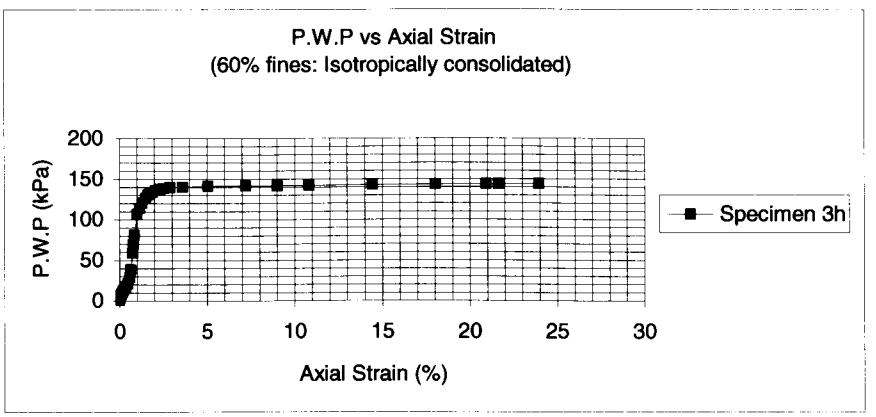
Proof ring properties		Strain gauge properties	
Proof ring No.	1800	1 strain division (mm)	0.01
Proof ring factor (dN/div)	14.846		

Strain Gauge (divs)	Axial Strain	Axial Strain (%)	Change Prf. ring (divs)	Change P.W.P (kPa)	q (Uncortd) (kPa)	Membrn. Corrctn. (kPa)	q (kPa)	t (kPa)	p' (kPa)	s' (kPa)
0	0.0000	0.0000	0.0	0.0	0.0	0.0	0.0	0.0	150.0	150.0
2	0.0001	0.0144	21.2	3.5	8.1	0.0	8.1	4.1	149.2	150.6
5	0.0004	0.0361	30.4	6.0	11.7	0.0	11.6	5.8	147.9	149.8
15	0.0011	0.1082	39.6	8.0	15.2	0.1	15.1	7.6	147.0	149.6
25	0.0018	0.1804	51.7	11.0	19.8	0.1	19.7	9.9	145.6	148.9
35	0.0025	0.2526	61.1	14.0	23.4	0.1	23.3	11.6	143.8	147.6
50	0.0036	0.3608	72.3	17.5	27.6	0.2	27.5	13.7	141.7	146.2
65	0.0047	0.4691	83.2	21.0	31.8	0.2	31.5	15.8	139.5	144.8
80	0.0058	0.5773	98.8	29.0	37.7	0.3	37.4	18.7	133.5	139.7
90	0.0065	0.6495	121.2	38.5	46.2	0.3	45.9	22.9	126.8	134.4
105	0.0076	0.7577	149.9	59.0	57.1	0.4	56.7	28.4	109.9	119.4
110	0.0079	0.7938	160.5	69.0	61.1	0.4	60.7	30.4	101.2	111.4
120	0.0087	0.8660	173.5	81.0	66.0	0.4	65.6	32.8	90.9	101.8
140	0.0101	1.0103	161.8	106.5	61.5	0.5	61.0	30.5	63.8	74.0
160	0.0115	1.1546	150.4	114.0	57.1	0.6	56.5	28.2	54.8	64.2
180	0.0130	1.2990	138.6	120.5	52.5	0.6	51.9	25.9	46.8	55.4
210	0.0152	1.5154	122.1	126.5	46.2	0.8	45.4	22.7	38.6	46.2
225	0.0162	1.6237	109.5	130.5	41.3	0.8	40.5	20.3	33.0	39.8
240	0.0173	1.7319	104.3	132.0	39.3	0.9	38.5	19.2	30.8	37.2
260	0.0188	1.8763	97.5	133.5	36.7	0.9	35.8	17.9	28.4	34.4
290	0.0209	2.0928	87.9	136.0	33.0	1.0	32.0	16.0	24.7	30.0
320	0.0231	2.3092	83.1	137.5	31.2	1.0	30.2	15.1	22.6	27.6
350	0.0253	2.5257	77.8	138.5	29.1	1.0	28.1	14.1	20.9	25.6
400	0.0289	2.8866	74.5	139.5	27.8	1.0	26.8	13.4	19.4	23.9

Strain Gauge (divs)	Axial Strain	Axial Strain (%)	Change Prf. ring (divs)	Change P.W.P (kPa)	q (Uncortd) (kPa)	Membrn. Corrctn. (kPa)	q (kPa)	t (kPa)	p' (kPa)	s' (kPa)
500	0.0361	3.6082	71.0	140.0	26.3	1.0	25.3	12.6	18.4	22.6
700	0.0505	5.0515	68.1	141.0	24.8	1.0	23.8	11.9	16.9	20.9
1000	0.0722	7.2164	68.1	141.5	24.3	1.0	23.3	11.6	16.3	20.1
1250	0.0902	9.0205	68.1	141.5	23.8	1.0	22.8	11.4	16.1	19.9
1500	0.1082	10.8246	68.1	142.0	23.3	1.0	22.3	11.2	15.4	19.2
2000	0.1443	14.4328	68.1	142.5	22.4	1.0	21.4	10.7	14.6	18.2
2500	0.1804	18.0410	68.1	143.0	21.4	1.0	20.4	10.2	13.8	17.2
2900	0.2093	20.9276	68.1	143.5	20.7	1.0	19.7	9.8	13.1	16.3
3000	0.2165	21.6492	68.1	143.5	20.5	1.0	19.5	9.7	13.0	16.2
3320	0.2396	23.9585	68.1	144.0	19.9	1.0	18.9	9.4	12.3	15.4







APPENDIX D

TEST RESULTS FOR SPECIMENS UNDER CASE 2 TESTS

Table D1 Summary of results of monotonic undrained compression triaxial tests performed on anisotropically consolidated Merriespruit gold tailings

Specimen No.	Fines Content	Initial stress state			Void ratio		Behavior	Peak shear resistance			Steady-state strength			L_P	L_R
		q_0	p'_0	K0	Setup	Final		q_P	p'_P	ϕ'_P	q_{ss}	p'_{ss}	ϕ'_{ss}		
	(%)	(kPa)	(kPa)					(kPa)	(kPa)	(Degrees)	(kPa)	(kPa)	(Degrees)		(kPa)
K0-1	0	133.7	224.6	0.57	1.473	1.106	Liquefaction	174.8	168.3	26.3	99.8	65.3	37.5	4.6	41.0
K0-2	0	53.1	90.2	0.58	1.491	1.154	Liquefaction	76.4	89.0	22.1	12.8	7.8	40.2	19.7	23.3
K0-9	0	78.4	156.1	0.62	1.469	1.146	Liquefaction	128.5	132.8	24.6	65.6	43.4	37.2	5.0	50.0
K0-10	0	63.2	121.1	0.61	1.512	1.131	Liquefaction	103.5	104.5	25.2	26.7	14.9	43.6	15.7	40.3
K0-13	0	72.2	134.1	0.60	1.561	1.089	Liquefaction	112.6	119.5	24.0	47.8	27.9	41.7	8.2	40.4
K0-14	0	137.1	245.7	0.59	1.544	1.134	Liquefaction	197.8	190.9	26.2	116.4	76.3	37.5	4.3	60.6
K0-19	0	294.4	548.1	0.60	1.525	1.060	Liquefaction	436.1	385.4	28.4	257.2	168.7	37.4	4.4	141.7
K0-20	0	221.9	374.0	0.57	1.508	1.042	Liquefaction	295.6	298.5	25.1	191.0	130.7	36.0	3.5	73.7
K0-24	0	156.1	302.0	0.62	1.503	1.077	Liquefaction	228.0	226.0	25.6	142.9	91.1	38.4	4.7	71.8
K0-3	20	105.1	195.0	0.60	1.478	1.137	Liquefaction	170.8	180.4	24.1	109.3	80.9	33.4	2.6	65.7
K0-4	20	140.1	226.7	0.56	1.497	1.099	Liquefaction	228.4	217.1	26.6	147.7	110.7	33.1	1.9	88.3
K0-11	20	69.5	112.2	0.56	1.413	1.156	Liquefaction	106.0	116.8	23.2	48.1	45.5	26.7	2.0	36.5
K0-18	20	63.1	96.0	0.54	1.436	1.239	Liquefaction	84.7	93.2	23.2	10.3	8.4	30.5	14.0	21.7
K0-21	20	87.4	161.1	0.60	1.385	1.224	Liquefaction	136.8	153.6	22.8	20.5	16.8	30.4	12.2	49.4
K0-25	20	123.7	205.2	0.57	1.392	1.108	Liquefaction	173.5	195.8	22.7	68.3	64.8	26.7	2.9	49.9
K0-26	20	171.3	269.1	0.55	1.358	1.033	Liquefaction	237.3	241.1	25.0	166.1	125.4	32.9	2.0	66.0
K0-33	20	194.8	321.9	0.57	1.423	1.052	Liquefaction	255.5	267.2	24.4	172.9	122.6	34.8	3.0	60.6
K0-34	20	187.1	332.4	0.59	1.446	1.061	Liquefaction	259.9	282.1	23.5	167.2	122.7	33.7	3.0	72.9
K0-5	30	72.6	114.2	0.55	1.437	0.973	Liquefaction	102.0	112.0	23.3	14.0	11.7	29.9	11.9	29.4
K0-6	30	148.3	231.4	0.55	1.418	0.964	Liquefaction	233.0	234.2	25.3	139.9	97.1	35.5	2.6	84.7
K0-12	30	93.3	168.1	0.60	1.365	0.935	Liquefaction	155.1	163.2	24.2	69.9	48.3	35.7	4.5	61.8
K0-16	30	114.3	190.1	0.57	1.399	0.901	Liquefaction	199.2	192.9	26.1	118.5	84.5	34.6	2.4	84.9
K0-22	30	186.4	322.1	0.58	1.448	0.916	Liquefaction	269.3	281.3	24.4	159.2	108.1	36.3	3.7	82.9
K0-27	30	204.3	368.1	0.59	1.469	0.940	Liquefaction	285.0	285.0	25.4	167.3	117.8	35.0	3.8	80.7
K0-28	30	81.7	147.2	0.60	1.509	0.892	Liquefaction	126.0	127.0	25.2	61.8	46.1	33.2	3.7	44.4
K0-32	30	134.4	244.8	0.60	1.426	0.908	Liquefaction	242.5	247.8	24.9	147.4	108.1	33.7	2.4	108.1
K0-35	30	159.1	270.0	0.58	1.555	0.863	Liquefaction	243.7	272.7	22.9	153.0	126.0	30.3	1.9	84.6
K0-7	60	103.7	174.6	0.57	1.351	0.754	Liquefaction	148.1	139.4	26.8	79.8	49.6	39.4	5.1	44.4

Specimen No.	Fines Content (%)	Initial stress state			Void ratio		Behavior	Peak shear resistance			Steady-state strength			L_P	L_R (kPa)
		q_0 (kPa)	p'_0 (kPa)	K0	Setup	Final		q_P (kPa)	p'_P (kPa)	ϕ'_P (Degrees)	q_{SS} (kPa)	p'_{SS} (kPa)	ϕ'_{SS} (Degrees)		
K0-8	60	56.3	102.8	0.60	1.302	0.748	Liquefaction	86.0	100.7	22.0	26.4	23.8	27.9	4.6	29.7
K0-15	60	66.1	137.0	0.63	1.300	0.785	Liquefaction	108.1	116.0	23.8	53.3	29.8	43.6	8.6	41.9
K0-17	60	128.5	212.8	0.57	1.227	0.762	Lim liqfction	183.7	161.2	28.6	99.3	62.6	38.9	4.8	55.2
K0-23	60	219.8	423.3	0.61	1.180	0.753	Lim liqfction	296.5	308.8	24.4	193.9	129.6	36.8	4.4	76.7
K0-29	60	245.3	481.8	0.62	1.136	0.727	Lim liqfction	308.6	332.9	23.7	214.7	133.6	39.3	5.5	63.3
K0-30	60	158.1	302.7	0.61	1.160	0.758	Lim liqfction	226.5	215.5	26.6	142.2	85.4	40.7	5.6	68.4
K0-31	60	200.3	366.8	0.60	1.111	0.750	Lim liqfction	264.4	258.1	25.9	174.5	101.2	42.1	6.0	64.1
K0-36	60	140.4	246.8	0.59	1.180	0.771	Liquefaction	196.6	175.5	28.2	127.1	78.9	39.4	4.5	56.2

Test	**Case 2: Monotonic Undrained Compression of One-Dimensionally Consolidated Specimens**		
Cell No.	3 (Big)	Fines content (%)	0
Specimen	K0-1	Specific gravity (g/cm^3)	2.72

1.) Sample physical properties

Wet mass before test (g)	841.609	m.c before test (%)	9.65	Height (mm)	151.25	Volume (cm^3)	697.926
Wet mass after test (g)	974.854	m.c. after test (%)	27.01	Diameter (mm)	76.65		
Dry mass (g)	767.541	Dry density (kg/m^3)	1100	Area (cm^2)	46.144	Void ratio (e_0)	1.473

2.) Saturation / Consolidation

Proof ring properties		Strain gauge properties		Loading ram properties	
Proof ring No.	5153	1 strain division (mm)	0.01	Area [ram]$_1$ (cm^2)	7.905
Proof ring factor (dN/div)	7.512			Area [ram]$_2$ (cm^2)	5.004

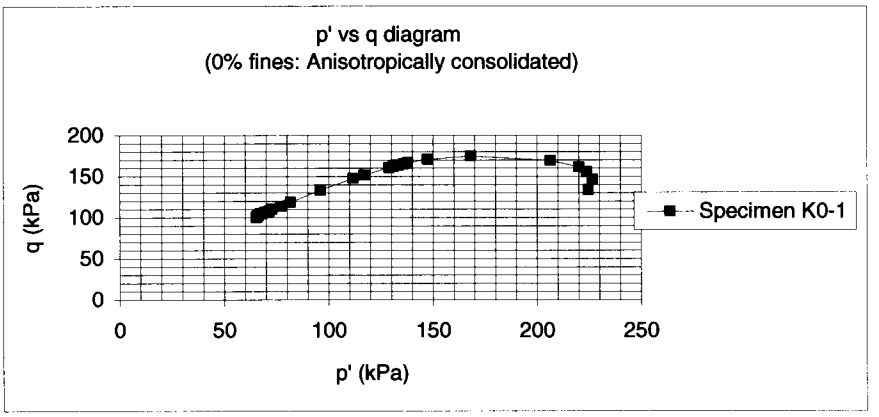
Date	Strain Gauge (divs)	Change Length (mm)	Cell Pressure (kPa)	Proof Ring (div)	Pore Pressure (kPa)	P_1 (kPa)	P'_3 (kPa)	P'_1 (kPa)	q (kPa)	p' (kPa)	K0	Volume Gauge (cm^3)	Cell Expansn (cm^3)
3/3	0	0.000	0	0.0	0.0						\	0.00	0.00
3/3	0	0.000	12.5		8.0	A I R - F L U S H I N G					\	8.00	0.00
3/3	195	1.950	50	125.0	40.0	61.8	10	21.8	11.8	13.9	0.46	33.41	6.08
4/3	324	3.240	100	168.2	90.0	110.3	10	20.3	10.3	13.4	0.49	52.13	8.77
5/3	512	5.120	150	202.1	140.0	157.2	10	17.2	7.2	12.4	0.58	62.00	10.65
6/3	694	6.940	200	250.5	190.0	206.5	10	16.5	6.5	12.2	0.61	69.57	12.00
7/3	826	8.260	250	305.2	240.0	256.9	10	16.9	6.9	12.3	0.59	74.49	13.63
8/3	933	9.330	300	362.7	290.0	307.7	10	17.7	7.7	12.6	0.57	78.03	15.06
9/3	1103	11.030	350	412.3	340.0	357.2	10	17.2	7.2	12.4	0.58	81.95	16.08
10/3	1255	12.550	400	650.0	350.0	437.3	50	87.3	37.3	62.4	0.57	86.49	18.12
11/3	1404	14.040	450	853.3	350.0	511.8	100	161.8	61.8	120.6	0.62	90.07	19.91
12/3	1700	17.000	550	1400.0	370.0	683.7	180	313.7	133.7	224.6	0.57	117.55	22.28

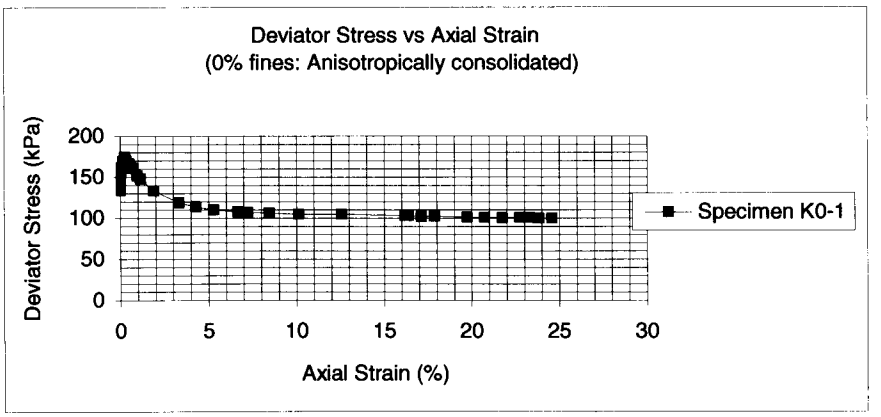
3.) Shear data

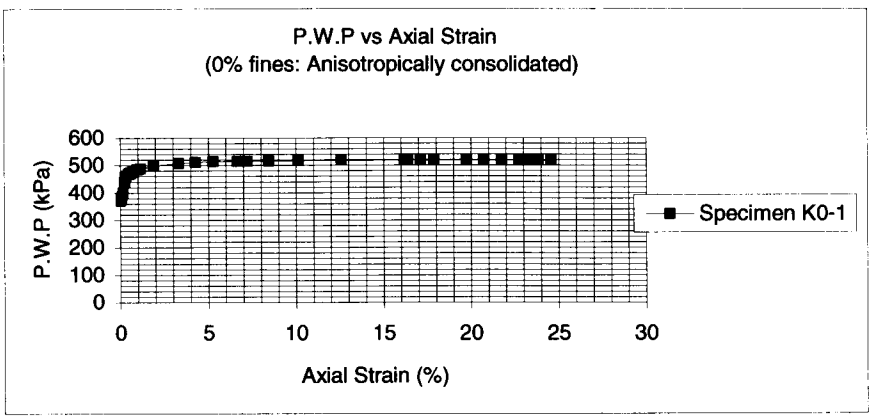
Volume change 1:		Volume change 2:		Sample Vol. change (cm^3)	103.78	B value	0.99
Air Flushing (cm^3)	8.00	Sat/Cons. (cm^3)	109.55	L_{cons} (mm)	134.25	K0	0.57
Cell Expsn. (cm^3)	0.00	Cell Expsn. (cm^3)	22.28	A_{cons} (cm^2)	46.144	Void ratio (e_1)	1.106
		Ram into cell (cm^3)	8.51				

Strain Gauge (divs)	Axial Strain (%)	Cell Press. (kPa)	Proof Ring (divs)	Pore Pressure (kPa)	Membrane Correction (kPa)	P_1 (kPa)	q (kPa)	t (kPa)	p' (kPa)	s' (kPa)
0	0.0000	550	1400.2	370.0	0.0	683.7	133.7	66.9	224.6	246.9
2	0.0149	550	1475.7	372.0	0.0	696.0	146.0	73.0	226.7	251.0
6	0.0447	550	1535.0	378.0	0.0	705.6	155.6	77.8	223.9	249.8
13	0.0968	550	1570.5	383.5	0.0	711.2	161.2	80.6	220.2	247.1
22	0.1639	550	1620.7	400.0	0.1	719.3	169.3	84.6	206.4	234.6
35	0.2607	550	1655.9	440.0	0.1	724.8	174.8	87.4	168.3	197.4
45	0.3352	550	1632.4	459.5	0.2	720.8	170.8	85.4	147.4	175.9
65	0.4842	550	1607.5	467.5	0.2	716.4	166.4	83.2	138.0	165.7
70	0.5214	550	1600.0	469.0	0.3	715.1	165.1	82.6	136.0	163.6
75	0.5587	550	1591.3	471.0	0.3	713.6	163.6	81.8	133.5	160.8
80	0.5959	550	1580.2	473.0	0.3	711.8	161.8	80.9	130.9	157.9
95	0.7076	550	1575.1	474.5	0.4	710.7	160.7	80.3	129.1	155.8
130	0.9683	550	1521.7	483.5	0.5	701.5	151.5	75.8	117.0	142.3
155	1.1546	550	1500.0	487.5	0.6	697.7	147.7	73.8	111.7	136.3
255	1.8994	550	1418.6	498.5	0.9	683.2	133.2	66.6	95.9	118.1
445	3.3147	550	1340.5	508.0	1.0	668.9	118.9	59.4	81.6	101.4
575	4.2831	550	1315.9	511.0	1.0	663.9	113.9	56.9	77.0	95.9
710	5.2886	550	1300.1	514.0	1.0	660.2	110.2	55.1	72.7	91.1
895	6.6667	550	1295.5	514.5	1.0	657.9	107.9	54.0	71.5	89.5
970	7.2253	550	1292.4	515.0	1.0	656.8	106.8	53.4	70.6	88.4
1135	8.4544	550	1298.0	516.0	1.0	656.2	106.2	53.1	69.4	87.1
1360	10.1304	550	1302.3	517.0	1.0	654.9	104.9	52.4	68.0	85.4
1690	12.5885	550	1320.4	517.5	1.0	654.5	104.5	52.3	67.3	84.8
2175	16.2011	550	1340.7	518.0	1.0	652.9	102.9	51.5	66.3	83.5

Strain Gauge (divs)	Axial Strain (%)	Cell Press. (kPa)	Proof Ring (divs)	Pore Pressure (kPa)	Membrane Correction (kPa)	P_1 (kPa)	q (kPa)	t (kPa)	p' (kPa)	s' (kPa)
2200	16.3873	550	1342.3	518.0	1.0	652.9	102.9	51.5	66.3	83.5
2300	17.1322	550	1343.2	518.0	1.0	652.1	102.1	51.1	66.0	83.1
2400	17.8771	550	1350.4	518.0	1.0	652.2	102.2	51.1	66.1	83.1
2650	19.7393	550	1360.0	518.0	1.0	651.1	101.1	50.5	65.7	82.5
2785	20.7449	550	1367.2	518.0	1.0	650.7	100.7	50.4	65.6	82.4
2920	21.7505	550	1373.8	518.0	1.0	650.3	100.3	50.1	65.4	82.1
3055	22.7561	550	1386.9	518.0	1.0	650.6	100.6	50.3	65.5	82.3
3125	23.2775	550	1393.0	518.0	1.0	650.7	100.7	50.3	65.6	82.3
3200	23.8361	550	1393.7	518.0	1.0	650.0	100.0	50.0	65.3	82.0
3300	24.5810	550	1400.0	518.0	1.0	649.8	99.8	49.9	65.3	81.9







Test	**Case 2: Monotonic Undrained Compression of One-Dimensionally Consolidated Specimens**		
Cell No.	2 (Big)	Fines content (%)	0
Specimen	K0-2	Specific gravity (g/cm^3)	2.72

1.) Sample physical properties

Wet mass before test (g)	840.860	m.c before test (%)	8.99	Height (mm)	152.55	Volume (cm^3)	706.683
Wet mass after test (g)	957.743	m.c. after test (%)	24.14	Diameter (mm)	76.80		
Dry mass (g)	771.502	Dry density (kg/m^3)	1092	Area (cm^2)	46.325	Void ratio (e_0)	1.491

2.) Saturation / Consolidation

Proof ring properties		Strain gauge properties		Loading ram properties	
Proof ring No.	4541	1 strain division (mm)	0.01	Area [ram]$_1$ (cm^2)	7.905
Proof ring factor (dN/div)	25.77			Area [ram]$_2$ (cm^2)	5.004

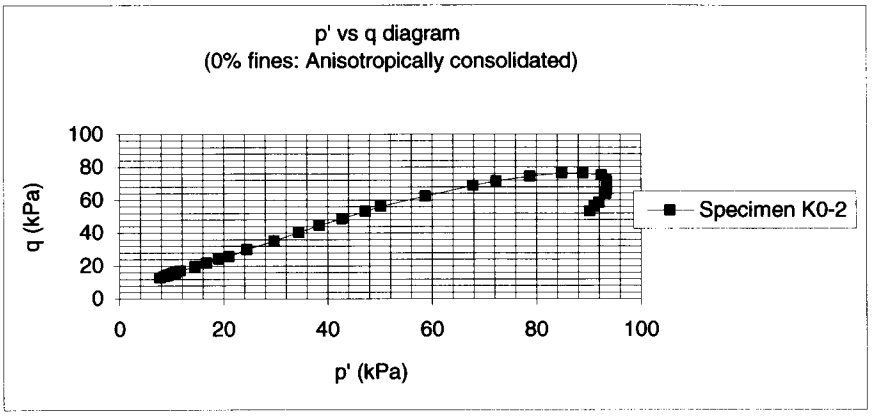
Date	Strain Gauge (divs)	Change Length (mm)	Cell Pressure (kPa)	Proof Ring (div)	Pore Pressure (kPa)	P_1 (kPa)	P'_3 (kPa)	P'_1 (kPa)	q (kPa)	p' (kPa)	K0	Volume Gauge (cm^3)	Cell Expansn (cm^3)
3/3	0	0.000	0	0.0	0.0						\	0.00	0.00
3/3	0	0.000	9.8		6.5	A I R - F L U S H I N G					\	6.25	0.00
3/3	214	2.140	50	50.2	40.0	69.4	10	29.4	19.4	16.5	0.34	31.27	7.06
4/3	400	4.000	100	55.4	90.0	113.7	10	23.7	13.7	14.6	0.42	48.52	9.79
5/3	586	5.860	150	65.0	140.0	160.6	10	20.6	10.6	13.5	0.49	58.93	11.63
6/3	723	7.230	200	74.1	190.0	207.1	10	17.1	7.1	12.4	0.59	71.34	13.02
7/3	879	8.790	250	89.0	240.0	256.8	10	16.8	6.8	12.3	0.59	82.16	14.57
8/3	995	9.950	300	105.8	290.0	307.7	10	17.7	7.7	12.6	0.57	92.48	16.03
9/3	1174	11.740	350	120.6	340.0	357.4	10	17.4	7.4	12.5	0.58	96.79	17.22
10/3	1320	13.200	400	200.9	350.0	443.5	50	93.5	43.5	64.5	0.53	101.55	19.30
11/3	1459	14.590	450	233.5	377.5	503.1	73	125.6	53.1	90.2	0.58	109.25	20.93

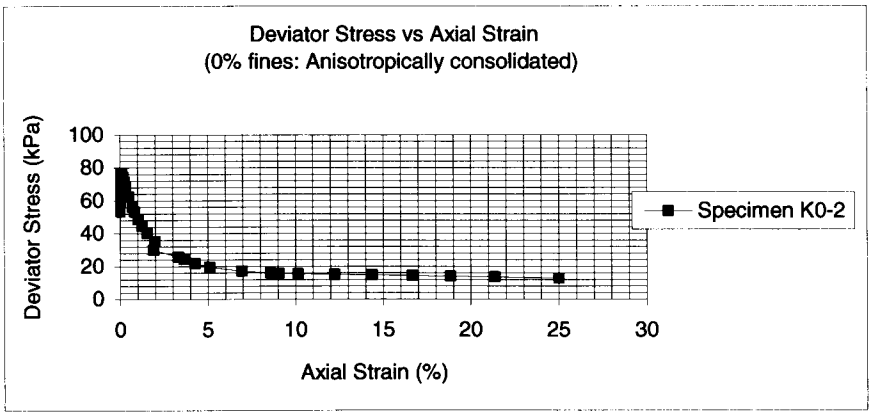
3.) Shear data

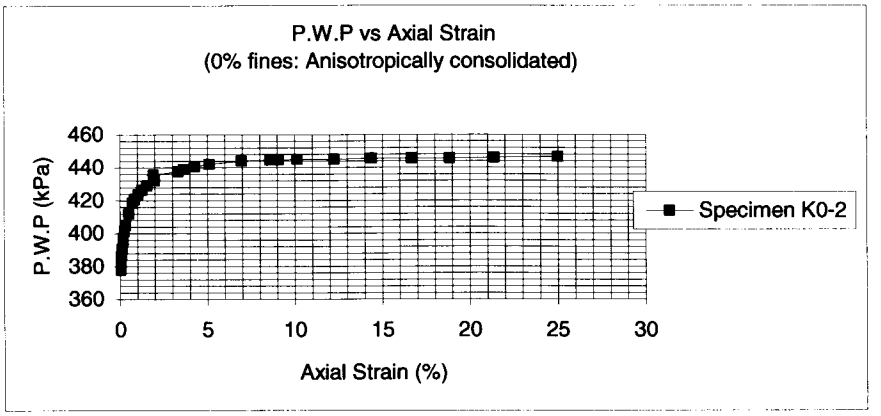
Volume change 1:		Volume change 2:		Sample Vol. change (cm^3)	95.62	B value	0.98
Air Flushing (cm^3)	6.25	Sat/Cons. (cm^3)	103.00	L_{cons} (mm)	137.96	K0	0.58
Cell Expsn. (cm^3)	0.00	Cell Expsn. (cm^3)	20.93	A_{cons} (cm^2)	46.325	Void ratio (e_1)	1.154
		Ram into cell (cm^3)	7.30				

Strain Gauge (divs)	Axial Strain (%)	Cell Press. (kPa)	Proof Ring (divs)	Pore Pressure (kPa)	Membrane Correction (kPa)	P_1 (kPa)	q (kPa)	t (kPa)	p' (kPa)	s' (kPa)
0	0.0000	450	233.5	377.5	0.0	503.1	53.1	26.6	90.2	99.1
1	0.0072	450	238.7	377.5	0.0	506.0	56.0	28.0	91.2	100.5
2	0.0145	450	243.2	377.5	0.0	508.5	58.5	29.2	92.0	101.7
3	0.0217	450	252.9	378.0	0.0	513.9	63.9	31.9	93.3	103.9
4	0.0290	450	256.5	378.5	0.0	515.9	65.9	32.9	93.5	104.4
5	0.0362	450	267.2	380.5	0.0	521.8	71.8	35.9	93.4	105.4
7	0.0522	450	272.8	382.5	0.0	524.9	74.9	37.5	92.5	105.0
12	0.0848	450	275.5	386.5	0.0	526.4	76.4	38.2	89.0	101.7
17	0.1210	450	275.5	390.5	0.1	526.3	76.3	38.2	84.9	97.7
25	0.1812	450	272.1	396.0	0.1	524.4	74.4	37.2	78.8	91.2
35	0.2537	450	267.0	401.5	0.1	521.4	71.4	35.7	72.3	84.2
45	0.3262	450	262.2	405.0	0.2	518.7	68.7	34.3	67.9	79.3
70	0.5074	450	250.9	412.0	0.3	512.2	62.2	31.1	58.7	69.1
100	0.7248	450	240.1	418.5	0.4	506.0	56.0	28.0	50.2	59.5
115	0.8336	450	235.2	420.5	0.4	503.2	53.2	26.6	47.2	56.1
145	1.0489	450	227.5	423.5	0.5	498.7	48.7	24.4	42.7	50.9
175	1.2685	450	220.3	426.5	0.6	494.5	44.5	22.3	38.3	45.8
215	1.5584	450	213.0	429.0	0.8	490.3	40.3	20.1	34.4	41.1
275	1.9933	450	204.4	432.0	1.0	485.2	35.2	17.6	29.7	35.6
265	1.9208	450	194.6	435.5	1.0	479.9	29.9	15.0	24.5	29.5
460	3.3343	450	187.5	437.5	1.0	475.6	25.6	12.8	21.0	25.3
505	3.6605	450	185.2	439.0	1.0	474.3	24.3	12.1	19.1	23.1
590	4.2766	450	180.8	440.5	1.0	471.8	21.8	10.9	16.8	20.4
705	5.1102	450	177.0	442.0	1.0	469.6	19.6	9.8	14.5	17.8

Strain Gauge (divs)	Axial Strain (%)	Cell Press. (kPa)	Proof Ring (divs)	Pore Pressure (kPa)	Membrane Correction (kPa)	P_1 (kPa)	q (kPa)	t (kPa)	p' (kPa)	s' (kPa)
960	6.9585	450	172.7	444.0	1.0	466.9	16.9	8.5	11.6	14.5
1185	8.5894	450	171.0	444.5	1.0	465.8	15.8	7.9	10.8	13.4
1250	9.0606	450	171.0	444.5	1.0	465.7	15.7	7.8	10.7	13.3
1400	10.1479	450	171.0	445.0	1.0	465.5	15.5	7.7	10.2	12.7
1690	12.2499	450	171.0	445.0	1.0	465.1	15.1	7.5	10.0	12.5
1985	14.3882	450	171.0	445.5	1.0	464.7	14.7	7.3	9.4	11.8
2300	16.6715	450	171.0	445.5	1.0	464.3	14.3	7.1	9.3	11.6
2600	18.8460	450	171.0	445.5	1.0	463.9	13.9	6.9	9.1	11.4
2950	21.3830	450	171.0	446.0	1.0	463.4	13.4	6.7	8.5	10.7
3450	25.0072	450	171.0	446.5	1.0	462.8	12.8	6.4	7.8	9.9







Test	**Case 2: Monotonic Undrained Compression of One-Dimensionally Consolidated Specimens**		
Cell No.	2 (Big)	Fines content (%)	0
Specimen	K0-9	Specific gravity (g/cm^3)	2.72

1.) Sample physical properties

Wet mass before test (g)	846.129	m.c before test (%)	10.05	Height (mm)	150.85	Volume (cm^3)	697.898
Wet mass after test (g)	948.464	m.c. after test (%)	23.36	Diameter (mm)	76.75		
Dry mass (g)	768.859	Dry density (kg/m^3)	1102	Area (cm^2)	46.264	Void ratio (e_0)	1.469

2.) Saturation / Consolidation

Proof ring properties		Strain gauge properties		Loading ram properties	
Proof ring No.	4541	1 strain division (mm)	0.01	Area [ram]$_1$ (cm^2)	7.905
Proof ring factor (dN/div)	25.77			Area [ram]$_2$ (cm^2)	5.004

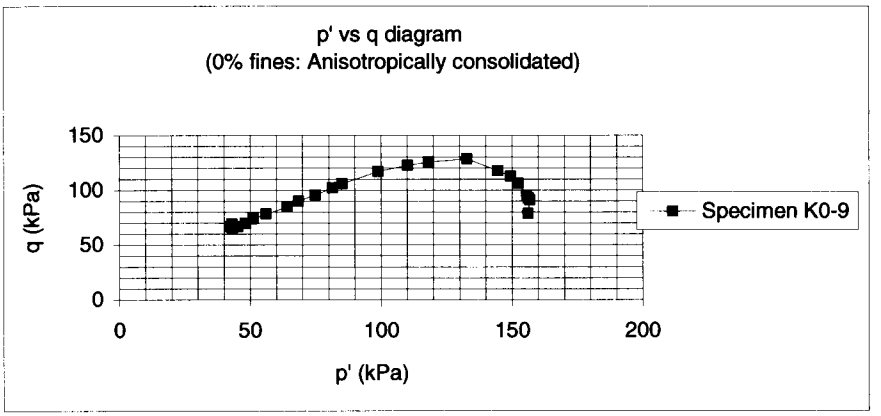
Date	Strain Gauge (divs)	Change Length (mm)	Cell Pressure (kPa)	Proof Ring (div)	Pore Pressure (kPa)	P_1 (kPa)	P'_3 (kPa)	P'_1 (kPa)	q (kPa)	p' (kPa)	K0	Volume Gauge (cm^3)	Cell Expansn (cm^3)
19/4	0	0.000	0	0.0	0.0						\	0.00	0.00
19/4	0	0.000	10.0		8.4	A I R - F L U S H I N G					\	9.60	0.00
19/4	244	2.440	50	33.1	40.0	59.9	10	19.9	9.9	13.3	0.50	34.12	7.06
20/4	463	4.630	100	45.0	90.0	108.0	10	18.0	8.0	12.7	0.56	51.23	9.79
21/4	589	5.890	150	58.6	140.0	157.0	10	17.0	7.0	12.3	0.59	60.05	11.63
22/4	700	7.000	200	74.5	190.0	207.3	10	17.3	7.3	12.4	0.58	67.41	13.02
23/4	842	8.420	250	88.3	240.0	256.5	10	16.5	6.5	12.2	0.61	72.31	14.57
24/4	961	9.610	300	105.8	290.0	307.7	10	17.7	7.7	12.6	0.57	76.98	16.03
25/4	1054	10.540	350	119.1	340.0	356.5	10	16.5	6.5	12.2	0.60	81.12	17.22
26/4	1122	11.220	400	136.9	390.0	407.9	10	17.9	7.9	12.6	0.56	86.04	19.30
27/4	1214	12.140	450	150.2	440.0	456.8	10	16.8	6.8	12.3	0.60	89.97	20.93
28/4	1300	13.000	500	166.4	490.0	507.3	10	17.3	7.3	12.4	0.58	96.30	22.85
29/4	1535	15.350	650	340.0	520.0	728.3	130	208.3	78.3	156.1	0.62	110.05	26.33

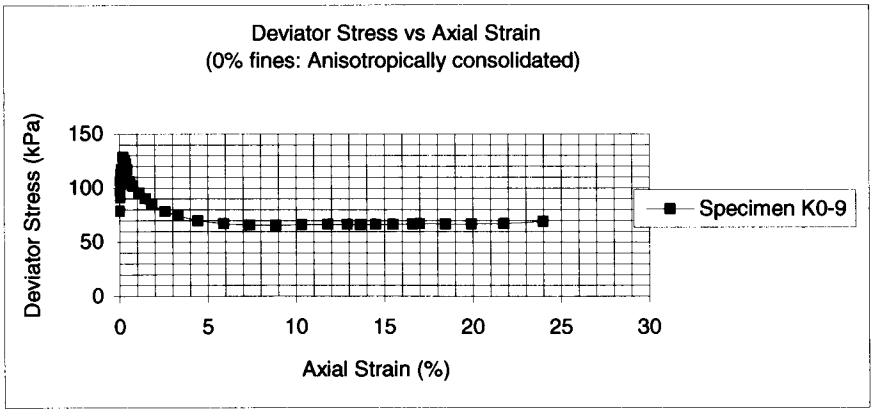
3.) Shear data

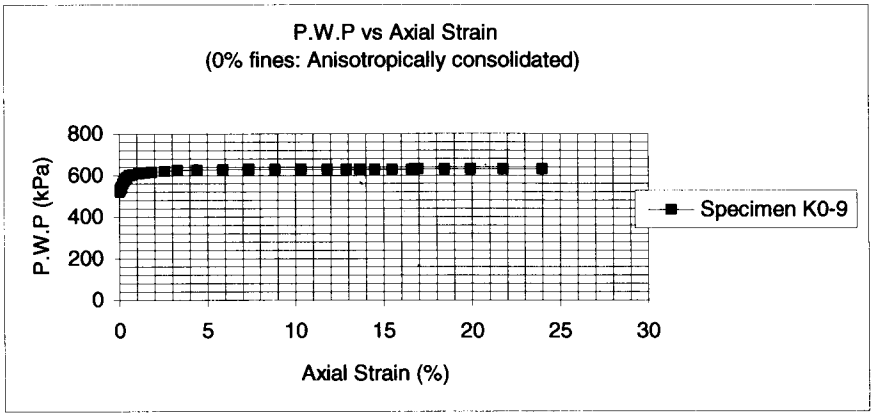
Volume change 1:		Volume change 2:		Sample Vol. change (cm^3)	91.40	B value	0.99
Air Flushing (cm^3)	9.60	Sat/Cons. (cm^3)	100.45	L_{cons} (mm)	135.50	K0	0.62
Cell Expsn. (cm^3)	0.00	Cell Expsn. (cm^3)	26.33	A_{cons} (cm^2)	46.264	Void ratio (e_1)	1.146
		Ram into cell (cm^3)	7.68				

Strain Gauge (divs)	Axial Strain (%)	Cell Press. (kPa)	Proof Ring (divs)	Pore Pressure (kPa)	Membrane Correction (kPa)	P_1 (kPa)	q (kPa)	t (kPa)	p' (kPa)	s' (kPa)
0	0.0000	650	340.2	520.0	0.0	728.4	78.4	39.2	156.1	169.2
2	0.0148	650	362.7	523.5	0.0	740.9	90.9	45.5	156.8	172.0
4	0.0295	650	365.5	524.5	0.0	742.5	92.5	46.2	156.3	171.7
6	0.0443	650	370.4	526.0	0.0	745.2	95.2	47.6	155.7	171.6
10	0.0738	650	390.1	533.0	0.0	756.1	106.1	53.1	152.4	170.1
15	0.1107	650	401.9	538.0	0.1	762.6	112.6	56.3	149.5	168.3
20	0.1476	650	410.5	544.5	0.1	767.3	117.3	58.7	144.6	164.2
30	0.2214	650	430.7	560.0	0.1	778.5	128.5	64.2	132.8	154.2
40	0.2952	650	425.3	573.5	0.1	775.3	125.3	62.7	118.3	139.2
50	0.3690	650	420.2	580.5	0.2	772.4	122.4	61.2	110.3	130.7
60	0.4428	650	410.5	590.0	0.2	766.9	116.9	58.4	99.0	118.4
80	0.5904	650	390.8	600.0	0.3	755.7	105.7	52.8	85.2	102.8
100	0.7380	650	384.6	602.5	0.4	752.0	102.0	51.0	81.5	98.5
150	1.1070	650	373.8	607.0	0.6	745.5	95.5	47.8	74.8	90.8
200	1.4760	650	364.7	611.5	0.7	740.0	90.0	45.0	68.5	83.5
250	1.8450	650	355.6	614.0	0.9	734.5	84.5	42.2	64.2	78.2
350	2.5830	650	345.4	620.0	1.0	728.2	78.2	39.1	56.1	69.1
450	3.3210	650	338.6	623.5	1.0	724.0	74.0	37.0	51.2	63.5
600	4.4280	650	332.1	625.0	1.0	719.7	69.7	34.8	48.2	59.8
800	5.9041	650	329.0	627.0	1.0	716.9	66.9	33.5	45.3	56.5
1000	7.3801	650	329.0	628.5	1.0	715.9	65.9	32.9	43.5	54.4
1200	8.8561	650	330.5	628.5	1.0	715.6	65.6	32.8	43.4	54.3
1400	10.3321	650	333.7	628.5	1.0	716.1	66.1	33.0	43.5	54.5
1600	11.8081	650	336.8	629.0	1.0	716.5	66.5	33.3	43.2	54.3

Strain Gauge (divs)	Axial Strain (%)	Cell Press. (kPa)	Proof Ring (divs)	Pore Pressure (kPa)	Membrane Correction (kPa)	P_1 (kPa)	q (kPa)	t (kPa)	p' (kPa)	s' (kPa)
1750	12.9151	650	338.6	629.0	1.0	716.5	66.5	33.3	43.2	54.3
1850	13.6531	650	339.1	629.0	1.0	716.2	66.2	33.1	43.1	54.1
1965	14.5018	650	340.8	629.0	1.0	716.3	66.3	33.2	43.1	54.2
2100	15.4982	650	342.3	629.0	1.0	716.3	66.3	33.1	43.1	54.1
2250	16.6052	650	345.4	629.0	1.0	716.8	66.8	33.4	43.3	54.4
2300	16.9742	650	346.5	629.5	1.0	717.0	67.0	33.5	42.8	54.0
2500	18.4502	650	348.6	629.5	1.0	716.8	66.8	33.4	42.8	53.9
2700	19.9262	650	350.9	629.5	1.0	716.6	66.6	33.3	42.7	53.8
2950	21.7712	650	355.1	630.0	1.0	716.9	66.9	33.4	42.3	53.4
3250	23.9852	650	365.2	630.0	1.0	719.2	69.2	34.6	43.1	54.6







Test	Case 2: Monotonic Undrained Compression of One-Dimensionally Consolidated Specimens		
Cell No.	3 (Big)	Fines content (%)	0
Specimen	K0-10	Specific gravity (g/cm^3)	2.72

1.) Sample physical properties

Wet mass before test (g)	828.194	m.c before test (%)	9.66	Height (mm)	150.95	Volume (cm^3)	697.451
Wet mass after test (g)	949.712	m.c. after test (%)	25.75	Diameter (mm)	76.70		
Dry mass (g)	755.238	Dry density (kg/m^3)	1083	Area (cm^2)	46.204	Void ratio (e_0)	1.512

2.) Saturation / Consolidation

Proof ring properties		Strain gauge properties		Loading ram properties	
Proof ring No.	5153	1 strain division (mm)	0.01	Area [ram]$_1$ (cm^2)	7.905
Proof ring factor (dN/div)	7.512			Area [ram]$_2$ (cm^2)	5.004

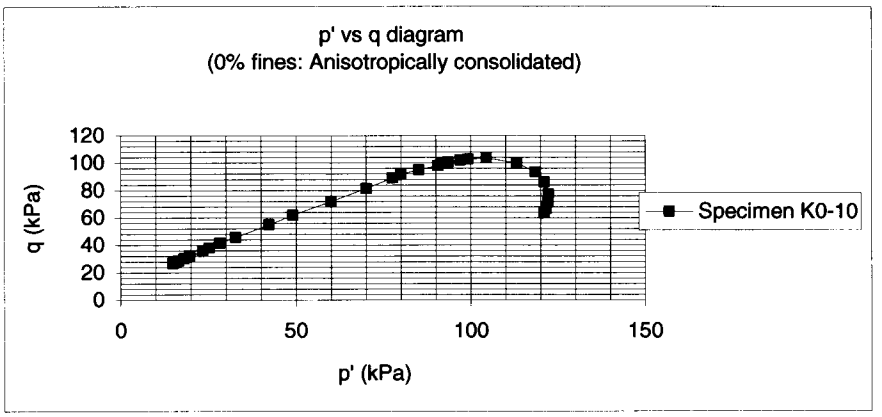
Date	Strain Gauge (divs)	Change Length (mm)	Cell Pressure (kPa)	Proof Ring (div)	Pore Pressure (kPa)	P_1 (kPa)	P'_3 (kPa)	P'_1 (kPa)	q (kPa)	p' (kPa)	K0	Volume Gauge (cm^3)	Cell Expansn (cm^3)
19/4	0	0.000	0	0.0	0.0						\	0.00	0.00
19/4	0	0.000	7.5		5.0	A I R - F L U S H I N G					\	8.35	0.00
19/4	212	2.120	50	136.6	40.0	63.7	10	23.7	13.7	14.6	0.42	35.10	6.08
20/4	417	4.170	100	167.0	90.0	110.0	10	20.0	10.0	13.3	0.50	54.87	8.77
21/4	562	5.620	150	217.8	140.0	159.7	10	19.7	9.7	13.2	0.51	67.92	10.65
22/4	671	6.710	200	262.4	190.0	208.4	10	18.4	8.4	12.8	0.54	76.05	12.00
23/4	786	7.860	250	308.5	240.0	257.4	10	17.4	7.4	12.5	0.58	84.12	13.63
24/4	891	8.910	300	358.2	290.0	306.9	10	16.9	6.9	12.3	0.59	92.11	15.06
25/4	999	9.990	350	412.3	340.0	357.2	10	17.2	7.2	12.4	0.58	98.96	16.08
26/4	1102	11.020	400	461.1	390.0	406.5	10	16.5	6.5	12.2	0.60	105.44	18.12
27/4	1212	12.120	450	709.6	390.0	488.4	60	98.4	38.4	72.8	0.61	109.84	19.91
28/4	1410	14.100	500	915.0	400.0	563.2	100	163.2	63.2	121.1	0.61	120.40	21.79

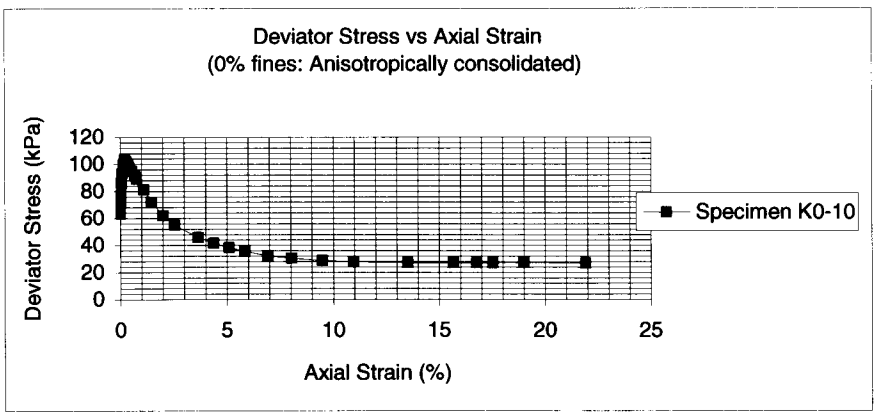
3.) Shear data

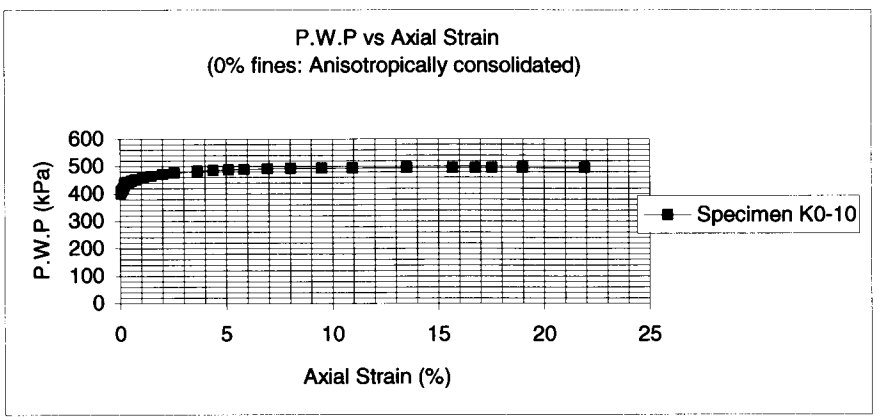
Volume change 1:		Volume change 2:		Sample Vol. change (cm^3)	105.67	B value	0.97
Air Flushing (cm^3)	8.35	Sat/Cons. (cm^3)	112.05	L_{cons} (mm)	136.85	K0	0.61
Cell Expsn. (cm^3)	0.00	Cell Expsn. (cm^3)	21.79	A_{cons} (cm^2)	46.204	Void ratio (e_1)	1.131
		Ram into cell (cm^3)	7.06				

Strain Gauge (divs)	Axial Strain (%)	Cell Press. (kPa)	Proof Ring (divs)	Pore Pressure (kPa)	Membrane Correction (kPa)	P_1 (kPa)	q (kPa)	t (kPa)	p' (kPa)	s' (kPa)
0	0.0000	500	914.7	400.0	0.0	563.2	63.2	31.6	121.1	131.6
1	0.0073	500	935.0	400.5	0.0	566.5	66.5	33.2	121.7	132.7
3	0.0219	500	964.5	401.5	0.0	571.2	71.2	35.6	122.2	134.1
5	0.0365	500	1002.3	403.5	0.0	577.4	77.4	38.7	122.3	135.2
9	0.0658	500	1055.1	407.5	0.0	585.9	85.9	43.0	121.1	135.5
15	0.1096	500	1100.2	412.5	0.1	593.2	93.2	46.6	118.6	134.1
22	0.1608	500	1141.2	420.0	0.1	599.8	99.8	49.9	113.3	129.9
28	0.2046	500	1164.6	430.0	0.1	603.5	103.5	51.7	104.5	121.7
30	0.2192	500	1160.0	435.0	0.1	602.7	102.7	51.4	99.2	116.4
38	0.2777	500	1156.3	437.0	0.1	602.0	102.0	51.0	97.0	114.0
45	0.3288	500	1147.9	440.0	0.2	600.6	100.6	50.3	93.5	110.3
50	0.3654	500	1140.4	441.5	0.2	599.3	99.3	49.7	91.6	108.2
55	0.4019	500	1132.5	442.0	0.2	598.0	98.0	49.0	90.7	107.0
75	0.5480	500	1114.8	446.5	0.3	594.9	94.9	47.5	85.1	101.0
95	0.6942	500	1095.2	450.5	0.3	591.5	91.5	45.8	80.0	95.3
105	0.7673	500	1079.9	452.0	0.4	589.0	89.0	44.5	77.7	92.5
150	1.0961	500	1034.6	457.0	0.5	581.2	81.2	40.6	70.1	83.6
200	1.4615	500	979.7	464.0	0.7	571.9	71.9	36.0	60.0	72.0
275	2.0095	500	920.4	471.5	1.0	561.8	61.8	30.9	49.1	59.4
350	2.5575	500	878.3	476.0	1.0	554.8	54.8	27.4	42.3	51.4
500	3.6536	500	824.1	482.5	1.0	545.7	45.7	22.8	32.7	40.3
600	4.3844	500	798.9	485.5	1.0	541.4	41.4	20.7	28.3	35.2
700	5.1151	500	779.5	487.5	1.0	538.1	38.1	19.0	25.2	31.5
800	5.8458	500	765.0	488.5	1.0	535.6	35.6	17.8	23.4	29.3

Strain Gauge (divs)	Axial Strain (%)	Cell Press. (kPa)	Proof Ring (divs)	Pore Pressure (kPa)	Membrane Correction (kPa)	P_1 (kPa)	q (kPa)	t (kPa)	p' (kPa)	s' (kPa)
950	6.9419	500	744.8	491.0	1.0	532.1	32.1	16.0	19.7	25.0
1100	8.0380	500	735.6	492.0	1.0	530.3	30.3	15.2	18.1	23.2
1300	9.4995	500	727.2	493.0	1.0	528.6	28.6	14.3	16.5	21.3
1500	10.9609	500	724.3	493.5	1.0	527.7	27.7	13.8	15.7	20.3
1850	13.5185	500	725.0	494.0	1.0	527.0	27.0	13.5	15.0	19.5
2145	15.6741	500	730.1	494.0	1.0	527.0	27.0	13.5	15.0	19.5
2295	16.7702	500	733.3	494.0	1.0	527.0	27.0	13.5	15.0	19.5
2400	17.5374	500	735.1	494.0	1.0	527.0	27.0	13.5	15.0	19.5
2600	18.9989	500	740.4	494.0	1.0	527.2	27.2	13.6	15.1	19.6
3000	21.9218	500	744.6	494.0	1.0	526.7	26.7	13.4	14.9	19.4







Test	**Case 2: Monotonic Undrained Compression of One-Dimensionally Consolidated Specimens**		
Cell No.	3 (Big)	Fines content (%)	0
Specimen	K0-13	Specific gravity (g/cm^3)	2.72

1.) Sample physical properties

Wet mass before test (g)	820.927	m.c before test (%)	10.11	Height (mm)	152.35	Volume (cm^3)	702.085
Wet mass after test (g)	935.518	m.c. after test (%)	25.48	Diameter (mm)	76.60		
Dry mass (g)	745.552	Dry density (kg/m^3)	1062	Area (cm^2)	46.084	Void ratio (e_0)	1.561

2.) Saturation / Consolidation

Proof ring properties		Strain gauge properties		Loading ram properties	
Proof ring No.	5153	1 strain division (mm)	0.01	Area [ram]$_1$ (cm^2)	7.905
Proof ring factor (dN/div)	7.512			Area [ram]$_2$ (cm^2)	5.004

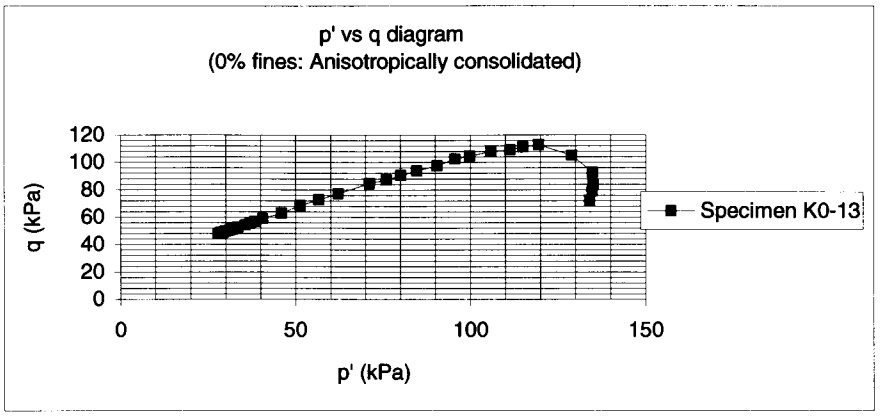
Date	Strain Gauge (divs)	Change Length (mm)	Cell Pressure (kPa)	Proof Ring (div)	Pore Pressure (kPa)	P_1 (kPa)	P'_3 (kPa)	P'_1 (kPa)	q (kPa)	p' (kPa)	K0	Volume Gauge (cm^3)	Cell Expansn (cm^3)
13/5	0	0.000	0	0.0	0.0						\	0.00	0.00
13/5	0	0.000	8.5		5.5	A I R - F L U S H I N G					\	7.95	0.00
13/5	284	2.840	50	135.6	40.0	63.5	10	23.5	13.5	14.5	0.43	39.54	6.08
14/5	482	4.820	100	165.2	90.0	109.8	10	19.8	9.8	13.3	0.51	64.21	8.77
15/5	593	5.930	150	211.7	140.0	158.8	10	18.8	8.8	12.9	0.53	76.38	10.65
16/5	700	7.000	200	252.0	190.0	206.8	10	16.8	6.8	12.3	0.60	86.84	12.00
17/5	799	7.990	250	308.5	240.0	257.4	10	17.4	7.4	12.5	0.57	95.47	13.63
18/5	888	8.880	300	358.1	290.0	306.9	10	16.9	6.9	12.3	0.59	102.00	15.06
19/5	980	9.800	350	407.4	340.0	356.4	10	16.4	6.4	12.1	0.61	106.54	16.08
20/5	1075	10.750	400	463.0	390.0	406.9	10	16.9	6.9	12.3	0.59	112.71	18.12
21/5	1168	11.680	450	510.2	440.0	456.0	10	16.0	6.0	12.0	0.63	118.60	19.91
22/5	1555	15.550	600	1075.5	490.0	672.4	110	182.4	72.4	134.1	0.60	144.65	23.05

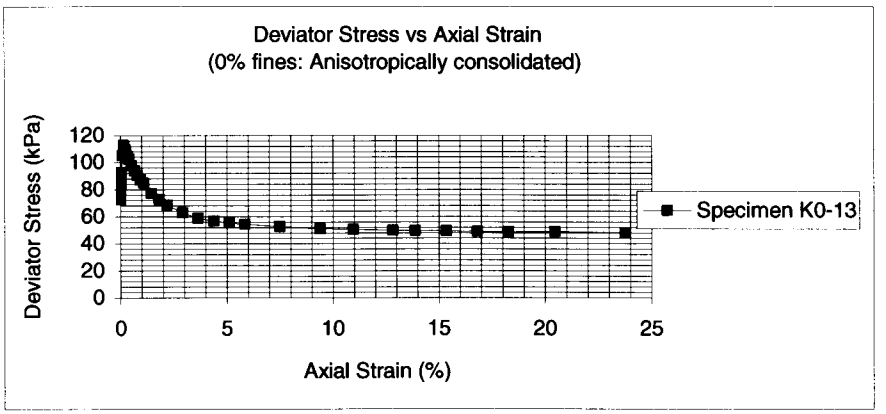
3.) Shear data

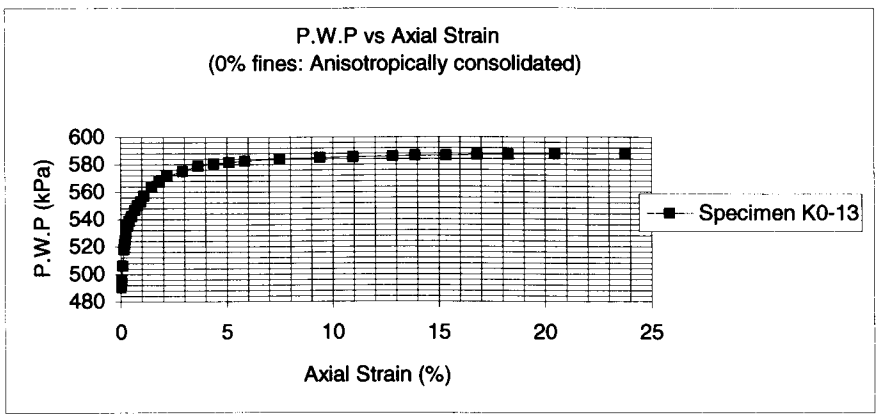
Volume change 1:		Volume change 2:		Sample Vol. change (cm^3)	129.38	B value	0.98
Air Flushing (cm^3)	7.95	Sat/Cons. (cm^3)	136.70	L_{cons} (mm)	136.80	K0	0.60
Cell Expsn. (cm^3)	0.00	Cell Expsn. (cm^3)	23.05	A_{cons} (cm^2)	46.084	Void ratio (e_1)	1.089
		Ram into cell (cm^3)	7.78				

Strain Gauge (divs)	Axial Strain (%)	Cell Press. (kPa)	Proof Ring (divs)	Pore Pressure (kPa)	Membrane Correction (kPa)	P_1 (kPa)	q (kPa)	t (kPa)	p' (kPa)	s' (kPa)
0	0.0000	600	1074.4	490.0	0.0	672.2	72.2	36.1	134.1	146.1
2	0.0146	600	1116.0	491.5	0.0	679.0	79.0	39.5	134.8	148.0
4	0.0292	600	1148.5	493.0	0.0	684.3	84.3	42.1	135.1	149.1
6	0.0439	600	1199.6	496.0	0.0	692.6	92.6	46.3	134.9	150.3
12	0.0877	600	1276.1	506.0	0.0	705.0	105.0	52.5	129.0	146.5
20	0.1462	600	1323.9	518.0	0.1	712.6	112.6	56.3	119.5	138.3
25	0.1827	600	1314.7	522.0	0.1	711.1	111.1	55.5	115.0	133.5
30	0.2193	600	1302.6	525.0	0.1	709.1	109.1	54.5	111.4	129.5
35	0.2558	600	1295.4	530.0	0.1	707.8	107.8	53.9	105.9	123.9
45	0.3289	600	1276.2	535.0	0.2	704.6	104.6	52.3	99.9	117.3
55	0.4020	600	1263.3	538.5	0.2	702.4	102.4	51.2	95.6	112.7
70	0.5117	600	1234.8	542.0	0.3	697.6	97.6	48.8	90.5	106.8
90	0.6579	600	1212.7	546.5	0.3	693.8	93.8	46.9	84.8	100.4
110	0.8041	600	1193.9	550.0	0.4	690.6	90.6	45.3	80.2	95.3
130	0.9503	600	1174.1	553.0	0.5	687.2	87.2	43.6	76.1	90.6
150	1.0965	600	1159.8	557.0	0.5	684.6	84.6	42.3	71.2	85.3
200	1.4620	600	1116.1	563.5	0.7	677.1	77.1	38.6	62.2	75.1
250	1.8275	600	1090.6	567.5	0.9	672.6	72.6	36.3	56.7	68.8
300	2.1930	600	1066.9	571.5	1.0	668.4	68.4	34.2	51.3	62.7
400	2.9240	600	1034.3	575.0	1.0	662.8	62.8	31.4	45.9	56.4
500	3.6550	600	1012.8	579.0	1.0	658.9	58.9	29.5	40.6	50.5
600	4.3860	600	1001.7	580.5	1.0	656.7	56.7	28.4	38.4	47.9
700	5.1170	600	995.6	581.5	1.0	655.3	55.3	27.7	36.9	46.2
800	5.8480	600	991.1	582.5	1.0	654.2	54.2	27.1	35.6	44.6

Strain Gauge (divs)	Axial Strain (%)	Cell Press. (kPa)	Proof Ring (divs)	Pore Pressure (kPa)	Membrane Correction (kPa)	P_1 (kPa)	q (kPa)	t (kPa)	p' (kPa)	s' (kPa)
1025	7.4927	600	986.5	584.0	1.0	652.6	52.6	26.3	33.5	42.3
1285	9.3933	600	984.0	585.0	1.0	651.1	51.1	25.5	32.0	40.5
1500	10.9649	600	986.5	585.5	1.0	650.5	50.5	25.3	31.3	39.8
1755	12.8289	600	989.6	586.0	1.0	649.9	49.9	25.0	30.6	39.0
1900	13.8889	600	992.1	586.5	1.0	649.6	49.6	24.8	30.0	38.3
2100	15.3509	600	996.7	586.5	1.0	649.4	49.4	24.7	30.0	38.2
2300	16.8129	600	999.8	587.0	1.0	649.0	49.0	24.5	29.3	37.5
2500	18.2749	600	1003.6	587.0	1.0	648.6	48.6	24.3	29.2	37.3
2800	20.4678	600	1015.4	587.5	1.0	648.8	48.8	24.4	28.8	36.9
3250	23.7573	600	1024.1	588.0	1.0	647.8	47.8	23.9	27.9	35.9







Test	**Case 2: Monotonic Undrained Compression of One-Dimensionally Consolidated Specimens**		
Cell No.	2 (Big)	Fines content (%)	0
Specimen	K0-14	Specific gravity (g/cm^3)	2.72

1.) Sample physical properties

Wet mass before test (g)	826.208	m.c before test (%)	9.98	Height (mm)	152.05	Volume (cm^3)	702.533
Wet mass after test (g)	951.289	m.c. after test (%)	26.63	Diameter (mm)	76.70		
Dry mass (g)	751.235	Dry density (kg/m^3)	1069	Area (cm^2)	46.204	Void ratio (e_0)	1.544

2.) Saturation / Consolidation

Proof ring properties		Strain gauge properties		Loading ram properties	
Proof ring No.	4541	1 strain division (mm)	0.01	Area [ram]$_1$ (cm^2)	7.905
Proof ring factor (dN/div)	25.77			Area [ram]$_2$ (cm^2)	5.004

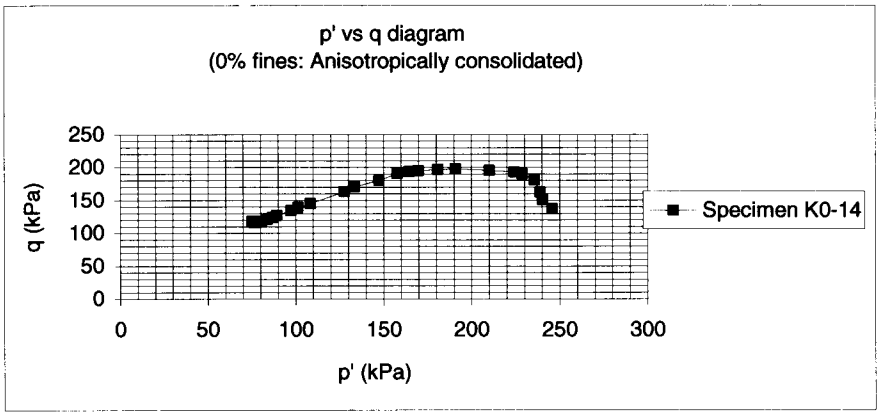
Date	Strain Gauge (divs)	Change Length (mm)	Cell Pressure (kPa)	Proof Ring (div)	Pore Pressure (kPa)	P_1 (kPa)	P'_3 (kPa)	P'_1 (kPa)	q (kPa)	p' (kPa)	K0	Volume Gauge (cm^3)	Cell Expansn (cm^3)
13/5	0	0.000	0	0.0	0.0						\	0.00	0.00
13/5	0	0.000	10.0		6.5	A I R - F L U S H I N G					\	10.50	0.00
13/5	219	2.190	50	44.2	40.0	66.1	10	26.1	16.1	15.4	0.38	41.21	7.06
14/5	413	4.130	100	55.0	90.0	113.6	10	23.6	13.6	14.5	0.42	58.02	9.79
15/5	547	5.470	150	66.8	140.0	161.6	10	21.6	11.6	13.9	0.46	70.50	11.63
16/5	665	6.650	200	78.3	190.0	209.5	10	19.5	9.5	13.2	0.51	79.89	13.02
17/5	766	7.660	250	90.1	240.0	257.5	10	17.5	7.5	12.5	0.57	86.17	14.57
18/5	869	8.690	300	104.9	290.0	307.2	10	17.2	7.2	12.4	0.58	90.98	16.03
19/5	963	9.630	350	120.5	340.0	357.3	10	17.3	7.3	12.4	0.58	96.11	17.22
20/5	1055	10.550	400	135.4	390.0	407.1	10	17.1	7.1	12.4	0.59	101.05	19.30
21/5	1134	11.340	450	150.5	440.0	457.0	10	17.0	7.0	12.3	0.59	104.96	20.93
22/5	1619	16.190	700	460.6	500.0	837.1	200	337.1	137.1	245.7	0.59	130.38	25.46

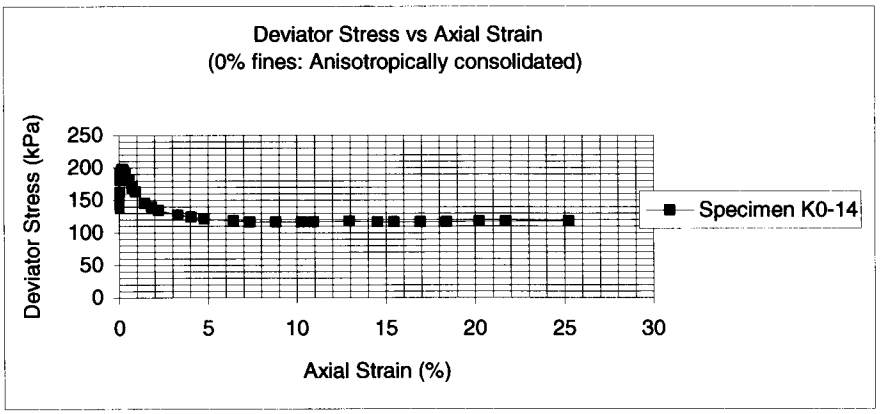
3.) Shear data

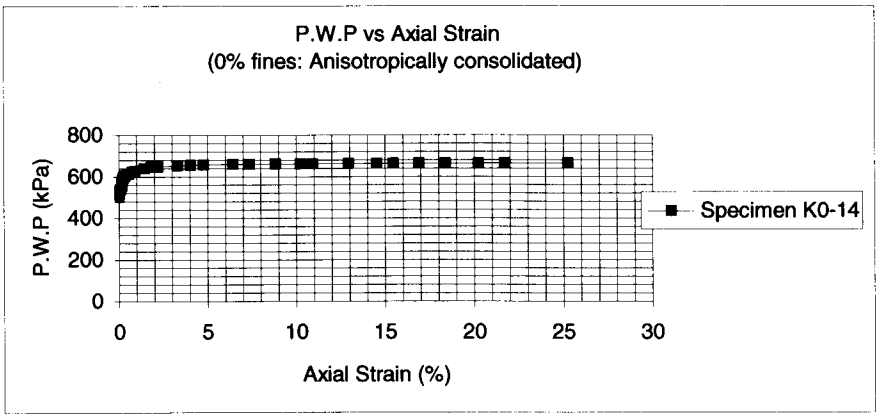
Volume change 1:		Volume change 2:		Sample Vol. change (cm^3)	113.02	B value	0.97
Air Flushing (cm^3)	10.50	Sat/Cons. (cm^3)	119.88	L_{cons} (mm)	135.86	K0	0.59
Cell Expsn. (cm^3)	0.00	Cell Expsn. (cm^3)	25.46	A_{cons} (cm^2)	46.204	Void ratio (e_1)	1.134
		Ram into cell (cm^3)	8.10				

Strain Gauge (divs)	Axial Strain (%)	Cell Press. (kPa)	Proof Ring (divs)	Pore Pressure (kPa)	Membrane Correction (kPa)	P_1 (kPa)	q (kPa)	t (kPa)	p' (kPa)	s' (kPa)
0	0.0000	700	460.6	500.0	0.0	837.1	137.1	68.6	245.7	268.6
1	0.0074	700	485.5	510.0	0.0	851.0	151.0	75.5	240.3	265.5
3	0.0221	700	505.4	515.0	0.0	862.1	162.1	81.0	239.0	266.0
5	0.0368	700	538.8	524.5	0.0	880.7	180.7	90.3	235.7	265.8
10	0.0736	700	555.9	534.5	0.0	890.1	190.1	95.1	228.9	260.6
15	0.1104	700	560.7	540.0	0.1	892.7	192.7	96.3	224.2	256.3
21	0.1546	700	565.5	555.0	0.1	895.3	195.3	97.6	210.1	242.6
25	0.1840	700	570.1	575.0	0.1	897.8	197.8	98.9	190.9	223.9
30	0.2208	700	568.2	584.5	0.1	896.6	196.6	98.3	181.0	213.8
35	0.2576	700	565.5	595.0	0.1	895.0	195.0	97.5	170.0	202.5
40	0.2944	700	562.6	600.0	0.1	893.3	193.3	96.7	164.4	196.7
50	0.3680	700	557.4	605.5	0.2	890.2	190.2	95.1	157.9	189.6
75	0.5520	700	540.1	612.5	0.3	880.2	180.2	90.1	147.6	177.6
100	0.7361	700	522.8	623.0	0.4	870.2	170.2	85.1	133.7	162.1
125	0.9201	700	510.9	626.5	0.5	863.2	163.2	81.6	127.9	155.1
195	1.4353	700	480.1	640.0	0.7	845.2	145.2	72.6	108.4	132.6
250	1.8401	700	470.7	645.0	0.9	839.2	139.2	69.6	101.4	124.6
300	2.2082	700	462.6	647.5	1.0	834.2	134.2	67.1	97.2	119.6
450	3.3122	700	452.0	653.0	1.0	827.0	127.0	63.5	89.3	110.5
550	4.0483	700	448.6	654.5	1.0	824.2	124.2	62.1	86.9	107.6
650	4.7843	700	445.0	656.5	1.0	821.3	121.3	60.6	83.9	104.1
875	6.4405	700	443.4	659.0	1.0	818.3	118.3	59.2	80.4	100.2
1000	7.3605	700	442.1	660.0	1.0	816.5	116.5	58.2	78.8	98.2
1200	8.8326	700	445.8	661.0	1.0	816.5	116.5	58.2	77.8	97.2

Strain Gauge (divs)	Axial Strain (%)	Cell Press. (kPa)	Proof Ring (divs)	Pore Pressure (kPa)	Membrane Correction (kPa)	P_1 (kPa)	q (kPa)	t (kPa)	p' (kPa)	s' (kPa)
1395	10.2679	700	449.8	661.5	1.0	816.7	116.7	58.3	77.4	96.8
1485	10.9304	700	451.6	661.5	1.0	816.7	116.7	58.3	77.4	96.8
1760	12.9545	700	458.7	662.0	1.0	817.4	117.4	58.7	77.1	96.7
1975	14.5370	700	461.7	662.5	1.0	816.7	116.7	58.4	76.4	95.9
2100	15.4571	700	464.1	662.5	1.0	816.6	116.6	58.3	76.4	95.8
2300	16.9292	700	468.2	662.5	1.0	816.4	116.4	58.2	76.3	95.7
2500	18.4013	700	473.3	663.0	1.0	816.7	116.7	58.3	75.9	95.3
2750	20.2414	700	481.4	663.0	1.0	817.6	117.6	58.8	76.2	95.8
2950	21.7135	700	486.5	664.0	1.0	817.7	117.7	58.8	75.2	94.8
3430	25.2466	700	500.2	664.0	1.0	818.0	118.0	59.0	75.3	95.0







Test	**Case 2: Monotonic Undrained Compression of One-Dimensionally Consolidated Specimens**		
Cell No.	3 (Big)	Fines content (%)	0
Specimen	K0-19	Specific gravity (g/cm^3)	2.72

1.) Sample physical properties

Wet mass before test (g)	820.688	m.c before test (%)	9.21	Height (mm)	151.20	Volume (cm^3)	697.696
Wet mass after test (g)	945.283	m.c. after test (%)	25.79	Diameter (mm)	76.65		
Dry mass (g)	751.477	Dry density (kg/m^3)	1077	Area (cm^2)	46.144	Void ratio (e_0)	1.525

2.) Saturation / Consolidation

Proof ring properties		Strain gauge properties		Loading ram properties	
Proof ring No.	4541	1 strain division (mm)	0.01	Area [ram]$_1$ (cm^2)	7.905
Proof ring factor (dN/div)	25.77			Area [ram]$_2$ (cm^2)	5.004

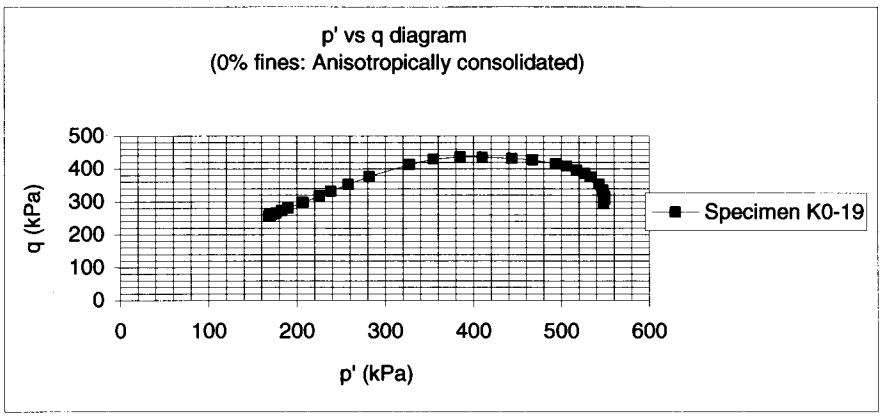
Date	Strain Gauge (divs)	Change Length (mm)	Cell Pressure (kPa)	Proof Ring (div)	Pore Pressure (kPa)	P_1 (kPa)	P'_3 (kPa)	P'_1 (kPa)	q (kPa)	p' (kPa)	K0	Volume Gauge (cm^3)	Cell Expansn (cm^3)
19/6	0	0.000	0	0.0	0.0						\	0.00	0.00
19/6	0	0.000	9.4		5.0	A I R - F L U S H I N G					\	7.20	0.00
19/6	233	2.330	50	38.8	40.0	63.1	10	23.1	13.1	14.4	0.43	36.87	6.08
20/6	439	4.390	100	48.1	90.0	109.7	10	19.7	9.7	13.2	0.51	55.84	8.77
21/6	591	5.910	150	60.0	140.0	157.8	10	17.8	7.8	12.6	0.56	69.06	10.65
22/6	694	6.940	200	73.2	190.0	206.6	10	16.6	6.6	12.2	0.60	77.95	12.00
23/6	795	7.950	250	87.7	240.0	256.2	10	16.2	6.2	12.1	0.62	83.52	13.63
24/6	890	8.900	300	105.0	290.0	307.2	10	17.2	7.2	12.4	0.58	88.67	15.06
25/6	983	9.830	350	120.8	340.0	357.5	10	17.5	7.5	12.5	0.57	92.84	16.08
26/6	1077	10.770	400	135.4	390.0	407.1	10	17.1	7.1	12.4	0.59	98.13	18.12
27/6	1170	11.700	450	150.9	440.0	457.2	10	17.2	7.2	12.4	0.58	103.29	19.91
28/6	1766	17.660	950	818.8	500.0	1244.5	450	744.5	294.5	548.2	0.60	145.41	25.74

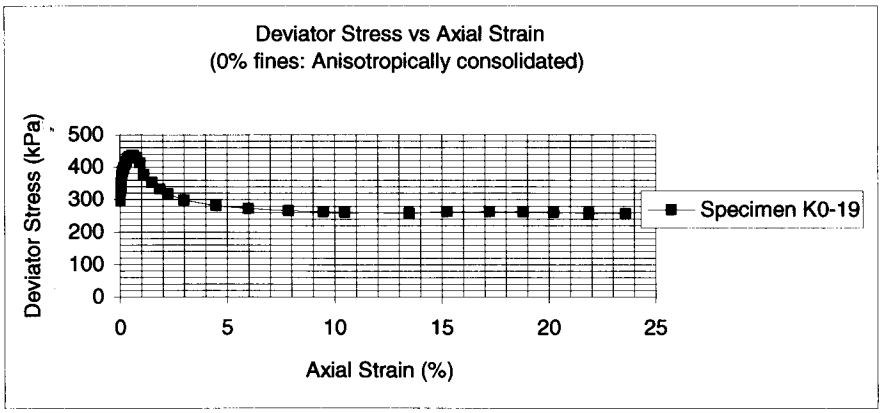
3.) Shear data

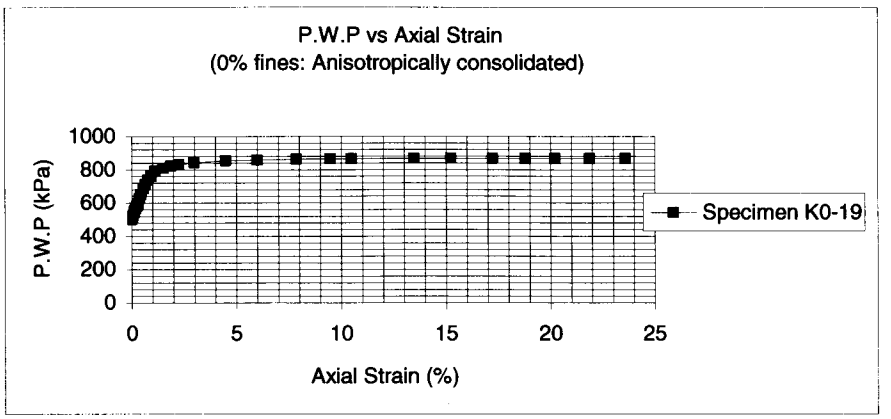
Volume change 1:		Volume change 2:		Sample Vol. change (cm^3)	128.51	B value	0.98
Air Flushing (cm^3)	7.20	Sat/Cons. (cm^3)	138.21	L_{cons} (mm)	133.54	K0	0.60
Cell Expsn. (cm^3)	0.00	Cell Expsn. (cm^3)	25.74	A_{cons} (cm^2)	46.144	Void ratio (e_1)	1.060
		Ram into cell (cm^3)	8.84				

Strain Gauge (divs)	Axial Strain (%)	Cell Press. (kPa)	Proof Ring (divs)	Pore Pressure (kPa)	Membrane Correction (kPa)	P_1 (kPa)	q (kPa)	t (kPa)	p' (kPa)	s' (kPa)
0	0.0000	950	818.6	500.0	0.0	1244.4	294.4	147.2	548.1	597.2
1	0.0075	950	843.1	503.0	0.0	1258.1	308.1	154.0	549.7	601.0
2	0.0150	950	858.2	506.0	0.0	1266.5	316.5	158.2	549.5	602.2
3	0.0225	950	872.8	510.0	0.0	1274.6	324.6	162.3	548.2	602.3
7	0.0524	950	893.7	515.0	0.0	1286.2	336.2	168.1	547.1	603.1
10	0.0749	950	924.2	525.0	0.0	1303.1	353.1	176.5	542.7	601.5
14	0.1048	950	963.5	542.0	0.1	1324.9	374.9	187.4	533.0	595.4
18	0.1348	950	984.0	552.0	0.1	1336.2	386.2	193.1	526.7	591.1
24	0.1797	950	1003.4	565.0	0.1	1346.8	396.8	198.4	517.3	583.4
33	0.2471	950	1024.7	580.0	0.1	1358.4	408.4	204.2	506.1	574.2
40	0.2995	950	1038.4	595.0	0.1	1365.8	415.8	207.9	493.6	562.9
50	0.3744	950	1059.1	625.0	0.2	1376.9	426.9	213.5	467.3	538.5
60	0.4493	950	1068.7	650.0	0.2	1381.9	431.9	216.0	444.0	516.0
75	0.5616	950	1076.7	685.0	0.3	1385.8	435.8	217.9	410.3	482.9
85	0.6365	950	1077.9	710.0	0.3	1386.1	436.1	218.1	385.4	458.1
105	0.7863	950	1066.8	738.0	0.4	1379.2	429.2	214.6	355.1	426.6
125	0.9360	950	1038.5	760.0	0.5	1362.9	412.9	206.4	327.6	396.4
150	1.1233	950	975.6	794.0	0.6	1327.2	377.2	188.6	281.7	344.6
200	1.4977	950	933.4	809.5	0.7	1302.4	352.4	176.2	258.0	316.7
250	1.8721	950	898.2	822.0	0.9	1281.6	331.6	165.8	238.5	293.8
300	2.2465	950	874.1	830.5	1.0	1267.1	317.1	158.6	225.2	278.1
400	2.9954	950	843.2	842.0	1.0	1247.9	297.9	149.0	207.3	257.0
600	4.4930	950	818.8	853.5	1.0	1230.3	280.3	140.1	189.9	236.6
800	5.9907	950	813.0	858.0	1.0	1222.8	272.8	136.4	182.9	228.4

Strain Gauge (divs)	Axial Strain (%)	Cell Press. (kPa)	Proof Ring (divs)	Pore Pressure (kPa)	Membrane Correction (kPa)	P_1 (kPa)	q (kPa)	t (kPa)	p' (kPa)	s' (kPa)
1050	7.8628	950	810.2	862.0	1.0	1215.9	265.9	133.0	176.6	221.0
1265	9.4728	950	813.3	864.0	1.0	1212.9	262.9	131.4	173.6	217.4
1400	10.4838	950	816.1	865.0	1.0	1211.3	261.3	130.7	172.1	215.7
1800	13.4791	950	828.2	866.0	1.0	1208.4	258.4	129.2	170.1	213.2
2035	15.2389	950	847.8	867.0	1.0	1212.4	262.4	131.2	170.5	214.2
2300	17.2233	950	861.6	867.0	1.0	1212.6	262.6	131.3	170.5	214.3
2510	18.7959	950	870.9	867.0	1.0	1211.8	261.8	130.9	170.3	213.9
2700	20.2187	950	879.1	867.0	1.0	1210.8	260.8	130.4	169.9	213.4
2920	21.8661	950	885.2	867.0	1.0	1208.1	258.1	129.1	169.0	212.1
3150	23.5884	950	896.4	867.0	1.0	1207.2	257.2	128.6	168.7	211.6







Test	**Case 2: Monotonic Undrained Compression of One-Dimensionally Consolidated Specimens**		
Cell No.	2 (Big)	Fines content (%)	0
Specimen	K0-20	Specific gravity (g/cm^3)	2.72

1.) Sample physical properties

Wet mass before test (g)	832.484	m.c before test (%)	8.98	Height (mm)	152.45	Volume (cm^3)	704.382
Wet mass after test (g)	976.324	m.c. after test (%)	27.81	Diameter (mm)	76.70		
Dry mass (g)	763.887	Dry density (kg/m^3)	1084	Area (cm^2)	46.204	Void ratio (e_0)	1.508

2.) Saturation / Consolidation

Proof ring properties		Strain gauge properties		Loading ram properties	
Proof ring No.	5153	1 strain division (mm)	0.01	Area [ram]$_1$ (cm^2)	7.905
Proof ring factor (dN/div)	7.512			Area [ram]$_2$ (cm^2)	5.004

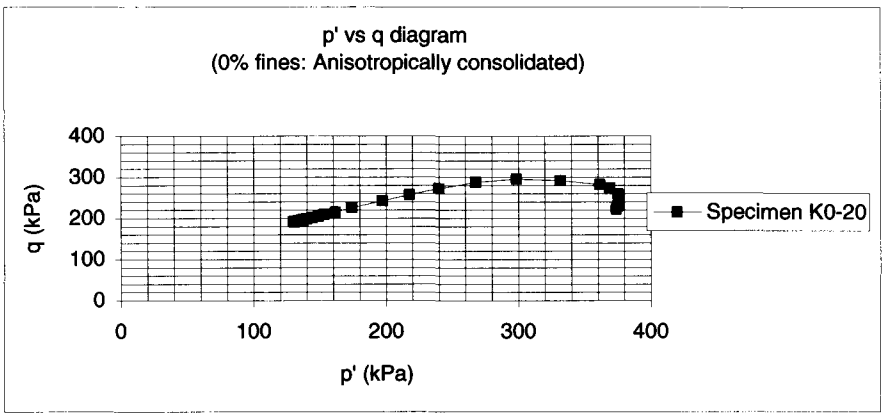
Date	Strain Gauge (divs)	Change Length (mm)	Cell Pressure (kPa)	Proof Ring (div)	Pore Pressure (kPa)	P_1 (kPa)	P'_3 (kPa)	P'_1 (kPa)	q (kPa)	p' (kPa)	K0	Volume Gauge (cm^3)	Cell Expansn (cm^3)
19/6	0	0.000	0	0.0	0.0						\	0.00	0.00
19/6	0	0.000	11.0		6.5	A I R - F L U S H I N G					\	8.40	0.00
19/6	205	2.050	50	130.7	40.0	62.7	10	22.7	12.7	14.2	0.44	41.00	7.06
20/6	402	4.020	100	169.3	90.0	110.4	10	20.4	10.4	13.5	0.49	61.21	9.79
21/6	593	5.930	150	208.0	140.0	158.2	10	18.2	8.2	12.7	0.55	74.62	11.63
22/6	715	7.150	200	253.2	190.0	206.9	10	16.9	6.9	12.3	0.59	85.57	13.02
23/6	835	8.350	250	301.9	240.0	256.3	10	16.3	6.3	12.1	0.61	92.55	14.57
24/6	930	9.300	300	358.8	290.0	307.0	10	17.0	7.0	12.3	0.59	97.96	16.03
25/6	1017	10.170	350	407.1	340.0	356.3	10	16.3	6.3	12.1	0.61	102.12	17.22
26/6	1094	10.940	400	457.8	390.0	406.0	10	16.0	6.0	12.0	0.63	107.23	19.30
27/6	1164	11.640	450	513.0	440.0	456.4	10	16.4	6.4	12.1	0.61	112.34	20.93
28/6	1233	12.330	500	564.5	490.0	506.2	10	16.2	6.2	12.1	0.62	117.51	22.85
29/6	1648	16.480	850	2259.7	550.0	1072.0	300	522.0	222.0	374.0	0.57	150.67	27.95

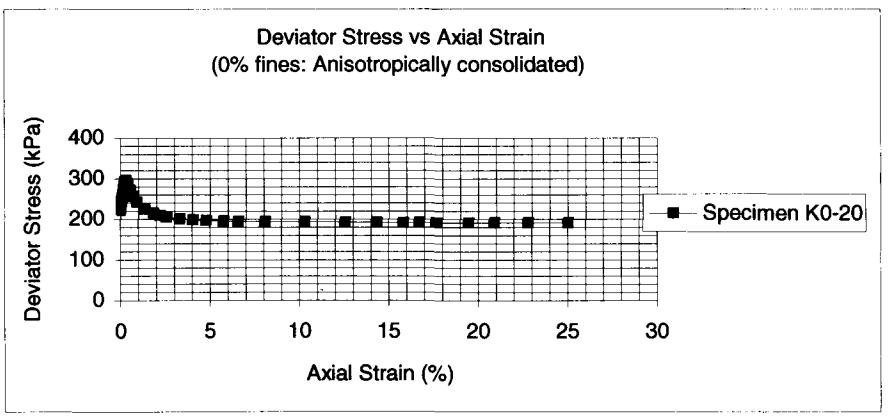
3.) Shear data

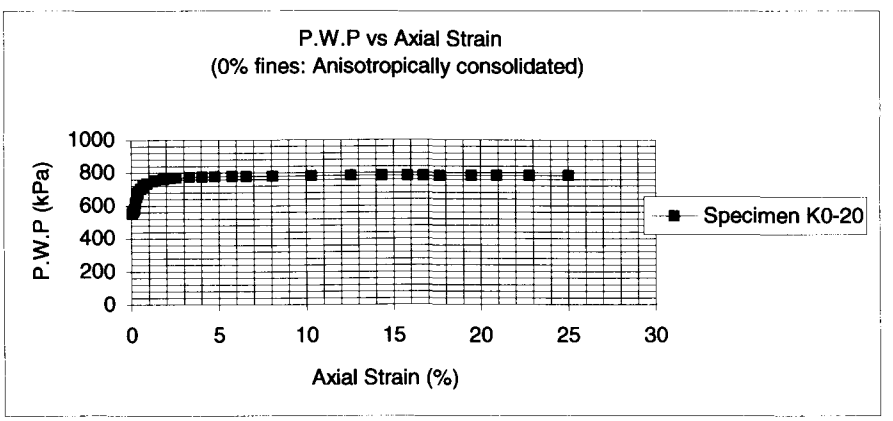
Volume change 1:		Volume change 2:		Sample Vol. change (cm^3)	130.97	B value	0.97
Air Flushing (cm^3)	8.40	Sat/Cons. (cm^3)	142.27	L_{cons} (mm)	135.97	K0	0.57
Cell Expsn. (cm^3)	0.00	Cell Expsn. (cm^3)	27.95	A_{cons} (cm^2)	46.204	Void ratio (e_1)	1.042
		Ram into cell (cm^3)	8.25				

Strain Gauge (divs)	Axial Strain (%)	Cell Press. (kPa)	Proof Ring (divs)	Pore Pressure (kPa)	Membrane Correction (kPa)	P_1 (kPa)	q (kPa)	t (kPa)	p' (kPa)	s' (kPa)
0	0.0000	850	2259.0	550.0	0.0	1071.9	221.9	110.9	374.0	410.9
2	0.0147	850	2308.5	551.5	0.0	1079.9	229.9	114.9	375.1	413.4
4	0.0294	850	2354.7	553.5	0.0	1087.3	237.3	118.7	375.6	415.2
8	0.0588	850	2397.1	555.0	0.0	1094.1	244.1	122.1	376.4	417.1
12	0.0883	850	2445.2	558.0	0.0	1101.9	251.9	125.9	376.0	417.9
18	0.1324	850	2494.1	561.5	0.1	1109.7	259.7	129.8	375.1	418.3
25	0.1839	850	2578.5	572.0	0.1	1123.2	273.2	136.6	369.1	414.6
30	0.2206	850	2633.7	582.5	0.1	1132.0	282.0	141.0	361.5	408.5
35	0.2574	850	2694.6	615.5	0.1	1141.8	291.8	145.9	331.8	380.4
45	0.3310	850	2719.4	650.0	0.2	1145.6	295.6	147.8	298.5	347.8
55	0.4045	850	2670.9	678.0	0.2	1137.4	287.4	143.7	267.8	315.7
75	0.5516	850	2578.0	700.5	0.3	1121.9	271.9	136.0	240.1	285.5
95	0.6987	850	2489.3	718.0	0.3	1107.1	257.1	128.6	217.7	260.6
125	0.9193	850	2400.5	733.5	0.5	1092.1	242.1	121.1	197.2	237.6
185	1.3606	850	2304.9	751.0	0.7	1075.5	225.5	112.8	174.2	211.8
250	1.8386	850	2247.1	760.0	0.9	1065.0	215.0	107.5	161.7	197.5
300	2.2064	850	2217.2	766.5	1.0	1059.3	209.3	104.7	153.3	188.2
350	2.5741	850	2193.0	769.5	1.0	1054.7	204.7	102.3	148.7	182.8
450	3.3096	850	2178.5	773.0	1.0	1050.9	200.9	100.4	144.0	177.4
550	4.0450	850	2172.9	776.0	1.0	1048.4	198.4	99.2	140.1	173.2
650	4.7805	850	2171.3	778.0	1.0	1046.7	196.7	98.3	137.6	170.3
785	5.7733	850	2174.4	779.0	1.0	1045.1	195.1	97.5	136.0	168.5
895	6.5823	850	2183.5	777.5	1.0	1044.8	194.8	97.4	137.4	169.9
1100	8.0900	850	2198.7	779.0	1.0	1043.9	193.9	96.9	135.6	167.9

Strain Gauge (divs)	Axial Strain (%)	Cell Press. (kPa)	Proof Ring (divs)	Pore Pressure (kPa)	Membrane Correction (kPa)	P_1 (kPa)	q (kPa)	t (kPa)	p' (kPa)	s' (kPa)
1400	10.2964	850	2227.6	780.5	1.0	1043.4	193.4	96.7	134.0	166.2
1710	12.5763	850	2259.8	783.0	1.0	1043.1	193.1	96.5	131.4	163.5
1950	14.3414	850	2283.2	783.0	1.0	1042.4	192.4	96.2	131.1	163.2
2150	15.8123	850	2302.1	784.0	1.0	1041.7	191.7	95.8	129.9	161.8
2275	16.7316	850	2319.0	781.5	1.0	1041.9	191.9	95.9	132.5	164.4
2400	17.6510	850	2332.5	782.0	1.0	1041.5	191.5	95.8	131.8	163.8
2650	19.4896	850	2361.1	783.0	1.0	1041.0	191.0	95.5	130.7	162.5
2845	20.9237	850	2388.6	783.0	1.0	1041.1	191.1	95.5	130.7	162.5
3100	22.7991	850	2427.8	783.0	1.0	1041.5	191.5	95.7	130.8	162.7
3405	25.0423	850	2474.4	783.0	1.0	1041.5	191.5	95.8	130.8	162.8







Test	**Case 2: Monotonic Undrained Compression of One-Dimensionally Consolidated Specimens**		
Cell No.	3 (Big)	Fines content (%)	0
Specimen	K0-24	Specific gravity (g/cm^3)	2.72

1.) Sample physical properties

Wet mass before test (g)	837.737	m.c before test (%)	10.24	Height (mm)	151.75	Volume (cm^3)	699.320
Wet mass after test (g)	938.275	m.c. after test (%)	23.47	Diameter (mm)	76.60		
Dry mass (g)	759.921	Dry density (kg/m^3)	1087	Area (cm^2)	46.084	Void ratio (e_0)	1.503

2.) Saturation / Consolidation

Proof ring properties		Strain gauge properties		Loading ram properties	
Proof ring No.	5153	1 strain division (mm)	0.01	Area [ram]$_1$ (cm^2)	7.905
Proof ring factor (dN/div)	7.512			Area [ram]$_2$ (cm^2)	5.004

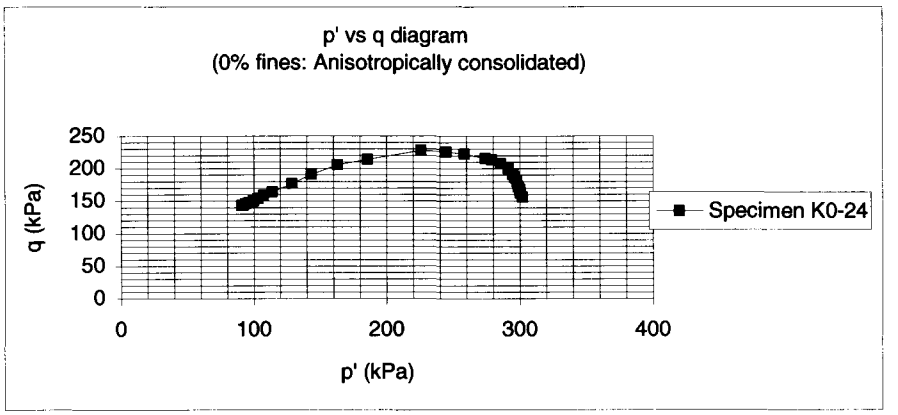
Date	Strain Gauge (divs)	Change Length (mm)	Cell Pressure (kPa)	Proof Ring (div)	Pore Pressure (kPa)	P_1 (kPa)	P'_3 (kPa)	P'_1 (kPa)	q (kPa)	p' (kPa)	K0	Volume Gauge (cm^3)	Cell Expansn (cm^3)
15/7	0	0.000	0	0.0	0.0						\	0.00	0.00
15/7	0	0.000	10.7		6.0	A I R - F L U S H I N G					\	8.30	0.00
15/7	185	1.850	50	123.5	40.0	61.6	10	21.6	11.6	13.9	0.46	37.12	6.08
16/7	333	3.330	100	156.0	90.0	108.3	10	18.3	8.3	12.8	0.55	57.21	8.77
17/7	442	4.420	150	202.6	140.0	157.3	10	17.3	7.3	12.4	0.58	71.95	10.65
18/7	547	5.470	200	251.8	190.0	206.7	10	16.7	6.7	12.2	0.60	80.21	12.00
19/7	645	6.450	250	306.7	240.0	257.1	10	17.1	7.1	12.4	0.58	84.93	13.63
20/7	740	7.400	300	364.4	290.0	307.9	10	17.9	7.9	12.6	0.56	89.88	15.06
21/7	837	8.370	350	412.6	340.0	357.2	10	17.2	7.2	12.4	0.58	95.05	16.08
22/7	936	9.360	400	467.9	390.0	407.7	10	17.7	7.7	12.6	0.57	100.07	18.12
23/7	1033	10.330	450	517.3	440.0	457.1	10	17.1	7.1	12.4	0.58	104.86	19.91
24/7	1132	11.320	500	569.4	490.0	507.1	10	17.1	7.1	12.4	0.59	111.24	21.79
25/7	1588	15.880	800	1800.1	550.0	956.2	250	406.2	156.2	302.1	0.62	136.33	25.12

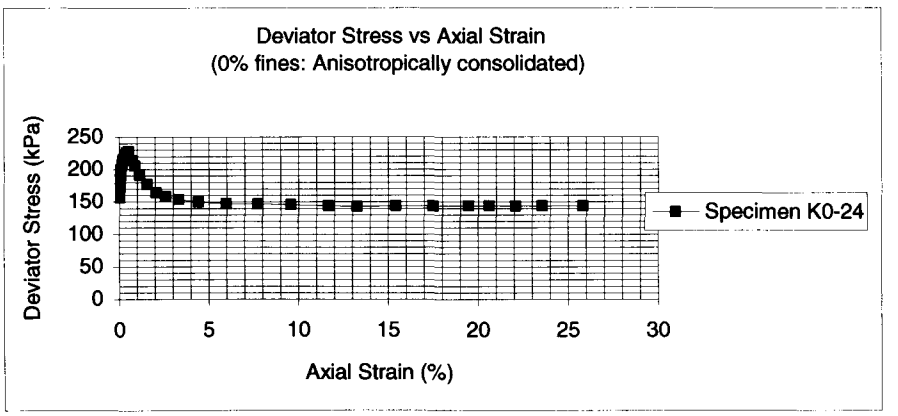
3.) Shear data

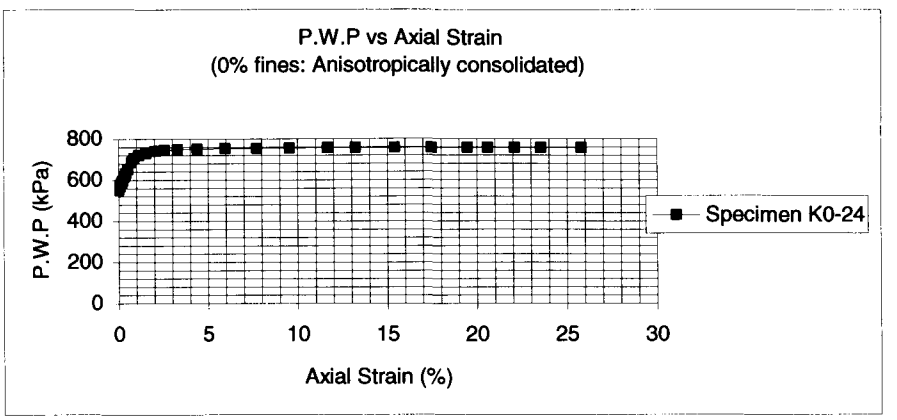
Volume change 1:		Volume change 2:		Sample Vol. change (cm^3)	119.16	B value	0.99
Air Flushing (cm^3)	8.30	Sat/Cons. (cm^3)	128.03	L_{cons} (mm)	135.87	K0	0.62
Cell Expsn. (cm^3)	0.00	Cell Expsn. (cm^3)	25.12	A_{cons} (cm^2)	46.084	Void ratio (e_1)	1.077
		Ram into cell (cm^3)	7.95				

Strain Gauge (divs)	Axial Strain (%)	Cell Press. (kPa)	Proof Ring (divs)	Pore Pressure (kPa)	Membrane Correction (kPa)	P_1 (kPa)	q (kPa)	t (kPa)	p' (kPa)	s' (kPa)
0	0.0000	800	1799.5	550.0	0.0	956.1	156.1	78.1	302.0	328.1
1	0.0074	800	1836.4	553.5	0.0	962.1	162.1	81.1	300.5	327.6
2	0.0147	800	1872.9	556.0	0.0	968.0	168.0	84.0	300.0	328.0
4	0.0294	800	1898.5	558.5	0.0	972.2	172.2	86.1	298.9	327.6
6	0.0442	800	1946.7	562.0	0.0	980.0	180.0	90.0	298.0	328.0
8	0.0589	800	1985.0	565.5	0.0	986.2	186.2	93.1	296.6	327.6
12	0.0883	800	2014.6	568.5	0.0	991.0	191.0	95.5	295.2	327.0
15	0.1104	800	2069.5	575.0	0.1	999.8	199.8	99.9	291.6	324.9
22	0.1619	800	2116.1	583.5	0.1	1007.3	207.3	103.6	285.6	320.1
30	0.2208	800	2154.3	592.0	0.1	1013.4	213.4	106.7	279.1	314.7
35	0.2576	800	2168.5	597.5	0.1	1015.6	215.6	107.8	274.4	310.3
45	0.3312	800	2212.3	615.5	0.2	1022.5	222.5	111.2	258.7	295.7
55	0.4048	800	2234.2	630.5	0.2	1025.8	225.8	112.9	244.8	282.4
70	0.5152	800	2249.1	650.0	0.3	1028.0	228.0	114.0	226.0	264.0
100	0.7360	800	2167.0	685.5	0.4	1014.1	214.1	107.0	185.9	221.5
120	0.8832	800	2116.3	705.5	0.4	1005.5	205.5	102.7	163.0	197.2
155	1.1408	800	2029.6	720.0	0.6	990.8	190.8	95.4	143.6	175.4
210	1.5456	800	1948.5	730.0	0.8	976.8	176.8	88.4	128.9	158.4
280	2.0608	800	1876.6	740.5	1.0	964.2	164.2	82.1	114.2	141.6
350	2.5760	800	1847.0	745.5	1.0	958.6	158.6	79.3	107.4	133.8
450	3.3120	800	1822.6	748.0	1.0	953.6	153.6	76.8	103.2	128.8
600	4.4160	800	1807.9	750.0	1.0	949.5	149.5	74.8	99.8	124.8
810	5.9616	800	1809.8	752.5	1.0	947.4	147.4	73.7	96.6	121.2
1050	7.7280	800	1824.6	753.0	1.0	946.8	146.8	73.4	95.9	120.4

Strain Gauge (divs)	Axial Strain (%)	Cell Press. (kPa)	Proof Ring (divs)	Pore Pressure (kPa)	Membrane Correction (kPa)	P_1 (kPa)	q (kPa)	t (kPa)	p' (kPa)	s' (kPa)
1300	9.5680	800	1838.1	754.5	1.0	945.9	145.9	72.9	94.1	118.4
1585	11.6656	800	1847.4	755.5	1.0	943.8	143.8	71.9	92.4	116.4
1800	13.2480	800	1859.3	756.5	1.0	942.9	142.9	71.4	91.1	114.9
2095	15.4192	800	1890.5	756.5	1.0	943.6	143.6	71.8	91.4	115.3
2375	17.4799	800	1915.8	756.5	1.0	943.5	143.5	71.7	91.3	115.2
2645	19.4671	800	1943.1	756.5	1.0	943.6	143.6	71.8	91.4	115.3
2800	20.6079	800	1959.9	756.5	1.0	943.7	143.7	71.8	91.4	115.3
3000	22.0799	800	1978.6	756.5	1.0	943.4	143.4	71.7	91.3	115.2
3200	23.5519	800	2003.7	756.5	1.0	943.8	143.8	71.9	91.4	115.4
3505	25.7967	800	2039.3	756.5	1.0	943.8	143.8	71.9	91.4	115.4







Test	**Case 2: Monotonic Undrained Compression of One-Dimensionally Consolidated Specimens**		
Cell No.	2 (Big)	Fines content (%)	20
Specimen	K0-3	Specific gravity (g/cm^3)	2.72

1.) Sample physical properties

Wet mass before test (g)	841.824	m.c before test (%)	9.33	Height (mm)	151.65	Volume (cm^3)	701.599
Wet mass after test (g)	960.787	m.c. after test (%)	24.78	Diameter (mm)	76.75		
Dry mass (g)	769.984	Dry density (kg/m^3)	1097	Area (cm^2)	46.264	Void ratio (e_0)	1.478

2.) Saturation / Consolidation

Proof ring properties		Strain gauge properties		Loading ram properties	
Proof ring No.	5153	1 strain division (mm)	0.01	Area [ram]$_1$ (cm^2)	7.905
Proof ring factor (dN/div)	7.512			Area [ram]$_2$ (cm^2)	5.004

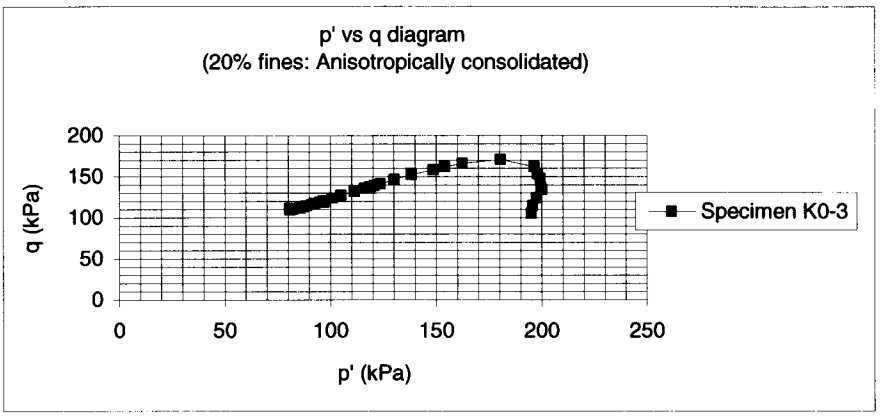
Date	Strain Gauge (divs)	Change Length (mm)	Cell Pressure (kPa)	Proof Ring (div)	Pore Pressure (kPa)	P_1 (kPa)	P'_3 (kPa)	P'_1 (kPa)	q (kPa)	p' (kPa)	K0	Volume Gauge (cm^3)	Cell Expansn (cm^3)
14/3	0	0.000	0	0.0	0.0						\	0.00	0.00
14/3	0	0.000	7.8		3.0	A I R - F L U S H I N G					\	9.55	0.00
14/3	236	2.360	50	135.1	40.0	63.4	10	23.4	13.4	14.5	0.43	33.94	7.06
15/3	450	4.500	100	181.2	90.0	112.3	10	22.3	12.3	14.1	0.45	52.01	9.79
16/3	633	6.330	150	205.6	140.0	157.8	10	17.8	7.8	12.6	0.56	63.22	11.63
17/3	790	7.900	200	254.0	190.0	207.1	10	17.1	7.1	12.4	0.59	72.24	13.02
18/3	914	9.140	250	302.3	240.0	256.4	10	16.4	6.4	12.1	0.61	82.15	14.57
19/3	1026	10.260	300	356.4	290.0	306.6	10	16.6	6.6	12.2	0.60	88.96	16.03
20/3	1135	11.350	350	405.7	340.0	356.1	10	16.1	6.1	12.0	0.62	94.88	17.22
21/3	1241	12.410	400	653.3	340.0	437.7	60	97.7	37.7	72.6	0.61	101.97	19.30
22/3	1353	13.530	450	888.5	340.0	517.4	110	177.4	67.4	132.5	0.62	106.20	20.93
23/3	1505	15.050	500	1173.4	340.0	605.1	160	265.1	105.1	195.0	0.60	112.09	22.85

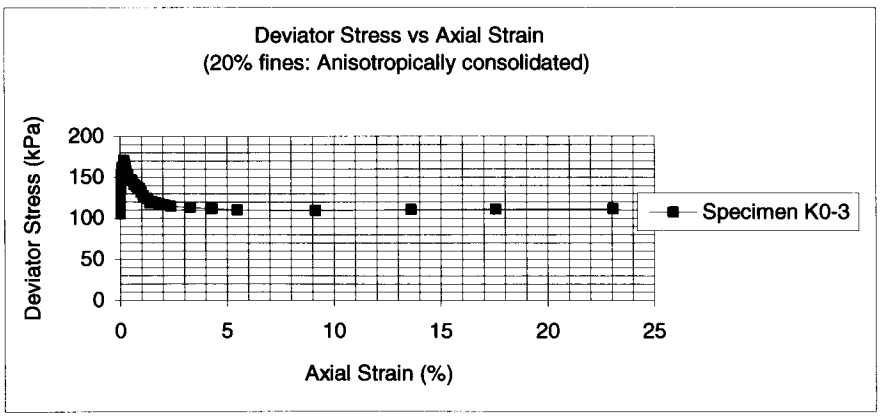
3.) Shear data

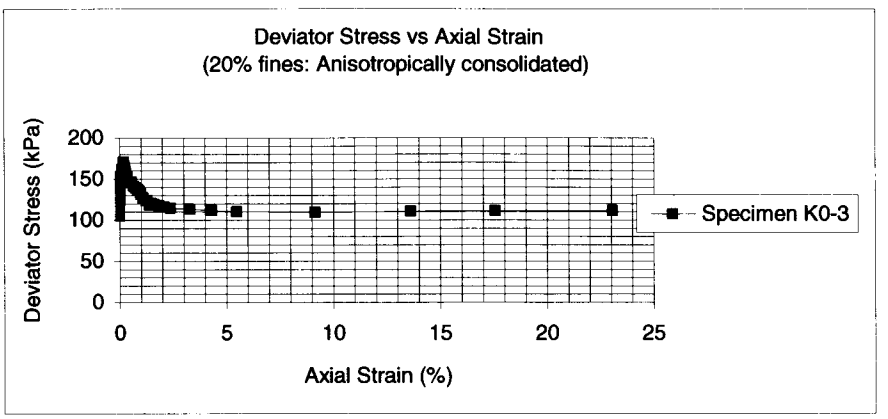
Volume change 1:		Volume change 2:		Sample Vol. change (cm^3)	96.77	B value	0.97
Air Flushing (cm^3)	9.55	Sat/Cons. (cm^3)	102.54	L_{cons} (mm)	136.60	K0	0.60
Cell Expsn. (cm^3)	0.00	Cell Expsn. (cm^3)	22.85	A_{cons} (cm^2)	46.264	Void ratio (e_1)	1.137
		Ram into cell (cm^3)	7.53				

Strain Gauge (divs)	Axial Strain (%)	Cell Press. (kPa)	Proof Ring (divs)	Pore Pressure (kPa)	Membrane Correction (kPa)	P_1 (kPa)	q (kPa)	t (kPa)	p' (kPa)	s' (kPa)
0	0.0000	500	1173.4	340.0	0.0	605.1	105.1	52.5	195.0	212.5
1	0.0073	500	1231.6	342.5	0.0	614.5	114.5	57.3	195.7	214.8
2	0.0110	500	1292.0	344.0	0.0	624.3	124.3	62.2	197.4	218.2
3	0.0220	500	1350.4	344.5	0.0	633.8	133.8	66.9	200.1	222.4
4	0.0293	500	1369.6	346.0	0.0	636.9	136.9	68.4	199.6	222.4
6	0.0461	500	1436.9	350.0	0.0	647.8	147.8	73.9	199.3	223.9
9	0.0622	500	1470.4	353.0	0.0	653.2	153.2	76.6	198.1	223.6
14	0.0988	500	1523.6	357.5	0.0	661.7	161.7	80.9	196.4	223.4
25	0.1830	500	1580.6	376.5	0.1	670.8	170.8	85.4	180.4	208.9
30	0.2196	500	1552.1	393.0	0.1	666.1	166.1	83.1	162.4	190.1
35	0.2562	500	1525.6	400.0	0.1	661.7	161.7	80.9	153.9	180.9
40	0.2928	500	1503.2	404.0	0.1	658.0	158.0	79.0	148.7	175.0
50	0.3660	500	1468.7	412.5	0.2	652.3	152.3	76.2	138.3	163.7
75	0.5490	500	1434.9	418.5	0.3	646.5	146.5	73.2	130.3	154.7
90	0.6589	500	1402.6	423.5	0.3	641.0	141.0	70.5	123.5	147.0
105	0.7687	500	1391.3	425.5	0.4	639.0	139.0	69.5	120.8	144.0
115	0.8419	500	1383.5	427.0	0.4	637.6	137.6	68.8	118.9	141.8
125	0.9151	500	1374.1	429.0	0.5	636.0	136.0	68.0	116.3	139.0
135	0.9883	500	1348.9	432.5	0.5	631.8	131.8	65.9	111.4	133.4
150	1.0981	500	1322.6	437.5	0.5	627.4	127.4	63.7	105.0	126.2
175	1.2811	500	1303.5	440.5	0.6	624.0	124.0	62.0	100.8	121.5
190	1.3909	500	1269.5	442.5	0.7	618.3	118.3	59.2	96.9	116.7
205	1.5007	500	1283.2	443.5	0.8	620.3	120.3	60.2	96.6	116.7
225	1.6471	500	1275.0	444.5	0.8	618.8	118.8	59.4	95.1	114.9

Strain Gauge (divs)	Axial Strain (%)	Cell Press. (kPa)	Proof Ring (divs)	Pore Pressure (kPa)	Membrane Correction (kPa)	P_1 (kPa)	q (kPa)	t (kPa)	p' (kPa)	s' (kPa)
250	1.8302	500	1269.2	446.5	0.9	617.5	117.5	58.8	92.7	112.3
285	2.0864	500	1262.3	447.5	1.0	616.0	116.0	58.0	91.2	110.5
325	2.3792	500	1255.5	449.5	1.0	614.6	114.6	57.3	88.7	107.8
450	3.2943	500	1254.7	450.5	1.0	613.4	113.4	56.7	87.3	106.2
590	4.3192	500	1252.6	451.5	1.0	611.9	111.9	55.9	85.8	104.4
750	5.4905	500	1250.9	454.5	1.0	610.2	110.2	55.1	82.2	100.6
1250	9.1508	500	1273.9	455.5	1.0	609.3	109.3	54.7	80.9	99.2
1860	13.6164	500	1320.1	456.0	1.0	610.4	110.4	55.2	80.8	99.2
2400	17.5695	500	1361.7	456.0	1.0	610.8	110.8	55.4	80.9	99.4
3150	23.0600	500	1425.5	456.5	1.0	611.4	111.4	55.7	80.6	99.2







Test	**Case 2: Monotonic Undrained Compression of One-Dimensionally Consolidated Specimens**		
Cell No.	3 (Big)	Fines content (%)	20
Specimen	K0-4	Specific gravity (g/cm^3)	2.72

1.) Sample physical properties

Wet mass before test (g)	848.547	m.c before test (%)	10.44	Height (mm)	152.05	Volume (cm^3)	705.284
Wet mass after test (g)	982.775	m.c. after test (%)	27.91	Diameter (mm)	76.85		
Dry mass (g)	768.333	Dry density (kg/m^3)	1089	Area (cm^2)	46.385	Void ratio (e_0)	1.497

2.) Saturation / Consolidation

Proof ring properties		Strain gauge properties		Loading ram properties	
Proof ring No.	4541	1 strain division (mm)	0.01	Area [ram]$_1$ (cm^2)	7.905
Proof ring factor (dN/div)	25.77			Area [ram]$_2$ (cm^2)	5.004

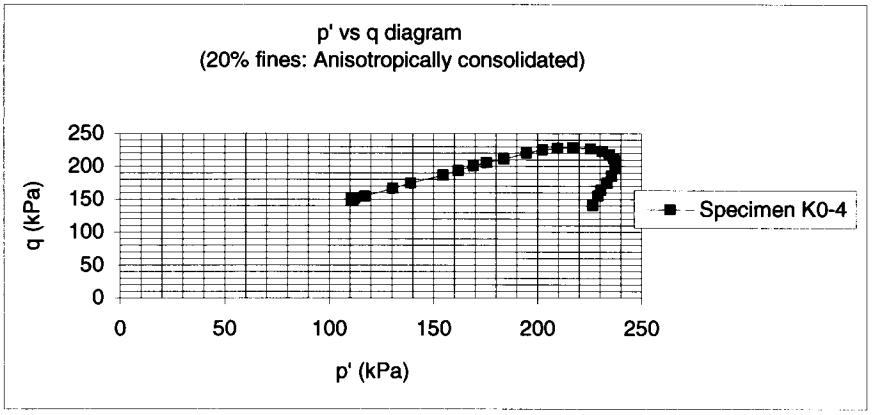
Date	Strain Gauge (divs)	Change Length (mm)	Cell Pressure (kPa)	Proof Ring (div)	Pore Pressure (kPa)	P_1 (kPa)	P'_3 (kPa)	P'_1 (kPa)	q (kPa)	p' (kPa)	K0	Volume Gauge (cm^3)	Cell Expansn (cm^3)
14/3	0	0.000	0	0.0	0.0						\	0.00	0.00
14/3	0	0.000	9.2		8.4	A I R - F L U S H I N G					\	10.42	0.00
14/3	202	2.020	50	50.0	40.0	69.3	10	29.3	19.3	16.4	0.34	41.25	6.08
15/3	412	4.120	100	59.8	90.0	116.2	10	26.2	16.2	15.4	0.38	58.91	8.77
16/3	624	6.240	150	65.2	140.0	160.7	10	20.7	10.7	13.6	0.48	69.87	10.65
17/3	821	8.210	200	75.4	190.0	207.8	10	17.8	7.8	12.6	0.56	77.63	12.00
18/3	996	9.960	250	88.9	240.0	256.8	10	16.8	6.8	12.3	0.60	84.90	13.63
19/3	1163	11.630	300	105.5	290.0	307.5	10	17.5	7.5	12.5	0.57	91.21	15.06
20/3	1308	13.080	350	120.6	340.0	357.4	10	17.4	7.4	12.5	0.58	96.65	16.08
21/3	1439	14.390	400	180.3	350.0	432.0	50	82.0	32.0	60.7	0.61	102.54	18.12
22/3	1574	15.740	450	235.5	360.0	504.1	90	144.1	54.1	108.0	0.62	108.00	19.91
23/3	1823	18.230	550	420.8	370.0	690.1	180	320.1	140.1	226.7	0.56	125.42	22.28

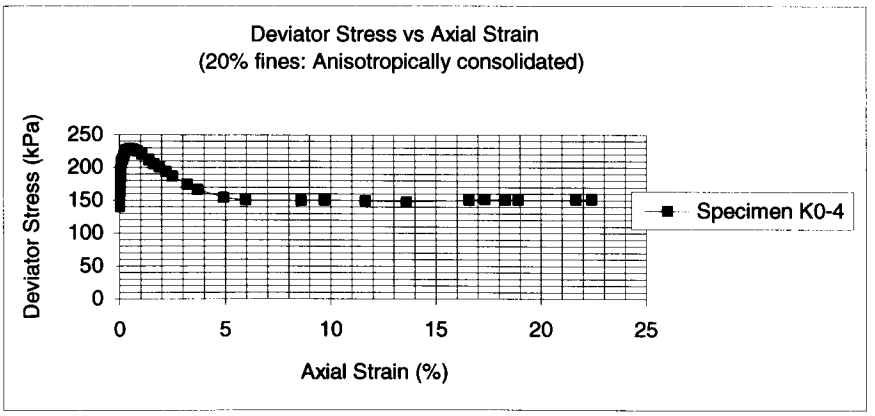
3.) Shear data

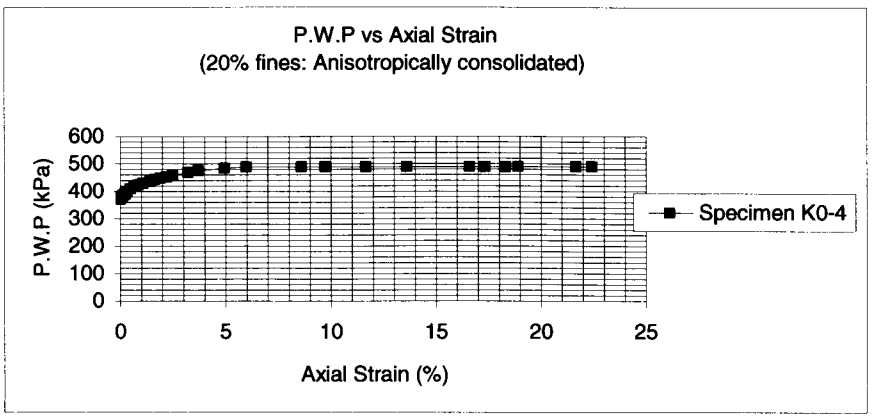
Volume change 1:		Volume change 2:		Sample Vol. change (cm^3)	112.26	B value	0.97
Air Flushing (cm^3)	10.42	Sat/Cons. (cm^3)	115.00	L_{cons} (mm)	133.82	K0	0.56
Cell Expsn. (cm^3)	0.00	Cell Expsn. (cm^3)	22.28	A_{cons} (cm^2)	46.385	Void ratio (e_1)	1.099
		Ram into cell (cm^3)	9.12				

Strain Gauge (divs)	Axial Strain (%)	Cell Press. (kPa)	Proof Ring (divs)	Pore Pressure (kPa)	Membrane Correction (kPa)	P_1 (kPa)	q (kPa)	t (kPa)	p' (kPa)	s' (kPa)
0	0.0000	550	420.8	370.0	0.0	690.1	140.1	70.0	226.7	250.0
3	0.0202	550	447.3	372.5	0.0	704.7	154.7	77.4	229.1	254.9
4	0.0291	550	463.1	374.0	0.0	713.5	163.5	81.7	230.5	257.7
6	0.0426	550	482.5	374.5	0.0	724.2	174.2	87.1	233.6	262.6
8	0.0628	550	501.9	376.0	0.0	735.0	185.0	92.5	235.7	266.5
10	0.0747	550	522.3	378.0	0.0	746.3	196.3	98.1	237.4	270.1
15	0.1121	550	543.2	381.5	0.1	757.8	207.8	103.9	237.8	272.4
20	0.1495	550	551.1	384.0	0.1	762.1	212.1	106.0	236.7	272.0
30	0.2242	550	562.0	388.0	0.1	767.9	217.9	108.9	234.6	270.9
35	0.2615	550	570.9	393.0	0.1	772.7	222.7	111.4	231.2	268.4
45	0.3363	550	578.0	400.0	0.2	776.5	226.5	113.2	225.5	263.2
65	0.4857	550	582.2	409.0	0.2	778.4	228.4	114.2	217.1	255.2
90	0.6725	550	581.3	416.0	0.3	777.3	227.3	113.7	209.8	247.7
115	0.8594	550	578.3	422.5	0.4	775.2	225.2	112.6	202.6	240.1
145	1.0835	550	570.0	428.5	0.5	770.0	220.0	110.0	194.8	231.5
190	1.4198	550	555.3	436.5	0.7	761.0	211.0	105.5	183.8	219.0
220	1.6440	550	546.5	443.0	0.8	755.6	205.6	102.8	175.5	209.8
255	1.9055	550	538.4	447.5	1.0	750.5	200.5	100.3	169.3	202.8
295	2.2045	550	526.7	452.5	1.0	743.5	193.5	96.8	162.0	194.3
335	2.5034	550	514.6	457.5	1.0	736.4	186.4	93.2	154.6	185.7
430	3.2133	550	495.2	469.0	1.0	724.6	174.6	87.3	139.2	168.3
495	3.6990	550	482.0	475.0	1.0	716.6	166.6	83.3	130.5	158.3
660	4.9320	550	463.2	484.5	1.0	704.5	154.5	77.3	117.0	142.8
800	5.9782	550	458.3	488.5	1.0	700.3	150.3	75.1	111.6	136.6

Strain Gauge (divs)	Axial Strain (%)	Cell Press. (kPa)	Proof Ring (divs)	Pore Pressure (kPa)	Membrane Correction (kPa)	P_1 (kPa)	q (kPa)	t (kPa)	p' (kPa)	s' (kPa)
1150	8.5936	550	465.7	488.5	1.0	699.8	149.8	74.9	111.4	136.4
1300	9.7145	550	470.9	488.5	1.0	700.6	150.6	75.3	111.7	136.8
1560	11.6575	550	474.9	488.5	1.0	699.3	149.3	74.6	111.3	136.1
1820	13.6004	550	478.6	488.5	1.0	697.7	147.7	73.9	110.7	135.4
2220	16.5894	550	495.7	488.5	1.0	700.5	150.5	75.3	111.7	136.8
2320	17.3367	550	501.9	488.5	1.0	702.0	152.0	76.0	112.2	137.5
2450	18.3082	550	503.5	488.5	1.0	700.9	150.9	75.5	111.8	137.0
2530	18.9060	550	506.1	489.5	1.0	701.0	151.0	75.5	110.8	136.0
2900	21.6709	550	518.2	489.5	1.0	701.1	151.1	75.5	110.9	136.0
3000	22.4182	550	522.1	489.5	1.0	701.3	151.3	75.7	110.9	136.2







Test	**Case 2: Monotonic Undrained Compression of One-Dimensionally Consolidated Specimens**		
Cell No.	2 (Big)	Fines content (%)	20
Specimen	K0-11	Specific gravity (g/cm^3)	2.72

1.) Sample physical properties

Wet mass before test (g)	861.797	m.c before test (%)	9.10	Height (mm)	151.45	Volume (cm^3)	700.674
Wet mass after test (g)	997.899	m.c. after test (%)	26.33	Diameter (mm)	76.75		
Dry mass (g)	789.915	Dry density (kg/m^3)	1127	Area (cm^2)	46.264	Void ratio (e_0)	1.413

2.) Saturation / Consolidation

Proof ring properties		Strain gauge properties		Loading ram properties	
Proof ring No.	4541	1 strain division (mm)	0.01	Area [ram]$_1$ (cm^2)	7.905
Proof ring factor (dN/div)	25.77			Area [ram]$_2$ (cm^2)	5.004

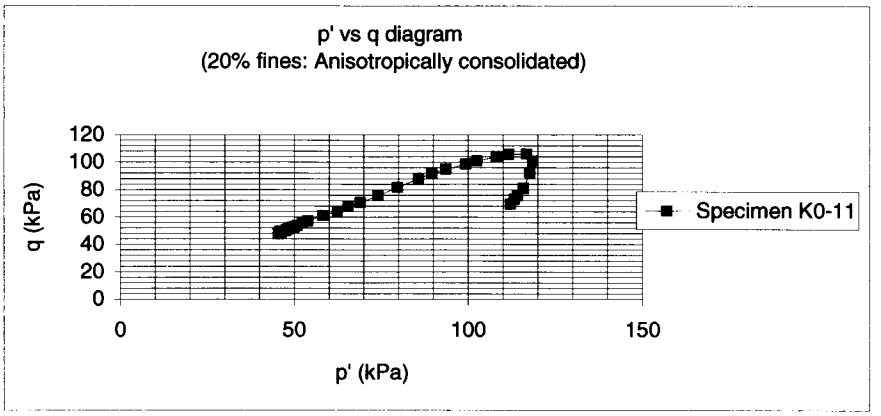
Date	Strain Gauge (divs)	Change Length (mm)	Cell Pressure (kPa)	Proof Ring (div)	Pore Pressure (kPa)	P_1 (kPa)	P'_3 (kPa)	P'_1 (kPa)	q (kPa)	p' (kPa)	K0	Volume Gauge (cm^3)	Cell Expansn (cm^3)
1/5	0	0.000	0	0.0	0.0						\	0.00	0.00
1/5	0	0.000	9.8		4.5	A I R - F L U S H I N G					\	7.97	0.00
1/5	192	1.920	50	45.0	40.0	66.5	10	26.5	16.5	15.5	0.38	28.31	7.06
2/5	361	3.610	100	50.2	90.0	110.9	10	20.9	10.9	13.6	0.48	42.87	9.79
3/5	480	4.800	150	58.6	140.0	157.0	10	17.0	7.0	12.3	0.59	51.29	11.63
4/5	577	5.770	200	75.4	190.0	207.8	10	17.8	7.8	12.6	0.56	57.74	13.02
5/5	670	6.700	250	89.3	240.0	257.0	10	17.0	7.0	12.3	0.59	62.64	14.57
6/5	765	7.650	300	105.9	290.0	307.7	10	17.7	7.7	12.6	0.56	66.19	16.03
7/5	859	8.590	350	122.7	340.0	358.5	10	18.5	8.5	12.8	0.54	69.58	17.22
8/5	950	9.500	400	136.5	390.0	407.7	10	17.7	7.7	12.6	0.57	73.82	19.30
9/5	1033	10.330	450	149.8	440.0	456.6	10	16.6	6.6	12.2	0.60	77.64	20.93
10/5	1121	11.210	500	165.6	490.0	506.8	10	16.8	6.8	12.3	0.59	82.01	22.85
11/5	1509	15.090	798	369.5	709.0	867.5	89	158.5	69.5	112.2	0.56	95.17	28.25

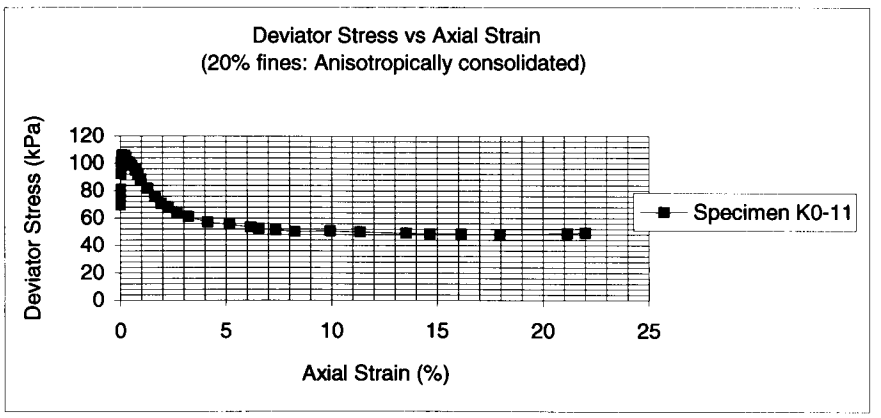
3.) Shear data

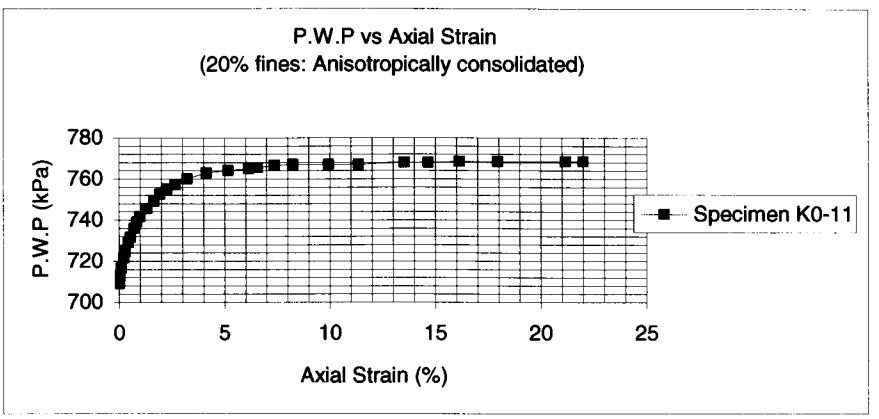
Volume change 1:		Volume change 2:		Sample Vol. change (cm^3)	74.47	B value	0.98
Air Flushing (cm^3)	7.97	Sat/Cons. (cm^3)	87.20	L_{cons} (mm)	136.36	K0	0.56
Cell Expsn. (cm^3)	0.00	Cell Expsn. (cm^3)	28.25	A_{cons} (cm^2)	46.264	Void ratio (e_1)	1.156
		Ram into cell (cm^3)	7.55				

Strain Gauge (divs)	Axial Strain (%)	Cell Press. (kPa)	Proof Ring (divs)	Pore Pressure (kPa)	Membrane Correction (kPa)	P_1 (kPa)	q (kPa)	t (kPa)	p' (kPa)	s' (kPa)
0	0.0000	798	369.5	709.0	0.0	867.5	69.5	34.7	112.2	123.7
1	0.0059	798	375.6	709.0	0.0	870.9	72.9	36.4	113.3	125.4
2	0.0147	798	380.4	709.0	0.0	873.5	75.5	37.8	114.2	126.8
3	0.0220	798	390.0	709.0	0.0	878.9	80.9	40.4	116.0	129.4
4	0.0293	798	410.8	711.0	0.0	890.4	92.4	46.2	117.8	133.2
6	0.0433	798	425.7	713.0	0.0	898.7	100.7	50.4	118.6	135.4
15	0.1100	798	435.4	716.5	0.1	904.0	106.0	53.0	116.8	134.5
30	0.2200	798	435.0	721.5	0.1	903.6	105.6	52.8	111.7	129.3
40	0.2933	798	432.3	724.5	0.1	902.0	104.0	52.0	108.2	125.5
60	0.4400	798	427.0	729.0	0.2	898.8	100.8	50.4	102.6	119.4
75	0.5500	798	423.1	731.5	0.3	896.5	98.5	49.3	99.3	115.8
100	0.7334	798	417.3	736.0	0.4	893.0	95.0	47.5	93.7	109.5
115	0.8434	798	412.1	739.0	0.4	890.0	92.0	46.0	89.7	105.0
135	0.9900	798	405.0	741.5	0.5	885.9	87.9	43.9	85.8	100.4
180	1.3200	798	394.5	745.5	0.7	879.6	81.6	40.8	79.7	93.3
225	1.6500	798	384.0	749.0	0.8	873.4	75.4	37.7	74.1	86.7
265	1.9434	798	375.8	752.5	1.0	868.6	70.6	35.3	69.0	80.8
310	2.2734	798	370.9	755.0	1.0	865.7	67.7	33.8	65.6	76.8
365	2.6767	798	365.1	757.0	1.0	862.2	64.2	32.1	62.4	73.1
440	3.2268	798	359.8	760.0	1.0	859.0	61.0	30.5	58.3	68.5
565	4.1434	798	353.2	763.0	1.0	854.9	56.9	28.4	54.0	63.4
705	5.1701	798	351.3	764.0	1.0	853.3	55.3	27.6	52.4	61.6
840	6.1602	798	349.0	765.0	1.0	851.5	53.5	26.7	50.8	59.7
895	6.5635	798	347.8	765.5	1.0	850.6	52.6	26.3	50.0	58.8

Strain Gauge (divs)	Axial Strain (%)	Cell Press. (kPa)	Proof Ring (divs)	Pore Pressure (kPa)	Membrane Correction (kPa)	P_1 (kPa)	q (kPa)	t (kPa)	p' (kPa)	s' (kPa)
1005	7.3702	798	346.4	766.5	1.0	849.4	51.4	25.7	48.6	57.2
1125	8.2502	798	345.0	767.0	1.0	848.2	50.2	25.1	47.7	56.1
1355	9.9369	798	347.9	767.0	1.0	848.7	50.7	25.4	47.9	56.4
1550	11.3670	798	348.1	767.0	1.0	848.0	50.0	25.0	47.7	56.0
1845	13.5304	798	348.5	768.0	1.0	847.0	49.0	24.5	46.3	54.5
2000	14.6671	798	349.0	768.0	1.0	846.5	48.5	24.3	46.2	54.3
2200	16.1338	798	350.3	768.5	1.0	846.3	48.3	24.1	45.6	53.6
2450	17.9671	798	352.2	768.5	1.0	846.1	48.1	24.0	45.5	53.5
2885	21.1572	798	358.3	768.5	1.0	846.9	48.9	24.4	45.8	53.9
3000	22.0006	798	360.4	768.5	1.0	847.2	49.2	24.6	45.9	54.1







Test	Case 2: Monotonic Undrained Compression of One-Dimensionally Consolidated Specimens		
Cell No.	2 (Big)	Fines content (%)	20
Specimen	K0-18	Specific gravity (g/cm^3)	2.72

1.) Sample physical properties

Wet mass before test (g)	855.509	m.c before test (%)	10.05	Height (mm)	150.50	Volume (cm^3)	696.279
Wet mass after test (g)	984.477	m.c. after test (%)	26.64	Diameter (mm)	76.75		
Dry mass (g)	777.382	Dry density (kg/m^3)	1116	Area (cm^2)	46.264	Void ratio (e_0)	1.436

2.) Saturation / Consolidation

Proof ring properties		Strain gauge properties		Loading ram properties	
Proof ring No.	5153	1 strain division (mm)	0.01	Area [ram]$_1$ (cm^2)	7.905
Proof ring factor (dN/div)	7.512			Area [ram]$_2$ (cm^2)	5.004

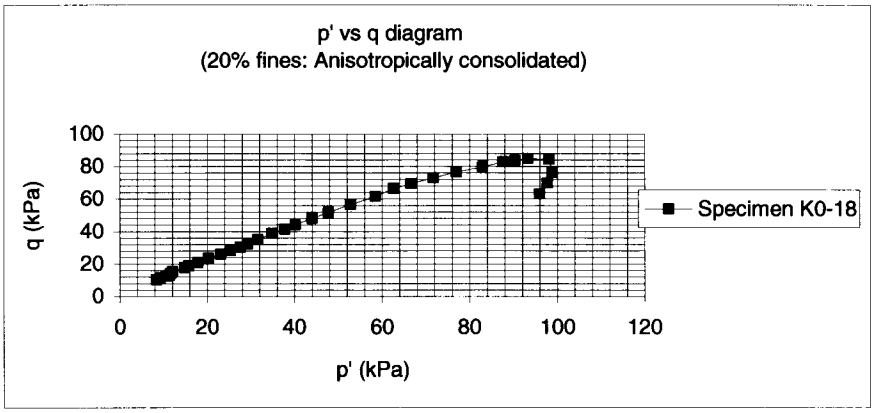
Date	Strain Gauge (divs)	Change Length (mm)	Cell Pressure (kPa)	Proof Ring (div)	Pore Pressure (kPa)	P_1 (kPa)	P'_3 (kPa)	P'_1 (kPa)	q (kPa)	p' (kPa)	K0	Volume Gauge (cm^3)	Cell Expansn (cm^3)
6/6	0	0.000	0	0.0	0.0						\	0.00	0.00
6/6	0	0.000	10.5		5.0	A I R - F L U S H I N G					\	9.88	0.00
6/6	223	2.230	50	134.5	40.0	63.3	10	23.3	13.3	14.4	0.43	25.21	7.06
7/6	432	4.320	100	155.7	90.0	108.2	10	18.2	8.2	12.7	0.55	33.41	9.79
8/6	629	6.290	150	202.3	140.0	157.2	10	17.2	7.2	12.4	0.58	39.50	11.63
9/6	801	8.010	200	251.1	190.0	206.6	10	16.6	6.6	12.2	0.60	44.13	13.02
10/6	922	9.220	250	305.5	240.0	256.9	10	16.9	6.9	12.3	0.59	47.52	14.57
11/6	1038	10.380	300	363.9	290.0	307.8	10	17.8	7.8	12.6	0.56	51.09	16.03
12/6	1154	11.540	350	408.6	340.0	356.5	10	16.5	6.5	12.2	0.60	54.22	17.22
13/6	1320	13.200	400	654.4	350.0	437.9	50	87.9	37.9	62.6	0.57	64.89	19.30
14/6	1444	14.440	450	861.9	375.0	513.1	75	138.1	63.1	96.0	0.54	69.93	20.93

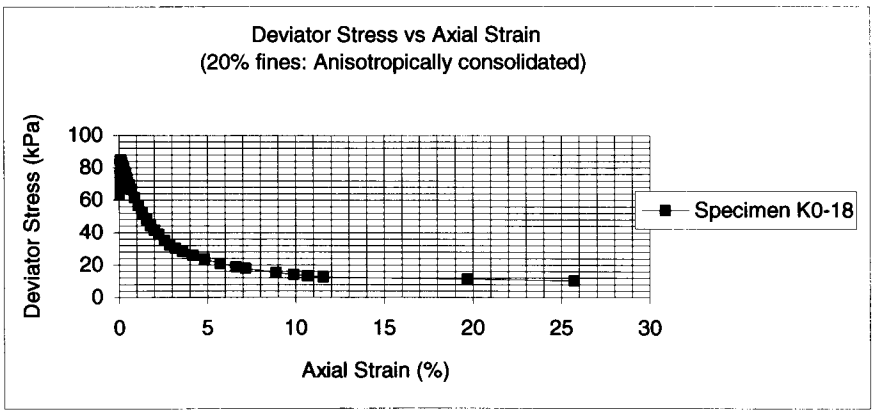
3.) Shear data

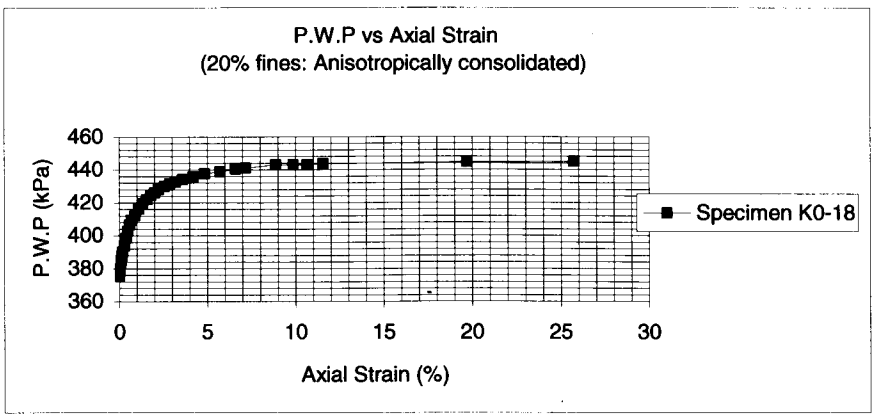
Volume change 1:		Volume change 2:		Sample Vol. change (cm^3)	56.23	B value	0.97
Air Flushing (cm^3)	9.88	Sat/Cons. (cm^3)	60.05	L_{cons} (mm)	136.06	K0	0.54
Cell Expsn. (cm^3)	0.00	Cell Expsn. (cm^3)	20.93	A_{cons} (cm^2)	46.264	Void ratio (e_1)	1.239
		Ram into cell (cm^3)	7.23				

Strain Gauge (divs)	Axial Strain (%)	Cell Press. (kPa)	Proof Ring (divs)	Pore Pressure (kPa)	Membrane Correction (kPa)	P_1 (kPa)	q (kPa)	t (kPa)	p' (kPa)	s' (kPa)
0	0.0000	450	861.9	375.0	0.0	513.1	63.1	31.5	96.0	106.5
1	0.0037	450	903.1	375.5	0.0	519.7	69.7	34.9	97.7	109.4
2	0.0125	450	942.5	376.5	0.0	526.1	76.1	38.1	98.9	111.6
8	0.0617	450	994.2	380.0	0.0	534.5	84.5	42.2	98.2	112.2
15	0.1102	450	996.4	385.0	0.1	534.7	84.7	42.4	93.2	107.4
20	0.1470	450	989.3	387.5	0.1	533.5	83.5	41.8	90.3	104.3
25	0.1837	450	985.1	390.0	0.1	532.8	82.8	41.4	87.6	101.4
40	0.2940	450	966.2	393.5	0.1	529.6	79.6	39.8	83.0	96.3
55	0.4042	450	947.4	398.5	0.2	526.4	76.4	38.2	77.0	89.7
65	0.4777	450	925.8	402.5	0.2	522.8	72.8	36.4	71.8	83.9
80	0.5880	450	905.2	406.5	0.3	519.4	69.4	34.7	66.6	78.2
95	0.6982	450	888.1	409.5	0.3	516.5	66.5	33.2	62.7	73.7
120	0.8820	450	857.8	412.0	0.4	511.4	61.4	30.7	58.5	68.7
152	1.1149	450	828.6	416.0	0.6	506.5	56.5	28.2	52.8	62.2
180	1.3229	450	801.1	419.5	0.7	501.8	51.8	25.9	47.8	56.4
215	1.5802	450	779.0	422.0	0.8	498.0	48.0	24.0	44.0	52.0
245	1.8007	450	755.8	424.5	0.9	494.1	44.1	22.1	40.2	47.6
275	2.0212	450	739.5	426.0	1.0	491.3	41.3	20.7	37.8	44.7
305	2.2417	450	723.6	428.0	1.0	488.7	38.7	19.3	34.9	41.3
350	2.5724	450	701.1	430.0	1.0	485.0	35.0	17.5	31.7	37.5
390	2.8664	450	684.7	431.5	1.0	482.3	32.3	16.2	29.3	34.7
435	3.1971	450	671.9	432.5	1.0	480.2	30.2	15.1	27.6	32.6
490	3.6014	450	658.7	434.0	1.0	478.0	28.0	14.0	25.3	30.0
570	4.1893	450	646.4	435.5	1.0	475.9	25.9	12.9	23.1	27.4

Strain Gauge (divs)	Axial Strain (%)	Cell Press. (kPa)	Proof Ring (divs)	Pore Pressure (kPa)	Membrane Correction (kPa)	P_1 (kPa)	q (kPa)	t (kPa)	p' (kPa)	s' (kPa)
660	4.8508	450	632.6	437.5	1.0	473.6	23.6	11.8	20.4	24.3
780	5.7328	450	615.8	439.0	1.0	470.8	20.8	10.4	17.9	21.4
900	6.6147	450	604.3	440.5	1.0	468.8	18.8	9.4	15.8	18.9
975	7.1660	450	598.2	441.0	1.0	467.8	17.8	8.9	14.9	17.9
1210	8.8931	450	583.5	443.0	1.0	465.3	15.3	7.6	12.1	14.6
1345	9.8853	450	575.6	443.0	1.0	463.9	13.9	7.0	11.6	14.0
1450	10.6571	450	570.5	443.0	1.0	463.1	13.1	6.5	11.4	13.5
1575	11.5758	450	567.8	443.5	1.0	462.5	12.5	6.3	10.7	12.8
2680	19.6972	450	567.5	444.5	1.0	461.3	11.3	5.6	9.3	11.1
3500	25.7239	450	567.5	445.0	1.0	460.3	10.3	5.2	8.4	10.2







Test	**Case 2: Monotonic Undrained Compression of One-Dimensionally Consolidated Specimens**		
Cell No.	2 (Big)	Fines content (%)	20
Specimen	K0-21	Specific gravity (g/cm^3)	2.72

1.) Sample physical properties

Wet mass before test (g)	874.672	m.c before test (%)	9.37	Height (mm)	151.55	Volume (cm^3)	701.137
Wet mass after test (g)	997.911	m.c. after test (%)	24.78	Diameter (mm)	76.75		
Dry mass (g)	799.737	Dry density (kg/m^3)	1141	Area (cm^2)	46.264	Void ratio (e_0)	1.385

2.) Saturation / Consolidation

Proof ring properties		Strain gauge properties		Loading ram properties	
Proof ring No.	4541	1 strain division (mm)	0.01	Area [ram]$_1$ (cm^2)	7.905
Proof ring factor (dN/div)	25.77			Area [ram]$_2$ (cm^2)	5.004

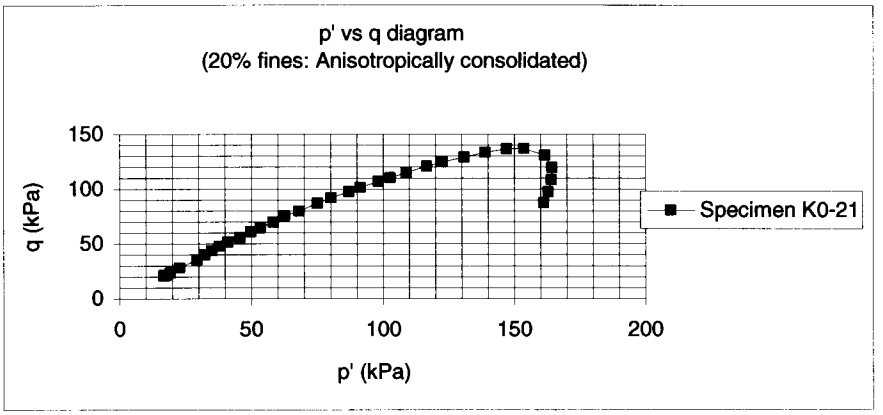
Date	Strain Gauge (divs)	Change Length (mm)	Cell Pressure (kPa)	Proof Ring (div)	Pore Pressure (kPa)	P_1 (kPa)	P'_3 (kPa)	P'_1 (kPa)	q (kPa)	p' (kPa)	K0	Volume Gauge (cm^3)	Cell Expansn (cm^3)
2/7	0	0.000	0	0.0	0.0						\	0.00	0.00
2/7	0	0.000	10.7		7.5	A I R - F L U S H I N G					\	11.10	0.00
2/7	223	2.230	50	54.9	40.0	72.0	10	32.0	22.0	17.3	0.31	24.27	7.06
3/7	428	4.280	100	59.4	90.0	116.0	10	26.0	16.0	15.3	0.38	30.84	9.79
4/7	610	6.100	150	69.5	140.0	163.1	10	23.1	13.1	14.4	0.43	35.11	11.63
5/7	749	7.490	200	74.4	190.0	207.3	10	17.3	7.3	12.4	0.58	38.30	13.02
6/7	869	8.690	250	88.7	240.0	256.7	10	16.7	6.7	12.2	0.60	40.98	14.57
7/7	983	9.830	300	105.0	290.0	307.2	10	17.2	7.2	12.4	0.58	43.01	16.03
8/7	1087	10.870	350	119.8	340.0	356.9	10	16.9	6.9	12.3	0.59	44.96	17.22
9/7	1194	11.940	400	134.4	390.0	406.5	10	16.5	6.5	12.2	0.61	47.62	19.30
10/7	1299	12.990	450	151.2	440.0	457.3	10	17.3	7.3	12.4	0.58	49.89	20.93
11/7	1687	16.870	600	341.0	468.0	687.4	132	219.4	87.4	161.1	0.60	62.95	24.27

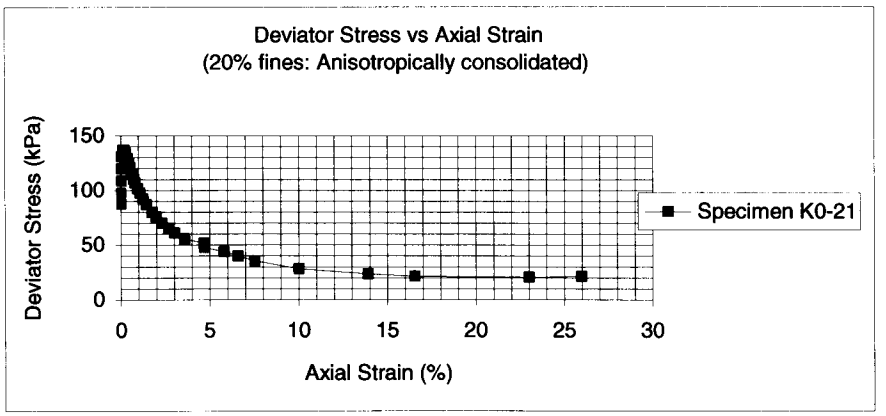
3.) Shear data

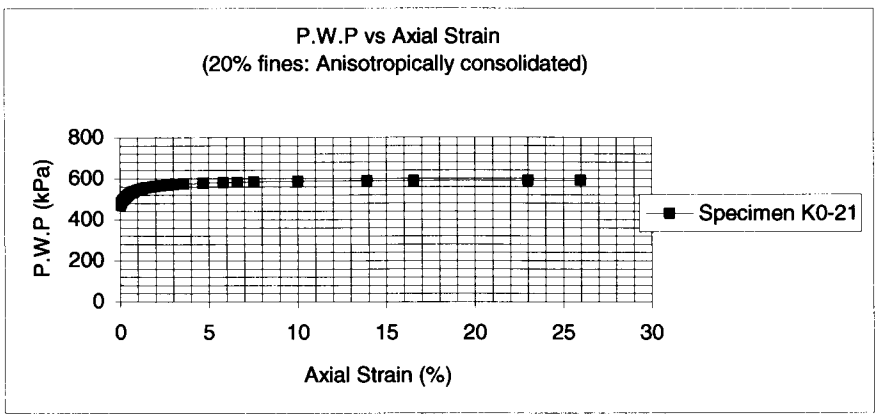
Volume change 1:		Volume change 2:		Sample Vol. change (cm^3)	47.12	B value	0.99
Air Flushing (cm^3)	11.10	Sat/Cons. (cm^3)	51.85	L_{cons} (mm)	134.68	K0	0.60
Cell Expsn. (cm^3)	0.00	Cell Expsn. (cm^3)	24.27	A_{cons} (cm^2)	46.264	Void ratio (e_1)	1.224
		Ram into cell (cm^3)	8.44				

Strain Gauge (divs)	Axial Strain (%)	Cell Press. (kPa)	Proof Ring (divs)	Pore Pressure (kPa)	Membrane Correction (kPa)	P_1 (kPa)	q (kPa)	t (kPa)	p' (kPa)	s' (kPa)
0	0.0000	600	341.0	468.0	0.0	687.4	87.4	43.7	161.1	175.7
1	0.0082	600	358.8	469.5	0.0	697.3	97.3	48.7	162.9	179.2
3	0.0200	600	378.7	472.0	0.0	708.4	108.4	54.2	164.1	182.2
5	0.0371	600	398.6	475.5	0.0	719.4	119.4	59.7	164.3	184.2
10	0.0743	600	418.9	482.0	0.0	730.7	130.7	65.3	161.6	183.3
20	0.1485	600	430.2	492.0	0.1	736.8	136.8	68.4	153.6	176.4
30	0.2228	600	429.8	498.5	0.1	736.5	136.5	68.2	147.0	169.7
40	0.2970	600	424.1	505.5	0.1	733.2	133.2	66.6	138.9	161.1
50	0.3713	600	416.8	512.0	0.2	729.0	129.0	64.5	131.0	152.5
60	0.4455	600	409.2	519.0	0.2	724.6	124.6	62.3	122.5	143.3
70	0.5198	600	402.1	523.5	0.3	720.6	120.6	60.3	116.7	136.8
85	0.6311	600	392.3	529.5	0.3	715.0	115.0	57.5	108.8	128.0
100	0.7425	600	383.8	534.0	0.4	710.1	110.1	55.0	102.7	121.0
110	0.8168	600	378.5	537.5	0.4	707.0	107.0	53.5	98.2	116.0
130	0.9653	600	368.6	542.5	0.5	701.3	101.3	50.7	91.3	108.2
145	1.0766	600	362.0	545.5	0.5	697.5	97.5	48.8	87.0	103.3
170	1.2623	600	352.4	550.5	0.6	692.0	92.0	46.0	80.2	95.5
195	1.4479	600	344.0	554.0	0.7	687.1	87.1	43.5	75.0	89.5
240	1.7820	600	331.6	558.5	0.9	679.8	79.8	39.9	68.1	81.4
270	2.0048	600	324.1	562.5	1.0	675.4	75.4	37.7	62.6	75.2
315	2.3389	600	314.3	565.0	1.0	669.9	69.9	34.9	58.3	69.9
365	2.7101	600	305.5	568.0	1.0	664.8	64.8	32.4	53.6	64.4
410	3.0443	600	298.6	570.5	1.0	660.9	60.9	30.4	49.8	59.9
485	3.6011	600	289.7	573.0	1.0	655.7	55.7	27.9	45.6	54.9

Strain Gauge (divs)	Axial Strain (%)	Cell Press. (kPa)	Proof Ring (divs)	Pore Pressure (kPa)	Membrane Correction (kPa)	P_1 (kPa)	q (kPa)	t (kPa)	p' (kPa)	s' (kPa)
630	4.6778	600	282.8	576.0	1.0	651.4	51.4	25.7	41.1	49.7
635	4.7149	600	276.0	578.0	1.0	647.8	47.8	23.9	37.9	45.9
785	5.8286	600	269.1	579.5	1.0	643.6	43.6	21.8	35.0	42.3
890	6.6083	600	262.8	581.0	1.0	640.0	40.0	20.0	32.3	39.0
1015	7.5364	600	255.0	582.5	1.0	635.5	35.5	17.8	29.3	35.3
1350	10.0238	600	242.0	586.5	1.0	628.0	28.0	14.0	22.8	27.5
1875	13.9219	600	234.9	588.5	1.0	623.4	23.4	11.7	19.3	23.2
2230	16.5578	600	232.3	589.5	1.0	621.4	21.4	10.7	17.6	21.2
3100	23.0175	600	234.2	590.0	1.0	620.5	20.5	10.3	16.8	20.3
3500	25.9875	600	238.0	590.0	1.0	621.2	21.2	10.6	17.1	20.6







Test	**Case 2: Monotonic Undrained Compression of One-Dimensionally Consolidated Specimens**		
Cell No.	2 (Big)	Fines content (%)	20
Specimen	K0-25	Specific gravity (g/cm^3)	2.72

1.) Sample physical properties

Wet mass before test (g)	878.859	m.c before test (%)	9.54	Height (mm)	152.90	Volume (cm^3)	705.540
Wet mass after test (g)	1014.451	m.c. after test (%)	26.44	Diameter (mm)	76.65		
Dry mass (g)	802.318	Dry density (kg/m^3)	1137	Area (cm^2)	46.144	Void ratio (e_o)	1.392

2.) Saturation / Consolidation

Proof ring properties		Strain gauge properties		Loading ram properties	
Proof ring No.	4541	1 strain division (mm)	0.01	Area [ram]$_1$ (cm^2)	7.905
Proof ring factor (dN/div)	25.77			Area [ram]$_2$ (cm^2)	5.004

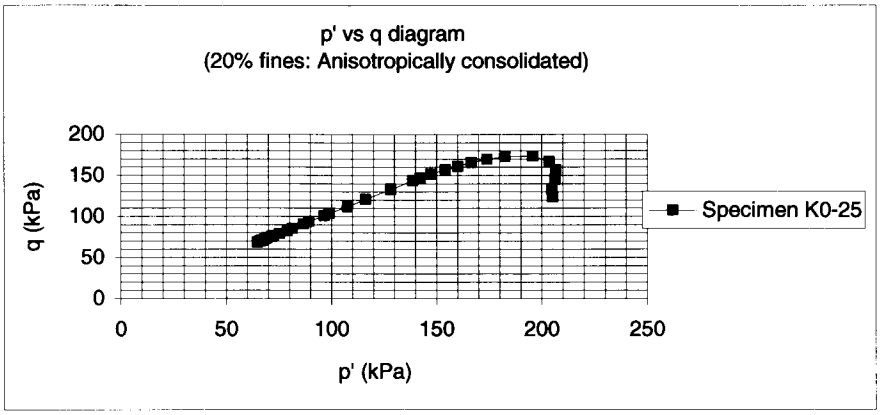
Date	Strain Gauge (divs)	Change Length (mm)	Cell Pressure (kPa)	Proof Ring (div)	Pore Pressure (kPa)	P_1 (kPa)	P'_3 (kPa)	P'_1 (kPa)	q (kPa)	p' (kPa)	K0	Volume Gauge (cm^3)	Cell Expansn (cm^3)
27/7	0	0.000	0	0.0	0.0						\	0.00	0.00
27/7	0	0.000	11.2		6.5	A I R - F L U S H I N G					\	10.24	0.00
27/7	192	1.920	50	35.0	40.0	61.0	10	21.0	11.0	13.7	0.48	32.10	7.06
28/7	365	3.650	100	44.7	90.0	107.8	10	17.8	7.8	12.6	0.56	46.89	9.79
29/7	533	5.330	150	61.2	140.0	158.5	10	18.5	8.5	12.8	0.54	56.14	11.63
30/7	671	6.710	200	75.4	190.0	207.8	10	17.8	7.8	12.6	0.56	62.95	13.02
31/7	802	8.020	250	88.5	240.0	256.6	10	16.6	6.6	12.2	0.60	68.05	14.57
1/8	914	9.140	300	105.0	290.0	307.2	10	17.2	7.2	12.4	0.58	71.94	16.03
2/8	1012	10.120	350	120.6	340.0	357.4	10	17.4	7.4	12.5	0.57	76.19	17.22
3/8	1100	11.000	400	147.6	380.0	413.9	20	33.9	13.9	24.6	0.59	81.35	19.30
4/8	1373	13.730	550	390.0	386.0	673.6	164	287.6	123.6	205.2	0.57	99.87	22.97

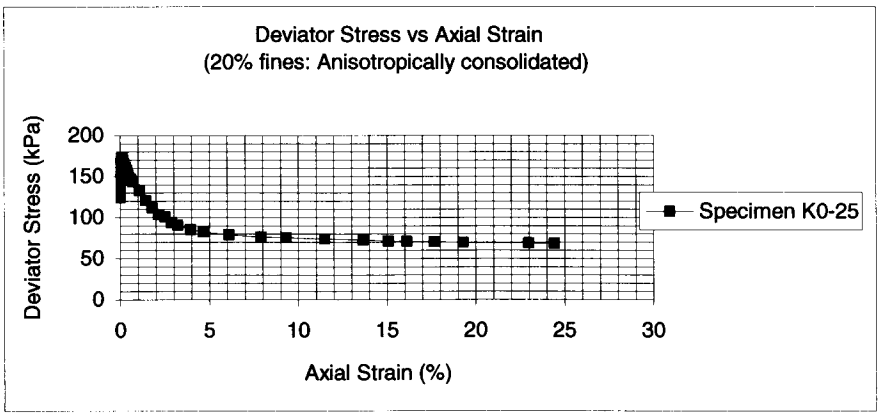
3.) Shear data

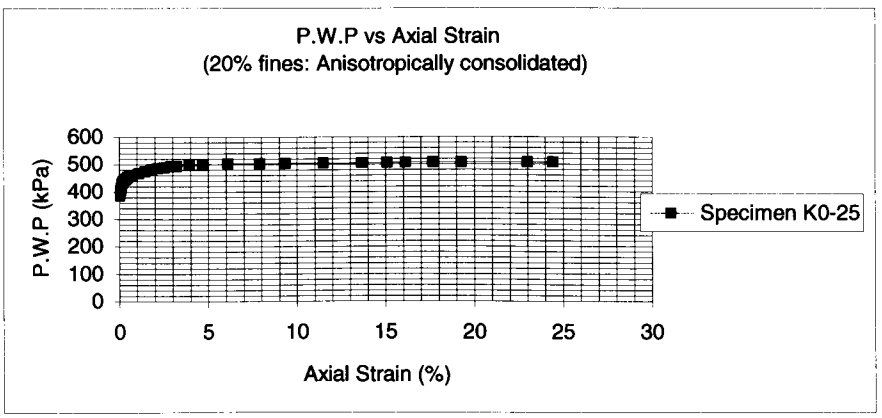
Volume change 1:		Volume change 2:		Sample Vol. change (cm^3)	83.77	B value	0.98
Air Flushing (cm^3)	10.24	Sat/Cons. (cm^3)	89.63	L_{cons} (mm)	139.17	K0	0.57
Cell Expsn. (cm^3)	0.00	Cell Expsn. (cm^3)	22.97	A_{cons} (cm^2)	46.144	Void ratio (e_1)	1.108
		Ram into cell (cm^3)	6.87				

Strain Gauge (divs)	Axial Strain (%)	Cell Press. (kPa)	Proof Ring (divs)	Pore Pressure (kPa)	Membrane Correction (kPa)	P_1 (kPa)	q (kPa)	t (kPa)	p' (kPa)	s' (kPa)
0	0.0000	550	390.2	386.0	0.0	673.7	123.7	61.8	205.2	225.8
2	0.0144	550	406.5	389.5	0.0	682.8	132.8	66.4	204.8	226.9
4	0.0287	550	428.6	392.0	0.0	695.1	145.1	72.5	206.4	230.5
8	0.0575	550	449.7	395.5	0.0	706.8	156.8	78.4	206.8	232.9
10	0.0719	550	467.5	402.0	0.0	716.7	166.7	83.4	203.6	231.4
15	0.1078	550	479.9	412.0	0.1	723.5	173.5	86.8	195.8	224.8
20	0.1437	550	478.7	425.0	0.1	722.8	172.8	86.4	182.6	211.4
25	0.1796	550	473.3	432.5	0.1	719.7	169.7	84.9	174.1	202.4
30	0.2156	550	466.0	438.5	0.1	715.6	165.6	82.8	166.7	194.3
45	0.3233	550	458.4	443.5	0.2	711.1	161.1	80.5	160.2	187.0
55	0.3952	550	451.3	448.0	0.2	707.0	157.0	78.5	154.3	180.5
65	0.4671	550	441.5	453.0	0.2	701.4	151.4	75.7	147.5	172.7
85	0.6108	550	433.0	456.5	0.3	696.4	146.4	73.2	142.3	166.7
100	0.7185	550	427.7	459.0	0.4	693.2	143.2	71.6	138.7	162.6
150	1.0778	550	410.2	466.0	0.5	682.9	132.9	66.4	128.3	150.4
200	1.4371	550	389.0	474.0	0.7	670.5	120.5	60.3	116.2	136.3
250	1.7964	550	374.2	479.5	0.9	661.8	111.8	55.9	107.8	126.4
300	2.1556	550	359.8	485.5	1.0	653.4	103.4	51.7	99.0	116.2
350	2.5149	550	355.4	487.0	1.0	650.6	100.6	50.3	96.5	113.3
400	2.8742	550	343.7	492.0	1.0	643.9	93.9	47.0	89.3	105.0
450	3.2335	550	338.5	493.5	1.0	640.8	90.8	45.4	86.8	101.9
550	3.9520	550	329.4	497.0	1.0	635.2	85.2	42.6	81.4	95.6
650	4.6705	550	325.2	498.5	1.0	632.3	82.3	41.2	78.9	92.7
850	6.1076	550	321.3	501.0	1.0	629.0	79.0	39.5	75.3	88.5

Strain Gauge (divs)	Axial Strain (%)	Cell Press. (kPa)	Proof Ring (divs)	Pore Pressure (kPa)	Membrane Correction (kPa)	P_1 (kPa)	q (kPa)	t (kPa)	p' (kPa)	s' (kPa)
1100	7.9040	550	318.7	503.0	1.0	626.1	76.1	38.1	72.4	85.1
1300	9.3411	550	319.5	503.5	1.0	625.3	75.3	37.7	71.6	84.2
1600	11.4967	550	320.1	505.0	1.0	623.8	73.8	36.9	69.6	81.9
1900	13.6524	550	321.1	505.5	1.0	622.5	72.5	36.2	68.7	80.7
2100	15.0895	550	321.0	506.0	1.0	621.2	71.2	35.6	67.7	79.6
2245	16.1314	550	322.1	506.5	1.0	620.8	70.8	35.4	67.1	78.9
2460	17.6762	550	323.7	507.0	1.0	620.3	70.3	35.1	66.4	78.1
2685	19.2930	550	325.2	507.0	1.0	619.5	69.5	34.8	66.2	77.8
3200	22.9935	550	330.5	508.0	1.0	618.6	68.6	34.3	64.9	76.3
3400	24.4306	550	333.0	508.0	1.0	618.3	68.3	34.2	64.8	76.2







Test	**Case 2: Monotonic Undrained Compression of One-Dimensionally Consolidated Specimens**		
Cell No.	3 (Big)	Fines content (%)	20
Specimen	K0-26	Specific gravity (g/cm^3)	2.72

1.) Sample physical properties

Wet mass before test (g)	882.010	m.c before test (%)	9.34	Height (mm)	151.15	Volume (cm^3)	699.286
Wet mass after test (g)	1024.467	m.c. after test (%)	27.00	Diameter (mm)	76.75		
Dry mass (g)	806.667	Dry density (kg/m^3)	1154	Area (cm^2)	46.264	Void ratio (e_0)	1.358

2.) Saturation / Consolidation

Proof ring properties		Strain gauge properties		Loading ram properties	
Proof ring No.	5153	1 strain division (mm)	0.01	Area [ram]$_1$ (cm^2)	7.905
Proof ring factor (dN/div)	7.512			Area [ram]$_2$ (cm^2)	5.004

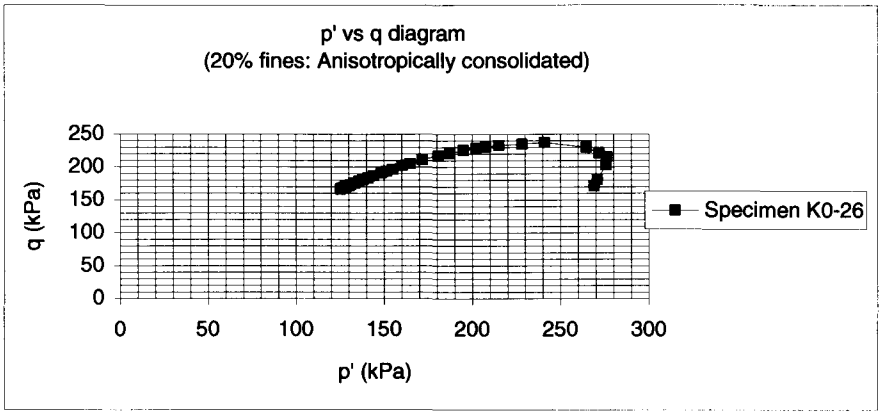
Date	Strain Gauge (divs)	Change Length (mm)	Cell Pressure (kPa)	Proof Ring (div)	Pore Pressure (kPa)	P_1 (kPa)	P'_3 (kPa)	P'_1 (kPa)	q (kPa)	p' (kPa)	K0	Volume Gauge (cm^3)	Cell Expansn (cm^3)
27/7	0	0.000	0	0.0	0.0						\	0.00	0.00
27/7	0	0.000	10.2		6.5	A I R - F L U S H I N G					\	8.76	0.00
27/7	201	2.010	50	121.1	40.0	61.1	10	21.1	11.1	13.7	0.47	31.95	6.08
28/7	394	3.940	100	151.2	90.0	107.5	10	17.5	7.5	12.5	0.57	47.89	8.77
29/7	536	5.360	150	190.6	140.0	155.3	10	15.3	5.3	11.8	0.65	58.48	10.65
30/7	659	6.590	200	251.0	190.0	206.6	10	16.6	6.6	12.2	0.60	64.12	12.00
31/7	778	7.780	250	310.8	240.0	257.7	10	17.7	7.7	12.6	0.56	69.01	13.63
1/8	891	8.910	300	358.9	290.0	307.0	10	17.0	7.0	12.3	0.59	72.79	15.06
2/8	1002	10.020	350	410.2	340.0	356.8	10	16.8	6.8	12.3	0.60	75.89	16.08
3/8	1100	11.000	400	456.6	390.0	405.8	10	15.8	5.8	11.9	0.63	79.96	18.12
4/8	1199	11.990	450	523.4	440.0	458.1	10	18.1	8.1	12.7	0.55	84.71	19.91
5/8	1300	13.000	500	610.7	480.0	513.7	20	33.7	13.7	24.6	0.59	88.23	21.79
6/8	1599	15.990	700	1791.5	488.0	871.3	212	383.3	171.3	269.1	0.55	113.03	24.78

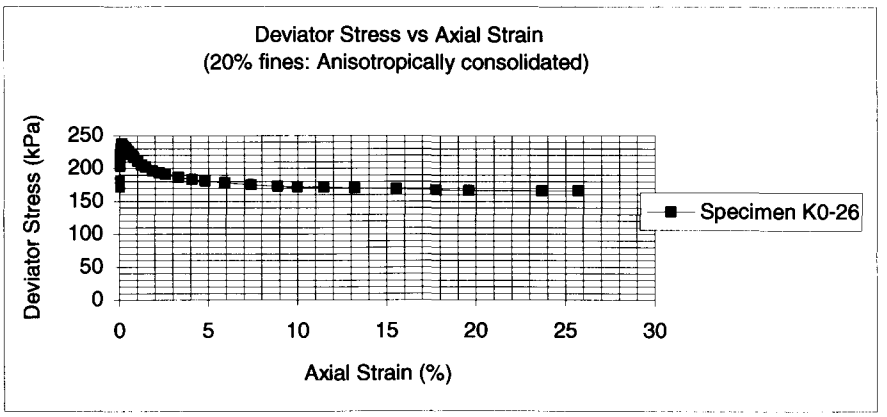
3.) Shear data

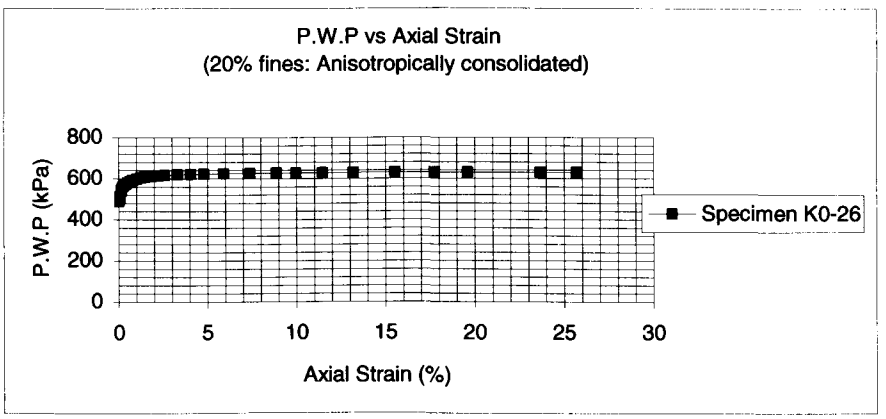
Volume change 1:		Volume change 2:		Sample Vol. change (cm^3)	96.25	B value	0.98
Air Flushing (cm^3)	8.76	Sat/Cons. (cm^3)	104.27	L_{cons} (mm)	135.16	K0	0.55
Cell Expsn. (cm^3)	0.00	Cell Expsn. (cm^3)	24.78	A_{cons} (cm^2)	46.264	Void ratio (e_1)	1.033
		Ram into cell (cm^3)	8.00				

Strain Gauge (divs)	Axial Strain (%)	Cell Press. (kPa)	Proof Ring (divs)	Pore Pressure (kPa)	Membrane Correction (kPa)	P_1 (kPa)	q (kPa)	t (kPa)	p' (kPa)	s' (kPa)
0	0.0000	700	1791.5	488.0	0.0	871.3	171.3	85.6	269.1	297.6
1	0.0074	700	1851.6	489.5	0.0	881.0	181.0	90.5	270.8	301.0
4	0.0296	700	1989.3	492.0	0.0	903.3	203.3	101.7	275.8	309.7
6	0.0444	700	2065.4	495.5	0.0	915.6	215.6	107.8	276.4	312.3
9	0.0666	700	2100.1	502.0	0.0	921.2	221.2	110.6	271.7	308.6
13	0.0962	700	2154.3	512.0	0.0	929.9	229.9	115.0	264.6	303.0
19	0.1406	700	2200.5	538.0	0.1	937.3	237.3	118.6	241.1	280.6
25	0.1850	700	2185.9	550.0	0.1	934.8	234.8	117.4	228.3	267.4
35	0.2590	700	2176.7	562.5	0.1	933.1	233.1	116.5	215.2	254.0
45	0.3329	700	2160.4	569.0	0.2	930.2	230.2	115.1	207.7	246.1
55	0.4069	700	2151.6	574.0	0.2	928.6	228.6	114.3	202.2	240.3
70	0.5179	700	2133.6	580.0	0.3	925.4	225.4	112.7	195.1	232.7
90	0.6659	700	2110.1	586.5	0.3	921.2	221.2	110.6	187.2	224.1
110	0.8139	700	2085.3	591.5	0.4	916.8	216.8	108.4	180.8	216.9
140	1.0358	700	2052.2	598.5	0.5	910.9	210.9	105.4	171.8	206.9
170	1.2578	700	2020.8	603.5	0.6	905.3	205.3	102.6	164.9	199.1
200	1.4797	700	2003.9	607.0	0.7	902.0	202.0	101.0	160.3	194.0
250	1.8497	700	1975.1	610.5	0.9	896.5	196.5	98.2	155.0	187.7
300	2.2196	700	1961.7	613.0	1.0	893.5	193.5	96.8	151.5	183.8
350	2.5895	700	1949.6	615.0	1.0	890.9	190.9	95.4	148.6	180.4
450	3.3294	700	1930.2	618.0	1.0	886.4	186.4	93.2	144.1	175.2
550	4.0693	700	1920.0	620.0	1.0	883.3	183.3	91.7	141.1	171.7
650	4.8091	700	1912.6	622.0	1.0	880.8	180.8	90.4	138.3	168.4
800	5.9189	700	1908.7	623.5	1.0	878.0	178.0	89.0	135.8	165.5

Strain Gauge (divs)	Axial Strain (%)	Cell Press. (kPa)	Proof Ring (divs)	Pore Pressure (kPa)	Membrane Correction (kPa)	P_1 (kPa)	q (kPa)	t (kPa)	p' (kPa)	s' (kPa)
1000	7.3986	700	1910.0	625.0	1.0	875.4	175.4	87.7	133.5	162.7
1200	8.8784	700	1912.4	626.5	1.0	873.0	173.0	86.5	131.2	160.0
1350	9.9882	700	1919.8	627.0	1.0	871.9	171.9	86.0	130.3	159.0
1550	11.4679	700	1937.5	627.5	1.0	871.6	171.6	85.8	129.7	158.3
1785	13.2066	700	1950.0	628.0	1.0	870.0	170.0	85.0	128.7	157.0
2100	15.5371	700	1976.3	629.0	1.0	869.0	169.0	84.5	127.3	155.5
2400	17.7567	700	2000.0	629.5	1.0	867.7	167.7	83.9	126.4	154.4
2650	19.6064	700	2020.1	630.0	1.0	866.5	166.5	83.3	125.5	153.3
3200	23.6756	700	2085.0	630.0	1.0	866.1	166.1	83.1	125.4	153.1
3475	25.7103	700	2123.0	630.0	1.0	866.2	166.2	83.1	125.4	153.1







Test	**Case 2: Monotonic Undrained Compression of One-Dimensionally Consolidated Specimens**		
Cell No.	2 (Big)	Fines content (%)	20
Specimen	K0-33	Specific gravity (g/cm^3)	2.72

1.) Sample physical properties

Wet mass before test (g)	870.689	m.c before test (%)	10.21	Height (mm)	151.95	Volume (cm^3)	703.903
Wet mass after test (g)	992.195	m.c. after test (%)	25.59	Diameter (mm)	76.80		
Dry mass (g)	790.027	Dry density (kg/m^3)	1122	Area (cm^2)	46.325	Void ratio (e_0)	1.423

2.) Saturation / Consolidation

Proof ring properties		Strain gauge properties		Loading ram properties	
Proof ring No.	4541	1 strain division (mm)	0.01	Area [ram]$_1$ (cm^2)	7.905
Proof ring factor (dN/div)	25.77			Area [ram]$_2$ (cm^2)	5.004

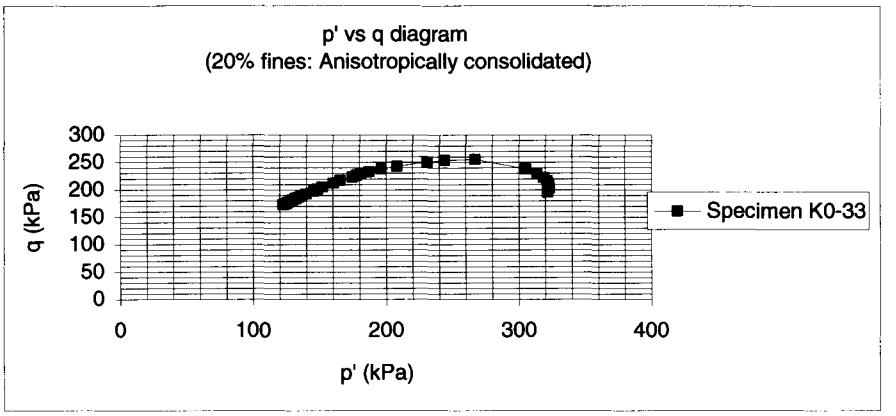
Date	Strain Gauge (divs)	Change Length (mm)	Cell Pressure (kPa)	Proof Ring (div)	Pore Pressure (kPa)	P_1 (kPa)	P'_3 (kPa)	P'_1 (kPa)	q (kPa)	p' (kPa)	K0	Volume Gauge (cm^3)	Cell Expansn (cm^3)
15/9	0	0.000	0	0.0	0.0						\	0.00	0.00
15/9	0	0.000	12.0		8.0	A I R - F L U S H I N G					\	9.30	0.00
15/9	205	2.050	50	35.3	40.0	61.1	10	21.1	11.1	13.7	0.47	32.02	7.06
16/9	384	3.840	100	45.0	90.0	108.0	10	18.0	8.0	12.7	0.56	44.87	9.79
17/9	525	5.250	150	58.9	140.0	157.2	10	17.2	7.2	12.4	0.58	55.21	11.63
18/9	653	6.530	200	73.5	190.0	206.8	10	16.8	6.8	12.3	0.60	62.58	13.02
19/9	749	7.490	250	91.1	240.0	258.0	10	18.0	8.0	12.7	0.55	69.74	14.57
20/9	842	8.420	300	104.9	290.0	307.2	10	17.2	7.2	12.4	0.58	74.38	16.03
21/9	930	9.300	350	117.6	340.0	355.7	10	15.7	5.7	11.9	0.64	78.45	17.22
22/9	1024	10.240	400	135.8	390.0	407.3	10	17.3	7.3	12.4	0.58	84.19	19.30
23/9	1118	11.180	450	152.4	440.0	458.0	10	18.0	8.0	12.7	0.56	88.23	20.93
24/9	1549	15.490	850	611.0	593.0	1044.8	257	451.8	194.8	321.9	0.57	127.25	27.13

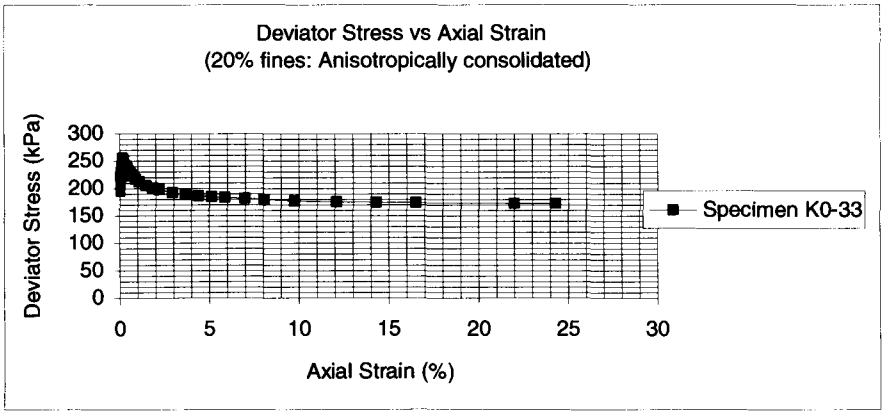
3.) Shear data

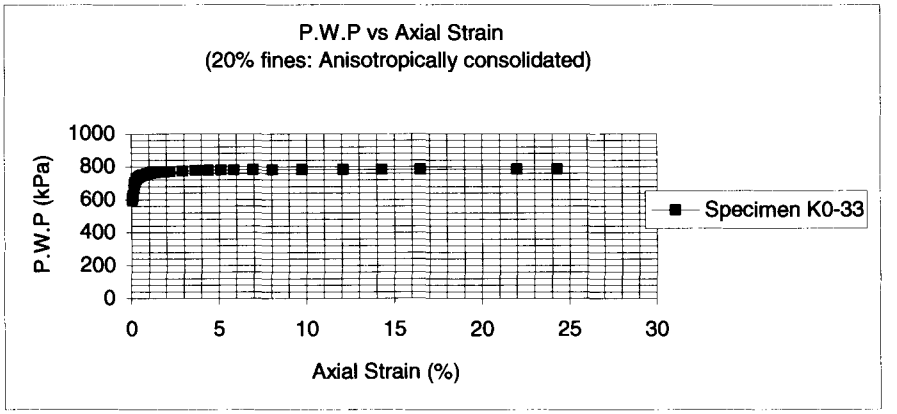
Volume change 1:		Volume change 2:		Sample Vol. change (cm^3)	107.87	B value	0.97
Air Flushing (cm^3)	9.30	Sat/Cons. (cm^3)	117.95	L_{cons} (mm)	136.46	K0	0.57
Cell Expsn. (cm^3)	0.00	Cell Expsn. (cm^3)	27.13	A_{cons} (cm^2)	46.325	Void ratio (e_1)	1.052
		Ram into cell (cm^3)	7.75				

Strain Gauge (divs)	Axial Strain (%)	Cell Press. (kPa)	Proof Ring (divs)	Pore Pressure (kPa)	Membrane Correction (kPa)	P_1 (kPa)	q (kPa)	t (kPa)	p' (kPa)	s' (kPa)
0	0.0000	850	611.0	593.0	0.0	1044.8	194.8	97.4	321.9	354.4
1	0.0081	850	625.3	594.5	0.0	1052.8	202.8	101.4	323.1	356.9
3	0.0198	850	637.5	597.0	0.0	1059.5	209.5	104.8	322.8	357.8
5	0.0366	850	649.6	600.5	0.0	1066.2	216.2	108.1	321.6	357.6
9	0.0660	850	660.4	605.0	0.0	1072.2	222.2	111.1	319.1	356.1
12	0.0879	850	673.1	612.5	0.0	1079.1	229.1	114.6	313.9	352.1
16	0.1173	850	689.3	624.0	0.1	1088.1	238.1	119.0	305.4	345.0
22	0.1612	850	720.9	668.0	0.1	1105.5	255.5	127.7	267.2	309.7
25	0.1832	850	718.0	690.5	0.1	1103.8	253.8	126.9	244.1	286.4
30	0.2198	850	712.3	702.5	0.1	1100.5	250.5	125.3	231.0	272.8
40	0.2931	850	698.6	722.5	0.1	1092.7	242.7	121.4	208.4	248.9
55	0.4030	850	690.3	732.5	0.2	1087.8	237.8	118.9	196.8	236.4
65	0.4763	850	681.0	740.0	0.2	1082.4	232.4	116.2	187.5	226.2
75	0.5496	850	675.2	745.0	0.3	1079.0	229.0	114.5	181.3	219.5
85	0.6229	850	670.8	747.5	0.3	1076.4	226.4	113.2	178.0	215.7
95	0.6962	850	665.2	749.5	0.3	1073.1	223.1	111.5	174.9	212.0
120	0.8794	850	655.3	756.5	0.4	1067.1	217.1	108.6	165.9	202.1
150	1.0992	850	647.1	760.0	0.5	1062.0	212.0	106.0	160.7	196.0
200	1.4656	850	635.8	766.0	0.7	1054.9	204.9	102.4	152.3	186.4
250	1.8320	850	630.6	768.5	0.9	1051.1	201.1	100.5	148.5	182.0
300	2.1984	850	625.1	770.0	1.0	1047.2	197.2	98.6	145.7	178.6
400	2.9313	850	618.5	774.0	1.0	1042.2	192.2	96.1	140.1	172.1
500	3.6641	850	614.7	776.5	1.0	1038.7	188.7	94.3	136.4	167.8
600	4.3969	850	613.0	777.5	1.0	1036.3	186.3	93.2	134.6	165.7

Strain Gauge (divs)	Axial Strain (%)	Cell Press. (kPa)	Proof Ring (divs)	Pore Pressure (kPa)	Membrane Correction (kPa)	P_1 (kPa)	q (kPa)	t (kPa)	p' (kPa)	s' (kPa)
700	5.1297	850	611.9	779.0	1.0	1034.3	184.3	92.2	132.4	163.2
800	5.8625	850	612.4	779.5	1.0	1033.2	183.2	91.6	131.6	162.1
950	6.9617	850	613.2	780.5	1.0	1031.4	181.4	90.7	130.0	160.2
1100	8.0610	850	613.9	781.5	1.0	1029.6	179.6	89.8	128.4	158.3
1330	9.7464	850	615.2	782.5	1.0	1027.0	177.0	88.5	126.5	156.0
1650	12.0915	850	621.4	783.0	1.0	1025.4	175.4	87.7	125.5	154.7
1950	14.2899	850	629.1	783.5	1.0	1024.6	174.6	87.3	124.7	153.8
2250	16.4883	850	636.9	784.0	1.0	1023.8	173.8	86.9	123.9	152.9
3000	21.9845	850	661.4	785.0	1.0	1022.9	172.9	86.4	122.6	151.4
3315	24.2928	850	673.6	785.0	1.0	1022.9	172.9	86.4	122.6	151.4







Test	**Case 2: Monotonic Undrained Compression of One-Dimensionally Consolidated Specimens**		
Cell No.	3 (Big)	Fines content (%)	20
Specimen	K0-34	Specific gravity (g/cm^3)	2.72

1.) Sample physical properties

Wet mass before test (g)	859.216	m.c before test (%)	10.00	Height (mm)	152.00	Volume (cm^3)	702.302
Wet mass after test (g)	1000.284	m.c. after test (%)	28.06	Diameter (mm)	76.70		
Dry mass (g)	781.105	Dry density (kg/m^3)	1112	Area (cm^2)	46.204	Void ratio (e_0)	1.446

2.) Saturation / Consolidation

Proof ring properties		Strain gauge properties		Loading ram properties	
Proof ring No.	5153	1 strain division (mm)	0.01	Area [ram]$_1$ (cm^2)	7.905
Proof ring factor (dN/div)	7.512			Area [ram]$_2$ (cm^2)	5.004

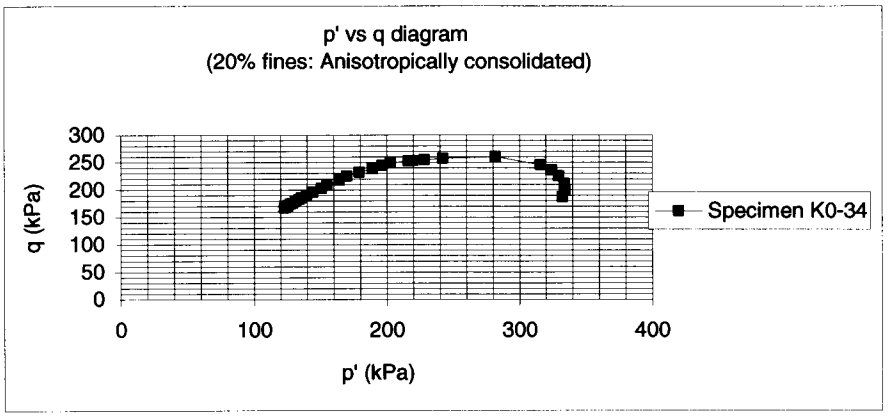
Date	Strain Gauge (divs)	Change Length (mm)	Cell Pressure (kPa)	Proof Ring (div)	Pore Pressure (kPa)	P_1 (kPa)	P'_3 (kPa)	P'_1 (kPa)	q (kPa)	p' (kPa)	K0	Volume Gauge (cm^3)	Cell Expansn (cm^3)
15/9	0	0.000	0	0.0	0.0						\	0.00	0.00
15/9	0	0.000	11.9		8.5	A I R - F L U S H I N G					\	9.55	0.00
15/9	211	2.110	50	125.5	40.0	61.8	10	21.8	11.8	13.9	0.46	36.21	6.08
16/9	400	4.000	100	156.4	90.0	108.3	10	18.3	8.3	12.8	0.55	49.05	8.77
17/9	545	5.450	150	198.9	140.0	156.7	10	16.7	6.7	12.2	0.60	60.18	10.65
18/9	653	6.530	200	254.1	190.0	207.1	10	17.1	7.1	12.4	0.58	65.87	12.00
19/9	748	7.480	250	302.5	240.0	256.4	10	16.4	6.4	12.1	0.61	72.24	13.63
20/9	836	8.360	300	366.2	290.0	308.2	10	18.2	8.2	12.7	0.55	78.13	15.06
21/9	928	9.280	350	420.3	340.0	358.5	10	18.5	8.5	12.8	0.54	82.22	16.08
22/9	1021	10.210	400	460.0	390.0	406.4	10	16.4	6.4	12.1	0.61	87.55	18.12
23/9	1123	11.230	450	511.1	440.0	456.1	10	16.1	6.1	12.0	0.62	92.34	19.91
24/9	1610	16.100	950	2150.0	680.0	1137.0	270	457.0	187.0	332.3	0.59	129.19	26.78

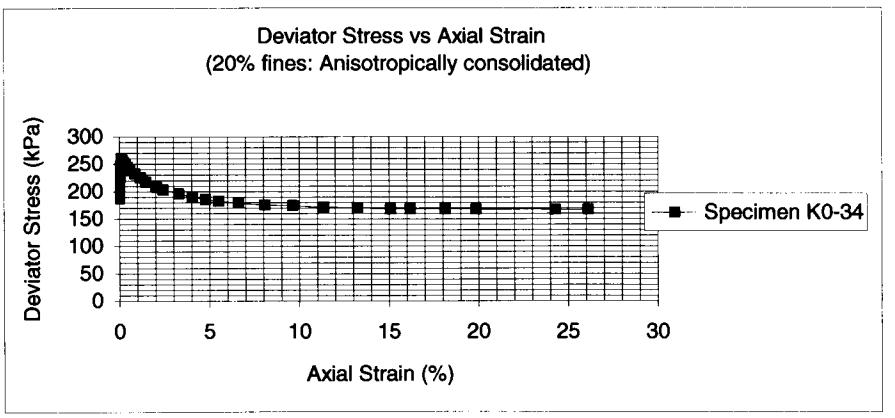
3.) Shear data

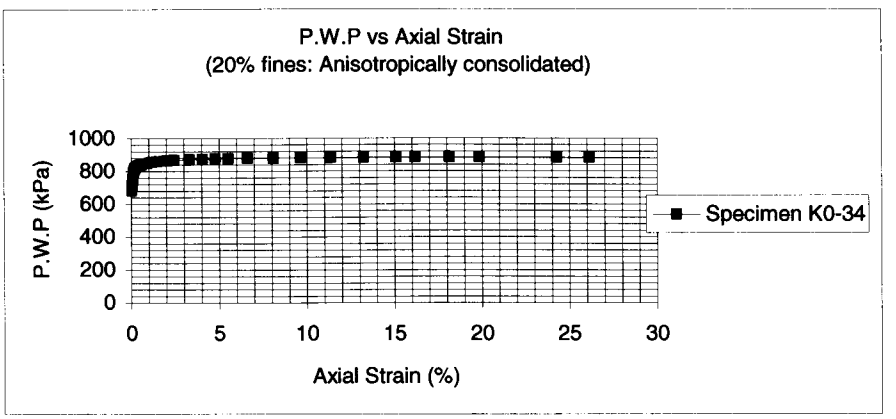
Volume change 1:		Volume change 2:		Sample Vol. change (cm^3)	110.47	B value	0.99
Air Flushing (cm^3)	9.55	Sat/Cons. (cm^3)	119.64	L_{cons} (mm)	135.90	K0	0.59
Cell Expsn. (cm^3)	0.00	Cell Expsn. (cm^3)	26.78	A_{cons} (cm^2)	46.204	Void ratio (e_1)	1.061
		Ram into cell (cm^3)	8.06				

Strain Gauge (divs)	Axial Strain (%)	Cell Press. (kPa)	Proof Ring (divs)	Pore Pressure (kPa)	Membrane Correction (kPa)	P_1 (kPa)	q (kPa)	t (kPa)	p' (kPa)	s' (kPa)
0	0.0000	950	2150.3	680.0	0.0	1137.1	187.1	93.5	332.4	363.5
2	0.0147	950	2222.6	682.0	0.0	1148.8	198.8	99.4	334.3	367.4
3	0.0221	950	2298.9	686.5	0.0	1161.2	211.2	105.6	333.9	369.1
6	0.0442	950	2385.4	695.5	0.0	1175.2	225.2	112.6	329.6	367.1
8	0.0589	950	2452.8	704.5	0.0	1186.1	236.1	118.0	324.2	363.5
10	0.0736	950	2510.5	716.0	0.0	1195.4	245.4	122.7	315.8	356.7
15	0.1104	950	2600.6	754.5	0.1	1209.9	259.9	130.0	282.1	325.5
21	0.1545	950	2585.1	793.5	0.1	1207.3	257.3	128.6	242.3	285.1
25	0.1840	950	2572.3	806.5	0.1	1205.1	255.1	127.6	228.5	271.1
29	0.2134	950	2560.8	814.5	0.1	1203.2	253.2	126.6	219.9	262.1
33	0.2428	950	2555.9	818.0	0.1	1202.3	252.3	126.1	216.1	258.1
45	0.3311	950	2533.7	830.0	0.2	1198.4	248.4	124.2	202.8	244.2
60	0.4415	950	2509.5	835.0	0.2	1194.2	244.2	122.1	196.4	237.1
80	0.5887	950	2478.1	840.5	0.3	1188.7	238.7	119.3	189.1	228.8
120	0.8830	950	2440.7	848.0	0.4	1181.8	231.8	115.9	179.3	217.9
160	1.1773	950	2402.5	855.0	0.6	1174.8	224.8	112.4	169.9	207.4
200	1.4717	950	2362.4	858.5	0.7	1167.6	217.6	108.8	164.0	200.3
280	2.0603	950	2314.0	864.5	1.0	1158.3	208.3	104.1	154.9	189.6
330	2.4283	950	2285.6	867.0	1.0	1153.0	203.0	101.5	150.7	184.5
450	3.3113	950	2251.0	871.0	1.0	1145.7	195.7	97.9	144.2	176.9
550	4.0471	950	2222.8	873.5	1.0	1139.8	189.8	94.9	139.8	171.4
650	4.7829	950	2201.5	876.0	1.0	1135.0	185.0	92.5	135.7	166.5
750	5.5188	950	2193.6	877.0	1.0	1132.4	182.4	91.2	133.8	164.2
900	6.6225	950	2184.9	878.5	1.0	1128.9	178.9	89.5	131.1	161.0

Strain Gauge (divs)	Axial Strain (%)	Cell Press. (kPa)	Proof Ring (divs)	Pore Pressure (kPa)	Membrane Correction (kPa)	P_1 (kPa)	q (kPa)	t (kPa)	p' (kPa)	s' (kPa)
1100	8.0942	950	2178.6	879.5	1.0	1125.2	175.2	87.6	128.9	158.1
1310	9.6394	950	2190.0	880.5	1.0	1123.9	173.9	86.9	127.5	156.4
1545	11.3687	950	2194.6	881.5	1.0	1121.2	171.2	85.6	125.6	154.1
1800	13.2450	950	2210.0	882.0	1.0	1119.7	169.7	84.9	124.6	152.9
2050	15.0846	950	2222.0	882.5	1.0	1117.8	167.8	83.9	123.4	151.4
2200	16.1884	950	2241.3	882.5	1.0	1118.2	168.2	84.1	123.6	151.6
2465	18.1383	950	2268.9	882.5	1.0	1117.9	167.9	84.0	123.5	151.5
2700	19.8675	950	2293.1	882.5	1.0	1117.5	167.5	83.8	123.3	151.3
3300	24.2826	950	2366.5	883.0	1.0	1117.3	167.3	83.6	122.8	150.6
3550	26.1221	950	2400.0	883.0	1.0	1117.2	167.2	83.6	122.7	150.6







Test	**Case 2: Monotonic Undrained Compression of One-Dimensionally Consolidated Specimens**		
Cell No.	3 (Big)	Fines content (%)	30
Specimen	K0-5	Specific gravity (g/cm^3)	2.72

1.) Sample physical properties

Wet mass before test (g)	861.429	m.c before test (%)	9.87	Height (mm)	152.05	Volume (cm^3)	702.533
Wet mass after test (g)	988.209	m.c. after test (%)	26.04	Diameter (mm)	76.70		
Dry mass (g)	784.044	Dry density (kg/m^3)	1116	Area (cm^2)	46.204	Void ratio (e_0)	1.437

2.) Saturation / Consolidation

Proof ring properties		Strain gauge properties		Loading ram properties	
Proof ring No.	5153	1 strain division (mm)	0.01	Area [ram]$_1$ (cm^2)	7.905
Proof ring factor (dN/div)	7.512			Area [ram]$_2$ (cm^2)	5.004

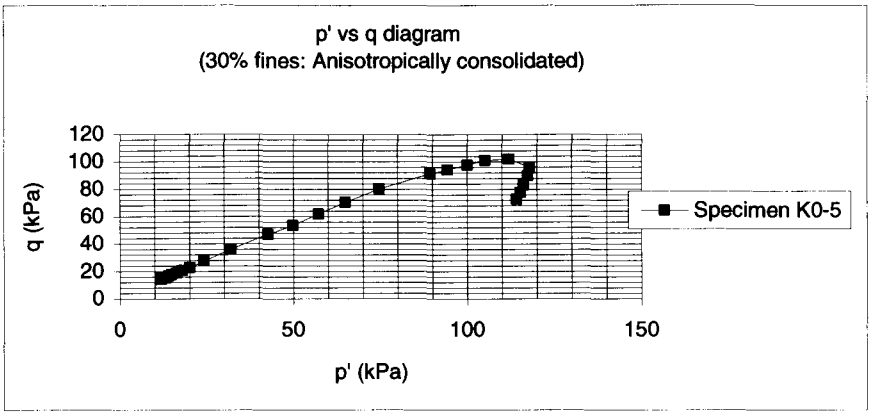
Date	Strain Gauge (divs)	Change Length (mm)	Cell Pressure (kPa)	Proof Ring (div)	Pore Pressure (kPa)	P_1 (kPa)	P'_3 (kPa)	P'_1 (kPa)	q (kPa)	p' (kPa)	K0	Volume Gauge (cm^3)	Cell Expansn (cm^3)
26/3	0	0.000	0	0.0	0.0						\	0.00	0.00
26/3	0	0.000	11.0		7.5	A I R - F L U S H I N G					\	9.12	0.00
26/3	201	2.010	50	118.7	40.0	60.7	10	20.7	10.7	13.6	0.48	42.57	6.08
27/3	390	3.900	100	156.5	90.0	108.3	10	18.3	8.3	12.8	0.55	67.23	8.77
28/3	575	5.750	150	205.8	140.0	157.8	10	17.8	7.8	12.6	0.56	83.97	10.65
29/3	738	7.380	200	263.3	190.0	208.6	10	18.6	8.6	12.9	0.54	95.62	12.00
30/3	886	8.860	250	306.7	240.0	257.1	10	17.1	7.1	12.4	0.59	105.22	13.63
31/3	1013	10.130	300	356.9	290.0	306.7	10	16.7	6.7	12.2	0.60	114.38	15.06
1/4	1138	11.380	350	414.5	340.0	357.5	10	17.5	7.5	12.5	0.57	123.99	16.08
2/4	1302	13.020	400	632.1	350.0	434.3	50	84.3	34.3	61.4	0.59	135.05	18.12
3/4	1472	14.720	450	920.1	360.0	522.6	90	162.6	72.6	114.2	0.55	146.50	19.91

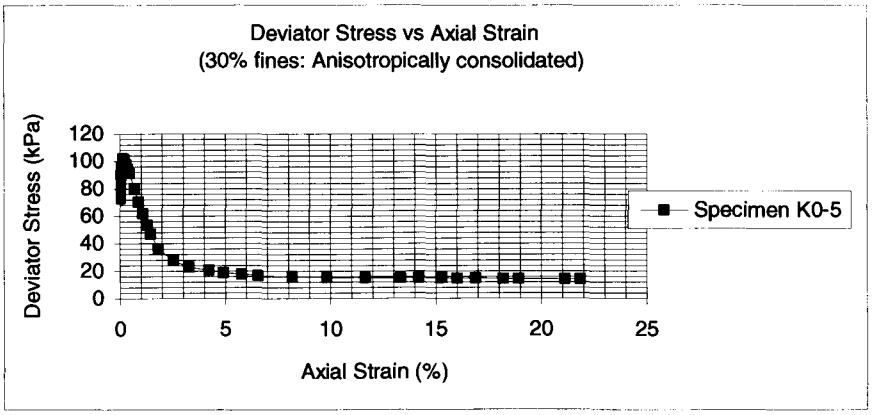
3.) Shear data

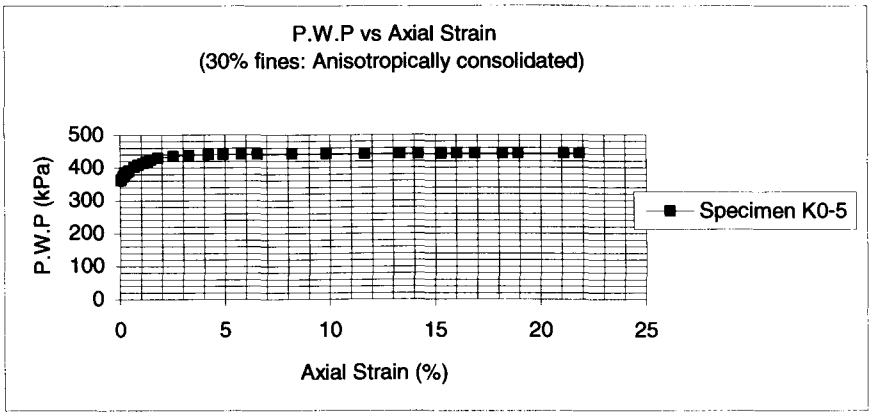
Volume change 1:		Volume change 2:		Sample Vol. change (cm^3)	133.96	B value	0.98
Air Flushing (cm^3)	9.12	Sat/Cons. (cm^3)	137.38	L_{cons} (mm)	137.33	K0	0.55
Cell Expsn. (cm^3)	0.00	Cell Expsn. (cm^3)	19.91	A_{cons} (cm^2)	46.204	Void ratio (e_1)	0.973
		Ram into cell (cm^3)	7.37				

Strain Gauge (divs)	Axial Strain (%)	Cell Press. (kPa)	Proof Ring (divs)	Pore Pressure (kPa)	Membrane Correction (kPa)	P_1 (kPa)	q (kPa)	t (kPa)	p' (kPa)	s' (kPa)
0	0.0000	450	920.1	360.0	0.0	522.6	72.6	36.3	114.2	126.3
3	0.0218	450	950.3	360.5	0.0	527.5	77.5	38.7	115.3	128.2
5	0.0364	450	984.5	361.5	0.0	533.0	83.0	41.5	116.2	130.0
6	0.0437	450	1026.4	362.5	0.0	539.8	89.8	44.9	117.4	132.4
10	0.0728	450	1065.0	364.0	0.0	546.1	96.1	48.0	118.0	134.0
20	0.1456	450	1102.1	372.0	0.1	552.0	102.0	51.0	112.0	129.0
30	0.2185	450	1096.7	378.5	0.1	551.0	101.0	50.5	105.2	122.0
40	0.2913	450	1077.6	382.5	0.1	547.8	97.8	48.9	100.1	116.4
50	0.3641	450	1056.4	387.0	0.2	544.2	94.2	47.1	94.4	110.1
60	0.4369	450	1038.3	391.0	0.2	541.2	91.2	45.6	89.4	104.6
95	0.6918	450	972.8	402.0	0.3	530.3	80.3	40.1	74.8	88.1
120	0.8738	450	912.4	408.5	0.4	520.3	70.3	35.1	64.9	76.6
150	1.0923	450	862.3	413.5	0.5	512.0	62.0	31.0	57.2	67.5
180	1.3107	450	810.0	418.0	0.7	503.3	53.3	26.7	49.8	58.7
200	1.4563	450	771.2	423.0	0.7	497.0	47.0	23.5	42.7	50.5
250	1.8204	450	705.1	430.0	0.9	486.1	36.1	18.0	32.0	38.0
350	2.5486	450	653.5	435.0	1.0	477.5	27.5	13.8	24.2	28.8
450	3.2768	450	625.0	437.5	1.0	472.8	22.8	11.4	20.1	23.9
580	4.2234	450	612.6	439.0	1.0	470.7	20.7	10.3	17.9	21.3
675	4.9152	450	601.8	440.0	1.0	468.8	18.8	9.4	16.3	19.4
795	5.7890	450	594.2	441.0	1.0	467.5	17.5	8.7	14.8	17.7
900	6.5536	450	589.9	441.5	1.0	466.7	16.7	8.3	14.1	16.8
1125	8.1919	450	585.7	442.0	1.0	465.7	15.7	7.9	13.2	15.9
1350	9.8303	450	585.0	442.0	1.0	465.3	15.3	7.7	13.1	15.7

Strain Gauge (divs)	Axial Strain (%)	Cell Press. (kPa)	Proof Ring (divs)	Pore Pressure (kPa)	Membrane Correction (kPa)	P_1 (kPa)	q (kPa)	t (kPa)	p' (kPa)	s' (kPa)
1600	11.6508	450	585.0	442.0	1.0	465.0	15.0	7.5	13.0	15.5
1830	13.3256	450	587.4	442.5	1.0	465.0	15.0	7.5	12.5	15.0
1950	14.1994	450	589.0	442.5	1.0	465.1	15.1	7.6	12.5	15.1
2100	15.2916	450	589.1	442.5	1.0	464.9	14.9	7.5	12.5	15.0
2200	16.0198	450	587.9	443.0	1.0	464.6	14.6	7.3	11.9	14.3
2320	16.8936	450	589.5	443.0	1.0	464.7	14.7	7.3	11.9	14.3
2500	18.2043	450	588.3	443.0	1.0	464.3	14.3	7.1	11.8	14.1
2600	18.9325	450	589.0	443.0	1.0	464.2	14.2	7.1	11.7	14.1
2900	21.1170	450	591.2	443.0	1.0	464.1	14.1	7.0	11.7	14.0
3000	21.8452	450	591.2	443.0	1.0	464.0	14.0	7.0	11.7	14.0







Test	**Case 2: Monotonic Undrained Compression of One-Dimensionally Consolidated Specimens**		
Cell No.	2 (Big)	Fines content (%)	30
Specimen	K0-6	Specific gravity (g/cm^3)	2.72

1.) Sample physical properties

Wet mass before test (g)	864.622	m.c before test (%)	10.05	Height (mm)	151.15	Volume (cm^3)	698.375
Wet mass after test (g)	975.558	m.c. after test (%)	24.17	Diameter (mm)	76.70		
Dry mass (g)	785.663	Dry density (kg/m^3)	1125	Area (cm^2)	46.204	Void ratio (e_0)	1.418

2.) Saturation / Consolidation

Proof ring properties		Strain gauge properties		Loading ram properties	
Proof ring No.	4145	1 strain division (mm)	0.01	Area [ram]$_1$ (cm^2)	7.905
Proof ring factor (dN/div)	25.77			Area [ram]$_2$ (cm^2)	5.004

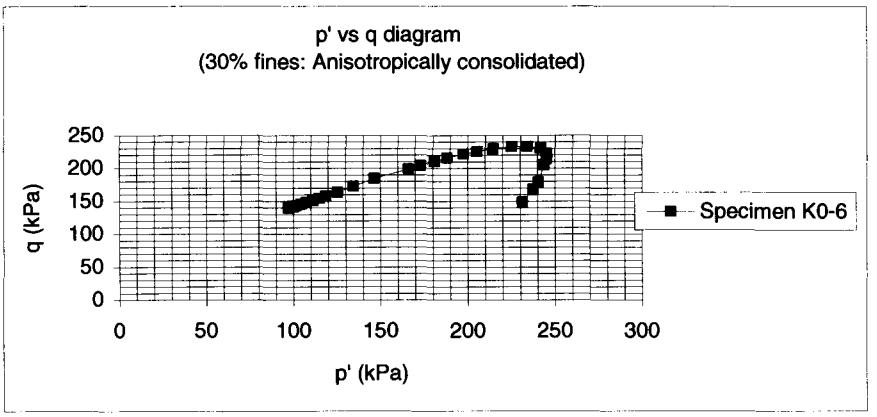
Date	Strain Gauge (divs)	Change Length (mm)	Cell Pressure (kPa)	Proof Ring (div)	Pore Pressure (kPa)	P_1 (kPa)	P'_3 (kPa)	P'_1 (kPa)	q (kPa)	p' (kPa)	K0	Volume Gauge (cm^3)	Cell Expansn (cm^3)
26/3	0	0.000	0	0.0	0.0						\	0.00	0.00
26/3	0	0.000	8.5		4.0	A I R - F L U S H I N G					\	8.33	0.00
26/3	206	2.060	50	50.1	40.0	69.4	10	29.4	19.4	16.5	0.34	40.13	7.06
27/3	399	3.990	100	56.3	90.0	114.3	10	24.3	14.3	14.8	0.41	62.00	9.79
28/3	557	5.570	150	60.8	140.0	158.2	10	18.2	8.2	12.7	0.55	78.32	11.63
29/3	690	6.900	200	74.6	190.0	207.4	10	17.4	7.4	12.5	0.58	91.19	13.02
30/3	852	8.520	250	88.2	240.0	256.4	10	16.4	6.4	12.1	0.61	99.51	14.57
31/3	988	9.880	300	105.0	290.0	307.2	10	17.2	7.2	12.4	0.58	107.10	16.03
1/4	1113	11.130	350	121.4	340.0	357.8	10	17.8	7.8	12.6	0.56	113.22	17.22
2/4	1220	12.200	400	135.5	390.0	407.1	10	17.1	7.1	12.4	0.58	120.01	19.30
3/4	1548	15.480	600	450.0	418.0	748.3	182	330.3	148.3	231.4	0.55	147.02	23.74

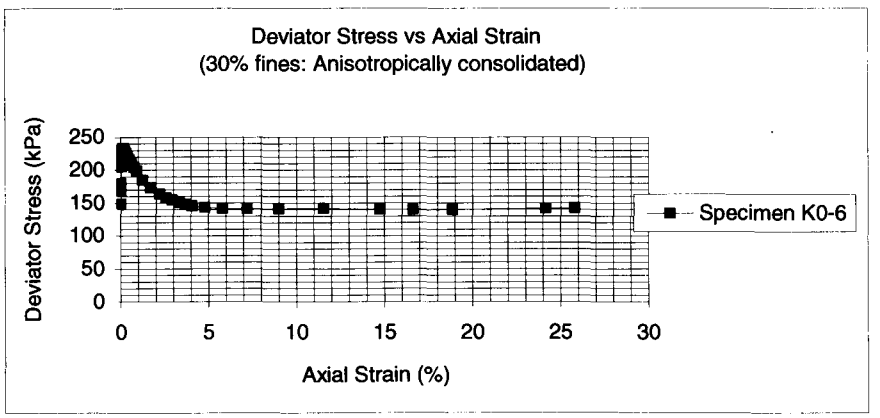
3.) Shear data

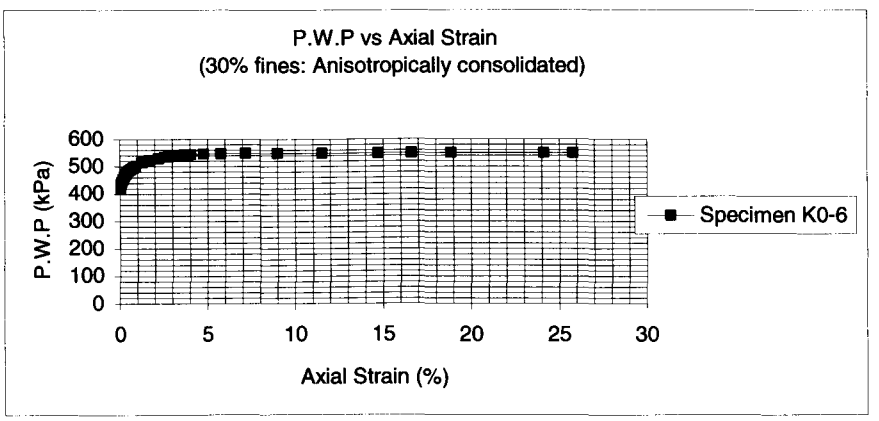
Volume change 1:		Volume change 2:		Sample Vol. change (cm^3)	131.03	B value	0.99
Air Flushing (cm^3)	8.33	Sat/Cons. (cm^3)	138.69	L_{cons} (mm)	135.67	K0	0.55
Cell Expsn. (cm^3)	0.00	Cell Expsn. (cm^3)	23.74	A_{cons} (cm^2)	46.204	Void ratio (e_1)	0.964
		Ram into cell (cm^3)	7.75				

Strain Gauge (divs)	Axial Strain (%)	Cell Press. (kPa)	Proof Ring (divs)	Pore Pressure (kPa)	Membrane Correction (kPa)	P_1 (kPa)	q (kPa)	t (kPa)	p' (kPa)	s' (kPa)
0	0.0000	600	450.0	418.0	0.0	748.3	148.3	74.2	231.4	256.2
2	0.0147	600	485.2	418.5	0.0	767.9	167.9	84.0	237.5	265.5
3	0.0221	600	505.1	419.0	0.0	779.0	179.0	89.5	240.7	270.5
4	0.0295	600	552.3	424.5	0.0	805.3	205.3	102.7	243.9	278.2
5	0.0369	600	567.6	426.0	0.0	813.8	213.8	106.9	245.3	280.9
6	0.0442	600	582.4	428.5	0.0	822.1	222.1	111.0	245.5	282.5
11	0.0811	600	597.3	435.0	0.0	830.3	230.3	115.1	241.8	280.1
17	0.1253	600	602.5	443.5	0.1	833.0	233.0	116.5	234.2	273.0
25	0.1843	600	602.6	452.5	0.1	832.9	232.9	116.5	225.1	264.0
35	0.2580	600	597.0	462.0	0.1	829.6	229.6	114.8	214.5	252.8
45	0.3317	600	590.5	470.0	0.2	825.8	225.8	112.9	205.3	242.9
55	0.4054	600	583.2	476.0	0.2	821.5	221.5	110.8	197.8	234.8
70	0.5160	600	573.1	483.5	0.3	815.6	215.6	107.8	188.4	224.3
85	0.6265	600	564.6	489.0	0.3	810.6	210.6	105.3	181.2	216.3
105	0.7739	600	553.4	495.0	0.4	804.0	204.0	102.0	173.0	207.0
125	0.9214	600	544.1	500.0	0.5	798.5	198.5	99.3	166.2	199.3
170	1.2530	600	520.0	515.0	0.6	784.4	184.4	92.2	146.5	177.2
230	1.6953	600	500.5	523.0	0.8	772.7	172.7	86.3	134.6	163.3
300	2.2112	600	485.7	529.0	1.0	763.5	163.5	81.8	125.5	152.8
350	2.5798	600	476.4	534.0	1.0	757.9	157.9	78.9	118.6	144.9
400	2.9483	600	470.8	536.5	1.0	754.2	154.2	77.1	114.9	140.6
450	3.3169	600	465.6	539.0	1.0	750.8	150.8	75.4	111.3	136.4
500	3.6854	600	461.3	542.0	1.0	747.9	147.9	74.0	107.3	132.0
550	4.0540	600	458.0	544.0	1.0	745.6	145.6	72.8	104.5	128.8

Strain Gauge (divs)	Axial Strain (%)	Cell Press. (kPa)	Proof Ring (divs)	Pore Pressure (kPa)	Membrane Correction (kPa)	P_1 (kPa)	q (kPa)	t (kPa)	p' (kPa)	s' (kPa)
650	4.7910	600	455.2	546.0	1.0	743.0	143.0	71.5	101.7	125.5
785	5.7861	600	455.8	547.0	1.0	741.8	141.8	70.9	100.3	123.9
975	7.1866	600	458.4	548.5	1.0	741.0	141.0	70.5	98.5	122.0
1220	8.9924	600	464.1	548.5	1.0	741.2	141.2	70.6	98.6	122.1
1565	11.5353	600	472.9	549.0	1.0	741.5	141.5	70.8	98.2	121.8
2000	14.7417	600	480.5	549.0	1.0	740.0	140.0	70.0	97.7	121.0
2255	16.6212	600	487.0	549.5	1.0	739.9	139.9	69.9	97.1	120.4
2560	18.8693	600	495.4	549.5	1.0	739.9	139.9	69.9	97.1	120.4
3275	24.1395	600	520.6	550.0	1.0	741.4	141.4	70.7	97.1	120.7
3500	25.7979	600	530.3	550.0	1.0	742.3	142.3	71.1	97.4	121.1







Test	**Case 2: Monotonic Undrained Compression of One-Dimensionally Consolidated Specimens**		
Cell No.	3 (Big)	Fines content (%)	30
Specimen	K0-12	Specific gravity (g/cm^3)	2.72

1.) Sample physical properties

Wet mass before test (g)	872.904	m.c before test (%)	8.96	Height (mm)	150.55	Volume (cm^3)	696.510
Wet mass after test (g)	1018.548	m.c. after test (%)	27.14	Diameter (mm)	76.75		
Dry mass (g)	801.123	Dry density (kg/m^3)	1150	Area (cm^2)	46.264	Void ratio (e_0)	1.365

2.) Saturation / Consolidation

Proof ring properties		Strain gauge properties		Loading ram properties	
Proof ring No.	5153	1 strain division (mm)	0.01	Area [ram]$_1$ (cm^2)	7.905
Proof ring factor (dN/div)	7.512			Area [ram]$_2$ (cm^2)	5.004

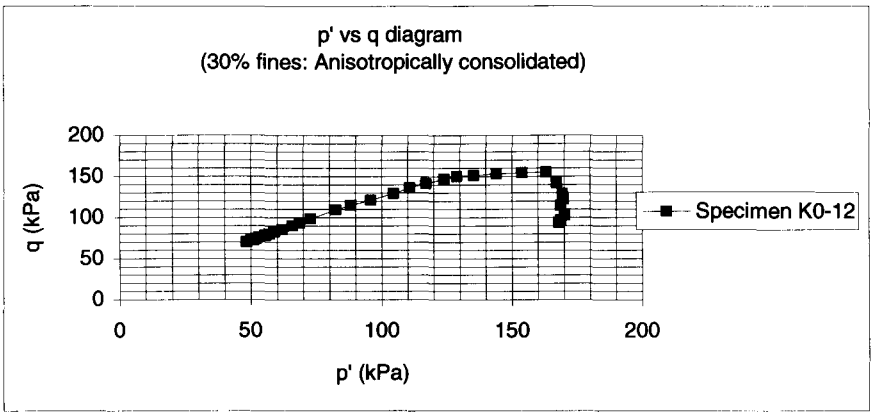
Date	Strain Gauge (divs)	Change Length (mm)	Cell Pressure (kPa)	Proof Ring (div)	Pore Pressure (kPa)	P_1 (kPa)	P'_3 (kPa)	P'_1 (kPa)	q (kPa)	p' (kPa)	K0	Volume Gauge (cm^3)	Cell Expansn (cm^3)
1/5	0	0.000	0	0.0	0.0						\	0.00	0.00
1/5	0	0.000	10.5		6.0	A I R - F L U S H I N G					\	7.89	0.00
1/5	222	2.220	50	115.8	40.0	60.3	10	20.3	10.3	13.4	0.49	38.00	6.08
2/5	421	4.210	100	152.5	90.0	107.7	10	17.7	7.7	12.6	0.57	60.94	8.77
3/5	605	6.050	150	200.2	140.0	156.9	10	16.9	6.9	12.3	0.59	74.85	10.65
4/5	786	7.860	200	251.3	190.0	206.6	10	16.6	6.6	12.2	0.60	86.53	12.00
5/5	923	9.230	250	304.9	240.0	256.8	10	16.8	6.8	12.3	0.60	95.28	13.63
6/5	1050	10.500	300	358.8	290.0	307.0	10	17.0	7.0	12.3	0.59	103.21	15.06
7/5	1168	11.680	350	415.0	340.0	357.6	10	17.6	7.6	12.5	0.57	110.15	16.08
8/5	1300	13.000	400	600.5	350.0	429.2	50	79.2	29.2	59.7	0.63	120.17	18.12
9/5	1622	16.220	500	1100.0	363.0	593.2	137	230.2	93.2	168.1	0.60	139.38	21.02

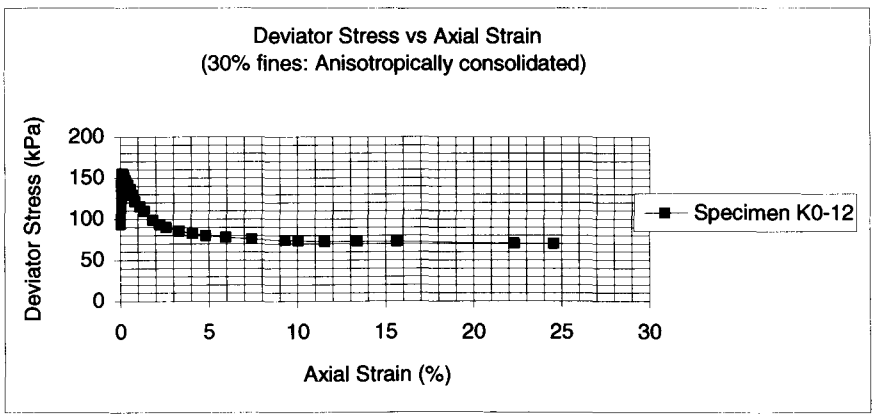
3.) Shear data

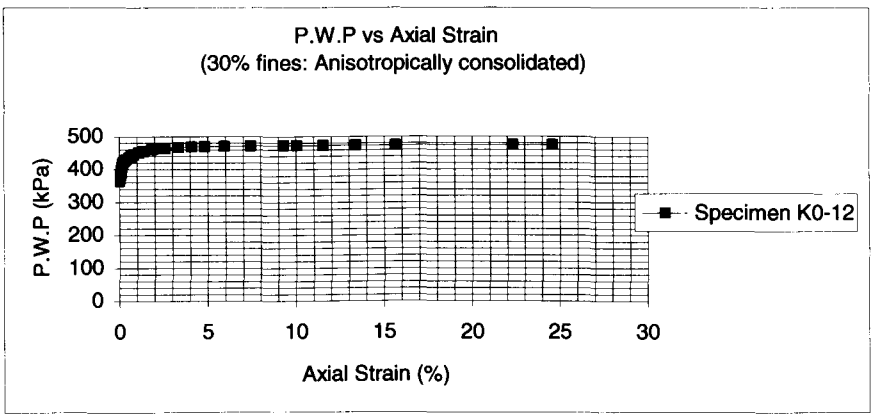
Volume change 1:		Volume change 2:		Sample Vol. change (cm^3)	126.48	B value	0.98
Air Flushing (cm^3)	7.89	Sat/Cons. (cm^3)	131.49	L_{cons} (mm)	134.33	K0	0.60
Cell Expsn. (cm^3)	0.00	Cell Expsn. (cm^3)	21.02	A_{cons} (cm^2)	46.264	Void ratio (e_1)	0.935
		Ram into cell (cm^3)	8.12				

Strain Gauge (divs)	Axial Strain (%)	Cell Press. (kPa)	Proof Ring (divs)	Pore Pressure (kPa)	Membrane Correction (kPa)	P_1 (kPa)	q (kPa)	t (kPa)	p' (kPa)	s' (kPa)
0	0.0000	500	1100.6	363.0	0.0	593.3	93.3	46.6	168.1	183.6
1	0.0074	500	1122.4	363.5	0.0	596.8	96.8	48.4	168.8	184.9
2	0.0149	500	1158.8	364.0	0.0	602.7	102.7	51.4	170.2	187.4
3	0.0223	500	1231.2	369.5	0.0	614.4	114.4	57.2	168.6	187.7
4	0.0298	500	1280.1	371.0	0.0	622.4	122.4	61.2	169.8	190.2
5	0.0372	500	1319.8	373.5	0.0	628.8	128.8	64.4	169.4	190.9
10	0.0744	500	1400.3	380.0	0.0	641.8	141.8	70.9	167.3	190.9
15	0.1117	500	1482.7	388.5	0.1	655.1	155.1	77.5	163.2	189.0
18	0.1340	500	1478.5	397.5	0.1	654.4	154.4	77.2	154.0	179.7
22	0.1638	500	1472.0	407.0	0.1	653.2	153.2	76.6	144.1	169.6
25	0.1861	500	1459.5	415.0	0.1	651.2	151.2	75.6	135.4	160.6
30	0.2233	500	1451.8	421.0	0.1	649.9	149.9	74.9	129.0	153.9
40	0.2978	500	1435.1	425.0	0.1	647.0	147.0	73.5	124.0	148.5
55	0.4094	500	1402.3	430.0	0.2	641.5	141.5	70.7	117.2	140.7
75	0.5583	500	1370.5	434.5	0.3	636.1	136.1	68.0	110.9	133.5
90	0.6700	500	1329.5	438.5	0.3	629.2	129.2	64.6	104.6	126.1
110	0.8189	500	1281.5	444.5	0.4	621.2	121.2	60.6	95.9	116.1
150	1.1167	500	1244.4	450.0	0.6	614.8	114.8	57.4	88.3	107.4
180	1.3400	500	1213.6	454.0	0.7	609.5	109.5	54.7	82.5	100.7
250	1.8611	500	1148.9	460.0	0.9	598.3	98.3	49.2	72.8	89.2
300	2.2333	500	1120.5	462.5	1.0	593.4	93.4	46.7	68.6	84.2
350	2.6055	500	1099.8	464.0	1.0	589.7	89.7	44.9	65.9	80.9
450	3.3500	500	1075.1	466.5	1.0	585.1	85.1	42.6	61.9	76.1
550	4.0944	500	1061.2	468.5	1.0	582.3	82.3	41.2	58.9	72.7

Strain Gauge (divs)	Axial Strain (%)	Cell Press. (kPa)	Proof Ring (divs)	Pore Pressure (kPa)	Membrane Correction (kPa)	P_1 (kPa)	q (kPa)	t (kPa)	p' (kPa)	s' (kPa)
650	4.8388	500	1049.6	469.5	1.0	579.9	79.9	39.9	57.1	70.4
800	5.9555	500	1042.4	470.5	1.0	577.8	77.8	38.9	55.4	68.4
1000	7.4444	500	1036.3	472.0	1.0	575.7	75.7	37.8	53.2	65.8
1250	9.3054	500	1033.0	472.5	1.0	573.6	73.6	36.8	52.0	64.3
1350	10.0499	500	1034.5	473.0	1.0	573.2	73.2	36.6	51.4	63.6
1550	11.5387	500	1035.9	473.0	1.0	572.2	72.2	36.1	51.1	63.1
1800	13.3998	500	1048.9	473.5	1.0	572.5	72.5	36.3	50.7	62.8
2100	15.6331	500	1063.2	474.0	1.0	572.6	72.6	36.3	50.2	62.3
3000	22.3331	500	1091.9	475.0	1.0	570.3	70.3	35.2	48.4	60.2
3300	24.5664	500	1105.0	475.0	1.0	569.9	69.9	34.9	48.3	59.9







Test	**Case 2: Monotonic Undrained Compression of One-Dimensionally Consolidated Specimens**		
Cell No.	3 (Big)	Fines content (%)	30
Specimen	K0-16	Specific gravity (g/cm^3)	2.72

1.) Sample physical properties

Wet mass before test (g)	886.909	m.c before test (%)	11.03	Height (mm)	152.65	Volume (cm^3)	704.386
Wet mass after test (g)	1025.102	m.c. after test (%)	28.33	Diameter (mm)	76.65		
Dry mass (g)	798.801	Dry density (kg/m^3)	1134	Area (cm^2)	46.144	Void ratio (e_0)	1.399

2.) Saturation / Consolidation

Proof ring properties		Strain gauge properties		Loading ram properties	
Proof ring No.	4541	1 strain division (mm)	0.01	Area [ram]$_1$ (cm^2)	7.905
Proof ring factor (dN/div)	25.77			Area [ram]$_2$ (cm^2)	5.004

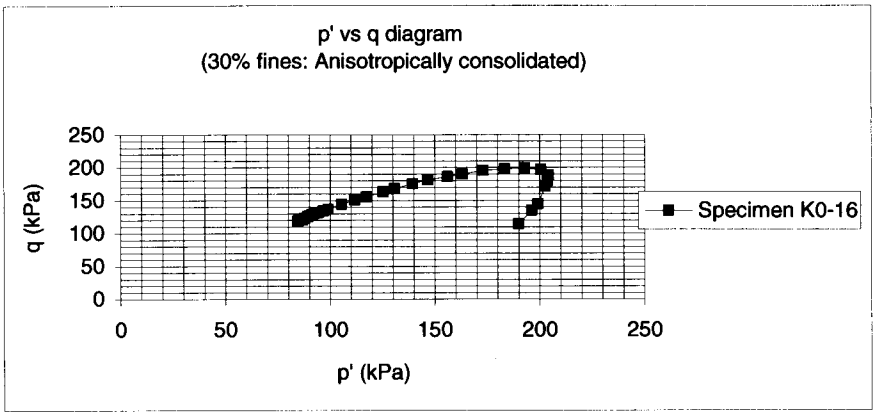
Date	Strain Gauge (divs)	Change Length (mm)	Cell Pressure (kPa)	Proof Ring (div)	Pore Pressure (kPa)	P_1 (kPa)	P'_3 (kPa)	P'_1 (kPa)	q (kPa)	p' (kPa)	K0	Volume Gauge (cm^3)	Cell Expansn (cm^3)
25/5	0	0.000	0	0.0	0.0						\	0.00	0.00
25/5	0	0.000	12.0		7.5	A I R - F L U S H I N G					\	9.25	0.00
25/5	221	2.210	50	50.0	40.0	69.4	10	29.4	19.4	16.5	0.34	42.15	6.08
26/5	412	4.120	100	57.2	90.0	114.8	10	24.8	14.8	14.9	0.40	63.78	8.77
27/5	585	5.850	150	65.4	140.0	160.8	10	20.8	10.8	13.6	0.48	74.35	10.65
28/5	726	7.260	200	74.6	190.0	207.4	10	17.4	7.4	12.5	0.57	82.96	12.00
29/5	840	8.400	250	88.8	240.0	256.8	10	16.8	6.8	12.3	0.60	88.97	13.63
30/5	943	9.430	300	105.0	290.0	307.2	10	17.2	7.2	12.4	0.58	95.12	15.06
31/5	1035	10.350	350	119.8	340.0	356.9	10	16.9	6.9	12.3	0.59	100.33	16.08
1/6	1124	11.240	400	134.5	390.0	406.6	10	16.6	6.6	12.2	0.60	105.02	18.12
2/6	1241	12.410	450	151.1	440.0	457.3	10	17.3	7.3	12.4	0.58	109.54	19.91
3/6	1704	17.040	800	450.0	648.0	914.3	152	266.3	114.3	190.1	0.57	161.62	24.18

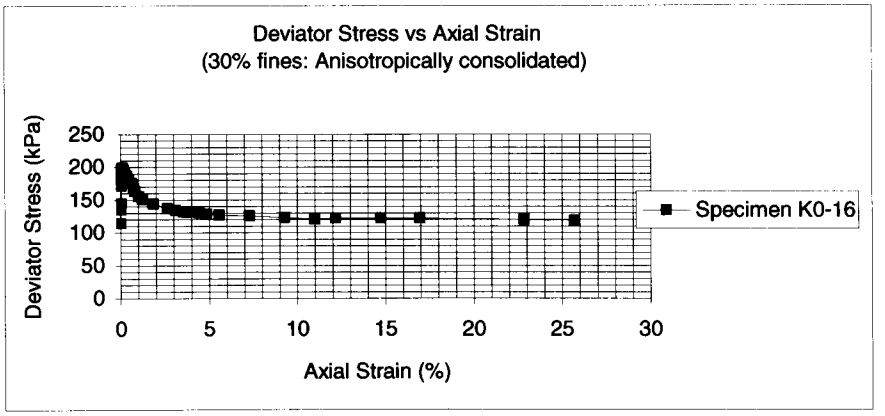
3.) Shear data

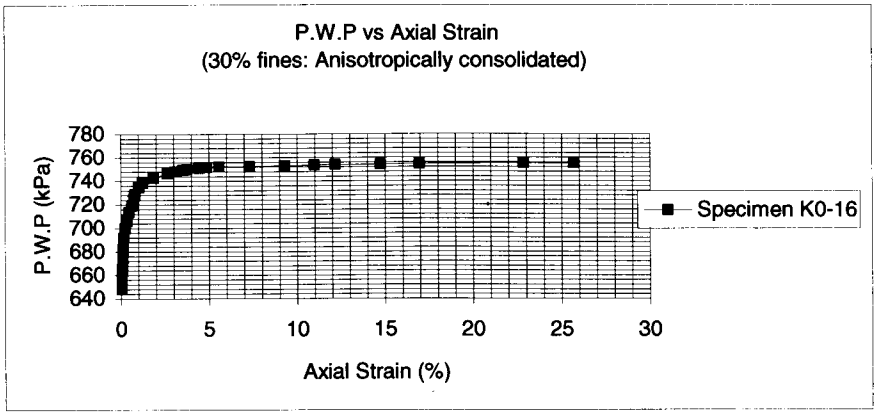
Volume change 1:		Volume change 2:		Sample Vol. change (cm^3)	145.97	B value	0.97
Air Flushing (cm^3)	9.25	Sat/Cons. (cm^3)	152.37	L_{cons} (mm)	135.61	K0	0.57
Cell Expsn. (cm^3)	0.00	Cell Expsn. (cm^3)	24.18	A_{cons} (cm^2)	46.144	Void ratio (e_1)	0.901
		Ram into cell (cm^3)	8.53				

Strain Gauge (divs)	Axial Strain (%)	Cell Press. (kPa)	Proof Ring (divs)	Pore Pressure (kPa)	Membrane Correction (kPa)	P_1 (kPa)	q (kPa)	t (kPa)	p' (kPa)	s' (kPa)
0	0.0000	800	450.0	648.0	0.0	914.3	114.3	57.1	190.1	209.1
2	0.0147	800	486.6	648.5	0.0	934.7	134.7	67.3	196.4	218.8
4	0.0295	800	504.5	649.0	0.0	944.6	144.6	72.3	199.2	223.3
5	0.0369	800	552.3	654.5	0.0	971.3	171.3	85.7	202.6	231.2
6	0.0442	800	567.2	656.0	0.0	979.6	179.6	89.8	203.9	233.8
8	0.0590	800	582.9	658.5	0.0	988.3	188.3	94.2	204.3	235.7
10	0.0737	800	598.1	665.0	0.0	996.8	196.8	98.4	200.6	233.4
15	0.1106	800	602.6	673.5	0.1	999.2	199.2	99.6	192.9	226.1
18	0.1327	800	600.0	682.5	0.1	997.7	197.7	98.9	183.4	216.4
25	0.1844	800	595.5	692.0	0.1	995.1	195.1	97.5	173.0	205.5
35	0.2581	800	586.7	700.0	0.1	990.0	190.0	95.0	163.3	195.0
50	0.3687	800	580.3	706.0	0.2	986.2	186.2	93.1	156.1	187.1
65	0.4793	800	571.5	713.5	0.2	981.0	181.0	90.5	146.8	177.0
85	0.6268	800	562.1	719.0	0.3	975.4	175.4	87.7	139.5	168.7
100	0.7374	800	548.8	725.0	0.4	967.8	167.8	83.9	130.9	158.9
110	0.8111	800	540.4	729.0	0.4	963.0	163.0	81.5	125.3	152.5
140	1.0324	800	527.6	734.5	0.5	955.5	155.5	77.7	117.3	143.2
170	1.2536	800	519.8	738.5	0.6	950.7	150.7	75.3	111.7	136.8
250	1.8435	800	509.5	742.5	0.9	943.9	143.9	71.9	105.5	129.4
360	2.6547	800	498.7	746.5	1.0	936.7	136.7	68.4	99.1	121.9
420	3.0971	800	495.6	748.0	1.0	934.4	134.4	67.2	96.8	119.2
480	3.5396	800	492.1	749.5	1.0	931.9	131.9	65.9	94.5	116.4
510	3.7608	800	491.3	750.0	1.0	931.2	131.2	65.6	93.7	115.6
600	4.4245	800	490.9	751.0	1.0	930.0	130.0	65.0	92.3	114.0

Strain Gauge (divs)	Axial Strain (%)	Cell Press. (kPa)	Proof Ring (divs)	Pore Pressure (kPa)	Membrane Correction (kPa)	P_1 (kPa)	q (kPa)	t (kPa)	p' (kPa)	s' (kPa)
660	4.8669	800	489.0	751.5	1.0	928.4	128.4	64.2	91.3	112.7
755	5.5674	800	488.1	752.0	1.0	927.0	127.0	63.5	90.3	111.5
990	7.3003	800	489.5	752.5	1.0	925.4	125.4	62.7	89.3	110.2
1260	9.2914	800	490.0	753.0	1.0	922.9	122.9	61.5	88.0	108.5
1490	10.9874	800	490.5	753.5	1.0	920.8	120.8	60.4	86.8	106.9
1650	12.1672	800	495.8	754.0	1.0	921.8	121.8	60.9	86.6	106.9
2000	14.7482	800	503.6	754.0	1.0	921.9	121.9	61.0	86.6	107.0
2300	16.9604	800	510.4	754.5	1.0	921.9	121.9	60.9	86.1	106.4
3100	22.8597	800	525.9	755.0	1.0	919.8	119.8	59.9	84.9	104.9
3485	25.6987	800	533.5	755.0	1.0	918.5	118.5	59.3	84.5	104.3







Test	**Case 2: Monotonic Undrained Compression of One-Dimensionally Consolidated Specimens**		
Cell No.	3 (Big)	Fines content (%)	30
Specimen	K0-22	Specific gravity (g/cm^3)	2.72

1.) Sample physical properties

Wet mass before test (g)	852.617	m.c before test (%)	9.91	Height (mm)	151.10	Volume (cm^3)	698.144
Wet mass after test (g)	961.531	m.c. after test (%)	23.95	Diameter (mm)	76.70		
Dry mass (g)	775.741	Dry density (kg/m^3)	1111	Area (cm^2)	46.204	Void ratio (e_0)	1.448

2.) Saturation / Consolidation

Proof ring properties		Strain gauge properties		Loading ram properties	
Proof ring No.	5153	1 strain division (mm)	0.01	Area [ram]$_1$ (cm^2)	7.905
Proof ring factor (dN/div)	7.512			Area [ram]$_2$ (cm^2)	5.004

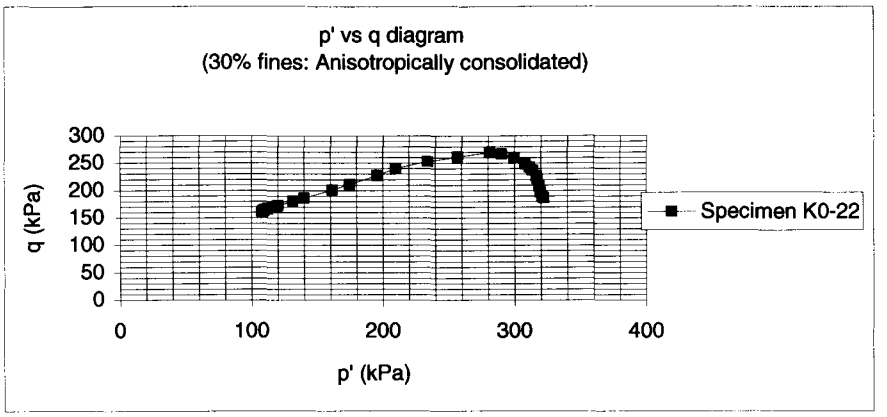
Date	Strain Gauge (divs)	Change Length (mm)	Cell Pressure (kPa)	Proof Ring (div)	Pore Pressure (kPa)	P_1 (kPa)	P'_3 (kPa)	P'_1 (kPa)	q (kPa)	p' (kPa)	K0	Volume Gauge (cm^3)	Cell Expansn (cm^3)
2/7	0	0.000	0	0.0	0.0						\	0.00	0.00
2/7	0	0.000	11.2		7.5	A I R - F L U S H I N G					\	10.00	0.00
2/7	197	1.970	50	150.0	40.0	65.8	10	25.8	15.8	15.3	0.39	45.71	6.08
3/7	380	3.800	100	182.3	90.0	112.5	10	22.5	12.5	14.2	0.44	65.22	8.77
4/7	558	5.580	150	222.7	140.0	160.5	10	20.5	10.5	13.5	0.49	79.10	10.65
5/7	701	7.010	200	250.9	190.0	206.6	10	16.6	6.6	12.2	0.60	87.84	12.00
6/7	823	8.230	250	307.5	240.0	257.2	10	17.2	7.2	12.4	0.58	93.99	13.63
7/7	942	9.420	300	354.8	290.0	306.4	10	16.4	6.4	12.1	0.61	100.15	15.06
8/7	1050	10.500	350	411.2	340.0	357.0	10	17.0	7.0	12.3	0.59	105.17	16.08
9/7	1154	11.540	400	464.6	390.0	407.1	10	17.1	7.1	12.4	0.58	112.09	18.12
10/7	1522	15.220	650	1830.0	390.0	836.3	260	446.3	186.3	322.1	0.58	167.29	23.11

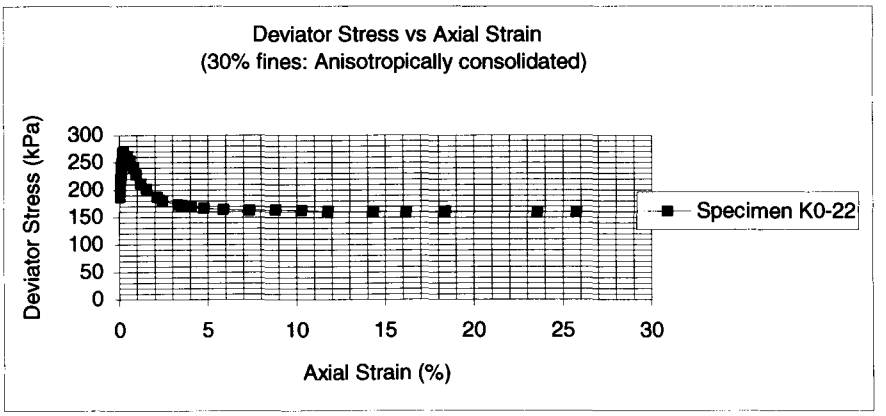
3.) Shear data

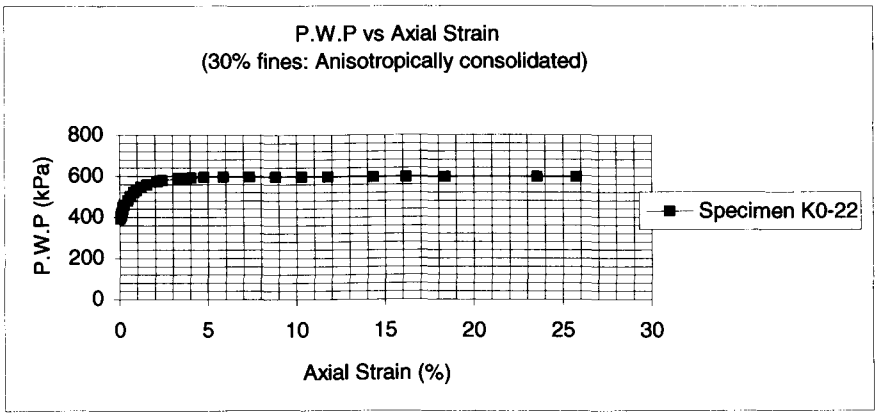
Volume change 1:		Volume change 2:		Sample Vol. change (cm^3)	151.80	B value	0.97
Air Flushing (cm^3)	10.00	Sat/Cons. (cm^3)	157.29	L_{cons} (mm)	135.88	K0	0.58
Cell Expsn. (cm^3)	0.00	Cell Expsn. (cm^3)	23.11	A_{cons} (cm^2)	46.204	Void ratio (e_1)	0.916
		Ram into cell (cm^3)	7.62				

Strain Gauge (divs)	Axial Strain (%)	Cell Press. (kPa)	Proof Ring (divs)	Pore Pressure (kPa)	Membrane Correction (kPa)	P_1 (kPa)	q (kPa)	t (kPa)	p' (kPa)	s' (kPa)
0	0.0000	650	1830.6	390.0	0.0	836.4	186.4	93.2	322.1	353.2
2	0.0147	650	1843.4	392.0	0.0	838.5	188.5	94.2	320.8	352.2
6	0.0442	650	1895.3	396.0	0.0	846.8	196.8	98.4	319.6	352.4
8	0.0589	650	1964.0	400.5	0.0	858.0	208.0	104.0	318.8	353.5
12	0.0883	650	2040.7	406.0	0.0	870.3	220.3	110.2	317.4	354.2
14	0.1030	650	2076.9	408.5	0.1	876.2	226.2	113.1	316.9	354.6
16	0.1178	650	2140.4	415.0	0.1	886.4	236.4	118.2	313.8	353.2
17	0.1251	650	2177.1	419.5	0.1	892.4	242.4	121.2	311.3	351.7
21	0.1545	650	2215.0	424.5	0.1	898.5	248.5	124.2	308.3	349.7
25	0.1840	650	2280.5	436.5	0.1	909.0	259.0	129.5	299.8	343.0
28	0.2061	650	2326.6	448.5	0.1	916.4	266.4	133.2	290.3	334.7
35	0.2576	650	2345.5	458.5	0.1	919.3	269.3	134.7	281.3	326.2
65	0.4784	650	2300.1	480.0	0.2	911.3	261.3	130.6	257.1	300.6
85	0.6219	650	2251.0	500.0	0.3	902.9	252.9	126.4	234.3	276.4
110	0.8095	650	2175.3	520.0	0.4	890.1	240.1	120.0	210.0	250.0
130	0.9567	650	2100.0	530.0	0.5	877.5	227.5	113.8	195.8	233.8
165	1.2143	650	2002.2	545.5	0.6	861.1	211.1	105.6	174.9	210.1
210	1.5455	650	1943.4	555.5	0.8	850.8	200.8	100.4	161.4	194.9
290	2.1342	650	1861.1	572.0	1.0	836.3	186.3	93.1	140.1	171.1
330	2.4286	650	1828.0	578.5	1.0	830.5	180.5	90.2	131.7	161.7
450	3.3117	650	1785.8	587.0	1.0	822.2	172.2	86.1	120.4	149.1
480	3.5325	650	1782.6	588.0	1.0	821.3	171.3	85.7	119.1	147.7
550	4.0477	650	1771.8	590.0	1.0	818.7	168.7	84.4	116.2	144.4
650	4.7836	650	1764.3	593.0	1.0	816.2	166.2	83.1	112.4	140.1

Strain Gauge (divs)	Axial Strain (%)	Cell Press. (kPa)	Proof Ring (divs)	Pore Pressure (kPa)	Membrane Correction (kPa)	P_1 (kPa)	q (kPa)	t (kPa)	p' (kPa)	s' (kPa)
800	5.8875	650	1763.4	595.0	1.0	814.2	164.2	82.1	109.7	137.1
1000	7.3594	650	1770.0	595.0	1.0	812.6	162.6	81.3	109.2	136.3
1200	8.8313	650	1792.2	595.0	1.0	813.3	163.3	81.6	109.4	136.6
1400	10.3032	650	1803.7	595.0	1.0	812.3	162.3	81.1	109.1	136.1
1600	11.7751	650	1810.2	595.0	1.0	810.5	160.5	80.3	108.5	135.3
1950	14.3509	650	1842.1	595.0	1.0	810.3	160.3	80.1	108.4	135.1
2200	16.1908	650	1859.9	595.0	1.0	809.2	159.2	79.6	108.1	134.6
2500	18.3986	650	1904.3	595.0	1.0	810.9	160.9	80.4	108.6	135.4
3200	23.5502	650	1977.6	595.0	1.0	809.8	159.8	79.9	108.3	134.9
3500	25.7580	650	2015.4	595.0	1.0	809.7	159.7	79.9	108.2	134.9







Test	**Case 2: Monotonic Undrained Compression of One-Dimensionally Consolidated Specimens**		
Cell No.	2 (Big)	Fines content (%)	30
Specimen	K0-27	Specific gravity (g/cm^3)	2.72

1.) Sample physical properties

Wet mass before test (g)	840.888	m.c before test (%)	8.77	Height (mm)	152.30	Volume (cm^3)	701.855
Wet mass after test (g)	979.348	m.c. after test (%)	26.68	Diameter (mm)	76.60		
Dry mass (g)	773.088	Dry density (kg/m^3)	1101	Area (cm^2)	46.084	Void ratio (e_0)	1.469

2.) Saturation / Consolidation

Proof ring properties		Strain gauge properties		Loading ram properties	
Proof ring No.	5153	1 strain division (mm)	0.01	Area [ram]$_1$ (cm^2)	7.905
Proof ring factor (dN/div)	7.512			Area [ram]$_2$ (cm^2)	5.004

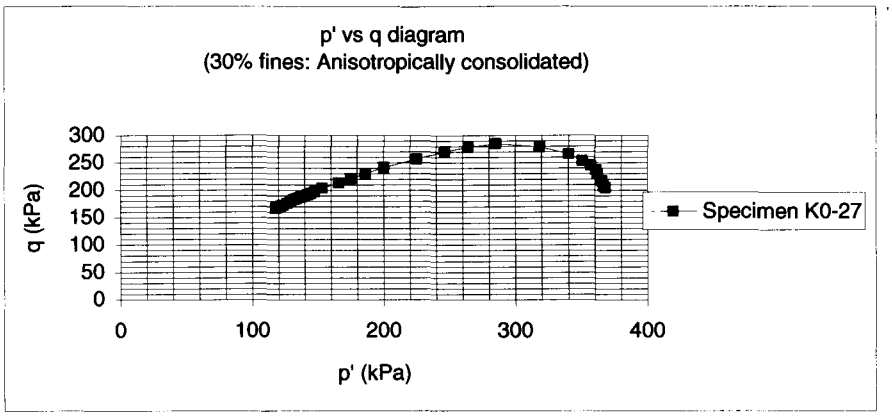
Date	Strain Gauge (divs)	Change Length (mm)	Cell Pressure (kPa)	Proof Ring (div)	Pore Pressure (kPa)	P_1 (kPa)	P'_3 (kPa)	P'_1 (kPa)	q (kPa)	p' (kPa)	K0	Volume Gauge (cm^3)	Cell Expansn (cm^3)
9/8	0	0.000	0	0.0	0.0						\	0.00	0.00
9/8	0	0.000	9.7		4.5	A I R - F L U S H I N G					\	8.75	0.00
9/8	200	2.000	50	133.6	40.0	63.2	10	23.2	13.2	14.4	0.43	37.89	7.06
10/8	374	3.740	100	164.5	90.0	109.7	10	19.7	9.7	13.2	0.51	54.67	9.79
11/8	512	5.120	150	201.8	140.0	157.2	10	17.2	7.2	12.4	0.58	69.01	11.63
12/8	608	6.080	200	249.7	190.0	206.4	10	16.4	6.4	12.1	0.61	81.28	13.02
13/8	700	7.000	250	304.4	240.0	256.7	10	16.7	6.7	12.2	0.60	88.19	14.57
14/8	793	7.930	300	358.2	290.0	306.9	10	16.9	6.9	12.3	0.59	94.22	16.03
15/8	877	8.770	350	415.9	340.0	357.8	10	17.8	7.8	12.6	0.56	101.31	17.22
16/8	961	9.610	400	472.3	390.0	408.4	10	18.4	8.4	12.8	0.54	108.03	19.30
17/8	1045	10.450	450	515.3	440.0	456.8	10	16.8	6.8	12.3	0.59	114.12	20.93
18/8	1168	11.680	500	564.5	490.0	506.3	10	16.3	6.3	12.1	0.62	120.24	22.85
19/8	1535	15.350	900	2200.0	600.0	1104.2	300	504.2	204.2	368.1	0.59	168.43	25.72

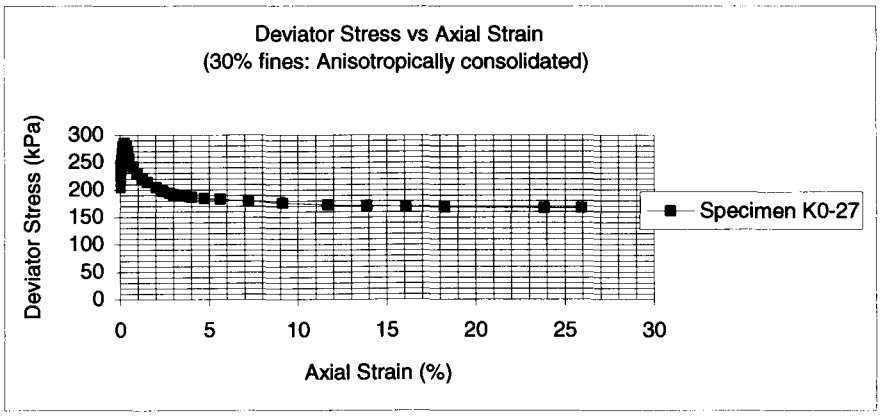
3.) Shear data

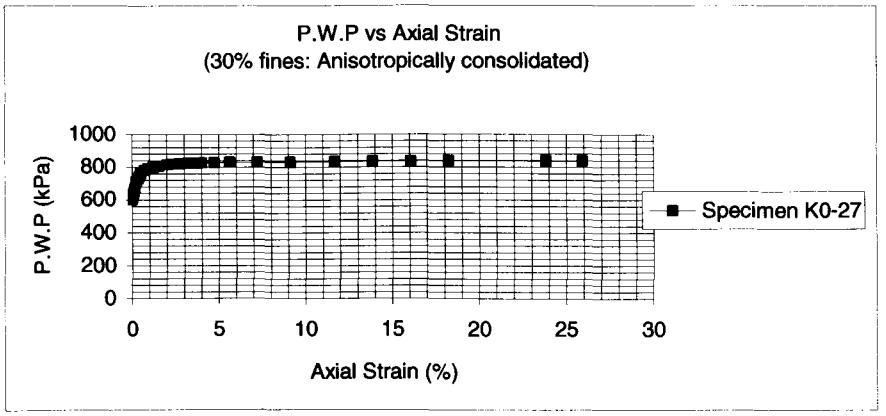
Volume change 1:		Volume change 2:		Sample Vol. change (cm^3)	150.39	B value	0.97
Air Flushing (cm^3)	8.75	Sat/Cons. (cm^3)	159.68	L_{cons} (mm)	136.95	K0	0.59
Cell Expsn. (cm^3)	0.00	Cell Expsn. (cm^3)	25.72	A_{cons} (cm^2)	46.084	Void ratio (e_1)	0.940
		Ram into cell (cm^3)	7.68				

Strain Gauge (divs)	Axial Strain (%)	Cell Press. (kPa)	Proof Ring (divs)	Pore Pressure (kPa)	Membrane Correction (kPa)	P_1 (kPa)	q (kPa)	t (kPa)	p' (kPa)	s' (kPa)
0	0.0000	900	2200.3	600.0	0.0	1104.3	204.3	102.1	368.1	402.1
1	0.0073	900	2218.9	602.5	0.0	1107.3	207.3	103.7	366.6	401.2
3	0.0219	900	2282.5	607.0	0.0	1117.6	217.6	108.8	365.5	401.8
4	0.0292	900	2349.7	614.0	0.0	1128.6	228.6	114.3	362.2	400.3
7	0.0511	900	2400.8	618.0	0.0	1136.8	236.8	118.4	360.9	400.4
9	0.0657	900	2450.1	624.5	0.0	1144.8	244.8	122.4	357.1	397.9
12	0.0876	900	2500.9	633.5	0.0	1153.0	253.0	126.5	350.8	393.0
18	0.1314	900	2580.2	648.0	0.1	1165.8	265.8	132.9	340.6	384.9
25	0.1789	900	2660.4	674.5	0.1	1178.7	278.7	139.3	318.4	364.8
35	0.2519	900	2700.6	710.0	0.1	1185.0	285.0	142.5	285.0	332.5
50	0.3651	900	2660.1	728.5	0.2	1178.0	278.0	139.0	264.2	310.5
60	0.4381	900	2615.0	743.5	0.2	1170.5	270.5	135.2	246.7	291.7
70	0.5075	900	2530.3	760.0	0.3	1156.5	256.5	128.3	225.5	268.3
100	0.7302	900	2440.6	780.0	0.4	1141.3	241.3	120.7	200.4	240.7
130	0.9493	900	2375.5	790.5	0.5	1130.2	230.2	115.1	186.2	224.6
170	1.2413	900	2322.1	798.5	0.6	1120.7	220.7	110.4	175.1	211.9
210	1.5334	900	2279.4	805.0	0.8	1113.1	213.1	106.5	166.0	201.5
280	2.0445	900	2230.8	814.5	1.0	1104.0	204.0	102.0	153.5	187.5
330	2.4096	900	2191.3	818.0	1.0	1096.9	196.9	98.5	147.6	180.5
380	2.7747	900	2175.7	820.0	1.0	1093.7	193.7	96.9	144.6	176.9
410	2.9938	900	2164.6	821.5	1.0	1091.5	191.5	95.8	142.3	174.3
460	3.3589	900	2156.4	823.5	1.0	1089.5	189.5	94.8	139.7	171.3
500	3.6510	900	2152.1	825.0	1.0	1088.3	188.3	94.1	137.8	169.1
550	4.0161	900	2145.2	826.0	1.0	1086.5	186.5	93.2	136.2	167.2

Strain Gauge (divs)	Axial Strain (%)	Cell Press. (kPa)	Proof Ring (divs)	Pore Pressure (kPa)	Membrane Correction (kPa)	P_1 (kPa)	q (kPa)	t (kPa)	p' (kPa)	s' (kPa)
650	4.7463	900	2140.0	828.0	1.0	1084.2	184.2	92.1	133.4	164.1
770	5.6225	900	2140.4	829.5	1.0	1082.6	182.6	91.3	131.4	161.8
990	7.2289	900	2140.3	830.5	1.0	1079.4	179.4	89.7	129.3	159.2
1250	9.1274	900	2140.0	832.0	1.0	1075.7	175.7	87.9	126.6	155.9
1600	11.6831	900	2151.7	834.0	1.0	1072.4	172.4	86.2	123.5	152.2
1900	13.8737	900	2172.3	835.0	1.0	1071.0	171.0	85.5	122.0	150.5
2200	16.0643	900	2191.1	836.0	1.0	1069.2	169.2	84.6	120.4	148.6
2500	18.2548	900	2218.2	837.0	1.0	1068.4	168.4	84.2	119.1	147.2
3265	23.8408	900	2302.5	838.0	1.0	1067.3	167.3	83.6	117.8	145.6
3550	25.9219	900	2340.6	838.0	1.0	1067.3	167.3	83.6	117.8	145.6







Test	**Case 2: Monotonic Undrained Compression of One-Dimensionally Consolidated Specimens**		
Cell No.	3 (Big)	Fines content (%)	30
Specimen	K0-28	Specific gravity (g/cm^3)	2.72

1.) Sample physical properties

Wet mass before test (g)	827.065	m.c before test (%)	8.66	Height (mm)	151.55	Volume (cm^3)	702.050
Wet mass after test (g)	950.447	m.c. after test (%)	24.87	Diameter (mm)	76.80		
Dry mass (g)	761.149	Dry density (kg/m^3)	1084	Area (cm^2)	46.325	Void ratio (e_0)	1.509

2.) Saturation / Consolidation

Proof ring properties		Strain gauge properties		Loading ram properties	
Proof ring No.	4541	1 strain division (mm)	0.01	Area [ram]$_1$ (cm^2)	7.905
Proof ring factor (dN/div)	25.77			Area [ram]$_2$ (cm^2)	5.004

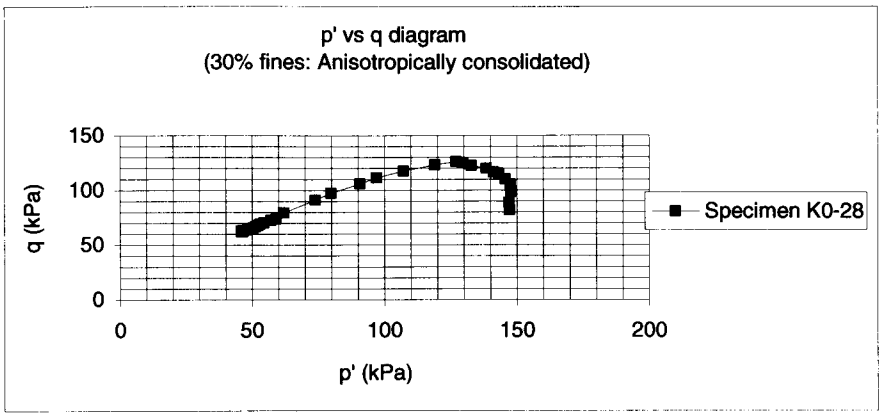
Date	Strain Gauge (divs)	Change Length (mm)	Cell Pressure (kPa)	Proof Ring (div)	Pore Pressure (kPa)	P_1 (kPa)	P'_3 (kPa)	P'_1 (kPa)	q (kPa)	p' (kPa)	K0	Volume Gauge (cm^3)	Cell Expansn (cm^3)
9/8	0	0.000	0	0.0	0.0						\	0.00	0.00
9/8	0	0.000	8.8		3.5	A I R - F L U S H I N G					\	9.81	0.00
9/8	204	2.040	50	48.6	40.0	68.5	10	28.5	18.5	16.2	0.35	44.22	6.08
10/8	385	3.850	100	54.3	90.0	113.1	10	23.1	13.1	14.4	0.43	68.34	8.77
11/8	540	5.400	150	60.2	140.0	157.9	10	17.9	7.9	12.6	0.56	87.51	10.65
12/8	677	6.770	200	74.0	190.0	207.0	10	17.0	7.0	12.3	0.59	103.24	12.00
13/8	785	7.850	250	92.3	240.0	258.7	10	18.7	8.7	12.9	0.54	114.05	13.63
14/8	900	9.000	300	104.9	290.0	307.2	10	17.2	7.2	12.4	0.58	124.51	15.06
15/8	1024	10.240	350	118.2	340.0	356.0	10	16.0	6.0	12.0	0.62	133.85	16.08
16/8	1142	11.420	400	144.5	380.0	412.1	20	32.1	12.1	24.0	0.62	144.54	18.12
17/8	1410	14.100	500	300.0	380.0	581.6	120	201.6	81.6	147.2	0.60	186.46	21.02

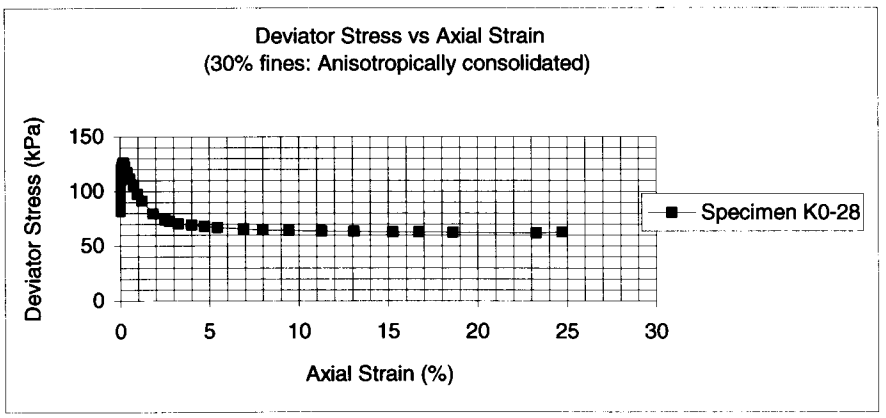
3.) Shear data

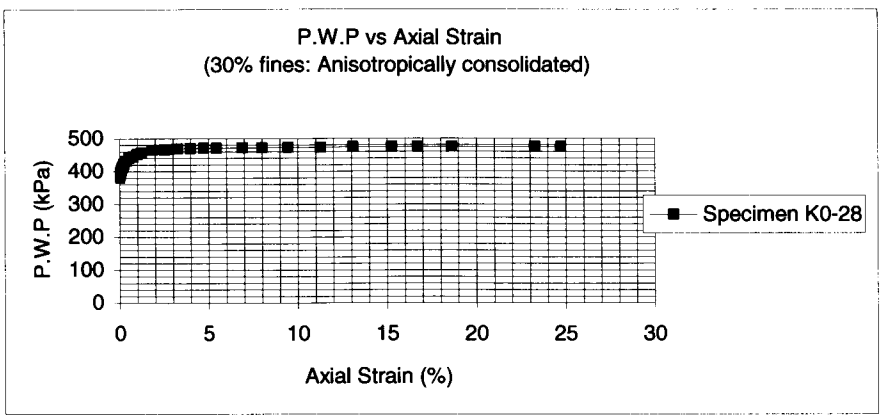
Volume change 1:		Volume change 2:		Sample Vol. change (cm^3)	172.50	B value	0.98
Air Flushing (cm^3)	9.81	Sat/Cons. (cm^3)	176.65	L_{cons} (mm)	137.45	K0	0.60
Cell Expsn. (cm^3)	0.00	Cell Expsn. (cm^3)	21.02	A_{cons} (cm^2)	46.325	Void ratio (e_1)	0.892
		Ram into cell (cm^3)	7.06				

Strain Gauge (divs)	Axial Strain (%)	Cell Press. (kPa)	Proof Ring (divs)	Pore Pressure (kPa)	Membrane Correction (kPa)	P_1 (kPa)	q (kPa)	t (kPa)	p' (kPa)	s' (kPa)
0	0.0000	500	300.2	380.0	0.0	581.7	81.7	40.8	147.2	160.8
1	0.0073	500	312.5	382.5	0.0	588.5	88.5	44.3	147.0	161.8
2	0.0146	500	330.4	385.0	0.0	598.5	98.5	49.2	147.8	164.2
3	0.0218	500	342.3	387.5	0.0	605.1	105.1	52.5	147.5	165.0
5	0.0364	500	351.0	391.0	0.0	609.9	109.9	54.9	145.6	163.9
7	0.0509	500	359.8	395.0	0.0	614.7	114.7	57.4	143.2	162.4
9	0.0655	500	362.7	397.5	0.0	616.3	116.3	58.2	141.3	160.7
13	0.0946	500	369.2	401.5	0.0	619.9	119.9	60.0	138.5	158.5
18	0.1310	500	374.0	408.0	0.1	622.5	122.5	61.3	132.8	153.3
23	0.1673	500	378.1	412.0	0.1	624.7	124.7	62.4	129.6	150.4
28	0.2037	500	380.6	415.0	0.1	626.0	126.0	63.0	127.0	148.0
35	0.2546	500	375.4	422.0	0.1	623.1	123.1	61.5	119.0	139.5
55	0.4001	500	365.6	432.0	0.2	617.4	117.4	58.7	107.1	126.7
75	0.5457	500	355.2	440.0	0.3	611.4	111.4	55.7	97.1	115.7
105	0.7639	500	345.7	444.5	0.4	605.8	105.8	52.9	90.8	108.4
135	0.9822	500	330.8	452.5	0.5	597.2	97.2	48.6	79.9	96.1
170	1.2332	500	320.4	456.5	0.6	591.2	91.2	45.6	73.9	89.1
255	1.8552	500	300.6	464.5	0.9	579.5	79.5	39.7	62.0	75.2
345	2.5100	500	291.5	465.5	1.0	573.9	73.9	37.0	59.1	71.5
380	2.7646	500	289.4	467.0	1.0	572.6	72.6	36.3	57.2	69.3
450	3.2739	500	286.1	469.0	1.0	570.4	70.4	35.2	54.5	66.2
550	4.0015	500	284.9	470.0	1.0	569.2	69.2	34.6	53.1	64.6
650	4.7290	500	283.5	470.5	1.0	568.0	68.0	34.0	52.2	63.5
750	5.4565	500	282.4	471.0	1.0	566.9	66.9	33.4	51.3	62.4

Strain Gauge (divs)	Axial Strain (%)	Cell Press. (kPa)	Proof Ring (divs)	Pore Pressure (kPa)	Membrane Correction (kPa)	P_1 (kPa)	q (kPa)	t (kPa)	p' (kPa)	s' (kPa)
950	6.9116	500	281.8	471.5	1.0	565.5	65.5	32.8	50.3	61.3
1100	8.0029	500	281.0	472.0	1.0	564.3	64.3	32.2	49.4	60.2
1300	9.4580	500	282.6	472.5	1.0	564.1	64.1	32.0	48.9	59.5
1550	11.2768	500	284.0	473.0	1.0	563.5	63.5	31.7	48.2	58.7
1800	13.0957	500	286.1	474.5	1.0	563.2	63.2	31.6	46.6	57.1
2100	15.2783	500	288.8	474.5	1.0	562.8	62.8	31.4	46.4	56.9
2300	16.7334	500	290.7	474.5	1.0	562.6	62.6	31.3	46.4	56.8
2560	18.6250	500	293.6	474.5	1.0	562.5	62.5	31.2	46.3	56.7
3200	23.2812	500	300.5	474.5	1.0	561.8	61.8	30.9	46.1	56.4
3400	24.7363	500	305.7	475.0	1.0	562.8	62.8	31.4	45.9	56.4







Test	**Case 2: Monotonic Undrained Compression of One-Dimensionally Consolidated Specimens**		
Cell No.	3 (Big)	Fines content (%)	30
Specimen	K0-32	Specific gravity (g/cm^3)	2.72

1.) Sample physical properties

Wet mass before test (g)	869.687	m.c before test (%)	10.32	Height (mm)	151.95	Volume (cm^3)	702.987
Wet mass after test (g)	978.871	m.c. after test (%)	24.17	Diameter (mm)	76.75		
Dry mass (g)	788.331	Dry density (kg/m^3)	1121	Area (cm^2)	46.264	Void ratio (e_0)	1.426

2.) Saturation / Consolidation

Proof ring properties		Strain gauge properties		Loading ram properties	
Proof ring No.	4541	1 strain division (mm)	0.01	Area [ram]$_1$ (cm^2)	7.905
Proof ring factor (dN/div)	25.77			Area [ram]$_2$ (cm^2)	5.004

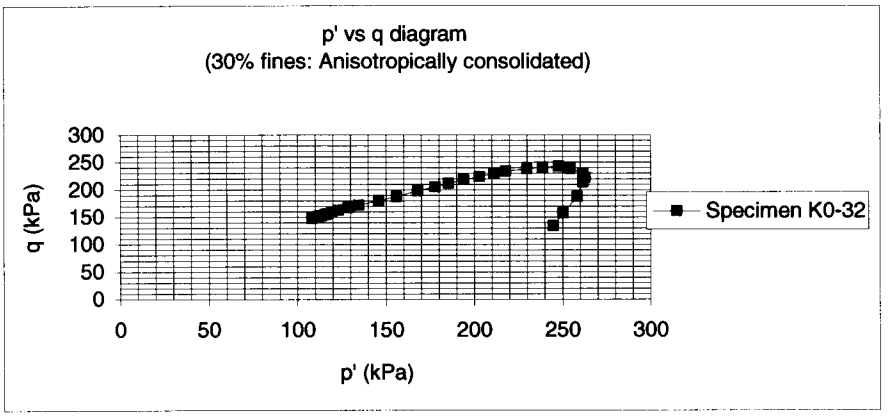
Date	Strain Gauge (divs)	Change Length (mm)	Cell Pressure (kPa)	Proof Ring (div)	Pore Pressure (kPa)	P_1 (kPa)	P'_3 (kPa)	P'_1 (kPa)	q (kPa)	p' (kPa)	K0	Volume Gauge (cm^3)	Cell Expansn (cm^3)
3/9	0	0.000	0	0.0	0.0						\	0.00	0.00
3/9	0	0.000	8.6		4.0	A I R - F L U S H I N G					\	7.55	0.00
3/9	239	2.390	50	51.2	40.0	70.0	10	30.0	20.0	16.7	0.33	38.87	6.08
4/9	421	4.210	100	56.4	90.0	114.3	10	24.3	14.3	14.8	0.41	62.15	8.77
5/9	585	5.850	150	61.7	140.0	158.7	10	18.7	8.7	12.9	0.53	78.84	10.65
6/9	714	7.140	200	75.4	190.0	207.8	10	17.8	7.8	12.6	0.56	90.87	12.00
7/9	830	8.300	250	88.3	240.0	256.5	10	16.5	6.5	12.2	0.61	102.22	13.63
8/9	956	9.560	300	103.5	290.0	306.4	10	16.4	6.4	12.1	0.61	110.55	15.06
9/9	1085	10.850	350	120.0	340.0	357.0	10	17.0	7.0	12.3	0.59	118.61	16.08
10/9	1200	12.000	400	180.6	350.0	432.3	50	82.3	32.3	60.8	0.61	125.96	18.12
11/9	1547	15.470	550	410.0	350.0	684.4	200	334.4	134.4	244.8	0.60	163.85	21.51

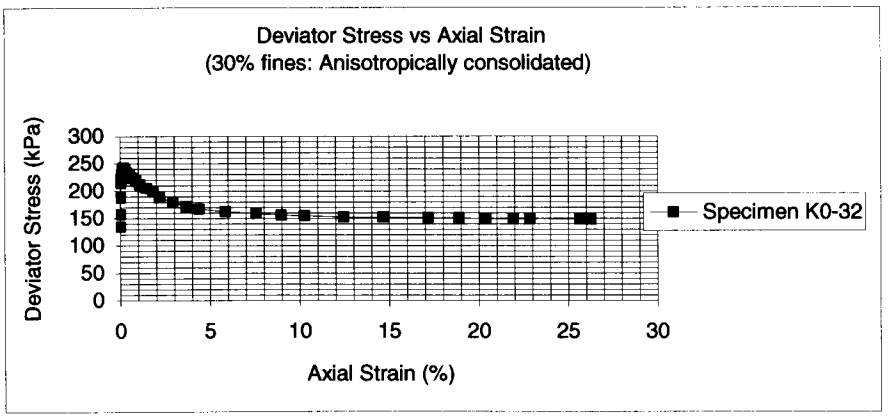
3.) Shear data

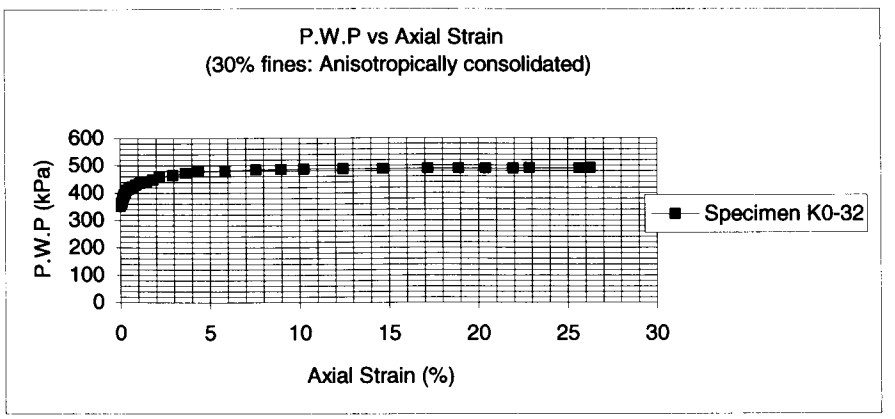
Volume change 1:		Volume change 2:		Sample Vol. change (cm^3)	150.08	B value	0.97
Air Flushing (cm^3)	7.55	Sat/Cons. (cm^3)	156.30	L_{cons} (mm)	136.48	K0	0.60
Cell Expsn. (cm^3)	0.00	Cell Expsn. (cm^3)	21.51	A_{cons} (cm^2)	46.264	Void ratio (e_1)	0.908
		Ram into cell (cm^3)	7.74				

Strain Gauge (divs)	Axial Strain (%)	Cell Press. (kPa)	Proof Ring (divs)	Pore Pressure (kPa)	Membrane Correction (kPa)	P_1 (kPa)	q (kPa)	t (kPa)	p' (kPa)	s' (kPa)
0	0.0000	550	410.0	350.0	0.0	684.4	134.4	67.2	244.8	267.2
1	0.0073	550	450.6	352.0	0.0	707.0	157.0	78.5	250.3	276.5
3	0.0220	550	505.4	354.0	0.0	737.5	187.5	93.7	258.5	289.7
5	0.0366	550	552.5	359.5	0.0	763.7	213.7	106.8	261.7	297.3
10	0.0733	550	567.3	361.0	0.0	771.8	221.8	110.9	262.9	299.9
15	0.1099	550	582.7	365.0	0.1	780.3	230.3	115.1	261.8	300.1
20	0.1465	550	597.3	375.0	0.1	788.3	238.3	119.2	254.4	294.2
25	0.1832	550	605.0	383.0	0.1	792.5	242.5	121.2	247.8	288.2
30	0.2198	550	602.6	391.5	0.1	791.0	241.0	120.5	238.8	279.0
40	0.2931	550	597.8	399.5	0.1	788.2	238.2	119.1	229.9	269.6
50	0.3664	550	590.3	410.0	0.2	783.8	233.8	116.9	217.9	256.9
70	0.5129	550	583.2	415.0	0.3	779.4	229.4	114.7	211.5	249.7
90	0.6594	550	573.8	421.5	0.3	773.8	223.8	111.9	203.1	240.4
120	0.8792	550	564.1	428.5	0.4	767.9	217.9	108.9	194.1	230.4
150	1.0991	550	553.4	435.0	0.5	761.4	211.4	105.7	185.5	220.7
200	1.4654	550	544.1	440.5	0.7	755.3	205.3	102.7	177.9	212.2
250	1.8318	550	532.8	448.0	0.9	748.2	198.2	99.1	168.1	201.1
300	2.1981	550	515.0	456.5	1.0	737.6	187.6	93.8	156.0	187.3
400	2.9308	550	503.5	464.0	1.0	730.0	180.0	90.0	146.0	176.0
500	3.6635	550	490.5	472.5	1.0	721.7	171.7	85.8	134.7	163.3
600	4.3962	550	484.7	477.0	1.0	717.3	167.3	83.6	128.8	156.6
800	5.8617	550	480.3	481.0	1.0	712.4	162.4	81.2	123.1	150.2
1035	7.5835	550	478.6	483.5	1.0	708.5	158.5	79.3	119.3	145.8
1225	8.9757	550	478.1	485.0	1.0	705.9	155.9	77.9	117.0	142.9

Strain Gauge (divs)	Axial Strain (%)	Cell Press. (kPa)	Proof Ring (divs)	Pore Pressure (kPa)	Membrane Correction (kPa)	P_1 (kPa)	q (kPa)	t (kPa)	p' (kPa)	s' (kPa)
1400	10.2579	550	480.0	486.0	1.0	704.6	154.6	77.3	115.5	141.3
1700	12.4560	550	482.9	487.0	1.0	702.2	152.2	76.1	113.7	139.1
2000	14.6542	550	491.5	487.5	1.0	702.5	152.5	76.2	113.3	138.7
2345	17.1820	550	498.0	488.5	1.0	700.9	150.9	75.5	111.8	137.0
2580	18.9039	550	503.7	488.5	1.0	700.3	150.3	75.2	111.6	136.7
2785	20.4059	550	508.4	489.0	1.0	699.6	149.6	74.8	110.9	135.8
2995	21.9446	550	514.6	489.0	1.0	699.4	149.4	74.7	110.8	135.7
3120	22.8605	550	518.1	489.5	1.0	699.1	149.1	74.6	110.2	135.1
3500	25.6448	550	528.8	490.0	1.0	698.1	148.1	74.1	109.4	134.1
3585	26.2676	550	530.0	491.0	1.0	697.4	147.4	73.7	108.1	132.7







Test	**Case 2: Monotonic Undrained Compression of One-Dimensionally Consolidated Specimens**		
Cell No.	2 (Big)	Fines content (%)	30
Specimen	K0-35	Specific gravity (g/cm^3)	2.72

1.) Sample physical properties

Wet mass before test (g)	818.949	m.c before test (%)	9.35	Height (mm)	152.25	Volume (cm^3)	703.458
Wet mass after test (g)	915.111	m.c. after test (%)	22.19	Diameter (mm)	76.70		
Dry mass (g)	748.925	Dry density (kg/m^3)	1065	Area (cm^2)	46.204	Void ratio (e_0)	1.555

2.) Saturation / Consolidation

Proof ring properties		Strain gauge properties		Loading ram properties	
Proof ring No.	4541	1 strain division (mm)	0.01	Area [ram]$_1$ (cm^2)	7.905
Proof ring factor (dN/div)	25.77			Area [ram]$_2$ (cm^2)	5.004

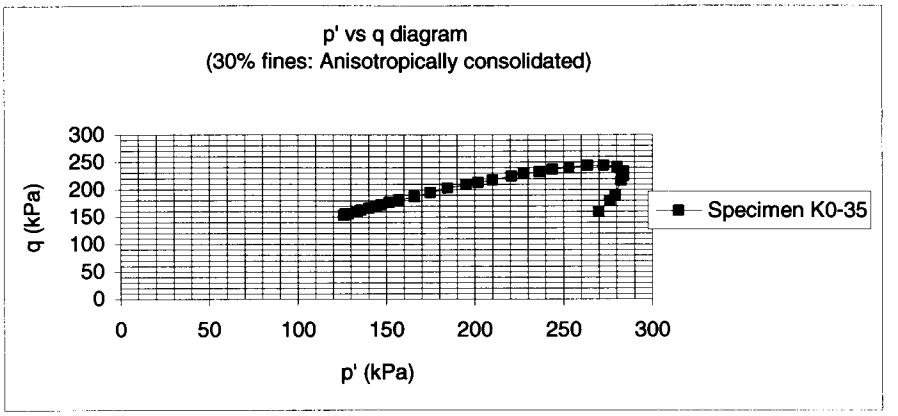
Date	Strain Gauge (divs)	Change Length (mm)	Cell Pressure (kPa)	Proof Ring (div)	Pore Pressure (kPa)	P_1 (kPa)	P'_3 (kPa)	P'_1 (kPa)	q (kPa)	p' (kPa)	K0	Volume Gauge (cm^3)	Cell Expansn (cm^3)
27/9	0	0.000	0	0.0	0.0						\	0.00	0.00
27/9	0	0.000	11.2		8.5	A I R - F L U S H I N G					\	9.00	0.00
27/9	235	2.350	50	50.2	40.0	69.4	10	29.4	19.4	16.5	0.34	49.05	7.06
28/9	433	4.330	100	55.5	90.0	113.8	10	23.8	13.8	14.6	0.42	71.95	9.79
29/9	588	5.880	150	60.7	140.0	158.2	10	18.2	8.2	12.7	0.55	91.22	11.63
30/9	722	7.220	200	75.2	190.0	207.7	10	17.7	7.7	12.6	0.56	104.17	13.02
1/10	848	8.480	250	91.2	240.0	258.1	10	18.1	8.1	12.7	0.55	115.04	14.57
2/10	975	9.750	300	104.6	290.0	307.0	10	17.0	7.0	12.3	0.59	125.11	16.03
3/10	1096	10.960	350	121.3	340.0	357.8	10	17.8	7.8	12.6	0.56	133.56	17.22
4/10	1220	12.200	400	134.6	390.0	406.6	10	16.6	6.6	12.2	0.60	141.45	19.30
5/10	1340	13.400	450	149.8	440.0	456.6	10	16.6	6.6	12.2	0.60	150.24	20.93
6/10	1658	16.580	700	500.0	483.0	859.1	217	376.1	159.1	270.0	0.58	207.55	25.46

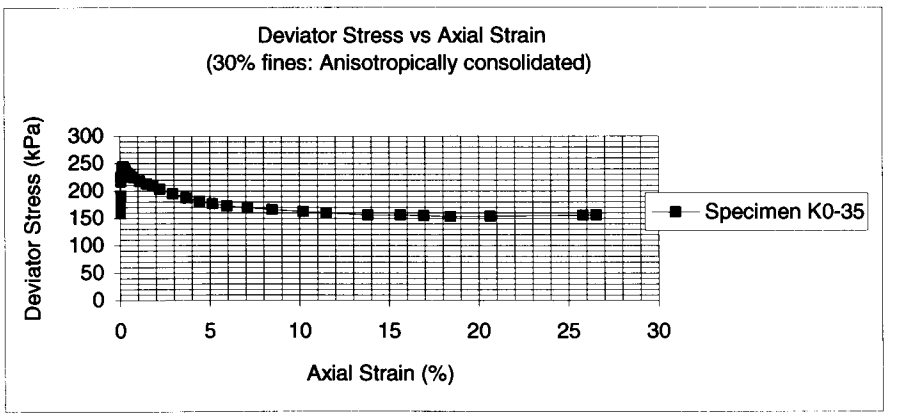
3.) Shear data

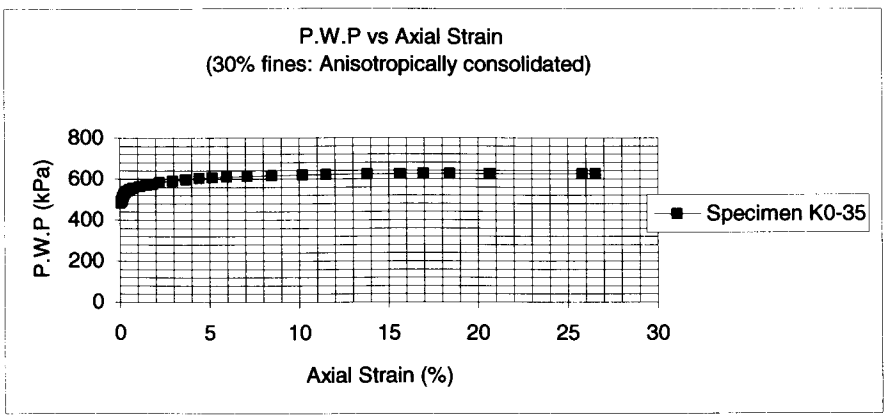
Volume change 1:		Volume change 2:		Sample Vol. change (cm^3)	190.39	B value	0.98
Air Flushing (cm^3)	9.00	Sat/Cons. (cm^3)	198.55	L_{cons} (mm)	135.67	K0	0.58
Cell Expsn. (cm^3)	0.00	Cell Expsn. (cm^3)	25.46	A_{cons} (cm^2)	46.204	Void ratio (e_1)	0.863
		Ram into cell (cm^3)	8.30				

Strain Gauge (divs)	Axial Strain (%)	Cell Press. (kPa)	Proof Ring (divs)	Pore Pressure (kPa)	Membrane Correction (kPa)	P_1 (kPa)	q (kPa)	t (kPa)	p' (kPa)	s' (kPa)
0	0.0000	700	500.0	483.0	0.0	859.1	159.1	79.6	270.0	296.6
1	0.0074	700	535.2	483.5	0.0	878.7	178.7	89.4	276.1	305.9
4	0.0295	700	555.1	484.0	0.0	889.8	189.8	94.9	279.3	310.9
6	0.0442	700	602.9	489.5	0.0	916.4	216.4	108.2	282.6	318.7
9	0.0663	700	617.7	491.0	0.0	924.6	224.6	112.3	283.9	321.3
17	0.1253	700	632.3	493.5	0.1	932.5	232.5	116.3	284.0	322.8
20	0.1474	700	647.3	500.0	0.1	940.8	240.8	120.4	280.3	320.4
23	0.1695	700	652.6	508.5	0.1	943.7	243.7	121.9	272.7	313.4
30	0.2211	700	652.6	517.5	0.1	943.6	243.6	121.8	263.7	304.3
35	0.2580	700	647.3	527.0	0.1	940.5	240.5	120.3	253.2	293.3
40	0.2948	700	640.3	535.0	0.1	936.5	236.5	118.3	243.8	283.3
55	0.4054	700	633.2	541.0	0.2	932.3	232.3	116.1	236.4	275.1
75	0.5528	700	628.0	548.5	0.3	929.0	229.0	114.5	227.8	266.0
100	0.7371	700	620.3	554.0	0.4	924.2	224.2	112.1	220.7	258.1
150	1.1056	700	610.0	562.5	0.6	917.5	217.5	108.7	210.0	246.2
200	1.4742	700	602.8	569.0	0.7	912.5	212.5	106.3	201.8	237.3
250	1.8427	700	597.1	574.5	0.9	908.4	208.4	104.2	195.0	229.7
300	2.2112	700	588.0	583.0	1.0	902.6	202.6	101.3	184.5	218.3
400	2.9483	700	576.3	590.0	1.0	894.7	194.7	97.4	174.9	207.4
500	3.6854	700	565.0	596.5	1.0	887.2	187.2	93.6	165.9	197.1
600	4.4225	700	555.8	603.0	1.0	880.8	180.8	90.4	157.3	187.4
700	5.1596	700	549.5	607.0	1.0	876.1	176.1	88.0	151.7	181.0
810	5.9704	700	544.6	610.0	1.0	872.0	172.0	86.0	147.3	176.0
965	7.1128	700	543.7	612.0	1.0	869.4	169.4	84.7	144.5	172.7

Strain Gauge (divs)	Axial Strain (%)	Cell Press. (kPa)	Proof Ring (divs)	Pore Pressure (kPa)	Membrane Correction (kPa)	P_1 (kPa)	q (kPa)	t (kPa)	p' (kPa)	s' (kPa)
1150	8.4765	700	541.5	615.0	1.0	865.8	165.8	82.9	140.3	167.9
1385	10.2086	700	540.5	618.5	1.0	862.2	162.2	81.1	135.6	162.6
1560	11.4985	700	541.2	620.0	1.0	860.2	160.2	80.1	133.4	160.1
1875	13.8203	700	541.3	623.5	1.0	856.0	156.0	78.0	128.5	154.5
2120	15.6262	700	547.5	624.0	1.0	855.6	155.6	77.8	127.9	153.8
2300	16.9529	700	550.6	624.5	1.0	854.6	154.6	77.3	127.0	152.8
2500	18.4271	700	553.1	625.0	1.0	853.0	153.0	76.5	126.0	151.5
2800	20.6383	700	564.0	625.0	1.0	853.6	153.6	76.8	126.2	151.8
3500	25.7979	700	592.5	625.0	1.0	855.3	155.3	77.7	126.8	152.7
3600	26.5350	700	598.0	625.0	1.0	856.0	156.0	78.0	127.0	153.0







Test	**Case 2: Monotonic Undrained Compression of One-Dimensionally Consolidated Specimens**		
Cell No.	2 (Big)	Fines content (%)	60
Specimen	K0-7	Specific gravity (g/cm^3)	2.72

1.) Sample physical properties

Wet mass before test (g)	892.451	m.c before test (%)	10.04	Height (mm)	151.75	Volume (cm^3)	701.147
Wet mass after test (g)	1016.943	m.c. after test (%)	25.39	Diameter (mm)	76.70		
Dry mass (g)	811.024	Dry density (kg/m^3)	1157	Area (cm^2)	46.204	Void ratio (e_0)	1.351

2.) Saturation / Consolidation

Proof ring properties		Strain gauge properties		Loading ram properties	
Proof ring No.	4541	1 strain division (mm)	0.01	Area [ram]$_1$ (cm^2)	7.905
Proof ring factor (dN/div)	25.77			Area [ram]$_2$ (cm^2)	5.004

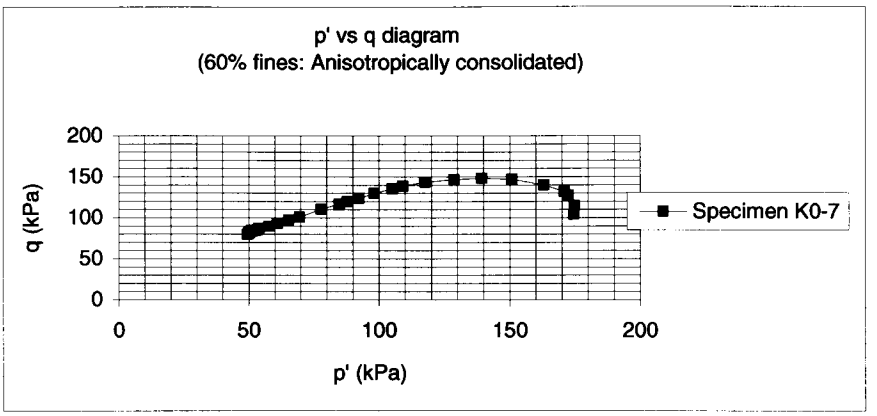
Date	Strain Gauge (divs)	Change Length (mm)	Cell Pressure (kPa)	Proof Ring (div)	Pore Pressure (kPa)	P_1 (kPa)	P'_3 (kPa)	P'_1 (kPa)	q (kPa)	p' (kPa)	K0	Volume Gauge (cm^3)	Cell Expansn (cm^3)
8/4	0	0.000	0	0.0	0.0						\	0.00	0.00
8/4	0	0.000	10.3		6.5	A I R - F L U S H I N G					\	10.25	0.00
8/4	231	2.310	50	54.5	40.0	71.8	10	31.8	21.8	17.3	0.31	51.34	7.06
9/4	433	4.330	100	60.3	90.0	116.5	10	26.5	16.5	15.5	0.38	78.41	9.79
10/4	620	6.200	150	63.5	140.0	159.8	10	19.8	9.8	13.3	0.51	98.05	11.63
11/4	752	7.520	200	75.1	190.0	207.7	10	17.7	7.7	12.6	0.57	113.27	13.02
12/4	865	8.650	250	91.2	240.0	258.1	10	18.1	8.1	12.7	0.55	124.54	14.57
13/4	990	9.900	300	106.3	290.0	308.0	10	18.0	8.0	12.7	0.56	134.95	16.03
14/4	1102	11.020	350	118.6	340.0	356.3	10	16.3	6.3	12.1	0.61	145.65	17.22
15/4	1225	12.250	400	135.0	390.0	406.9	10	16.9	6.9	12.3	0.59	152.14	19.30
16/4	1350	13.500	450	151.2	440.0	457.3	10	17.3	7.3	12.4	0.58	160.00	20.93
17/4	1635	16.350	600	370.0	460.0	703.7	140	243.7	103.7	174.6	0.57	194.31	24.27

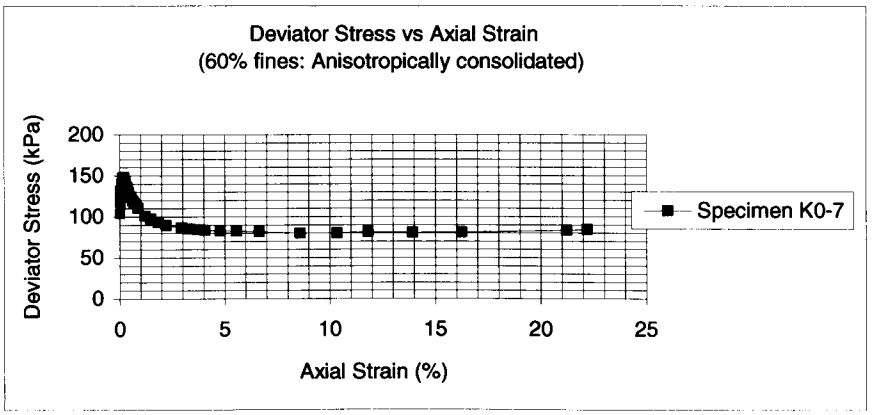
3.) Shear data

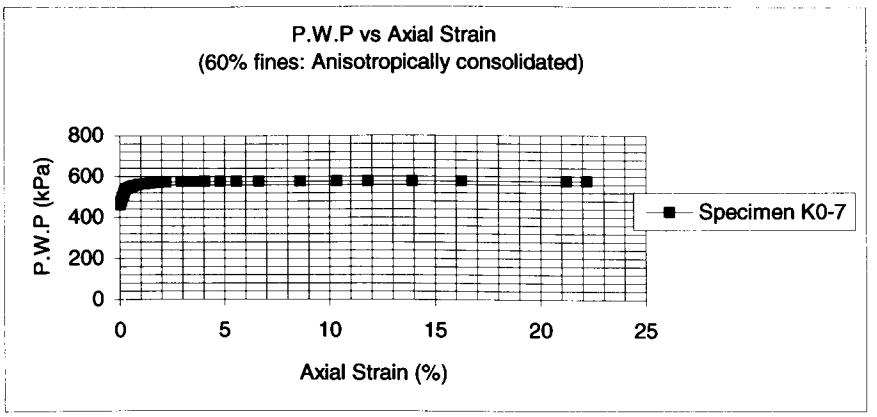
Volume change 1:		Volume change 2:		Sample Vol. change (cm^3)	178.22	B value	0.97
Air Flushing (cm^3)	10.25	Sat/Cons. (cm^3)	184.06	L_{cons} (mm)	135.40	K0	0.57
Cell Expsn. (cm^3)	0.00	Cell Expsn. (cm^3)	24.27	A_{cons} (cm^2)	46.204	Void ratio (e_1)	0.754
		Ram into cell (cm^3)	8.18				

Strain Gauge (divs)	Axial Strain (%)	Cell Press. (kPa)	Proof Ring (divs)	Pore Pressure (kPa)	Membrane Correction (kPa)	P_1 (kPa)	q (kPa)	t (kPa)	p' (kPa)	s' (kPa)
0	0.0000	600	370.0	460.0	0.0	703.7	103.7	51.9	174.6	191.9
3	0.0222	600	390.1	463.5	0.0	714.9	114.9	57.4	174.8	193.9
4	0.0295	600	412.5	470.0	0.0	727.4	127.4	63.7	172.5	193.7
8	0.0591	600	420.6	473.0	0.0	731.8	131.8	65.9	170.9	192.9
14	0.1034	600	435.0	483.5	0.1	739.8	139.8	69.9	163.1	186.4
19	0.1403	600	447.8	498.0	0.1	746.8	146.8	73.4	150.9	175.4
25	0.1846	600	450.3	510.0	0.1	748.1	148.1	74.1	139.4	164.1
29	0.2142	600	447.5	520.0	0.1	746.5	146.5	73.3	128.8	153.3
35	0.2585	600	441.9	530.0	0.1	743.3	143.3	71.7	117.8	141.7
40	0.2954	600	433.7	537.0	0.1	738.7	138.7	69.3	109.2	132.3
50	0.3693	600	428.5	540.0	0.2	735.7	135.7	67.8	105.2	127.8
60	0.4431	600	418.1	545.0	0.2	729.7	129.7	64.9	98.2	119.9
75	0.5539	600	408.0	549.0	0.3	723.9	123.9	62.0	92.3	113.0
85	0.6278	600	400.2	552.0	0.3	719.5	119.5	59.7	87.8	107.7
95	0.7016	600	395.5	554.0	0.4	716.8	116.8	58.4	84.9	104.4
120	0.8863	600	384.8	559.0	0.4	710.5	110.5	55.3	77.8	96.3
165	1.2186	600	368.3	564.0	0.6	700.9	100.9	50.5	69.6	86.5
200	1.4771	600	362.7	567.0	0.7	697.4	97.4	48.7	65.5	81.7
250	1.8464	600	355.6	570.0	0.9	693.0	93.0	46.5	61.0	76.5
300	2.2157	600	350.1	572.0	1.0	689.6	89.6	44.8	57.9	72.8
400	2.9542	600	345.9	575.0	1.0	686.6	86.6	43.3	53.9	68.3
450	3.3235	600	344.0	575.0	1.0	685.2	85.2	42.6	53.4	67.6
500	3.6928	600	343.2	575.5	1.0	684.5	84.5	42.2	52.7	66.7
550	4.0620	600	342.1	576.5	1.0	683.6	83.6	41.8	51.4	65.3

Strain Gauge (divs)	Axial Strain (%)	Cell Press. (kPa)	Proof Ring (divs)	Pore Pressure (kPa)	Membrane Correction (kPa)	P_1 (kPa)	q (kPa)	t (kPa)	p' (kPa)	s' (kPa)
650	4.8006	600	342.0	577.0	1.0	682.9	82.9	41.4	50.6	64.4
755	5.5761	600	342.5	577.0	1.0	682.4	82.4	41.2	50.5	64.2
900	6.6470	600	342.6	577.0	1.0	681.6	81.6	40.8	50.2	63.8
1165	8.6041	600	342.5	577.0	1.0	679.8	79.8	39.9	49.6	62.9
1400	10.3397	600	346.4	577.0	1.0	680.2	80.2	40.1	49.7	63.1
1600	11.8168	600	351.3	577.0	1.0	681.3	81.3	40.6	50.1	63.6
1885	13.9217	600	353.8	577.0	1.0	680.5	80.5	40.2	49.8	63.2
2200	16.2482	600	358.9	577.0	1.0	680.7	80.7	40.3	49.9	63.3
2875	21.2334	600	375.4	577.0	1.0	683.1	83.1	41.5	50.7	64.5
3005	22.1935	600	380.7	577.0	1.0	684.3	84.3	42.2	51.1	65.2







Test	Case 2: Monotonic Undrained Compression of One-Dimensionally Consolidated Specimens		
Cell No.	3 (Big)	Fines content (%)	60
Specimen	K0-8	Specific gravity (g/cm^3)	2.72

1.) Sample physical properties

Wet mass before test (g)	900.686	m.c before test (%)	9.50	Height (mm)	150.85	Volume (cm^3)	696.081
Wet mass after test (g)	1015.760	m.c. after test (%)	23.49	Diameter (mm)	76.65		
Dry mass (g)	822.544	Dry density (kg/m^3)	1182	Area (cm^2)	46.144	Void ratio (e_0)	1.302

2.) Saturation / Consolidation

Proof ring properties		Strain gauge properties		Loading ram properties	
Proof ring No.	5153	1 strain division (mm)	0.01	Area [ram]$_1$ (cm^2)	7.905
Proof ring factor (dN/div)	7.512			Area [ram]$_2$ (cm^2)	5.004

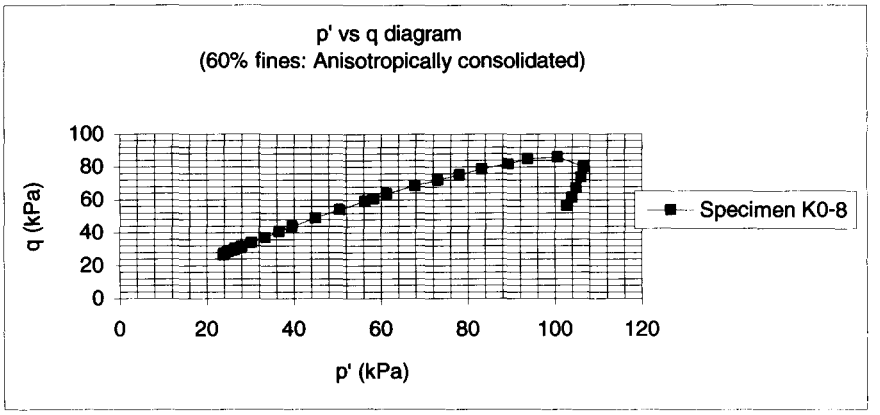
Date	Strain Gauge (divs)	Change Length (mm)	Cell Pressure (kPa)	Proof Ring (div)	Pore Pressure (kPa)	P_1 (kPa)	P'_3 (kPa)	P'_1 (kPa)	q (kPa)	p' (kPa)	K0	Volume Gauge (cm^3)	Cell Expansn (cm^3)
8/4	0	0.000	0	0.0	0.0						\	0.00	0.00
8/4	0	0.000	9.1		5.0	A I R - F L U S H I N G					\	6.58	0.00
8/4	255	2.550	50	122.0	40.0	61.3	10	21.3	11.3	13.8	0.47	43.96	6.08
9/4	469	4.690	100	153.5	90.0	107.9	10	17.9	7.9	12.6	0.56	74.05	8.77
10/4	663	6.630	150	215.4	140.0	159.4	10	19.4	9.4	13.1	0.52	97.12	10.65
11/4	800	8.000	200	253.8	190.0	207.1	10	17.1	7.1	12.4	0.59	115.24	12.00
12/4	905	9.050	250	299.7	240.0	256.0	10	16.0	6.0	12.0	0.63	131.85	13.63
13/4	1024	10.240	300	361.2	290.0	307.4	10	17.4	7.4	12.5	0.57	148.88	15.06
14/4	1140	11.400	350	408.9	340.0	356.6	10	16.6	6.6	12.2	0.60	162.20	16.08
15/4	1263	12.630	400	641.2	350.0	435.9	50	85.9	35.9	62.0	0.58	170.05	18.12
16/4	1457	14.570	450	820.1	366.0	506.4	84	140.4	56.4	102.8	0.60	180.08	19.91

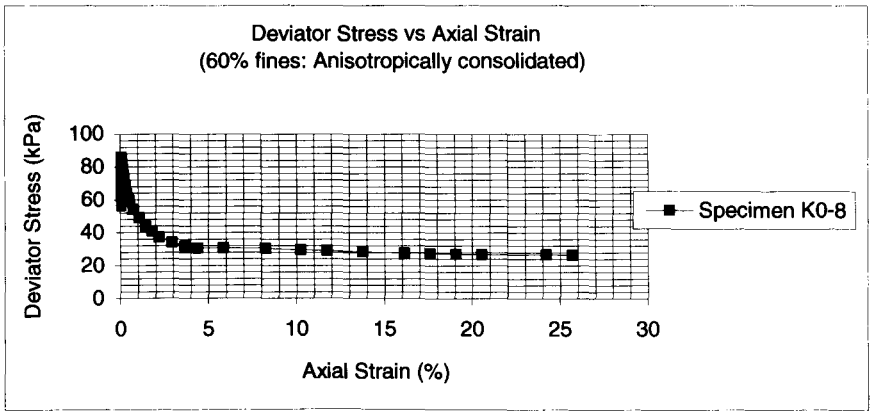
3.) Shear data

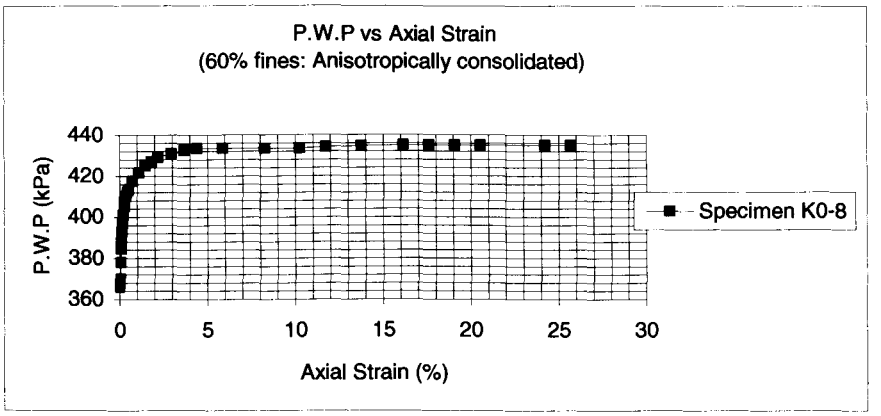
Volume change 1:		Volume change 2:		Sample Vol. change (cm^3)	167.46	B value	0.98
Air Flushing (cm^3)	6.58	Sat/Cons. (cm^3)	173.50	L_{cons} (mm)	136.28	K0	0.60
Cell Expsn. (cm^3)	0.00	Cell Expsn. (cm^3)	19.91	A_{cons} (cm^2)	46.144	Void ratio (e_1)	0.748
		Ram into cell (cm^3)	7.29				

Strain Gauge (divs)	Axial Strain (%)	Cell Press. (kPa)	Proof Ring (divs)	Pore Pressure (kPa)	Membrane Correction (kPa)	P_1 (kPa)	q (kPa)	t (kPa)	p' (kPa)	s' (kPa)
0	0.0000	450	819.3	366.0	0.0	506.3	56.3	28.1	102.8	112.1
1	0.0073	450	850.3	366.5	0.0	511.3	61.3	30.7	103.9	114.2
2	0.0147	450	885.5	367.5	0.0	517.0	67.0	33.5	104.8	116.0
4	0.0294	450	925.9	368.5	0.0	523.6	73.6	36.8	106.0	118.3
6	0.0440	450	965.0	370.0	0.0	530.0	80.0	40.0	106.7	120.0
8	0.0587	450	1002.1	378.0	0.0	536.0	86.0	43.0	100.7	115.0
12	0.0881	450	995.7	384.5	0.0	534.9	84.9	42.4	93.8	107.9
15	0.1101	450	977.6	388.0	0.1	531.9	81.9	41.0	89.3	103.0
20	0.1468	450	958.4	393.0	0.1	528.7	78.7	39.4	83.2	96.4
25	0.1834	450	937.4	397.0	0.1	525.3	75.3	37.6	78.1	90.6
30	0.2201	450	918.2	401.0	0.1	522.1	72.1	36.1	73.0	85.1
40	0.2935	450	896.8	405.0	0.1	518.6	68.6	34.3	67.9	79.3
50	0.3669	450	867.2	410.0	0.2	513.7	63.7	31.8	61.2	71.8
60	0.4403	450	850.0	412.0	0.2	510.8	60.8	30.4	58.3	68.4
70	0.5136	450	842.2	413.5	0.3	509.5	59.5	29.7	56.3	66.2
100	0.7338	450	810.1	417.5	0.4	504.0	54.0	27.0	50.5	59.5
150	1.1007	450	781.5	421.5	0.6	499.0	49.0	24.5	44.8	53.0
200	1.4676	450	750.8	425.0	0.7	493.7	43.7	21.9	39.6	46.9
250	1.8345	450	734.2	427.0	0.9	490.7	40.7	20.4	36.6	43.4
300	2.2014	450	713.5	429.0	1.0	487.2	37.2	18.6	33.4	39.6
400	2.9351	450	695.5	431.0	1.0	484.1	34.1	17.0	30.4	36.0
500	3.6689	450	682.1	432.5	1.0	481.7	31.7	15.9	28.1	33.4
600	4.4027	450	675.6	433.5	1.0	480.4	30.4	15.2	26.6	31.7
800	5.8703	450	680.4	433.5	1.0	480.7	30.7	15.4	26.7	31.9

Strain Gauge (divs)	Axial Strain (%)	Cell Press. (kPa)	Proof Ring (divs)	Pore Pressure (kPa)	Membrane Correction (kPa)	P_1 (kPa)	q (kPa)	t (kPa)	p' (kPa)	s' (kPa)
1125	8.2551	450	682.7	433.5	1.0	480.2	30.2	15.1	26.6	31.6
1395	10.2363	450	682.8	433.5	1.0	479.6	29.6	14.8	26.4	31.3
1600	11.7405	450	682.9	434.0	1.0	479.1	29.1	14.5	25.7	30.5
1875	13.7584	450	682.0	434.5	1.0	478.3	28.3	14.1	24.9	29.6
2200	16.1432	450	682.2	435.0	1.0	477.5	27.5	13.7	24.2	28.7
2400	17.6108	450	684.5	435.0	1.0	477.3	27.3	13.6	24.1	28.6
2600	19.0784	450	686.3	435.0	1.0	477.0	27.0	13.5	24.0	28.5
2800	20.5459	450	688.1	435.0	1.0	476.8	26.8	13.4	23.9	28.4
3300	24.2149	450	698.8	435.0	1.0	476.8	26.8	13.4	23.9	28.4
3500	25.6824	450	700.3	435.0	1.0	476.4	26.4	13.2	23.8	28.2







Test	**Case 2: Monotonic Undrained Compression of One-Dimensionally Consolidated Specimens**		
Cell No.	2 (Big)	Fines content (%)	60
Specimen	K0-15	Specific gravity (g/cm^3)	2.72

1.) Sample physical properties

Wet mass before test (g)	912.592	m.c before test (%)	9.65	Height (mm)	152.15	Volume (cm^3)	703.912
Wet mass after test (g)	1053.746	m.c. after test (%)	26.61	Diameter (mm)	76.75		
Dry mass (g)	832.277	Dry density (kg/m^3)	1182	Area (cm^2)	46.264	Void ratio (e_0)	1.300

2.) Saturation / Consolidation

Proof ring properties		Strain gauge properties		Loading ram properties	
Proof ring No.	5153	1 strain division (mm)	0.01	Area [ram]$_1$ (cm^2)	7.905
Proof ring factor (dN/div)	7.512			Area [ram]$_2$ (cm^2)	5.004

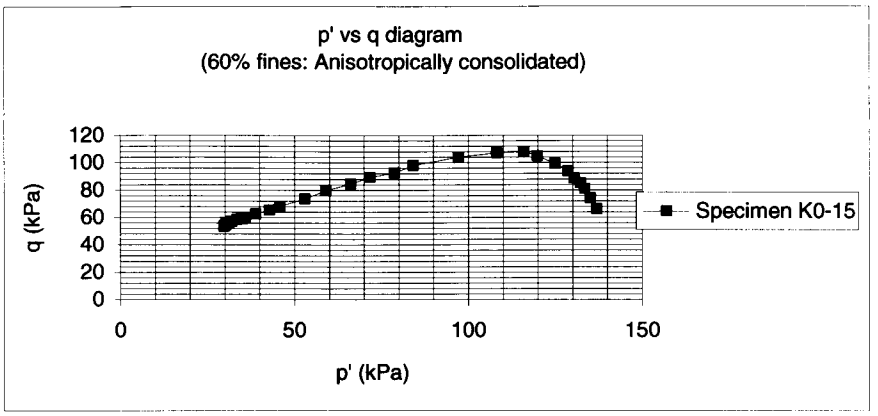
Date	Strain Gauge (divs)	Change Length (mm)	Cell Pressure (kPa)	Proof Ring (div)	Pore Pressure (kPa)	P_1 (kPa)	P'_3 (kPa)	P'_1 (kPa)	q (kPa)	p' (kPa)	K0	Volume Gauge (cm^3)	Cell Expansn (cm^3)
25/5	0	0.000	0	0.0	0.0						\	0.00	0.00
25/5	0	0.000	7.9		3.0	A I R - F L U S H I N G					\	8.25	0.00
25/5	221	2.210	50	124.3	40.0	61.6	10	21.6	11.6	13.9	0.46	48.59	7.06
26/5	422	4.220	100	155.4	90.0	108.1	10	18.1	8.1	12.7	0.55	74.66	9.79
27/5	618	6.180	150	206.6	140.0	157.9	10	17.9	7.9	12.6	0.56	91.05	11.63
28/5	803	8.030	200	254.9	190.0	207.2	10	17.2	7.2	12.4	0.58	101.92	13.02
29/5	974	9.740	250	304.8	240.0	256.8	10	16.8	6.8	12.3	0.60	112.28	14.57
30/5	1122	11.220	300	358.5	290.0	307.0	10	17.0	7.0	12.3	0.59	122.36	16.03
31/5	1255	12.550	350	413.3	340.0	357.3	10	17.3	7.3	12.4	0.58	131.10	17.22
1/6	1388	13.880	400	460.7	390.0	406.5	10	16.5	6.5	12.2	0.61	141.51	19.30
2/6	1522	15.220	450	550.0	430.0	462.4	20	32.4	12.4	24.1	0.62	151.42	20.93
3/6	1902	19.020	550	986.6	435.0	616.2	115	181.2	66.2	137.1	0.63	171.82	23.50

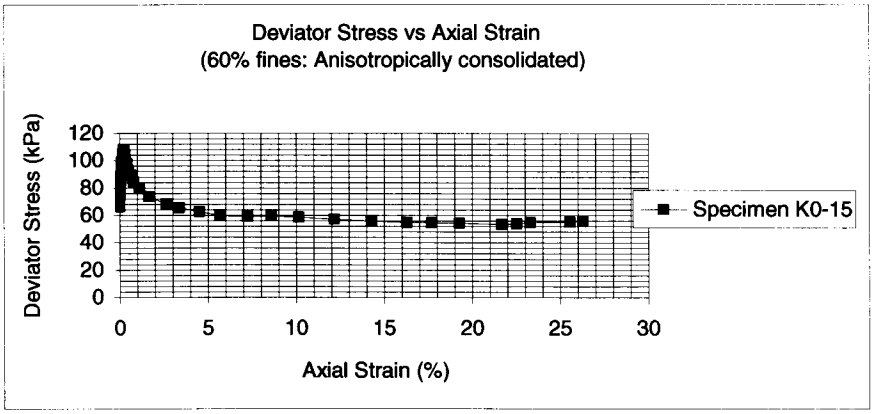
3.) Shear data

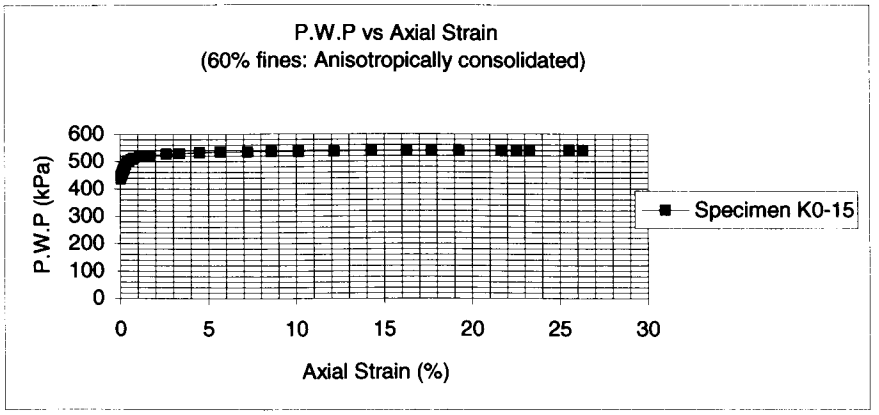
Volume change 1:		Volume change 2:		Sample Vol. change (cm^3)	157.84	B value	0.97
Air Flushing (cm^3)	8.25	Sat/Cons. (cm^3)	163.57	L_{cons} (mm)	133.13	K0	0.63
Cell Expsn. (cm^3)	0.00	Cell Expsn. (cm^3)	23.50	A_{cons} (cm^2)	46.264	Void ratio (e_1)	0.785
		Ram into cell (cm^3)	9.52				

Strain Gauge (divs)	Axial Strain (%)	Cell Press. (kPa)	Proof Ring (divs)	Pore Pressure (kPa)	Membrane Correction (kPa)	P_1 (kPa)	q (kPa)	t (kPa)	p' (kPa)	s' (kPa)
0	0.0000	550	986.1	435.0	0.0	616.1	66.1	33.1	137.0	148.1
2	0.0150	550	1035.3	439.5	0.0	624.1	74.1	37.1	135.2	147.6
5	0.0376	550	1077.5	443.5	0.0	630.9	80.9	40.5	133.5	147.0
7	0.0526	550	1102.9	446.0	0.0	635.0	85.0	42.5	132.3	146.5
10	0.0751	550	1124.6	449.0	0.0	638.5	88.5	44.3	130.5	145.3
15	0.1127	550	1156.8	452.5	0.1	643.7	93.7	46.8	128.7	144.3
18	0.1352	550	1191.1	458.0	0.1	649.2	99.2	49.6	125.1	141.6
23	0.1728	550	1225.2	465.0	0.1	654.7	104.7	52.3	119.9	137.3
28	0.2103	550	1246.4	470.0	0.1	658.1	108.1	54.0	116.0	134.0
35	0.2629	550	1241.5	477.5	0.1	657.2	107.2	53.6	108.2	126.1
40	0.3005	550	1223.1	487.5	0.2	654.2	104.2	52.1	97.2	114.6
55	0.4131	550	1186.0	498.5	0.2	648.0	98.0	49.0	84.2	100.5
65	0.4882	550	1153.3	502.0	0.2	642.6	92.6	46.3	78.9	94.3
85	0.6385	550	1134.0	508.0	0.3	639.3	89.3	44.6	71.8	86.6
105	0.7887	550	1105.7	512.0	0.4	634.5	84.5	42.2	66.2	80.2
150	1.1267	550	1078.6	517.5	0.6	629.7	79.7	39.8	59.1	72.3
220	1.6525	550	1044.1	521.5	0.8	623.5	73.5	36.7	53.0	65.2
350	2.6290	550	1016.5	527.0	1.0	618.2	68.2	34.1	45.7	57.1
450	3.3802	550	1002.6	529.0	1.0	615.5	65.5	32.7	42.8	53.7
600	4.5069	550	988.5	532.0	1.0	612.5	62.5	31.3	38.8	49.3
755	5.6711	550	975.2	534.0	1.0	609.7	59.7	29.9	35.9	45.9
965	7.2486	550	977.1	534.5	1.0	609.0	59.0	29.5	35.2	45.0
1145	8.6006	550	986.4	535.0	1.0	609.5	59.5	29.7	34.8	44.7
1350	10.1405	550	986.5	536.0	1.0	608.5	58.5	29.2	33.5	43.2

Strain Gauge (divs)	Axial Strain (%)	Cell Press. (kPa)	Proof Ring (divs)	Pore Pressure (kPa)	Membrane Correction (kPa)	P_1 (kPa)	q (kPa)	t (kPa)	p' (kPa)	s' (kPa)
1620	12.1686	550	986.7	537.0	1.0	607.2	57.2	28.6	32.1	41.6
1900	14.2718	550	986.8	537.5	1.0	605.8	55.8	27.9	31.1	40.4
2170	16.2999	550	990.2	538.0	1.0	604.9	54.9	27.5	30.3	39.5
2355	17.6895	550	994.3	538.0	1.0	604.5	54.5	27.3	30.2	39.3
2565	19.2669	550	1000.6	538.0	1.0	604.3	54.3	27.1	30.1	39.1
2885	21.6705	550	1006.0	538.0	1.0	603.3	53.3	26.7	29.8	38.7
3000	22.5344	550	1015.1	538.0	1.0	603.9	53.9	26.9	30.0	38.9
3100	23.2855	550	1027.0	538.0	1.0	604.8	54.8	27.4	30.3	39.4
3400	25.5389	550	1042.7	538.0	1.0	605.1	55.1	27.5	30.4	39.5
3500	26.2901	550	1050.8	538.0	1.0	605.5	55.5	27.7	30.5	39.7







Test	**Case 2: Monotonic Undrained Compression of One-Dimensionally Consolidated Specimens**		
Cell No.	3 (Big)	Fines content (%)	60
Specimen	K0-17	Specific gravity (g/cm^3)	2.72

1.) Sample physical properties

Wet mass before test (g)	940.780	m.c before test (%)	9.48	Height (mm)	152.25	Volume (cm^3)	703.458
Wet mass after test (g)	1059.967	m.c. after test (%)	23.35	Diameter (mm)	76.70		
Dry mass (g)	859.317	Dry density (kg/m^3)	1222	Area (cm^2)	46.204	Void ratio (e_0)	1.227

2.) Saturation / Consolidation

Proof ring properties		Strain gauge properties		Loading ram properties	
Proof ring No.	4541	1 strain division (mm)	0.01	Area [ram]$_1$ (cm^2)	7.905
Proof ring factor (dN/div)	25.77			Area [ram]$_2$ (cm^2)	5.004

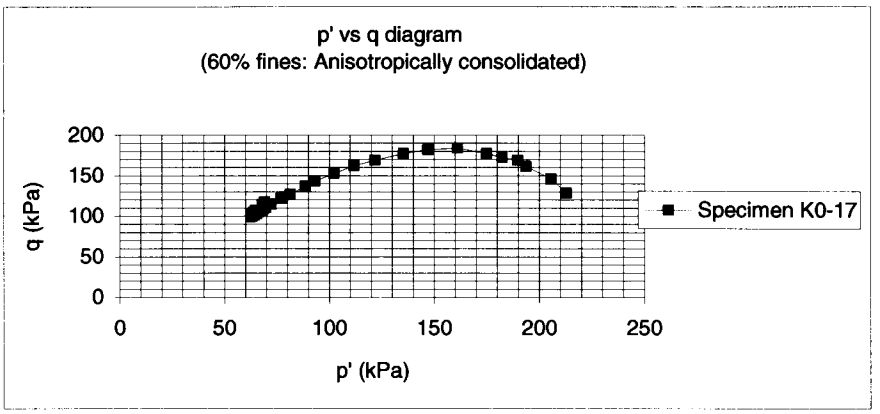
Date	Strain Gauge (divs)	Change Length (mm)	Cell Pressure (kPa)	Proof Ring (div)	Pore Pressure (kPa)	P_1 (kPa)	P'_3 (kPa)	P'_1 (kPa)	q (kPa)	p' (kPa)	K0	Volume Gauge (cm^3)	Cell Expansn (cm^3)
6/6	0	0.000	0	0.0	0.0						\	0.00	0.00
6/6	0	0.000	8.7		3.5	A I R - F L U S H I N G					\	6.98	0.00
6/6	221	2.210	50	34.5	40.0	60.7	10	20.7	10.7	13.6	0.48	41.12	6.08
7/6	402	4.020	100	48.0	90.0	109.7	10	19.7	9.7	13.2	0.51	62.89	8.77
8/6	584	5.840	150	59.1	140.0	157.3	10	17.3	7.3	12.4	0.58	76.16	10.65
9/6	705	7.050	200	74.8	190.0	207.5	10	17.5	7.5	12.5	0.57	86.05	12.00
10/6	802	8.020	250	88.2	240.0	256.4	10	16.4	6.4	12.1	0.61	95.00	13.63
11/6	915	9.150	300	105.3	290.0	307.4	10	17.4	7.4	12.5	0.57	104.27	15.06
12/6	1024	10.240	350	120.7	340.0	357.4	10	17.4	7.4	12.5	0.57	113.54	16.08
13/6	1157	11.570	400	135.9	390.0	407.4	10	17.4	7.4	12.5	0.58	123.35	18.12
14/6	1258	12.580	450	150.0	440.0	456.7	10	16.7	6.7	12.2	0.60	132.22	19.91
15/6	1545	15.450	650	430.2	480.0	778.7	170	298.7	128.7	212.9	0.57	162.98	23.88

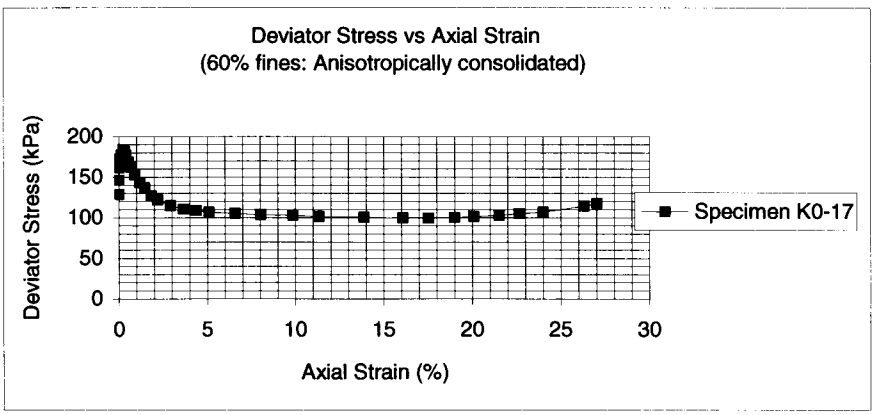
3.) Shear data

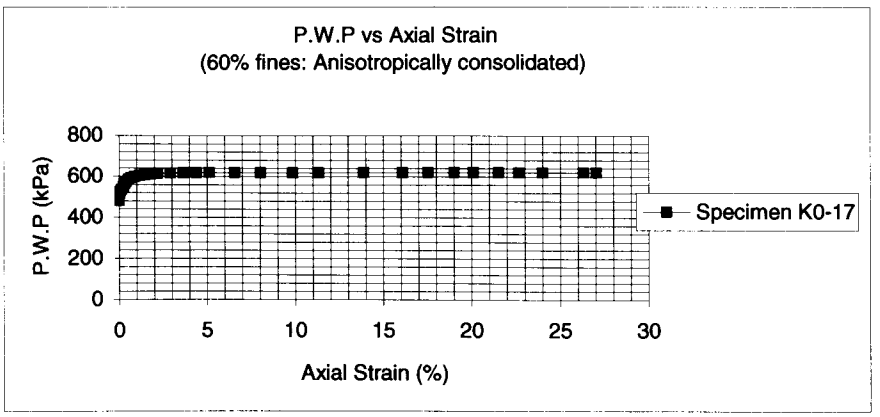
Volume change 1:		Volume change 2:		Sample Vol. change (cm^3)	146.83	B value	0.97
Air Flushing (cm^3)	6.98	Sat/Cons. (cm^3)	156.00	L_{cons} (mm)	136.80	K0	0.57
Cell Expsn. (cm^3)	0.00	Cell Expsn. (cm^3)	23.88	A_{cons} (cm^2)	46.204	Void ratio (e_1)	0.762
		Ram into cell (cm^3)	7.73				

Strain Gauge (divs)	Axial Strain (%)	Cell Press. (kPa)	Proof Ring (divs)	Pore Pressure (kPa)	Membrane Correction (kPa)	P_1 (kPa)	q (kPa)	t (kPa)	p' (kPa)	s' (kPa)
0	0.0000	650	429.8	480.0	0.0	778.5	128.5	64.3	212.8	234.3
1	0.0073	650	461.2	493.0	0.0	796.0	146.0	73.0	205.7	230.0
3	0.0219	650	488.5	510.0	0.0	811.2	161.2	80.6	193.7	220.6
5	0.0365	650	502.2	516.5	0.0	818.8	168.8	84.4	189.8	217.9
10	0.0731	650	508.1	525.0	0.0	822.0	172.0	86.0	182.3	211.0
20	0.1462	650	517.7	534.0	0.1	827.2	177.2	88.6	175.1	204.6
35	0.2558	650	529.8	550.0	0.1	833.7	183.7	91.8	161.2	191.8
45	0.3289	650	526.6	563.5	0.2	831.7	181.7	90.9	147.1	177.4
55	0.4020	650	518.2	573.5	0.2	826.9	176.9	88.5	135.5	165.0
75	0.5482	650	504.4	584.5	0.3	818.9	168.9	84.5	121.8	150.0
95	0.6944	650	492.5	592.0	0.3	812.0	162.0	81.0	112.0	139.0
125	0.9137	650	476.2	598.5	0.5	802.5	152.5	76.3	102.3	127.8
165	1.2061	650	460.1	604.5	0.6	793.1	143.1	71.5	93.2	117.0
200	1.4620	650	449.7	607.0	0.7	786.8	136.8	68.4	88.6	111.4
250	1.8275	650	433.0	611.0	0.9	777.0	127.0	63.5	81.3	102.5
300	2.1930	650	424.6	613.5	1.0	771.9	121.9	60.9	77.1	97.4
400	2.9240	650	412.6	616.0	1.0	764.4	114.4	57.2	72.1	91.2
500	3.6550	650	406.7	617.0	1.0	760.4	110.4	55.2	69.8	88.2
600	4.3860	650	404.9	617.5	1.0	758.6	108.6	54.3	68.7	86.8
700	5.1170	650	402.7	618.0	1.0	756.6	106.6	53.3	67.5	85.3
900	6.5789	650	402.8	618.5	1.0	755.0	105.0	52.5	66.5	84.0
1100	8.0409	650	403.2	619.0	1.0	753.5	103.5	51.8	65.5	82.8
1350	9.8684	650	405.9	619.0	1.0	752.8	102.8	51.4	65.3	82.4
1550	11.3304	650	406.3	619.5	1.0	751.3	101.3	50.7	64.3	81.2

Strain Gauge (divs)	Axial Strain (%)	Cell Press. (kPa)	Proof Ring (divs)	Pore Pressure (kPa)	Membrane Correction (kPa)	P_1 (kPa)	q (kPa)	t (kPa)	p' (kPa)	s' (kPa)
1900	13.8889	650	410.4	620.0	1.0	750.3	100.3	50.2	63.4	80.2
2200	16.0819	650	414.1	620.0	1.0	749.5	99.5	49.7	63.2	79.7
2400	17.5439	650	417.5	620.5	1.0	749.3	99.3	49.7	62.6	79.2
2600	19.0058	650	423.2	620.5	1.0	750.1	100.1	50.1	62.9	79.6
2750	20.1023	650	428.6	621.0	1.0	751.1	101.1	50.6	62.7	79.6
2945	21.5278	650	436.7	621.0	1.0	752.9	102.9	51.4	63.3	80.4
3100	22.6608	650	444.8	621.0	1.0	754.9	104.9	52.4	64.0	81.4
3285	24.0132	650	453.9	621.0	1.0	756.9	106.9	53.4	64.6	82.4
3600	26.3158	650	479.8	620.0	1.0	764.2	114.2	57.1	68.1	87.1
3700	27.0468	650	490.0	620.0	1.0	767.2	117.2	58.6	69.1	88.6







Test	**Case 2: Monotonic Undrained Compression of One-Dimensionally Consolidated Specimens**		
Cell No.	2 (Big)	Fines content (%)	60
Specimen	K0-23	Specific gravity (g/cm^3)	2.72

1.) Sample physical properties

Wet mass before test (g)	955.789	m.c before test (%)	8.99	Height (mm)	151.90	Volume (cm^3)	702.756
Wet mass after test (g)	1125.830	m.c. after test (%)	28.38	Diameter (mm)	76.75		
Dry mass (g)	876.951	Dry density (kg/m^3)	1248	Area (cm^2)	46.264	Void ratio (e_0)	1.180

2.) Saturation / Consolidation

Proof ring properties		Strain gauge properties		Loading ram properties	
Proof ring No.	4541	1 strain division (mm)	0.01	Area [ram]$_1$ (cm^2)	7.905
Proof ring factor (dN/div)	25.77			Area [ram]$_2$ (cm^2)	5.004

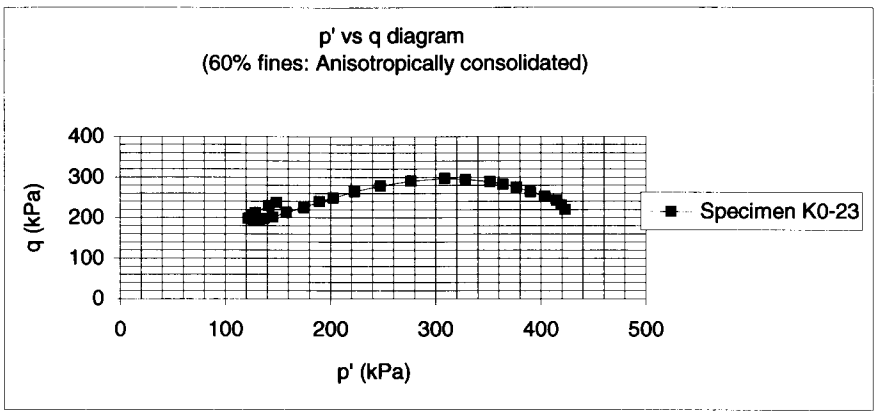
Date	Strain Gauge (divs)	Change Length (mm)	Cell Pressure (kPa)	Proof Ring (div)	Pore Pressure (kPa)	P_1 (kPa)	P'_3 (kPa)	P'_1 (kPa)	q (kPa)	p' (kPa)	K0	Volume Gauge (cm^3)	Cell Expansn (cm^3)
15/7	0	0.000	0	0.0	0.0						\	0.00	0.00
15/7	0	0.000	12.5		8.5	A I R - F L U S H I N G					\	9.60	0.00
15/7	190	1.900	50	40.2	40.0	63.8	10	23.8	13.8	14.6	0.42	39.91	7.06
16/7	365	3.650	100	47.8	90.0	109.5	10	19.5	9.5	13.2	0.51	57.18	9.79
17/7	530	5.300	150	59.1	140.0	157.3	10	17.3	7.3	12.4	0.58	69.55	11.63
18/7	633	6.330	200	77.0	190.0	208.7	10	18.7	8.7	12.9	0.53	81.25	13.02
19/7	728	7.280	250	90.4	240.0	257.6	10	17.6	7.6	12.5	0.57	90.98	14.57
20/7	823	8.230	300	104.8	290.0	307.1	10	17.1	7.1	12.4	0.58	101.24	16.03
21/7	920	9.200	350	120.3	340.0	357.2	10	17.2	7.2	12.4	0.58	112.02	17.22
22/7	1012	10.120	400	135.2	390.0	407.0	10	17.0	7.0	12.3	0.59	116.34	19.30
23/7	1100	11.000	450	150.4	440.0	456.9	10	16.9	6.9	12.3	0.59	121.32	20.93
24/7	1477	14.770	800	640.0	450.0	1019.8	350	569.8	219.8	423.3	0.61	157.55	27.43

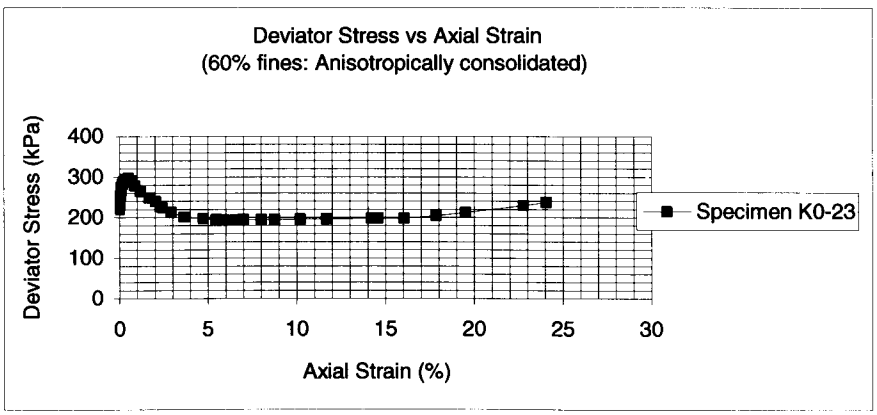
3.) Shear data

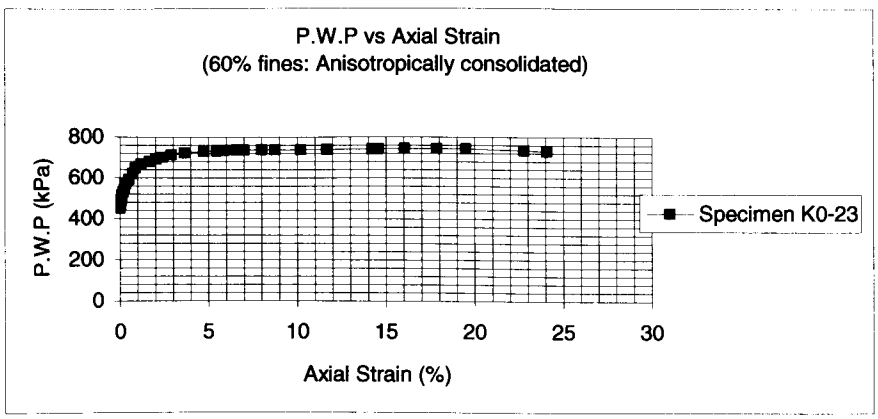
Volume change 1:		Volume change 2:		Sample Vol. change (cm^3)	137.51	B value	0.99
Air Flushing (cm^3)	9.60	Sat/Cons. (cm^3)	147.95	L_{cons} (mm)	137.13	K0	0.61
Cell Expsn. (cm^3)	0.00	Cell Expsn. (cm^3)	27.43	A_{cons} (cm^2)	46.264	Void ratio (e_1)	0.753
		Ram into cell (cm^3)	7.39				

Strain Gauge (divs)	Axial Strain (%)	Cell Press. (kPa)	Proof Ring (divs)	Pore Pressure (kPa)	Membrane Correction (kPa)	P_1 (kPa)	q (kPa)	t (kPa)	p' (kPa)	s' (kPa)
0	0.0000	800	640.0	450.0	0.0	1019.8	219.8	109.9	423.3	459.9
2	0.0146	800	659.5	457.5	0.0	1030.6	230.6	115.3	419.4	457.8
4	0.0292	800	681.6	466.0	0.0	1042.9	242.9	121.4	415.0	455.4
8	0.0583	800	698.1	480.0	0.0	1052.0	252.0	126.0	404.0	446.0
12	0.0875	800	717.8	497.5	0.0	1062.9	262.9	131.4	390.1	433.9
15	0.1094	800	740.3	515.0	0.1	1075.3	275.3	137.7	376.8	422.7
25	0.1823	800	752.9	530.0	0.1	1082.1	282.1	141.0	364.0	411.0
35	0.2552	800	765.4	544.5	0.1	1088.8	288.8	144.4	351.8	399.9
45	0.3282	800	775.0	569.5	0.2	1093.9	293.9	146.9	328.5	377.4
70	0.5105	800	780.8	590.0	0.3	1096.5	296.5	148.2	308.8	358.2
100	0.7292	800	770.1	620.0	0.4	1089.8	289.8	144.9	276.6	324.9
120	0.8751	800	750.3	645.0	0.4	1078.3	278.3	139.2	247.8	294.2
165	1.2032	800	725.8	665.0	0.6	1063.8	263.8	131.9	222.9	266.9
230	1.6772	800	700.2	680.0	0.8	1048.2	248.2	124.1	202.7	244.1
280	2.0419	800	685.6	690.0	1.0	1039.2	239.2	119.6	189.7	229.6
330	2.4065	800	660.5	700.0	1.0	1024.7	224.7	112.3	174.9	212.3
400	2.9169	800	640.0	712.5	1.0	1012.4	212.4	106.2	158.3	193.7
500	3.6462	800	622.1	722.0	1.0	1001.2	201.2	100.6	145.1	178.6
650	4.7400	800	618.7	729.0	1.0	997.1	197.1	98.5	136.7	169.5
750	5.4693	800	616.3	732.0	1.0	994.3	194.3	97.1	132.8	165.1
810	5.9068	800	617.2	735.0	1.0	993.9	193.9	96.9	129.6	161.9
900	6.5631	800	620.0	735.5	1.0	994.0	194.0	97.0	129.2	161.5
960	7.0007	800	622.5	736.0	1.0	994.3	194.3	97.2	128.8	161.2
1100	8.0216	800	626.7	737.0	1.0	994.4	194.4	97.2	127.8	160.2

Strain Gauge (divs)	Axial Strain (%)	Cell Press. (kPa)	Proof Ring (divs)	Pore Pressure (kPa)	Membrane Correction (kPa)	P_1 (kPa)	q (kPa)	t (kPa)	p' (kPa)	s' (kPa)
1200	8.7508	800	630.1	737.0	1.0	994.5	194.5	97.3	127.8	160.3
1400	10.2093	800	637.9	738.0	1.0	995.3	195.3	97.7	127.1	159.7
1600	11.6678	800	645.4	739.0	1.0	995.8	195.8	97.9	126.3	158.9
1950	14.2201	800	660.7	740.5	1.0	997.4	197.4	98.7	125.3	158.2
2000	14.5847	800	662.1	742.5	1.0	997.3	197.3	98.6	123.3	156.1
2200	16.0432	800	670.2	744.0	1.0	997.7	197.7	98.8	121.9	154.8
2450	17.8663	800	693.6	743.0	1.0	1004.1	204.1	102.0	125.0	159.0
2675	19.5070	800	720.0	742.0	1.0	1011.8	211.8	105.9	128.6	163.9
3125	22.7886	800	780.9	735.0	1.0	1029.3	229.3	114.7	141.4	179.7
3300	24.0648	800	807.8	730.0	1.0	1036.9	236.9	118.4	149.0	188.4







Test	**Case 2: Monotonic Undrained Compression of One-Dimensionally Consolidated Specimens**		
Cell No.	2 (Big)	Fines content (%)	60
Specimen	K0-29	Specific gravity (g/cm^3)	2.72

1.) Sample physical properties

Wet mass before test (g)	965.385	m.c before test (%)	8.32	Height (mm)	151.45	Volume (cm^3)	699.761
Wet mass after test (g)	1092.386	m.c. after test (%)	22.57	Diameter (mm)	76.70		
Dry mass (g)	891.234	Dry density (kg/m^3)	1274	Area (cm^2)	46.204	Void ratio (e_0)	1.136

2.) Saturation / Consolidation

Proof ring properties		Strain gauge properties		Loading ram properties	
Proof ring No.	5153	1 strain division (mm)	0.01	Area [ram]$_1$ (cm^2)	7.905
Proof ring factor (dN/div)	7.512			Area [ram]$_2$ (cm^2)	5.004

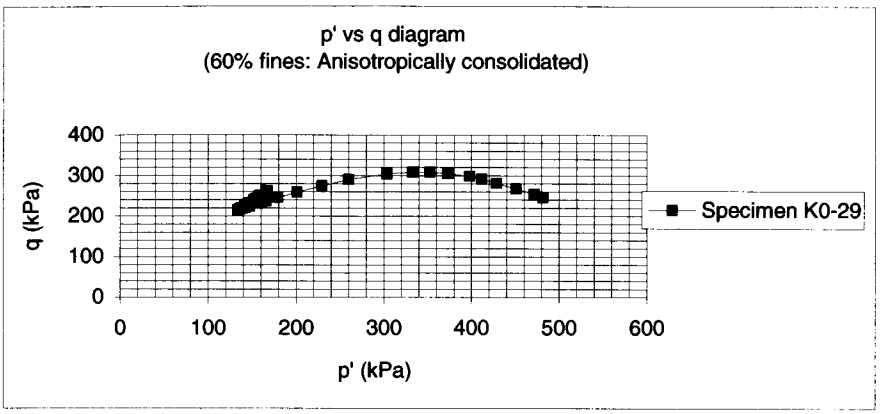
Date	Strain Gauge (divs)	Change Length (mm)	Cell Pressure (kPa)	Proof Ring (div)	Pore Pressure (kPa)	P_1 (kPa)	P'_3 (kPa)	P'_1 (kPa)	q (kPa)	p' (kPa)	K0	Volume Gauge (cm^3)	Cell Expansn (cm^3)
22/8	0	0.000	0	0.0	0.0						\	0.00	0.00
22/8	0	0.000	11.0		6.5	A I R - F L U S H I N G					\	8.64	0.00
22/8	202	2.020	50	134.5	40.0	63.3	10	23.3	13.3	14.4	0.43	34.21	7.06
23/8	400	4.000	100	151.1	90.0	107.5	10	17.5	7.5	12.5	0.57	49.00	9.79
24/8	551	5.510	150	194.4	140.0	155.9	10	15.9	5.9	12.0	0.63	58.94	11.63
25/8	644	6.440	200	251.7	190.0	206.7	10	16.7	6.7	12.2	0.60	66.32	13.02
26/8	740	7.400	250	296.2	240.0	255.4	10	15.4	5.4	11.8	0.65	72.18	14.57
27/8	833	8.330	300	353.9	290.0	306.2	10	16.2	6.2	12.1	0.62	78.09	16.03
28/8	925	9.250	350	407.0	340.0	356.3	10	16.3	6.3	12.1	0.61	83.21	17.22
29/8	1005	10.050	400	463.5	390.0	406.9	10	16.9	6.9	12.3	0.59	89.10	19.30
30/8	1100	11.000	450	516.6	440.0	457.0	10	17.0	7.0	12.3	0.59	95.14	20.93
31/8	1187	11.870	500	564.0	490.0	506.2	10	16.2	6.2	12.1	0.62	100.28	22.85
1/9	1580	15.800	900	2456.6	500.0	1145.4	400	645.4	245.4	481.8	0.62	154.12	28.25

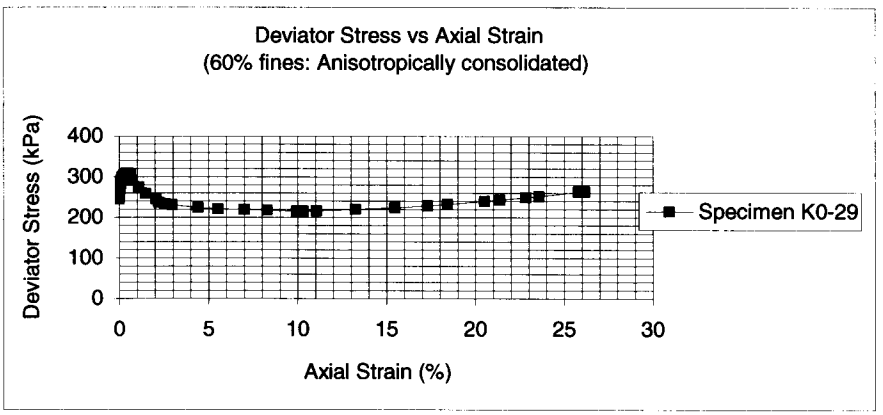
3.) Shear data

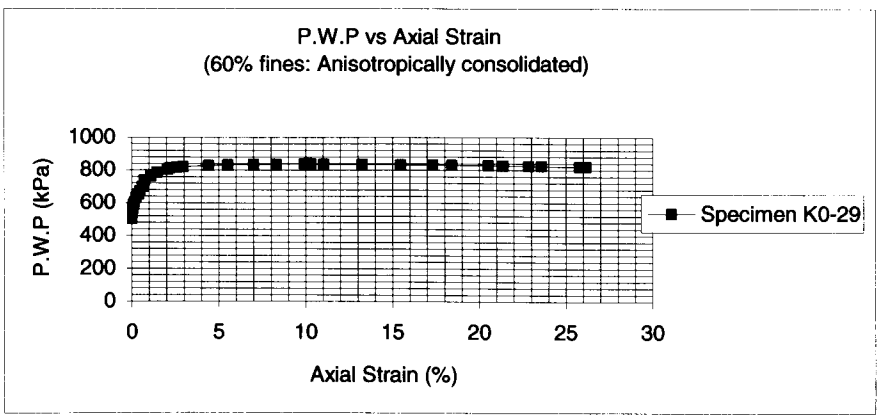
Volume change 1:		Volume change 2:		Sample Vol. change (cm^3)	133.78	B value	0.98
Air Flushing (cm^3)	8.64	Sat/Cons. (cm^3)	145.48	L_{cons} (mm)	135.65	K0	0.62
Cell Expsn. (cm^3)	0.00	Cell Expsn. (cm^3)	28.25	A_{cons} (cm^2)	46.204	Void ratio (e_1)	0.727
		Ram into cell (cm^3)	7.91				

Strain Gauge (divs)	Axial Strain (%)	Cell Press. (kPa)	Proof Ring (divs)	Pore Pressure (kPa)	Membrane Correction (kPa)	P_1 (kPa)	q (kPa)	t (kPa)	p' (kPa)	s' (kPa)
0	0.0000	900	2455.8	500.0	0.0	1145.3	245.3	122.6	481.8	522.6
3	0.0221	900	2506.3	512.5	0.0	1153.4	253.4	126.7	472.0	514.2
6	0.0442	900	2590.5	538.0	0.0	1167.1	267.1	133.5	451.0	495.5
10	0.0737	900	2675.1	565.0	0.0	1180.7	280.7	140.4	428.6	475.4
15	0.1106	900	2739.9	585.0	0.1	1191.1	291.1	145.6	412.0	460.6
22	0.1622	900	2785.7	601.5	0.1	1198.4	298.4	149.2	398.0	447.7
35	0.2580	900	2824.5	628.5	0.1	1204.3	304.3	152.2	372.9	423.7
55	0.4055	900	2852.3	650.0	0.2	1208.3	308.3	154.1	352.8	404.1
65	0.4792	900	2855.9	670.0	0.2	1208.6	308.6	154.3	332.9	384.3
85	0.6266	900	2830.1	697.5	0.3	1203.9	303.9	152.0	303.8	354.5
100	0.7372	900	2746.7	736.5	0.4	1190.1	290.1	145.0	260.2	308.5
150	1.1058	900	2654.3	761.5	0.6	1173.9	273.9	137.0	229.8	275.5
200	1.4744	900	2566.6	785.0	0.7	1158.7	258.7	129.3	201.2	244.3
280	2.0641	900	2493.4	802.5	1.0	1145.2	245.2	122.6	179.2	220.1
300	2.2116	900	2440.5	813.0	1.0	1136.4	236.4	118.2	165.8	205.2
350	2.5802	900	2423.8	816.5	1.0	1132.9	232.9	116.4	161.1	199.9
400	2.9488	900	2415.1	820.0	1.0	1130.6	230.6	115.3	156.9	195.3
600	4.4231	900	2393.0	827.5	1.0	1123.7	223.7	111.8	147.1	184.3
750	5.5289	900	2389.4	831.5	1.0	1120.5	220.5	110.3	142.0	178.8
950	7.0033	900	2401.8	833.5	1.0	1119.0	219.0	109.5	139.5	176.0
1125	8.2934	900	2410.6	836.0	1.0	1117.2	217.2	108.6	136.4	172.6
1350	9.9521	900	2420.7	838.0	1.0	1114.7	214.7	107.4	133.6	169.4
1400	10.3207	900	2431.2	837.5	1.0	1115.4	215.4	107.7	134.3	170.2
1500	11.0579	900	2445.7	836.0	1.0	1115.7	215.7	107.9	135.9	171.9

Strain Gauge (divs)	Axial Strain (%)	Cell Press. (kPa)	Proof Ring (divs)	Pore Pressure (kPa)	Membrane Correction (kPa)	P_1 (kPa)	q (kPa)	t (kPa)	p' (kPa)	s' (kPa)
1800	13.2694	900	2512.5	835.0	1.0	1119.7	219.7	109.9	138.2	174.9
2100	15.4810	900	2584.4	833.0	1.0	1124.0	224.0	112.0	141.7	179.0
2350	17.3240	900	2655.0	831.5	1.0	1128.6	228.6	114.3	144.7	182.8
2500	18.4298	900	2706.5	830.0	1.0	1132.3	232.3	116.2	147.4	186.2
2785	20.5308	900	2808.9	828.0	1.0	1139.6	239.6	119.8	151.9	191.8
2900	21.3785	900	2855.3	826.5	1.0	1142.9	242.9	121.5	154.5	195.0
3100	22.8529	900	2940.5	825.0	1.0	1149.0	249.0	124.5	158.0	199.5
3200	23.5901	900	2979.6	824.0	1.0	1151.5	251.5	125.8	159.8	201.8
3500	25.8017	900	3131.2	820.5	1.0	1162.5	262.5	131.2	167.0	210.7
3550	26.1703	900	3140.0	820.0	1.0	1162.2	262.2	131.1	167.4	211.1







Test	**Case 2: Monotonic Undrained Compression of One-Dimensionally Consolidated Specimens**		
Cell No.	3 (Big)	Fines content (%)	60
Specimen	K0-30	Specific gravity (g/cm^3)	2.72

1.) Sample physical properties

Wet mass before test (g)	963.694	m.c before test (%)	9.18	Height (mm)	151.30	Volume (cm^3)	700.892
Wet mass after test (g)	1091.592	m.c. after test (%)	23.67	Diameter (mm)	76.80		
Dry mass (g)	882.665	Dry density (kg/m^3)	1259	Area (cm^2)	46.325	Void ratio (e_0)	1.160

2.) Saturation / Consolidation

Proof ring properties		Strain gauge properties		Loading ram properties	
Proof ring No.	4541	1 strain division (mm)	0.01	Area [ram]$_1$ (cm^2)	7.905
Proof ring factor (dN/div)	25.77			Area [ram]$_2$ (cm^2)	5.004

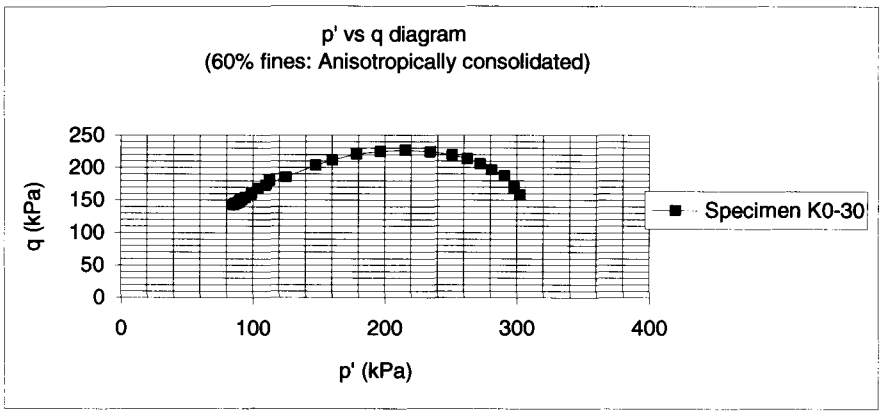
Date	Strain Gauge (divs)	Change Length (mm)	Cell Pressure (kPa)	Proof Ring (div)	Pore Pressure (kPa)	P_1 (kPa)	P'_3 (kPa)	P'_1 (kPa)	q (kPa)	p' (kPa)	K0	Volume Gauge (cm^3)	Cell Expansn (cm^3)
22/8	0	0.000	0	0.0	0.0						\	0.00	0.00
22/8	0	0.000	10.2		6.0	A I R - F L U S H I N G					\	9.12	0.00
22/8	190	1.900	50	37.8	40.0	62.5	10	22.5	12.5	14.2	0.44	36.55	6.08
23/8	351	3.510	100	50.0	90.0	110.8	10	20.8	10.8	13.6	0.48	52.79	8.77
24/8	457	4.570	150	59.3	140.0	157.4	10	17.4	7.4	12.5	0.57	65.01	10.65
25/8	550	5.500	200	74.5	190.0	207.3	10	17.3	7.3	12.4	0.58	72.20	12.00
26/8	645	6.450	250	90.1	240.0	257.5	10	17.5	7.5	12.5	0.57	78.51	13.63
27/8	742	7.420	300	107.2	290.0	308.4	10	18.4	8.4	12.8	0.54	83.94	15.06
28/8	830	8.300	350	120.7	340.0	357.4	10	17.4	7.4	12.5	0.57	89.20	16.08
29/8	924	9.240	400	135.4	390.0	407.1	10	17.1	7.1	12.4	0.59	95.41	18.12
30/8	1021	10.210	450	150.0	440.0	456.7	10	16.7	6.7	12.2	0.60	102.54	19.91
31/8	1100	11.000	500	166.3	490.0	507.2	10	17.2	7.2	12.4	0.58	109.67	21.79
1/9	1412	14.120	750	514.5	500.0	908.2	250	408.2	158.2	302.7	0.61	148.03	24.85

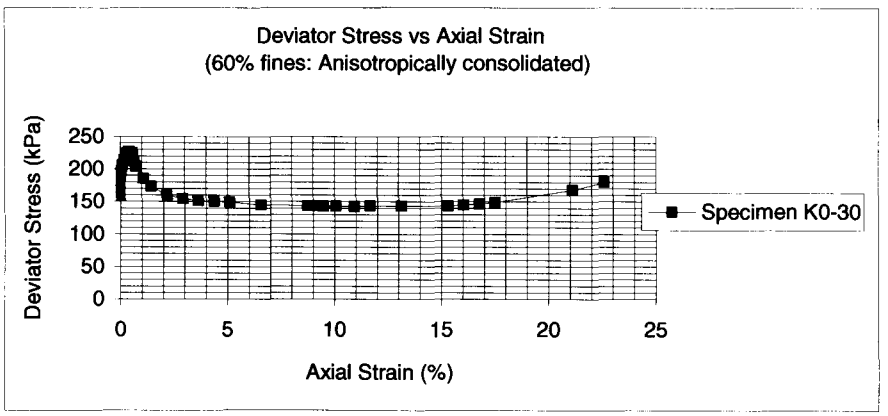
3.) Shear data

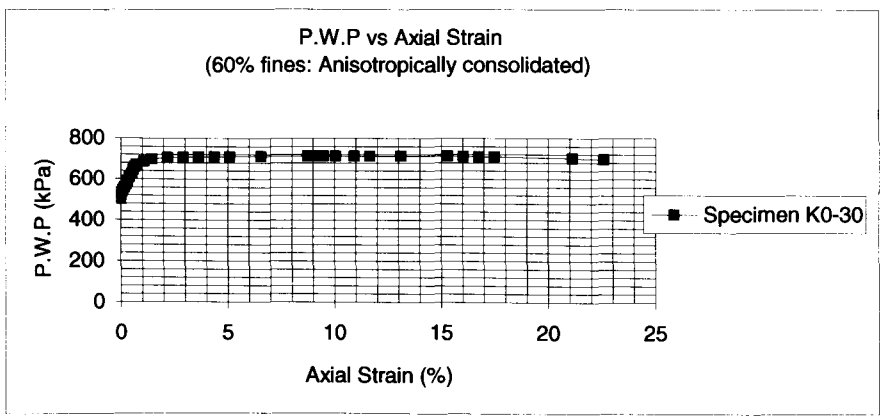
Volume change 1:		Volume change 2:		Sample Vol. change (cm^3)	130.25	B value	0.97
Air Flushing (cm^3)	9.12	Sat/Cons. (cm^3)	138.91	L_{cons} (mm)	137.18	K0	0.61
Cell Expsn. (cm^3)	0.00	Cell Expsn. (cm^3)	24.85	A_{cons} (cm^2)	46.325	Void ratio (e_1)	0.758
		Ram into cell (cm^3)	7.07				

Strain Gauge (divs)	Axial Strain (%)	Cell Press. (kPa)	Proof Ring (divs)	Pore Pressure (kPa)	Membrane Correction (kPa)	P_1 (kPa)	q (kPa)	t (kPa)	p' (kPa)	s' (kPa)
0	0.0000	750	514.3	500.0	0.0	908.1	158.1	79.1	302.7	329.1
1	0.0073	750	535.0	508.5	0.0	919.6	169.6	84.8	298.0	326.3
3	0.0219	750	566.4	521.5	0.0	937.1	187.1	93.5	290.9	322.0
9	0.0656	750	583.8	534.5	0.0	946.6	196.6	98.3	281.0	313.8
15	0.1093	750	599.9	546.0	0.1	955.5	205.5	102.7	272.5	306.7
25	0.1822	750	614.6	558.5	0.1	963.4	213.4	106.7	262.6	298.2
35	0.2551	750	626.0	572.0	0.1	969.6	219.6	109.8	251.2	287.8
45	0.3280	750	635.1	590.0	0.2	974.4	224.4	112.2	234.8	272.2
55	0.4009	750	639.3	610.0	0.2	976.5	226.5	113.3	215.5	253.3
75	0.5467	750	636.6	628.0	0.3	974.6	224.6	112.3	196.9	234.3
80	0.5832	750	629.7	645.0	0.3	970.7	220.7	110.4	178.6	215.4
90	0.6561	750	612.9	660.0	0.3	961.2	211.2	105.6	160.4	195.6
100	0.7290	750	599.2	670.0	0.4	953.5	203.5	101.7	147.8	181.7
150	1.0935	750	568.0	686.5	0.5	935.4	185.4	92.7	125.3	156.2
200	1.4579	750	546.8	697.5	0.7	922.9	172.9	86.5	110.1	139.0
300	2.1869	750	524.9	704.0	1.0	909.4	159.4	79.7	99.1	125.7
400	2.9159	750	517.6	707.0	1.0	904.3	154.3	77.1	94.4	120.1
500	3.6448	750	514.3	708.5	1.0	901.4	151.4	75.7	92.0	117.2
600	4.3738	750	514.1	709.0	1.0	900.1	150.1	75.0	91.0	116.0
700	5.1028	750	514.6	709.5	1.0	899.2	149.2	74.6	90.2	115.1
900	6.5607	750	510.2	711.5	1.0	894.6	144.6	72.3	86.7	110.8
1200	8.7476	750	514.5	712.0	1.0	893.4	143.4	71.7	85.8	109.7
1250	9.1121	750	515.4	712.0	1.0	893.3	143.3	71.6	85.8	109.6
1300	9.4766	750	515.9	712.0	1.0	892.9	142.9	71.5	85.6	109.5

Strain Gauge (divs)	Axial Strain (%)	Cell Press. (kPa)	Proof Ring (divs)	Pore Pressure (kPa)	Membrane Correction (kPa)	P_1 (kPa)	q (kPa)	t (kPa)	p' (kPa)	s' (kPa)
1380	10.0598	750	517.2	712.0	1.0	892.7	142.7	71.3	85.6	109.3
1500	10.9345	750	519.0	712.0	1.0	892.2	142.2	71.1	85.4	109.1
1600	11.6635	750	523.7	712.0	1.0	893.3	143.3	71.6	85.8	109.6
1800	13.1214	750	528.3	712.0	1.0	893.1	143.1	71.6	85.7	109.6
2100	15.3084	750	535.8	712.0	1.0	893.0	143.0	71.5	85.7	109.5
2200	16.0373	750	542.0	711.0	1.0	894.7	144.7	72.4	87.2	111.4
2300	16.7663	750	548.4	710.0	1.0	896.4	146.4	73.2	88.8	113.2
2400	17.4953	750	556.6	709.5	1.0	898.9	148.9	74.4	90.1	114.9
2900	21.1401	750	614.9	702.0	1.0	917.8	167.8	83.9	103.9	131.9
3100	22.5980	750	650.0	697.0	1.0	929.8	179.8	89.9	112.9	142.9







Test	**Case 2: Monotonic Undrained Compression of One-Dimensionally Consolidated Specimens**		
Cell No.	2 (Big)	Fines content (%)	60
Specimen	K0-31	Specific gravity (g/cm^3)	2.72

1.) Sample physical properties

Wet mass before test (g)	992.312	m.c before test (%)	10.11	Height (mm)	151.60	Volume (cm^3)	699.541
Wet mass after test (g)	1115.146	m.c. after test (%)	23.74	Diameter (mm)	76.65		
Dry mass (g)	901.201	Dry density (kg/m^3)	1288	Area (cm^2)	46.144	Void ratio (e_0)	1.111

2.) Saturation / Consolidation

Proof ring properties		Strain gauge properties		Loading ram properties	
Proof ring No.	5153	1 strain division (mm)	0.01	Area [ram]$_1$ (cm^2)	7.905
Proof ring factor (dN/div)	7.512			Area [ram]$_2$ (cm^2)	5.004

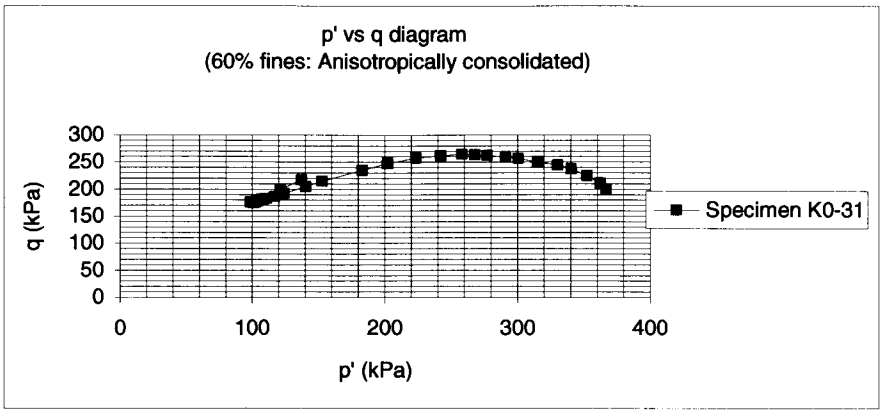
Date	Strain Gauge (divs)	Change Length (mm)	Cell Pressure (kPa)	Proof Ring (div)	Pore Pressure (kPa)	P_1 (kPa)	P'_3 (kPa)	P'_1 (kPa)	q (kPa)	p' (kPa)	K0	Volume Gauge (cm^3)	Cell Expansn (cm^3)
3/9	0	0.000	0	0.0	0.0						\	0.00	0.00
3/9	0	0.000	8.8		4.0	A I R - F L U S H I N G					\	10.05	0.00
3/9	201	2.010	50	110.0	40.0	59.3	10	19.3	9.3	13.1	0.52	33.85	7.06
4/9	387	3.870	100	152.3	90.0	107.7	10	17.7	7.7	12.6	0.57	46.92	9.79
5/9	516	5.160	150	199.9	140.0	156.8	10	16.8	6.8	12.3	0.59	56.20	11.63
6/9	632	6.320	200	249.2	190.0	206.3	10	16.3	6.3	12.1	0.61	62.18	13.02
7/9	724	7.240	250	300.0	240.0	256.0	10	16.0	6.0	12.0	0.62	68.00	14.57
8/9	815	8.150	300	354.3	290.0	306.3	10	16.3	6.3	12.1	0.61	74.23	16.03
9/9	911	9.110	350	412.6	340.0	357.2	10	17.2	7.2	12.4	0.58	79.61	17.22
10/9	1000	10.000	400	462.4	390.0	406.8	10	16.8	6.8	12.3	0.60	86.54	19.30
11/9	1094	10.940	450	518.7	440.0	457.4	10	17.4	7.4	12.5	0.58	92.40	20.93
12/9	1563	15.630	850	2125.2	550.0	1050.4	300	500.4	200.4	366.8	0.60	138.99	27.13

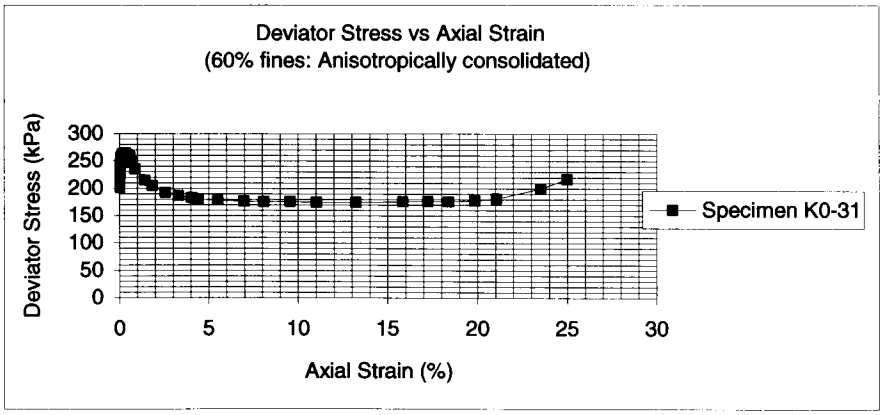
3.) Shear data

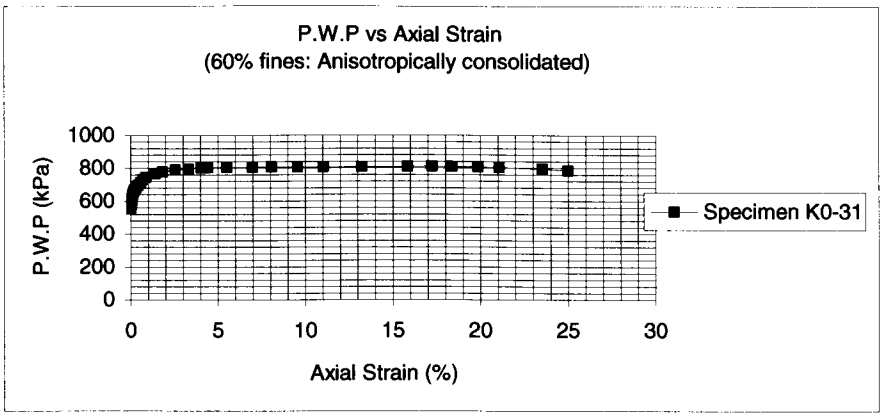
Volume change 1:		Volume change 2:		Sample Vol. change (cm^3)	119.68	B value	0.97
Air Flushing (cm^3)	10.05	Sat/Cons. (cm^3)	128.94	L_{cons} (mm)	135.97	K0	0.60
Cell Expsn. (cm^3)	0.00	Cell Expsn. (cm^3)	27.13	A_{cons} (cm^2)	46.144	Void ratio (e_1)	0.750
		Ram into cell (cm^3)	7.82				

Strain Gauge (divs)	Axial Strain (%)	Cell Press. (kPa)	Proof Ring (divs)	Pore Pressure (kPa)	Membrane Correction (kPa)	P_1 (kPa)	q (kPa)	t (kPa)	p' (kPa)	s' (kPa)
0	0.0000	850	2125.0	550.0	0.0	1050.3	200.3	100.2	366.8	400.2
2	0.0147	850	2191.3	558.0	0.0	1061.1	211.1	105.5	362.4	397.5
4	0.0294	850	2275.5	572.5	0.0	1074.7	224.7	112.4	352.4	389.9
8	0.0588	850	2352.4	588.5	0.0	1087.2	237.2	118.6	340.6	380.1
10	0.0735	850	2396.0	601.0	0.0	1094.2	244.2	122.1	330.4	371.1
12	0.0883	850	2428.6	618.0	0.0	1099.5	249.5	124.7	315.2	356.7
14	0.1030	850	2472.7	635.0	0.1	1106.6	256.6	128.3	300.5	343.3
19	0.1397	850	2485.9	645.0	0.1	1108.6	258.6	129.3	291.2	334.3
25	0.1839	850	2506.3	660.0	0.1	1111.8	261.8	130.9	277.3	320.9
33	0.2427	850	2517.5	670.0	0.1	1113.5	263.5	131.7	267.8	311.7
46	0.3383	850	2525.3	680.0	0.2	1114.4	264.4	132.2	258.1	302.2
60	0.4413	850	2508.2	695.0	0.2	1111.3	261.3	130.7	242.1	285.7
80	0.5884	850	2484.5	712.0	0.3	1107.0	257.0	128.5	223.7	266.5
100	0.7355	850	2425.0	730.0	0.4	1097.0	247.0	123.5	202.3	243.5
120	0.8825	850	2352.9	745.0	0.4	1084.9	234.9	117.4	183.3	222.4
195	1.4341	850	2236.0	768.5	0.7	1064.5	214.5	107.3	153.0	188.8
250	1.8386	850	2180.4	777.5	0.9	1054.6	204.6	102.3	140.7	174.8
350	2.5741	850	2113.7	790.0	1.0	1042.4	192.4	96.2	124.1	156.2
450	3.3096	850	2084.5	795.0	1.0	1036.3	186.3	93.2	117.1	148.2
550	4.0450	850	2069.7	800.0	1.0	1032.6	182.6	91.3	110.9	141.3
600	4.4127	850	2062.3	802.0	1.0	1030.7	180.7	90.4	108.2	138.4
750	5.5159	850	2060.5	805.0	1.0	1028.4	178.4	89.2	104.5	134.2
950	6.9868	850	2063.9	805.5	1.0	1026.1	176.1	88.0	103.2	132.5
1100	8.0900	850	2076.4	806.0	1.0	1025.8	175.8	87.9	102.6	131.9

Strain Gauge (divs)	Axial Strain (%)	Cell Press. (kPa)	Proof Ring (divs)	Pore Pressure (kPa)	Membrane Correction (kPa)	P_1 (kPa)	q (kPa)	t (kPa)	p' (kPa)	s' (kPa)
1300	9.5609	850	2095.8	807.0	1.0	1025.9	175.9	87.9	101.6	130.9
1500	11.0318	850	2108.4	807.5	1.0	1024.8	174.8	87.4	100.8	129.9
1800	13.2382	850	2137.1	807.0	1.0	1024.5	174.5	87.3	101.2	130.3
2155	15.8491	850	2185.6	808.0	1.0	1025.9	175.9	87.9	100.6	129.9
2345	17.2465	850	2210.7	810.0	1.0	1026.3	176.3	88.2	98.8	128.2
2500	18.3864	850	2223.3	808.0	1.0	1025.6	175.6	87.8	100.5	129.8
2700	19.8573	850	2260.7	806.0	1.0	1027.3	177.3	88.6	103.1	132.6
2865	21.0708	850	2311.9	803.0	1.0	1031.1	181.1	90.6	107.4	137.6
3200	23.5346	850	2506.9	795.0	1.0	1049.7	199.7	99.9	121.6	154.9
3400	25.0055	850	2680.2	785.0	1.0	1067.0	217.0	108.5	137.3	173.5







Test	**Case 2: Monotonic Undrained Compression of One-Dimensionally Consolidated Specimens**		
Cell No.	3 (Big)	Fines content (%)	60
Specimen	K0-36	Specific gravity (g/cm^3)	2.72

1.) Sample physical properties

Wet mass before test (g)	957.173	m.c before test (%)	8.97	Height (mm)	152.35	Volume (cm^3)	703.920
Wet mass after test (g)	1132.410	m.c. after test (%)	28.92	Diameter (mm)	76.70		
Dry mass (g)	878.382	Dry density (kg/m^3)	1248	Area (cm^2)	46.204	Void ratio (e_0)	1.180

2.) Saturation / Consolidation

Proof ring properties		Strain gauge properties		Loading ram properties	
Proof ring No.	5153	1 strain division (mm)	0.01	Area [ram]$_1$ (cm^2)	7.905
Proof ring factor (dN/div)	7.512			Area [ram]$_2$ (cm^2)	5.004

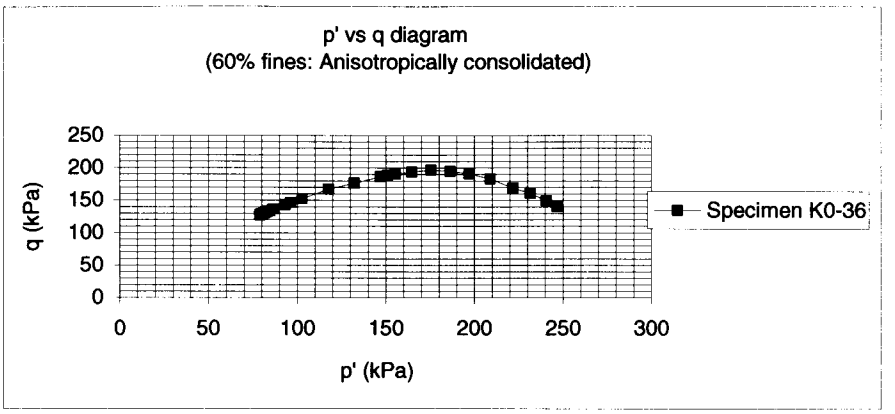
Date	Strain Gauge (divs)	Change Length (mm)	Cell Pressure (kPa)	Proof Ring (div)	Pore Pressure (kPa)	P_1 (kPa)	P'_3 (kPa)	P'_1 (kPa)	q (kPa)	p' (kPa)	K0	Volume Gauge (cm^3)	Cell Expansn (cm^3)
27/9	0	0.000	0	0.0	0.0						\	0.00	0.00
27/9	0	0.000	8.0		3.5	A I R - F L U S H I N G					\	9.47	0.00
27/9	235	2.350	50	103.2	40.0	58.2	10	18.2	8.2	12.7	0.55	38.41	6.08
28/9	433	4.330	100	148.9	90.0	107.1	10	17.1	7.1	12.4	0.58	60.05	8.77
29/9	600	6.000	150	201.1	140.0	157.0	10	17.0	7.0	12.3	0.59	73.20	10.65
30/9	741	7.410	200	257.4	190.0	207.6	10	17.6	7.6	12.5	0.57	82.18	12.00
1/10	855	8.550	250	304.5	240.0	256.7	10	16.7	6.7	12.2	0.60	90.16	13.63
2/10	958	9.580	300	354.0	290.0	306.2	10	16.2	6.2	12.1	0.62	95.54	15.06
3/10	1045	10.450	350	412.9	340.0	357.3	10	17.3	7.3	12.4	0.58	102.61	16.08
4/10	1147	11.470	400	463.5	390.0	406.9	10	16.9	6.9	12.3	0.59	107.97	18.12
5/10	1235	12.350	450	513.8	440.0	456.5	10	16.5	6.5	12.2	0.60	114.99	19.91
6/10	1600	16.000	700	1602.3	500.0	840.7	200	340.7	140.7	246.9	0.59	147.68	23.84

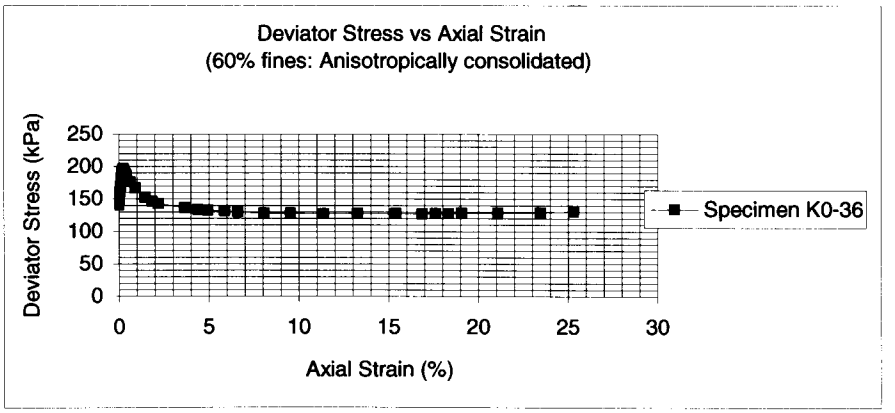
3.) Shear data

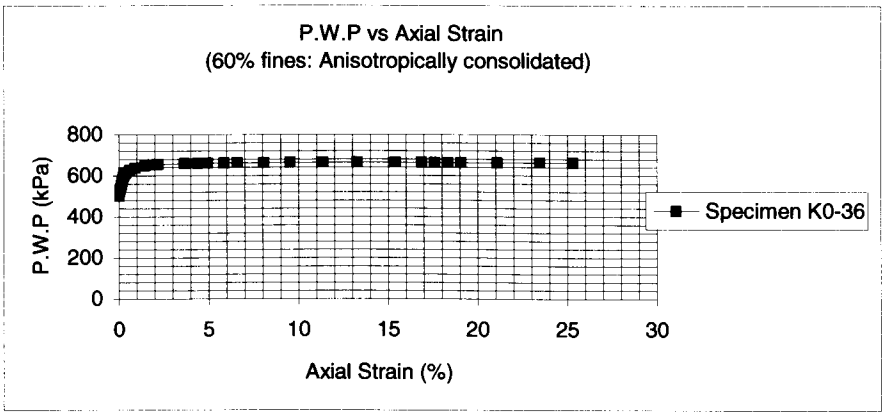
Volume change 1:		Volume change 2:		Sample Vol. change (cm^3)	131.85	B value	0.97
Air Flushing (cm^3)	9.47	Sat/Cons. (cm^3)	138.21	L_{cons} (mm)	136.35	K0	0.59
Cell Expsn. (cm^3)	0.00	Cell Expsn. (cm^3)	23.84	A_{cons} (cm^2)	46.204	Void ratio (e_1)	0.771
		Ram into cell (cm^3)	8.01				

Strain Gauge (divs)	Axial Strain (%)	Cell Press. (kPa)	Proof Ring (divs)	Pore Pressure (kPa)	Membrane Correction (kPa)	P_1 (kPa)	q (kPa)	t (kPa)	p' (kPa)	s' (kPa)
0	0.0000	700	1600.2	500.0	0.0	840.4	140.4	70.2	246.8	270.2
3	0.0220	700	1653.8	509.0	0.0	849.1	149.1	74.5	240.7	265.5
8	0.0587	700	1725.0	522.0	0.0	860.6	160.6	80.3	231.5	258.3
12	0.0880	700	1778.6	534.5	0.0	869.2	169.2	84.6	221.9	250.1
20	0.1467	700	1864.1	552.0	0.1	883.0	183.0	91.5	209.0	239.5
25	0.1834	700	1911.5	566.5	0.1	890.6	190.6	95.3	197.0	228.8
30	0.2200	700	1935.9	578.5	0.1	894.4	194.4	97.2	186.3	218.7
35	0.2567	700	1950.0	590.0	0.1	896.6	196.6	98.3	175.5	208.3
40	0.2934	700	1933.2	600.0	0.1	893.8	193.8	96.9	164.6	196.9
45	0.3300	700	1912.2	608.0	0.2	890.3	190.3	95.2	155.4	187.2
50	0.3667	700	1900.5	612.0	0.2	888.4	188.4	94.2	150.8	182.2
55	0.4034	700	1886.7	615.0	0.2	886.0	186.0	93.0	147.0	178.0
85	0.6234	700	1831.4	626.5	0.3	876.6	176.6	88.3	132.4	161.8
125	0.9168	700	1775.6	638.0	0.5	866.9	166.9	83.5	117.6	145.5
200	1.4668	700	1692.4	648.0	0.7	852.4	152.4	76.2	102.8	128.2
250	1.8335	700	1659.9	652.5	0.9	846.4	146.4	73.2	96.3	120.7
300	2.2002	700	1641.7	654.5	1.0	842.9	142.9	71.5	93.1	117.0
500	3.6670	700	1613.3	659.0	1.0	836.3	136.3	68.2	86.4	109.2
600	4.4004	700	1600.8	660.0	1.0	833.3	133.3	66.7	84.4	106.7
675	4.9505	700	1600.1	661.0	1.0	832.4	132.4	66.2	83.1	105.2
800	5.8673	700	1600.5	661.5	1.0	831.2	131.2	65.6	82.2	104.1
900	6.6007	700	1600.3	662.0	1.0	830.2	130.2	65.1	81.4	103.1
1100	8.0675	700	1600.4	663.0	1.0	828.1	128.1	64.1	79.7	101.1
1300	9.5343	700	1613.7	663.5	1.0	828.0	128.0	64.0	79.2	100.5

Strain Gauge (divs)	Axial Strain (%)	Cell Press. (kPa)	Proof Ring (divs)	Pore Pressure (kPa)	Membrane Correction (kPa)	P_1 (kPa)	q (kPa)	t (kPa)	p' (kPa)	s' (kPa)
1550	11.3678	700	1625.9	663.5	1.0	827.1	127.1	63.6	78.9	100.1
1810	13.2747	700	1648.9	663.5	1.0	827.6	127.6	63.8	79.0	100.3
2100	15.4015	700	1670.1	663.5	1.0	827.4	127.4	63.7	79.0	100.2
2300	16.8684	700	1685.0	663.5	1.0	827.2	127.2	63.6	78.9	100.1
2400	17.6018	700	1696.8	663.0	1.0	827.6	127.6	63.8	79.5	100.8
2500	18.3352	700	1705.1	663.0	1.0	827.6	127.6	63.8	79.5	100.8
2600	19.0686	700	1718.9	663.0	1.0	828.3	128.3	64.1	79.8	101.1
2875	21.0854	700	1746.3	662.5	1.0	828.5	128.5	64.3	80.3	101.8
3200	23.4690	700	1781.3	662.5	1.0	829.0	129.0	64.5	80.5	102.0
3450	25.3025	700	1820.8	662.0	1.0	830.7	130.7	65.3	81.6	103.3







APPENDIX E

TEST RESULTS FOR SPECIMENS UNDER CASE 3 TESTS

Table E1 Summary of results of undrained compression triaxial tests performed on anisotropically consolidated Merriespruit gold tailings
(Loading was by reducing the cell pressure while keeping either the deviator stress or the effective mean normal stress constant)

Specimen No.	Fines Content	Initial stress state			Void ratio		Behavior	Peak shear resistance			Steady-state strength			L_P	L_R
		q_0	p'_0	K0	Setup	Final		q_P	p'_P	ϕ'_P	q_{ss}	p'_{ss}	ϕ'_{ss}		
	(%)	(kPa)	(kPa)					(kPa)	(kPa)	(Degrees)	(kPa)	(kPa)	(Degrees)		(kPa)
BW-1	20	109.3	186.3	0.58	1.507	1.148	Liquefaction	113.2	142.4	20.5	53.2	40.0	33.0	5.7	3.9
BW-2	20	193.1	385.5	0.62	1.473	1.050	Liquefaction	372.2	369.3	25.6	257.0	193.2	33.0	2.0	179.1
BW-3	20	166.2	306.6	0.60	1.466	1.131	Liquefaction	167.5	163.6	25.9	90.4	65.7	34.0	6.1	1.3
BW-4	20	184.5	331.1	0.59	1.442	1.071	Liquefaction	200.4	191.7	26.4	109.3	83.3	32.6	4.8	15.9
BW-5	20	179.1	340.1	0.61	1.394	1.011	Liquefaction	349.6	350.0	25.4	266.5	204.8	32.3	1.4	170.5

Test	**Case 3: Constant Deviator Stress Undrained Loading, One-Dimensionally Consolidated**		
Cell No.	Bishop-Wesley stress path cell	Fines content (%)	20
Sample	Specimen BW-1	Specific gravity (g/cm^3)	2.72

1.) Sample physical properties

Wet mass before test (g)	102.753	m.c before test (%)	9.66	Height (mm)	75.95	Volume (cm^3)	86.363
Wet mass after test (g)	124.229	m.c. after test (%)	32.58	Diameter (mm)	38.05		
Dry mass (g)	93.701	Dry density (kg/m^3)	1085	Area (cm^2)	11.371	Void ratio (e_0)	1.507

2.) Saturation / Consolidation

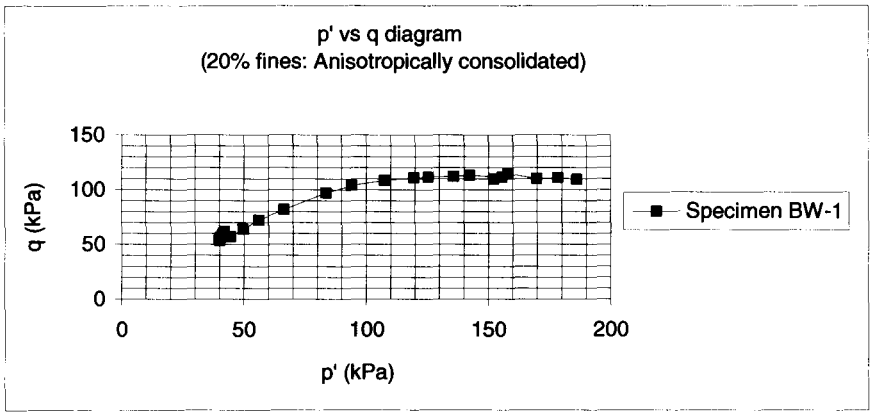
Observed Data								Processed Data								
Date	Cell Press Trd (mV)	Pore Press Trd (mV)	Axial LVDT (V)	Volume change transducer: measrd. (V)	cell expans. (V)	piston movmnt. (V)	Load Trd (V)	Cell Press. (kPa)	Proof Ring (div)	Pore Press. (kPa)	P_1 (kPa)	P'_3 (kPa)	P'_1 (kPa)	q (kPa)	p' (kPa)	K0
8/3			-2.788	-2.976	0.000	0.000		0.0	0.0	0.0						\
8/3	A I R - F L U S H I N G							9.8		4.1						\
8/3	5.58	3.88	-2.592	-2.896	0.296	0.415	0.241	50.0	12.4	40.5	78.2	9.5	37.6	28.1	18.9	0.25
9/3	10.59	8.85	-2.463	-2.710	0.583	0.688	0.152	99.9	5.2	90.1	111.8	9.9	21.7	11.8	13.8	0.46
10/3	15.64	13.90	-2.394	-2.477	0.856	0.834	0.189	150.2	5.5	140.4	162.6	9.8	22.2	12.4	14.0	0.44
11/3	20.66	18.89	-2.322	-2.321	1.111	0.987	0.181	200.2	3.3	190.2	207.7	10.1	17.6	7.5	12.6	0.57
12/3	25.63	23.88	-2.265	-2.120	1.404	1.108	0.197	249.7	2.7	239.9	255.9	9.8	16.0	6.1	11.9	0.62
13/3	30.69	28.93	-2.193	-1.971	1.677	1.260	0.230	300.1	3.2	290.3	307.5	9.9	17.2	7.3	12.3	0.57
14/3	35.70	33.93	-2.156	-1.765	1.928	1.339	0.251	350.0	3.3	340.1	357.5	9.9	17.4	7.4	12.4	0.57
15/3	40.70	38.98	-2.112	-1.600	2.163	1.432	0.268	399.8	3.2	390.5	407.2	9.4	16.7	7.4	11.8	0.56
16/3	45.76	44.00	-2.071	-1.437	2.391	1.519	0.280	450.2	3.1	440.5	457.3	9.7	16.8	7.0	12.1	0.58
17/3	70.86	55.02	-1.732	-0.998	3.421	2.237	1.087	700.2	48.2	550.4	809.4	149.9	259.0	109.1	186.2	0.58

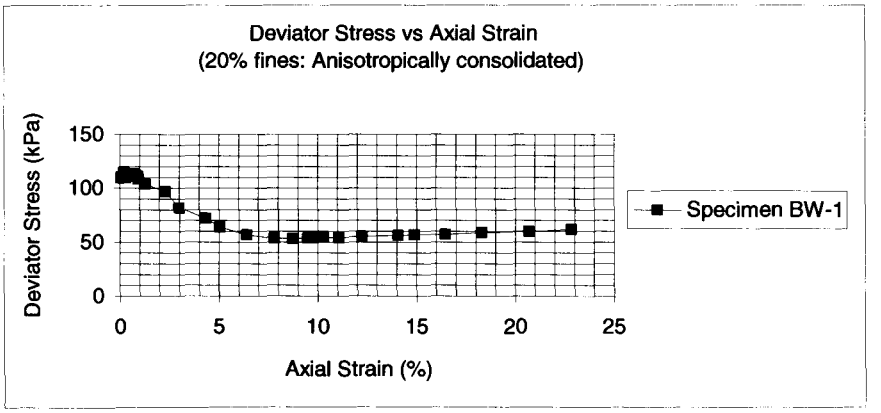
3.) Shear data

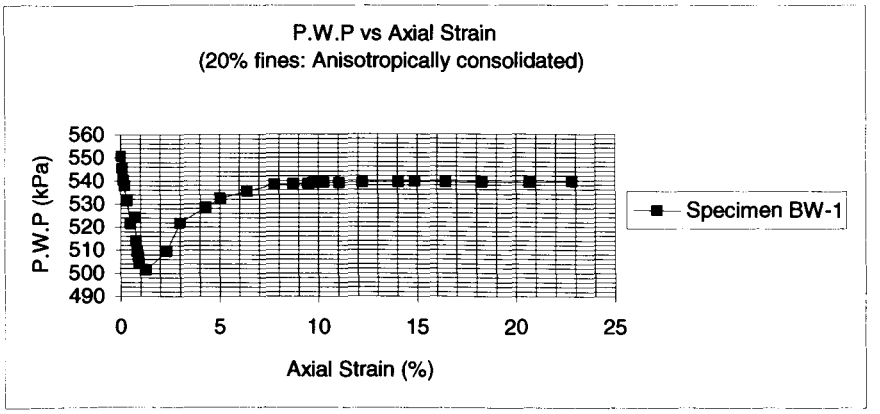
Volume change 1:		Volume change 2:		Sample Vol. change (cm^3)	12.357	K0	0.58		
Air Flushing (cm^3)	2.050	Sat/Cons. (cm^3)	25.688	L_{cons} (mm)	71.02			Void ratio (e_1)	1.148
Cell Expsn. (cm^3)	0.000	Cell Expsn.(cm^3)	44.429	A_{cons} (cm^2)	11.371	B value	0.99		
		Piston pen.(cm^3)	29.047						

Raw Data				Processed Data									
Cell Press Trd (mV)	Pore Press Trd (mV)	Axial LVDT (V)	Load Trd (V)	Change in Length (mm)	Axial Strain (%)	Cell Press (kPa)	Proof Ring (div)	Pore Press (kPa)	P_1 (kPa)	q (kPa)	t (kPa)	p' (kPa)	s' (kPa)
70.88	55.04	-1.732	1.088	0.000	0.000	700.4	48.2	550.6	809.7	109.3	54.6	186.3	204.5
69.52	54.51	-1.718	1.100	0.065	0.092	686.9	48.9	545.3	797.5	110.6	55.3	178.5	196.9
68.17	54.01	-1.710	1.096	0.103	0.145	673.5	48.6	540.3	783.5	110.0	55.0	169.8	188.1
66.60	53.76	-1.701	1.130	0.145	0.204	657.8	50.6	537.8	772.2	114.4	57.2	158.1	177.2
65.52	53.10	-1.685	1.094	0.220	0.309	647.1	48.5	531.2	756.6	109.5	54.8	152.3	170.6
64.80	52.11	-1.655	1.111	0.360	0.506	639.9	49.5	521.4	751.3	111.4	55.7	155.7	174.2
63.69	52.39	-1.622	1.127	0.514	0.723	628.8	50.5	524.2	742.0	113.2	56.6	142.4	161.3
62.06	51.37	-1.613	1.117	0.556	0.783	612.6	50.0	514.0	724.5	111.9	56.0	135.9	154.6
60.57	50.90	-1.604	1.112	0.598	0.842	597.8	49.7	509.3	709.1	111.3	55.7	125.6	144.1
59.77	50.67	-1.595	1.107	0.640	0.901	589.8	49.5	507.0	700.5	110.7	55.3	119.7	138.1
58.38	50.42	-1.588	1.089	0.673	0.947	575.9	48.5	504.5	684.4	108.4	54.2	107.6	125.6
56.87	50.10	-1.534	1.055	0.925	1.302	560.9	46.7	501.3	664.6	103.7	51.9	94.1	111.4
56.85	50.90	-1.380	1.013	1.644	2.315	560.7	44.2	509.3	657.6	96.9	48.5	83.7	99.9
56.88	52.14	-1.276	0.898	2.130	2.999	561.0	37.6	521.7	642.6	81.6	40.8	66.5	80.1
56.87	52.84	-1.077	0.830	3.059	4.308	560.9	33.6	528.6	632.9	72.0	36.0	56.3	68.2
56.88	53.23	-0.965	0.769	3.582	5.044	561.0	30.1	532.5	624.8	63.8	31.9	49.7	60.4
56.88	53.52	-0.758	0.719	4.549	6.406	561.0	27.2	535.4	617.8	56.8	28.4	44.5	54.0
56.85	53.82	-0.546	0.698	5.539	7.800	560.7	26.0	538.4	614.1	53.4	26.7	40.1	49.0
56.86	53.83	-0.405	0.701	6.198	8.727	560.8	26.2	538.5	614.0	53.2	26.6	40.0	48.9
56.87	53.85	-0.289	0.708	6.740	9.490	560.9	26.6	538.7	614.5	53.6	26.8	40.0	49.0
56.86	53.87	-0.252	0.711	6.913	9.734	560.8	26.8	538.9	614.6	53.8	26.9	39.8	48.8
56.89	53.89	-0.168	0.718	7.305	10.286	561.1	27.2	539.1	615.4	54.3	27.1	40.1	49.1
56.89	53.88	-0.050	0.721	7.856	11.062	561.1	27.3	539.0	615.2	54.1	27.1	40.1	49.2

Raw Data				Processed Data									
Cell Press Trd (mV)	Pore Press Trd (mV)	Axial LVDT (V)	Load Trd (V)	Change in Length (mm)	Axial Strain (%)	Cell Press (kPa)	Proof Ring (div)	Pore Press (kPa)	P_1 (kPa)	q (kPa)	t (kPa)	p' (kPa)	s' (kPa)
56.87	53.89	0.131	0.736	8.702	12.253	560.9	28.2	539.1	616.0	55.1	27.6	40.2	49.3
56.88	53.91	0.407	0.756	9.991	14.068	561.0	29.4	539.3	617.2	56.2	28.1	40.4	49.8
56.91	53.93	0.533	0.765	10.579	14.897	561.3	29.9	539.5	618.0	56.6	28.3	40.7	50.1
56.90	53.90	0.771	0.778	11.691	16.462	561.2	30.6	539.2	618.2	57.0	28.5	41.0	50.5
56.87	53.91	1.053	0.806	13.008	18.316	560.9	32.3	539.3	619.6	58.7	29.4	41.2	51.0
56.85	53.89	1.414	0.833	14.694	20.691	560.7	33.8	539.1	620.5	59.8	29.9	41.5	51.5
56.86	53.93	1.742	0.870	16.226	22.848	560.8	36.0	539.5	622.7	61.9	30.9	41.9	52.2







Test	**Case 3: Constant Effecive Mean Normal Stress Undrained Loading, One-Dimensionally Consolidated**		
Cell No.	Bishop-Wesley stress path cell	Fines content (%)	20
Sample	Specimen BW-2	Specific gravity (g/cm^3)	2.72

1.) Sample physical properties

Wet mass before test (g)	104.492	m.c before test (%)	10.00	Height (mm)	76.15	Volume (cm^3)	86.363
Wet mass after test (g)	127.338	m.c. after test (%)	34.05	Diameter (mm)	38.00		
Dry mass (g)	94.993	Dry density (kg/m^3)	1100	Area (cm^2)	11.341	Void ratio (e_0)	1.473

2.) Saturation / Consolidation

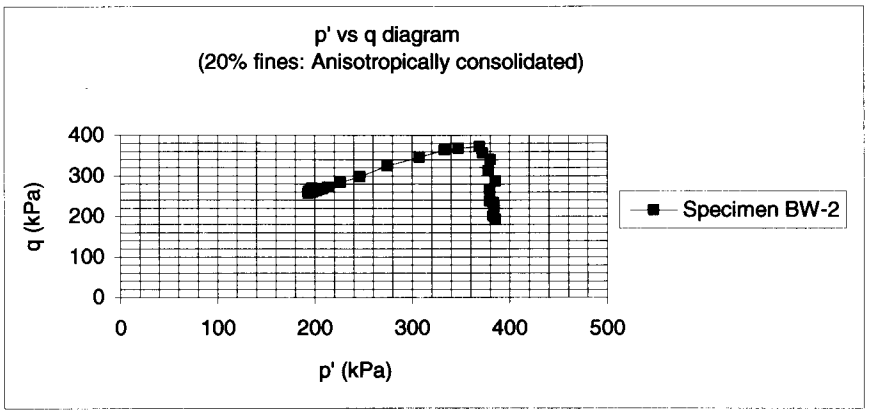
Observed Data								Processed Data							
Date	Cell Press Trd (mV)	Pore Press Trd (mV)	Axial LVDT (V)	Volume change transducer measrd. (V)	Volume change transducer cell expans. (V)	Volume change transducer piston movmnt. (V)	Load Trd (V)	Cell Press. (kPa)	Proof Ring (div)	Pore Press. (kPa)	P_1 (kPa)	P'_3 (kPa)	P'_1 (kPa)	q (kPa)	p' (kPa)	K0
15/1			-2.786	-2.532	0.000	0.000		0.0	0.0	0.0						\
15/1	A I R - F L U S H I N G							7.5		3.0						\
15/1	5.54	3.73	-2.401	-2.525	0.296	0.815	0.107	49.6	4.7	39.0	60.3	10.6	21.3	10.6	14.2	0.50
16/1	10.64	8.87	-2.127	-2.518	0.583	1.396	0.123	100.4	3.5	90.3	108.4	10.2	18.2	8.0	12.8	0.56
17/1	15.61	13.85	-2.015	-2.450	0.856	1.633	0.140	149.9	2.6	139.9	155.9	10.0	16.0	6.0	12.0	0.63
18/1	20.68	18.92	-1.829	-2.443	1.111	2.027	0.181	200.4	3.3	190.5	207.9	10.0	17.5	7.5	12.5	0.57
19/1	25.60	23.94	-1.787	-2.202	1.404	2.116	0.195	249.4	2.6	240.5	255.3	8.9	14.8	5.9	10.9	0.60
20/1	30.63	28.90	-1.726	-2.041	1.677	2.245	0.212	299.5	2.2	290.0	304.6	9.6	14.6	5.0	11.3	0.66
21/1	35.65	33.91	-1.698	-1.844	1.928	2.304	0.250	349.5	3.2	339.9	356.9	9.6	17.0	7.3	12.1	0.57
22/1	40.74	37.98	-1.657	-1.690	2.163	2.391	0.313	400.2	5.8	380.5	413.5	19.8	33.0	13.3	24.2	0.60
23/1	70.97	37.99	-1.461	-1.522	2.820	2.806	1.724	701.3	85.0	380.6	894.4	320.8	513.9	193.1	385.1	0.62

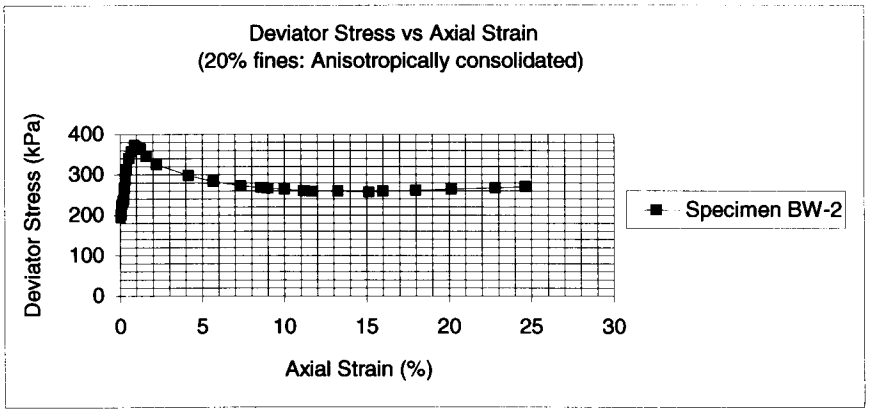
3.) Shear data

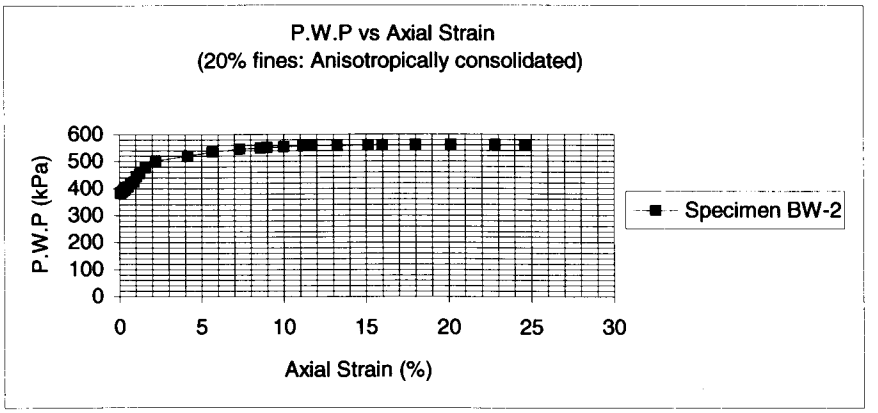
Volume change 1:		Volume change 2:		Sample Vol. change (cm^3)	14.784	K0	0.62		
Air Flushing (cm^3)	1.850	Sat/Cons. (cm^3)	13.112	L_{cons} (mm)	69.96			Void ratio (e_1)	1.050
Cell Expsn. (cm^3)	0.000	Cell Expsn.(cm^3)	36.623	A_{cons} (cm^2)	11.341	B value	0.97		
		Piston pen.(cm^3)	36.446						

Raw Data				Processed Data									
Cell Press Trd (mV)	Pore Press Trd (mV)	Axial LVDT (V)	Load Trd (V)	Change in Length (mm)	Axial Strain (%)	Cell Press (kPa)	Proof Ring (div)	Pore Press (kPa)	P_1 (kPa)	q (kPa)	t (kPa)	p' (kPa)	s' (kPa)
71.02	38.00	-1.461	1.724	0.000	0.000	701.8	85.0	380.7	894.9	193.1	96.5	385.5	417.7
70.85	38.32	-1.449	1.783	0.056	0.080	700.1	88.4	383.9	900.8	200.6	100.3	383.1	416.6
70.32	38.40	-1.445	1.954	0.075	0.107	694.9	98.3	384.7	917.8	223.0	111.5	384.5	421.7
70.06	38.61	-1.434	2.038	0.126	0.180	692.3	103.1	386.8	926.1	233.8	116.9	383.4	422.4
69.70	38.78	-1.426	2.074	0.163	0.234	688.7	105.2	388.5	927.0	238.3	119.2	379.7	419.4
69.32	39.33	-1.420	2.289	0.191	0.274	684.9	117.6	393.9	951.3	266.4	133.2	379.8	424.1
69.03	39.15	-1.412	2.447	0.229	0.327	682.0	126.7	392.2	968.9	286.9	143.4	385.5	433.3
68.50	40.21	-1.403	2.644	0.271	0.387	676.7	138.1	402.7	989.2	312.4	156.2	378.2	430.2
68.11	40.51	-1.380	2.857	0.378	0.541	672.9	150.4	405.7	1012.6	339.7	169.8	380.4	437.0
67.88	41.66	-1.356	2.991	0.490	0.701	670.6	158.2	417.2	1027.1	356.5	178.3	372.2	431.7
67.62	42.22	-1.328	3.117	0.621	0.888	668.0	165.5	422.8	1040.2	372.2	186.1	369.3	431.3
67.61	44.24	-1.303	3.089	0.738	1.055	667.9	163.8	442.9	1035.7	367.8	183.9	347.6	408.9
67.62	45.54	-1.273	3.061	0.878	1.255	668.0	162.2	455.9	1031.3	363.4	181.7	333.2	393.8
67.66	47.57	-1.223	2.935	1.112	1.589	668.4	154.9	476.1	1014.0	345.7	172.8	307.5	365.1
67.62	50.11	-1.126	2.789	1.565	2.237	668.0	146.5	501.4	992.4	324.4	162.2	274.7	328.8
67.60	52.00	-0.838	2.628	2.910	4.159	667.8	137.2	520.3	965.5	297.8	148.9	246.8	296.4
67.59	53.50	-0.613	2.544	3.961	5.661	667.7	132.3	535.2	950.4	282.7	141.3	226.7	273.8
67.60	54.50	-0.362	2.500	5.133	7.337	667.8	129.8	545.2	940.1	272.3	136.1	213.3	258.7
67.62	54.90	-0.175	2.492	6.007	8.586	668.0	129.3	549.2	935.6	267.6	133.8	208.0	252.6
67.58	55.18	-0.113	2.492	6.296	8.999	667.6	129.3	552.0	934.0	266.4	133.2	204.4	248.8
67.62	55.33	0.039	2.492	7.006	10.014	668.0	129.3	553.5	931.4	263.4	131.7	202.3	246.2
67.61	55.60	0.213	2.492	7.819	11.176	667.9	129.3	556.2	927.9	260.0	130.0	198.4	241.7
67.63	55.80	0.295	2.493	8.202	11.723	668.1	129.4	558.2	926.6	258.5	129.3	196.1	239.2

Raw Data				Processed Data									
Cell Press Trd (mV)	Pore Press Trd (mV)	Axial LVDT (V)	Load Trd (V)	Change in Length (mm)	Axial Strain (%)	Cell Press (kPa)	Proof Ring (div)	Pore Press (kPa)	P_1 (kPa)	q (kPa)	t (kPa)	p' (kPa)	s' (kPa)
67.61	55.72	0.526	2.539	9.281	13.265	667.9	132.0	557.4	927.1	259.2	129.6	196.9	240.1
67.59	56.00	0.805	2.569	10.584	15.128	667.7	133.8	560.1	924.7	257.0	128.5	193.2	236.0
67.61	56.00	0.934	2.609	11.186	15.989	667.9	136.1	560.1	926.7	258.8	129.4	194.0	237.1
67.57	56.05	1.235	2.683	12.592	17.999	667.5	140.4	560.6	928.0	260.6	130.3	193.7	237.1
67.64	56.05	1.555	2.781	14.087	20.135	668.2	146.0	560.6	932.2	264.0	132.0	195.5	239.5
67.58	56.05	1.957	2.900	15.965	22.819	667.6	152.9	560.6	934.8	267.2	133.6	196.0	240.5
67.61	56.05	2.226	2.989	17.221	24.615	667.9	158.1	560.6	937.6	269.7	134.9	197.1	242.1







Test	**Case 3: Constant Deviator Stress Undrained Loading, One-Dimensionally Consolidated**		
Cell No.	Bishop-Wesley stress path cell	Fines content (%)	20
Sample	Specimen BW-3	Specific gravity (g/cm^3)	2.72

1.) Sample physical properties

Wet mass before test (g)	103.677	m.c before test (%)	9.33	Height (mm)	76.00	Volume (cm^3)	85.966
Wet mass after test (g)	123.553	m.c. after test (%)	30.29	Diameter (mm)	37.95		
Dry mass (g)	94.829	Dry density (kg/m^3)	1103	Area (cm^2)	11.311	Void ratio (e_0)	1.466

2.) Saturation / Consolidation

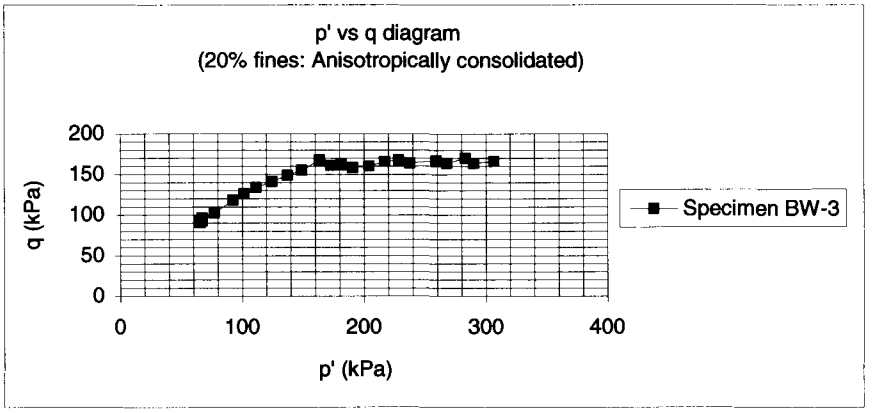
Observed Data								Processed Data								
Date	Cell Press Trd (mV)	Pore Press Trd (mV)	Axial LVDT (V)	Volume change transducer measrd. (V)	cell expans. (V)	piston movmnt. (V)	Load Trd (V)	Cell Press. (kPa)	Proof Ring (div)	Pore Press. (kPa)	P_1 (kPa)	P'_3 (kPa)	P'_1 (kPa)	q (kPa)	p' (kPa)	K0
2/2			-2.781	-2.873	0.000	0.000		0.0	0.0	0.0						\
2/2	A I R - F L U S H I N G							7.5		3.0						\
2/2	5.62	3.91	-2.533	-2.835	0.296	0.525	0.123	50.4	5.6	40.8	63.1	9.6	22.3	12.7	13.9	0.43
3/2	10.58	8.89	-2.338	-2.811	0.583	0.938	0.170	99.8	6.3	90.5	114.1	9.4	23.6	14.2	14.1	0.40
4/2	15.61	13.83	-2.225	-2.697	0.856	1.178	0.194	149.9	5.8	139.7	163.1	10.2	23.4	13.1	14.6	0.44
5/2	20.61	18.87	-2.146	-2.550	1.111	1.345	0.203	199.7	4.6	190.0	210.2	9.8	20.2	10.4	13.3	0.48
6/2	25.69	23.95	-2.022	-2.493	1.404	1.608	0.211	250.3	3.5	240.6	258.3	9.7	17.7	8.0	12.4	0.55
7/2	30.67	28.90	-1.936	-2.378	1.677	1.790	0.227	299.9	3.1	290.0	306.9	10.0	17.0	7.0	12.3	0.59
8/2	35.73	33.98	-1.821	-2.344	1.928	2.033	0.258	350.3	3.7	340.6	358.7	9.7	18.1	8.4	12.5	0.54
9/2	40.76	38.91	-1.757	-2.225	2.163	2.169	0.274	400.4	3.6	389.8	408.6	10.7	18.8	8.2	13.4	0.57
10/2	76.01	50.02	-1.419	-1.242	3.767	2.885	1.512	751.5	72.9	500.5	917.7	251.0	417.2	166.2	306.4	0.60

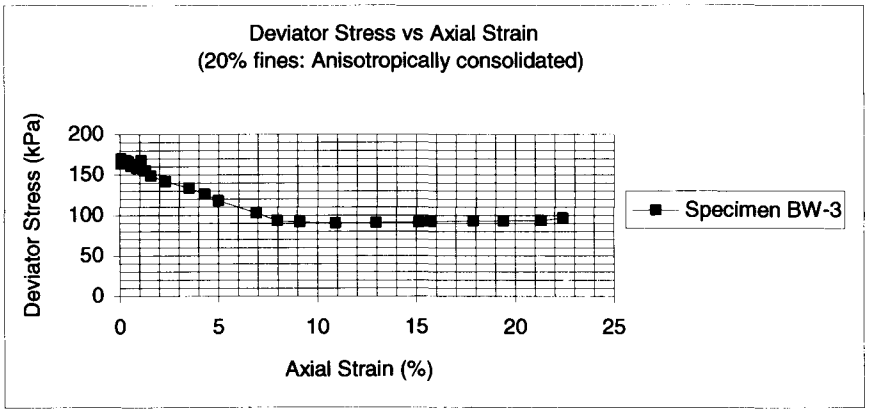
3.) Shear data

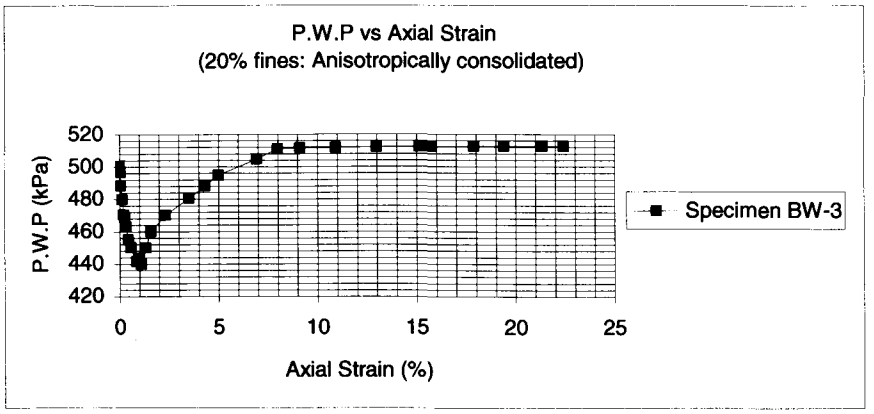
Volume change 1:		Volume change 2:		Sample Vol. change (cm^3)	11.674	K0	0.60		
Air Flushing (cm^3)	1.950	Sat/Cons. (cm^3)	21.182	L_{cons} (mm)	69.64			Void ratio (e_1)	1.131
Cell Expsn. (cm^3)	0.000	Cell Expsn.(cm^3)	48.922	A_{cons} (cm^2)	11.311	B value	0.97		
		Piston pen.(cm^3)	37.464						

Raw Data				Processed Data									
Cell Press Trd (mV)	Pore Press Trd (mV)	Axial LVDT (V)	Load Trd (V)	Change in Length (mm)	Axial Strain (%)	Cell Press (kPa)	Proof Ring (div)	Pore Press (kPa)	P_1 (kPa)	q (kPa)	t (kPa)	p' (kPa)	s' (kPa)
76.02	50.01	-1.419	1.512	0.000	0.000	751.6	72.9	500.4	917.8	166.2	83.1	306.6	334.3
74.06	49.63	-1.413	1.495	0.028	0.040	732.1	71.8	496.6	895.7	163.6	81.8	290.0	317.3
72.33	48.80	-1.411	1.545	0.037	0.054	714.9	74.7	488.4	884.9	170.0	85.0	283.2	311.5
70.16	47.94	-1.399	1.500	0.093	0.134	693.3	72.0	479.8	857.1	163.8	81.9	268.1	295.4
68.24	46.99	-1.391	1.523	0.131	0.188	674.2	73.3	470.3	840.8	166.6	83.3	259.4	287.2
66.00	46.84	-1.380	1.501	0.182	0.262	651.8	72.1	468.8	815.4	163.6	81.8	237.6	264.8
64.35	46.25	-1.371	1.532	0.224	0.322	635.4	73.9	462.9	803.0	167.6	83.8	228.3	256.3
62.49	45.46	-1.354	1.519	0.304	0.436	616.9	73.2	455.1	782.6	165.8	82.9	217.1	244.7
60.91	44.98	-1.335	1.478	0.392	0.563	601.1	70.9	450.3	761.4	160.3	80.1	204.3	231.0
58.76	44.10	-1.290	1.463	0.603	0.865	579.7	70.1	441.5	737.6	157.9	79.0	190.9	217.2
57.90	44.31	-1.277	1.492	0.663	0.952	571.2	71.8	443.6	732.8	161.6	80.8	181.4	208.4
56.94	44.20	-1.271	1.487	0.691	0.993	561.6	71.6	442.5	722.7	161.1	80.5	172.8	199.6
55.55	43.95	-1.257	1.536	0.757	1.087	547.8	74.6	440.0	715.2	167.5	83.7	163.6	191.5
55.52	44.95	-1.224	1.443	0.911	1.308	547.5	69.2	450.0	702.4	154.9	77.5	149.1	174.9
55.55	45.95	-1.184	1.398	1.098	1.576	547.8	66.6	459.9	696.3	148.5	74.3	137.3	162.1
55.54	46.98	-1.074	1.352	1.611	2.314	547.7	63.9	470.2	688.9	141.3	70.6	124.5	148.1
55.53	48.02	-0.895	1.304	2.447	3.515	547.6	61.2	480.6	681.0	133.4	66.7	111.4	133.7
55.55	48.76	-0.777	1.254	2.999	4.306	547.8	58.3	488.0	673.8	126.0	63.0	101.8	122.8
55.56	49.43	-0.675	1.198	3.475	4.990	547.9	55.0	494.6	666.0	118.1	59.1	92.6	112.3
55.55	50.44	-0.386	1.091	4.825	6.928	547.8	48.8	504.7	650.3	102.6	51.3	77.2	94.3
55.53	51.08	-0.229	1.021	5.558	7.981	547.6	44.8	511.1	640.5	92.9	46.5	67.4	82.9
55.50	51.12	-0.058	1.020	6.357	9.128	547.3	44.7	511.5	638.9	91.6	45.8	66.3	81.6
55.51	51.15	0.209	1.025	7.604	10.919	547.4	45.0	511.8	637.7	90.4	45.2	65.7	80.8

Raw Data				Processed Data									
Cell Press Trd (mV)	Pore Press Trd (mV)	Axial LVDT (V)	Load Trd (V)	Change in Length (mm)	Axial Strain (%)	Cell Press (kPa)	Proof Ring (div)	Pore Press (kPa)	P_1 (kPa)	q (kPa)	t (kPa)	p' (kPa)	s' (kPa)
55.53	51.18	0.516	1.047	9.038	12.978	547.6	46.3	512.1	638.3	90.8	45.4	65.7	80.9
55.55	51.20	0.837	1.070	10.537	15.131	547.8	47.6	512.3	638.8	91.1	45.5	65.8	81.0
55.55	51.21	0.926	1.083	10.953	15.728	547.8	48.4	512.4	639.6	91.9	45.9	66.0	81.3
55.54	51.22	1.249	1.117	12.461	17.895	547.7	50.3	512.5	640.8	93.2	46.6	66.2	81.8
55.56	51.23	1.475	1.133	13.517	19.410	547.9	51.3	512.6	641.0	93.1	46.6	66.3	81.8
55.54	51.23	1.762	1.158	14.858	21.335	547.7	52.7	512.6	641.1	93.5	46.7	66.2	81.8
55.53	51.23	1.924	1.200	15.614	22.422	547.6	55.1	512.6	644.0	96.5	48.2	67.1	83.2







Test	**Case 3: Constant Deviator Stress Undrained Loading, One-Dimensionally Consolidated**		
Cell No.	Bishop-Wesley stress path cell	Fines content (%)	20
Sample	Specimen BW-4	Specific gravity (g/cm^3)	2.72

1.) Sample physical properties

Wet mass before test (g)	103.455	m.c before test (%)	8.27	Height (mm)	76.05	Volume (cm^3)	85.796
Wet mass after test (g)	122.604	m.c. after test (%)	28.31	Diameter (mm)	37.90		
Dry mass (g)	95.553	Dry density (kg/m^3)	1114	Area (cm^2)	11.282	Void ratio (e_0)	1.442

2.) Saturation / Consolidation

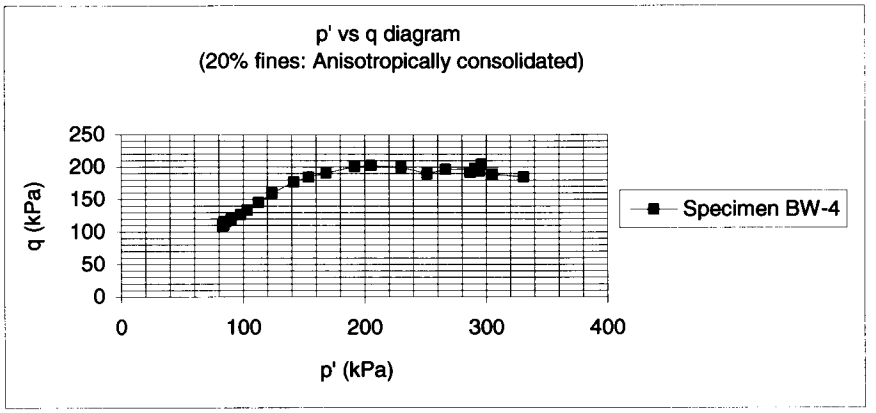
Observed Data								Processed Data								
Date	Cell Press Trd (mV)	Pore Press Trd (mV)	Axial LVDT (V)	Volume change transducer: measrd. (V)	cell expans. (V)	piston movmnt. (V)	Load Trd (V)	Cell Press. (kPa)	Proof Ring (div)	Pore Press. (kPa)	P_1 (kPa)	P'_3 (kPa)	P'_1 (kPa)	q (kPa)	p' (kPa)	K0
15/2			-2.785	-2.661	0.000	0.000		0.0	0.0	0.0						\
15/2	A I R - F L U S H I N G							7.5		3.0						\
15/2	5.51	3.81	-2.526	-2.631	0.296	0.549	0.102	49.3	4.4	39.8	59.4	9.5	19.6	10.0	12.9	0.49
16/2	10.62	8.92	-2.424	-2.387	0.583	0.765	0.152	100.2	5.2	90.8	112.1	9.5	21.4	11.9	13.4	0.44
17/2	15.67	13.91	-2.332	-2.210	0.856	0.959	0.167	150.5	4.2	140.5	160.1	10.0	19.6	9.5	13.2	0.51
18/2	20.64	18.84	-2.216	-2.133	1.111	1.205	0.195	200.0	4.1	189.7	209.4	10.4	19.8	9.4	13.5	0.53
19/2	25.70	23.92	-2.144	-1.939	1.404	1.358	0.213	250.4	3.6	240.3	258.7	10.1	18.4	8.2	12.9	0.55
20/2	30.63	28.94	-2.017	-1.915	1.677	1.627	0.227	299.5	3.1	290.4	306.6	9.2	16.2	7.0	11.5	0.57
21/2	35.74	33.95	-1.938	-1.796	1.928	1.794	0.248	350.4	3.1	340.3	357.5	10.1	17.2	7.1	12.5	0.59
22/2	40.68	37.98	-1.859	-1.700	2.163	1.961	0.320	399.6	6.3	380.5	413.9	19.2	33.5	14.3	23.9	0.57
23/2	65.81	37.98	-1.426	-1.485	3.222	2.878	1.653	649.9	80.8	380.5	834.6	269.5	454.1	184.7	331.0	0.59

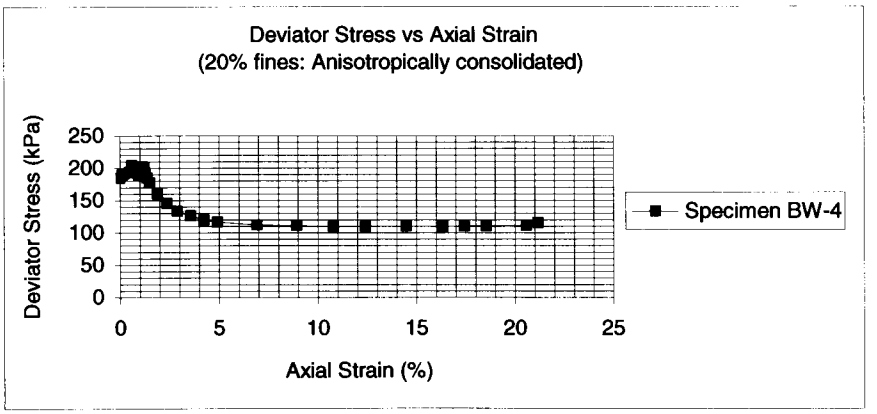
3.) Shear data

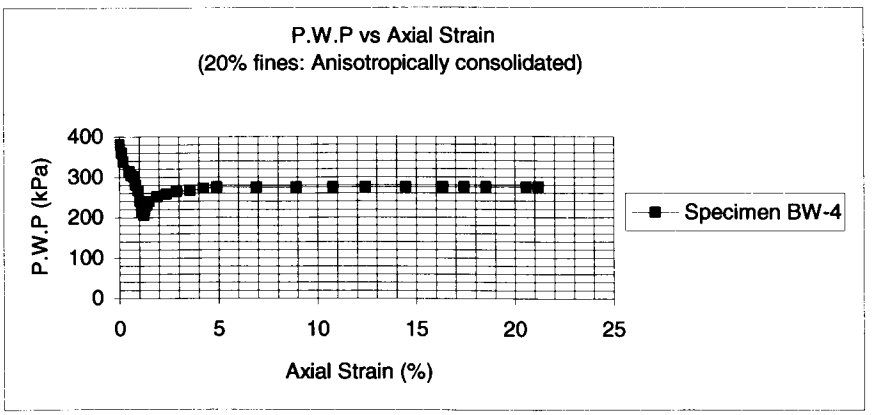
Volume change 1:		Volume change 2:		Sample Vol. change (cm^3)	13.060	K0	0.59		
Air Flushing (cm^3)	2.250	Sat/Cons. (cm^3)	15.273	L_{cons} (mm)	69.70			Void ratio (e_1)	1.071
Cell Expsn. (cm^3)	0.000	Cell Expsn.(cm^3)	41.844	A_{cons} (cm^2)	11.282	B value	0.97		
		Piston pen.(cm^3)	37.381						

Raw Data				Processed Data									
Cell Press Trd (mV)	Pore Press Trd (mV)	Axial LVDT (V)	Load Trd (V)	Change in Length (mm)	Axial Strain (%)	Cell Press (kPa)	Proof Ring (div)	Pore Press (kPa)	P_1 (kPa)	q (kPa)	t (kPa)	p' (kPa)	s' (kPa)
65.83	37.99	-1.426	1.652	0.000	0.000	650.1	80.8	380.6	834.7	184.5	92.3	331.1	361.8
61.02	35.90	-1.408	1.685	0.084	0.121	602.2	82.8	359.7	791.2	188.9	94.5	305.5	336.9
56.85	33.67	-1.397	1.700	0.135	0.194	560.7	83.9	337.5	752.0	191.3	95.6	286.9	318.8
55.23	31.36	-1.354	1.720	0.336	0.482	544.6	85.2	314.5	738.1	193.5	96.7	294.6	326.8
53.96	30.28	-1.337	1.800	0.416	0.596	531.9	90.0	303.7	735.9	204.0	102.0	296.2	330.2
53.34	29.98	-1.314	1.753	0.523	0.751	525.7	87.3	300.7	723.3	197.6	98.8	290.9	323.8
48.95	27.96	-1.305	1.734	0.565	0.811	482.0	86.7	280.6	678.1	196.0	98.0	266.8	299.4
46.24	26.55	-1.286	1.681	0.654	0.938	455.0	84.0	266.5	644.7	189.6	94.8	251.7	283.3
41.06	23.87	-1.270	1.744	0.729	1.045	403.4	88.5	239.8	602.9	199.5	99.8	230.1	263.4
35.72	21.09	-1.257	1.745	0.789	1.132	350.2	89.6	212.1	552.1	201.8	100.9	205.4	239.1
33.73	20.43	-1.243	1.728	0.855	1.226	330.4	89.1	205.5	530.8	200.4	100.2	191.7	225.1
32.94	21.66	-1.235	1.652	0.892	1.280	322.6	84.9	217.8	513.3	190.8	95.4	168.4	200.2
32.91	22.86	-1.220	1.605	0.962	1.380	322.3	82.2	229.7	506.7	184.4	92.2	154.0	184.7
32.93	23.86	-1.203	1.551	1.042	1.494	322.5	79.0	239.7	499.6	177.1	88.6	141.8	171.3
32.91	25.06	-1.143	1.423	1.322	1.896	322.3	71.7	251.7	481.9	159.6	79.8	123.8	150.4
32.89	25.66	-1.073	1.319	1.649	2.365	322.1	65.6	257.7	467.5	145.4	72.7	112.9	137.1
32.96	26.27	-0.993	1.232	2.022	2.902	322.8	60.6	263.7	456.2	133.4	66.7	103.5	125.7
32.95	26.56	-0.893	1.184	2.489	3.572	322.7	57.8	266.6	449.0	126.4	63.2	98.2	119.2
32.93	27.09	-0.793	1.138	2.957	4.242	322.5	55.2	271.9	442.1	119.7	59.8	90.4	110.4
32.91	27.38	-0.693	1.118	3.424	4.912	322.3	54.0	274.8	438.6	116.3	58.2	86.2	105.6
32.88	27.40	-0.393	1.101	4.825	6.922	322.0	53.0	275.0	433.7	111.8	55.9	84.2	102.8
32.90	27.39	-0.093	1.112	6.226	8.932	322.2	53.7	274.9	432.8	110.7	55.3	84.1	102.6
32.91	27.41	0.185	1.122	7.525	10.795	322.3	54.3	275.1	431.8	109.6	54.8	83.7	101.9

Raw Data				Processed Data									
Cell Press Trd (mV)	Pore Press Trd (mV)	Axial LVDT (V)	Load Trd (V)	Change in Length (mm)	Axial Strain (%)	Cell Press (kPa)	Proof Ring (div)	Pore Press (kPa)	P_1 (kPa)	q (kPa)	t (kPa)	p' (kPa)	s' (kPa)
32.89	27.42	0.428	1.139	8.660	12.424	322.1	55.2	275.2	431.6	109.5	54.8	83.4	101.6
32.92	27.41	0.734	1.167	10.089	14.474	322.4	56.9	275.1	432.4	110.1	55.0	83.9	102.3
32.90	27.43	1.014	1.182	11.397	16.350	322.2	57.7	275.3	431.5	109.3	54.7	83.3	101.5
32.93	27.40	1.175	1.200	12.149	17.429	322.5	58.8	275.0	432.3	109.8	54.9	84.1	102.4
32.94	27.39	1.341	1.218	12.924	18.541	322.6	59.8	274.9	432.8	110.3	55.1	84.4	102.8
32.91	27.41	1.645	1.251	14.344	20.579	322.3	61.7	275.1	433.2	111.0	55.5	84.1	102.6
32.88	27.40	1.736	1.301	14.769	21.188	322.0	64.6	275.0	437.3	115.3	57.7	85.4	104.6







Test	**Case 3: Constant Effecive Mean Normal Stress Undrained Loading, One-Dimensionally Consolidated**		
Cell No.	Bishop-Wesley stress path cell	Fines content (%)	20
Sample	Specimen BW-5	Specific gravity (g/cm^3)	2.72

1.) Sample physical properties

Wet mass before test (g)	107.823	m.c before test (%)	10.04	Height (mm)	75.85	Volume (cm^3)	86.249
Wet mass after test (g)	124.970	m.c. after test (%)	27.54	Diameter (mm)	38.05		
Dry mass (g)	97.985	Dry density (kg/m^3)	1136	Area (cm^2)	11.371	Void ratio (e_0)	1.394

2.) Saturation / Consolidation

Observed Data								Processed Data							
Date	Cell Press Trd (mV)	Pore Press Trd (mV)	Axial LVDT (V)	Volume change transducer: measrd. (V)	cell expans. (V)	piston movmnt. (V)	Load Trd (V)	Cell Press. (kPa)	Proof Ring (div)	Pore Press. (kPa)	P_1 (kPa)	P'_3 (kPa)	P'_1 (kPa)	q (kPa)	p' (kPa)	K0
25/2			-2.788	-3.127	0.000	0.000		0.0	0.0	0.0						\
25/2	A I R - F L U S H I N G							7.5		3.0						\
25/2	5.64	3.83	-2.452	-3.121	0.296	0.712	0.105	50.6	4.5	40.0	60.9	10.6	20.9	10.2	14.0	0.51
26/2	10.67	8.82	-2.257	-2.954	0.583	1.125	0.111	100.7	2.8	89.8	107.1	11.0	17.4	6.4	13.1	0.63
27/2	15.60	13.92	-2.136	-2.785	0.856	1.381	0.148	149.8	3.1	140.6	156.9	9.2	16.3	7.0	11.6	0.57
28/2	20.66	18.94	-2.031	-2.652	1.111	1.603	0.180	200.2	3.2	190.7	207.6	9.6	16.9	7.3	12.0	0.57
1/3	25.61	23.90	-1.946	-2.438	1.404	1.783	0.208	249.5	3.3	240.1	257.1	9.4	17.0	7.6	12.0	0.55
2/3	30.72	28.88	-1.867	-2.289	1.677	1.951	0.230	300.4	3.2	289.8	307.8	10.7	18.0	7.3	13.1	0.59
3/3	35.68	33.89	-1.822	-2.077	1.928	2.046	0.243	349.8	2.8	339.7	356.2	10.1	16.5	6.4	12.3	0.61
4/3	40.69	38.91	-1.688	-2.054	2.163	2.330	0.258	399.7	2.7	389.8	405.8	10.0	16.0	6.0	12.0	0.62
5/3	80.90	52.03	-1.258	-1.685	3.767	3.241	1.612	800.2	79.1	520.6	979.5	279.7	458.9	179.2	339.4	0.61

3.) Shear data

Volume change 1:		Volume change 2:		Sample Vol. change (cm^3)	13.790	K0	0.61		
Air Flushing (cm^3)	1.900	Sat/Cons. (cm^3)	18.727	L_{cons} (mm)	68.70			Void ratio (e_1)	1.011
Cell Expsn. (cm^3)	0.000	Cell Expsn.(cm^3)	48.922	A_{cons} (cm^2)	11.371	B value	0.98		
		Piston pen.(cm^3)	42.085						

Raw Data				Processed Data									
Cell Press Trd (mV)	Pore Press Trd (mV)	Axial LVDT (V)	Load Trd (V)	Change in Length (mm)	Axial Strain (%)	Cell Press (kPa)	Proof Ring (div)	Pore Press (kPa)	P_1 (kPa)	q (kPa)	t (kPa)	p' (kPa)	s' (kPa)
80.90	51.96	-1.685	1.611	0.000	0.000	800.2	79.0	519.9	979.3	179.1	89.5	340.1	369.9
80.02	51.52	-1.672	1.763	0.061	0.088	791.5	87.7	515.5	990.1	198.6	99.3	342.2	375.3
78.33	50.67	-1.661	1.942	0.112	0.163	774.6	97.9	507.0	996.2	221.5	110.8	341.5	378.4
76.09	49.91	-1.655	2.097	0.140	0.204	752.3	106.8	499.4	993.7	241.3	120.7	333.4	373.6
74.79	49.18	-1.634	2.258	0.238	0.347	739.4	116.0	492.2	1001.2	261.8	130.9	334.5	378.1
72.95	47.31	-1.627	2.363	0.271	0.394	721.1	122.0	473.5	996.2	275.1	137.6	339.3	385.1
71.19	46.15	-1.609	2.509	0.355	0.517	703.5	130.4	461.9	997.2	293.7	146.8	339.5	388.4
68.85	43.65	-1.596	2.670	0.416	0.605	680.2	139.6	437.0	994.4	314.2	157.1	347.9	400.3
67.22	42.32	-1.577	2.863	0.504	0.734	664.0	150.8	423.8	1002.8	338.8	169.4	353.2	409.6
64.94	40.72	-1.557	2.950	0.598	0.870	641.3	155.8	407.8	990.9	349.6	174.8	350.0	408.3
64.91	42.64	-1.554	2.924	0.612	0.891	641.0	154.3	426.9	987.2	346.2	173.1	329.4	387.1
64.89	44.64	-1.534	2.846	0.705	1.027	640.8	149.8	446.9	976.3	335.5	167.8	305.7	361.7
64.94	46.64	-1.494	2.756	0.892	1.298	641.3	144.6	466.8	964.1	322.8	161.4	282.1	335.9
64.92	47.34	-1.450	2.693	1.098	1.598	641.1	141.0	473.8	954.7	313.6	156.8	271.8	324.1
64.91	49.64	-1.290	2.579	1.845	2.685	641.0	134.4	496.7	936.4	295.4	147.7	242.7	291.9
64.91	50.04	-1.244	2.549	2.060	2.998	641.0	132.6	500.7	931.6	290.6	145.3	237.1	285.6
64.88	50.84	-0.982	2.541	3.284	4.779	640.7	132.2	508.7	924.9	284.3	142.1	226.7	274.1
64.95	52.19	-0.907	2.435	3.634	5.289	641.4	126.1	522.2	911.0	269.6	134.8	209.1	254.0
64.92	52.41	-0.807	2.437	4.101	5.969	641.1	126.2	524.4	909.0	267.9	133.9	206.0	250.7
64.91	52.48	-0.607	2.458	5.035	7.329	641.0	127.4	525.1	907.5	266.5	133.3	204.8	249.2
64.93	52.58	-0.31	2.525	6.436	9.368	641.2	131.3	526.0	909.8	268.6	134.3	204.7	249.4
64.90	52.61	-0.01	2.579	7.837	11.408	640.9	134.4	526.3	909.7	268.8	134.4	204.1	248.9
64.89	52.66	0.208	2.641	8.842	12.869	640.8	138.0	526.8	912.2	271.4	135.7	204.4	249.7

Raw Data				Processed Data									
Cell Press Trd (mV)	Pore Press Trd (mV)	Axial LVDT (V)	Load Trd (V)	Change in Length (mm)	Axial Strain (%)	Cell Press (kPa)	Proof Ring (div)	Pore Press (kPa)	P_1 (kPa)	q (kPa)	t (kPa)	p' (kPa)	s' (kPa)
64.88	52.68	0.36	2.665	9.542	13.889	640.7	139.4	527.0	911.6	271.0	135.5	204.0	249.1
64.94	52.73	0.51	2.692	10.257	14.929	641.3	140.9	527.5	912.0	270.7	135.3	204.0	249.1
64.93	52.75	0.76	2.758	11.411	16.608	641.2	144.7	527.7	913.7	272.5	136.3	204.3	249.7
64.94	52.78	0.96	2.799	12.345	17.968	641.3	147.1	528.0	913.8	272.5	136.2	204.1	249.5
64.96	52.73	1.26	2.889	13.746	20.007	641.5	152.3	527.5	916.6	275.1	137.6	205.6	251.5
64.92	52.71	1.66	2.993	15.614	22.727	641.1	158.3	527.3	917.3	276.2	138.1	205.8	251.9
64.94	52.75	1.69	3.076	15.782	22.972	641.3	163.1	527.7	925.0	283.7	141.9	208.1	255.4

